

Durham E-Theses

The role of the C-terminal extension of α B-crystallin upon structure and function and the relationship with disease

Hayes, Victoria.H.

How to cite:

Hayes, Victoria.H. (2008) *The role of the C-terminal extension of α B-crystallin upon structure and function and the relationship with disease*, Durham theses, Durham University. Available at Durham E-Theses Online: <http://etheses.dur.ac.uk/2929/>

Use policy

The full-text may be used and/or reproduced, and given to third parties in any format or medium, without prior permission or charge, for personal research or study, educational, or not-for-profit purposes provided that:

- a full bibliographic reference is made to the original source
- a [link](#) is made to the metadata record in Durham E-Theses
- the full-text is not changed in any way

The full-text must not be sold in any format or medium without the formal permission of the copyright holders.

Please consult the [full Durham E-Theses policy](#) for further details.

Academic Support Office, Durham University, University Office, Old Elvet, Durham DH1 3HP
e-mail: e-theses.admin@dur.ac.uk Tel: +44 0191 334 6107
<http://etheses.dur.ac.uk>

**The Role of the C-terminal Extension of
 α B-crystallin upon Structure and Function
and the Relationship with Disease**

BY

VICTORIA H. HAYES

The copyright of this thesis rests with the author or the university to which it was submitted. No quotation from it, or information derived from it may be published without the prior written consent of the author or university, and any information derived from it should be acknowledged.

**A thesis submitted at the University of Durham
for the degree of Doctor of Philosophy**

School of Biological and Biomedical Sciences


University of Durham, September 2008

13 NOV 2008



DECLARATION

I declare that the experiments described in this thesis were carried out by myself in the School of Biological and Biomedical Sciences, University of Durham, under the supervision of Prof. Roy A. Quinlan. This thesis has been composed by myself and is a record of work that has not been submitted previously for a higher degree. All references have been consulted by myself unless stated otherwise.

A handwritten signature in blue ink, appearing to read 'Victoria H. Hayes', with a long horizontal flourish extending to the right.

Victoria H. Hayes

I certify that, the work reported in this thesis has been performed by Victoria H. Hayes, who during the period of study has fulfilled the conditions of the Ordinance and regulations governing the Degree of Doctor of Philosophy.

A handwritten signature in blue ink, appearing to read 'Roy A. Quinlan', with a stylized, cursive script.

Roy A. Quinlan

ACKNOWLEDGEMENTS

I would like to acknowledge the help of the following people:

My parents Raymond and Denise Hayes for their infinite help and support throughout my studies.

My supervisor Prof. Roy Quinlan for his constant help and guidance and for always making time for me.

Everybody in ICBL who all at some point have been there to discuss my problems and help me as much as possible.

Ming der Perng for always being so kind and helpful and Shu Fang Wen also for her great kindness and for always listening.

Glyn Devlin for being my great host in Cambridge on several occasions and introducing me to the world of CD.

Terry Gibbons for his molecular cloning master classes.

Michael Gardner and Dave Laurie at ImmunoDiagnostic Systems (IDS) Ltd for their time and financial support.

DEDICATION

“Give me the strength to change the things I can change, the courage to let go of the things I need to let go, and the wisdom to know the difference”

Lisa Gardner

TABLE OF CONTENTS

1. INTRODUCTION.....	1
1.1. THE LENS.....	2
1.2. α -CRYSTALLIN.....	5
1.3. THE STRUCTURE OF α -CRYSTALLIN.....	8
1.4. α -CRYSTALLIN AS A MOLECULAR CHAPERONE.....	11
1.5. THE FUNCTIONS OF α B-CRYSTALLIN.....	12
1.5.1. Modulators of Intermediate Filament (IF) assembly.....	12
1.5.2. Regulators of apoptosis.....	14
1.5.3. Transcriptional Regulators.....	14
1.5.4. Genome stability and hyperproliferation.....	15
1.5.5. Proteosome function.....	15
1.6. α B-CRYSTALLIN AND CATARACT.....	17
1.6.1. Age related Cataract.....	17
1.6.2. Disease related Cataract: The risk factors of cataractogenesis.....	18
1.6.3. Congenital cataract.....	19
1.7. NATURALLY OCCURRING MUTATIONS OF α B-CRYSTALLIN.....	21
1.7.1. R120G α B-crystallin.....	22
1.7.2. 450delA α B-crystallin.....	23
1.7.3. Q151X α B-crystallin and 464delCT α B-crystallin.....	24
1.7.4. Post Translational Modifications (PTM).....	25
1.7.5. R157H α B-crystallin.....	27
1.7.6. D140N α B-crystallin.....	28
1.7.7. P20S α B-crystallin.....	28
1.8. HYPOTHESIS AND AIMS OF THE STUDY.....	31

2. MATERIAL AND METHODS.....	33
2.1. CHEMICALS.....	34
2.2. CONSTRUCTION OF α B-CRYSTALLIN MUTANTS.....	34
2.2.1. Primer Design.....	34
2.2.2. Construction of Q151X α B-crystallin mutant using SDM.....	36
2.2.3. Construction of E165X α B-crystallin mutant using SDM.....	39
2.2.4. Construction of 464delCT, E164X, K174X and A171X α B-crystallin mutants.....	40
2.2.5. Sub cloning of mutant DNA into mammalian Expression vector pCDNA3.1(-) from pET23d (+).....	45
2.3. TRANSFORMATION OF PLASMID DNA AND PREPARATION OF INOCULUM FOR BATCH CULTURE.....	46
2.4. BATCH FERMENTATION OF <i>E. COLI</i> BL-21 (PLYSS) CELLS.....	47
2.5. CELL HARVESTING, HOMOGENISATION AND RECOVERY OF THE α B-CRYSTALLIN PROTEIN FRACTION.....	47
2.6. PURIFICATION OF SOLUBLE PROTEIN WILD TYPE α B-CRYSTALLIN.....	48
2.6.1. Removal of DNA from the Wild Type α B-crystallin soluble protein fraction.....	48
2.6.2. Ion Exchange Chromatography.....	49
2.6.3. Size Exclusion Chromatography.....	50
2.6.4. Large scale (6L) α B-crystallin purification.....	51
2.7. PURIFICATION OF MUTANT α B-CRYSTALLIN AS INCLUSION BODIES.....	51
2.7.1. Inclusion body extraction and solubilisation.....	51
2.7.2. Ion Exchange Chromatography.....	52
2.7.3. Refolding of the mutant α B-crystallin.....	53
2.8. CHARACTERISATION OF α B-CRYSTALLIN MUTANTS.....	56
2.8.1. In Vitro protein chaperone assays.....	56
2.8.2. Analytical Size exclusion chromatography.....	57
2.8.3. Mass Spectrometry for molecular weight determination.....	59

2.8.4. Circular Dichroism Spectroscopy.....	59
2.8.5. Thermal Stability Assay.....	61
2.8.6. In Vitro Desmin Filament Assembly and Cosedimentation Assay.....	61
2.8.7. Cross-linking of α B-crystallin.....	63
2.8.8. Dynamic Light Scattering.....	63
2.8.9. bis-ANS fluorescence measurements.....	64
2.9. CELL CULTURES AND TRANSIENT TRANSFECTION ASSAYS.....	64
2.9.1. Protein extraction and cell fractionation.....	65
2.9.2. Immunofluorescence Microscopy.....	66
2.10. ONE DIMENSIONAL SDS PAGE ANALYSIS.....	67
2.11. IMMUNOBLOTTING.....	68
2.12. ANTIBODY PURIFICATION.....	69
2.12.1. Monoclonal α B-crystallin antibody from cell culture supernatant.....	69
2.12.2. Polyclonal α B-crystallin antibody from rabbit serum.....	71
2.13. ANTIBODY CONJUGATION.....	72
2.13.1. HRP Conjugation.....	72
2.13.2. Antibody-Biotin Conjugation.....	74
2.14. PLATE COATING WITH PURIFIED MAB AND PAB ANTIBODIES.....	74
2.15. ENZYME LINKED IMMUNOSORBANT ASSAY FOR DETECTION AND QUANTITATION OF α B-CRYSTALLIN.....	75
2.15.1. Calibrator and sample preparation using Ab: HRP conjugate.....	75
2.15.2. Calibrator and sample preparation using Ab: Biotin conjugate.....	76
2.15.3. Simultaneous ELISA for α B-crystallin detection and quantitation.....	77
2.15.4. Split ELISA for α B-crystallin detection and quantitation.....	78

RESULTS.....	79
---------------------	-----------

.

3. THE FLEXIBLE C-TERMINAL ‘TAIL’ PLAYS AN IMPORTANT ROLE IN MAINTANING THE SOLUBILITY OF αB-CRYSTALLIN OLIGOMER.....	79
--	-----------

3.1. AIMS.....	80
3.2. INTRODUCTION.....	81
3.3. RESULTS.....	86
3.3.1. Assembly of mutant α B-crystallin constructs.....	86
3.3.2. The effect of the c-terminal mutations on the solubility of α B-crystallin mutant proteins expressed in bacterial and mammalian cells.....	90
3.3.3. Purification of recombinant α B-crystallin mutants.....	98
3.3.4. The effect of the C-terminal mutations on the ability of the α B-crystallin mutants to refold.....	121
3.4. DISCUSSION.....	138
3.4.1. The role of the C-terminal ‘tail’ in the solubilisation of α B-crystallin.....	139
3.5. CHAPTER’S CONCLUSIONS.....	143

4. THE ROLE OF THE C-TERMINAL EXTENSION IN THE OLIGOMERISATION AND CHAPERONE FUNCTION OF αB-CRYSTALLIN.....	144
--	------------

4.1. AIMS.....	145
4.2. INTRODUCTION.....	146
4.3. RESULTS.....	155
4.3.1. Truncation of the C-terminal Extension reduces α B-crystallin oligomerisation.....	155
4.3.2. Effect of the C-terminal mutations upon the secondary structure and oligomerisation of α B-crystallin.....	159

4.3.3. Loss in Heat Stability of α B-crystallin correlates with changes in secondary structure.....	162
4.3.4. Effect of the C-terminal extension mutations upon α B-crystallin chaperone activity.....	164
4.3.5. Ability of the disease causing mutants to inhibit desmin filament aggregation.....	168
4.4. DISCUSSION.....	175
4.4.1. Removal of the C-terminal extension reduces α B-crystallin oligomerisation, but not chaperone activity.....	177
4.4.2. The C-terminal extension is not essential for chaperone activity and is inhibitory for some client proteins.....	178
4.4.3. Aggregation of α B-crystallin is encouraged by the removal of the C-terminal extension.....	180
4.4.4. Reduced protein stability and uncontrolled self-aggregation underlies the molecular basis of the Q151X, 450delA and 464delCT mutations.....	181
4.5. CHAPTER'S CONCLUSIONS.....	183

5. THE RELATIONSHIP BETWEEN SUBUNIT DYNAMICS AND THE OLIGOMERISATION OF WILD TYPE α B-CRYSTALLIN.....184

5.1. AIMS.....	185
5.2. INTRODUCTION.....	186
5.2.1. Theories for the role of oligomerisation and subunit dynamics in chaperone activity.....	187
5.2.2. Influential factors affecting subunit dynamics and chaperone activity.....	190
5.3. RESULTS.....	197
5.3.1. The effect of α B-crystallin concentration upon oligomerisation and polydispersity.....	199
5.3.2. Identification of an unknown Mwt α B-crystallin species.....	205
5.3.3. Characterisation of the unknown Mwt α B-crystallin species.....	211

5.4.	DISCUSSION.....	231
5.4.1.	The polydispersity of the wild type α B-crystallin oligomer is dependant upon concentration.....	231
5.4.2.	A low Mwt α B-crystallin species isolated from the α B-crystallin Oligomer could potentially be the active unit of chaperone activity.....	237
5.5.	CHAPTER'S CONCLUSIONS.....	241
6.	CONCLUSION.....	242
6.1.	STUDY SUMMARY.....	243
6.2.	IMPLICATIONS FOR THE CELLULAR FUNCTIONS OF α B-CRYSTALLIN.....	245
6.2.1.	Cytoplasmic Effects.....	246
6.2.2.	Nuclear Effects.....	248
6.3.	POTENTIAL MECHANISMS OF PHENOTYPIC HETEROGENEITY ASSOCIATED WITH α B-CRYSTALLIN.....	250
6.4.	FUTURE WORK.....	255
6.4.1.	Phenotypic Heterogeneity.....	255
6.4.2.	Additional congenital α B-crystallin mutant characterisation.....	256
6.4.3.	Refolding efficiency.....	256
6.4.4.	The effect of α B-crystallin concentration upon oligomerisation and polydispersity.....	257
6.4.5.	Characterisation of the potential unit of chaperone activity.....	257

APPENDICES.....	259
 1. APPENDIX 1-ASSEMBLY AND BLAST ANALYSIS OF MUTANT αB-CRYSTALLIN BACTERIAL AND MAMMALIAN EXPRESSION CONSTRUCTS FOR CHAPTER 3.....	 259
A1.1 THE PROMOTER AND MULTIPLE CLONING SEQUENCES OF VECTORS USED FOR MUTAGENESIS AND CLONING.....	260
A1.2 ASSEMBLY OF Q151X αB-CRYSTALLIN CONSTRUCT BY SDM.....	263
A1.3 ASSEMBLY OF E165X αB-CRYSTALLIN BY SDM.....	266
A1.4 ASSEMBLY OF 464DELCT αB-CRYSTALLIN.....	270
A1.5 ASSEMBLY OF E164X αB-CRYSTALLIN.....	274
A1.6 ASSEMBLY OF A171X αB-CRYSTALLIN.....	278
A1.7 ASSEMBLY OF K174X αB-CRYSTALLIN.....	282
A1.8 SUBCLONING αB-CRYSTALLIN CONSTRUCTS INTO THE MAMMALIAN EXPRESSION VECTOR PCDNA3.1(-).....	286
 2. APPENDIX 2-CALIBRATION OF ANALYTICAL SEC COLUMN AND MOLECULAR WEIGHT DETERMINATION OF αB-CRYSTALLIN MUTANTS FOR CHAPTER 4 (SECTION 4.3.1).....	 296
A2.1 CALIBRATION OF SUPEROSE 6 ANALYTICAL SEC COLUMN.....	297
A2.2 MOLECULAR WEIGHT DETERMINATION OF αB-CRYSTALLIN MUTANTS.....	300
 3. APPENDIX 3-CHAPERONE ASSAY DATA SETS FOR CHAPTER 4 (SECTION 4.3.4).....	 302
A3.1 CITRATE SYNTHASE ASSAY TRIPLICATE DATA SETS FOR FIGURE 4.7.....	303
A3.2 INSULIN ASSAY TRIPLICATE DATA SETS FOR FIGURE 4.8.....	305

TABLE OF FIGURES

Figure 1.1. Schematic drawing of a sagittal section through a vertebrate lens.....	3
Figure 1.2. Secondary structure the hsp 16.9 subunit with an ordered N-terminus.....	8
Figure 1.3. Structural Alignment of α B-crystallin mutations.....	30
Figure. 2.1. α B-crystallin ELISA plate map.....	77
Figure 3.1. Structural alignment of the C-terminal extensions α -crystallins and sHSPs.....	82
Figure 3.2. Solubility of α B-crystallin mutants expressed in BL-21 <i>E.coli</i> cells.....	92
Figure 3.3. Formation of cytoplasmic aggregates by selected α B-crystallin mutants in MCF7 cells.....	95/96
Figure 3.4. The solubility of α B-crystallin mutants in populations of transiently transfected MCF7 cells.....	97
Figure 3.5. IEX Chromatography of Wild type α B-crystallin and fraction analysis.....	100
Figure 3.6. SEC Chromatography of Wild type α B-crystallin and fraction analysis.....	101
Figure 3.7. Analysis of additional species in the Wild type α B-crystallin SEC pool.....	102
Figure 3.8. Dynamic Light Scattering analyses of α B-crystallin wild type.....	103
Figure 3.9. IEX Chromatography of K174X α B-crystallin and fraction analysis.....	105
Figure 3.10. SEC Chromatography of K174X α B-crystallin and fraction analysis.....	106
Figure 3.11. IEX Chromatography of A171X α B-crystallin and fraction analysis.....	108
Figure 3.12. SEC Chromatography of A171X α B-crystallin and fraction analysis.....	109
Figure 3.13. IEX Chromatography of 450delA α B-crystallin and fraction analysis.....	111
Figure 3.14. Analysis of additional proteins present in the 450delA α B-crystallin IEX pool by Immunoblotting.....	112
Figure 3.15. IEX Chromatography of 464delCT α B-crystallin and fraction analysis.....	114
Figure 3.16. IEX Chromatography of E164X α B-crystallin and fraction analysis.....	116
Figure 3.17. IEX Chromatography of E165X α B-crystallin and fraction analysis.....	118
Figure 3.18. IEX Chromatography of Q151X α B-crystallin and fraction analysis.....	120
Figure 3.19. The 450delA α B-crystallin refolding procedure using a one step dialysis....	122
Figure 3.20. Refolding 450delA α B-crystallin in association with the wild type α B-crystallin.....	123

Figure 3.21. The effect of protein and urea concentration on soluble Q151X α B-crystallin yield	125
Figure 3.22. Refold of 450delA/ Wild type α B-crystallin using diluted protocol.....	129
Figure 3.23. Optimisation of the 464delCT α B-crystallin refold process.....	131
Figure 3.24. Refolding efficiency of E164X under the diluted and direct dialysis protocols.....	133
Figure 3.25. Characterisation of the bacterially expressed and purified mutants used in this study by SDS-PAGE.....	137
Figure 4.1. Interactive regions of α B crystallin important for chaperone function and oligomerisation	149/150
Figure 4.2. Interactive sites of α B-crystallin associated with functional and structural activity.....	153
Figure 4.3. Effect of C-terminal mutations upon the oligomerisation of α B-crystallin.....	157
Figure 4.4. Native gel electrophoresis of the Q151X α B-crystallin oligomer.....	158
Figure 4.5. Circular Dichroism of wild type α B-crystallin and the C-terminal extension Mutants.....	160
Figure 4.6. Bis-ANS fluorescence binding properties of the α B-crystallin mutants.....	161
Figure 4.7. Thermal stability of wild type and C-terminal extension mutants of α B-crystallin.....	163
Figure 4.8. Aggregation of Citrate Synthase in the presence of wild type and mutant α B-crystallins.	166
Figure 4.9. Aggregation of Insulin in the presence of wild type and mutant α B-crystallins.	167
Figure 4.10. Sedimentation assay to investigate the prevention of desmin filament aggregation in the presence of various α B-crystallins at 37°C.....	170
Figure 4.11. Desmin Filament assembly in the presence of wild type and Q151X α B-crystallin.....	171
Figure 4.12. Sedimentation assay to investigate the prevention of desmin filament aggregation in the presence of various α B-crystallins at 20°C.....	173
Figure 4.13. Sedimentation assay to investigate the prevention of desmin filament aggregation in the presence of various α B-crystallins at 44°C.....	174

Figure 5.1. The effect of decreasing concentration upon the oligomerisation of wild type α B-crystallin at ambient temperature (20°C).....	199
Figure 5.2. The effect of decreasing concentration upon the oligomerisation of wild type α B-crystallin at 4°C.....	201
Figure 5.3. The effect of decreasing concentration upon the oligomerisation of wild type α B-crystallin at 20°C.....	203
Figure 5.4. Characterisation of tail material from a 2mg/ml α B-crystallin load onto a 23ml Superose 6 column.....	207
Figure 5.5. Characterisation of tail material from a 2 mg/ml α B-crystallin load onto a HW55s 23ml column.....	209
Figure 5.6. Large Scale purification of wild type α B-crystallin.....	215
Figure 5.7. Characterisation of tail material from a 31.25mg/ml α B-crystallin load onto a HW55s 413ml column.....	217
Figure 5.8. Rechromatography of the unknown α B-crystallin.....	220
Figure 5.9. Cross-linked α B-crystallin wild type oligomer by DMS.....	223
Figure 5.10. Cross-linking of α B-crystallin wild type oligomer by gluteraldehyde...224/225	
Figure 5.11. Immunoblotting of Cross-linked α B-crystallin wild type oligomer by gluteraldehyde.....	227
Figure 5.12. Immunoblotting of Cross-linked α B-crystallin unknown Mwt species.....	229
Figure 5.13. Schematic representation of the possible oligomeric assembly of α B-crystallin.....	236
Figure 6.1. Effect of coaggregation upon the physiological function of α B-crystallin.....	245
Figure A1.1. The promoter and multiple cloning sequences of pGEM®-T Easy.....	260
Figure A1.2. The promoter and multiple cloning sequences of pET23d(+)......	261
Figure A1.3. The promoter and multiple cloning sequences of pcDNA3.1(-)......	262
Figure A1.4. SDM PCR for insertion of mutant α B-crystallin into pET23d(+) bacterial expression vector.....	264
Figure A1.5. BLAST data for Q151X insert in pET23d(+) Construct 1.....	265
Figure A1.6. BLAST data for Q151X insert in pET23d(+) Construct 2.....	265
Figure A1.7. PCR mutagenesis of E165X mutant construct assembly.....	267
Figure A1.8. BLAST data for E165X insert in pET23d(+) Construct 2.....	268

Figure A1.9. BLAST data for E165X insert in pET23d(+) Construct 10.....	269
Figure A1.10. Assembly of 464delCT α B-crystallin construct using pGEM®-T Easy vector system.....	271
Figure A1.11. BLAST data for 464delCT insert in pGEM-T Easy-Construct 8.....	272
Figure A1.12. BLAST data for 464delCT insert in pET23d(+)-Construct 2.....	273
Figure A1.13. Assembly of E164X α B-crystallin construct using pGEM®-T Easy vector system.....	275
Figure A1.14. BLAST data for E164X insert in pGEM-T Easy-Construct 4.....	276
Figure A1.15. BLAST data for E164X insert in pET23d(+)-Construct 1.....	277
Figure A1.16. Assembly of A171X α B-crystallin construct using pGEM®-T Easy vector system.....	279
Figure A1.17. BLAST data for A171X insert in pGEM-T Easy-Construct 2.....	280
Figure A1.18. BLAST data for A171X insert in pET23d(+)-Construct 2.....	281
Figure A1.19. Assembly of K174X α B-crystallin construct using pGEM®-T Easy vector system.....	283
Figure A1.20. BLAST data for K174X insert in pGEM-T Easy-Construct 2.....	284
Figure A1.21. BLAST data for K174X insert in pET23d(+)-Construct 1.....	285
Figure A1.22. Subcloning of α B-crystallin constructs from pET23d(+) into the vector pcDNA3.1(-).....	288
Figure A1.23. BLAST data for 464delCT insert in pcDNA3.1(-) - Construct 2.....	289
Figure A1.24. BLAST data for 450delA insert in pcDNA3.1(-) - Construct 3.....	290
Figure A1.25. BLAST data for K174X insert in pcDNA3.1(-) - Construct 1.....	291
Figure A1.26. BLAST data for Q151X insert in pcDNA3.1(-) - Construct 1.....	292
Figure A1.27. BLAST data for E164X insert in pcDNA3.1(-) - Construct 4.....	293
Figure A1.28. BLAST data for A171X insert in pcDNA3.1(-) - Construct 2.....	294
Figure A1.29. BLAST data for E165X insert in pcDNA3.1(-) - Construct 1.....	295
Figure A2.1. The SEC calibrator profiles for calibration of the Analytical SEC column.....	297/298/299
Figure A2.2. SEC calibration curves for MW determination.....	300/301
Figure A3.1. Triplicate data set of Citrate synthase assays.....	303
Figure A3.2. Triplicate data set of Insulin assays.....	305

Figure A4.1. The effect of decreasing concentration upon the oligomerisation of wild type α B-crystallin under conditions of 1M NaCl.....	309
Figure A4.2. Analysis of the 93 min peak of the Superose 6 SEC analytical column.....	312
Figure A4.3. The effect of the injection upon the presence of the 93 min peak.....	314
Figure A5.1. A typical sandwich ELISA assay.....	317
Figure A5.2. Titration Pab HRP conjugates on plates with 0-100 ng/ml α B-crystallin.....	320
Figure A5.3. Titration of Mab HRP conjugates on plates with 0-100 ng/ml α B-crystallin.....	320
Figure A5.4. The specific signal of a Poly capture assay with titrated Mab Biotin and Av-HRP levels.....	322
Figure A5.5. Optimisation of the α B-crystallin Mab Biotin Simultaneous ELISA.....	324
Figure A5.6. A typical 500 μ g SEC elution profile.....	326

TABLE OF TABLES

Table 1.1. Mutations of the CRYAB gene.....	21
Table 2.1. Oligonucleotide primer sequence details used for introduction of the α B-crystallin mutations.....	35
Table 2.2. Q151X α B-crystallin mutant reaction mixture for PCR.....	36
Table 2.3. Q151X α B-crystallin mutant PCR cycling condition.....	37
Table 2.4. E165X α B-crystallin mutant reaction mixture for PCR.....	39
Table 2.5. E165X α B-crystallin mutant PCR cycling conditions.....	40
Table 2.6. Easy A PCR reaction mixture.....	41
Table 2.7. Easy A PCR cycling conditions.....	42
Table 2.8. Ligation reactions using the pGEM-T Easy (Promega) ligation kit.....	43
Table 2.9. Mixture for restriction enzyme digestion	44
Table 2.10. Ligation reaction for sub cloning into pET23d(+).	45
Table 2.11. Mixture for restriction enzyme digestion	46
Table 2.12. Extinction Coefficients of α B-crystallin mutants used for concentration determinations.....	54
Table 2.13. Details of the Calibration of the Superose 6 SEC column.....	58
Table 2.14. Far and Near UVCD spectra assay parameters.....	60
Table 3.1. Optimisation of the urea and mutant concentration for successful refolding	124
Table 3.2. Yield of Q151X α B-crystallin over the diluted refolding process from 1.2mg.....	126
Table 3.3. Yield of Q151X α B-crystallin over the diluted refolding process from 12 mg.....	127
Table 3.4. Refolding efficiency of Q151X/ Wild type using the diluted protocol.....	128
Table 3.5. Yield of 450delA: wild type α B-crystallin over a 1.2 mg diluted refolding process.....	130
Table 3.6. Yield of E165X α B-crystallin from direct one step dialysis.....	130
Table 3.7. Refolding efficiency of 464delCT/ wild type α B-crystallin using the diluted protocol.....	132

Table 3.8. Refolding efficiency of 464delCT/ wild type α B-crystallin using the direct dialysis protocol.....	132
Table 3.9. Refolding efficiency of E164X using the diluted protocol.....	134
Table 3.10. Refolding efficiency of E164X using the direct dialysis protocol.....	134
Table 3.11. Summary of refold efficiency of α B-crystallin mutants.....	135
Table 4.1. Interactive sites of α B-crystallin and their numerous functions.....	148
Table 5.1. Integration data for Figure 5.1.....	200
Table 5.2. Integration data for Figure 5.2.....	201
Table 5.3. Integration data for Figure 5.3.....	203
Table 5.4. Comparison of unknown Mwt species between 125 mg and 0.5 mg SEC runs.....	218
Table A3.1. Inhibition data for the Citrate Synthase assay.....	304
Table A3.2. Inhibition data for the Insulin assay.....	306
Table A4.1. Integration data for Figure A4.1.....	310
Table A4.2. Relative peak heights of 93 min peaks from Figure A4.2.....	313
Table A5.1. Quantitation of Oligomer and 93min peak material from 500 μ g α B-crystallin load using Mab: HRP.....	327
Table A5.2. Quantitation of Oligomer and 93min peak material from 125 μ g α B-crystallin load using Mab: HRP.....	328
Table A5.3. Quantitation of Oligomer and 93min peak material from 500 μ g α B-crystallin load using Mab: Biotin.....	329
Table A5.4. Quantitation of 93min peak material from 125 μ g α B-crystallin load using Mab: Biotin.....	331

LIST OF ABBREVIATIONS

Ab	antibody
a.a	Amino Acid
A β	Amyloid- β peptide
AD	Alzheimer's Disease
ADCC	Autosomal Dominant Congenital Cataract
Ag(s)	Antigens
ALS1	Amyotrophic lateral sclerosis 1
ATP	Adenosine triphosphate
Av	Avidin
Av-HRP	Avidin labelled with Horse Radish Peroxidase
BCA	Bicinchoninic Acid
Biotin LC NHS	Succinimidyl - (biotinamido) hexanoate-biotin
bis-ANS	4,4'-dianilino-1,1'-binaphthyl-5,5'-disulfonic acid
BLAST	Basic Local Alignment Search Tool
BSA	Bovine serum albumin
BQ-HRP	Benzoquinone-HRP
CD	Circular Dichroism
CMT	Charcot-Marie-Tooth
CIP	Cleaning in place
CMAPS	Compound motor action potentials
CNS	Central nervous system
CS	Chaperone site
CSS	Calibrator Stock Solution
CV	Column volume
DAPI	4'-6-diamidino-2-phenylindole
DMEM	Dulbecco's Minimum Eagle's Medium
DMF	Dimethyl Formamide
DNA	Deoxyribonucleic acid
DCM	Dilated cardiomyopathy
dHMN	Distal hereditary motor neuropathy

DRM	Desmin related myopathy
dSMA-V	Distal spinal muscular atrophy type V
DTT	Dithiothreitol
DLS	Dynamic Light Scattering
DMS	Dimethyl Suberimide•2 HCl
DTBP	Dimethyl 3,3' – dithiobispropionimide•2 HCl
EACC	European Animal Cell Culture Collection
EDTA	Ethylenediaminetetraacetic acid
EGF	Epithelial growth factor
EGTA	Ethylene glycol tetraacetic acid
ELISA	Enzyme Linked ImmunoSorbant Assay
EGF	Epithelial growth factor
FBX4	F-box protein 4
FCS	Fetal calf serum
FFL	Feed-forward loops
FPLC	Fast Performance Liquid Chromatography
GA	Gluteraldehyde
GARS	Glycyl tRNA synthetase gene
Gdn-HCl	Guanidinium hydrochloride
GFAP	Glial fibrillary acidic protein
GFC	Gel filtration chromatography
HCl	Hydrochloric acid
HCM	Hypertrophic cardiomyopathy
HPLC	High Performance Liquid Chromatography
HRP	Horse radish Peroxidase
HSC	Hepatic stellate cell
IEX	Ion exchange chromatography
IF	Intermediate Filaments
IgG	Immunoglobulin
IPTG	Isopropyl-beta-D-Thiogalactopyranoside
JNK	c-Jun amino-terminal kinases
KARS	lysyl tRNA synthetase

LB	Luria-Bertani
Mab	Monoclonal Antibody
MgCl ₂	Magnesium Chloride
MALDI-TOF	Matrix-assisted laser desorption/ ionization- Time of Flight
MAP	Mitogen activated protein
MAPKAP	Mitogen activated protein kinase activated protein
MAPs	Microtubule Associated Proteins
MECs	Mammary epithelial cells
mRNA	messenger Ribonucleic Acid
MS	Multiple Sclerosis
MW	Molecular Weight
MWCO	Molecular weight cut off
NaCl	Sodium Chloride
NaOH	Sodium hydroxide
NSB	Non specific binding
NMR	Nuclear magnetic resonance
OD	Optical density
Pab	Polyclonal Antibody
PBH	Packed bed height
PBS	Phosphate Buffered Saline
PCO	Posterior capsular opacification
PCR	Polymerase Chain Reaction
PEI	Polyethylimine
PES	Polyethersulphone
PI	Protease Inhibitor
PMSF	Phenylmethanesulphonylfluoride
PROPOR PES	Proportional Polyethersulphone
PTM	Post translational modifications
Q-TOF MS	Quadrupole Time of Flight Mass Spectrometry
RS	Recognition sequence
RNA	Ribonucleic acid
SCF complex	Skp1-Cullin-F-box containing complex

SDS PAGE	sodium dodecyl (lauryl) sulfate-polyacrylamide gel electrophoresis
SEC	Size Exclusion Chromatography
SDM	Site Directed Mutagenesis
sHSPs	Small heat shock proteins
s-IBM	Inclusion body mitosis
SNAPS	Sensory nerve action potentials
SOD1	Superoxide dismutase 1 gene
SPF	Soluble protein fraction
SPR	Surface plasmon resonance
TAE	40mM Tris-acetate, 1mM EDTA pH 8.0
TBS	20mM Tris HCl, 150mM NaCl, pH 7.4
TBST	20mM Tris HCl, 150mM NaCl, 0.2% Tween 20, pH 7.4,
TMAE	Trimethylammoniummethyl
TMB	3,3',5,5'-Tetramethylbenzidine
TRIS HCl	Tris(hydroxymethyl)methylamine hydrochloride
UV	Ultra Violet

ABSTRACT

The eye lens protein α B-crystallin plays an important role in maintaining the refractive index of the lens, however is also found in many non-lenticular tissues suggest that it has general cellular functions over and above its role in light refraction. The role of the C-terminal extension of α B-crystallin upon solubility, structure and function and the relationship with disease has not been investigated. In this study, the systematic analysis of the role of the C-terminal extension of α B-crystallin aimed to investigate the hypothesis that the C-terminal region in α B-crystallin is important for solubility, structure and function of the protein. This study also aimed to find a link between the role of the C-terminal and the symptoms of disease, thus providing a potential explanation of whether the three congenital mutations (450delA, Q151X and 464delCT), which alter the C-terminal extension of α B-crystallin, cause the various diseases via the loss of chaperone function or perhaps by a different mechanism. Further more this study aimed to elucidate the mechanism of phenotypic heterogeneity associated with these α B-crystallin mutations.

I compared the three C-terminal α B-crystallin mutants (450delA, Q151X and 464delCT) to a series of C-terminal truncations (E164X, E165X, K174X and A171X) and found that the C-terminal extension was essential for oligomerisation but not chaperone function, infact the removal of the entire C-terminal extension actually enhanced chaperone activity, however significantly destabilized α B-crystallin causing it to self-aggregate. This instability was supported by refolding analysis, where the 450delA and 464delCT mutants could only be refolded and assayed as a complex with wild type α B-crystallin, however the Q151X α B-crystallin could be refolded alone. From these studies, I conclude that all three disease-causing mutations (450delA, 464delCT and Q151X) in the C-terminal extension destabilise α B-crystallin and increase its tendency to self-aggregate. I propose that it is this, rather than a catastrophic loss of chaperone activity, that is a major factor in disease development.

CHAPTER 1

INTRODUCTION



1.1. THE LENS

The function of the eye lens fulfils two requirements; it has to provide transparency and a high refractive index, i.e. low light scattering and high solubility of its cytoplasmic proteins (Bloemendal et al., 2004). The lens is an encapsulated structure consisting almost entirely of a large number of rigid, elongated cells known as lens fibres or fibre cells (Jacob et al., 2000). These cells are produced via the terminal differentiation of a monolayer of epithelial cells, located just beneath the anterior lens capsule (Rafferty, 1985), and include the programmed removal of cytoplasmic organelles (Piatigorsky, 1981). This is accompanied by the expression of an extensive range of lens fibre cell-specific proteins including α -, β - and γ -crystallins and membrane-associated proteins (Jacob et al., 2000; Mörner, 1894; Perng and Quinlan, 2005). Despite these alterations, the differentiated lens fibre cells maintain a well-organised lenticular cytoskeleton comprising actin-containing microfilaments, microtubules and at least two different Intermediate Filament networks (Meriin et al., 1998), one based on vimentin and the other based on a copolymer of lens-specific intermediate filament proteins (Meriin et al., 1998; Sandilands et al., 1995).

In the mature lens, hexagonally packed, long ribbon-like fibre cells, which in man are up to 10 mm long, are arranged in concentric shells, with the oldest cells at the centre and the youngest on the outside (Maisel, 1985) (see Figure 1). This process begins early in embryogenesis and continues throughout life (Grainger, 1992), resulting in the deposition of one layer of fibre cells upon another (Bron et al., 2000). As new layers of fibre cells are produced, existing layers are displaced toward the centre of the lens (Jacob et al., 2000). The absence of cell nuclei, of deoxyribonucleic acid (DNA) and ribonucleic acid (RNA) means that the fibre cells are unable to renew or replace their proteins or replace damaged proteins (Harding, 1991). Successful organogenesis results in a transparent biconvex lens suspended in the eye by zonular ligaments, between the aqueous humour and the vitreous body. Exchange of waste products and nutrients occurs with the aqueous humour across the semi-permeable lens capsule (Rafferty, 1985).

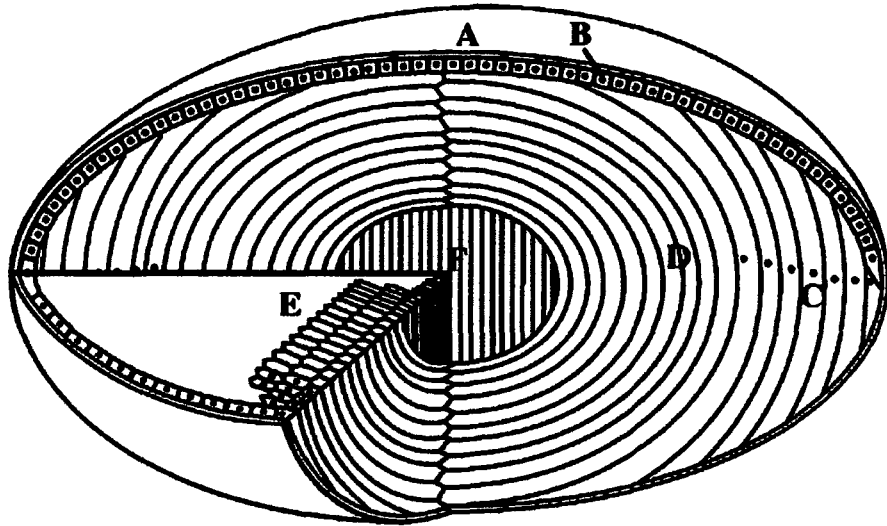


Figure 1. Schematic view of the eye lens showing the main features and regions. The lens of the eye is enclosed by lens capsule (A) and the anterior surface of the lens is covered with a single layer of epithelial cells (B). The lens fibre cells are formed from epithelial cells at the lens equator (C) as part of their differentiation pathway. The epithelia elongate until their ends reach the two lens poles and are joined at the lens sutures. One of the striking features of the lens differentiation process at this stage is the removal of membrane-bound organelles (D) including nuclei, as indicated here as black dots. A cross section of the lens reveals the elongated fibre cells with characteristic hexagonal shape (E). The bulk of the lens thus consists of long, ribbon-like fibre cells arranged as concentric layer with the primary fibre cells at the centre of the lens (F). (Reprinted from (Perng et al., 2007) Copyright 2007, with permission from Elsevier).

The shape of the fibre cells is determined and maintained by an extensive cytoskeleton (Alizadeh et al., 2002) consisting of the type III IFs. IFs are ubiquitous cytoskeletal elements generally considered as one of the most insoluble and resilient structures of the eukaryotic cell (Nicholl and Quinlan, 1994). The cells of the eye lens contain type III IF vimentin (present in both differentiated and undifferentiated lens epithelium) (Geisler and Weber, 1981; Ramaekers et al., 1982; Ramaekers et al., 1980) as well as two other IF proteins phakinin and filensin (Maisel and Perry, 1972). Interestingly, vimentin appeared to be absent from older fibre cells (Bradley et al., 1979; Ramaekers et al., 1980) and phakinin and filensin appear to be unique to the differentiated lens fibre cell (Gounari et al., 1993; Hess et al., 1993; Hess et al., 1996; Hess et al., 1998; Masaki and Watanabe, 1992; Orii et al., 1993; Sandilands et al., 1995).

Thus, secondary lens fibre elongation and compaction are accompanied by alterations in the expression of several components of the cytoskeletal architecture. In the

mature lens fibre cell, keratin and vimentin are not expressed but instead, phakinin and filensin assemble to form a novel cytoskeletal structure referred to as the beaded filament (Maisel and Perry, 1972; Perng et al., 2007). The critical role played by the exact architecture of the cytoskeleton is indicated by the fact that a lens lacking the lens-specific intermediate filament proteins phakinin and filensin is opaque even though the overall fibre cell morphology is normal (Alizadeh et al., 2002; Sandilands et al., 1995; Sandilands et al., 2003). The beaded filament appears to have the ability to interact with the chaperone protein α -crystallin (Iwaki et al., 1989; Kato et al., 1992; Lowe et al., 1992) and implicates chaperones in the remodelling of IF during development and cell differentiation (Nicholl and Quinlan, 1994).

1.2. α -CRYSTALLIN

The human lens fibre cells have an unusually high protein concentration of approx. 0.32 g/ml (Bloemendal et al., 2004), and consist mostly of abundant water-soluble crystallins (Augusteyn, 2004), which account for 90% of total lens proteins (Thampi et al., 2002). The lens crystallins play a crucial role in maintaining the clarity of the lens and its refractive properties (Thampi et al., 2002). For the lens to be able to retain life-long transparency in the absence of protein turnover, the crystallins must meet not only the requirement of solubility associated with high cellular concentration but that of longevity as well. For proteins, longevity is commonly assumed to be correlated with long-term retention of native structure, which in turn can be due to inherent thermodynamic stability, efficient capture and refolding of non-native protein by chaperones, or a combination of both (Bloemendal et al., 2004).

The crystallins were first identified as the major proteins of the eye lens and their subsequent classification into α -, β - and γ -crystallins (Mörner, 1894), allowed different functional properties to be assigned to the α - and the $\beta\gamma$ -crystallin groups. The α -crystallin functions as a molecular chaperone (Horwitz, 1992) as well as a structural protein (Nicholl and Quinlan, 1994) and β - and γ -crystallins are structural proteins (Bloemendal et al., 2004; Bloemendal and de Jong, 1991).

In its native state, α -crystallin is a large water-soluble aggregate, with an average molecular weight (Mwt) of approximately 800 kDa (Groenen et al., 1994) and is comprised of two polypeptides, α A-crystallins and α B-crystallins each encoded by a different gene, which share 60% sequence homology (Bloemendal and de Jong, 1991). In humans, the α A-crystallin gene (CRYAA), which is located on chromosome 21, encodes a polypeptide of 173 residues. The α B-crystallin gene (CRYAB), which is located on chromosome 11, encodes a 175-residue polypeptide (Horwitz, 1992). Urea denaturation studies showed α -crystallin to be 50% unfolded at about 2.9 M urea, whilst the C-terminal domain of α B-crystallin, started unfolding at 2.5 M urea and the N-terminal domain at 4.0 M urea. For unfolding of the C-terminal domain of α A-crystallin 4 M urea (at pH 3.9) is required indicating that α B-crystallin is less stable than α A-crystallin and is stabilized in the α -crystallin assembly by its interaction with α A-crystallin (Sun et al., 1998).

These two homologous subunits constitute about 30% of the proteins in young human lenses and in the outer cortex of the adult human lens (Bhat and Nagineni, 1989; Dubin et al., 1989). These proteins share a common central domain of about 90 residues (the 'α-crystallin domain') with variable N- and C-terminal extensions (Augusteyn, 2004). In its native state in the lens, α-crystallin is always found as a heterogeneous oligomeric assembly consisting of a 3:1 ratio of αA to αB-crystallin subunits (Siezen et al., 1978) (2:1 in the foetal lens (Ma et al., 1998)), that self-associate to form polydisperse assemblies with a wide Mwt distribution of 300000 to over one million (Horwitz, 1993). With a similar Mwt of 19909Da and 20159Da for αA- and αB-crystallin respectively, the native complex with an average Mwt of 800kDa (Groenen et al., 1994) may consist of between 15-50 subunits (Groenen et al., 1994; Horwitz, 2003).

Sequence comparisons of α-crystallin with other proteins found homologies between small heat shock proteins (sHSPs) and α-crystallins, suggesting that α-crystallin is a member of the heat shock protein family (de Jong et al., 1988; Ingolia and Craig, 1982; Nene et al., 1986) and functions as a molecular chaperone (Horwitz et al., 1992; Klemenz et al., 1991).

Until about 1985, it was generally accepted that the α-crystallins were lens specific, however since that time, evidence has accumulated that show α-crystallins exist in many non-lenticular tissues (Inaguma et al., 1995; Lewis et al., 1988; Moscona et al., 1985). The expression of αB-crystallin has been found in non-lenticular tissues with high oxidative activity such as heart, striated muscle, lung, spinal cord, brain, retina and kidney (Bhat and Nagineni, 1989; Dubin et al., 1989; Iwaki et al., 1989), but also in degenerative disorders of the nervous system. Reports show an over expression of αB-crystallin in the development of benign tumours associated with tuberous sclerosis, neuromuscular disorders, and other neurological diseases, such as Alexander disease (Head et al., 1993; Johnson and Bettica, 1989; Tomokane et al., 1991), Alzheimer's (Renkawek et al., 1994; Shinohara et al., 1993), Parkinson's diseases (Lowe et al., 1992; Renkawek et al., 1999), and multiple sclerosis (Lowe et al., 1992; Renkawek et al., 1999; van Noort et al., 1995; Van Noort et al., 1998). αB-crystallin is frequently found co-localised with amyloid plaques *in vivo* (Sun and MacRae, 2005) and amyloid has been connected with a wide range of disorders including Alzheimers, Creutzfeld-Jakob disease and type II diabetes (Raso, 2000; Selkoe, 2003a; Selkoe, 2003b). A recent study suggested that a fine balance

may be at play *in vivo* between a natively aggregated functional α B-crystallin and a misfolded aggregate in the form of amyloid fibrils (Meehan et al., 2007). Naturally occurring mutations of α B-crystallin have been associated with the onset of diseases such as cataract (Berry et al., 2001; Liu et al., 2006b; Vicart et al., 1998), desmin related myopathy (DRM) (Selcen and Engel, 2003; Vicart et al., 1998) and dilated cardiomyopathy (DCM) (Inagaki et al., 2006) (see Section 1.6).

The extra lenticular expression of α B-crystallin has been reported in many tissues but α A-crystallin is mainly lenticular and divergence in the promoter region of α A-crystallin means it is not stress induced (Derham and Harding, 1999). The protein α A-crystallin however, has been found in non-lenticular tissues such as the rat spleen and the thymus in trace amounts (Jimenez-Asensio et al., 1999; Kato et al., 1991). Deretic *et al.* (1994) directly demonstrated α A-crystallin is synthesized outside of the lens in retinal cells of frogs (Deretic et al., 1994), and has more recently been found in the mouse retina (Xi et al., 2003). Reports show an over expression of α A-crystallin in transgenic mice resulted in myelin degradation and axonal dystrophy and developed hind limb paralysis after 8 weeks of age with large α A-crystallin deposits in the astrocytes of the spinal cord and Schwann cells of the sciatic nerve (De Rijk et al., 2000; Van Rijk et al., 2003). The naturally occurring mutation R116C was associated with autosomal dominant congenital cataract associated with a missense mutation in the human α A-crystallin gene CRYAA (Litt et al., 1998).

1.3. THE STRUCTURE OF α -CRYSTALLIN

The polydisperse nature of α -crystallin is thought to have been the main obstacle to acquisition of high resolution X-ray crystallographic data to determine its structure. Over many years several models for the tertiary and quaternary structure of α -crystallin have been proposed using a variety of analytical techniques (Peterson et al., 2004).

Kim et al. (1998) reported the crystal structure of sHSP 16.5 from *Methanococcus jannaschii*, a hyperthermophilic archaeon (Kim et al., 1998), which provided some insight into the structure of sHSPs assembly (van Montfort et al., 2001). Van Montfort et al. (2001), presented the first crystal structure of a eukaryotic sHSP, cytosolic class I HSP16.9 from wheat, (see Figure 1.2), whose homology to α A- and α B-crystallin via the highly conserved α -domain, allowed some insight into the structure of α -crystallin.

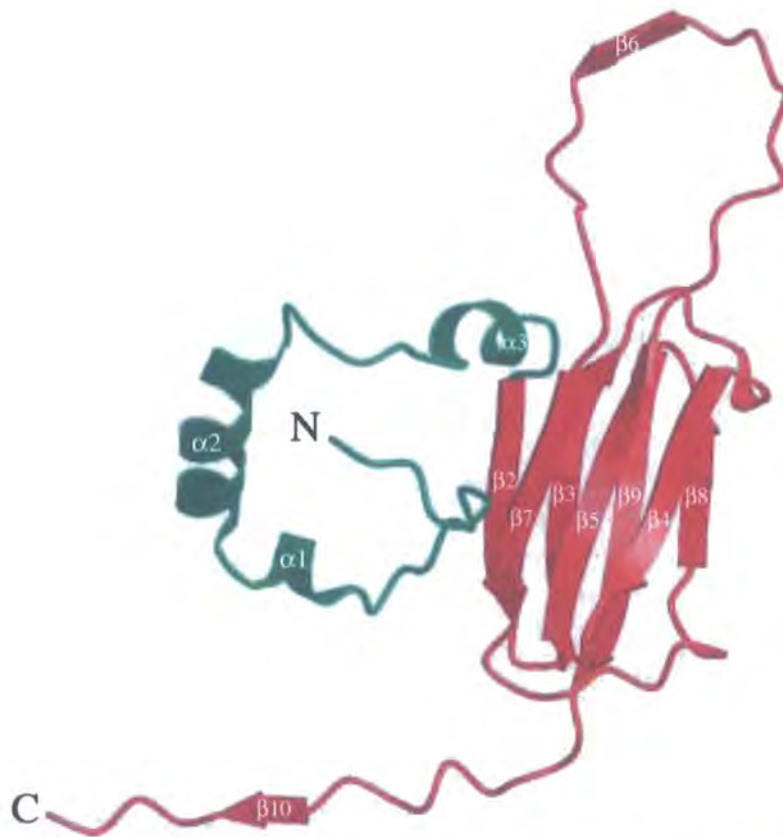


Figure 1.2. Secondary structure of the HSP 16.9 subunit with an ordered N-terminus. Ribbon diagram of the monomer with the ordered N-terminal arm shown in green and the α -crystallin domain and the C-terminal extension shown in red. (Reprinted by permission from Macmillan Publishers Ltd: Nature Structural and Molecular Biology ((van Montfort et al., 2001), copyright 2001).

The N-terminal domain contains three helical segments, in half of the subunits. The remaining subunits in HSP16.9 and all subunits in HSP16.5 have unstructured N-termini. The α -crystallin domain consists of a seven-stranded β -sandwich, an interdomain loop containing one β -strand and a C-terminal extension (at the bottom), which is largely unstructured except for the short β 10 strand (Augusteyn, 2004).

The 2.7 Å structure of wheat HSP16.9 indicates how its α -crystallin domain and flanking extensions assemble into a dodecameric double disk. The folding of the monomer and assembly of the oligomer are mutually interdependent involving strand exchange, helix swapping, loose knots and hinged extensions. In support of the chaperone mechanism, the substrate bound dimers in temperature dependant equilibrium with higher assembly forms have unfolded N-terminal arms and exposed conserved hydrophobic binding sites on the α -crystallin domain (van Montfort et al., 2001).

Boelens et al. found that the N-terminal domain of α B-crystallin does not detectably bind to α B crystallin or with one of its two domains. The N terminus is involved in the formation of larger complexes but can only do so in the presence of the C-terminal domain. It would seem that the highly conserved C-terminal domain forms the building blocks, which associate into large complexes through interactions between the N-terminal domains (Boelens et al., 1998).

The C terminal extensions of α A- and α B-crystallin are 34 and 32 residues, respectively. Both α A- and α B-crystallin have polar, flexible C-terminal extensions that have been implicated in the chaperone-like activity of these crystallins and are thought to contribute to the solubility of these crystallins (Carver and Lindner), because of a preponderance of charged amino acids.. Harrington et al. (2004), suggests that both N- and C-terminal regions are important for proper folding of α -crystallin, subunit interactions between α A- and α B-crystallin, and chaperone activity.

While α B-crystallin contains the same three structural domains found in *M.jannaschii* HSP16.5 and wheat HSP16.9, the complex assembly of human α B-crystallin is larger and more polydisperse than the two sHSPs that have been crystallised and cryo-electron microscopy studies showed that α B-crystallin has an asymmetric variable quaternary structure consisting of 32 subunits with a central cavity (Feil et al., 2001; Haley et al., 1998). An alternative model consisting of a tetramer of tetramers is

consistent with many observations of the protein (Augusteyn, 2004; Augusteyn, 1998). A similar model has been suggested for the murine HSP 25 (Ehrnsperger et al., 1999).

1.4. α -CRYSTALLIN AS A MOLECULAR CHAPERONE

While its lenticular function is also structural, both α B- and α A-crystallin and the hetero-oligomer α -crystallin have been shown to display molecular chaperone activity *in vitro* (Horwitz, 1992). Fundamental cellular processes such as protein synthesis, transport and turnover involve unfolded or partially denatured proteins. These processes and stress expose hydrophobic regions, which may interact incorrectly even at low concentration, thus molecular chaperones sequester unfolded polypeptides to prevent aggregation and allow for refolding (Derham and Harding, 1999). Molecular chaperones assist the correct non-covalent assembly of other polypeptide containing structures *in vivo*, but are not components of these assembled structures when they are performing their normal biological function. The predominant function of molecular chaperones is the prevention of incorrect associations and aggregation of unfolded polypeptides (Dahlman et al., 2005), by suppressing the unfolding of proteins or by mediating in the refolding of unfolded proteins (Thampi et al., 2002). α -crystallin can recognize and bind unfolded proteins over a range of temperatures and hence its chaperone function is maintained over a range of conformations (including sizes) (Bloemendal et al., 2004), however, unlike adenosine triphosphate (ATP)-dependent chaperones, the α -crystallins and other sHSPs are not thought to actively refold non-native proteins but rather to incorporate them into large complexes, thereby preventing their nonspecific aggregation (Aquilina et al., 2004). The function of α -crystallin as a chaperone protein has been linked to the dynamics of mammalian cytoskeleton assembly because correct folding of cytoskeletal proteins is dependent upon its presence (Nicholl and Quinlan, 1994).

1.5. THE FUNCTIONS OF α B-CRYSTALLIN

The expression of α B-crystallin in a variety of tissues outside the lens and its ability to prevent thermal aggregation of proteins in a manner similar to molecular chaperones (Horwitz, 1992; Klemenz et al., 1991), suggest that it has general cellular functions over and above its role in light refraction (Andley et al., 2002). A number of physiological functions have been identified.

1.5.1. MODULATORS OF IF ASSEMBLY

Within the lens, the α -crystallins are intimately associated with the lens cytoskeleton (Nicholl and Quinlan, 1994). The function of this association is not clear, but it may be important in facilitating the chaperone activity of α -crystallins by providing a solid phase support in the form of IFs (Perng and Quinlan, 2005). Previous studies on the lens cytoskeleton have demonstrated that α -crystallins associate with and directly inhibit vimentin IF assembly *in vitro* and induce filament disassembly (Nicholl and Quinlan, 1994). These observations provide the first evidence that α -crystallins have the potential to influence IF assembly, which may participate in modulating the dynamic aspect of IF organisation and structure (Nicholl and Quinlan, 1994). During lens maturation, such a mechanism may also contribute to the selective removal of vimentin IF networks and rearrangement of the phakinin/filensin IF networks. Perng et al. (1999) suggested that one of the functions of α B-crystallin is to help manage IF network by controlling filament-filament interactions (Perng et al., 1999) and recently demonstrated the ability of α B-crystallin to assist the formation of IF networks in living cells (Perng and Quinlan, 2005).

Thus, α B-crystallin participates in the dynamic assembly, disassembly reorganisation and stabilisation of the filamentous cytoskeleton. In normal tissues α -crystallin interacts directly with a number of filamentous proteins including phakinin, filensin (CP119), desmin, glial fibrillary acidic protein (GFAP) and vimentin where it functions in the organisation and stabilisation of the filament networks formed by these proteins (Bennardini et al., 1992; Ghosh et al., 2007; Vicart et al., 2006). One of the major functions of the association of sHSPs with IFs is to help manage the interactions

that occur between filaments in their cellular networks and a link was found suggesting that α B-crystallin regulates cell division through the stabilization of cytoskeleton filaments (Andley et al., 2001; Andley et al., 2000; Fujita et al., 2004). This is achieved by protecting filaments against those non covalent interactions that result when they come into close proximity and which have the potential to induce IF aggregation as seen in some disease pathologies (Perng et al., 1999). Other functions suggested have been protection of tubulin subunits of microtubules (Arai and Atomi, 1997), and association with actin in ischemic cardiac cells, where it may prevent aggregation of filaments (Chiesi et al., 1990). α B-crystallin regulates actin filament dynamics, stabilises them in a phosphorylation dependant manner and protects the integrity of IFs against extracellular stress. Disturbance of the cytoskeleton leads by converging signalling pathways to the phosphorylation of α B-crystallin, which probably acts as a protective effector of the cytoskeleton (Launay et al., 2006).

Disruption of cytoskeletal assembly is one of the early effects of any stress that can ultimately lead to cell death. Singh et al. (2007) demonstrated that α B-crystallin can prevent stress-induced aggregation of actin *in vitro* and regulate actin filament dynamics and protects cells from stress-induced death *in vivo*. Association of α B-crystallin with actin helps maintenance of pinocytosis, a physiological function essential for survival of cells (Singh et al., 2007). α B-crystallin also associates with the tubulin cytoskeleton as shown by Xi et al., (2006) where the mitotic spindle is abnormally assembled in a number of α A- and α B-crystallin knockout lens epithelial cells (Xi, 2006). The study suggested that the α B-crystallin interacts with microtubule associated proteins (MAPs) to inhibit aggregation of microtubules in lens epithelial cells therefore affecting microtubule assembly by maintaining the pool of unassembled tubulin (Xi, 2006).

1.5.2. REGULATORS OF APOPTOSIS

The ability of α B-crystallin to inhibit apoptosis was demonstrated by Kamradt et al. They showed that α B-crystallin is a novel negative regulator of myogenic apoptosis whose expression is selectively induced in surviving myoblasts during an early stage of their differentiation *in vitro*, and provided a direct and previously unrecognized link between the myogenic differentiation program and the acquisition of apoptosis resistance (Kamradt et al., 2002). α B-crystallin also antagonizes myogenic apoptosis by inhibiting the activation of caspase-3, which is consistent with previous findings in cancer cells that α B-crystallin inhibits caspase-3 activation by disrupting its proteolytic maturation (Kamradt et al., 2002). As caspase-3 plays a central role in the execution of apoptosis (Cryns and Yuan, 1998) α B-crystallin may participate broadly in the regulation of muscle cell death (Kamradt et al., 2002).

1.5.3. TRANSCRIPTIONAL REGULATORS

Both α B-crystallin and HSP27, are identified as nuclear speckle components in unstressed cells in tissue culture (van den IJssel et al., 2003). This new finding suggests a constitutive function for these sHSP chaperones in the nucleus and suggests a new perspective on the cardiomyopathy-causing mutation for α B-crystallin (R120G) that could involve transcriptional splicing effects. Both α B-crystallin and HSP27 were immunolocalised to nuclear speckles (interchromatin granule clusters), whilst HSP27 was also seen associated with the nucleolar compartment, indicating a subtle difference between these closely related sHSPs. Phosphorylation was not required for nuclear localisation of α B-crystallin. This was confirmed by the transient transfection of HeLa cells with a phosphorylation-defective α B-crystallin (van den IJssel et al., 2003). Mutations of α B-crystallin would potentially have nuclear as well as cytoplasmic consequences.

1.5.4. GENOME STABILITY AND HYPERPROLIFERATION

Preservation of genomic stability encompasses many factors, such as the maintenance of primary DNA sequence and the preservation of chromosomal ploidy and structure (Hartwell et al., 1994). Primary cultures of CRYAB knockout (-/-) lens epithelial cells show genome instability and hyperproliferation, suggesting that α B-crystallin regulates cell division through the stabilization of cytoskeleton filaments (Andley et al., 2001; Andley et al., 2000; Fujita et al., 2004).

Genomic instability is a hallmark of cancer cells, the over expression of α B-crystallin during oncogene expression and in tumours of neuroectodermal origin suggests that the protein may accumulate as a stress response to maintain chromosomal integrity during cellular evolution from a normal to a cancer cell. This notion is consistent with the current finding that CRYAB-/- cells demonstrate genomic instability. The mechanism by which the loss of α B-crystallin enhances genomic instability needs further investigation (Andley et al., 2001).

1.5.5. PROTEOSOME FUNCTION

The α B-crystallin protein plays a role in the proteasome-mediated degradation of selected proteins (Parcellier et al., 2005). Degradation of a protein by the ubiquitin system involves two distinct and successive steps. Firstly, multiple ubiquitin molecules covalently attach to the target protein then the tagged protein is degraded by the 26S proteasome (Ciechanover, 1998). The ubiquitin-protein isopeptide ligase SCF (SKP1/CUL1/F-box) complex captures the target protein via the F-box protein (Cenciarelli et al., 1999). Den Engelsman et al, (2003) identified the F-box protein FBX4 as an interactor with α B-crystallin (den Engelsman et al., 2003). The interaction with FBX4 seems to depend on the phosphorylation status of α B-crystallin, but is also enhanced by the mutation R120G α B-crystallin. Binding of FBX4 to α B-crystallin stimulates the ubiquitination of a detergent-insoluble protein, which probably destines this protein for ubiquitin-dependent degradation (den Engelsman et al., 2003).

Cytoplasmic inclusions containing α B-crystallin found in various neurological disorders, such as Alzheimer's, Parkinson's, Huntington's, Alexander's, and diffuse Lewy

body disease (Head and Goldman, 2000; Kato et al., 2001; Tamaoka et al., 1995), have been shown to consistently contain ubiquitin-positive proteins (Rideout et al., 2001) suggesting that the proteins responsible for aggregate formation may have a role in ubiquitin-dependent degradation (Ciechanover, 2001).

Other functions suggested included the regulation of platelet function. Aggregation of human platelets were dose-dependently inhibited by α B-crystallin and induced by thrombin or botrocetin. α B-crystallin can act intercellularly to regulate platelet functions. These results may provide the basis for a novel defence system against thrombus formation in vivo (Matsuno and Kozawa, 2003).

1.6. α B-CRYSTALLIN AND CATARACT

Cataract, or opacification of all or part of the lens of the eye reduces optical performance most commonly manifested by decreased visual acuity, glare and decreased contrast sensitivity. While age-related cataract is the commonest cause of visual impairment worldwide, most advances have been made in understanding the genetic basis of its congenital counterpart (Francis et al., 1999). Cataract is a pathological opacity interfering with transparency caused either by disturbances to the regular cytoplasm-membrane lattice repeat of the lens, or by perturbations of the local short-range order of the crystallins in the interior of the fibre cells (Bloemendal et al., 2004).

There are three primary causes of cataract including age related, exposure to certain risk factors and congenital cataracts as detailed below. The consequences of the three primary causes of cataract suggest that cataractogenesis could be considered as a protein folding disease; due to unfolding of lens proteins, or be the consequence of a loss of solubility due to altered interaction of native proteins (Bloemendal et al., 2004).

1.6.1. AGE RELATED CATARACT

The incidence of three kinds of cataract increase with age and include nuclear, cortical and posterior subcapsular cataract (Klein et al., 2002). The theories of aging include firstly, the evolutionary theory, which regards aging as a result of natural selection becoming weaker with age (Medawar, 1952) and secondly the disposable soma theory of aging suggesting that ageing is a consequence of the progressive accumulation of molecular and cellular damage (Kirkwood and Austad, 2000).

The exceptionally long lifetime of lenticular proteins means that the α -crystallins are susceptible to the accumulation of a variety of posttranslational modifications that are thought to disrupt their structure and include disulfide bonding, oxidation, backbone cleavage, proteolysis, aggregation, cross-linking, deamidation, methylation and glycosylation (Bloemendal et al., 2004). For α B-crystallin in the lens, the major modification has been identified as phosphorylation at serine residues 19, 45, and 59 (Aquilina et al., 2004). Another modification is deamidation, which introduces a negative charge, and is believed to cause alterations in protein tertiary structure, affecting their

structural and functional properties (Gupta and Srivastava, 2004). Therefore, the posttranslational modifications inhibit potential chaperone capabilities and lead to protein insolubilization and consequently cataract development.

Age-related cataract derives from two distinct molecular routes: protein unfolding resulting in protein aggregation and/or altered interaction and association between native crystallins resulting in lesser solubility. With increasing age the incidence of lens opacities increases and visual acuity lessens. Ultimately, the only way to restore sight is cataract surgery, however post surgery cataract can occur if the lens epithelial cells remain in the capsular bag following surgery (Lois et al., 2003). Four types of post surgery cataract have been recorded and include Fibrous posterior capsular opacification (PCO) Soemmering's ring (Apple et al., 2000), Elschnig pearls (Cheng et al., 2001) and liquefied PCO (Miyake et al., 1998).

1.6.2. DISEASE RELATED CATARACT: THE RISK FACTORS OF CATARACTOGENESIS

Cataract can be one of the symptoms of systemic disease (Shinohara et al., 2007). Data from epidemiological and case control studies have suggested various risk factors (Shah et al., 2007; Virgolici and Popescu, 2006). These risk factors include diabetes (Iwamoto et al., 2004; Jacob, 1999; Thampi et al., 2002), steroid use (Dickerson et al., 1997; Hamamichi et al., 2003; Kojima et al., 2002; Nakamura et al., 2003; Patteau et al., 2003; Shibata et al., 2003), smoking (Hiller et al., 1997; Kelly et al., 2005; Klein et al., 1993; Krishnaiah et al., 2005; Raju et al., 2006; Shalini et al., 1994; Sulochana et al., 2002; West and Valmadrid, 1995), UV radiation (Hayashi, 1998; McCarty and Taylor, 2002; Pastor-Valero et al., 2007), nutrition and oxidative stress (Christen et al., 2007; Delcourt et al., 2005; Fain, 2004; Reddy et al., 2002; Taylor et al., 1989; Valero et al., 2002), diarrhoea (Minassian et al., 1984; Zodpey et al., 1999) and alcohol consumption (Lindblad et al., 2007).

1.6.3. CONGENITAL CATARACT

Congenital cataract is a result of a mutation in one of the lenticular proteins and is usually already present at birth or develops shortly thereafter. It is responsible for 10% of childhood blindness worldwide (Francis et al., 2000) and if left untreated permanent visual loss usually occurs (Zhang et al., 2007).

Congenital cataract shows wide phenotypic variation reflecting its genetic heterogeneity (Francis et al., 1999). Current literature recognises several classifications of congenital cataract phenotypes taking into account the location and appearance of the opacity within the lens. The classifications include anterior polar, posterior polar, nuclear, lamellar (zonular), coralliform (coral-like appearance), blue-dot (cerulean), cortical, pulverulent (opacities have a 'pulverized' dust-like appearance) and total cataract (Francis et al., 1999). Posterior polar cataract is located at the back of the lens and is proximal to the optical centre of the eye, therefore can result in a marked effect on visual acuity (Berry et al., 2001).

Inherited cataracts account for up to half of all congenital cataracts and are clinically heterogeneous, with the most common mode of inheritance being autosomal dominant congenital cataract (ADCC). The less common autosomal recessive and X-linked forms are also observed (Berry et al., 2001). Thus far seventeen functionally diversified genes have been identified to cause isolated ADCC (Zhang et al., 2007). A study by Vicart et al, (1998) reported the first defect in the α B-crystallin gene (CRYAB) at locus 11q22.3-q23.1, which caused the human muscle disorder of desmin related myopathy (DRM) (Vicart et al., 1998). Similarly in the α A-crystallin gene (CRYAA) an ADCC gene was mapped to chromosome 21q22.3 and sequencing identified a missense mutation R116C associated with ADCC (Litt et al., 1998).

The observation has been made that clinical phenotypes might be caused by mutations in different genes, in contrast, mutations in the same gene do not necessarily lead to the same phenotype (Graw, 2003). This indicated the importance of as yet unknown modulators of gene expression or function. For example, mutations of the

CRYAB gene cause ADCC (Liu et al., 2006b; Vicart et al., 1998) as well as DRM (Selcen and Engel, 2003; Vicart et al., 1998) and DCM (Inagaki et al., 2006). Graw (2003) suggested that the detailed molecular analysis of allelic series of mutations will allow detailed genotype–phenotype correlations to be made, which should help understand the function of particular domains of the mutated proteins (Graw, 2003).

1.7. NATURALLY OCCURRING MUTATIONS OF α B-CRYSTALLIN

Naturally occurring mutations have been found in both α A- and α B-crystallin. The regions affected by these specific mutations helped to identify single amino acid substitutions that would drastically alter protein structure and eliminate chaperone like activity (Bova et al., 1999; Pras et al., 2000; Shroff et al., 2000). Mutations found in α A-crystallin result only in cataract, however the mutations associated with α B-crystallin specifically are of more interest as high expression levels of α B-crystallin in non lenticular tissues and the lens leads to a variety of tissues displaying a phenotype associated with the α B-crystallin mutation (see Table 1.1).

Table 1.1. Mutations of the CRYAB gene

Mutation	Symptoms	Reference
R120G	Desmin Related Myopathy (DRM), Cardiomyopathy, cataracts	(Vicart et al., 1998)
450delA	Isolated congenital cataract	(Berry et al., 2001)
Q151X	Myofibrillar myopathy (MM)	(Selcen and Engel, 2003)
464delCT	Myofibrillar myopathy	(Selcen and Engel, 2003)
D140N	ADCC	(Liu et al., 2006b)
R157H*	Dilated Cardiomyopathy (DCM)	(Inagaki et al., 2006)
P20S	ADCC	(Liu et al., 2006a)

*- The R157H mutation was not analysed in this study. Although the C-terminal region was affected, the mutation was reported late into the study and as the mutation caused a base substitution without altering the length of the C-terminal extension it was deemed indirectly comparable to the remainder of the mutants studied.

Mutations found in the α B-crystallin CRYAB gene result in a modified/truncated C-terminal region with the exception of the P20S, R120G and D140N mutation. Previous reports show that the removal of C-terminal extensions of 32 residues from α B-crystallins lead to improper folding, reduced chaperone activity, and formation of trimers or tetramers (Gupta and Srivastava, 2004), therefore the discovery of the CRYAB mutations will help further understand the role of specific and/or sequences of amino acids in the C-terminal

region of the α B-crystallin on function, in terms of chaperone capability and solubility, and relationship between the mutant α B-crystallin and the expressed phenotypes. The known CRYAB mutations are discussed below.

1.7.1. R120G α B-CRYSTALLIN

The R120G missense mutation was the first case where a defect in a molecular chaperone was identified as a cause for an inherited human muscle disorder (Vicart et al., 1998). The patients affected by the R120G mutation had proximal and distal weakness with desmin accumulation in skeletal muscle, cardiomyopathy and cataracts, (Selcen, 2003 #31). Perng et al 2004 showed that the mutation alters the *in vitro* binding characteristics of α B-crystallin for desmin filaments (Perng et al., 2004) resulting in desmin aggregation. Desmin-related myopathies (DRM) are inherited neuromuscular disorders characterized by adult onset and delayed accumulation of aggregates of desmin, a protein belonging to the type III intermediate filament family, in the sarcoplasm of skeletal and cardiac muscles (Vicart et al., 1998). The adult onset of α B-crystallinopathy indicates that in the real physiological situation, the formation of the aggregates by R120G α B-Crystallin is a tightly regulated process. The delayed onset of the disease *in vivo* may be explained by co-polymerization with family members, assisted folding and targeted degradation (Chavez Zobel et al., 2003).

The R120G mutation occurs within the highly conserved α -crystallin domain (residues 68-151), which is believed to be engaged in the subunit-subunit interactions, but the individual amino acids in subunit interactions and chaperone activity have not been fully identified (Gupta and Srivastava, 2004). Studies have shown that patients with DRM display heterozygous expression of wild type and R120G α B-crystallin and that misfolded R120G α B-Crystallin could be rescued by wild-type α B-Crystallin (Chavez Zobel et al., 2003). The R120G mutation alters affected the secondary and tertiary structure of the α B-crystallin (Perng et al., 1999), causing a decreased β -sheet secondary structure and an altered aromatic residue environment compared with wild-type α B-crystallin (Bova et al., 1999), and leads to the appearance of intracellular aggregates containing both α B-crystallin and desmin in the muscles of affected individuals (Barral et al., 2004). Treweek

et al. (2005) indicated that R120G α B-crystallin exists as a larger oligomer than wild-type α B-crystallin, and its size increases with time. It is likely that removal of the positive charge from R120 of α B-crystallin causes partial unfolding, increased exposure of hydrophobic regions, and enhances its susceptibility to proteolysis, thus reducing its solubility and promoting its aggregation and complexation with other proteins. These characteristics may explain the involvement of R120G α B-crystallin with human disease states (Treweek et al., 2005). The appearance of similar aggregates in another form of DRM, caused by missense mutations in desmin itself, lends support to the notion that failure of and also to assist in folding and assembly of desmin into the intermediate filament cytoskeleton leads to the disease (Barral et al., 2004).

1.7.2. 450DELA α B-CRYSTALLIN

Berry et al. (2001) reported the first mutation to cause isolated congenital cataract in the CRYAB gene. Sequence analysis of the CRYAB gene revealed a deletion mutation 450delA in exon 3. This mutation co-segregated in a family with autosomal dominant posterior polar cataract who displayed a single well-defined plaque that was present at birth or developed during the first few months of life not progressing, with age to other regions of the lens. The mutation was not found in a panel of 100 normal unrelated individuals, excluding the possibility that it is a rare polymorphism.

The result of the mutation is the production of an extended protein of 184 residues with 35 novel amino acids at the C-terminus, starting at codon 154 of the protein, replacing several highly conserved residues. The C-terminal extension region is thought to be important for the chaperone function and solubility of α B-crystallin (Smulders et al., 1996). Since the 450delA mutation in CRYAB leads to the replacement of the C-terminal extension by novel residues, it is very likely to compromise the chaperone-like activity of α B-crystallin (Berry et al., 2001).

The constitutive expression of α B-crystallin in the lens and non-lenticular tissues raises the question, why the mutation results in isolated congenital cataract and shows no non lenticular symptoms like the R120G mutation, which displayed DRM and cataract. The major difference is the region in α B-crystallin where the mutation has occurred, resulting in a larger protein with significant alteration to the C-terminal residues. It is yet

to be understood the effect the 450delA mutant protein has on its interaction with substrate proteins relative to the wild type, to give rise to the isolated cataract.

1.7.3. Q151X α B-CRYSTALLIN AND 464DELCT α B-CRYSTALLIN

Selcen & Engel, (2003) reported further mutations of the CRYAB gene, which resulted in myofibrillar myopathy. Additional symptoms included adult onset proximal and distal leg muscle weakness, myopathic electromyogram with abnormal electrical irritability and muscle biopsy findings of myofibrillar myopathy and mild denervation (Selcen and Engel, 2003), however no cataracts were identified. The term myofibrillar myopathy was proposed in 1996 as a non-committal term for a pathological pattern of myofibrillar dissolution associated with the accumulation of myofibrillar degradation products and ectopic expression of multiple proteins that include desmin, α B-crystallin, dystrophin and congophilic amyloid material (Selcen et al., 2004).

1.7.3.1. Q151X α B-crystallin

The second mutation showed a C-to-T transition at position 451 (451C-T) that generates a stop codon (Q151X) and predicts a protein consisting of 150 residues with a molecular mass of 17.5kDa. This mutation results in the removal of the C-terminal extension, which consists of residues 149-175 (Selcen and Engel, 2003).

1.7.3.2. 464delCT α B-crystallin

The third mutation showed a 2bp deletion at position 464 (464delCT) that generates eight missense codons (RAHSHHP) followed by a stop codon. This mutation predicts a protein consisting of 162 instead of 175 residues with a molecular mass of 18.8kDa (Selcen and Engel, 2003).

Although the phenotype of the Q151X- and 464delCT α B-crystallin mutant affects non-lenticular tissues, the expression of the α B-crystallin protein is at its highest levels in the lens, but no evidence of cataract has been reported in patients with these mutations in α B-crystallin. Both wild type and mutant proteins are present in muscle, but

expression of the mutant moieties is less than of wild type. The decreased expression of the mutant protein could be a consequence of its relative instability, due to the truncation of the C-terminal region responsible for stabilisation of the α B-crystallin. Despite its reduced expression, the truncated proteins still result in pathological changes in skeletal muscle, consistent with a dominant negative effect (Selcen and Engel, 2003). Patients with the R120G missense mutation in α B-crystallin had cardiomyopathy, palatopharyngeal weakness, and cataracts (Vicart et al., 1998), all features not detected in patients with the Q151X or 464delCT mutations, and patients with 450delA mutation show isolated cataract and no neuromuscular degeneration. The differences in the expressed phenotype of the different CRYAB mutations may be related to functionally different regions of α B-crystallin itself, to single nucleotide polymorphisms in functionally related genes in the different patients (Selcen and Engel, 2003), or the presence of other chaperones in the eye lens, which associate with the mutant and prevent aggregation and thus cataractogenesis.

1.7.4. POST TRANSLATIONAL MODIFICATIONS (PTM)

Recent studies have identified a number of PTMs occurring in α B-crystallin, which result in a truncated C-terminal region by proteolytic digestion and lead to cataract formation. Comparisons can be made between the affect of these PTMs and the congenital mutations on the function and stability of the specific α B-crystallin.

Several post-translationally modified forms of α B-crystallin have been identified. Two degradation products, α B-crystallin (1-170) and α B-crystallin (1-174) (Jimenez-Asensio et al., 1999; Plater et al., 1996) each make up between 9.5-27% of the total α B-crystallin in Soemmerring's ring form of cataract and less than 1% in the normal lenses (Colvis et al., 2000). Other modified forms of α B-crystallin such as 1-163 are aberrant in the fibre cells of the Soemmerring's rings relative to normal lens. Soemmerring's ring is one form of secondary cataract that can occur following cataract surgery. The ring structure is formed by adherence of the anterior lens capsule to the posterior lens capsule. Epithelial cells, remaining after surgery, differentiate into lens fibre cells, but the resulting tissue mass does not remain transparent (Colvis et al., 2000; Ueda et al., 2002b).

1.7.4.1. α B-crystallin 1-174

An α B-crystallin fragment was detected in the cataract of a human lens and was preferentially phosphorylated over the wild type (Jimenez-Asensio et al., 1999). The fragment was identified as α B-crystallin minus the terminal lysine by Matrix-assisted laser desorption/ionisation-Time of Flight-mass spectrometry (MALDI-TOF-MS) in Soemmerring's ring cataract (Colvis et al., 2000). The mechanism involved in generating truncated α B-crystallin is not known, but a premature termination of the α B-crystallin gene was ruled out by sequencing the polymerase chain reaction products of the last exon for the α B-crystallin gene from lenses containing the fragment (Jimenez-Asensio et al., 1999). Recombinant truncated α B-crystallin was primarily soluble and the chaperone activity was comparable to that of the wild type α B-crystallin.

Plater et al. (1996) showed the effect of substituting the two terminal lysines of α B-crystallin with Leucine (L) or Glycine (G) residues. Plater et al. (1996) suggested that the effect of substituting the two terminal lysines resulted in a largely intact but less mobile C terminus. The absence of a strong hydrophilic positive charge at the end of the highly flexible C-terminal extension may result in the C terminus folding back on itself, losing its flexibility, and sterically hindering protein binding (Plater et al., 1996), thus explaining the significant reduction in chaperone activity.

1.7.4.2. α B-crystallin 1-170 and 1-163

The induction of diabetes resulted in a C-terminal truncated form of α B-crystallin 1-170 in rat lenses, however, not observed in the human lenses of diabetic sufferers (Thampi et al., 2002). Another study also showed the presence of the α B-crystallin 1-170 in vitro from rat lens nucleus using LP82 and M-calpain proteolysis and a second truncation 1-163, thus with 12 residues removed from the C-terminal (Ueda et al., 2002a). The 1-170 and 1-163 modified forms of α B-crystallin were observed in patients who display Soemmerring's ring cataract (Colvis et al., 2000; Ueda et al., 2002a). Proteolytic removal of the Thr171- Lys175 region did not affect α B-crystallin chaperone activity (Carver et al., 1995), which again supports the theory that there would be sufficient charge-charge interactions with the remainder of the C-terminal arm to ensure efficient

chaperone-like activity (Plater et al., 1996). This also suggests that the terminal five amino acids do not affect the solubility of the α B-crystallin and the complexes formed during chaperone activities. The effect of the removal of the 12 amino acid residues on chaperone activity and solubility is unknown.

The age related post-translational modifications of the C- terminal region, like the congenital mutations 450delA, 464delCT and Q151X show a relationship between the C-terminal structures of α B-crystallin and its subsequent solubility and function as a molecular chaperone, which ultimately lead to the onset of disease.

1.7.5. R157H α B-CRYSTALLIN

Dilated Cardiomyopathy (DCM) is a disease characterised by cardiac enlargement accompanied by systolic dysfunction and associated congestive heart failure (Richardson, 1996). A novel missense CRYAB mutation R157H was found in a familial DCM patient and affected one of the evolutionary conserved amino acid residues amongst α -crystallin (Inagaki et al., 2006). Mutations in the sarcomeric proteins such as titin/connectin are known to cause DCM (Gerull et al., 2002; Itoh-Satoh et al., 2002) and functional analysis revealed that the R157H mutation decreased the binding of α B-crystallin to titin/connectin heart specific N2B domain without affecting distribution of the mutant α B-crystallin in cardiomyocytes. In contrast the R120G mutation decreased the binding to both N2B and striated muscle-specific I26/27 domains and showed intracellular aggregates of the mutant protein. These observations by Inagaki et al. (2006) suggest that the R157H mutation disease causing mechanism is different from the R120G (Inagaki et al., 2006). This R157H mutation, which affects the C-terminal of α B-crystallin, alters the structural and functional integrity of α B-crystallin by hindering the ability of α B-crystallin to bind to client proteins.

1.7.6. D140N α B-CRYSTALLIN

Liu et al. (2006) reported a novel D140N mutation in the third exon of the CRYAB gene. The mutation was found to co-segregate with disease phenotype in a five generation ADCC family with isolated lamellar cataract, where opacity is limited to the layers of the lens external to the nucleus (Liu et al., 2006b). Characterisation of the mutant α B-crystallin, which affects the highly conserved α -domain of sHSPs, indicated that although the mutation had no effect upon secondary structure, alterations to the tertiary and/or quaternary structure were observed with changes in surface hydrophobicity. The D140N α B-crystallin aggregated into a larger complex than the wild type α B-crystallin, was more susceptible to thermal denaturation and not only lost its chaperone activity but displayed a dominant negative effect by inhibiting the chaperone activity of wild type α B-crystallin (Liu et al., 2006b). The D140N mutation results in similar structural changes to R120G yet the R120G causes myopathy as well as cataract phenotype. Liu et al. (2006) proposed that the altered tertiary and/or quaternary structure and the dominant negative effect of the D140N mutation underlie the molecular mechanism of cataractogenesis of this nature (Liu et al., 2006b).

1.7.7. P20S α B-CRYSTALLIN

The CRYAB mutation first associated with isolated congenital cataract was 450delA, however, Liu et al., (2006) identified a mutation, P20S, in the CRYAB gene in a large four-generation Chinese family with nonsyndromic posterior polar cataract (Liu et al., 2006a).

The disease gene of this Chinese family was mapped to chromosome 11 in region q22-22.3, where two small heat shock proteins CRYAB and HSPB2 are harboured. The expression of HSPB2 is not detectable in the lens so it is unlikely to be the candidate gene for ADCC (Iwaki A, 1997). Instead, mutation analysis of CRYAB identified a novel mutation P20S that cosegregated with all affected individuals, but was not present in unaffected members of the family or the 200 normal control subjects. The mutation occurs at an evolutionarily conserved residue P20 in the α B-crystallin. Although this is the second novel mutation in CRYAB that has been linked to isolated cataract, it is interesting

to note that the P20S mutation is located at the N terminus of CRYAB, whereas the previously identified 450delA mutation associated with cataract and other CRYAB mutations associated with myopathy are all located at the C terminus.

The relative effects of the α B-crystallin mutations upon the amino acid sequence of α B-crystallin are detailed in Figure 1.3. The sequence alignment shows the effect of congenital mutations 450delA, 464delCT, Q151X, D140N, R157H, P20S and R120G upon the C-terminal extension of α B-crystallin. Also shown are the PTM products E164X, K175X and A171X plus mutations of interest K174X and E165X that complete a series of C-terminal truncated mutants, which sequentially remove important regions of the C-terminal extension.

It is clear from the structural alignment that with the exception of P20S, R120G and D140N, all the disease causing mutations of α B-crystallin, are associated with an altered C-terminal extension. The 450delA, 464delCt and Q151X mutations resulted in a C-terminal extension that was altered from residue 150 onwards (450delA) (Berry et al., 2001), 155 onward (464delCT) or completely removed (Q151X) (Selcen and Engel, 2003). The deletion of a known substrate interaction site (157-164; (Ghosh, 2005 #157)) and a region important in the oligomerisation of α B-crystallin itself (155-166; (Ghosh, 2005 #157)) support the hypothesis that this region in α B-crystallin is important to the solubility, the structure and function of the protein. The pathology of the R157H mutation lends further support to this conclusion. Thus far, the effect of such extensive deletions (Q151X) combined with altered C-terminal sequences (450delA, 464CT) upon α B-crystallin solubility, structure and function have not been investigated. In α B-crystallin, there has not been any systematic analysis of the role of the C-terminal extension and therefore no potential explanation of whether the three mutations (450delA, Q151X and 464delCT) cause the various diseases via the loss of chaperone function or perhaps by a different mechanism.

R120G	MDIAIHHPWIRRPFFPFHSPSR LF DQFFGEHLLES DL FPTSTSLSPFYLRPPSFLRAPSW	60
D140N	MDIAIHHPWIRRPFFPFHSPSR LF DQFFGEHLLES DL FPTSTSLSPFYLRPPSFLRAPSW	60
Wild Type	MDIAIHHPWIRRPFFPFHSPSR LF DQFFGEHLLES DL FPTSTSLSPFYLRPPSFLRAPSW	60
K175X	MDIAIHHPWIRRPFFPFHSPSR LF DQFFGEHLLES DL FPTSTSLSPFYLRPPSFLRAPSW	60
K174X	MDIAIHHPWIRRPFFPFHSPSR LF DQFFGEHLLES DL FPTSTSLSPFYLRPPSFLRAPSW	60
A171X	MDIAIHHPWIRRPFFPFHSPSR LF DQFFGEHLLES DL FPTSTSLSPFYLRPPSFLRAPSW	60
R157H	MDIAIHHPWIRRPFFPFHSPSR LF DQFFGEHLLES DL FPTSTSLSPFYLRPPSFLRAPSW	60
E165X	MDIAIHHPWIRRPFFPFHSPSR LF DQFFGEHLLES DL FPTSTSLSPFYLRPPSFLRAPSW	60
E164X	MDIAIHHPWIRRPFFPFHSPSR LF DQFFGEHLLES DL FPTSTSLSPFYLRPPSFLRAPSW	60
464delCT	MDIAIHHPWIRRPFFPFHSPSR LF DQFFGEHLLES DL FPTSTSLSPFYLRPPSFLRAPSW	60
Q151X	MDIAIHHPWIRRPFFPFHSPSR LF DQFFGEHLLES DL FPTSTSLSPFYLRPPSFLRAPSW	60
450delA	MDIAIHHPWIRRPFFPFHSPSR LF DQFFGEHLLES DL FPTSTSLSPFYLRPPSFLRAPSW	60
P20S	MDIAIHHPWIRRPFFPFHSS SR LF DQ FFGEHLLES DL FPTSTSLSPFYLRPPSFLRAPSW	60
R120G	FDTGLSEMRLEKDRFSVNLDVKHFSPEELKVKVLGDVIEVHGKHEERQDEHGFISREFHG	120
D140N	FDTGLSEMRLEKDRFSVNLDVKHFSPEELKVKVLGDVIEVHGKHEERQDEHGFISREFHR	120
Wild Type	FDTGLSEMRLEKDRFSVNLDVKHFSPEELKVKVLGDVIEVHGKHEERQDEHGFISREFHR	120
K175X	FDTGLSEMRLEKDRFSVNLDVKHFSPEELKVKVLGDVIEVHGKHEERQDEHGFISREFHR	120
K174X	FDTGLSEMRLEKDRFSVNLDVKHFSPEELKVKVLGDVIEVHGKHEERQDEHGFISREFHR	120
A171X	FDTGLSEMRLEKDRFSVNLDVKHFSPEELKVKVLGDVIEVHGKHEERQDEHGFISREFHR	120
R157H	FDTGLSEMRLEKDRFSVNLDVKHFSPEELKVKVLGDVIEVHGKHEERQDEHGFISREFHR	120
E165X	FDTGLSEMRLEKDRFSVNLDVKHFSPEELKVKVLGDVIEVHGKHEERQDEHGFISREFHR	120
E164X	FDTGLSEMRLEKDRFSVNLDVKHFSPEELKVKVLGDVIEVHGKHEERQDEHGFISREFHR	120
464delCT	FDTGLSEMRLEKDRFSVNLDVKHFSPEELKVKVLGDVIEVHGKHEERQDEHGFISREFHR	120
Q151X	FDTGLSEMRLEKDRFSVNLDVKHFSPEELKVKVLGDVIEVHGKHEERQDEHGFISREFHR	120
450delA	FDTGLSEMRLEKDRFSVNLDVKHFSPEELKVKVLGDVIEVHGKHEERQDEHGFISREFHR	120
P20S	FDTGLSEMRLEKDRFSVNLDVKHFSPEELKVKVLGDVIEVHGKHEERQDEHGFISREFHR	120
R120G	KYRIPADVDP LT ITSS LSS DGVLTVNGPRKQVSGPERTIPITREEKPAVTAAPKK-----	175
D140N	KYRIPADVDP LT ITSS LSS NGVLTVNGPRKQVSGPERTIPITREEKPAVTAAPKK-----	175
Wild Type	KYRIPADVDP LT ITSS LSS DGVLTVNGPRKQVSGPERTIPITREEKPAVTAAPKK-----	175
K175X	KYRIPADVDP LT ITSS LSS DGVLTVNGPRKQVSGPERTIPITREEKPAVTAAPK-----	174
K174X	KYRIPADVDP LT ITSS LSS DGVLTVNGPRKQVSGPERTIPITREEKPAVTAAP-----	173
A171X	KYRIPADVDP LT ITSS LSS DGVLTVNGPRKQVSGPERTIPITREEKPAVT-----	170
R157H	KYRIPADVDP LT ITSS LSS DGVLTVNGPRKQVSGPEHTIPITREEKPAVTAAPKK-----	175
E165X	KYRIPADVDP LT ITSS LSS DGVLTVNGPRKQVSGPERTIPITRE-----	164
E164X	KYRIPADVDP LT ITSS LSS DGVLTVNGPRKQVSGPERTIPITR-----	163
464delCT	KYRIPADVDP LT ITSS LSS DGVLTVNGPRKQVSG----- <u>RAHSHHP</u> -----	162
Q151X	KYRIPADVDP LT ITSS LSS DGVLTVNGPRK-----	150
450delA	KYRIPADVDP LT ITSS LSS DGVLTVNGPRNRS LALS APFPSPVKRSLLSPQPPRNRCPFLNCIF	184
P20S	KYRIPADVDP LT ITSS LSS DGVLTVNGPRKQVSGPERTIPITREEKPAVTAAPKK-----	175

Figure 1.3. Structural alignment of the naturally occurring α B-crystallin mutations and specific mutations of interest. The structural alignment shows the effect of congenital mutations 450delA, 464delCT, Q151X, D140N, R157H, P20S and R120G upon the structure of α B-crystallin. Details are also shown of the PTM products E164X, K175X and A171X and for comparison a series of C-terminal truncated mutants, which sequentially remove important regions of the C-terminal extension. Small and hydrophobic amino acids (including aromatic -Y) are indicated in red, acidic (blue), basic (magenta), Hydroxyl +amine+basic-Q, (green) and other amino acids are indicated in grey. Novel amino acid sequences are underlined. (Alignment produced using ClustalW multiple sequence alignment programme at www.ebi.ac.uk/clustalw).

1.8. HYPOTHESIS AND AIMS OF THE STUDY

The systematic analysis of the role of the C-terminal extension aims to investigate the hypothesis that, the C-terminal region in α B-crystallin is important for solubility, structure and function of the protein, thus providing a potential explanation of whether the three mutations (450delA, Q151X and 464delCT) cause the various diseases via the loss of chaperone function or perhaps by a different mechanism.

In this study, I aim to analyse the effects of the Q151X, 464delCT and 450delA mutations upon the oligomerisation and chaperone activity of α B-crystallin. For comparison, I will also assess the activity of a series of α B-crystallin constructs truncated at residues K174, E165, A171 and E164 to sequentially remove important regions of the C-terminal extension and therefore help us understand the role it plays in the functional and structural integrity of α B-crystallin. The characterisation of these mutants also aims to provide understanding of the mechanism that allows mutations such as Q151X and 464delCT to express the phenotype of myofibrillar myopathy without any evidence of cataractogenesis, where as 450delA shows isolated congenital cataract with no muscular degeneration.

In Chapter 3, I have investigated the relationship between the C-terminal extension and the solubility of α B-crystallin, and its potential role in the mechanism that causes various disease states. This Chapter involved the cloning, expression and purification of the sequentially truncated C-terminal α B-crystallin mutants (K174X and E165X) along with the three naturally occurring disease causing mutants (450delA, Q151X and 464delCT) and the PTM truncations (E164X and A171X). The nature of expression and purification helped understand the role of specific regions of the C-terminal extension important in solubilisation of α B-crystallin oligomers, and provided the basis for further characterisation that was performed in Chapter 4.

In Chapter 4, I investigated the role of the C-terminal extension upon oligomerisation and chaperone activity by characterising the effects of these C-terminal extension mutants upon the structure and function of α B-crystallin. This further characterisation of the C-terminal extension aimed to elucidate the mechanism that links the C-terminal extension with the chaperone function, oligomerisation and solubility and how the three naturally occurring mutations of this C-terminal extension not only cause disease but also result in the varying pathology of isolated polar posterior cataract (450delA) and myofibrillar myopathy (464delCT and Q151X).

In Chapter 5, I wanted to focus on the mechanism that links chaperone activity with oligomerisation by investigating the relationship between the subunit dynamics of wild type α B-crystallin and oligomerisation, hoping to provide further understanding of the role this plays in efficient chaperoning of client proteins by wild type α B-crystallin. In this chapter, I analysed the effect of protein concentration of wild type α B-crystallin upon oligomerisation and also identified a low Mwt species of wild type α B-crystallin, which could potentially be an active unit of chaperone activity however further analysis is required.

CHAPTER 2

MATERIALS AND METHODS

2.1. CHEMICALS

All chemicals and reagents used were purchased from Merck Ltd (Poole, UK) or Sigma Aldrich (Poole, UK) and were of analytical grade unless otherwise stated. All restriction endonucleases were from New England Biolabs (Herts, UK) unless otherwise stated.

2.2. CONSTRUCTION OF α B-CRYSTALLIN MUTANTS

2.2.1. PRIMER DESIGN

Primers for α B-crystallin mutants (see Table 2.1) were designed based on the messenger RNA (mRNA) sequence for wild type human α B-crystallin (DDBJ/EMBL/GenBank entry NM_001885) (Sigma Genosys, UK). Unique restriction enzyme sites were incorporated into the primers to assist screening, using the software available at: http://www.dwalab.com/DNAProject/bin/DNA_Analysis_Frame.html and products amplified using wild type α B-crystallin as a template for PCR mutagenesis. With the exception of the Q151X and the E165X mutations, the amplified products were cloned into the vector pGEM®-T Easy (Promega, UK). After verification of the sequences the mutant α B-crystallin constructs were subcloned into the *NcoI* and *EcoRI* sites of the expression vector pET23d (New England Biolabs). The Q151X and E165X mutations were introduced into pET23d by Site Directed mutagenesis (SDM) (Stratagene, UK) using complementary primers, (see Table 2.1). Constructs were sequenced and compared for fidelity to the GenBank data base entry (accession no. NM001885).

Table 2.1. Oligonucleotide primer sequence details used for introduction of the α B-crystallin mutations

Mutant α B-crystallin	Restriction Enzyme site	Primer sequence (5'-3')
Q151X	<i>StuI</i>	Forward primer gtgaatggaccaaggaaat aggcct ctggccctgagcgcacc Reverse Primer ggtgcgctcagggccag aggcct tattccttggtccattcac
E165X	<i>HindIII</i>	Forward primer attcccatcaccggtgaataga aagctt gctgtcaccgcagccccc Reverse Primer gggggctgcggtgacagc aagctt ctattcacgggtgatgggaat
464delCT	<i>n/a</i>	Forward primer Taccatggacatcgccatccaccacc Reverse Primer tcacgggtgatgggaatggtgcgctcggccagagacctgtttcc
K174X	<i>SacII</i>	Forward primer Taccatggacatcgccatccaccacc Reverse Primer Ctaggggg ccgagg tgacagcaggcttc
A171X	<i>SacI</i>	Forward primer Taccatggacatcgccatccaccacc Reverse Primer gggcatctatttcttgg agctc aggtgacagcaggcttctc
E164X	<i>PstI</i>	Forward primer Taccatggacatcgccatccaccacc Reverse Primer cttgggagctgcggtga ctgcagg cttctcttaacgggtgatgggaatggt

The unique restriction enzyme sites incorporated into the primer design are highlighted in bold text. Q151X and E165X were introduced using SDM requiring complementary forward (5'-3') and reverse (3'-5) primers. The 464delCT, K174X, A171X and E164X mutant mRNA were amplified using a forward primer overlapping the

pET23d insertion site and the 5' end of the template wild type α B-crystallin. Reverse primers were complementary to the 3' end of the template wild type α B-crystallin and incorporated the mutation and the unique restriction site. A suitable restriction enzyme site was not available for the 464delCT mutation.

2.2.2. CONSTRUCTION OF Q151X α B-CRYSTALLIN MUTANT USING SDM

2.2.2.1. Polymerase Chain Reaction (PCR)

Initial attempts to incorporate the Q151X mutation into wild type α B-crystallin using SDM required optimisation of the magnesium chloride (MgCl_2) concentration and extension time during the PCR. The pfu Turbo polymerase supplied with the Stratagene kit utilised a proof reading function, however, comparison for fidelity to the GenBank data base entry (accession no. NM001885) identified random base changes, although the mutant sequence had been successfully cloned. Therefore, SDM was performed using Taq polymerase and a T7 Terminator primer. Table 2.2 details the reaction mixture and Table 2.3 details the cycling parameters utilised during the PCR stage of the SDM process.

Table 2.2. Q151X α B-crystallin mutant reaction mixture for PCR

Reagent	Volume
T7 terminator primer 10 μ M	1 μ l
Q151X forward primer 10 μ M	1 μ l
pET 23d vector with wild type α B-crystallin insert	100ng
10X buffer (Roche Diagnostics, Lewes, UK)	5 μ l
dNTP mix 10mM	1 μ l
DEPC Water (Invitrogen, Paisley, UK)	To final volume 50 μ l
25mM MgCl_2	3 μ l
Taq polymerase (Bioline, London, UK)	0.5 μ l

Table 2.3. Q151X α B-crystallin mutant PCR cycling condition

Stage	Temp (°C)	Time (min)	N ^o cycles
1	94	1	1
2	94	1	25
	60	1	
	72	4*	
3	72	2	1
4	4	Hold	1

*The extension time is representative of 1min/kb plasmid

The PCR product was digested for 1 h at 37°C with Dpn I (Stratagene, UK) to remove parental DNA from the product DNA. An agarose gel (0.6% w/v) was performed to confirm the product was of the required size (see 2.2.2.2).

2.2.2.2. Agarose gel electrophoresis

For a 0.6% (w/v) agarose gel, 0.3g of agarose was reconstituted in 50ml of 40mM Tris(hydroxymethyl)methylamine (Tris)-acetate, 1mM EDTA pH 8.0, (TAE), buffer and heated in the microwave until the agarose had completely melted. Once cooled to 50°C, a 2.5 μ l aliquot of 10 mg/ml ethidium Bromide was added and the gel cast. The gel was allowed to set for 30 min prior to sample loading. DNA samples for gel analysis require addition of 0.25% (w/v) Bromophenol blue, 0.25% (w/v) xylene cyanol, 30% (w/v) glycerol, (6X DNA running buffer) (Maniatis, 1989)). The gels were calibrated using DNA ladders, the first, 4 μ l of a GeneRuler® 100 bp DNA ladder (Fermentas, York, UK) consisting of 14 fragments ranging from 100-3000 bp. The second, 12 μ l of a 1000 bp marker (λ Pst I) consisting of fragments of Lambda DNA (New England BioLabs, UK) digested by Pst I (New England BioLabs, UK) ranging from 15 – 11501 bp. The DNA is resolved by 50V constant voltage and DNA products visualised using a Biorad Gel Doc 2000 and Quantity one v4.0.3 software (Biorad Laboratories, UK).

2.2.2.3. Transformation of mutant DNA

Confirmation of the correctly sized PCR product prompted transformation of the PCR product into DH5 α competent cells for proliferation, (see Section 2.3). The PCR product consists of the pET23d(+) vector containing the mutant α B-crystallin mRNA insert.

2.2.2.4. Cultivation and purification of plasmid DNA

A selection of suitable colonies were picked and placed into 5ml of Luria-Bertani (LB) media with 50 μ g/ml Carbenicillin and incubated overnight at 37°C at 225rpm. The plasmid DNA was purified using plasmid mini prep Kit (Sigma, Gillingham, UK) following the recommended protocol. Each 5ml culture was centrifuged for 15 min at 4000rpm at 4°C, and the supernatant discarded. The resulting pellet was resuspended in 400 μ l of resuspension buffer and separated into two 200 μ l volumes for further purification in 1.5ml eppendorf tubes. The cells were lysed by the addition of 200 μ l lysis buffer and gently inverted 6-8 times ensuring the neutralisation buffer was added (350 μ l) within 5 min of the Lysis buffer. The tubes were inverted 4-6 times and centrifuged in the microcentrifuge for 10 min at 12500rpm. The supernatant was added to a spin column, which was prepared by the addition of 500 μ l of column preparation buffer and centrifuged for 1 min at 12500 rpm and the flow through was discarded. With the plasmid DNA applied the spin column was centrifuged for 1 min at 12500 rpm and the flow through discarded. The 750 μ l of wash solution was added to the spin column and centrifuged for 1 min at 12500 rpm and flow through discarded. The column was spun for a further 2 min without any additional buffer, to ensure maximum removal of ethanol from the column membrane. The purified plasmid DNA was eluted with 50 μ l of sterile water, and the two aliquots per 5ml culture were recombined and stored at -20°C.

2.2.2.5. Screening for transformants

Purified plasmid DNA was digested with Nco I / Stu I. To 10 µl of DNA, 0.5 µl of each restriction enzyme was added with 1 µl of 1 mg/ml BSA (New England BioLabs, UK), 1 µl Buffer B digestion buffer (provided with the restriction enzyme) and 7 µl of sterile purified water. The mixture was incubated at 37°C for 1-2 h then analysed by agarose gel (see Section 2.2.22) to identify the constructs with fragments of the correct insert size. Constructs were sequenced and compared for sequence fidelity to the GenBank data base entry (accession no. NM001885).

2.2.3. CONSTRUCTION OF E165X α B-CRYSTALLIN MUTANT USING SDM

The pfu Turbo polymerase supplied with the Stratagene kit utilised a proof reading function, which failed to prevent the introduction of random base changes, however the mutant sequence had been successfully cloned. SDM was performed using Taq polymerase with an optimised annealing temperature and cycle number. Table 2.4 details the reaction mixture and Table 2.5 details the cycling parameters utilised during the PCR stage of the SDM process.

Table 2.4. E165X α B-crystallin mutant reaction mixture for PCR

Reagent	Volume (µl)
E165X Reverse primer 10µM	1µl
E165X forward primer 10µM	1µl
pET 23d vector with wild type α B-crystallin insert	100ng
10X buffer (Roche Diagnostics, Lewes, UK)	5µl
dNTP mix 10mM	1µl
DEPC Water (Invitrogen, Paisley, UK)	To final volume 50µl
25mm MgCl ₂	3µl
Taq polymerase (Bioline, London, UK)	0.5µl

Table 2.5 E165X α B-crystallin mutant PCR cycling conditions

Stage	Temp (°C)	Time (min)	Nº cycles
1	94	1	1
2	94	1	5
	55	1	
	72	4	
3	94	1	20
	60	1	
	72	4	
4	72	2	1
5	4	Hold	1

The PCR product was digested for 1 h at 37°C with *DpnI* to remove parental DNA from the product DNA. An agarose gel (0.6% w/v) was performed to confirm the product was of the required size (see Section 2.2.2.2).

Digested PCR product was transformed into DH5 α competent cells for proliferation, (see Section 2.3), resulting colonies picked, cultured overnight and plasmid DNA purified using plasmid mini prep Kit (Sigma, Gillingham, UK) (see Section 2.2.2.4). The purified plasmid DNA was digested with *NcoI*/ *HindIII* (see Section 2.2.2.5) and analysed by agarose gel (see Section 2.2.2.2) to identify the constructs with fragments of the correct insert size. Constructs were sequenced to confirm mutagenesis.

2.2.4. CONSTRUCTION OF 464DELCT, E164X, K174X AND A171X α B-CRYSTALLIN MUTANTS

Initial SDM experiments failed to produce PCR products of the correct size for the 464delCT, E164X, K174X and A171X α B-crystallin constructs. A different approach used primers for the amplification of PCR products using wild type α B-crystallin as a template for PCR mutagenesis. The amplified products were cloned into the vector pGEM®-T Easy (Promega, UK). After verification of the sequences the mutant α B-

crystallin constructs were subcloned into the *NcoI* and *EcoRI* sites of the expression vector pET23d (New England Biolabs).

2.2.4.1. Primer design

Primers for α B-crystallin mutants (Table 2.1; sigma Genosys, UK) were designed based on the mRNA sequence for wild type human α B-crystallin (DDBJ/EMBL/GenBank entry NM_001885). The first 4 bases of the forward primers consisted of pET23d(+) sequence, in which the wild type α B-crystallin gene was inserted. Unique restriction enzyme sites were incorporated into the primers to assist screening, using the software available at: http://www.dwalab.com/DNAProject/bin/DNA_Analysis_Frame.

2.2.4.2. PCR

The pGEM®-T Easy system required a PCR product with a 3' A overhang, which was generated using the EasyA high fidelity polymerase (Stratagene, UK). Table 2.6 details the reaction mixture and Table 2.7 details the cycling parameters utilised during the PCR mutagenesis.

Table 2.6. Easy A PCR reaction mixture

Reagent	Volume
Reverse primer 10 μ M	1 μ l
Forward primer 10 μ M	1 μ l
pET 23d vector with wild type α B-crystallin insert	100ng
10X buffer (Stratagene, UK)	5 μ l
dNTP mix 10mM	1 μ l
DEPC Water (Invitrogen, Paisley, UK)	To final volume 50 μ l
Easy A polymerase (Stratagene, UK)	0.5 μ l

Table 2.7. Easy A PCR cycling conditions

Stage	Temp (°C)	Time	No Cycles
1	95	2 min	1
2	95	40 sec	25
	72	30 sec	
	72	1 min	
4	72	7 min	1
5	4	Hold	1

2.2.4.3. PCR product Gel Extraction (QIAquick - Qiagen)

The PCR product of interest was resolved from other non-specific bands by 0.6% (w/v) agarose gel electrophoresis, (see Section 2.2.2.2). The DNA fragment was excised from the agarose gel with a clean sharp scalpel and it was ensured that exposure to UV was minimal in order to prevent mutation of the DNA. The size of the gel slice was minimised by removal of excess agarose. The gel slice was weighed and then solubilised by the addition of 3 volumes of buffer QG (Qiagen, Crawley, UK) to 1 volume of gel. To aid dissolution, heating at 50°C was utilised with intermittent vortexing. The sample was applied to a QIAquick spin column in a 2ml collection tube centrifuged for 1 min at 12500 rpm and the flow through discarded. The column was washed with 0.75 ml Buffer PE (Qiagen, Crawley, UK), centrifuged for 1 min at 12500 rpm and the flow through discarded. To ensure complete ethanol removal the column was centrifuged for a further 1 min at 12500 rpm and the QIAquick spin column placed into a clean tube. The DNA was eluted by application of 50 µl of sterile water onto the membrane and after being allowed to stand for 1 min, was centrifuged for 1 min at 12500 rpm. The purified DNA was ligated immediately.

2.2.4.4. Ligation into pGEM-T Easy vector system

Ligation reactions utilised the Promega pGEM-T Easy ligation kit (Promega WI, USA). The ligation reactions were performed using the reaction mixture detailed in Table 2.8.

Table 2.8. Ligation reactions using the pGEM-T Easy (Promega) ligation kit.

Reagent	Standard reaction	Positive Control	Background control
2X rapid ligation buffer	10µl	10µl	10µl
pGEM-T Easy vector	1µl	1µl	1µl
PCR product	5µl	-	-
Control insert	-	5µl	-
T4 DNA ligase	1µl	1µl	1µl
Sterile water	3µl	3µl	8µl

The ligation reaction mixtures were incubated for 3 h at room temperature or overnight at 4°C.

2.2.4.5. Transformation, cultivation and purification of plasmid DNA

The entire 20µl ligation reaction was transformed into DH5α competent cells performed as detailed in Section 2.3.

A selection of white colonies were picked and placed into 5ml of LB media with 50µg/ml carbenicillin and incubated overnight at 37°C at 225rpm. The DNA was purified using the plasmid mini prep Kit (Sigma, Gillingham, UK) and the recommended protocol (see 2.2.2.4).

2.2.4.6. Screening for transformants

Purified plasmid DNA was digested (see Section 2.2.2.5) with the appropriate restriction enzymes as shown in Table 2.9

Table 2.9. Mixture for restriction enzyme digestion

Construct	Restriction enzymes
464delCT	<i>NcoI/ EcoRI</i>
E164X	<i>NcoI/ PstI</i>
K174X	<i>NcoI/ SacII</i>
A171X	<i>NcoI/ SacI</i>

The mixture was incubated at 37°C for 1 - 2 h then analysed by agarose gel (see Section 2.2.2.2) to identify constructs of the correct size for sequencing analysis.

2.2.4.7. Sub cloning of mutant DNA into bacterial expression vector pET23d(+).

The mutant α B-crystallin sequence was cleaved from the pGEM-T easy vector using a double digest with *NcoI/ EcoRI* restriction enzymes (see Section 2.2.2.5). A second double digest was performed with the empty pET23d(+) expression vector with the same restriction for insertion of the excised fragment. The mixture was incubated at 37°C for 1 - 2 h then separated by Agarose gel electrophoresis (see Section 2.7.2.2). The pET23d(+) vector minus fragment and the cleaved α B-crystallin sequence cleaved from pGEM-T Easy are excised from the gel and undergo gel extraction purification, see 2.2.4.3. Once purified, the vector and fragment are ligated as detailed in Table 2.10.

Table 2.10. Ligation reaction for sub cloning into pET23d(+)

Reagent	Standard reaction	Positive control	Background control
10X rapid ligation buffer	2µl	2µl	2µl
pET23d(+)	1µl	1µl	1µl
PCR product	17µl	-	-
Control insert	-	5µl	-
T4 DNA ligase	1µl	1µl	1µl
Sterile water	3µl	3µl	8µl

The ligation reaction mixtures were incubated for 3 h at room temperature or overnight at 4°C, then either stored at 4°C or -20°C until further use. The entire 20µl ligation reaction was transformed into DH5α competent cells performed as detailed in Section 2.3. A selection of 12 colonies were picked and placed into 5ml of LB media with 50µg/ml Carbenicillin and incubated overnight at 37°C at 225rpm.

The DNA was purified using the plasmid mini prep Kit (Sigma, Gillingham, UK) and the recommended protocol (see Section 2.2.2.4). Purified plasmid DNA was digested with the appropriate restriction enzymes (Table 2.9) and screened as detailed in Section 2.2.4.6. Constructs with confirmation of the correct mutant sequence in pET23d(+), are suitable for expression in BL-21(pLysS) competent cells.

2.2.5. SUB-CLONING OF MUTANT DNA INTO MAMMALIAN EXPRESSION VECTOR pCDNA3.1(-) FROM PET23D (+)

The sub-cloning of mutant DNA from pET23d(+) to pcDNA3.1(-) follows the protocol detailed in Section 2.2.4.7 with restriction enzymes appropriate for ligation into pcDNA3.1(-). The enzymes required are specific to the vector pcDNA3.1(-) not the insert (Table 2.11).

Table 2.11. Mixture for restriction enzyme digestion

Reagent	Volume
<i>HindIII</i>	1µl
<i>XbaI</i>	1µl
Yellow Tango Buffer	2µl
Mutant DNA / pcDNA3.1(-)	17µl/ 500ng

The resulting digest fragments undergo gel extraction (see Section 2.2.4.3), ligation (see Section 2.2.4.7), transformation (see Section 2.3), cultivation, purification of plasmid DNA (see Section 2.2.2.4) and finally screening for transformants using restriction enzymes *ApaI*/ *HindIII*. This digest allows confirmation of the presence of a mutant fragment and transfer into the pcDNA3.1(-) vector as pET23d(+) has no *ApaI* site.

Confirmation of the presence of the required mutant DNA by sequencing preceded transient transfection of mutant α B-crystallin DNA in pcDNA3.1(-) into mammalian cells.

2.3. TRANSFORMATION OF PLASMID DNA AND PREPARATION OF INOCULUM FOR BATCH CULTURE.

Competent cells (BL-21/DH5 α) were thawed on ice and divided into pre cooled eppendorf tubes in 50µl aliquots, (50µl per transformation). A 2µl volume of plasmid DNA, (α B-crystallin insert in pET23d(+)), was added to the 50µl aliquot and mixed by gentle swirling. The transformation mixture was incubated on ice for 30 min, followed by incubation at 42°C for 45 sec, then incubation on ice for 2 min. A 500µl volume of LB media was added to the tube contents, and the transformation reaction was incubated at 37°C for 60 min at 225rpm. The reaction mixture was plated onto LB agar plates with 50µg/ml carbenicillin for growth of DH5 α colonies and 50µg/ml carbenicillin with 34µg/ml Chloramphenicol, for growth of BL-21 colonies. Plates were incubated overnight at 37°C. One colony was picked and placed into 10ml of LB media with suitable antibiotics (plus 0.05% (w/v) glucose for BL-21 cultures) and incubated overnight at 37°C at 225rpm.

2.4. BATCH FERMENTATION OF *E.COLI* BL-21 (PLYSS) CELLS

A 500ml flask of LB media containing 34 μ g/ml chloramphenicol, 50 μ g/ml carbenicillin and 0.05% (w/v) glucose was inoculated with a 10ml of a fresh overnight culture. The flask was mixed at 225rpm at 37°C and the optical density was monitored at OD₆₀₀ until a value of 0.6 ± 0.1 AU was observed, at which time protein expression was induced by adding 0.5mM Isopropyl-beta-D-Thiogalactopyranoside (IPTG) and the cells were cultured for a further 3 h.

2.5. CELL HARVESTING, HOMOGENISATION AND RECOVERY OF THE α B-CRYSTALLIN PROTEIN FRACTION

Following a 3 h post induction growth period, the cells were removed from the 37°C incubator and centrifuged at 4°C for 15 min at 4000 rpm. The supernatant was decanted and discarded. The pelleted material was resuspended in 20ml of 50mM Tris-hydrochloric acid (HCl), pH8.0, 1mM EDTA, 100mM sodium chloride (NaCl), 10mM MgCl₂ 0.2mM Phenylmethylsulphonylfluoride (PMSF) with the addition of a Complete™ protease inhibitor cocktail tablet (Roche Diagnostics, Lewes, UK). Cell lysis was initiated by 3 freeze thaw cycles at -20°C, after which, the cell resuspension was homogenised using a Dounce glass homogeniser, on ice, in order to prevent proteolysis. The cell lysate was centrifuged at 15000rpm for 30 min at 4°C. For soluble protein expression such as wild type α B-crystallin, the supernatant is retained and further purified. Expression of mutant α B-crystallin as inclusion bodies results in further purification of the pelleted material.

2.6. PURIFICATION OF SOLUBLE PROTEIN WILD TYPE α B-CRYSTALLIN

2.6.1. REMOVAL OF DNA FROM THE WILD TYPE α B-CRYSTALLIN SOLUBLE PROTEIN FRACTION

Benzonase® nuclease, (Novagen, Nottingham, UK) was added to a final conc. of 10 u/ml to the soluble protein fraction (SPF) to degrade endogenous nucleic acids that may have interfered with purification due to high viscosity. The SPF was mixed gently at ambient temperature for 30 min. The DNA material present in the SPF was precipitated by the addition of 0.1%(v/v) Polyethylimine (PEI) and was incubated on ice for 5min. Precipitated DNA material was removed by centrifugation at 15000rpm for 10min at 4°C. To remove the PEI, the supernatant was dialysed, overnight at 4°C against 20mM Tris HCl pH 7.4, 1mM MgCl₂, 1mM EDTA, 1mM Dithiothreitol (DTT), 0.2M PMSF, using 12K-14K molecular weight cut off, (MWCO) dialysis tubing (Medicell International Ltd, London, UK). The dialysate was concentrated to \leq 5ml using a 15ml Amicon spin concentrator, (Millipore UK, Watford, UK). The concentrated material was filtered using a 32mm Acrodisc® polyethersulphone (PES) syringe filter (Pall, Portsmouth, UK). Clarified SPF was stored at 4°C until further purification.

2.6.2. ION EXCHANGE CHROMATOGRAPHY

Further purification of the wild type α B-crystallin was performed using Fractogel® Trimethylammoniummethyl group (TMAE) (Merck Biosciences, West Drayton, UK) ion exchange chromatography (IEX) resin, (binding capacity for BSA 100mg/ml resin). A 10 ml column was poured with a packed bed height, (PBH) of 10 cm and underwent a cleaning in place, (CIP) and equilibration protocol using the Merck Hitachi Biochromatography High performance liquid chromatography (HPLC) system (Merck Hitachi Ltd, Tokyo, Japan).

- 2 h sanitisation with 0.5M sodium hydroxide, (NaOH).
- 3 column volumes (CV) of milliQ water
- 2 CV of 20mM Tris HCl pH 7.4, 1mM MgCl₂, 1M NaCl, 1mM EDTA, 1mM DTT, 0.2M PMSF, (Buffer B).
- 3 CV of 20mM Tris HCl pH 7.4, 1mM MgCl₂, 1mM EDTA, 1mM DTT, 0.2M PMSF, (Buffer A) or until OD_{280} reaches a stable baseline.

All HPLC buffers were degassed and vacuum filtered to 0.2 μ m using a Whatman Cellulose nitrate membrane disc filter (Whatman, Maidstone, UK). The load material was applied at 1ml/min to the column in 10 ml of Buffer A and was eluted with a 50 ml linear gradient of 0 - 0.5M NaCl (Buffer B). Residual bound protein was eluted over a 30 ml linear gradient of 0.5 – 1M NaCl (Buffer B). Eluted material was collected as 1ml fractions using a Biorad Model 2110 fraction collector (Biorad Laboratories, UK) and assayed by sodium dodecyl (lauryl) sulfate-polyacrylamide gel electrophoresis (SDS-PAGE) (see Section 2.10), using 12% (w/v) acrylamide gels. Fractions enriched with wild type α B-crystallin were pooled. The column was sanitised by a 2 h contact time with 0.5M NaOH followed by 30 ml of milliQ water. The column was stored in 20 ml of 20mM Tris HCl, 1M NaCl, 0.02% (v/v) sodium azide, pH 7.4. The data was analysed using Chromeleon 6.30 software (Sunnyvale, CA, USA).

2.6.3. SIZE EXCLUSION CHROMATOGRAPHY

Further purification of the wild type α B-crystallin pool was performed using, a 120 ml size exclusion (SEC) Fractogel EMD BioSEC Superperformance® column (60 x 1.6cm) (Merck, Darmstadt, Germany), which underwent the following CIP and equilibration protocol.

- 2 h sanitisation with 0.5M NaOH.
- 3 CV of milliQ water
- 2 CV of 20mM Tris HCl pH 7.4, 500mM NaCl
- 3 CV of 20mM Tris HCl pH 7.4, 100mM NaCl, (Buffer A) or until OD_{280} reaches a stable baseline.

All HPLC buffers were degassed and vacuum filtered to 0.2 μ M using a Whatman Cellulose nitrate membrane disc filter (Whatman, Maidstone, UK). The wild type α B-crystallin IEX pool (see Section 2.6.2) was dialysed for 16 h at 4°C into Buffer A using 12-14kDa MWCO dialysis tubing (Medicell International Ltd, London, UK) then concentrated to 0.5ml using an Amicon Ultra Centrifugal filter device 10K MWCO (Millipore, Watford, UK) and 0.2 μ M filtered using a 32mm Acrodisc® PES syringe filter (Pall, Portsmouth, UK). The concentrated pool was applied at 1ml/min to the column in Buffer A and was collected in the flow through as 1ml fractions. Fractions were assayed by SDS-PAGE, using 12% (w/v) acrylamide gels and those fractions enriched with wild type α B-crystallin were pooled, aliquoted and stored at -20°C. The column was sanitised by a 2 h contact time with 0.5M NaOH followed by 3 CV of milliQ water. The column was stored in 2 CV of 20mM Tris HCl, 1M NaCl, 0.02% (v/v) sodium azide, pH 7.4.

2.6.4. LARGE SCALE (6L) α B-CRYSTALLIN PURIFICATION

Large scale purification was performed as detailed in sections 2.5 and 2.6 with the appropriate 6x increase in process volumes. The IEX chromatography was performed using a 68 ml the strong anion exchange resin Fractogel ® TMAE EMD (s) column (13cm x 2.6cm) (Merck, Darmstadt, Germany). Sample application was performed via three 5ml injections and eluate was collected in 6 ml fractions. SEC purification was performed using a 415 ml HW55s (Tosoh, Japan) (78cm x 2.6cm) column with a Gilson Minipuls 2 peristaltic pump (Gilson, France) at 0.6 ml/min (7.5cm/h linear flowrate). The sample (5 ml ~ 1% CV) was applied directly to the top of the column bed and eluate collected in 6 ml fractions using a Biorad Model 2110 fraction collector (Biorad laboratories, UK).

2.7. PURIFICATION OF MUTANT α B-CRYSTALLIN AS INCLUSION BODIES

2.7.1. INCLUSION BODY EXTRACTION AND SOLUBILISATION

The inclusion body pellet was resuspended in 20ml of 20Mm Tris, 1% (v/v) Triton X-100, 150mM NaCl, 5mM EDTA, 1mM ethylene glycol tetraacetic acid (EGTA) 0.5mM DTT 0.2mM PMSF, pH 7.5 (Extract buffer 1). Benzonase® nuclease, was added to a final conc. of 10 u/ml to the resuspension, to degrades all forms of DNA and RNA, that may have interfered with purification due to high viscosity, while having no proteolytic activity, and was mixed gently at ambient temperature for 30 min. The inclusion body solution was centrifuged at 15000rpm for 30 min at 4°C, and the supernatant containing cell debris was discarded. The inclusion body pellet was resuspended in 20ml of 20mM Tris, 0.5% (v/v) Triton X-100, 600mM NaCl, 5mM EDTA, 1mM EGTA 0.5mM DTT 0.2mM PMSF, pH 7.5 (Extract buffer 2), and was mixed gently at ambient temperature for 30 min. The inclusion body solution was centrifuged at 15000rpm for 30 min at 4°C, and the supernatant containing cell debris was discarded. The inclusion body pellet was resuspended in 20ml of 10mM Tris pH 7.5, 150mM NaCl, 5mM EDTA, 1mM EGTA 0.5mM DTT 0.2mM PMSF (Extract buffer 3) and was mixed gently at ambient

temperature for 30 min. The inclusion body solution was centrifuged at 15000 rpm for 30 min at 4°C, and the supernatant containing cell debris was discarded. The resulting pellet was solubilised in 10 volumes of 10mM Tris, 6M urea, pH 8.0 1mM EDTA, 1mM DTT 0.2mM PMSF and incubated at 4°C with mixing for 4 h. The solubilised material was clarified by centrifugation at 15000 rpm for 30 min at 4°C, and the supernatant was decanted and dialysed against 10mM Tris, 6M urea, 1mM EDTA, pH 8.0, 1mM DTT 0.2mM PMSF overnight at 4°C using 12-14kDa MWCO dialysis tubing (Medicell International Ltd, London, UK) then concentrated to 0.5 ml

The dialysate was concentrated to ≤ 5 ml using a 15 ml Amicon Ultra Centrifugal filter device 10K MWCO (Millipore, Watford, UK). The concentrated material was 0.2 μ M filtered using 32 mm Acrodisc® PES syringe filter (Pall, Portsmouth, UK) and stored at 4°C until further purification.

2.7.2. IEX

Further purification of the mutant α B-crystallin was performed using the IEX column detailed in Section 2.6.2. and underwent the following CIP protocol and equilibration.

- 2 h sanitisation with 0.5M NaOH.
- 3 CV of milliQ water
- 2 CV of 10mM Tris HCl, 1mM EDTA, 6M urea, pH 8.0, 1M NaCl, 1mM DTT, 0.2M PMSF, (Buffer B).
- 3 CV of 10mM Tris HCl, 1mM EDTA, 6M urea, pH 8.0, 1mM DTT, 0.2M PMSF, (Buffer A) or until OD_{280} reaches a stable baseline.

All HPLC buffers were degassed and vacuum filtered to 0.2 μ m using a Whatman cellulose nitrate membrane disc filter (Whatman, Maidstone, UK). The mutant α B-crystallin was applied at 1 ml/min to the column in 10 ml of Buffer A and was eluted with a 50 ml linear gradient of 0-0.5M NaCl (Buffer B). Residual bound protein was eluted over 3 CV linear gradient of 0.5–1M NaCl, (Buffer B). Eluted material was collected as 1ml fractions and assayed by SDS-PAGE using 12% (w/v) acrylamide gels and those

fractions, which were wild type α B-crystallin enriched were pooled. The column was sanitised by a 2 h contact time with 0.5M NaOH followed by 3 CV of milliQ water. The column was stored in 2CV of 20mM Tris HCl, 1M NaCl, 0.02% (v/v) sodium azide, pH 7.4.

2.7.3. REFOLDING OF THE MUTANT α B-CRYSTALLIN

Aggregation prone mutant α B-crystallins (450delA, 464delCT and Q151X) required the presence of wild type α B-crystallin in order achieve a soluble refold product (see Section 2.7.3.1.). Further refolding was dependant upon the solubility characteristics of each specific mutant, where the 450delA/- and Q151X/ wild type α B-crystallin mixtures required a diluted refold for aggregation prone mutants (see Section 2.7.3.2) and the 464delCT/ wild type α B-crystallin required an undiluted refold for non aggregating mutants (see Section 2.7.3.3).

2.7.3.1. Association with wild type α B-crystallin

Mutants requiring association with the wild type α B-crystallin (450delA, 464delCT and Q151X α B-crystallin) are combined with the wild type α B-crystallin prior to refolding. Firstly, the wild type α B-crystallin was dialysed into the mutant α B-crystallin denaturing buffer conditions (10mM Tris, 6M urea, pH 8.0, 1mM DTT) for 16 h at 4°C. Protein concentrations of the denatured wild type and mutant α B-crystallin were determined by optical density (OD) OD₂₈₀. Extinction Coefficients were determined using the Emboss Pepstats programme (www.ebi.ac.uk/emboss/pepinfo/) and then the wild type and mutant α B-crystallin were mixed in a 1:1 molar ratio. The Extinction Coefficients for each mutant α B-crystallin are detailed in Table 2.12 and are derived from the quotient of the molar extinction coefficient for α B-crystallin of 13940 over the Mwt of the specific mutant.

Table 2.12. Extinction Coefficients of α B-crystallin mutants used for concentration determinations.

α B-crystallin	A280 Extinction Coefficient 1 mg/ml ($\text{mg}^{-1}\text{ml}^{-1}\text{cm}^{-1}$)
wild type	0.69
450delA	0.66
464delCT	0.74
Q151X	0.8
E164X	0.74
E165X	0.73
K174X	0.70
A171X	0.71
450delA/ wild type	0.675
464delCT/ wild type	0.715
Q151X/ wild type	0.745

2.7.3.2. Diluted refolding protocol for aggregation prone mutants

The diluted protocol was required for the refolding of 450delA/ wild type, Q151X/ wild type, Q151X and E164X α B-crystallin.

The protein was diluted to 0.25mg/ml (by OD_{280} using extinction coefficient specific to the mutant α B-crystallin (see Table 2.12)) with 10mM Tris, 6M-urea, pH 8.0 1mM EDTA, 1mM DTT and mixed gently at ambient temperature for 2 min. The addition of 1M-cystamine dihydrochloride to a final concentration of 1mM was followed by a 10 min mixing at ambient temperature. The urea concentration in the pooled material was diluted by an additional 6 fold dilution to 1M urea in refold buffer (10mM Tris-HCl, 5mM EDTA, 1mM EGTA, 150mM NaCl pH 7.5) and mixed gently at ambient temperature for 10 min. The mutant α B-crystallin was dialysed, for 4 h at 16°C against the refold buffer, using 12-14K MWCO dialysis tubing (Medicell International, Ltd, London, UK). The dialysate was partially concentrated using a 15ml Amicon Ultra Centrifugal filter device 10K MWCO (Millipore, Watford, UK) in a Jouan CR422 centrifuge at 16°C at 4000 rpm then centrifuged for 2 h at 4°C at 250000 (g) in the Beckman Optima MAX Ultracentrifuge, MLA-80 rotor (Beckman Instruments Inc, Fullerton, CA, USA). The supernatant was further concentrated at 4°C to a suitable volume. The concentrated material was stored at -80°C.

2.7.3.3. Undiluted refolding protocol for non aggregating mutants

The undiluted protocol was required for the refolding of 464delCT/ wild type and E165X α B-crystallin.

The protein mixture was dialysed into refold buffer for 4 h at 16°C and the resulting dialysate was centrifuged 2 h at 4°C at 2500000 (g) Beckman Optima MAX Ultracentrifuge, MLA-80 rotor and the supernatant concentrated using the Amicon Ultra Centrifugal filter device 10K MWCO (Millipore, Watford, UK) to a suitable volume in a Jouan CR422 centrifuge at 4°C.

2.8. CHARACTERISATION OF α B-CRYSTALLIN MUTANTS

2.8.1. *IN VITRO* PROTEIN CHAPERONE ASSAYS

2.8.1.1. Citrate Synthase chaperone activity assays

A 200 μ l aliquot of citrate synthase from porcine heart was dialysed for 16 h against 50mM Tris HCl, 2mM EDTA, pH 8.0 at 4°C, using 12-14 K MWCO dialysis tubing (Medicell International, Ltd, London, UK). Following dialysis the protein concentration was determined by Bicinchoninic acid (BCA) assay, (Pierce, UK), and the citrate synthase was diluted to achieve a stock concentration of 0.49 mg/ml. The assay mixture contained citrate synthase at a concentration of 0.196 mg/ml (88 μ l of a 0.49 mg/ml stock solution) and chaperone to produce varying citrate synthase: chaperone ratios in a final test volumes of 220 μ l. The time dependant light scattering was measured at 360 nm every 15 sec over a 30 min period using Beckman Tm cuvette (14mm high) for kinetic assays and a Beckman DU640 spectrophotometer (Beckman instruments Inc, CA, USA).

2.8.1.2. Insulin assay chaperone activity assays

A 20 mg aliquot of insulin from bovine pancreas was reconstituted in 5 ml of 100mM sodium sulphate (NaSO_4), 20mM sodium phosphate (NaPO_4) pH6.9 (Insulin buffer) and solubilised by the addition of 1 ml of acetic acid 30% (v/v) and gentle mixing for 15 min. The insulin solution was dialysed for 16 h against the Insulin buffer at 4°C, using 12-14K MWCO dialysis tubing (Medicell International, Ltd, London, UK). The dialysate was centrifuged for 1 min at 13000 rpm in an Eppendorf bench top centrifuge (5417R; Eppendorf, Hamburg, Germany). The insulin concentration was determined from the measured OD_{280} using its extinction coefficient, $((A_{280}/5840) \times 5600 = \text{mg/ml})$. The assay mixture contained, 20mM DTT, insulin at a concentration of 0.35mg/ml and chaperone to produce varying insulin: chaperone ratios in a final test volumes of 220 μ l. The time dependant light scattering was measured using a Beckman Tm cuvette (14mm high) at 360 nm every 15 sec over a 15 min period at 37°C using a Beckman DU640 spectrophotometer for (Beckman instruments Inc, CA, USA).

2.8.2. ANALYTICAL SEC

Purified and refolded α B-crystallin proteins were analysed using a Superose 6 column (290 x 10mm) with a maximum pressure limit of 10 bar at a flow rate of 0.2ml/min at room temperature using a Merck-Hitachi Biochromatography system (Merck Hitachi Ltd, Tokyo, Japan). The data was analysed using Chromeleon 6.30 software, (Sunnyvale, CA, USA). All HPLC buffers were degassed and vacuum filtered to 0.2 μ M using a Whatman Cellulose nitrate membrane disc filter (Whatman, Maidstone, UK).

2.8.2.1. Column preparation

The Superose 6 SEC column was sanitised at 0.2 ml/min using a 2 hr contact time with 0.5M NaOH. During periods of increased back pressure the flow rate was reduced accordingly. A 2 CV wash with purified water was followed by 2 CV of 10mM Tris, 1mM EGTA, 5mM EDTA, 1M NaCl, pH 7.5 (Buffer B). The column was equilibrated overnight at 0.2 ml/min in 10mM Tris, 1mM EGTA, 5mM EDTA, 150mM NaCl, pH 7.5 (Buffer A).

2.8.2.2. Mwt calibration of Superose 6 column

Mwt determination used a High MW calibration kit (Amersham Biosciences, UK). The components of this kit included a MW range from 2000 kDa (Blue Dextran 2000) to 150 kDa (Aldolase) with intermediate calibrators 440 kDa (Ferritin) and 232 kDa (Catalase). Additional low MW calibrators were included for a full range of calibration and included 66 kDa bovine serum albumin (BSA), 29 kDa Carbonic Anhydrase from Bovine erythrocytes (Sigma Aldrich, UK), and 12.4 kDa Cytochrome C from equine heart (Sigma Aldrich, UK). All high Mwt calibrators were reconstituted in Buffer A to a stock solution concentration of 10 mg/ml. To determine the void volume (V_0) of the column, Blue Dextran was loaded onto the column 1% of the geometrical column volume of 23 ml, (250 μ l of a 1 mg/ml solution). The high Mwt calibrators were analysed as mixtures recommended by the manufacturer to allow resolution of individual peaks. The mixtures and individual calibrators are detailed in Table 2.12. A 250 μ l blank injection (Buffer A) was performed in-between each calibrator run.

Table 2.13. Details of the Calibration of the Superose 6 SEC column

Run	Calibrator	Mwt (kDa)	Concentration (mg/ml)	Load volume (μ l)
1	Aldolase	158	5	100
	Ferritin	440	1	
2	Catalase	232	5	100
	Thyroglobulin	669	5	
3	BSA	66	5	100
4	Carbonic anhydrase	29	5	100
5	Cytochrome C	12.4	5	100

The data was analysed using Chromeleon 6.30 software, (Sunnyvale, CA, USA) and a calibration curve of K_{av} versus log molecular weight was prepared using the following equation:

$$K_{av} = \frac{V_e - V_o}{V_c - V_o}$$

Where V_e = elution volume as retention time, V_o = column void volume, V_c = geometric column volume.

Two calibration curves were prepared, one for the high Mwt calibrators and one for low Mwt calibrators due to the large separation range covered.

2.8.2.3. SEC of wild type and mutant α B-crystallin

Wild type α B-crystallin was dialysed into Buffer A for 16 h at 4°C using 12-14 kDa dialysis tubing (Medicell International Ltd, London, UK). The protein concentrations of the wild type and mutant α B-crystallin were determined using BCA protein assay kit (Pierce, UK) and the samples diluted accordingly in Buffer A to 0.2 mg/ml. The samples were injected in a 250 μ l volume to provide 0.2 % of the geometric column volume. The corresponding K_{av} for the α B-crystallin wild type and mutants were calculated and their molecular weight determined from the appropriate calibration curve prepared in Section 2.8.2.2.

2.8.2.4. Large scale (6L) analytical SEC

The chromatography conditions were as those detailed in section 2.6.4. The buffer used was 200mM ammonium Acetate and fractions were collected in 8 ml volumes using a Biorad Model 2110 fraction collector (Biorad Laboratories, UK).

2.8.3. MASS SPECTROMETRY FOR MOLECULAR WEIGHT DETERMINATION

The α B-crystallin mutants used for molecular weight determination was provided either refolded (wild type, K174X and A171X) or unfolded in 10mM Tris, 1mM EDTA, 6M urea, pH 8.0. Unfolded mutants were provided in this form due to their instability in aqueous buffer. The protein was loaded onto a MassPREP desalting cartridge (Waters, Elstree, Herts, UK) to remove buffer contaminants. The protein was eluted with 70% (v/v) acetonitrile, 0.5% (v/v) formic acid at 0.2 ml/min and introduced into a Waters Q-TOF Premier mass spectrometer operating in positive electrospray mode, with a cone voltage of 40V. Spectra were externally calibrated using sodium formate then corrected for drift using a leucine enkephalin lockspray. Multiply-charged protein ions were deconvoluted using the manufacturer-supplied, MaxEnt1 software, to determine protein mass.

2.8.4. CIRCULAR DICHROISM SPECTROSCOPY

Wild type α B-crystallin was dialysed into 10mM Tris, 1mM EGTA, 5mM EDTA, 150mM NaCl, pH 7.5 (CD buffer) for 16 h at 4°C using 12-14 kDa dialysis tubing (Medicell International Ltd, London, UK). Mutant α B-crystallins were thawed from storage at - 80°C and kept on ice prior to analysis. The Wild type and mutant α B-crystallins were centrifuged at 18000 x g for 1 min in a Bench Top centrifuge (5417R; Eppendorf, Hamburg, Germany) at room temperature. The protein concentrations of the wild type and mutant α B-crystallin were determined using BCA protein assay kit (Pierce, UK) and the samples diluted accordingly using circular dichroism (CD) Buffer to 0.2 – 0.3 mg/ml immediately prior to accumulation of spectra. Far ultra violet (UV) and near UV

circular dichroism spectra of wild type and mutant α B-crystallin were recorded in a cuvette with 0.1cm path length at room temperature using a Jasco J-810 spectropolarimeter. The optimised assay parameters are detailed in Table 2.13.

Table 2.14. Far and near UVCD spectra assay parameters

Parameter	Setting
Data pitch	0.5 nm
Response	4 sec
Band width	2
Sensitivity	100 mdeg
Speed	100 nm/min
Accumulations	4
Scanning mode	Continuous
Wavelength	350 -195 nm

The UVCD spectra were baseline corrected using spectra for CD buffer. The CD spectra were normalised and expressed as molar ellipticity using the following equation:

$$\text{Molar Ellipticity } (\Theta) = \frac{0.1 \times \theta_{\text{obs}}}{c \times l}$$

Where c = concentration (M), l = path length (cm) and θ_{obs} = CD mdeg

The near UVCD is represented by data collected between wavelengths 195 – 250 nm and far UVCD by data collected between wavelengths 250 – 350 nm.

2.8.5. THERMAL STABILITY ASSAY

Wild type α B-crystallin was dialysed into 10mM Tris, 1mM EGTA, 5mM EDTA, 150mM NaCl, pH 7.5 (assay buffer) for 16 h at 4°C using 12-14 kDa dialysis tubing (Medicell International Ltd, London, UK). Mutant α B-crystallins were thawed from storage at -80°C and kept on ice prior to analysis. The Wild type and mutant α B-crystallins were centrifuged at 18000 (g) for 1 min in a Bench Top centrifuge (5417R; Eppendorf, Hamburg, Germany) at room temperature. The protein concentrations of the wild type and mutant α B-crystallin were determined using BCA protein assay kit (Pierce, UK) and the samples diluted accordingly using assay Buffer to 0.1 mg/ml immediately prior to the assay. A 200 μ l volume of each sample was dispensed into a Beckman Tm cuvette for kinetic assays and the thermal stability monitored by observing changes in absorption at 360nm over a temperature gradient of 25-86°C at 1°C/min ramp rate using the Beckman DU640 spectrophotometer. Data were corrected for the assay buffer.

2.8.6. *IN VITRO* DESMIN FILAMENT ASSEMBLY AND CO-SEDIMENTATION ASSAY

In vitro assembly and cosedimentation assay were carried out using the technique developed by Dr Ming Der Perng (Durham, UK) (Perng et al., 1999; Perng et al., 2004).

2.8.6.1. Preparation of samples

Purified recombinant wild type desmin (a kind gift from Dr Ming Der Perng (Durham, UK) in 20mM Tris-HCl, pH 8.0, 1mMEDTA, 1mM EGTA, 1mM DTT, 0.2mM PMSF (Buffer A) was dialysed by step wise lowering of the urea concentration firstly to 10mM Tris-HCl, 3M urea, pH 8.0 (Buffer B) over 4 h at 4°C. Finally the desmin is dialysed into 10mM Tris-HCl, pH 8.0 (Buffer C) over 16 h at 4°C in parallel with wild type and mutant α B-crystallins in separate vessels using 12-14 kDa MWCO dialysis tubing (Medicell International Ltd, London, UK). Post dialysis, the desmin and Wild type and mutant α B-crystallins were centrifuged at 18000 (g) for 1 min in a Bench Top centrifuge (5417R; Eppendorf, Hamburg, Germany) at room temperature. The protein

concentrations were determined using BCA protein assay kit (Pierce, UK) and the samples diluted accordingly using Buffer C.

2.8.6.2. Desmin Filament assembly

Wild type or mutant α B-crystallin was mixed with desmin at pH 8.0 in Buffer C at a 1:1 mass ratio at 0.2 mg/ml into thick walled 2 ml centrifuge tubes for the TLS-55 rotor of the Beckman Optima MAX Ultracentrifuge, (Beckman Instruments Inc., Fullerton, CA, USA). Due to the limitations of the low refold yield, assays involving Q151X α B-crystallin were performed at concentrations of 0.1mg/ml. The assembly of desmin filament was initiated by the addition of a 20X concentrated assembly buffer at pH 6.8 to give a final concentration of 100mM Imidazole-HCl. A typical sample consisted of 95 μ l (desmin: α B-crystallin) plus 5 μ l assembly buffer. The appropriate control of 95 μ l of α B-crystallin plus 5 μ l assembly buffer was also prepared. The samples were mixed by gentle tapping avoiding liquid being displaced onto the wall of the centrifuge tube. The tubes were sealed with parafilm to avoid evaporation during the 1 h incubation at the required temperature of 20, 37 or 44°C.

2.8.6.3. Sedimentation Assays

After filament assembly an equal volume (100 μ l) of 0.85 M sucrose in assembly buffer was layered onto the protein samples. On addition of the sucrose cushion, care was taken to ensure the pipette tip was not immersed into the sample mixture to avoid contact with desmin filaments. Each sample was centrifuged at 80000 (g) for 30 min at 20°C in a Beckman Optima MAX Ultracentrifuge, TLS-55 rotor, (Beckman Instruments Inc., Fullerton, CA, USA) to pellet assembled desmin filament and associated α B-crystallin. To investigate the effect of α B-crystallin mutations upon aggregate formation in vitro, duplicate samples were prepared and subjected to a low-speed centrifugation at 2500 x g for 15 min in a Bench Top centrifuge (5417R; Eppendorf, Hamburg, Germany). The pellet and supernatant fraction volumes were solubilised in equal volumes of SDS-PAGE sample buffer (see Section 2.10). Pellet fractions were thoroughly resuspended in 250 μ l 1x SDS-PAGE sample buffer and supernatant fractions diluted with 50 μ l 5x SDS-PAGE

sample buffer. Great care was taken to ensure all material was solubilised in the SDS-PAGE sample buffer in order to achieve an accurate account of the distribution of protein between the pellet and the supernatant fraction. The samples were separated on 12% (w/v) SDS-PAGE and protein bands visualized by Coomassie Blue staining (see Section 2.10). The amount of protein in the supernatant and pellet fractions were analyzed by a luminescent image analyser (LAS-1000plus; Fuji Film, Tokyo, Japan) and quantified using the Image Gauge software (version 4.0; Fuji Film).

2.8.7. CROSS-LINKING OF α B-CRYSTALLIN

The optimised cross-linking of α B-crystallin was performed using glutaraldehyde at a final concentration of 0.01%. For best results, a 0.1% glutaraldehyde solution was added to the α B-crystallin solution to give a final concentration of 0.01% glutaraldehyde and a sample volume of 135 μ l. The mixture was incubated at room temperature for 1 h after which, 15 μ l stop solution (0.5M glycine) was added. The samples were concentrated by methanol chloroform precipitation (see Section 2.9.1.1), resuspended in 25 μ l SDS-PAGE sample buffer and analysed by SDS-PAGE (see Section 2.10).

2.8.8. DYNAMIC LIGHT SCATTERING

Dynamic light scattering (DLS) experiments were performed at 20°C using a Zetosizer Nano ZS (Malvern Instruments, Worcs. UK). The α B-crystallin samples (0.2 mg/ml) were 0.2 μ M filtered using a 32mm Acrodisc® PES syringe filter (Pall, Portsmouth, UK) and sealed with parafilm, into a 1ml disposable cuvette, (Fisher scientific, UK) blown out with nitrogen. Data collection utilised three data sets, each containing 5 accumulations, averaged using the Zetosizer Nano ZS software.

2.8.9. BIS-ANS FLUORESCENCE MEASUREMENTS

α B-crystallin variant proteins were incubated in 10mM Tris, 150mM NaCl, 5mM EDTA, 1mM EGTA, pH 7.5 at a protein concentration of 1 μ M and in the presence of a 10-fold molar excess of bis-ANS (4,4'-dianilino-1,1'-binaphthyl-5,5'-disulfonic acid, purchased from Invitrogen, Paisley, UK). Samples were allowed to equilibrate for 1 hour at room temperature prior to the acquisition of fluorescence spectra on a Varian Cary Eclipse fluorescence spectrophotometer. The excitation wavelength was 410 nm and emission was collected between 420 – 700 nm with excitation and emission slit-widths of 5 nm and a scan speed of 600 nm/min. All spectra are the average of 10 individual scans.

2.9. CELL CULTURES AND TRANSIENT TRANSFECTION ASSAYS

MCF7 cells, which contain no endogenous α B-crystallin thus avoiding the need to tag the protein for subsequent detection, were obtained from the European animal Cell Culture Collection (EACC, Portan Down, UK) and grown in Dulbeccos's minimum eagle's medium (DMEM) (Sigma-Aldrich, Poole, UK)), supplemented with 10% (v/v) fetal calf serum (FCS) (Sigma-Aldrich, Poole, UK) 2 mM L-glutamine, and antibiotics (100 U of penicillin and 0.1 mg of streptomycin). All cells were maintained at 37°C in a humidified incubator of 95% (v/v) air and 5% (v/v) CO₂. For transfection experiments, plasmid DNA containing wild type and mutant α B-crystallin in pcDNA3.1 (Invitrogen) (see 2.2.5) was prepared using MidiPrep kits (QIAGEN, Dorking, Surrey, United Kingdom). Cells were grown in 75 cm² flasks and seeded on 13-mm coverslips and 10cm petri dishes. The cells at a density of 50–60% confluence were transiently transfected with wild type or mutant α B-crystallin by GeneJuice transfection reagent (Novagen) according to manufacturer's protocol. Cells were incubated for 24 h before processing for cell fractionation (see Section 2.9.1), immunofluorescence microscopy (see Section 2.9.2), and immunoblotting (see Section 2.11)

2.9.1. PROTEIN EXTRACTION AND CELL FRACTIONATION

Cells grown on 10cm dishes were washed twice with phosphate buffered saline (PBS) (Sigma-Aldrich, Poole, UK) before being trypsinised for 5 min in 1 ml trypsin-ethylene diamine tetra acetate (EDTA) (Sigma-Aldrich, Poole, UK) and resuspended in 10ml DMEM for cell counting. Cultures were divided into aliquots containing 1×10^6 cells prior to protein extraction. The cells were washed twice with PBS before being lysed with 0.5ml of extraction buffer (PBS, 0.5% (v/v) Triton-X (Sigma-Aldrich, Poole, UK)) by ten times passage through a 25-gauge needle. Following incubation on ice for 15 min, the lysates were clarified by centrifugation $18000 \times g$ for 10 min at 4°C in a precooled Bench Top centrifuge (5417R; Eppendorf, Hamburg, Germany). The resulting supernatant and pellet fractions were further processed using separate techniques. This allowed the fraction volumes to be equalised before SDS-PAGE (see Section 2.11) and immunoblotting analysis (see Section 2.11).

2.9.1.1. Supernatant treatment

The supernatant fraction was concentrated by chloroform methanol precipitation (Wessel and Flugge, 1984), which involved the addition of 4 parts methanol: 1 part chloroform: 3 parts purified water, and sedimented by bench top centrifugation at room temperature for 2 min at 12500 rpm. The top layer of liquid was removed and a further 3 parts methanol added. The mixture was well mixed and centrifugation repeated. The pelleted soluble protein fraction was resuspended with 1x SDS-PAGE sample buffer in 50mM Tris-HCl, pH 6.8, 1% (w/v) SDS, 1mM EDTA to a 100 μl volume.

2.9.1.2. Pellet treatment

The pellet fraction was washed twice by resuspension in 1 ml PBS followed by centrifugation at room temperature for 1 min at 12500 rpm and disposal of the supernatant. The pellet was resuspended in a 200 μ l volume of 20mM Tris-HCl, pH 8.0, 10mM MgCl₂ containing 50U Benzonase® nuclease, and incubated at room temperature whilst mixing gently for 30 min. The pellet was recovered by centrifugation at 4°C for 5 min at 12500 rpm and resuspended in 100 μ l 1x SDS-PAGE sample buffer.

2.9.1.3. Primary and secondary antibodies

Primary antibodies included purified mouse monoclonal anti- α B-crystallin 2D2B6, (Inoue, 1994; Sawada et al., 1993) (see Section 2.12.1), polyclonal anti- α B-crystallin antibody (Sandilands, 1995; van den IJssel et al., 2003) (see Section 2.12.2) and monoclonal anti-HSP27 antibody, ER-D5, (King et al., 1987) diluted 1:1000. Secondary antibodies were horseradish Peroxidase (HRP) conjugated Goat anti-mouse Immunoglobulins (DakoCytomation) diluted 1:1000.

2.9.2. IMMUNOFLUORESCENCE MICROSCOPY

For immunofluorescence studies, cells grown on 13mm coverslips were washed twice with PBS and fixed with ice-cold methanol/acetone [1:1 (v/v)] for 20 min at room temperature, and washed three times with PBS containing 0.02% (w/v) BSA. Cells were then preblocked with 10% (v/v) goat serum in PBS/BSA for 30 min, washed three times in PBS/BSA, and then incubated with primary antibodies at room temperature for 1 h. The primary antibodies used in this study were, rabbit polyclonal anti- α B-crystallin (1:200; Chemicon Ab1546) (Sandilands, 1995; van den IJssel et al., 2003) and monoclonal mouse anti-keratin LE41, (1:1; CRUK). After washing three times with PBS/BSA, the primary antibodies were detected using Alexa 488 or Alexa 594 (1:500; Molecular Probes) HRP conjugated secondary antibodies. All antibodies were diluted in PBS/BSA buffer. Nuclear detection was achieved using 4'-6-diamidino-2-phenylindole DAPI (1:2000; Sigma). The glass coverslips were mounted on slides with the fluorescent protecting

agent Citifluor, (Citifluor Labs, London, United Kingdom) and observed with an Axioplan fluorescence microscope (Carl Zeiss, Jena, Germany) by using a 63X Plan-Apochromat 1.4 numerical aperture objective. Images were obtained through a cooled charge-coupled device camera (Digital Pixel, Brighton, United Kingdom) running IP Lab software. Alternatively, images were collected using a 63X oil immersion lens of the confocal Axiovert 200M microscope and LSM 510 META software (both Zeiss, Germany). Optical sections were set to $\sim 1.0 \mu\text{m}$. Images were processed and prepared for figures using Adobe Photoshop 8.0 (Adobe Systems). Quantitation of the αB -crystallin phenotypes was by visual assessment of the cells.

2.10. ONE-DIMENSIONAL SDS-PAGE ANALYSIS

One-dimensional SDS-PAGE analysis was performed essentially according to Laemmli (Laemmli, 1970), under reducing conditions. Slab gels of 12% (w/v) were used as a resolving gel and the concentrating gel was 3% (w/v). A pre-mixed acrylamide solution containing bis-acrylamide (33% (Biorad Laboratories, UK)) was used as a stock solution for One-dimensional SDS-PAGE analysis. A layer of water-saturated butanol was applied to ensure the concentrating gel interface was flat. The gels were calibrated using a PageRuler™ Prestained protein ladders (Fermentas, UK) containing a mixture of proteins with molecular weights of 11, 17, 24, 33, 40, 55, 72, 100, 130 and 170 kDa.

Samples for analysis were diluted in Laemmli's sample buffer, (50mM Tris-HCl pH 6.8, 100mM DTT, 2% (w/v) SDS, 0.1% (w/v) Bromophenol Blue, 10% (v/v) glycerol) (Laemmli, 1970) to the target concentration required for specific gel loading. Samples not containing urea were boiled for 5 min and allowed to cool before centrifugation for 3 sec at 12500 rpm in a microcentrifuge to concentrate the sample at the bottom of the tube. Gels were run at 200V constant voltage in running buffer (25mM Tris HCl, 200mM glycine, 0.1% SDS) (Kyhse-Andersen, 1984)

After electrophoresis, gels were fixed in 50% (v/v) methanol and 10% acetic acid then stained with 0.5% (w/v) Coomassie® brilliant blue R-250 (Merck-BDH, UK), solubilised in 50% (v/v) methanol and 10% (v/v) acetic acid for 15 min, and destained with several changes of 10% (v/v) methanol and 5% acetic acid. The gels were kept in 7% acetic acid.

2.11. IMMUNOBLOTTING

Immunoblotting was performed using the semidry blotting method (Kyhse-Andersen, 1984) according to the manufacturer's specifications (Bio-Rad Laboratories, UK). Following one-dimensional SDS-PAGE, proteins were transferred onto NitroBind 0.45 μ M nitrocellulose membrane, (VWR, UK). After blotting, protein transfer was assessed by Ponceau S (Sigma Aldrich, UK) staining of the nitrocellulose membrane followed by destaining in Tris-buffered saline (TBS) (20 mM Tris-HCl, pH 7.4, 150 mM NaCl). After incubation with blocking solution consisting of 5% (w/v) dried milk powder (Marvel, Tesco Ltd., UK) in TBS containing 0.2% (v/v) Tween 20 (TBST) for 1 h at room temperature with agitation, (or overnight, static at 4°C) the membranes were probed with a panel of primary antibodies in antibody buffer (1 part block solution: 2 parts TBS) for 2 h at room temperature with agitation. The nitrocellulose membrane was washed 3 times with TBST and once with TBS over a 30 min period then incubated with the appropriate horseradish peroxidase-conjugated secondary antibodies (DakoCytomation) diluted 1:1000 in antibody buffer for 1 h at room temperature with agitation. Antibody labelling was detected by enhanced chemilluminescence (Walker et al., 1995) using a luminescent image analyser (LAS-1000plus; Fuji Photo Film (UK), London, United Kingdom).

2.12. ANTIBODY PURIFICATION

2.12.1. MONOCLONAL α B-CRYSTALLIN ANTIBODY FROM CELL CULTURE SUPERNATANT

Hybridoma cells expressing α B-crystallin mouse monoclonal antibody (MAb) 2D2B6 clone generated to chicken α B-crystallin (Inoue, 1994) were cultured in DMEM with 10% FCS and 1% GPS until 50% cell death. The cell supernatant was centrifuged at 4°C for 10min at 3000r.p.m using a Sorvall RT 6000D centrifuge with H1000B rotor, followed by a 0.45 μ M filtration using a 32mm Acrodisc® PES syringe filter (Pall, Portsmouth, UK) The supernatant was left to achieve ambient temperature.

Purification of the α B-crystallin MAb was performed with a 5ml PROSEP® G (Millipore, Watford, UK) Affinity chromatography column (10 x 100mm Omnifit) on a Pharmacia fast performance liquid chromatography (FPLC) system comprising a Pharmacia high precision pump (P-500), a Pharmacia Fraction collector (Frac-100), UV-1 UV detector and a Labdata chart recorder (Amersham Biosciences, NJ, USA). All FPLC buffers were vacuum filtered to 0.2 μ M using PROPOR PES (proportional polyethersulphone) membrane discs (Domnick Hunter, UK). The column was equilibrated in 10 CV PBS to remove the storage buffer PBS 0.05% sodium azide (w/v). The α B-crystallin MAb was loaded via the sample load pump at 3ml/min and chased through with PBS. The column flow through was retained in order to reapply any unbound α B-crystallin MAb onto the PROSEP® G column.

The α B-crystallin MAb was eluted using the following gradient:

- 5 CV 100mM Citrate pH 7.0 at 5ml/min
- 10 CV 0-100% 100mM Citrate pH 3.0 at 3ml/min
- 10 CV 100mM Citrate pH 3.0
- 3 CV 100mM Citrate pH 7.0

Fractions were collected in 3ml volumes, neutralised by adding 0.8ml 0.5M di-sodium hydrogen phosphate (Na_2HPO_4), and pooled corresponding to the major peak

(eluted after approx 84% 100mM Citrate pH 3.0). The column was regenerated using 10CV PBS, 5-10 CV 30mM HCl and 5-10 CV PBS via the load pump at 3 ml/min. The purification was repeated using the unbound flow through as load material and fractions pooled as stated previously. The column was stored following sanitisation as detailed below and stored at 4°C.

- In upflow via the load pump at 3 ml/min
- 5 CV PBS
- 8 CV 6M Guanidine HCl
- 20 CV PBS 0.05% (w/v) sodium azide

An appropriate dilution of α B-crystallin MAb in PBS was performed and the absorbance read at 280nm. The extinction coefficient of 1.4mg/ml/cm was used to determine the amount of purified α B-crystallin MAb recovered from the purification. The α B-crystallin MAb pool was concentrated to 1 mg/ml using a 100kDa MWCO Vivaspinn centrifugal concentrator (Vivascience, Epsom, UK), rinsed in PBS prior to application of α B-crystallin MAb using a Sorvall RT 6000D centrifuge with H1000B rotor, and dialysed against 50 diavolumes of PBS for at least 6 hours or overnight at 4°C. The dialysis was repeated with fresh PBS.

The α B-crystallin MAb final yield was calculated using the extinction coefficient following a 0.2 μ M filtration using a 32mm Acrodisc® PES syringe filter (Pall, Portsmouth, UK) into a pre-weighed bottle and diluted to 1mg/ml in PBS prior to storage at -20°C in 1ml aliquots.

2.12.2. POLYCLONAL α B-CRYSTALLIN ANTIBODY FROM RABBIT SERUM

The α B-crystallin polyclonal antibody (PAb) was a rabbit polyclonal antibody 3148 generated to the decapeptide KPAVTAAPKK and coupled to keyhole limpet haemocyanin, by glutaraldehyde prior to immunisation (Sandilands, 1995; van den IJssel et al., 2003).

The ammonium sulphate technique for rabbit serum immunoglobulins (IgG) followed by rabbit antiserum purification was performed to isolate the α B-crystallin PAb. The α B-crystallin PAb serum was diluted 1:1 in PBS (10mM potassium phosphate 0.9% NaCl (w/v) pH 7.0 - 7.6) by gradual addition of PBS. The solution was mixed gently to avoid foaming and centrifuged if precipitate was present using Sorvall® RT 6000D centrifuge with H1000B rotor. For each 1ml of diluted serum, 0.67ml of saturated ammonium sulphate (70g of ammonium sulphate to 1ml of 1M NaOH in 75ml of deionised water) was added in four portions, vortexing gently after each addition. The mixture was incubated at 4°C for 30min and centrifuged at 4°C for 30min at 3000r.p.m using a Sorvall® RT 6000D centrifuge with H1000B rotor, (Sorvall®, USA). The supernatant was carefully decanted to waste.

The pellet was washed by resuspension with 40% saturated ammonium sulphate (1ml PBS to 0.67ml of saturated ammonium sulphate) to the same total volume achieved by addition of saturated ammonium sulphate. The centrifugation was repeated and the pellet was resuspended in two portions of deionised water to the original α B-crystallin PAb serum.

The ammonium sulphate was removed from the α B-crystallin PAb resuspension using a PD-10 Desalting column (Sephadex G-25 Medium, GE Healthcare, UK). An 8.3ml PD-10 desalting column was equilibrated with 5-10CV of PBS and α B-crystallin PAb was absorbed into the media following application to the top of the column. PBS was flowed by gravity through the column for 2.3ml (void volume) and the following 2ml containing the α B-crystallin PAb was collected in a separate tube. The α B-crystallin PAb yield was determined by extinction coefficient (see Section 2.12.1) and the α B-crystallin PAb was diluted to 1mg/ml in PBS for storage at -20°C in 1ml aliquots.

2.13. ANTIBODY CONJUGATION

2.13.1. HRP CONJUGATION

2.13.1.1. Benzoquinone–HRP antibody coupling

Benzoquinone–HRP (BQ-HRP) has a low level of activation, which avoids antibody cross-linking, as the BQ-HRP does not have multiple conjugation sites. A large excess of HRP was required to force the coupling process. For a MAb BQ-HRP conjugation 1mg MAb was added to 10mg BQ-HRP. This reaction ratio of 1:10 was suggested as a starting point for new MAb coupling as it gives a moderate level of HRP incorporation. Higher incorporation levels can usually be achieved by process optimisation. For a polyclonal BQ-HRP conjugation 0.5mg PAb was added to 10mg BQ-HRP. A 1:20 reaction ratio will usually provide high activity conjugate (approx 1:1 Ab:HRP), however high reaction ratios may inactivate the antibody.

The purified antibody solution (see Section 2.12) was added to the freeze dried BQ-HRP (IDS Ltd, Boldon, UK) allowed to reconstitute for 2-3 min prior to gentle vortexing. The antibody: BQ-HRP (Ab: BQ-HRP) coupling mixture was diluted with 100mM Sodium Bicarbonate (Coupling Buffer) to 0.5 mg/ml and incubated for 16-20 h at 2-8°C. The coupled antibody was precipitated by 1:1 addition of saturated ammonium sulphate (see Section 2.12.2) slowly in four portions, which was gently vortexed after each addition. The mixture was incubated at 4°C for 60 min and centrifuged at 4°C for 30 min at 3000r.p.m. The supernatant was carefully decanted to waste and the pellet was drained for 10-20 sec before addition of a minimum number of 100 µl portions of PBS.

2.13.1.2. Gel Filtration Chromatography to remove excess HRP

Purification of the Ab: BQ-HRP was performed using a 35ml Sephacryl S-100HR (Sigma-Aldrich, Poole, UK) Gel Filtration Chromatography (GFC) column (10 x 450mm Omnifit) on a Pharmacia FPLC system (Amersham Biosciences, NJ, USA). All FPLC buffers were vacuum filtered to 0.2 μ M using PROPOR PES membrane discs (Domnick Hunter, UK). The column was equilibrated in 10CV PBS to remove the storage buffer PBS 0.05% sodium azide (w/v) and the Ab: BQ-HRP was loaded directly onto the column bed and eluted in PBS at 0.5ml/min. The column was sanitised by equilibration with PBS 0.05% (w/v) sodium azide. Fractions were collected in 1ml volumes and fractions containing Ab: HRP were identified using an anti-(rabbit/mouse IgG) coated plate, (IDS Ltd, Boldon, UK). From each fraction, 10 μ l was diluted with 2ml of (10mM potassium phosphate, 0.9% NaCl, 0.05% Tween 20 (w/v), 0.5% BSA (w/v), 0.1% Proclin (v/v), 1% HRP stabilisers, (IDS Ltd, Boldon, UK) pH 7.0 - 7.6, (HRP basic buffer) and mixed thoroughly. A 20 μ l volume of each diluted fraction was combined with 100 μ l of basic HRP buffer in the well. The plate was covered and incubated for 30 min at ambient temperature, followed by a 3x wash with 10mM phosphate, 1.8% NaCl (w/v), 0.05% Tween 20 (w/v), 0.025% Proclin (v/v), pH 7.0 - 7.6, (AC wash) using a Thermo Wellwash® 4 MK2 plate washer (Thermo Electron Corporation, Vantaa, Finland). 3,3',5,5'-Tetramethylbenzidine (TMB) substrate reagent (BioFX Laboratories Inc., MD, USA) was added (100 μ l/well) and the plate incubated for 5–10 min before adding 0.5M HCl (Stop solution). The plate was read at 450nm using an Anthos Lucy microplate luminometer (Anthos Labtec Instruments, Salzburg, Austria) and fractions pooled with the highest absorbance readings. Fractions were excluded that had high 280nm absorbance (from GFC) but lower Ab-HRP activity as these fractions would contain the resolved excess HRP.

The Ab: HRP solution was 0.2 μ M filtered using Acrodisc 32mm syringe filters (Pall, Portsmouth, UK) into a pre-weighed container and the Ab: HRP concentration was determined (see Section 2.12.1). The Ab: HRP solution was diluted to 25 μ g/ml in Basic HRP buffer and the 0.2 μ M filtration was repeated prior to storage at -20°C in 1.5ml aliquots.

2.13.2. ANTIBODY-BIOTIN CONJUGATION

A 0.5mg aliquot of purified antibody solution (1 mg/ml) (see Section 2.12) was diluted to 0.5 mg/ml in 100mM sodium bicarbonate (pH 8.0-8.4) with care taken to ensure that the antibody solution was equilibrated to 20°C–23°C before the coupling reaction was initiated. Per 1 ml of the purified antibody solution, 50 µl succinimidyl-(biotinamido) hexanoate-biotin (Biotin LC NHS) was added during continuous mixing and the coupling mixture was incubated at 20°C – 23°C for 15 min. The biotin LC NHS solution (Sigma-Aldrich, Poole, UK) was prepared by reconstitution in dry Dimethyl Formamide (DMF) (Sigma-Aldrich, Poole, UK) to achieve 9.1mg/ml and used within 10 min. The coupling reaction was stopped on addition of 50µl/ml of 1M Ethanolamine pH 8.0 and the excess biotin was removed using a PD-10 Desalting column (see Section 2.12.2). The Ab: Biotin concentration was determined (see Section 2.12.1) and diluted to 25 µg/ml in 10mM potassium phosphate, 0.9% NaCl, 0.05% Tween 20 (w/v), 0.5% BSA (w/v), 0.09% sodium azide (w/v), pH 7.0 - 7.6 (Ab: Biotin Buffer). The Ab: Biotin solution 0.2µM filtered using a 32mm Acrodisc® PES syringe filter (Pall, Portsmouth, UK) prior to storage at -20°C in 1.5ml aliquots.

2.14. P LATE COATING WITH MAB AND PAB ANTIBODIES

The 96 well F8 Maxisorp plates (Nunc, Denmark) were coated at a 2 mg/L concentration of antibody. The purified antibody solution (1mg/ml) (see Section 2.12) was diluted 500x in PBS and a 1:4000 volume of Yoko yellow dye (IDS Ltd, Boldon, UK) was added. The coating solution was mixed for 15 min at ambient temperature then dispensed into the 96 well plates (200µl/well) for overnight incubation at room temperature. Post incubation the plates were washed 3x with AC wash (see Section 2.13.1.2), followed by the addition of 300µl of glaze solution/well (IDS Ltd, Boldon, UK). The plates were incubated for 30min at room temperature then aspirated to remove the glaze buffer, before overnight drying at 35°C. Plates are sealed in foil bags with silica gel and stored at 4°C.

2.15. ENZYME LINKED IMMUNOSORBANT ASSAY FOR DETECTION AND QUANTITATION OF α B-CRYSTALLIN

2.15.1. CALIBRATORS AND SAMPLE PREPARATION USING AB: HRP CONJUGATE

The Ab: HRP conjugate was used for detection of significant levels (> 0.1 mg/ml or 100000 ng/ml) of α B-crystallin by enzyme linked immunosorbant assay (ELISA). For greater sensitivity the Ab: Biotin conjugate was more appropriate. A five point calibration curve ranging from 100ng/ml to 1.27ng/ml was prepared by serial dilution of calibrator stock solution (CSS). The CSS consisted of purified wild type α B-crystallin (see Section 2.6) diluted to a concentration of 1 μ g/ml in 10mM potassium phosphate, 0.9% NaCl, 0.05% Tween 20 (w/v), 0.5% BSA (w/v), 0.1% Proclin (v/v), pH 7.0 - 7.6, filtered to 0.2 μ M and stored at 4°C (Assay Buffer). A typical dilution series used for calibrator preparation is shown below:

- Calibrator 5 - 0.2 ml CSS to 1.8 ml Assay Buffer (100 ng/ml)
- Calibrator 4 - 0.5 ml Calibrator 5 to 1 ml of Assay Buffer (33.3 ng/ml)
- Calibrator 3 - 0.5 ml Calibrator 4 to 1 ml of Assay Buffer (11.1 ng/ml)
- Calibrator 2 - 0.5 ml Calibrator 3 to 1 ml of Assay Buffer (3.7 ng/ml)
- Calibrator 1 - 0.5 ml Calibrator 2 to 1 ml of Assay Buffer (1.27 ng/ml)

Samples were diluted in Assay Buffer to fit the standard curve. The Ab: HRP conjugate (see Section 2.13.1.2) was diluted 100x to a concentration of 250 ng/ml in Basic HRP buffer (see Section 2.13.1.2) by adding 0.5 ml Ab: HRP conjugate (25 μ g/ml) to 49.5 ml Basic HRP buffer.

2.15.2. CALIBRATORS AND SAMPLE PREPARATION USING AB: BIOTIN CONJUGATE

The Ab: Biotin conjugate was used for detection (< 0.1 mg/ml or 1×10^8 pg/ml) of α B-crystallin by ELISA as it delivered greater sensitivity than the Ab: HRP conjugate.

A five-point calibration curve ranging from 5000 pg/ml to 128 pg/ml was prepared by serial dilution of CSS (see Section 2.15.1). A typical dilution series used for calibrator preparation is shown below:

Prepare a dilution series of wild type α B-crystallin to achieve a 5 point calibration curve ranging from 5000pg/ml to 128pg/ml as follows:

- Calibrator 5 - 0.025 ml CSS to 4.975 ml Assay Buffer (5000 pg/ml)
- Calibrator 4 - 0.8 ml Calibrator 5 to 1.2 ml of Assay Buffer (2000 pg/ml)
- Calibrator 3 - 0.4 ml Calibrator 4 to 0.6 ml of Assay Buffer (800 pg/ml)
- Calibrator 2 - 0.4 ml Calibrator 3 to 0.6 ml of Assay Buffer (320 pg/ml)
- Calibrator 1 - 0.4 ml Calibrator 2 to 0.6 ml of Assay Buffer (128 pg/ml)

Samples were diluted in Assay Buffer to fit the standard curve. The Ab: Biotin conjugate (see Section 2.13.2) was diluted 100x to a concentration of 250 ng/ml in Ab: Biotin buffer (see Section 2.13.2) by adding 0.5 ml Ab: Biotin conjugate (25 μ g/ml) to 49.5 ml Ab: Biotin buffer.

Assays utilising the Ab: Biotin conjugate, require an additional step, to allow binding of Avidin-HRP to Biotin prior to addition of substrate. The Avidin-HRP buffer consisted of equal amounts of labelled Avidin HRP (25 μ g/ml) (IDS Ltd, Boldon, UK) to unlabelled Avidin (25 μ g/ml) (IDS Ltd, Boldon, UK).

2.15.3. SIMULTANEOUS ELISA FOR α B-CRYSTALLIN DETECTION AND QUANTITATION

A simultaneous assay operates at moderate sensitivity. Figure 2.1. shows a typical plate map.

Figure. 2.1 Simultaneous α B-crystallin ELISA plate map

	1	2	3	4	5	6	7	8	9	10	11	12
A	Blank	Blank	2	2	6	6	10	10	14	14	18	18
B	Cal 1	Cal 1	2	2	6	6	10	10	14	14	18	18
C	Cal 2	Cal 2	3	3	7	7	11	11	15	15	19	19
D	Cal 3	Cal 3	3	3	7	7	11	11	15	15	19	19
E	Cal 4	Cal 4	4	4	8	8	12	12	16	16	20	20
F	Cal 5	Cal 5	4	4	8	8	12	12	16	16	20	20
G	1	1	5	5	9	9	13	13	17	17	21	21
H	1	1	5	5	9	9	13	13	17	17	21	21

High

Low

1 = sample 1

Each calibrator (Cal) was assayed in duplicate. A dilution resulting in a high and low concentration (conc.) (see Figure 2.1) of each sample (numbered cell) was prepared and assayed in duplicate to cover the range of the calibration curve, ensuring accurate quantitation. The calibrators and samples (100 μ l) were added to the appropriate wells (see Figure 2.1), to which 100 μ l of Ab: conjugate was added. The plates were covered and incubated for 2 h at room temperature followed by a 3x wash with AC wash buffer (see Section 2.13.1.2). At this point, separate protocols were followed depending on the Ab: conjugate in operation

For assays utilising Ab: HRP conjugates, TMB substrate solution (IDS Ltd, Boldon, UK) was added (200 μ l/well) to detect α B-crystallin and plates were incubated for 30 min at room temperature before 100 μ l 0.5M HCl (Stop solution) was added.

For assays utilising Ab: Biotin conjugates, 250 ng/ml Avidin/Avidin HRP (see Section 2.15.2) was added (200 μ l/well) and plates incubated for 30 min at room

temperature followed by a 3x wash with AC wash buffer. To detect the α B-crystallin, TMB substrate solution (IDS Ltd, Boldon, UK) was added (200 μ l/well) and plates were incubated for 30 min at room temperature before 100 μ l 0.5M HCl (Stop solution) was added.

The α B-crystallin signal produced by the TMB substrate was read at 450nm using an Anthos Lucy microplate luminometer (Anthos Labtec Instruments, Salzburg, Austria) and the amount of α B-crystallin quantified using a calibration curve of Mean absorbance versus log concentration.

2.15.4. SPLIT ELISA FOR α B-CRYSTALLIN DETECTION AND QUANTITATION

A split assay achieves greater sensitivity than the simultaneous assay, as twice the amount of analyte is present in the assay. The same sample and calibrator plate map was utilised for split assays (see Figure 2.1). The calibrators and samples (200 μ l) were added to the appropriate wells (see Figure 2.1). The plates were covered and incubated for 1.5 h at room temperature followed by a 3x wash with AC wash buffer (see Section 2.13.1.2). A 200 μ l volume of Ab: conjugate was added and the incubation and wash step was repeated. At this point, separate protocols detailed in Section 2.15.3 were followed depending on the Ab: conjugate in operation.

CHAPTER 3

THE FLEXIBLE C-TERMINAL ‘TAIL’ PLAYS AN IMPORTANT ROLE IN MAINTAINING THE SOLUBILITY OF THE α B-CRYSTALLIN OLIGOMER

3.1. AIMS

The flexible C-terminal ‘tail’ has been suggested to play an important role in solubilising the hydrophobic complexes formed between α -crystallin particles and denatured proteins (Smulders et al., 1996).

In this Chapter, I wanted to investigate the relationship between the C-terminal extension and the solubility of α B-crystallin, and its potential role in the mechanism that causes various disease states. This chapter, therefore aimed to clone, express and purify the sequentially truncated C-terminal α B-crystallin mutants (K174X and E165X) along with the three naturally occurring disease causing mutants (450delA, Q151X and 464delCT) and the post translational modification truncations (E164X and A171X). The nature of expression and purification will help further understand the role of specific regions of the C-terminal extension important in solubilisation of α B-crystallin oligomers, and will provide the basis for further characterisation aiming to understand the relationship between the C-terminal extension, the chaperone function, oligomerisation and the relationship with disease.

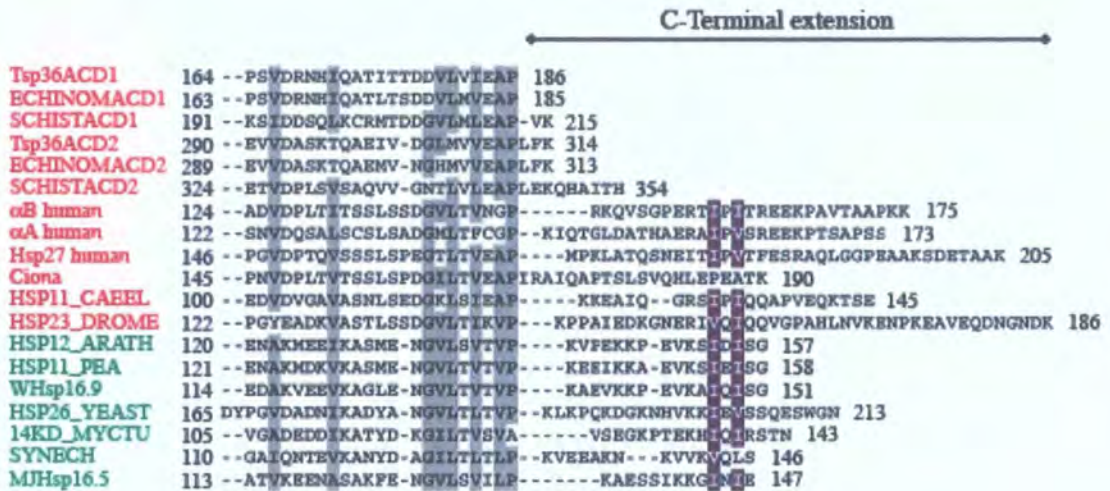
3.2. INTRODUCTION

The C-terminal extension is conserved amongst α A- and α B-crystallin and the family of sHSPs. Similar to the N-terminal domain, its sequence is of variable length and composition as shown by structural alignment (see Figure 3.1A) and according to nuclear magnetic resonance (NMR) analyses, the C-terminal 9 and 11 residues of α A- and α B-crystallin, respectively, appear to adopt the conformation of a flexible solvent-exposed random coil (Carver et al., 1992; Carver and Lindner, 1998)

The exposed nature of this random coil was in accord with the observation that the last 20 or so residues of the α -crystallin are especially liable to truncations and modifications (Jimenez-Asensio et al., 1999; Lin et al., 1997). For example, enzymatic truncation of the C terminal with calpain II or trypsin results in a decreased chaperone-like activity (Takemoto et al., 1992)

The solvent exposed random coil has been defined as a highly mobile 'tail' with regions of flexibility being pinpointed to the terminal 9 and 11 residues of Bovine α A and α B-crystallin as well as the terminal 16 residues of Human HSP27, the terminal 10 residues of Rat HSP20 and the terminal 18 residues of mouse HSP 25 (see Figure 3.1B) (Carver, 1999). The C-terminal flexibility is a common feature of mammalian sHSPs, and despite sharing little sequence similarity, they are characterised by being polar.

A



B

Bovine α A-crystallin REEKPSSAPSS 173
 Mole rat α A-crystallin QEEKPSSAPLF 173
 Bovine α B-crystallin REEKPAVTAAPKK 175
 Mouse Hsp25 FEARAQIGGPEAGKSEQSGAK 205
 Human Hsp27 FESRAQLGGPEAAKSDETAAK 205
 Rat Hsp20 -ASLSPPPAAK 162

Figure 3.1. Structural alignment of the C-terminal extensions α -crystallins and sHSPs. (A) Structural alignment of the C-terminal extensions of metazoan (red) and non-metazoan (green) sHSPs. Conserved and conservatively substituted residues are indicated in grey, except for the C-terminal motif (purple). The C-terminal extensions are indicated. Reprinted from (Stamler et al., 2005) Copyright (2005) with permission from Elsevier. (B) shows a sequence alignment including mammalian sHSPs and their regions of C-terminal flexibility (underlined). Reprinted from (Carver, 1999) Copyright (1999) with permission from Elsevier.

In α -crystallin, the primary role of the flexible C-terminal extension 'tail' is to offset the large degree of hydrophobicity exposed to the solution by the α -crystallin i.e the 'tail' acts as a solubilising agent for the relatively hydrophobic protein and any subsequent sHSP-client complexes, which form upon chaperone action (Lindner et al., 2000). Each sHSP subunit possesses this short, polar, highly flexible, hydrophilic and solvent-exposed C-terminal 'tail', whose composition is dominated by polar and charged amino acid

residues (Caspers et al., 1995). Interestingly, a mutant of α A-crystallin in which hydrophobicity was introduced into the C-terminal 'tail' had significantly reduced flexibility within this 'tail' and a corresponding reduction in solubility, heat stability and chaperone activity, compared with the wild type protein and supports the argument that the extensions may have a role in solubilising the hydrophobic complexes formed between α -crystallin particles and denatured proteins via electrostatic interactions (Smulders et al., 1996).

Lindner et al., (2000) suggested that the C-terminal 'tails' might serve as 'spacers' in preventing sHSP-client complexes from approaching one another (Lindner et al., 2000). Without their presence, hydrophobic interactions between the proteins would result in aggregation and precipitation, thus if the polarity and flexibility of the 'tails' are disrupted the stability and chaperone activity of the protein are reduced significantly (Lindner et al., 2000).

The role of the C-terminal as a 'solubiliser' has been well studied for α A-crystallin. As discussed earlier, the introduction of hydrophobic residues such as tryptophan in the C-terminal 'tail' of α A-crystallin affected structural and functional integrity, reducing chaperone activity, thermostability, and flexibility (Smulders et al., 1996).

Further evidence to suggest the role of the 'tail' as a solubiliser of the α -crystallin complex, was shown when its deletion from *Caenorhabditis elegans* HSP16.2 caused precipitation of the complex upon freeze-thawing (Leroux et al., 1997). Deletion of 17 residues from the C terminal of α A-crystallin (R157STOP), despite having spectroscopic properties similar to wild type protein, formed large insoluble aggregates with a marked reduction in chaperone-like activity (Andley et al., 1996). Similar results were observed for *Xenopus* HSP30C (Fernando, 2000). Complete removal of the flexible 'tail' was observed in a study, which investigated the influence of the $_{163}\text{REEK}_{166}$ region on α A-crystallin structure and function by the sequential removal of the $_{163}\text{REEK}_{166}$ residues. This resulted in a reduction in chaperone activity and oligomerisation without affecting the solubility. The study showed that the charged residues in the $_{163}\text{REEK}_{166}$ motif provide the electrostatic interactions in the C-terminal extension needed to form oligomeric complexes. In addition, the R163 residue was found to provide a positive

charge for intersubunit electrostatic interactions in the C-terminal extension (Rajan et al., 2006). Similar truncations in α A-crystallin have also shown no affect on the solubility, when recombinantly produced, but have been found in rat lenses (α A₁₋₁₅₁, α A₁₋₁₅₇, α A₁₋₁₆₂, α A₁₋₁₆₃ and α A₁₋₁₆₈) (Thampi and Abraham, 2003), in human lenses (α A₁₋₁₆₂ and α A₁₋₁₆₈) (Colvis et al., 2000) and diabetic human lenses (α A₁₋₁₇₂) (Thampi et al., 2002). Interestingly, the removal of the terminal serine resulted in aggregation of α A-crystallin (Aziz et al., 2007).

A study investigating the C-terminal ‘tail’ of α B-crystallin, looked at the proteolytic removal of the C-terminal Thr171 - Lys175 region. There was no significant affect on the solubility of the α B-crystallin complex (Carver et al., 1995) as there would be sufficient charge-charge interactions with the remainder of the C-terminal ‘tail’ to ensure efficient solubility and chaperone-like activity. Similarly, the removal (Liao et al., 2002) and substitution (Plater et al., 1996) of the terminal lysines of α B-crystallin resulted in a stable complex. It may be that the mutations resulted in a largely intact but less mobile C terminal. The absence of a strong hydrophilic positive charge at the end of the highly flexible C-terminal ‘tail’ may result in the C terminal folding back on itself, losing its flexibility, and sterically hindering protein binding (Plater et al., 1996). The formation of large insoluble aggregates observed with the α A-crystallin truncation (R157X) (Andley et al., 1996) would tend to suggest that a similar modification to the α B-crystallin C-terminal would also result in aggregation of the truncated α B-crystallin protein.

Interestingly, a recent study by Ghosh et.al, 2006 saw the removal of the polar C-terminal sequence (₁₅₅PERTIPITREE₁₆₅), which, resulted in poor solubility despite the retention of 10 of the 11 C-terminal ‘tail’ residues, plus limited or no chaperone activity. This study demonstrated the importance of C-terminal residues α B₁₅₅₋₁₆₅ in maintaining the solubility of unfolded substrates in a manner independent of the amount of substrate protein unfolding (Ghosh et al., 2006). It also suggested an additional influence on the solubilisation of α B-crystallin by the ₁₆₃REEK₁₆₆ motif and the highly conserved IX/(I/V) motif (₁₅₉IPI₁₆₁), both of which are important in intersubunit interactions and chaperone function (Pasta et al., 2004; Rajan et al., 2006). Mutations in the C-terminal lysines and glutamic acid residues resulted in altered oligomerisation and chaperone activity

Further investigation of the role of the C-terminal 'tail' in the solubility of α B-crystallin would require the creation of a series of sequentially truncated C-terminal mutants to help further characterise the effect of specific regions of the C-terminal extension 'tail' on the solubilisation function.

In addition, the discovery of three naturally occurring mutations, which affect the C-terminal extension of α B-crystallin are of interest firstly, due to their disease causing nature in both the lens and extra lenticular tissues. Secondly by their phenotypic heterogeneity, where the mutations result in either isolated posterior polar cataract (450delA) with no muscle phenotype, or Myofibrillar myopathy (464delCT and Q151X) with no cataract. Two post translation modifications have also been identified, which result in a truncated C-terminal extension and include α B₁₋₁₇₀ and α B₁₋₁₆₃. The α B₁₋₁₇₀ was found in diabetic rat lenses (Thampi et al., 2002) and was observed in patients who display Soemmerring's ring cataract (Colvis et al., 2000). The α B₁₋₁₆₃ was found in human lens fiber cells growing in lens capsules following cataract surgery (Colvis et al., 2000) and was identified as a fragment from LP82 and M-calpain proteolysis of the rat lens nucleus (Ueda et al., 2002). These observations further strengthen the argument suggesting the C-terminal extension plays an important role in the solubilisation of the α B-crystallin oligomer.

In α B-crystallin, there has been no systematic analysis of the role of the C-terminal extension and therefore no potential explanation of whether the three mutations (450delA, Q151X and 464delCT) cause the various diseases via a loss in solubility or perhaps a loss in chaperone function and oligomerisation or even by a completely different mechanism. Cloning, expression and purification of these α B-crystallin mutations along with sequential truncations of the C-terminal extension, will help further understand the role of specific amino acids important in the solubilisation of α B-crystallin oligomers. This study will provide the basis for further characterisation aiming to understand the relationship between the C-terminal extension and the chaperone function, oligomerisation and the relationship with disease.

3.3. RESULTS

The role of the C-terminal extension of α B-crystallin upon solubility has been characterised in this section. The relative solubility of expressed mutant α B-crystallin protein in both a bacterial and mammalian cell environment are shown in Section 3.3.2. The assembly of the C-terminal α B-crystallin mutant constructs are detailed in Section 3.3.1 and the subsequent purification of the bacterial recombinant α B-crystallin mutants are discussed in Section 3.3.3.

3.3.1. ASSEMBLY OF MUTANT α B-CRYSTALLIN CONSTRUCTS

The construction of all α B-crystallin mutants detailed in Section 2.2 involved a basic PCR mutagenesis system with the exception of Q151X and E165X α B-crystallin, which utilised SDM. All mutagenesis utilised specific mutagenic primers with unique restriction sites for digest screening (see Table 2.1). The 450delA construct in pET23d(+) was a kind gift from Dr Ming der Perng.

3.3.1.1. Q151X α B-crystallin mutant construct

The Q151X α B-crystallin construct was assembled by SDM using a mutagenic reverse primer in combination with a Taq promoter to incorporate the Q151X mutation into the wild type α B-crystallin template, present in the pET23d(+) vector. Proliferation of the PCR product allowed screening for the Q151X mutant using a unique restriction site incorporated in the primer (*Stu*I). Constructs which produced a fragment of 455bp were sequenced by the departmental sequencing facility, after which, the sequence obtained was checked by the nucleotide-nucleotide option of the Basic Local Alignment Search Tool (BLAST) software. The sequencing and BLAST analysis confirmed the presence of the mutant Q151X insert when compared to the GenBank data base entry (accession no. NM001885) for human α B-crystallin. (For further details of the cloning procedure and BLAST sequence, see Appendix 1, Section A1.2)

3.3.1.2. Assembly of E165X α B-crystallin mutant by SDM

The E165X α B-crystallin construct was assembled by SDM using complementary mutagenic primers to incorporate the E165X mutation. Subsequent screening for the E165X mutant utilised the unique *HindIII* restriction site. Constructs, which produced a fragment of 497bp were sequenced and checked by the BLAST software and confirmed the presence of the mutant E165X insert. (For further details of the cloning procedure and BLAST sequences see Appendix 1, Section A1.3)

3.3.1.3. Assembly of 464delCT α B-crystallin constructs

PCR mutagenesis utilised a mutagenic primer to generate the 464delCT α B-crystallin mutant insert (492bp) with 3'A overhangs for subsequent ligation into the pGEM®-T Easy vector. The presence of the 464delCT mutation was assessed using the *NcoI/EcoRI* digest on purified constructs to screen for fragments of expected size of 498bp. Following confirmation by sequencing, the construct was subcloned into pET23d(+) using *NcoI/EcoRI* digest. The multiple cloning region of pET23d(+) is shown in Appendix 1, Figure A8.2B. Further *NcoI/EcoRI* screening, sequencing and BLAST analysis confirmed the 464delCT insert had successfully been subcloned into the pET23d(+) vector and was viable for protein expression. (For further details of the cloning procedure and BLAST sequences see Appendix 1, Section A1.4).

3.3.1.4. Assembly of E164X α B-crystallin mutant

The E164X α B-crystallin construct was generated by PCR, using a mutagenic primer to generate a 528bp fragment, which was ligated into the pGEM®-T Easy vector. The E164X mutant contains a unique *PstI* restriction site downstream from the stop codon. DNA from selected transformants was purified and the presence of the E164X mutation was assessed using *NcoI/PstI* digest to screen for fragments of expected size of 506bp. The construct containing the E164X mutation was subcloned into pET23d(+) using *NcoI/EcoRI* digest. Further screening, sequencing and BLAST analysis confirmed the E164X insert had successfully been subcloned into the pET23d(+) vector. (For further details of the cloning procedure and BLAST sequences see Appendix 1, Section A1.5)

3.3.1.5. Assembly of A171X α B-crystallin mutant

The A171X α B-crystallin construct was assembled by PCR, using a mutagenic primer to generate a 540bp fragment. Ligation of the fragment into the pGEM®-T Easy vector was assessed using *NcoI/SacI* digest to screen for fragments of expected size 512bp and confirmed by sequencing. The construct containing the A171X mutation was subcloned into pET23d(+) using *NcoI/EcoRI* digest and confirmation was achieved by screening, sequencing and BLAST analysis. (For further details of the cloning procedure and BLAST sequences see Appendix 1, Section A1.6)

3.3.1.6. Assembly of K174X α B-crystallin mutant

The K174X α B-crystallin construct was generated by PCR, using a mutagenic primer to generate a 528bp fragment, which was ligated into the pGEM®-T Easy vector and assessed using *NcoI/SacII* digest to screen for fragments of expected size 514bp and confirmed by sequencing. The construct containing the K174X mutation was subcloned into pET23d(+) using *NcoI/EcoRI* digest and confirmation was achieved by screening, sequencing and BLAST analysis. (For further details of the cloning procedure and BLAST sequences see Appendix 1, Section A1.7)

3.3.1.7. Subcloning of α B-crystallin constructs into pcDNA3.1(-)

In order to express the α B-crystallin mutants in mammalian cells by transient transfection, the inserts were subcloned from the pET23d(+) bacterial expression vector into pcDNA3.1(-) using *XbaI/HindIII* digest. Subsequent screening utilised *Apal/HindIII* digest, where *Apal* is unique to the pcDNA3.1(-) vector, thus confirming the efficient ligation of the mutant insert, but also the presence of the target vector pcDNA3.1 (-). The multiple cloning region of pcDNA3.1(-) is shown in Appendix 1, Figure A8.3. The wild type α B-crystallin insert in pcDNA3.1(-) was a kind gift from Dr Ming der Perng. (For full details of the subcloning process and BLAST sequences, see Appendix 1, Section A1.8)

3.3.2. THE EFFECT OF THE C-TERMINAL MUTATIONS ON THE SOLUBILITY OF α B-CRYSTALLIN MUTANT PROTEINS EXPRESSED IN BACTERIAL AND MAMMALIAN CELLS

The C-terminal extension has been reported to be important for the solubility of α B-crystallin and its associated complexes, thus the sequential removal of the C-terminal arm should increase the insolubility of the α B-crystallin mutants.

The effect of the C-terminal mutations on the solubility of the various α B-crystallin mutants was assessed firstly, in bacterial *E.coli* strain BL-21 (pLysS) cells by transformation of the mutant α B-crystallin constructs cloned into the pET23d(+) vector and secondly, in mammalian epithelial breast carcinoma MCF7 cells by transient transfection of the constructs cloned into the pCDNA3.1(-) vector.

3.3.2.1. The solubility of α B-crystallin mutant constructs expressed in *E.coli* strain BL-21

The disease causing nature of the naturally occurring mutations 450delA, 464delCT and Q151X α B-crystallin and the age related cataract causing E164X α B-crystallin would tend to lead us to the conclusion that the mutants would be expressed as inclusion bodies (Berry et al., 2001; Colvis et al., 2000; Selcen and Engel, 2003; Ueda et al., 2002).

The mutant α B-crystallin constructs cloned into the pET23d(+) vector were transformed into *E.coli* strain BL-21 (pLysS) cells for protein expression and cultured. The level of expression and the solubility of the expressed mutant proteins were assessed initially by investigating whether the protein produced remained soluble when expressed recombinantly in *E.coli* (see Figure 3.2).

These mutants also are those where the C-terminal extension is the most modified. The four mutants are all expressed as inclusion bodies (see Figure 3.2A-D, lane 4) with the entire mutant protein present in the pellet fraction (P).

The predicted Mwts calculated from the amino acid sequences using Emboss Pepstats software are confirmed by the mobility of the mutant α B-crystallins in

comparison to the protein ladders (lane 1). The E165X α B-crystallin, being only one amino acid longer than E164X α B-crystallin is also expressed and present in inclusion bodies (see Figure 3.2E).

The remaining α B-crystallin mutants A171X and K174X (truncated by 5 and 2 amino acids respectively) are expressed as soluble protein similar to the wild type α B-crystallin (see Figure 3.2 (F-H) respectively, lane 3). The SDS-PAGE also suggests the expression of these mutants and the wild type α B-crystallin as inclusion bodies as there are significant levels of the respective proteins in the pellet fractions (lane 4). Inclusion bodies are condensed particles of protein that are formed within the bacterial cell when the cell is forced to make large amounts of protein and are the result of 'off pathway' aggregation or folding which could explain the presence of inclusions alongside soluble mutant protein. It is more likely, however that the pellet material is indicative of an inefficient lysis, where the whole cells, which have not been efficiently homogenised, continue to be sedimented by the centrifugation process required for fractionation.

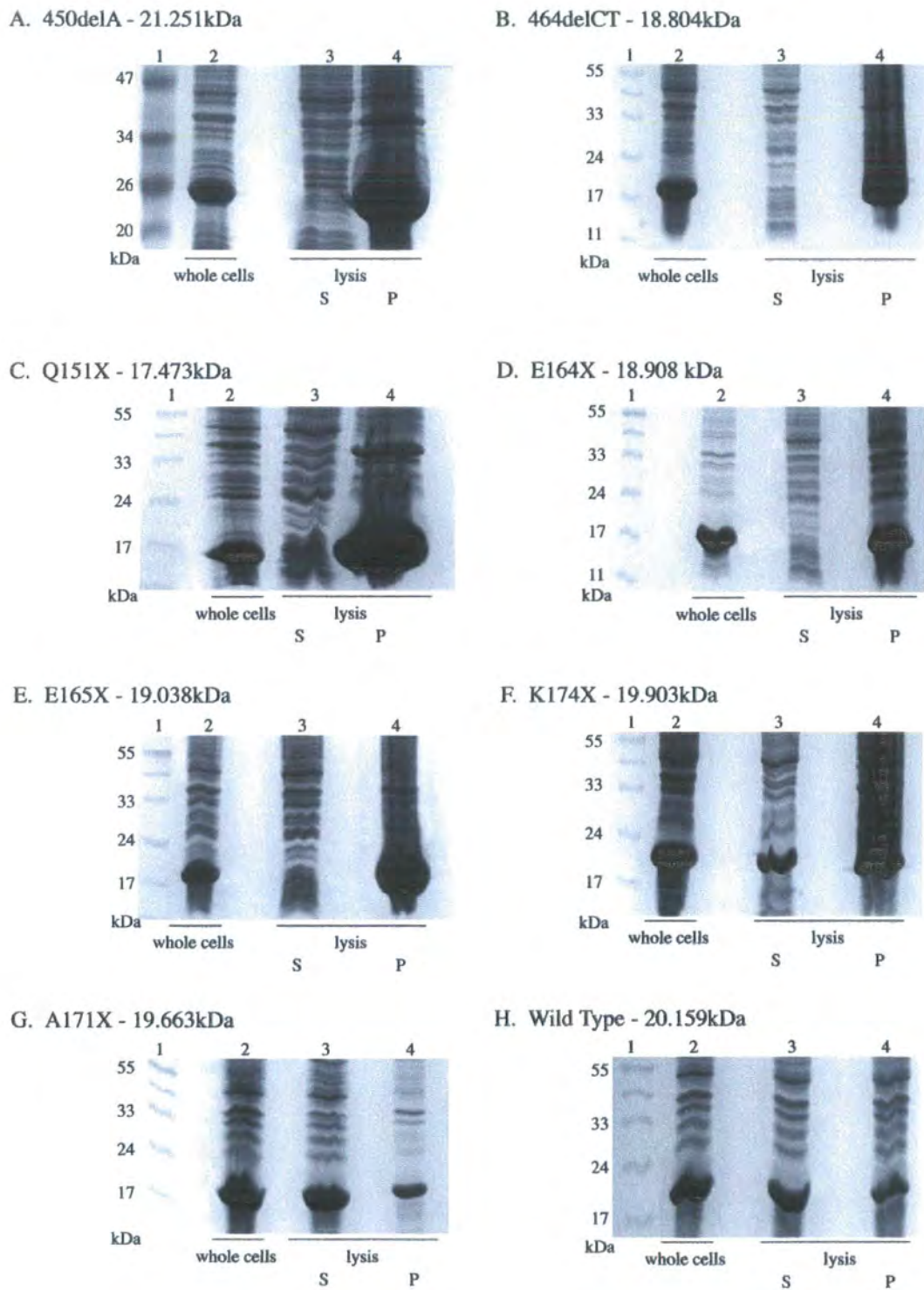


Figure 3.2. Solubility of α B-crystallin mutants expressed in BL-21 *E.coli* cells. The whole cells for each mutant and the wild type are shown in lane 2 (A-H). The soluble fractions (S) in lane 3 (A-H), and insoluble fractions (P) in lane 4 (A-H), from lysis show the distribution of the mutant protein. The predicted Mwt is shown as calculated from the amino acid sequence using the Emboss Pepstats software (www.ebi.ac.uk/emboss/pepstats).

3.3.2.2. The Solubility of α B-crystallin mutants expressed in mammalian MCF7 Cells

Transient transfection of α B-crystallin mutants into breast epithelial MCF7 cells was performed to investigate the relative solubility of the mutants in a mammalian cell environment. MCF7 cells have no endogenous α B-crystallin thus avoiding the need to tag the protein for subsequent detection but high levels of endogenous HSP27, a small heat shock protein chaperone that is known to form heterogeneous oligomers with α B-crystallin (Zantema et al., 1992)

Figure 3.3 illustrates the solubility and distribution of the specific mutants. Cells expressing wild type α B-crystallin (Figure 3.3.A; green channel), showed a homogenous cytoplasmic distribution. A similar distribution was observed for the E165X, A171X and K174X (Figure 3.3.F-H respectively)

In contrast, cells expressing Q151X, 464delCT, E164X and 450delA α B-crystallin were obvious by the presence of cytoplasmic aggregates that were immunopositive for α B-crystallin (Figure 3.3.B-E respectively), all of which have been shown to be extremely insoluble in *E. Coli* BL-21 expressions (see Section 3.3.2.1, Figure 3.3). The distribution of the 450delA and 464delCT aggregates were scattered throughout the cytoplasm whereas the Q151X and E164X α B-crystallin aggregates were perinuclear in distribution. This data has been complemented by a recent paper, which found that both the Q151X α B-crystallin and 464delCT α B-crystallin formed aggregates in transfected cells (Simon et al., 2007).

In order to provide an assessment of the solubility of the different α B-crystallin constructs in populations of transiently transfected MCF7 cells, cells were extracted and the presence of α B-crystallin in supernatant and pellet fractions was measured by sedimentation assay followed by SDS-PAGE and immunoblotting with monoclonal anti- α B-crystallin (see Figure 3.4). A second antibody, monoclonal anti-HSP27 antibody (ERD-5) was used as a control to detect the endogenous levels of HSP27.

Transfected wild type α B-crystallin was found almost entirely in the soluble fraction (see Figure 3.4, lane 1). Transfected Q151X, 464delCT and E164X α B-crystallin, however, were detected almost entirely in the pellet fractions, (see Figure 3.4, lanes 8, 4 and 10 respectively) with only a small proportion left in the supernatant

fractions (see Figure 3.4, lanes 7, 3 and 9 respectively). The K174X, A171X and E165X whose mutations involve the least truncation of the C-terminal extension, are all entirely present in the supernatant fractions similarly to the wild type α B-crystallin (see Figure 3.4, lane 11, 13 and 15 respectively). Interestingly, the E165X α B-crystallin was shown to be entirely insoluble in *E. Coli* BL-21 expressions (see Section 3.3.2.1, Figure 3.3.E). The 450delA α B-crystallin, which was expected to be present entirely in the pellet fraction, seems to show only a trace amount in the supernatant fraction (see Figure 3.4, lane 3). This could be a problem with the transfection conditions or the nature of the mutant in preventing efficient recovery of the 450delA α B-crystallin protein either during the transfection or the protein extraction stage.

The endogenous HSP27 was unable to prevent the formation of aggregates by the various mutant α B-crystallins and the presence of these aggregates did not cause a significant shift in the solubility of the endogenous HSP27 to the pellet fraction. These data support the hypothesis that the sequential loss of the C-terminal extension also results in a sequential loss of solubility even in a cellular environment.

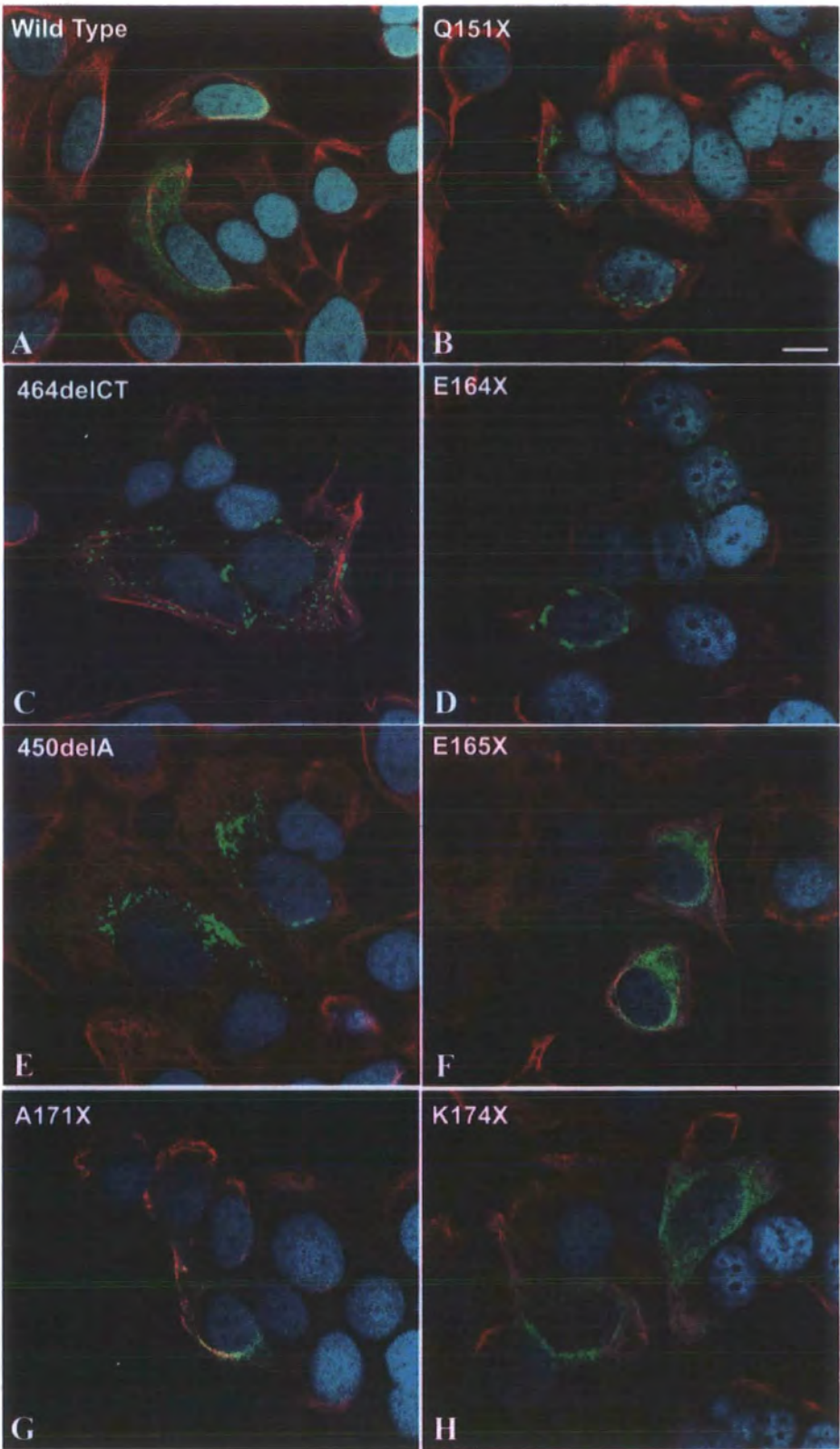


Figure 3.3. Formation of cytoplasmic aggregates by selected α B-crystallin mutants in MCF7 cells. MCF7 cells (A–D) transiently transfected with wild-type (A), Q151X (B), 464delCT (C) or E164X (D) α B-crystallin were fixed at 24 h post transfection and processed for immunofluorescence microscopy. The subcellular distribution of α B-crystallin and keratin were visualized by double labeling with monoclonal anti-keratin (red channel) and polyclonal anti- α B-crystallin antibodies (green channel). A–D are merged images showing the superimposition of the green, red and blue (DAPI staining) channels with areas of red and green overlap in yellow. Images are individual optical sections acquired using a confocal laser scanning microscope (Zeiss 510). Cells expressing wild type α B-crystallin (A). showed the expected cytoplasmic distribution of α B-crystallin. In contrast, cells expressing mutant α B-crystallin resulted in the formation of cytoplasmic aggregates of α B-crystallin (B–D). Notice that 464delCT and 450delA aggregates are scattered throughout the cytoplasm whereas the Q151X and E164X aggregates locate to the peripnuclear region of the cell. Bars, 10 μ m. Immunoblotting analysis (E), of α B-crystallin expressed in MCF7 cells, illustrating the insolubility of the mutant α B-crystallins. At 24 h posttransfection, cells were extracted with detergent buffer followed by centrifugation at $18,000 \times g$ for 10 min at 4°C. The resulting supernatant (S) and pellet (P) fractions were separated by SDS-PAGE followed by immunoblotting analysis by using anti-HSP27 and α B-crystallin antibodies as detailed in the Materials and Methods. The blot was developed using the enhanced chemiluminescence system. Whereas wild-type α B-crystallin was present almost entirely in the soluble fraction (E, lane 1, labeled S), Q151X (lane 4), 464delCT (lane 6) and E164X (lane 8) was found mostly in the pellet fraction, (labeled P). Mutant α B-crystallin bands are denoted by the arrow head (►). HSP27 Immuno-positive signals were detected mostly in the supernatant fractions (E lanes 2, 4, and 6, labeled P). These data are representative of three experiments.

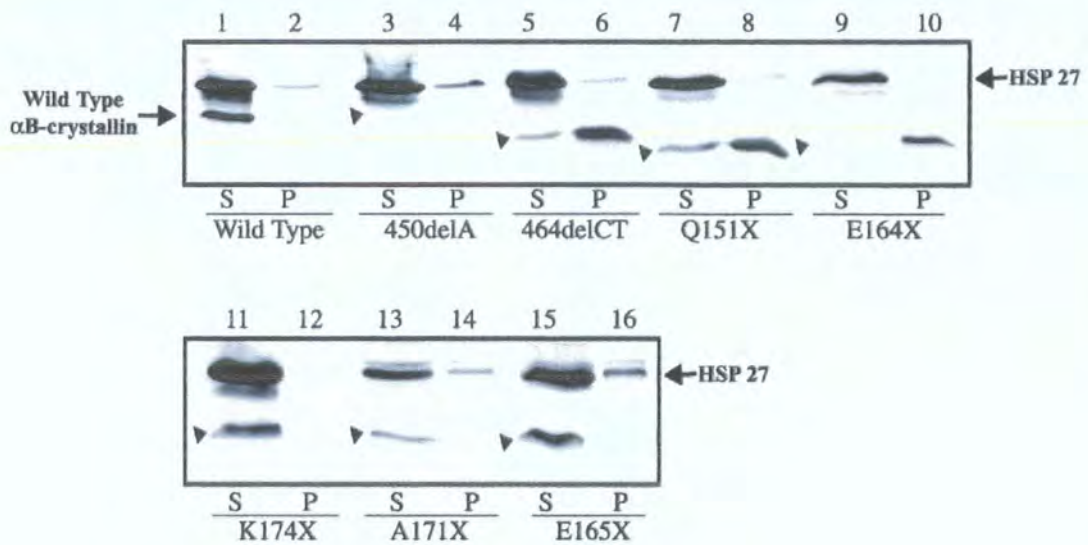


Figure 3.4. The solubility of α B-crystallin mutants in populations of transiently transfected MCF7 cells. This data illustrates the insolubility of the mutant α B-crystallins. At 24 h post transfection, cells were extracted with detergent buffer followed by centrifugation at $18,000 \times g$ for 10 min at 4°C . The resulting supernatant (S) and pellet (P) fractions were separated by SDS-PAGE followed by immunoblotting analysis by using anti-HSP27 and α B-crystallin antibodies. The blot was developed by enhanced chemilluminescence system. Whereas wild type α B-crystallin was present almost entirely in the soluble fraction (lane 1, labelled S), Q151X (lane 8), 464delCT (lane 6) and E164X (lane 10) was found mostly in the pellet fraction, (labelled P). The K174X (lane 11) A171X (lane 13) and E165X (lane 15) are present entirely in the supernatant fraction similar to the wild type α B-crystallin. The 450delA was expected to be completely insoluble, however the only band visible is in the supernatant (lane 3) and is very faint. Mutant α B-crystallin bands are denoted by the arrow head (\blacktriangleright). HSP27 Immuno-positive signals were detected mostly in the supernatant fractions. These data are representative of three experiments.

3.3.3. PURIFICATION OF RECOMBINANT α B-CRYSTALLIN MUTANTS

The various mutant α B-crystallins expressed in *E.coli* strain BL-21 (pLysS) cells were purified to allow further characterisation of the effect of a modified C-terminal extension on the structure and function of α B-crystallin.

The solubility of the expressed protein dictated the purification protocol utilised. Expression data shown in Section 3.3.2 confirmed that the disease mutants 450delA, 464delCT, Q151X and E164X were present as inclusion bodies along with the E165X mutant, therefore solubilisation in 6M urea was required to allow purification of the protein. The expression of soluble protein shown for the A171X and the K174X meant they would be purified using the wild type α B-crystallin purification protocol.

3.3.3.1. Wild type α B-crystallin

The wild type protein expressed (see Figure 3.2H) was purified following the protocol detailed in Section 2.6. The first chromatography step used Ion Exchange chromatography (IEX) to remove contaminating proteins and allow the isolation of the wild type protein. A typical IEX purification is shown in Figure 3.5A. Following SDS-PAGE analysis (see Figure 3.5B), fractions 3-23 inclusive were pooled. The pooling criteria excluded those fractions with additional contaminating proteins despite the presence of the wild type α B-crystallin.

The second stage of the purification was Size Exclusion Chromatography (SEC), which would further resolve wild type α B-crystallin from any contaminating proteins carried forward in the IEX pool. The IEX pool was concentrated from 21 ml to 0.5 ml prior to SEC. The SEC purification resulted in the recovery of 27mg of wild type α B-crystallin (see Figure 3.6A). The α B-crystallin was the major species present in the SEC profile, and SDS-PAGE analysis of these fractions (see Figure 3.6B) confirmed that fractions 35-49 were enriched and were subsequently pooled to give a total pool volume of 15ml. The SEC pool material was divided into 0.5ml aliquots and stored at -80°C.

A number of additional species were identified at 40 kDa, 28 kDa and several below the wild type band at approx. 17 kDa. These may be contaminating proteins or could potentially be a dimer (40 kDa) and breakdown products. The nature of these

additional bands was investigated by immunoblotting with α B-crystallin mouse monoclonal 2D2B6 clone generated to chicken α B-crystallin, (see Figure 3.7). The immunoblotting confirms that the bands at 28 kDa and 40 kDa are wild type α B-crystallin. A number of the low Mwt bands that were observed between the wild type band and 17 kDa in Figure 3.6B may be masked in Figure 3.7, by the large wild type band at 20 kDa. A very low intensity band at approx. 17 kDa shown in the Ponceau stain (see Figure 3.7) was not detected by the wild type α B-crystallin monoclonal antibody, suggesting that the band was a contaminant. The amount of the low Mwt band present in the 1.8 mg/ml SEC pool was negligible and would not be visible in SDS-PAGE analysis of wild type α B-crystallin under typical experimental conditions of 0.1-0.2 mg/ml.

Dynamic Light Scattering (DLS) was used to confirm the quality of the purified wild type α B-crystallin because it is a non-invasive, well-established technique for measuring the size of molecules and size distribution of particles typically in the sub micron region. Therefore DLS can confirm the purity of the wild type α B-crystallin SEC pool material and the data shows that the α B-crystallin is the only species present (see Figure 3.8).

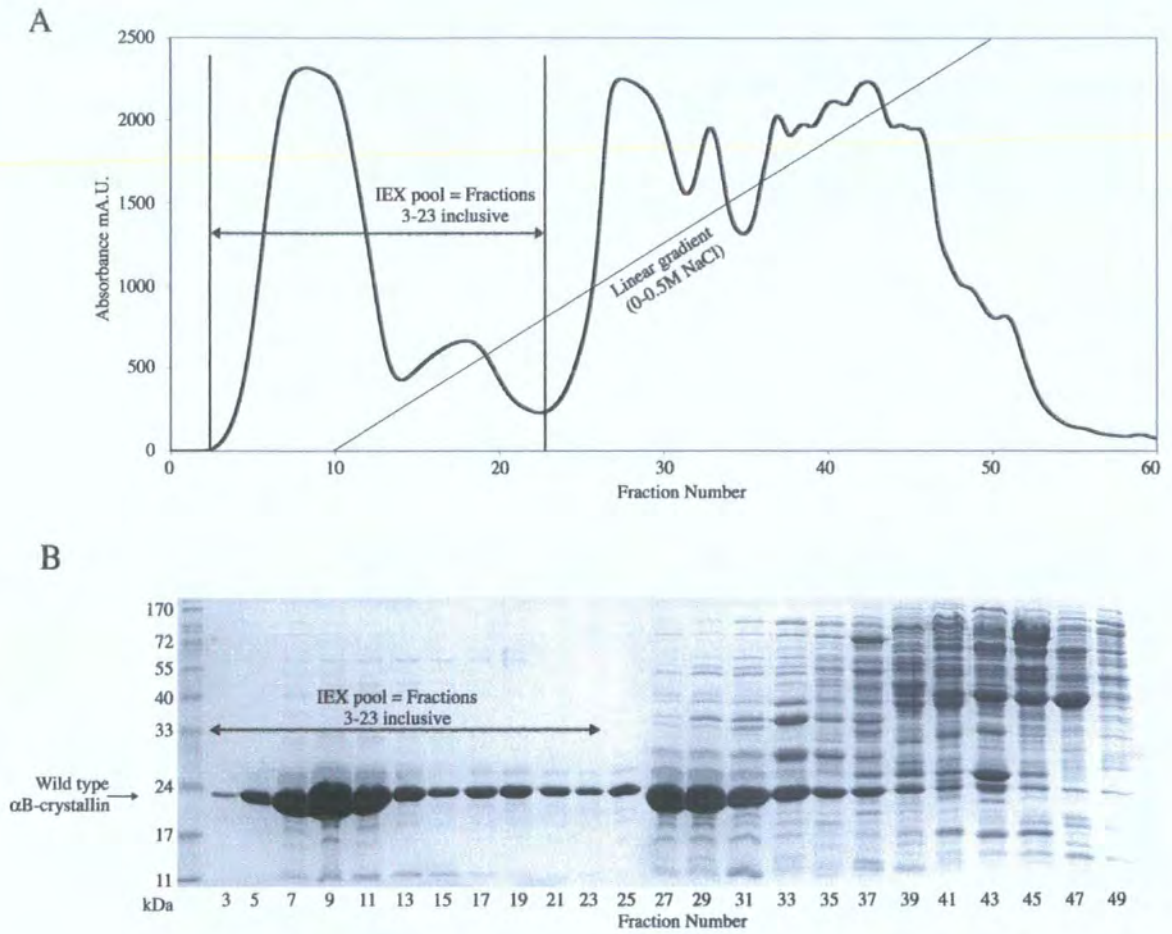
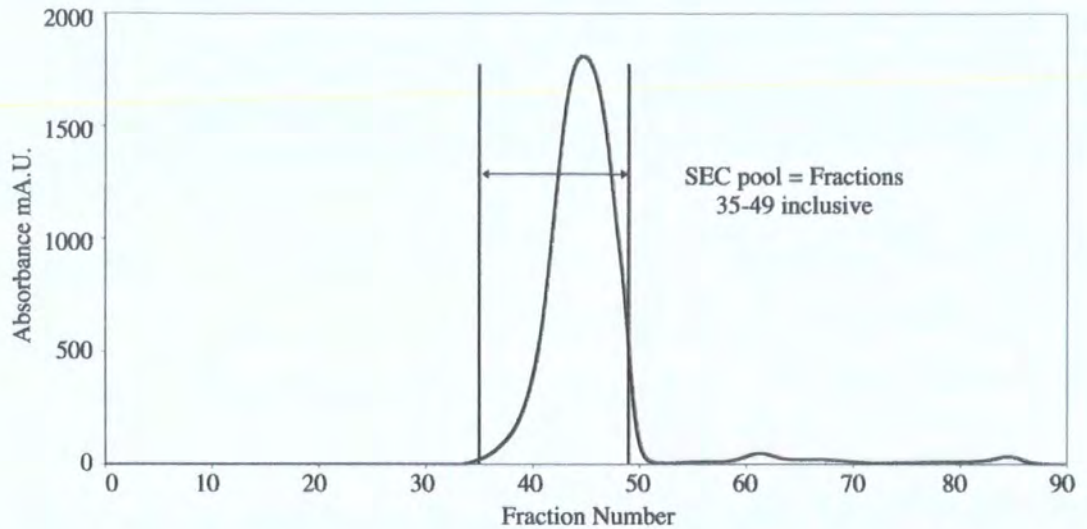


Figure 3.5. IEX Chromatography of wild type α B-crystallin and fraction analysis. The wild type α B-crystallin was initially purified by IEX (A), and the appropriate fractions for pooling were identified by reducing SDS-PAGE (B). Fractions 3-23 inclusive were enriched with α B-crystallin and were pooled to give a 21ml pool volume. The pool excluded contaminating proteins, which co-eluted with α B-crystallin in fractions 27 onwards under higher NaCl concentrations.

A



B

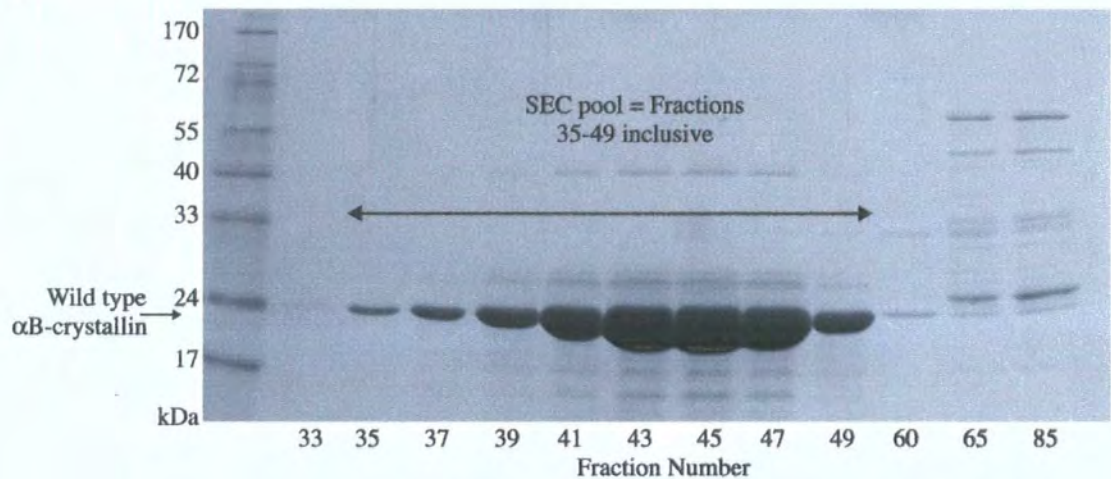


Figure 3.6. SEC Chromatography of wild type α B-crystallin and fraction analysis. The wild type α B-crystallin was further purified by SEC (A), and the appropriate fractions for pooling were identified by reducing SDS-PAGE (B). Fractions 35-49 inclusive were enriched with α B-crystallin and were pooled to give a 15ml pool volume of 1.82 mg/ml. A number of low intensity bands were present in the pooled material at low and high Mwt, which may be dimer (40 kDa) and breakdown products of the pool material.



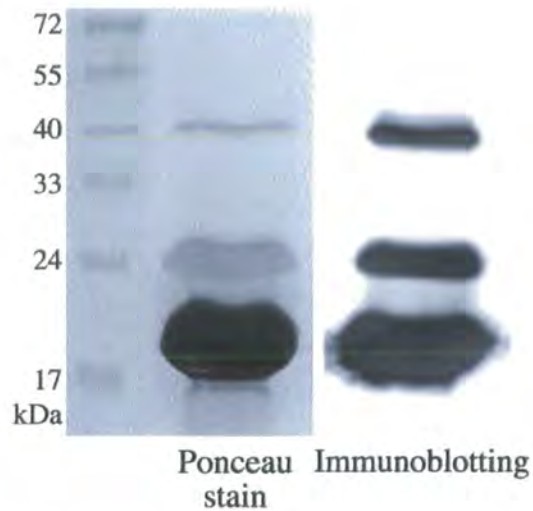


Figure 3.7. Analysis of additional species in the wild type α B-crystallin SEC pool. The Ponceau stain of the SEC pool identifies the wild type band at 20 kDa, showing the greatest intensity. Two additional bands are also evident at 28 kDa and 40 kDa. There is a trace amount of the lower Mwt proteins at 17 kDa, however is masked due to the large wild type band. The immunoblotting confirms that the bands at 28 kDa and 40 kDa are wild type α B-crystallin by showing a signal when probed with α B-crystallin mouse monoclonal 2D2B6 clone generated to chicken α B-crystallin. The bands at 17 kDa are not detected by the immunoblotting suggestive of a contaminant.

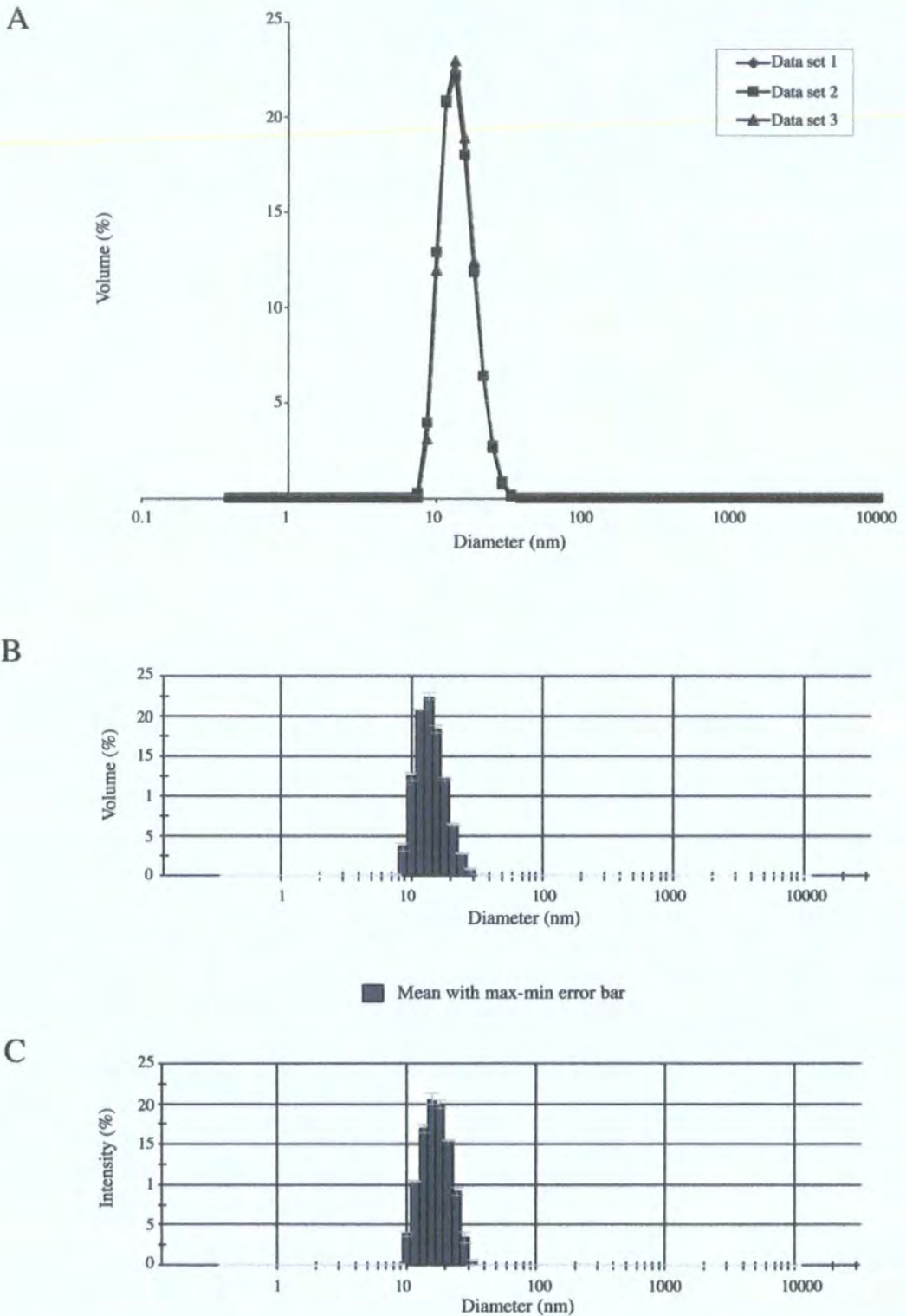


Figure 3.8. Dynamic Light Scattering analyses of α B-crystallin wild type. The data shown represents the average of 3 runs, each of which consisted of 5 data accumulations. Figure 3.8A shows the 3 data sets overlayed and confirms that the wild type oligomer accounts for 100% of the protein in the SEC pool. Figure 3.8B shows the corresponding histogram and (C) represents the intensity or level of light scattering produced by the α B-crystallin wild type.

3.3.3.2. K174X α B-crystallin

The K174X protein expressed (see Figure 3.2F) was purified following the protocol detailed in Section 2.6. The first chromatography step used IEX chromatography to remove contaminating proteins and allow the isolation of the K174X α B-crystallin. A typical IEX purification is shown in Figure 3.9. The K174X protein was co-eluted under higher NaCl concentrations with a range of contaminating proteins. This was identified by SDS-PAGE analysis of the appropriate fractions (see Figure 3.9B) and subsequently fractions 35-43 inclusive were pooled giving a 15ml pool volume. The pool criteria excluded those fractions (F44 onwards) with additional contaminating proteins despite the presence of the K174X α B-crystallin.

The second stage of the purification was SEC, which would further resolve K174X α B-crystallin from the contaminating proteins carried forward in the IEX pool. The IEX pool was concentrated to 0.5ml prior to SEC. The SEC purification resulted in the recovery of 4mg of K174X α B-crystallin (see Figure 3.10A). The K174X α B-crystallin was well resolved as a single species as shown in the SEC profile (see Figure 3.10A), and SDS-PAGE analysis of these fractions identified fractions 34-42 to be enriched and were subsequently pooled to give a total pool volume of 9ml at 0.4 mg/ml (see Figure 3.10B).

The yield was compromised by the exclusion of fractions from the SEC pool where the K174X was co eluted with a low level of contaminating bands (see Figure 3.10B, Fraction 44 and 46). The SEC was successful in resolving the majority of contaminating proteins that were carried forward from the IEX (see Figure 3.9). SEC pool material was divided into 0.5ml aliquots and stored at -80°C.

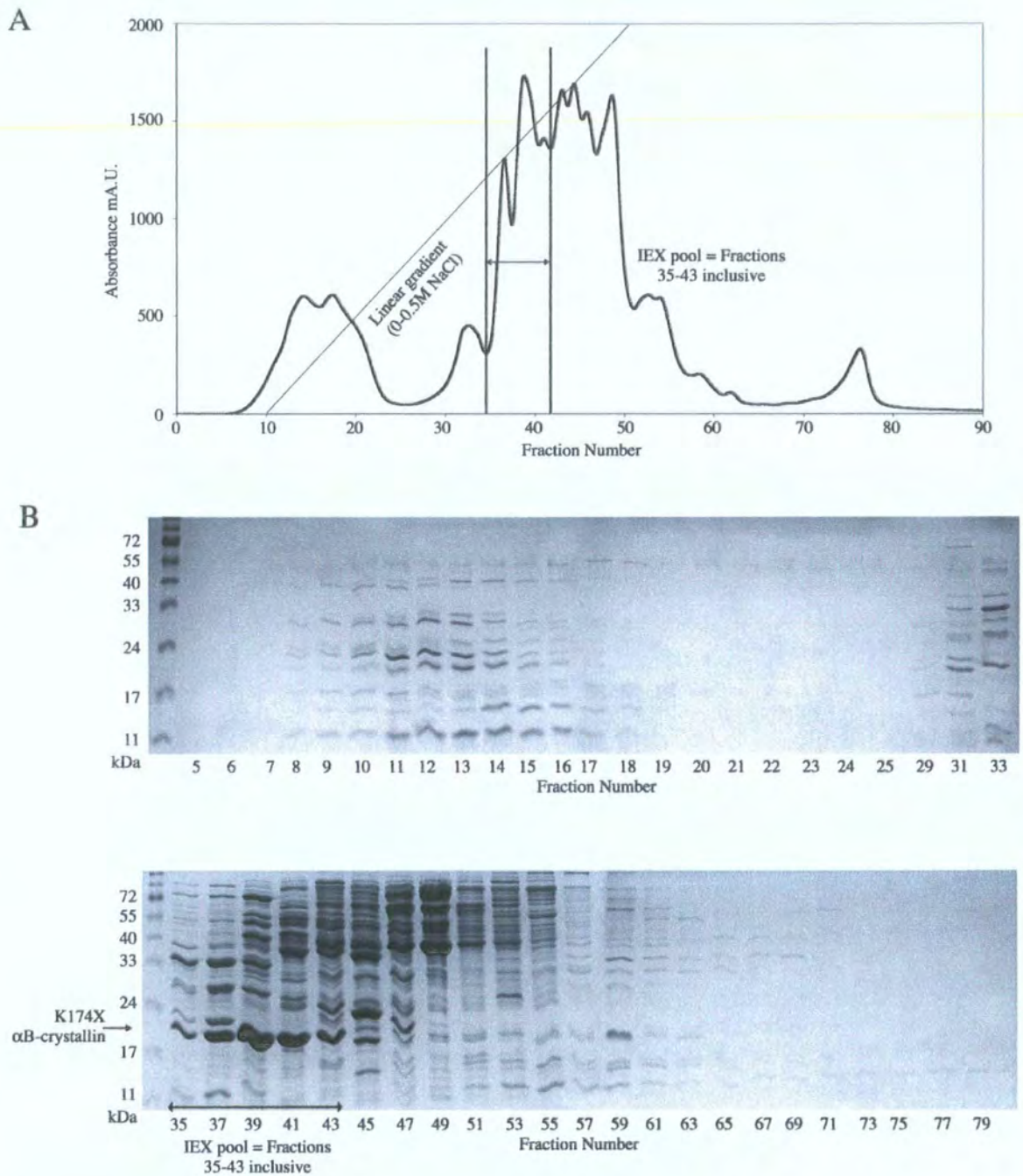


Figure 3.9. IEX Chromatography of K174X α B-crystallin and fraction analysis. The K174X α B-crystallin was initially purified by IEX (A), and the appropriate fractions for pooling were identified by reducing SDS-PAGE (B). Fractions 35-43 inclusive were enriched with α B-crystallin and were pooled to give a 9 ml pool volume. The pool excluded contaminating proteins, which co-eluted with α B-crystallin in fractions 45 onwards.

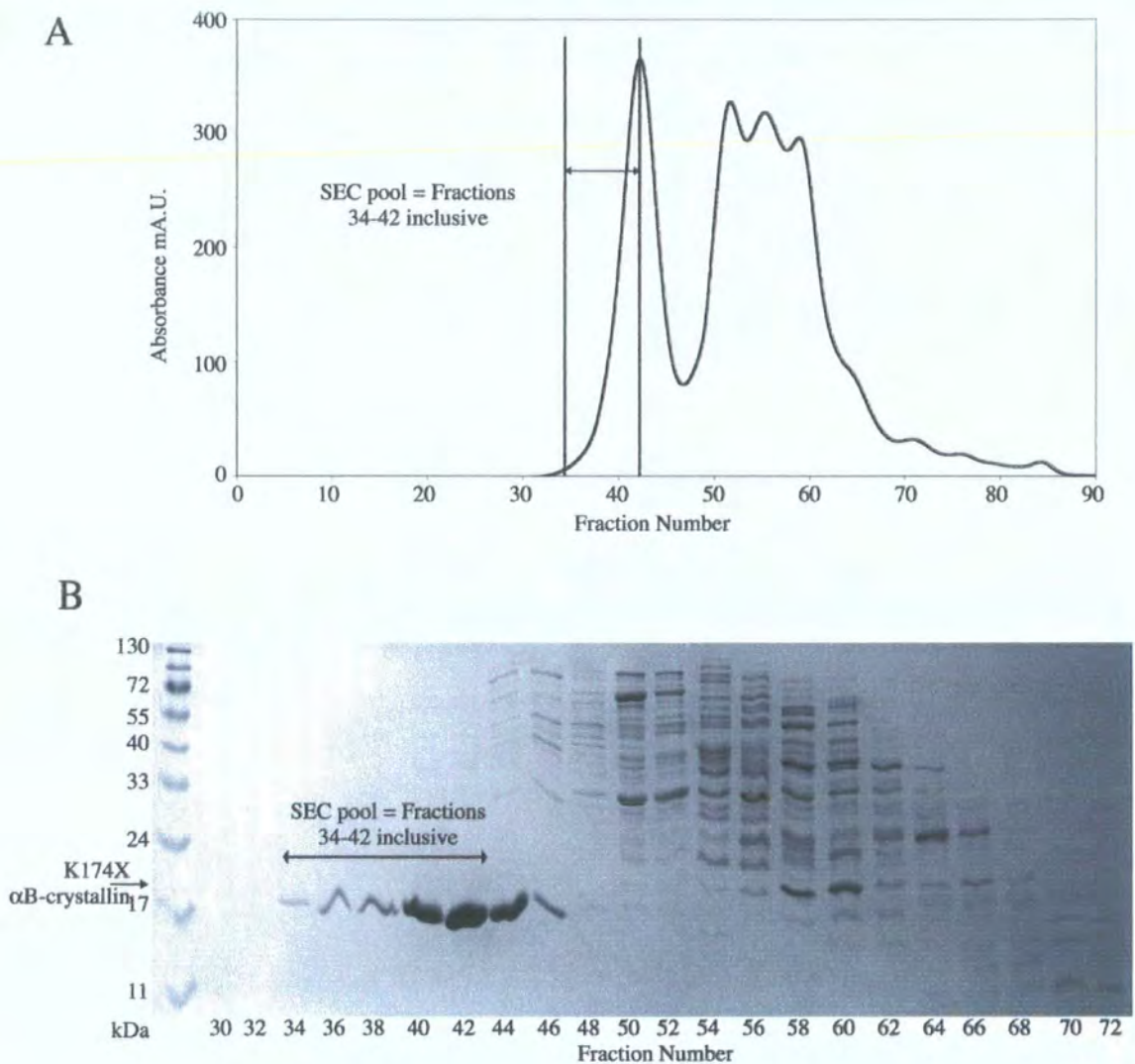


Figure 3.10. SEC Chromatography of K174X α B-crystallin and fraction analysis. The K174X α B-crystallin was further purified by SEC (A), and the appropriate fractions for pooling were identified by reducing SDS-PAGE (B). Fractions 34-42 inclusive were enriched with α B-crystallin and were pooled to give a 9ml pool volume of 0.4 mg/ml. Although fraction 44 and 46 contained K174X α B-crystallin, they were discarded due to the presence of high molecular weight contaminating proteins. The contaminating proteins carried forward in the IEX pool are removed subsequently in the latter stages of the SEC.

3.3.3.3. A171X α B-crystallin

The A171X protein expressed (see Figure 3.2G) was purified following the protocol for soluble protein detailed in Section 2.6. A typical IEX purification is shown in Figure 3.11A. The A171X protein was co-eluted under high NaCl concentrations with a range of contaminating proteins as shown by SDS-PAGE analysis of the appropriate fractions (see Figure 3.11B). Fractions 31-45 inclusive were pooled giving a 15ml pool volume. The pool criteria excluded those fractions (F46 onwards) with additional contaminating proteins despite the presence of the A171X α B-crystallin.

The SEC purification resulted in the recovery of 36mg of A171X α B-crystallin (see Figure 3.12A). The A171X α B-crystallin was resolved as a single species up to fraction 44, after which, the A171X was co-eluted with a number of contaminating proteins (see Figure 3.12B). Fractions 33-44 were enriched with A171X α B-crystallin and pooled to give a volume of 12ml at 3.0 mg/ml. The SEC was successful in resolving the majority of contaminating proteins that were carried forward from the IEX (see Figure 3.11). SEC pool material was divided into 0.5ml aliquots and stored at -80°C.

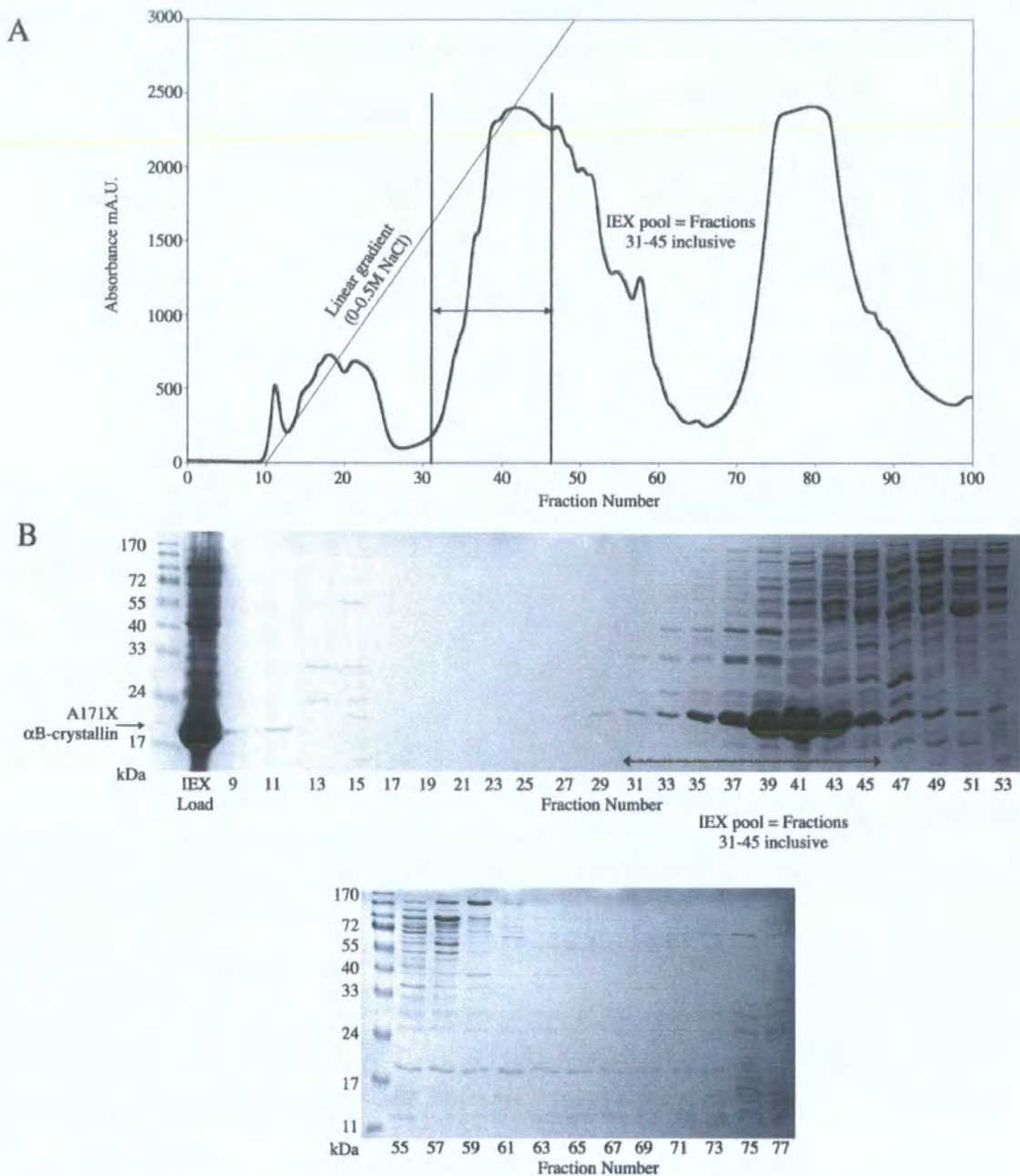


Figure 3.11. IEX Chromatography of A171X α B-crystallin and fraction analysis. The A171X α B-crystallin was initially purified by IEX (A), and the appropriate fractions for pooling were identified by reducing SDS-PAGE (B). Fractions 31-45 inclusive were enriched with α B-crystallin and were pooled to give a 15ml pool volume despite containing contaminating proteins. The pool excluded additional contaminating proteins, which co-eluted with α B-crystallin in fractions 46 onwards.

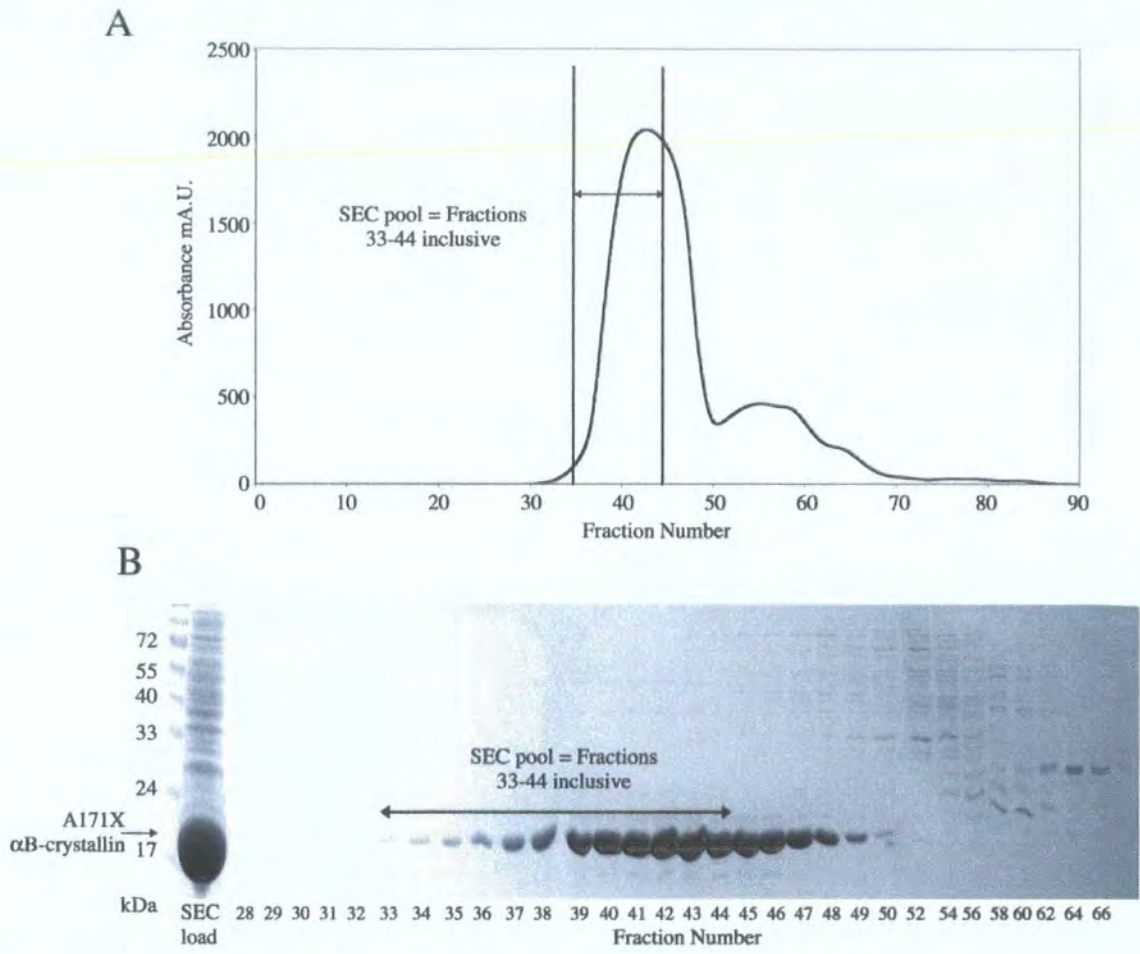


Figure 3.12. SEC Chromatography of A171X α B-crystallin and fraction analysis. The A171X α B-crystallin was further purified by SEC (A), and the appropriate fractions for pooling were identified by reducing SDS-PAGE (B). Fractions 33-44 inclusive were enriched with α B-crystallin and were pooled to give a 12ml pool volume of 3.0 mg/ml.

Although fraction 45-49 contained significant levels of A171X α B-crystallin, they were discarded due to the presence of high molecular weight contaminating proteins. The contaminating proteins carried forward in the IEX pool are removed subsequently in the latter stages of the SEC.

3.3.3.4. 450delA α B-crystallin

The 450delA α B-crystallin was expressed as inclusion bodies (see Figure 3.2A) and required solubilisation with 6M urea to facilitate further purification by IEX. Prior to urea solubilisation, the inclusion bodies were initially purified by washes using detergent Triton-X and NaCl to remove cell debris, an advantage of inclusion body expression. The washes resulted in white inclusion bodies, which are indicative of inclusions of high purity (see Section 2.7). The solubilisation of 450delA inclusion bodies in 6M urea required 4 h incubation whilst gently mixing. This insolubility supports the literature stating that the mutant is highly insoluble and is found in large plaques in the disease state, (Berry et al., 2001).

The solubilised 450delA α B-crystallin was purified by IEX, (see Figure 3.13A). The advantage of inclusion body purification is the ability to remove the majority of cell debris prior to the IEX, highlighted by the relatively low number of contaminating bands shown in the SDS-PAGE analysis of the IEX load (see Figure 3.13.B, IEX load). Fractions 3-19 inclusive were enriched with 450delA α B-crystallin and were subsequently pooled, giving a 17 ml pool volume containing 60mg of the mutant in 6M urea. The SDS-PAGE analysis revealed a higher Mwt protein migrating to approx. 42 kDa and a number of lower Mwt bands (see Figure 3.13.B).

The nature of these proteins was analysed by immunoblotting to assess whether they were of 450delA α B-crystallin origin or contaminants (see Figure 3.14). The 450delA α B-crystallin IEX pool was probed with the 2D2B6 monoclonal α B-crystallin antibody in parallel with the wild type SEC pool, which in previous analyses by immunoblotting confirmed bands at 40 kDa and 28 kDa were of wild type α B-crystallin origin (see Figure 3.7). Figure 3.14 clearly shows that the band migrating to approx. 42 kDa was immunopositive for 450delA α B-crystallin, thus suggesting a dimer. The lower Mwt bands were not detected therefore it was likely that these bands represented contaminating proteins. The proportion of the 3.5 mg/ml IEX pool represented by these low Mwt proteins was negligible and would not be visible in SDS-PAGE analysis of 450delA α B-crystallin under typical experimental conditions of 0.1-0.2 mg/ml.

One of the disadvantages of protein expression in inclusion bodies is the need to denature the protein to allow solubilisation and subsequent purification with 6 M urea.

The 450delA α B-crystallin IEX purified material was in a denatured form and needed refolding in order to obtain a functional protein that could be subsequently characterised. The refolding required buffer exchange into aqueous buffer and is detailed in Section 3.3.4.

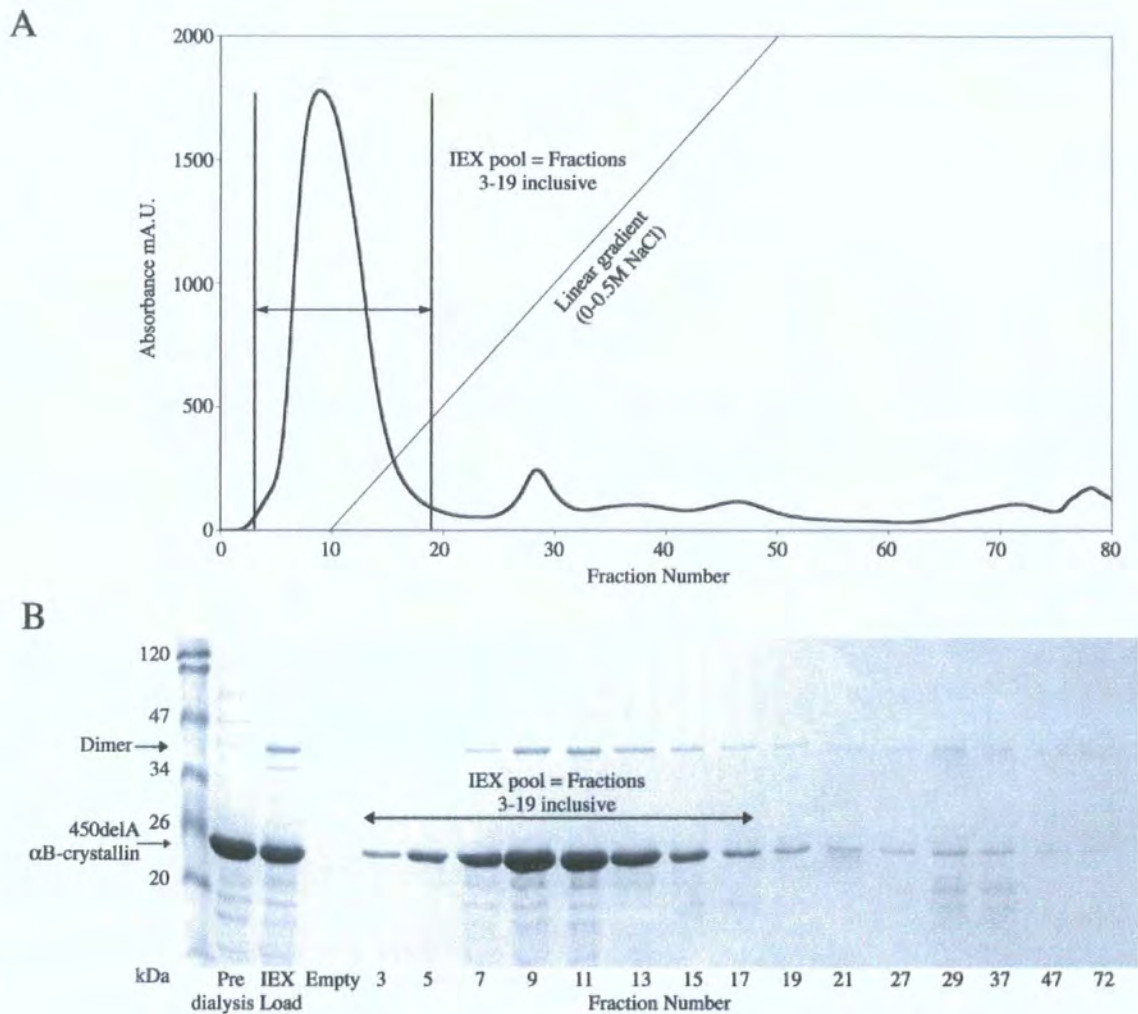


Figure 3.13. IEX Chromatography of 450delA α B-crystallin and fraction analysis. The 450delA α B-crystallin was initially purified by IEX (A), and the appropriate fractions for pooling were identified by reducing SDS-PAGE (B). Fractions 3-19 inclusive were enriched with α B-crystallin and were pooled to give a 17ml pool. The load material was relatively pure after detergent washes.

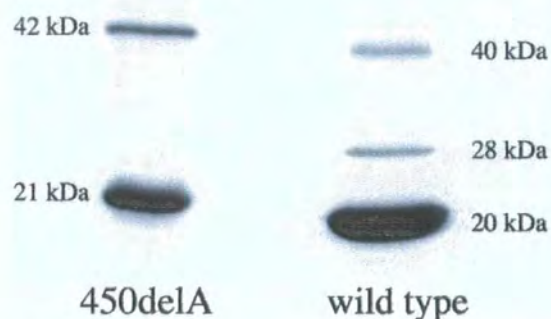


Figure 3.14. Analysis of additional proteins present in the 450delA α B-crystallin IEX pool by Immunoblotting. A higher Mwt band (approx. 42 kDa) in the 450delA α B-crystallin IEX pool was suggestive of a dimer. Confirmation that the protein was of 450delA α B-crystallin origin was achieved by immunoblotting with monoclonal wild type α B-crystallin antibody 2D2B6, which resulted in a signal for the monomer at 21 kDa and also the high Mwt band at 42 kDa. The wild type α B-crystallin SEC pool was also analysed in parallel as a marker, where dimer (40 kDa), a band at 28kDa and monomer (20 kDa) have been identified previously (see Figure 3.7).

3.3.3.5. 464delCT α B-crystallin

The 464delCT α B-crystallin like the 450delA α B-crystallin construct was expressed as inclusion bodies (see Figure 3.2B) therefore, subsequent purification also required the use of 6M urea to solubilise the inclusion bodies, thus facilitating further purification by IEX (see Section 2.7). The washes resulted in white inclusion bodies, which are indicative of inclusions of high purity (see Section 2.7). The solubilisation of 464delCT inclusion bodies in 6M urea required a 4 h incubation whilst gently mixing. This insolubility was similar to that experienced with the 450delA α B-crystallin and again supports the literature where the 464delCT mutant was found to accumulate as aggregates in muscle tissue of patients suffering from myofibrillar myopathy (MM) (Selcen and Engel, 2003). IEX chromatography was used to remove contaminating proteins and allow the isolation of the 464delCT protein. A typical IEX purification is shown in Figure 3.15.A. The 464delCT α B-crystallin was eluted at the start of the NaCl gradient however, the yield of 464delCT α B-crystallin was compromised by co elution with a protein of approx 26 kDa shown in fractions 19–22. SDS-PAGE analysis of the appropriate fractions (see Figure 3.15.B) identified fractions 23–32 inclusive to be enriched with 464delCT α B-crystallin and were subsequently pooled, giving a 10 ml pool volume containing 20mg of the mutant in 6M urea. Refolding of the 464delCT α B-crystallin is detailed in Section 3.3.4.

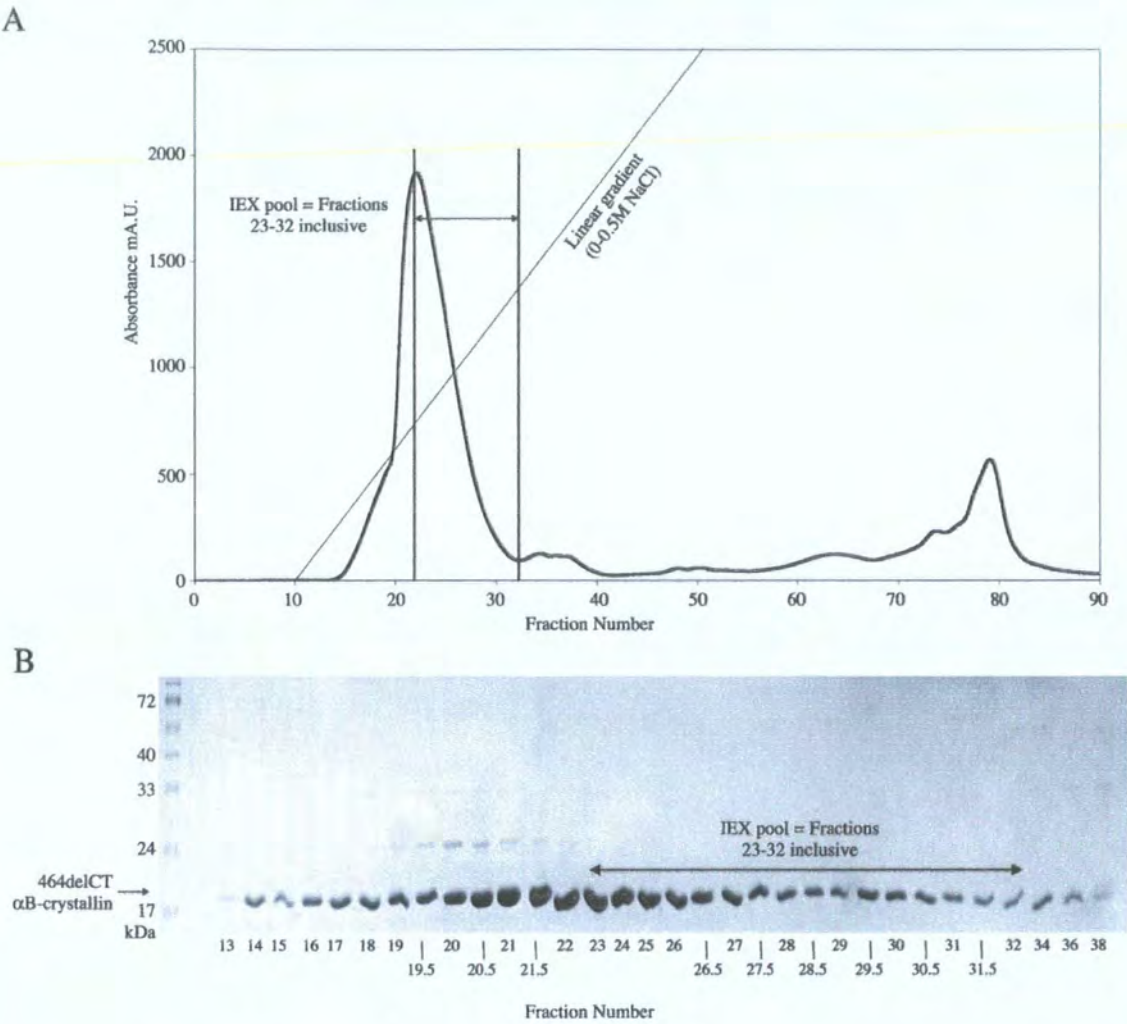
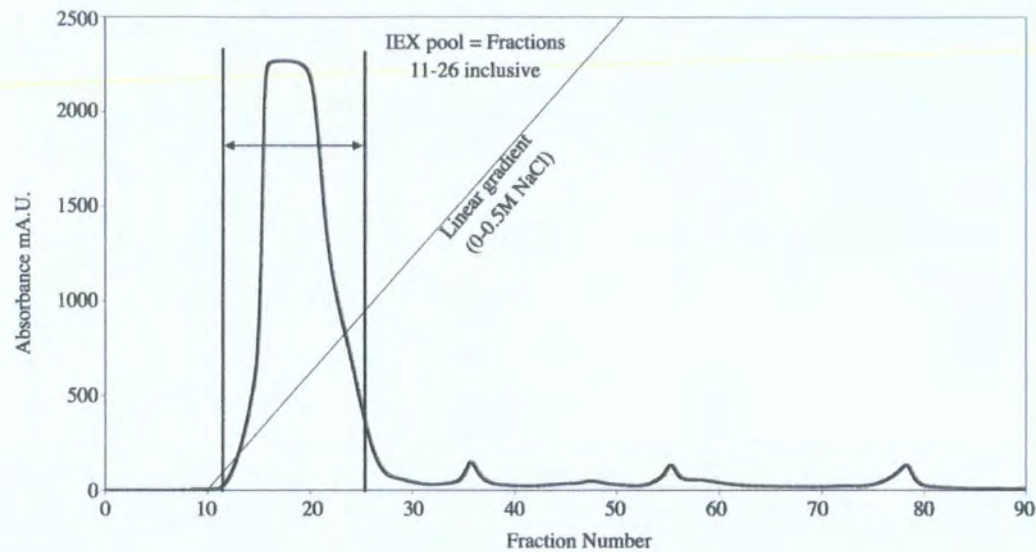


Figure 3.15. IEX Chromatography of 464delCT α B-crystallin and fraction analysis. The 464delCT α B-crystallin was initially purified by IEX (A), and the appropriate fractions for pooling were identified by reducing SDS-PAGE (B). Fractions 23-32 inclusive were enriched with α B-crystallin and were pooled to give a 10ml pool. Fractions 19-22 were excluded despite significant levels of 464delCT, due to the presence of a contaminating band at approx. 26 kDa.

3.3.3.6. E164X α B-crystallin

The E164X α B-crystallin was expressed as inclusion bodies (see Figure 3.2D) therefore, subsequent purification utilised the same protocol as the 450delA and 464delCT α B-crystallin (see Section 2.7). The detergent washes resulted in white inclusion bodies, which are indicative of inclusions of high purity (see Section 2.7). The E164X inclusion bodies were solubilised in 6 M urea more readily than the 450delA and 464delCT α B-crystallin inclusion bodies. The E164X mutation results in a 12 amino acid residue truncation, whereas the 450delA and 464delCT α B-crystallin mutations produce more extreme alterations to the C-terminal extension by the introduction of novel peptides, therefore the increased solubility observed for the E164X α B-crystallin inclusion bodies is representative of the severity of the C-terminal extension modifications and suggests an important role of the C-terminal extension in maintaining solubility. IEX chromatography was used to remove contaminating proteins and allow the isolation of the E164X protein. A typical IEX purification is shown in Figure 3.16.A. The E164X α B-crystallin was eluted at the start of the NaCl gradient followed by very low levels of contaminating protein, which peaked at 37, 56 and 78 min (see Figure 3.16.A). SDS-PAGE analysis (see Figure 3.16.B) shows that the IEX load was almost entirely pure except for a trace amount of a band at approx 27 kDa. SDS-PAGE analysis identified fractions 11-26 inclusive to be enriched with E164X α B-crystallin and were subsequently pooled (see Figure 3.22B), giving a 16 ml pool volume yielding 70 mg of the mutant in 6M urea. Refolding of the E164X α B-crystallin is investigated in Section 3.3.4.

A



B

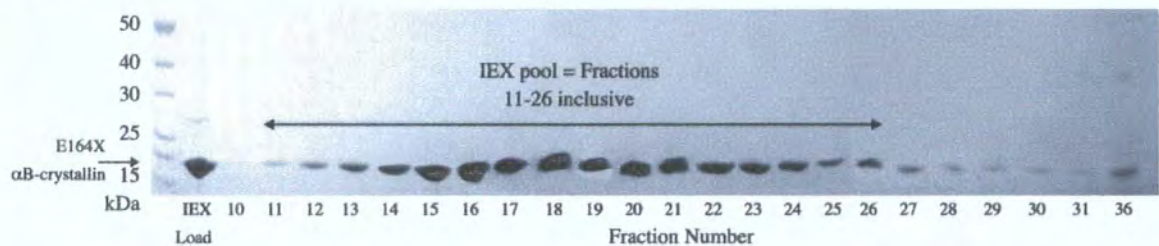


Figure 3.16. IEX Chromatography of E164X α B-crystallin and fraction analysis. The E164X α B-crystallin was initially purified by IEX (A), and the appropriate fractions for pooling were identified by reducing SDS-PAGE (B). Fractions 11-26 inclusive were enriched with α B-crystallin and were pooled to give a 10ml pool. The IEX load was almost entirely pure following the detergent washes.

3.3.3.7. E165X α B-crystallin

The E165X α B-crystallin was, like the E164X α B-crystallin construct, expressed as inclusion bodies (see Figure 3.2E) and was purified using the 6 M urea solubilisation. The E165X inclusion bodies were solubilised immediately when treated with 6M urea suggesting that extension of the E164X α B-crystallin C-terminal by just one glutamic acid can improve the solubility of α B-crystallin. This enhanced solubility correlates with the literature, where the E164X α B-crystallin mutation has been observed in the rat lens nucleus following proteolysis with LP82 and M-calpain (Ueda et al., 2002) and in human lens fiber cells growing in lens capsules following cataract surgery (Colvis et al., 2000), however removal of the terminal 11 amino acids is not disease causing for α B-crystallin but is observed for α A-crystallin in human diabetic lenses (Thampi et al., 2002).

A typical IEX purification is shown in Figure 3.17.A. SDS-PAGE analysis (see Figure 3.17.B) shows that the E165X α B-crystallin was co eluted with a band of approx 30kDa. Fractions 7-16 inclusive were enriched with E165X α B-crystallin and were subsequently pooled (see Figure 3.17.B), giving a 10 ml pool volume yielding 30 mg of the mutant in 6M urea. The pooling criteria excluded fractions 2-6 due to the presence of the contaminant band at 30 kDa. Refolding of the E165X α B-crystallin is investigated in Section 3.3.4.

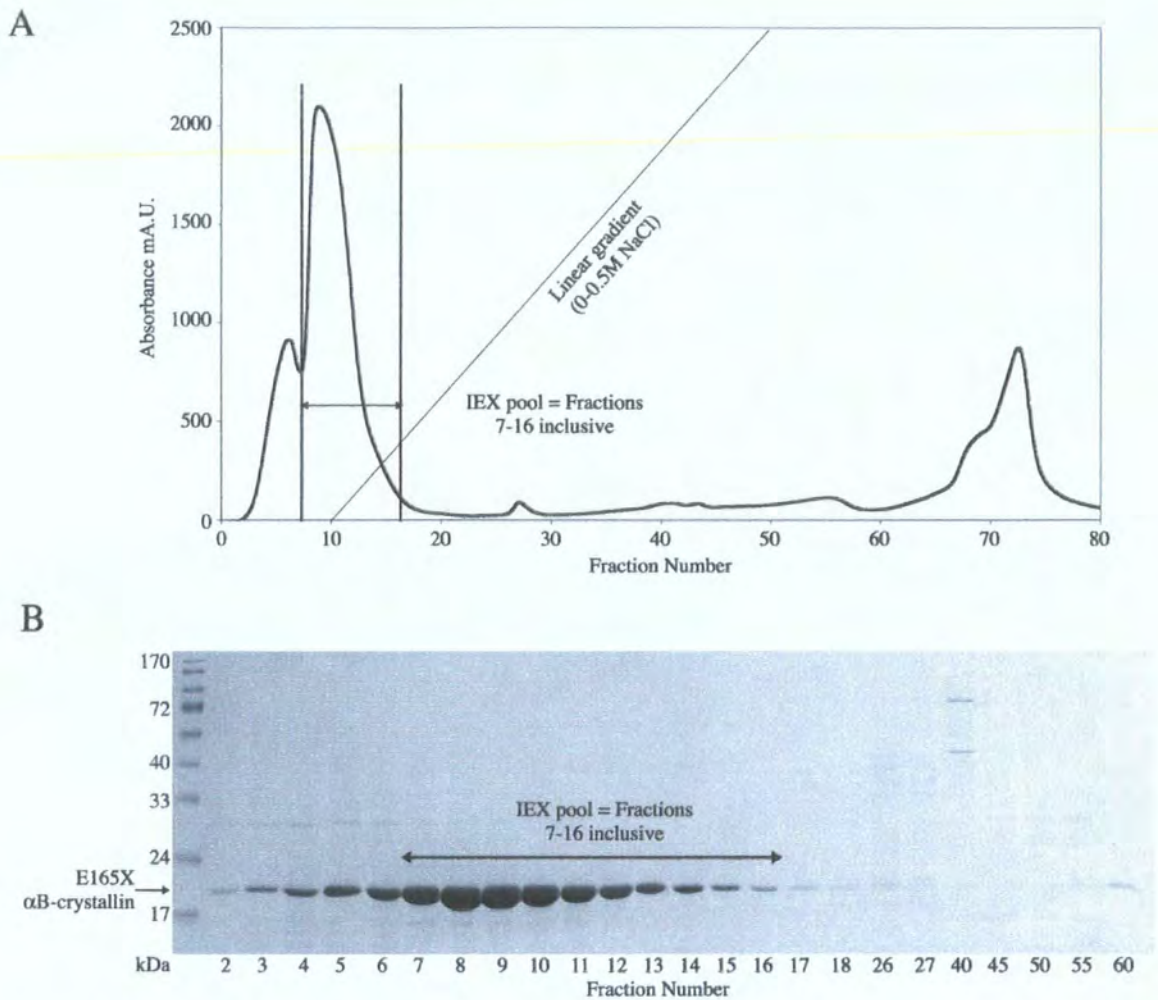


Figure 3.17. IEX Chromatography of E165X α B-crystallin and fraction analysis. The E165X α B-crystallin was purified initially by IEX (A), and the appropriate fractions for pooling were identified by SDS-PAGE (B). Fractions 7-16 inclusive were enriched with E165X α B-crystallin and were pooled to give a 10ml pool. Fractions 2-6 were excluded despite significant levels of E165X, due to the presence of a contaminating band at approx. 30kDa. Additional contaminant bands were resolved under high NaCl conditions shown in fractions 26 onwards.

3.3.3.8. Q151X α B-crystallin

The Q151X α B-crystallin is a naturally occurring mutation causing Myofibrillar myopathy (MM), like the 464delCT α B-crystallin, and was also expressed as inclusion bodies (see Figure 3.2C) therefore, subsequent purification also required the use of 6 M urea to solubilise the inclusion bodies, thus facilitating further purification by IEX (see Section 2.7). The Q151X α B-crystallin mutation involved a 25 amino acid truncation of the whole C-terminal extension so theoretically should be more insoluble than the E164X, however the Q151X inclusion bodies surprisingly were almost immediately solubilised in 6M urea compared to the 464delCT and 450delA α B-crystallin, which both required a 4h incubation to achieve solubilisation.

A typical IEX purification is shown in Figure 3.18.A and shows that the Q151X α B-crystallin was eluted under low NaCl conditions. SDS-PAGE analysis identified a very low intensity 30 kDa protein, which is difficult to visualise in Figure 3.18.B, however the protein co eluted with Q151X α B-crystallin over the leading edge of the Q151X peak and was represented by a shoulder (see Figure 3.18.A). The 30 kDa protein was resolved from fractions 14 onwards allowing fractions 14-24 inclusive to be pooled (see Figure 3.18.B), giving an 11 ml pool volume yielding 18 mg of the mutant in 6M urea. Refolding of the Q151X α B-crystallin is investigated in Section 3.3.4.

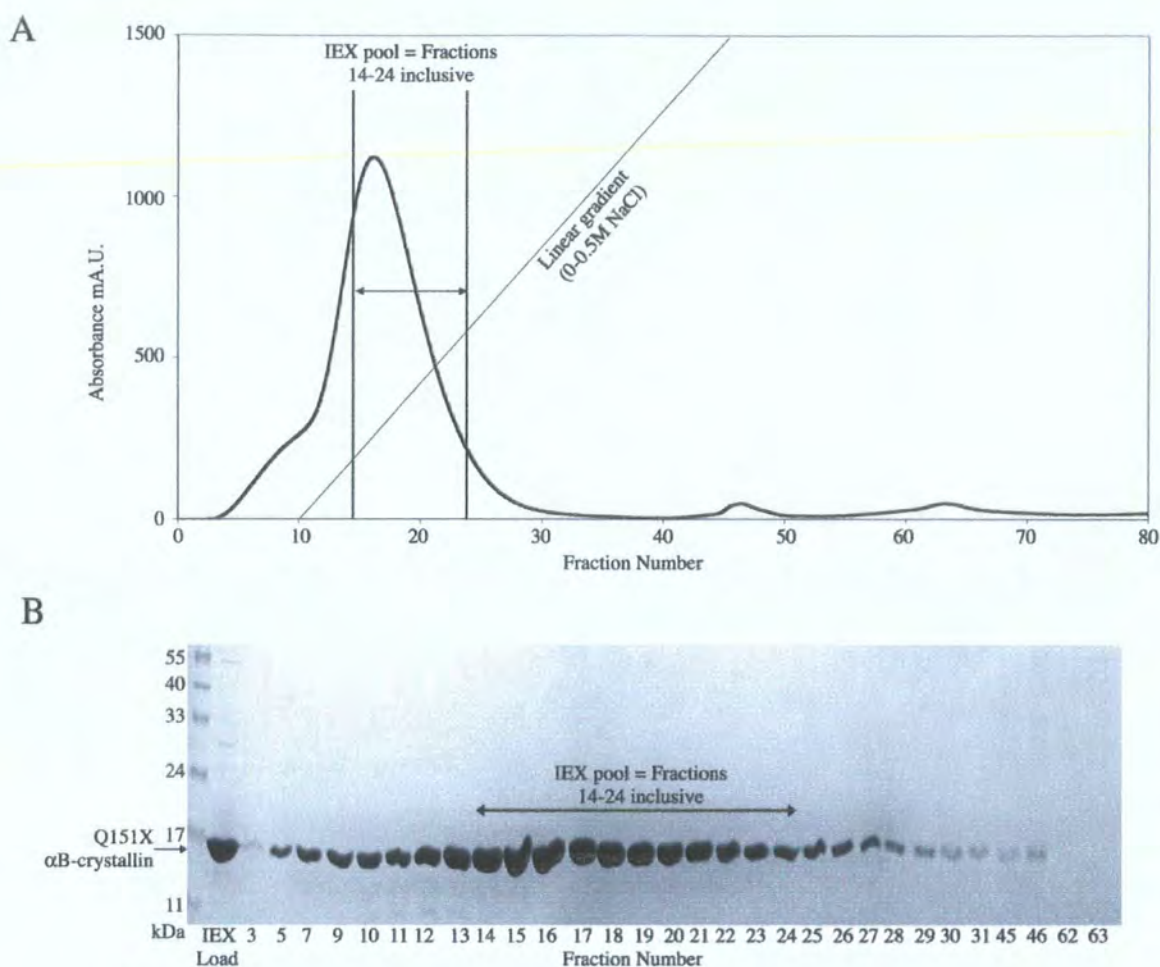


Figure 3.18. IEX Chromatography of Q151X α B-crystallin and fraction analysis. The Q151X α B-crystallin was purified initially by IEX (A), and the appropriate fractions for pooling were identified by reducing SDS-PAGE (B). Fractions 14-24 inclusive were enriched with α B-crystallin and were pooled to give a 11ml pool. Fractions 3-13 were excluded despite significant levels of Q151X, due to the presence of a contaminating band at approx. 30 kDa shown as a shoulder on the leading edge of the peak IEX. Additional contaminant bands were resolved under high NaCl conditions shown in fractions 45 onwards.

3.3.4. THE EFFECT OF THE C-TERMINAL MUTATIONS ON THE ABILITY OF THE α B-CRYSTALLIN MUTANTS TO REFOLD

The C-terminal mutations of wild type α B-crystallin have been suggested to be necessary for proper folding of α B-crystallin, subunit interactions and chaperone activity, (Harrington et al., 2004) and its solubility, (Carver et al., 1995). This suggested that the refolding of the 450delA, 464delCT, Q151X, E164X and E165X α B-crystallin, whose C-terminal were significantly altered and expression was in the form of inclusion bodies, may result in protein aggregation and precipitation.

Initial refolding analysis using 450delA α B-crystallin (see Section 3.3.4.1), was unsuccessful due to the extreme insolubility of the mutant. The refolding analysis, therefore was continued and finally optimised using Q151X α B-crystallin (see Section 3.3.4.2), after which the optimised conditions were applied to the 450delA α B-crystallin (see Section 3.3.4.3) and the other remaining α B-crystallin mutants (see Sections 3.3.4.4-3.3.4.6) to achieve the recovery of a soluble α B-crystallin mutant. The 450delA and 464delCT α B-crystallin could only be refolded successfully when associated with wild type α B-crystallin, highlighting their extreme propensity to aggregate. The refolding efficiency for each mutant α B-crystallin is summarised in Section 3.3.4.7.

3.3.4.1. Initial refold analysis using 450delA α B-crystallin

The basic refolding protocol required a one step dialysis of the IEX pool material into aqueous buffer (10mM Tris-HCl, 150mM NaCl, 1mM EGTA, 5mM EDTA, pH 7.5) over a 4 h period. This dialysis resulted in complete precipitation of the mutant α B-crystallins, with the exception of the E165X α B-crystallin, which yielded 54% soluble protein following the one-step dialysis procedure (see Section 3.3.4.4). Figure 3.19 shows an example of this complete precipitation observed for the 450delA α B-crystallin.

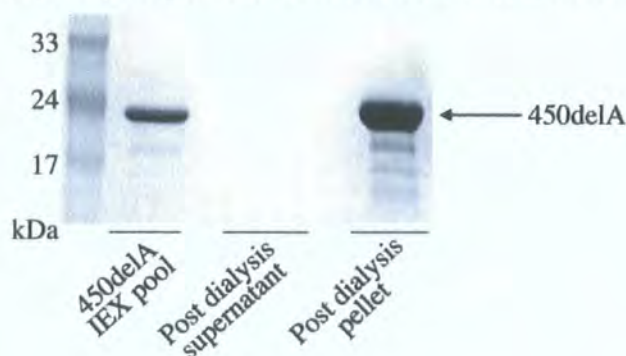


Figure 3.19. The 450delA α B-crystallin refolding procedure using a one step dialysis. The recovery of 450delA α B-crystallin is entirely in the insoluble pellet fraction, with no evidence of any 450delA in the supernatant fraction.

Optimisation of the refolding process was required in order to obtain soluble mutant α B-crystallin, thus allowing the characterisation of the 450delA, Q151X, 464delCT and E164X α B-crystallin.

Initial optimisation of the 450delA α B-crystallin refold, included varying the number of dialysis steps, dialysis temperature and duration of steps, but all failed to recover soluble 450delA α B-crystallin. Therefore, the chaperone capabilities of the wild type α B-crystallin were utilised to stabilise the 450delA α B-crystallin during the dialysis process.

The wild type and 450delA α B-crystallin were combined at a 1:1 molar ratio (10:1 ratio of wild type to 450delA α B-crystallin was investigated, but showed no improvement over the 1:1 combination). Initial combination experiments investigated the number and duration of dialysis steps. A dialysis utilising a 6-4-3-2-1-0M urea concentration step

reduction with a 12 h step interval duration at 4°C, yielded a 23% recovery of soluble 450delA α B-crystallin, (see Figure 3.20, post dialysis supernatant), however, the length of the procedure carried out to achieve the yield was not practical (60 h) and the amount of mutant was not sufficient to perform any characterisation work. Incorporating the 450delA/ wild type α B-crystallin into the one step dialysis (4 h duration) even resulted in the complete precipitation of the complex.

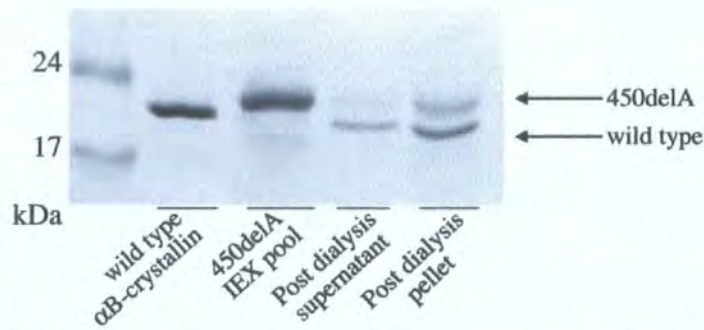


Figure 3.20. Refolding 450delA α B-crystallin in association with the wild type α B-crystallin. The step dialysis with 450delA combined with wild type, yields 23% recovery of soluble 450delA/ wild type.

This data confirmed that despite the presence of wild type α B-crystallin, it was actually the gradual reduction in urea concentration, which was successful in yielding soluble protein. Further optimisation looked to develop a refolding protocol, which would utilise an intermediate urea concentration, whilst maintaining a relatively short dialysis duration.

This optimisation was carried out with Q151X α B-crystallin due to the extreme insolubility of 450delA α B-crystallin as a homogenous solution. The recovery of a homogenous protein solution rather than a combination with wild type α B-crystallin would be preferred in order to achieve optimum characterisation of the α B-crystallin mutants.

3.3.4.2. Further refold optimisation using Q151X α B-crystallin: Analysis of the urea and protein concentration prior to dialysis

In section 3.3.4.1, I discussed how a gradual reduction of the urea concentration resulted in a more efficient refolding process. The C-terminal domain of α B-crystallin begins to fold at ≤ 2.5 M concentration of urea, (Sun et al., 1998). Therefore, the reduction of the urea concentration from 6M-1M would allow partial refolding to occur prior to dialysis, thus resulting in a relatively more stable protein being exposed to the aqueous buffer.

The relatively high protein concentrations of the mutant α B-crystallin prior to refolding (3-5 mg/ml) could be influential on the ability of the precipitation prone mutants to refold efficiently. High protein concentrations are known to affect reactions including folding and association of proteins resulting in irreversible aggregation, (Ellis and Minton, 2003), therefore, lowering the protein concentration prior to the reduction of the urea concentration may further improve the solubility during refolding, by reducing the frequency of collisions. The conditions investigated are detailed in Table 3.1 and looked to optimise both the protein concentration and the urea concentration prior to dialysis. The mutant used for the experiment was Q151X α B-crystallin.

Table 3.1. Optimisation of the urea and mutant concentration for successful refolding

Sample No.	Q151X α B-crystallin Conc. in 6M Urea (mg/ml)	Urea Conc. (M)
1	1.6	6
2	1.0	6
3	0.5	6
4	0.25	6
5	1.6	1
6	1.0	1
7	0.5	1
8	0.25	1

The samples were dialysed for 4 h at ambient temperature (16°C) and the dialysate clarified by centrifugation for 30 min at 4°C at 255000 x g. The OD₂₈₀ was measured for the soluble and insoluble fractions, from which the protein concentration was determined using the extinction coefficient for the Q151X α B-crystallin of 0.8mg⁻¹ml⁻¹cm⁻¹. Extinction Coefficients were determined from the amino acid sequence using the Emboss Pepstats programme (www.ebi.ac.uk/emboss/pepinfo/).

The yields of soluble Q151X α B-crystallin are shown in Figure 3.21 and represent the amount of soluble protein recovered in the centrifugation supernatant, as a percentage of the amount of Q151X α B-crystallin dialysed.

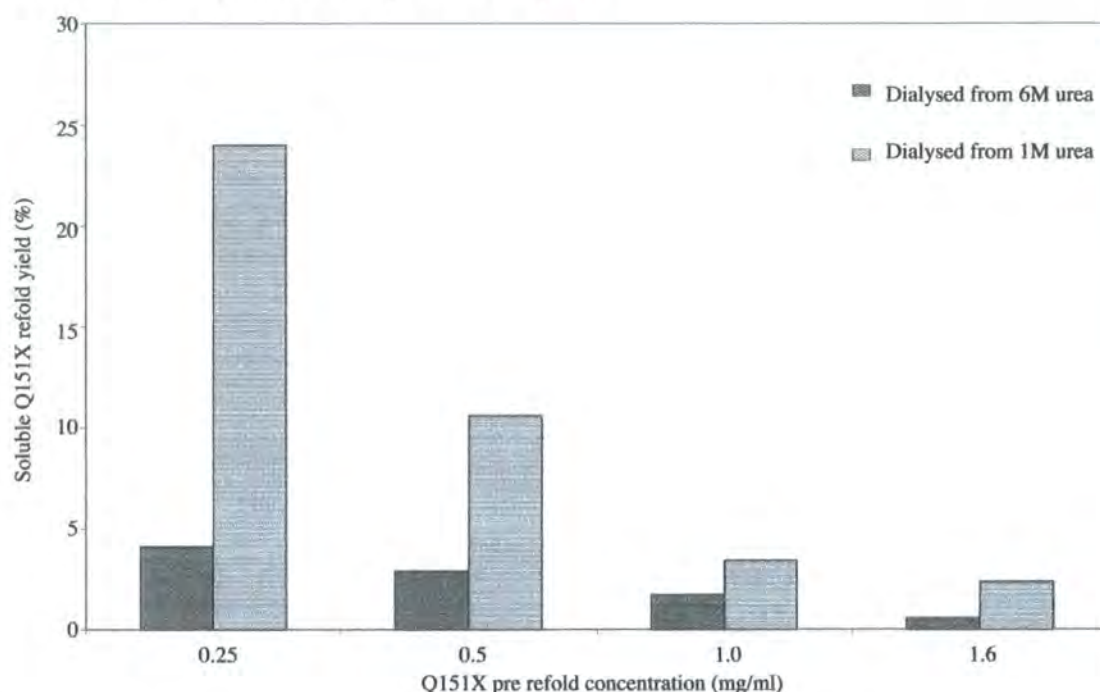


Figure 3.21. The effect of protein and urea concentration on soluble Q151X α B-crystallin yield. The optimisation of sample conditions required for successful refolding involved varying the urea concentration and the Q151X concentration in urea prior to refold dialysis.

Figure 3.21 shows that reducing the protein concentration results in an increased yield of soluble Q151X α B-crystallin, which is further increased by the dilution of urea from 6M to 1M prior to dialysis. For example, Q151X was diluted to 0.25mg/ml using 6M urea buffer, followed by a 6X dilution of urea to 1M, which produced a protein concentration of 0.04 mg/ml. These refolding conditions resulted in a soluble Q151X α B-crystallin yield of 24%.

This is significant as it allows characterisation of the mutant without the presence of other stabilising chaperones, however the resulting protein concentration of 0.013 mg/ml was too low to enable any characterisation of mutant α B-crystallin.

The refold was performed for a larger 1.2 mg scale with the aim to increase the amount of recovered soluble Q151X α B-crystallin. The refolding utilised the optimised conditions, where the Q151X α B-crystallin was diluted to 0.25 mg/ml using 6 M urea buffer, followed by a 6X dilution of the urea concentration to 1M prior to dialysis. The duration of the centrifugation step was increased to 2 h from 30 min to ensure all the aggregated Q151X α B-crystallin was sedimented. The soluble Q151X α B-crystallin was concentrated from 0.024 mg/ml using an Amicon spin concentrator (Millipore, Watford, UK) to 0.255 mg/ml, resulting in a 20-fold concentration factor. The yield of soluble Q151X α B-crystallin over the spin concentration was 66% resulting in an overall 17% yield. The resulting yields are summarised in Table 3.2.

Table 3.2. Yield of Q151X α B-crystallin over the diluted refolding process from 1.2 mg

Stage	Q151X conc. mg/ml	Volume ml	Total Q151X Mg	Yield	Step Yield
Protein dilution	0.25	4.853	1.2	100	100
Urea dilution	0.04	29.01	1.2	100	100
Post dialysis and clarification	0.013	24	0.31	25	25
Post concentration	0.26	0.17	0.20	17	66

The yield and concentration of the Q151X was sufficient for characterisation, however, with only 0.17 ml of the refolded mutant, the final volume is not sufficient for any subsequent experiments.

The refold was performed for a larger 12 mg scale with the aim to provide both the required concentration and volume of Q151X α B-crystallin. The scale up of the refold procedure was limiting due the large process volumes encountered upon dilution to 0.25 mg/ml and 1M urea. A starting amount of Q151X of 12 mg (7.3 mg/ml) resulted in a dialysis volume of approx. 300ml, therefore after the dialysis, a preliminary concentration

was required using an Amicon spin concentrator (Millipore, Watford, UK) to 48ml to accommodate the volumes held by the centrifuge. Following a 2 h centrifugation a final concentration was performed to a volume of 1ml. The yield of soluble Q151X α B-crystallin over the spin concentration was 4.6% resulting in an overall 0.91% yield. Despite this fall in yield compared to the 1.2 mg refold (see Table 3.4), the resulting Q151X α B-crystallin was at 0.11 mg/ml in 1ml volume, which was sufficient for further characterisation work. The resulting yields are summarised in Table 3.3.

Table 3.3. Yield of Q151X α B-crystallin over the diluted refolding process from 12mg

Stage	Q151X conc. mg/ml	Volume ml	Total Q151X mg	Yield	Step Yield
Protein dilution	0.25	46.72	12	100	100
Urea dilution	0.04	280.32	12	100	100
Post dialysis and clarification	0.035	48	1.7	14.2	14.2
Post concentration	0.11	1.0	0.11	0.91	4.6

The yield of 0.91% was very low and subsequently, an experiment combining the Q151X with wild type α B-crystallin at a 1:1 molar ratio was carried out to assess whether a greater yield of Q151X α B-crystallin could be achieved. Although the product would not be homogenous it would still be very useful to investigate the effect of the Q151X mutation upon the function of α B-crystallin.

Initially the refold of Q151X/ wild type was performed without any dilutions prior to dialysis (direct dialysis protocol), however resulted in complete precipitation of the Q151X/ wild type α B-crystallin. The optimised refolding conditions, which involved modification to the urea and protein concentration prior to dialysis (diluted protocol), were applied to the Q151X/ wild type α B-crystallin and the resulting yield data are shown in Table 3.4. The refolded complex of Q151X/ wild type α B-crystallin was shown by SDS-PAGE to maintain the 1:1 molar ratio throughout the refolding (data not shown), thus the yield data represents a 1:1 complex of wild type to Q151X α B-crystallin.

Table 3.4. Refolding efficiency of Q151X/ wild type using the diluted protocol.

Stage	Q151X/ wt conc. (mg/ml)	Volume (ml)	Total Q151X/ wt (mg)	Yield (%)
Pre dialysis	5.2	2.4	12.4	100
Protein dilution	0.25	50.0	12.4	100
Urea dilution	0.042	300	12.4	100
Post concentration	0.45	3.0	1.35	11

The refolding of Q151X associated with the wild type α B-crystallin, following the diluted protocol, resulted in a 10-fold increase of the yield of soluble Q151X/ wild type α B-crystallin (11 %) compared to the homogenous Q151X α B-crystallin (0.91 %) as shown in Table 3.5.

3.3.4.3. Refolding of 450delA α B-crystallin

The recovery of soluble homogeneous Q151X α B-crystallin using the diluted protocol (see Section 3.3.4.2, Figure 3.7) suggested the possibility that soluble homogeneous 450delA α B-crystallin may be obtained utilising this method. The optimised refolding conditions resulted in complete precipitation of the 450delA α B-crystallin as a homogeneous solution, however, yielded soluble 450delA α B-crystallin when combined with wild type α B-crystallin at a 1:1 molar ratio (see Figure 3.22).

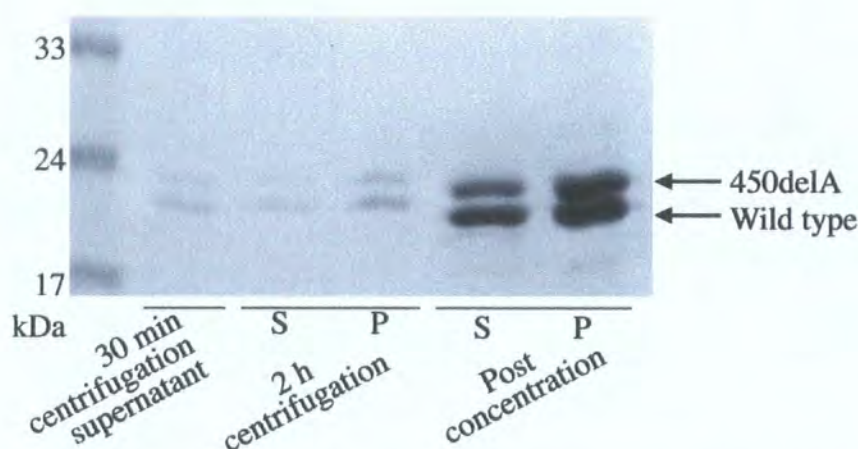


Figure 3.22. Refold of 450delA/ wild type α B-crystallin using diluted protocol. The centrifugation step was developed from 30 min to 2 h to ensure entire sedimentation of aggregated protein. The resulting 2 h supernatant was concentrated to 0.48 ml to achieve a sufficient protein concentration.

The soluble 450delA/ wild type α B-crystallin, (see Figure 3.26, post concentration supernatant), was concentrated using an Amicon spin concentrator (Millipore, Watford, UK) to achieve the required protein concentration. The yield of soluble 450delA/ wild type α B-crystallin is detailed in Table 3.5.

Table 3.5. Yield of 450delA: wild type α B-crystallin mixture (1:1 molar ratio) over a 1.2 mg diluted refolding process

Stage	450delA: WT conc. (mg/ml)	Volume (ml)	Total 450delA/ wt (mg)	Yield (%)	Step Yield (%)
Pre dialysis	1.62	0.75	1.2	100	100
Protein dilution	0.25	4.83	1.2	100	100
Urea dilution	0.042	29.16	1.2	100	100
Post centrifugation	0.024	27.5	0.66	55	55
Post concentration	0.361	0.48	0.159	13	24

The diluted protocol for refolding resulted in a 13% yield soluble 450delA/ wild type α B-crystallin, (0.361mg/ml), similar to the 17% yield of Q151X α B-crystallin, (0.255mg/ml). The significant difference however, is that the Q151X α B-crystallin could be refolded as a single protein solution, whereas the 450delA α B-crystallin required combination with the wild type α B-crystallin for soluble recovery.

3.3.4.4. Refolding of E165X α B-crystallin

Refolding of the E165X α B-crystallin was successful without any modifications to the urea and protein concentrations prior to dialysis. The dialysis showed no visible precipitate, typically seen with 450delA and Q151X α B-crystallin at this stage. Clarification by centrifugation at 4°C for 2h at 255000 x g produced a clear pellet. The yield of soluble E165X α B-crystallin was quantified by OD₂₈₀ measurements (see Table 3.6.)

Table 3.6. Yield of E165X α B-crystallin from direct one step dialysis

Stage	E165X conc. (mg/ml)	Volume (ml)	Total E165X (mg)	Yield (%)	Step Yield (%)
Pre dialysis	1.6	6	9.7	100	100
Post centrifugation	0.90	6	5.3	54	54

The yield of E165X α B-crystallin was 54% at a protein concentration of 0.9 mg/ml. The refolding data suggests that the modifications to the C-terminal extension introduced by the Q151X and 450delA mutations produced mutant α B-crystallin unable to refold by direct dialysis due to their extreme insolubility under aqueous conditions. In contrast, the E165X mutation produced a mutant α B-crystallin whose solubility was significantly greater thus was able to refold to achieve a 54 % yield of soluble E165X α B-crystallin.

3.3.4.5. Refolding of 464delCT α B-crystallin

Based on the refolding optimisation performed with Q151X α B-crystallin (see Section 3.3.4.2), an initial experiment was performed looking at the refolding efficiency of the 464delCT α B-crystallin as a homogeneous protein solution, using both the direct dialysis and diluted protocol. Both protocols resulted in complete aggregation of the 464delCT α B-crystallin, thus yielding no soluble protein. Therefore, the dialysis experiments were repeated with the 464delCT α B-crystallin in combination with the wild type α B-crystallin at a 1:1 molar ratio (see Figure 3.23).

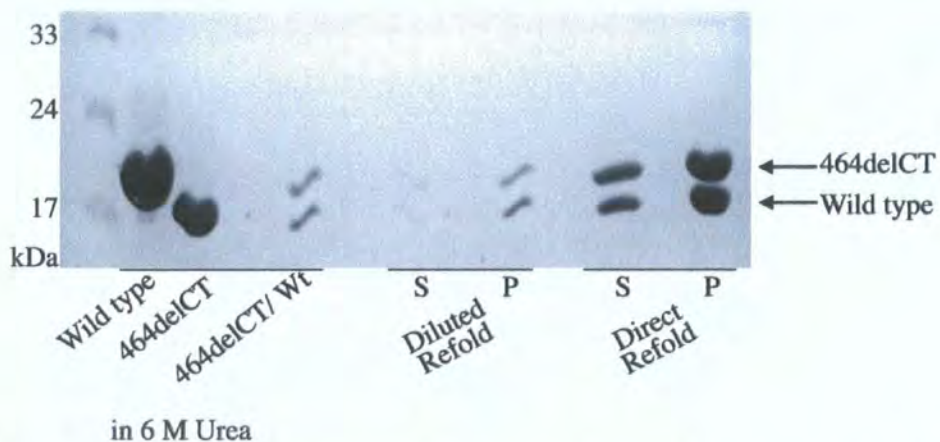


Figure 3.23. Optimisation of the 464delCT α B-crystallin refold process. The experiment investigated refolding in association with wild type α B-crystallin using both the diluted and the direct dialysis protocol. The association with wild type was successful in refolding 464delCT α B-crystallin using both dialysis protocols.

Figure 3.23 illustrates that the 464delCT α B-crystallin when associated with the wild type α B-crystallin can be successfully refolded to yield soluble protein without the need for dilution. The refold yields are detailed in Table 3.7 and 3.8.

Table 3.7. Refolding efficiency of 464delCT/ wild type α B-crystallin using the diluted protocol

Stage	464delCT/ Wt conc. (mg/ml)	Volume (ml)	Total 464delCT/ Wt (mg)	Yield (%)	Step Yield (%)
Pre dialysis	2.0	1.0	2.0	100	100
Protein dilution	0.25	8.0	2.0	100	100
Urea dilution	0.042	48.0	2.0	100	100
Post centrifugation	0.024	48.0	1.2	60	60
Post concentration	0.72	0.1	0.07	3.6	6

Table 3.8. Refolding efficiency of 464delCT/ wild type α B-crystallin using the direct dialysis protocol

Stage	464delCT/ Wt conc. (mg/ml)	Volume (ml)	Total 464delCT/ Wt (mg)	Yield (%)
Pre dialysis	2.0	1	2.0	100
Post centrifugation	0.25	1	0.25	12.5

The refold yield data clearly illustrates that although the diluted protocol yields a 0.72 mg/ml solution, the volume was only 0.1 ml, which was not sufficient for any subsequent experiments. The direct dialysis refold protocol with no dilution however, resulted in a relatively lower concentration of 0.25 mg/ml but in a 1 ml volume, which therefore achieves both objectives of sufficient concentration and volume to allow characterisation to be performed.

The 464delCT, can be successfully refolded without the need for dilution, however requires the presence of a 1:1 molar ratio of wild type α B-crystallin. This suggests although very unstable, the 464delCT mutation has a less severe effect on the solubility

than the 450delA (whose refold requires both dilution and combination with wild type) and a more severe effect than the Q151X, which can be successfully refolded as a homogenous protein solution using the diluted protocol.

3.3.4.6. Refolding of E164X α B-crystallin

As seen previously in Section 3.3.4.4, the E165X was successfully refolded as a homogenous solution without the need for dilution, therefore we should expect the E164X, with only one less amino acid, to have similar solubility characteristics. An experiment investigated the refolding efficiency of E164X α B-crystallin under the diluted and direct dialysis protocol as a homogenous protein (see, Figure 3.24).

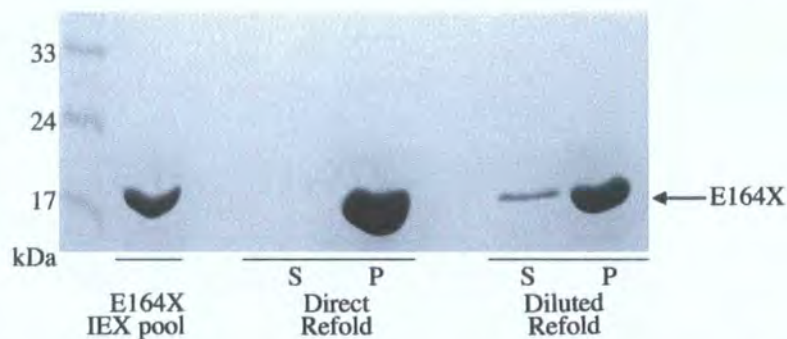


Figure 3.24. Refolding efficiency of E164X using the diluted and direct dialysis protocols. The E164X α B-crystallin was found entirely in the pellet fraction when using the direct dialysis protocol however, with the diluted protocol, E164X α B-crystallin was observed in the soluble fraction.

Figure 3.24 illustrates that the E164X α B-crystallin can be successfully refolded to yield soluble protein, but requires dilution of both the protein and urea concentration prior to dialysis. The refold yields are detailed in Table 3.9 and 3.10.

Table 3.9. Refolding efficiency of E164X using the diluted protocol

Stage	E164X conc. (mg/ml)	Volume (ml)	Total E164X (mg)	Yield (%)
Pre dialysis	4.5	0.4	1.8	100
Protein dilution	0.25	7.2	1.8	100
Urea dilution	0.042	43.2	1.8	100
Post centrifugation	0.021	43.2	0.87	48
Post concentration	0.21	0.5	0.11	13

Table 3.10. Refolding efficiency of E164X using the direct dialysis protocol

Stage	E164X conc. (mg/ml)	Volume (ml)	Total E164X (mg)	Yield (%)
Pre dialysis	4.5	1	4.5	100
Post centrifugation	0.08	1	0.08	1.8

Both Figure 3.24 and Tables 3.9 and 3.10 clearly illustrate that the refolding yield of homogenous E164X α B-crystallin was optimal when using the diluted protocol and resulted in a 0.5 ml volume at 0.21 mg/ml. Despite the E164X α B-crystallin being only one glutamic acid shorter than the E165X α B-crystallin, it showed refolding requirements similar to the highly insoluble Q151X α B-crystallin. This data strengthens the argument that the C-terminal extension is important for maintaining the solubility of α B-crystallin and those mutants, which, display extreme insolubility have been associated with various disease states.

3.3.4.7. Summary of refold optimisation for α B-crystallin mutants

The analysis of the refolding efficiency of the α B-crystallin mutants achieved optimised refolding protocols for each mutant α B-crystallin. These protocols were used for all future refolding as a means to provide material for characterisation experiments. Summaries of subsequent refolding procedures are detailed in Table 3.11 and show data from three separate refolds for each mutant α B-crystallin.

Table 3.11. Summary of refold efficiency of α B-crystallin mutants

α B-crystallin (Refold protocol)	Pre dialysis (mg)	Yield (mg)	Yield (%)	Standard Deviation (\pm)	Average Yield (%)
450delA/ wild type (Diluted)	7.7	0.4	4.8	1.8%	6.8
	12.4	1.0	7.9		
	12.4	1.0	7.8		
464delICT/ wild type (Direct)	12.3	1.2	9.6	1.6%	10.5
	2.0	0.2	9.6		
	2.0	0.2	12.4		
Q151X/ wild type (Diluted)	12.4	1.4	10.9	2.6%	10.2
	5.0	0.4	7.4		
	1.6	0.1	6.4		
Q151X (Diluted)	12.0	0.2	1.7	0.4%	1.4
	11.7	0.2	1.7		
	11.7	0.1	0.9		
E164X (Diluted)	12.0	1.2	10.2	2.5%	12.0
	12.0	1.3	10.9		
	12.0	1.8	14.8		
E165X (Direct)	6.3	0.7	10.6	1.6%	10.5
	1.2	0.1	8.9		
	6.3	0.8	12.0		

The purified and refolded α B-crystallin mutants are illustrated in Figure 3.25. The SDS-PAGE analysis highlights the relative changes in Mwt conferred by the mutations. The 450delA and 464delCT α B-crystallin are the only mutants whose insolubility required refolding in association with α B-crystallin wild type.

The Q151X was also refolded with the wild type to allow a direct comparison with the other disease mutants, however could be refolded as a homogenous complex. The 450delA mutation has a unique characteristic in that it does not form a 1:1 molar ratio with the wild type α B-crystallin similar to the 464delCT and the Q151X α B-crystallin. The SDS-PAGE analysis revealed that the wild type α B-crystallin is present in excess compared to the 450delA α B-crystallin.

In fact, this proved to be the maximum ratio compatible with protein solubility for the 450delA/ wild type α B-crystallin complex and is in stark contrast to 464delCT α B-crystallin, where a 1:1 mixture with wild type α B-crystallin resulted in a refolded protein mixture with a 1:1 molar ratio of wild type/ 464delCT α B-crystallin as shown by the equal intensity of the wild type and 464delCT α B-crystallin protein bands depicted in Figure 3.25.

The 450delA α B-crystallin is also unique in that the mutation introduces a novel extended C-terminal extension, which could potentially hinder the associations required to achieve a 1:1 ratio by physically masking the necessary binding sites.

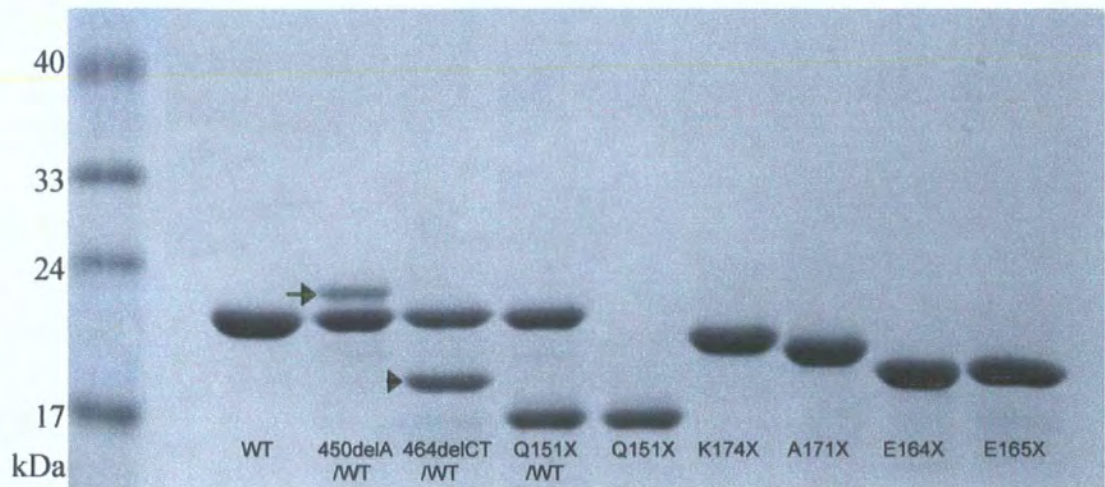


Figure 3.25. Characterisation of the bacterially expressed and purified mutants used in this study by SDS-PAGE. The 450delA (arrow) and 464delCT (arrowhead) mutants could not be produced as individual soluble proteins and therefore were refolded in the presence of wild type α B-crystallin.

3.4. DISCUSSION

The principal role of the C-terminal 'tail' had been identified as a polar solubilizing agent for the relatively hydrophobic sHSPs and the sHSP–client complex, which forms upon chaperone action, but are not involved in binding directly to the substrate (Smulders et al., 1996). They may also serve as 'spacers' in preventing subunits from approaching too close to one another which, without their presence, would result in aggregation and precipitation due to hydrophobic interactions between sHSP–client complexes. If the polarity and flexibility of the extensions are disrupted, the solubility and chaperone activity of the protein are reduced significantly (Lindner et al., 2000).

In α B-crystallin, there had not been any systematic analysis of the role of the C-terminal extension and therefore no potential explanation of how alterations to the C-terminal extension disrupt the solubility of the protein. In this Chapter, I have investigated a series of mutations including two truncated C-terminal α B-crystallin mutants of interest (K174X and E165X), along with the three naturally occurring disease causing mutants (450delA, Q151X and 464delCT) and the PTMs (E164X and A171X). This study investigated the role of specific regions of the C-terminal extension important in solubilisation of α B-crystallin oligomers, thus providing the basis for further characterisation of the relationship between the C-terminal extension, the chaperone function, oligomerisation and the relationship with disease.

3.4.1. The role of the C-terminal 'tail' in the solubilisation of α B-crystallin

The role played by the C-terminal 'tail' in solubilising the α B-crystallin complex, would suggest that the naturally occurring mutations 450delA, 464delCT and Q151X α B-crystallin, the post translational modification E164X and the truncation E165X α B-crystallin, would be expressed as insoluble inclusion bodies with the post translational modification A171X and truncation K174X being expressed as soluble protein similar to the wild type α B-crystallin. The nature of the disease mutants is to form aggregates within the lens (450delA, E164X) and muscle tissue (464delCT and Q151X) thus, providing a link between the effect of a severely altered C-terminal and the solubility of the expressed protein.

Expression of the α B-crystallin mutants in both bacterial and mammalian cells revealed an influence of the altered C-terminal on the solubility of α B-crystallin. In *E.coli* cells the 450delA, 464delCT, Q151X, E164X and E165X α B-crystallin were expressed as inclusion bodies with soluble expression being observed for K174X and A171X α B-crystallin. Similar effects were seen in mammalian MCF7 cells, where for the 450delA, 464delCT, Q151X and the E164X α B-crystallin clear cytoplasmic aggregates were observed. In contrast, however the E165X α B-crystallin displayed a homogenous cytoplasmic distribution of α B-crystallin similar to the K174X, A171X and wild type α B-crystallin.

Further effects of the C-terminal mutations were evident in the varying ability of the recombinant α B-crystallin mutants to refold efficiently without aggregation. Refolding directly from 6 M urea to aqueous buffer resulted in rapid and complete aggregation of the 450delA, 464delCT, Q151X and E164X α B-crystallin, all of which were expressed in *E.coli* as inclusion bodies. In contrast, however the E165X α B-crystallin remained soluble resulting in a refolded, soluble protein showing similar solubility characteristics to E165X α B-crystallin expressed in MCF7 cells.

The highly insoluble α B-crystallin mutants (the 450delA, 464delCT, Q151X and E164X) were successfully refolded by lowering of the urea and protein concentrations prior to dialysis, thus allowing the protein to partially refold before exposure to the aqueous buffer and preventing immediate aggregation.

It was evident that the C-terminal extension was playing a role in the solubility of these mutants and despite the expression of E165X α B-crystallin as inclusion bodies, once refolded it was a relatively soluble protein. Despite its inherent insolubility, the E164X α B-crystallin was successfully refolded as a homogenous complex by partial refolding before dialysis to remove the denaturing buffer, showing a greater propensity to aggregate than the E165X α B-crystallin despite being only one glutamic acid shorter.

The removal of the entire C-terminal extension by the Q151X mutation did not prevent the refolding and recovery of a soluble homogenous complex of the Q151X α B-crystallin. The yield however, was significantly lower than the E164X α B-crystallin, highlighting the important role of both the flexible and the non-flexible C-terminal in maintaining solubility. Combination of the Q151X with the wild type α B-crystallin resulted in a 10X increase in the refold yield.

Both the 450delA and 464delCT α B-crystallin could only be refolded in the presence of the wild type α B-crystallin, with the 464delCT α B-crystallin refolding by direct dialysis. The 450delA α B-crystallin proved the most difficult to refold from 6M urea and keep soluble as both a combination with the wild type and prior lowering of the urea and protein concentration was required in order to produce refolded 450delA α B-crystallin of a similar yield to the 464delCT α B-crystallin.

Expression and purification of the α B-crystallin mutants has revealed that a sequentially modified C-terminal extension results in an equally sequential loss of solubility of the respective mutants.

The data presented in this Chapter support the literature, which has shown that the terminal 11 residues of α B-crystallin are highly mobile and the maintenance of its polarity and flexibility facilitates solubilisation of the complex (Carver, 1999; Carver et al., 1992). Therefore, the 'tail' is present to offset the large degree of hydrophobicity exposed to solution by the α B crystallin.

The data in this Chapter identify specific regions of the C-terminal extension important in the solubilisation of α B-crystallin complex. All the α B-crystallin mutants whose C-terminal 'tail' had been removed or modified were highly insoluble but to varying degrees. The E164X, E165X and Q151X α B-crystallins are simple truncations removing the 'tail' region, whereas the 464delCT α B-crystallin incorporates an 8 codon missense mutation and a premature stop codon resulting in a 162 residue mutant. The 450delA α B-crystallin shows the greatest modification by the introduction of a novel 35 amino acid sequence producing a 184 residue protein. The relative solubility of the mutants is reflected by the nature of the specific mutation, with solubility diminishing as the C-terminal mutations become more severe. The A171X and K174X α B-crystallin mutants were soluble and were similar to the wild type suggesting that despite the truncations there were sufficient charge-charge interactions with the remainder of the C-terminal 'tail' to ensure sufficient solubility.

Most surprising are the differences in solubility between the E165X and the E164X α B-crystallin, where both are expressed as inclusions in *E.coli* but during refolding the E165X α B-crystallin proves to have a higher level of solubility. In a mammalian cell environment the E165X α B-crystallin shows homogeneous cytoplasmic distribution similar to the wild type α B-crystallin, however, the E164X α B-crystallin is highly insoluble and forms perinuclear aggregates similar to the Q151X α B-crystallin.

The E165X and E164X mutations both involve the removal of the entire flexible 'tail' ($_{165}\text{EKPAVTAAPKK}_{175}$) exposing the $_{163}\text{REEK}_{166}$ motif and the interface between the non-flexible and flexible part of the C-terminal extension. In addition, the removal of the entire $_{163}\text{REEK}_{166}$ motif (R163X) also resulted in highly insoluble protein aggregates (Treweek et al., 2007).

In contrast studies have shown that for α A-crystallin the sequential removal of this $_{163}\text{REEK}_{166}$ motif does not affect the solubility of the resulting α A-crystallin protein (Rajan et al., 2006) but does reduce the chaperone activity and oligomerisation. In contrast, other studies have shown the truncation of the terminal amino acid residue caused insolubility of α A-crystallin (Aziz et al., 2007) and complete removal of the $_{163}\text{REEK}_{166}$ motif by the R157X mutation (αA_{156}) resulted in the formation of large insoluble aggregates (Andley, U, 1996).

The Rajan, 2006 study identified an important role for the $_{163}\text{REEK}_{166}$ motif in the oligomerisation of αA -crystallin, especially the Arg_{163} which provides a positive charge for intersubunit electrostatic interactions in the C-terminal extension needed to form oligomeric complexes. (Rajan et al., 2006).

A recent study of αB -crystallin by Ghosh et.al, 2006 saw the removal of the polar C-terminal sequence ($_{155}\text{PERTIPITREE}_{165}$) (Ghosh et al., 2006), which involved the disturbance of the $_{163}\text{REEK}_{166}$ motif and saw removal of the highly conserved IX/(I/V) motif ($_{159}\text{IPI}_{161}$). The removal of these two motifs, both of which are found to participate in inter subunit interactions (Pasta et al., 2004; Rajan et al., 2006) resulted in poor solubility despite the retention of 10 of the terminal 11 'tail' residues and little or no chaperone activity. A very recent study, which involved mutations of the C-terminal lysines and glutamic acid residues, resulted in proteins with altered oligomerisation and enhanced chaperone activity against amyloid fibril formation (Treweek et al., 2007).

Therefore, the insolubility of E164X and E165X αB -crystallin during refolding is primarily caused by the deletion of the C-terminal 'tail' region, however additional insolubility of the E164X may be caused by the further disturbance of the $_{163}\text{REEK}_{166}$ motif. The recent studies (Ghosh et al., 2006; Pasta et al., 2004; Rajan et al., 2006) demonstrated the importance of both flexible and non-flexible C-terminal residues, in maintaining solubility and highlight the potential influence of the $_{163}\text{REEK}_{166}$ motif in the solubilisation of αB -crystallin, perhaps through a different mechanism involving the chaperone function and oligomerisation.

The effect of the disease causing C-terminal mutations on αB -crystallin solubility was as expected with high levels of aggregation being observed in both a bacterial and mammalian cell environment. However the mechanism, which causes a variation in pathology between the myofibrillar myopathy mutants (Q151X and 464delCT) and the posterior polar cataract mutant (450delA), remains unclear. The mutants display a varying level of insolubility during the refold process as a function of the severity of the alterations to the C-terminal extension, however this does not provide a link between the mutation and the disease mechanism.

3.5. CHAPTER'S CONCLUSIONS

In this Chapter, I wanted to investigate the relationship between the solubility of α B-crystallin and the C-terminal extension with the aim to provide further understanding of the mechanism that causes the phenotypic variation experienced with the disease mutants of α B-crystallin. It was clear that the flexible C-terminal 'tail' was essential to produce a stable α B-crystallin complex and that perhaps additional regions in the non flexible region of the C-terminal extension also conferred an additional level of solubility to the complex, through a mechanism that also involved the oligomerisation and chaperone function (Ghosh et al., 2006). The C-terminal extension can influence the structure and function of α B-crystallin apart from the solubilising function that is generally attributed to this region. Attempting to gain understanding of the mechanism of phenotypic variation by only investigating the solubility perhaps gives a one-dimensional view of the system involved. Further understanding of the disease mechanism requires characterisation of the chaperone activity and oligomerisation properties of these C-terminal mutations. This additional characterisation will help to provide a link between the structural and functional properties of the C-terminal mutants and the associated disease phenotypes.

CHAPTER 4

THE ROLE OF THE C-TERMINAL EXTENSION IN THE OLIGOMERISATION AND CHAPERONE FUNCTION OF α B-CRYSTALLIN

4.1. AIMS

In Chapter 3, I used the sequential truncations of the C-terminal extension (K174X and E165X), the PTM truncations (A171X and E164X) and the disease causing mutants (450delA, 464delCT and Q151X) to show how the flexible C-terminal ‘tail’ was essential to produce a stable α B-crystallin complex. The data suggested that perhaps additional regions in the non-flexible region of the C-terminal extension also conferred an additional level of solubility to the complex, through a mechanism that also involved the oligomerisation and chaperone activity.

In this chapter, I wanted to investigate the role of the C-terminal extension in oligomerisation and chaperone activity, thus characterising the effects of these C-terminal extension mutants upon the structure and function of α B-crystallin.

This further characterisation of the C-terminal extension aimed to elucidate the mechanism that links the C-terminal extension with the chaperone function, oligomerisation and solubility and how the three naturally occurring mutations of this C-terminal extension not only cause disease, but also result in the varying pathology of isolated polar posterior cataract (450delA) and MM (464delCT and Q151X).

4.2. INTRODUCTION

The C-terminal extension can influence the structure and function of α B-crystallin apart from the solubilising function that is generally attributed to this region. It appears that this region can have either inter- or intra-molecular tertiary interactions that contribute significantly to the chaperone function and oligomerisation characteristics (Pasta et al., 2002).

In its native state in the lens, α -crystallin is always found as a heterogeneous oligomeric assembly consisting of a 3:1 ratio of α A to α B-crystallin subunits that self-associate to form polydisperse assemblies with a wide Mwt distribution of 300000 to over one million Daltons (Horwitz, 1993). With a similar Mwt of 19909Da and 20159Da for α A- and α B-crystallin respectively, the native complex with an average molecular mass of 800 kDa (Groenen et al., 1994) may consist of between 15-50 subunits (Groenen et al., 1994; Horwitz, 2003). The α -crystallin oligomer shows self-interaction due to the interactions between the α A-crystallin subunits rather than the α B-crystallin subunits. On the other hand, the α B-crystallin had a stronger binding activity than α A-crystallin to β - and γ -crystallin (Kamei and Matsuura, 2002). Therefore, α A- and α B-crystallin may play different roles when α -crystallin displays chaperone-like activity, and also that the decreased chaperone-like activity of α -crystallin finally results in cataract formation following aggregation and insolubilization of lens proteins (Kamei and Matsuura, 2002).

The nature of the oligomers formed by α B-crystallin were determined by tandem mass spectrometry to reveal a distribution primarily of oligomers containing 24-33 subunits with a dominant species composed of 28 subunits. Additionally low levels of oligomers as small as 10 and as large as 40 subunits were observed (Aquilina et al., 2003). In extra lenticular tissues α B-crystallin forms heterogeneous oligomers with the small heat shock protein HSP27 (Zantema et al., 1992).

A number of interactive domains have been identified in human α B-crystallin and have been suggested to have a dual role in chaperone function and oligomerisation (see Table 4.1). These specific interactive domains are responsible for the recognition and selection mechanisms of α B-crystallin and other sHSPs for similar subunits, unfolding

substrate proteins, or assembling filament proteins (Ghosh et al., 2006b; Ghosh et al., 2006c).

Seven interactive domains for chaperone activity (CS1-CS7) have been identified (see Table 4.1 and Figure 4.1) and overlap five previously identified sites required for subunit interaction (Ghosh et al., 2005). In addition, other studies have identified numerous peptides such as mini α BC, RS-1, RS-2 and ATP1 (see Table 4.1), which are influential upon the chaperone activity and oligomerisation of α B-crystallin and represent partial regions of the seven interactive sites identified by Ghosh et al. (2005). These studies suggest that particular interactive regions of α B-crystallin have dual roles in oligomerisation and chaperone function. The location of these interactive regions in relation to the α B-crystallin C-terminal extension mutants (see Figure 4.1B.) also highlight the potential effect the mutations may have upon the structure and function of α B-crystallin.

Table 4.1. Interactive sites of α B-crystallin and their numerous functions. The interactive sites involved in the chaperone function are denoted CS. The recognition sequences (RS) involved in association of α B-crystallin with α A-crystallin are denoted RS. Mini α BC is a peptide of α B-crystallin found to display chaperone function. ATP1 is a sequence important in ATP binding.

Site Reference	Interactive chaperone Site	Secondary structure	Overlapping subunit site	Function(s) associated with the interactive site
CS1	9-20	None	None	Chaperone
CS2	43-58	α 3-turn- α 4 motif	37-54	Chaperone/subunit interaction
RS-1	42-57	α 3-turn- α 4 motif	37-54	α A-crystallin association/ subunit interaction/chaperone
RS-2	60-71	α 3-turn- α 4 motif	None	α A-crystallin association
Mini α BC	73-92	β 3 strand	75-82	Mini α B-crystallin/ chaperone/subunit interaction
CS3	75-82	β 3 strand	75-82	Chaperone/subunit interaction
ATP1	82-96	β 4- β 8 groove	75-82	ATP binding/Chaperone/subunit interaction
CS4	113-120	None	None	Chaperone
CS5	131-138	β 8 strand	131-138	Chaperone/subunit interaction
CS6	141-148	β 9 strand	141-148	Chaperone/subunit interaction
CS7	157-164	None	155-166	Chaperone/subunit interaction

The mini α B-crystallin peptide (α B₇₃₋₉₂), can still function as a molecular chaperone (Bhattacharyya et al., 2006), and overlaps the chaperone site CS-3 and subunit interaction site of α B₇₅₋₈₂ (Ghosh et al., 2005). In contrast, the site RS-1 (α B₄₂₋₅₇), which is required for the association of α B- with α A-crystallin (Sreelakshmi and Sharma, 2006), overlaps CS-2 (α B₄₃₋₅₈), but was shown to have no chaperone activity (Bhattacharyya et al., 2006).

Whilst the dual function mechanisms of these specific regions are not yet clear, the subunit interaction sequence of the N-terminus (α B₃₇₋₅₄) and the C-terminus (α B₁₅₅₋₁₆₅) have been linked with higher order assembly whilst sequences within the α -domain (α B₇₅₋

⁸², $\alpha B_{131-138}$ and $\alpha B_{141-148}$) are involved in the formation of the dimer interface (Ghosh et al., 2005), which is the unit of subunit exchange between closely related oligomers and the structural determinant for dimerisation (Koteiche and McHaourab, 2002; McHaourab et al., 2002). A truncated form of α B-crystallin (αB_{57-157}), which exists as a dimer, still displays chaperone activity, despite the loss of structure required for higher order assembly (Feil et al., 2001) as it is not dependant on 3D structure for binding unlike antibodies or enzymes (Ghosh and Clark, 2005)

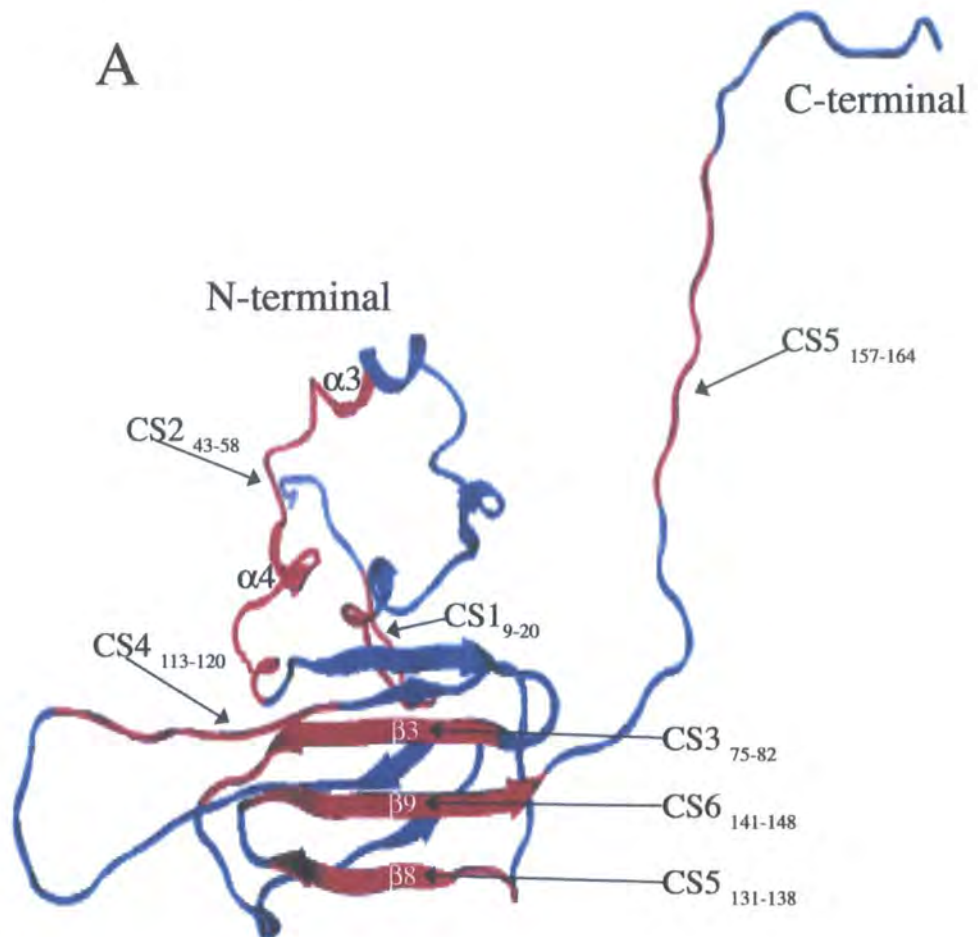


Figure legend on following page

B

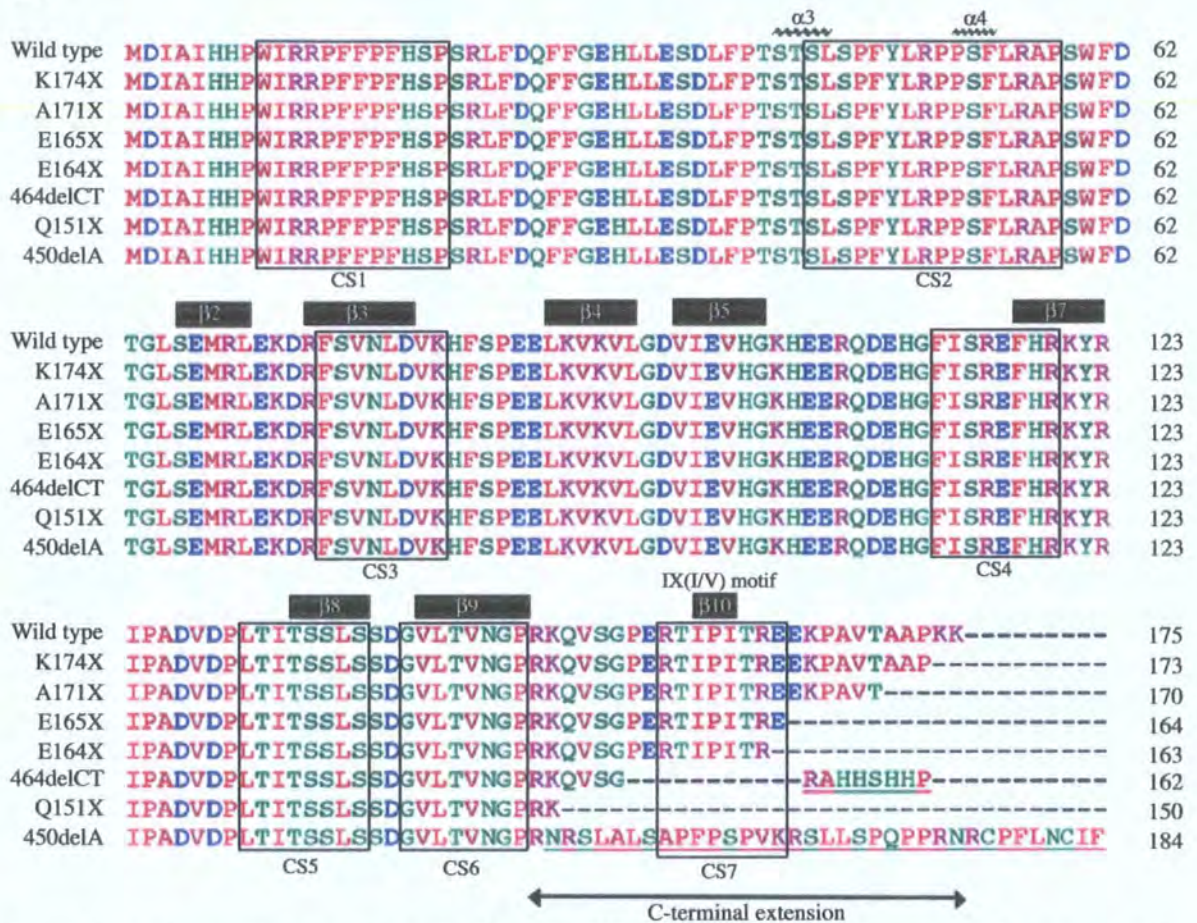


Figure 4.1. Interactive regions of α B crystallin important for chaperone function and oligomerisation. (A) Ribbon representation of the secondary and tertiary structure of human α B crystallin. Interactive chaperone sites of human α B-crystallin are coloured red, while non-interactive regions are coloured blue. The sequences CS1₉₋₂₀, CS4₁₁₃₋₁₂₀, and CS7₁₅₇₋₁₆₄ did not have secondary structure. The sequence CS2₄₃₋₅₈, formed the α 3-turn- α 4 motif, while the sequences CS3₇₅₋₈₂, CS5₁₃₁₋₁₃₈, and CS6₁₄₁₋₁₄₈ formed β strand motifs β 3, β 8, and β 9, respectively (Figure was modified from Ghosh et al. (2005) using Adobe Photoshop.CSv.8; Reprinted with permission from (Ghosh et al., 2005). Copyright 2005 American Chemical Society). The structural alignment of the C-terminal extension α B-crystallin mutants (B) shows the position of the interactive chaperone sites CS1-CS7 in relation to the C-terminal extension and highlights the potential consequences of the C-terminal mutations upon the chaperone and oligomerisation functions. The alignment includes α -helix-3 and α -helix-4 (wave) β -sheets and the IX(I/V) motif are indicated by black boxes. Small and hydrophobic amino acids (including aromatic -Y) are indicated in red, acidic (blue), basic (magenta), Hydroxyl +amine+basic-Q, (green) and other amino acids are indicated in grey. The β 2 sequence spans residues ₆₆SEMRLE₇₀, β 3-₇₄RFSVLND₈₀, β 4-₈₉LKVKVL₉₄, β 5-₉₇VIEVHG₁₀₂, β 7-₁₁₈FHRKYR₁₂₃, β 8-₁₃₄TSSLS₁₃₈ and the β 9 sequence spans residues ₁₄₂VLTVNGP₁₄₈ (Ghosh et al., 2005; Guruprasad and Kumari, 2003). The highly conserved IX(I/V) motif spans residues ₁₅₉IPI₁₆₁. The C-terminal extension consists of residues ₁₄₉RKQVSGPERTIPITREEKPAVTAAPKK₁₇₅

(Stamler et al., 2005). (Alignment produced using ClustalW multiple sequence alignment programme at www.ebi.ac.uk/clustalw).

The discovery of an ATP binding site (ATP1) of α B-crystallin is contradictory to previous literature that identified sHSP's as chaperones who function independently of ATP, however a recent study by Ghosh et al. (2006), identified the β 4- β 8 groove as an interaction site for ATP in α B-crystallin. The sequence α B₈₂₋₉₆ has been identified as a Walker B motif, (R/K-X₂₋₁₀-O-X-O-D) in human α B-crystallin, which is similar to the conserved Asp96 in HSP90. The α and β phosphate groups of ATP are positioned to interact with side chains of residues of the β 4 and β 8 strand. The binding of ATP to residues of the β 4 and β 8 groove has an affect on sub unit dynamics by disrupting the interaction between the C-terminal and the β 4- β 8 groove, thus affecting complex size and exposure of the interactive chaperone sites on the surface of the α B-crystallin (Ghosh et al., 2006c). The binding of ATP could potentially displace bound substrate protein releasing it to ATP dependant machinery allowing the subsequent disaggregation and refolding of the unfolded protein.

The C-terminal extension plays a role in α B-crystallin subunit interaction but is not involved in the formation of the heterogeneous oligomer of α -crystallin, whose assembly requires interaction between the N-terminal regions of the α A- and α B-crystallin subunits.

The study of subunit interactions between α A- and α B-crystallin identified sequences RS-1 (α B₄₂₋₅₇) (Sreelakshmi et al., 2004) and RS-2 (α B₆₀₋₇₁) (Sreelakshmi and Sharma, 2005) of α B-crystallin as the sites involved in association with α A-crystallin.

Inversion of the α B-crystallin sequence α B₅₄₋₆₀, which overlaps both RS-1 (α B₄₂₋₅₇) and the subunit interaction site α B₃₇₋₅₄, led to a two-fold reduction in the subunit exchange rate with α A-crystallin and saw α B-crystallin oligomers 38% smaller than the wild type. This suggested that the correct orientation was important for the formation of α B-crystallin oligomers and for the optimal subunit interaction and oligomerisation with α A-crystallins (Sreelakshmi and Sharma, 2006). A slight increase in α -helical content was observed and chaperone activity was similar to the wild type.

Mutations in the RS-2 region, W60R and S66G increased the oligomeric size of α B-crystallin by 1.6- and 2.7-fold respectively whereas an F61N mutation had no effect (Sreelakshmi and Sharma, 2005). The mutant W60R mutation had no effect on subunit exchange between α B- and α A-crystallin, whereas F61N slowed subunit exchange by 36%, and the S66G increased subunit exchange by 100%. Thus, the region RS-2 (α B₆₀₋₇₁) is important in the oligomerisation of α B-crystallin, in addition to subunit interactions between α A- and α B-crystallins (Sreelakshmi and Sharma, 2005). An increase in oligomeric size may not be correlated with an increase in chaperone activity or subunit exchange as shown by the deletion of the N-terminal sequence $_{21}\text{SRLFDQFFG}_{29}$, which lead to a reduction in the oligomeric size but an increase in subunit exchange and chaperone function (Sreelakshmi and Sharma, 2005).

Thus, the interactive sequences in the N-terminal are important for the formation of the α B-crystallin oligomer, the associations between the α A- and α B-crystallins and also contain the interactive sites CS-1 and CS-2 required for chaperone activity (α B₉₋₂₀, and α B₄₃₋₅₈ respectively).

The focus and experimental goals of this chapter aim to establish the relationship between the structure and function of α B-crystallin and the C-terminal extension. The emergence of the interactive sites in α B-crystallin for subunit interactions, chaperone function, ATP binding and α A-crystallin associations, combined with the further characterisation of the C-terminal α B-crystallin mutants will help elucidate the mechanisms involved in substrate binding and oligomerisation.

A number of recent studies by Ghosh et.al, (2006) looked further at the role of the α -domain β 3- β 8- β 9 surface as an interface for complex assembly and chaperone activity (Ghosh et al., 2006a) and the N-terminal region α B₄₁₋₅₈ and C-terminal region α B₁₅₅₋₁₆₅ in the recognition selection and solubility of unfolding substrate proteins during the chaperone process (Ghosh et al., 2006d). The studies revealed that chaperone activity is dependant on composition of interactive sequences in the α -domain, independent to complex size (Ghosh et al., 2006a), and characterized the importance of the exposed side chains of the non conserved Glu-78, Lys-82, and His-83 in the interactive β 3 sequence for chaperone function, which was influenced by the amount of unfolding of the target proteins and independent of complex size (Ghosh et al., 2006b).

Mutations or post-translational modifications of these interactive domains can shift the dynamic equilibrium to increase oligomerisation and reduce chaperone activity or lead to dissociation of the oligomeric assembly and formation of protective multimeric chaperone-substrate aggregates (Ghosh et al., 2006b; Ghosh et al., 2006c).

Complex assembly is the result of subunit-subunit interactions that involves an interaction of the C-terminal extension of one α B-crystallin molecule with the β 4- β 8 interface on the surface of the α -domain of a second α B-crystallin molecule (see Figure 4.2). Chaperone activity is the result of interactions between the β 3- β 8- β 9 interface on the surface of α B crystallin and the exposed residues of an unfolding target substrate protein (see Figure 4.2) (Ghosh et al., 2006a), however a more recent study also suggested that the polar C-terminal sequence α B₁₅₅₋₁₆₅ interacted with unfolding proteins to maintain solubility, independent of the amount of substrate protein unfolding (Ghosh et al., 2006d).

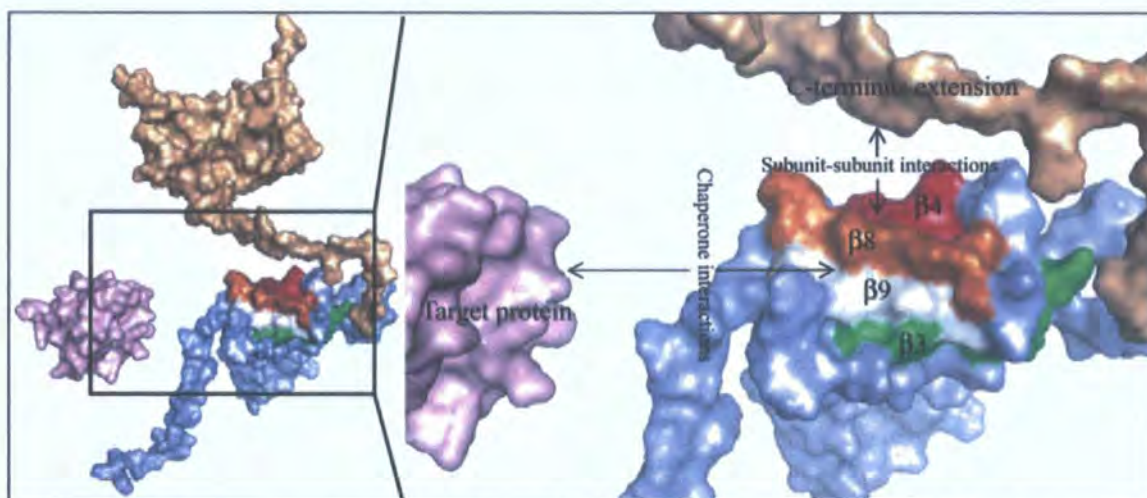


Figure 4.2 Interactive sites of α B-crystallin associated with functional and structural activity. A Ghosh (2006) 3-D computer model for the β 3- β 8- β 9 interface on the surface of the α crystallin core domain of human α B crystallin. In the space-filled model of human α B crystallin (blue), the exposed side chains of the β 3- β 8- β 9 interface are shown as green (β 3), orange (β 8), and white (β 9) surfaces. The exposed side chains of the β 4 strand are in red. Complex assembly is the result of subunit-subunit interactions that involves an interaction of the C-terminal extension of one α B crystallin molecule (tan) with the β 4- β 8 interface on the surface of the α crystallin core domain of a second α B crystallin molecule (blue). Chaperone activity is the result of interactions between the β 3- β 8- β 9 interface on the surface of α B crystallin (blue) and the exposed residues of an unfolding target substrate protein (purple). The exposed residues, Asn-78, Lys-82, and His-83 of the β 3 sequence, Leu-131, Thr-132, Thr-134, Ser-136, and Ser-138 of the β 8 sequence, and Gly-141 and Thr-144 of the β 9 sequence together form the β 3- β 8- β 9 chaperone interface on the surface of the α crystallin core domain (Reprinted with permission from (Ghosh et al., 2006a). Copyright 2006 American Chemical Society).

The role of the C-terminal and its relationship with chaperone activity and oligomerisation has been extensively studied by mutagenesis of selected residues in the interactive regions, which suggests that the C-terminal is not essential for chaperone activity, but has a primary role in subunit interaction and also interacts with unfolding proteins to maintain solubility (Ghosh and Clark, 2005; Ghosh et al., 2005; Ghosh et al., 2006a; Ghosh et al., 2006b; Ghosh et al., 2006d).

There has however, been no systematic analysis of the C-terminal extension and its role in chaperone function and oligomerisation or the relationship between the structural and functional relevance of the C-terminal extension and the pathology of C-terminal mutants 450delA, Q151X and 464delCT.

The α B-crystallin C-terminal mutants and their solubility have been discussed previously (see Chapter 3). It was concluded that in order to elucidate the mechanism responsible for the phenotypic heterogeneity observed with the C-terminal disease mutants, further characterisation of an altered C-terminal extension upon chaperone activity and oligomerisation was essential. This additional characterisation will provide a link between the structural and functional properties of the C-terminal extension mutants and the associated disease phenotypes. It will also provide further insight into the role the C-terminal extension plays in the chaperone function and oligomerisation of α B-crystallin and other sHSPs.

4.3. RESULTS

4.3.1. TRUNCATION OF THE C-TERMINAL EXTENSION REDUCES α B-CRYSTALLIN OLIGOMERISATION

The oligomerisation properties of α B-crystallin mutants were assessed using an analytical size exclusion column (see Figure 4.3A). Calibration curves covering a range of high and low Mwt calibrators allowed the Mwt determination of the mutants (see Appendix 2 Figure A2.1-2). Each mutant was analysed three times and the average retention time was used for Mwt determination (see Figure 4.3B). Wild type α B-crystallin formed oligomers that were equivalent to 564 kDa, agreeing with previously published data (Horwitz et al., 2004).

The sequential truncation of the C-terminal extension of α B-crystallin produces a steady decrease in oligomer size (see Figure 4.3A). The shortest construct, Q151X α B-crystallin produces a peak with a very significantly increased elution volume equivalent to 19 kDa (Figure 4.3B) and represents the most dramatic reduction in oligomerisation observed for all the constructs studied.

This effect on Q151X oligomerisation is obvious when the negative stained electron micrographs of wild type and Q151X α B-crystallin are compared (Fig 4.3C, D respectively). Notice the absence of particles in the Q151X sample (Figure 4.3D) relative to the wild type (Figure 4.3C). Deletion of the two C-terminal lysines (K174X) did not alter the oligomerisation of α B-crystallin, as previously reported (Plater et al., 1996), producing a 605 kDa complex. Removal of 5 C-terminal residues only reduced the apparent size of the main peak to 553 kDa, however the removal of both 11 (E165X) and 12 (E164X) residues resulted in oligomers of 454 kDa and 413 kDa respectively. In the case of the latter two truncation mutants, there is evidence of increased polydispersity as indicated by the very noticeable shoulder on the main peak for the E165X construct and the presence of an additional peak at the void volume of the column for the E164X construct. The reduction of mean complex size for α B-crystallin oligomers suggests that residues E164/E165 also contribute to α B-crystallin oligomerisation. The two frame-shift disease causing mutants 450delA and 464delCT remained insoluble unless they were refolded in the presence of wild type α B-crystallin (see Section 3.3.4). As seen from the

elution profiles in Figure 4.3A, the presence of these mutant proteins decreased the oligomer size of the wild type α B-crystallin to 491 kDa and 434 kDa in the presence of 450delA α B-crystallin and 464delCT α B-crystallin respectively.

SDS-PAGE analysis (Section 3.3.4, Figure 3.29) revealed that the wild type α B-crystallin is present in excess compared to 450delA α B-crystallin, yet this excess was not sufficient to retain the elution characteristics of the wild type protein. In fact, this proved to be the maximum ratio compatible with protein solubility for the 450delA/ wild type α B-crystallin complex and is in stark contrast to 464delCT α B-crystallin, where a 1:1 mixture with wild type α B-crystallin was entirely soluble. The presence of the 450delA α B-crystallin also increased the polydispersity of the main peak, as seen by the shoulder and the additional small peak with a predicted Mwt equivalent to α B-crystallin dimers. The 450delA mutation, introduces a unique 33 residue polypeptide completely unrelated to the C-terminal extension of wild type α B-crystallin and quite clearly this frameshift sequence has a significant effect upon the oligomerisation of α B-crystallin. It is, however, the Q151X mutation that has the most dramatic effect, with the complete removal of the single peak equivalent to the 564 kDa oligomer and the appearance of a peak with elution characteristics predicted to be equivalent to a monomer.

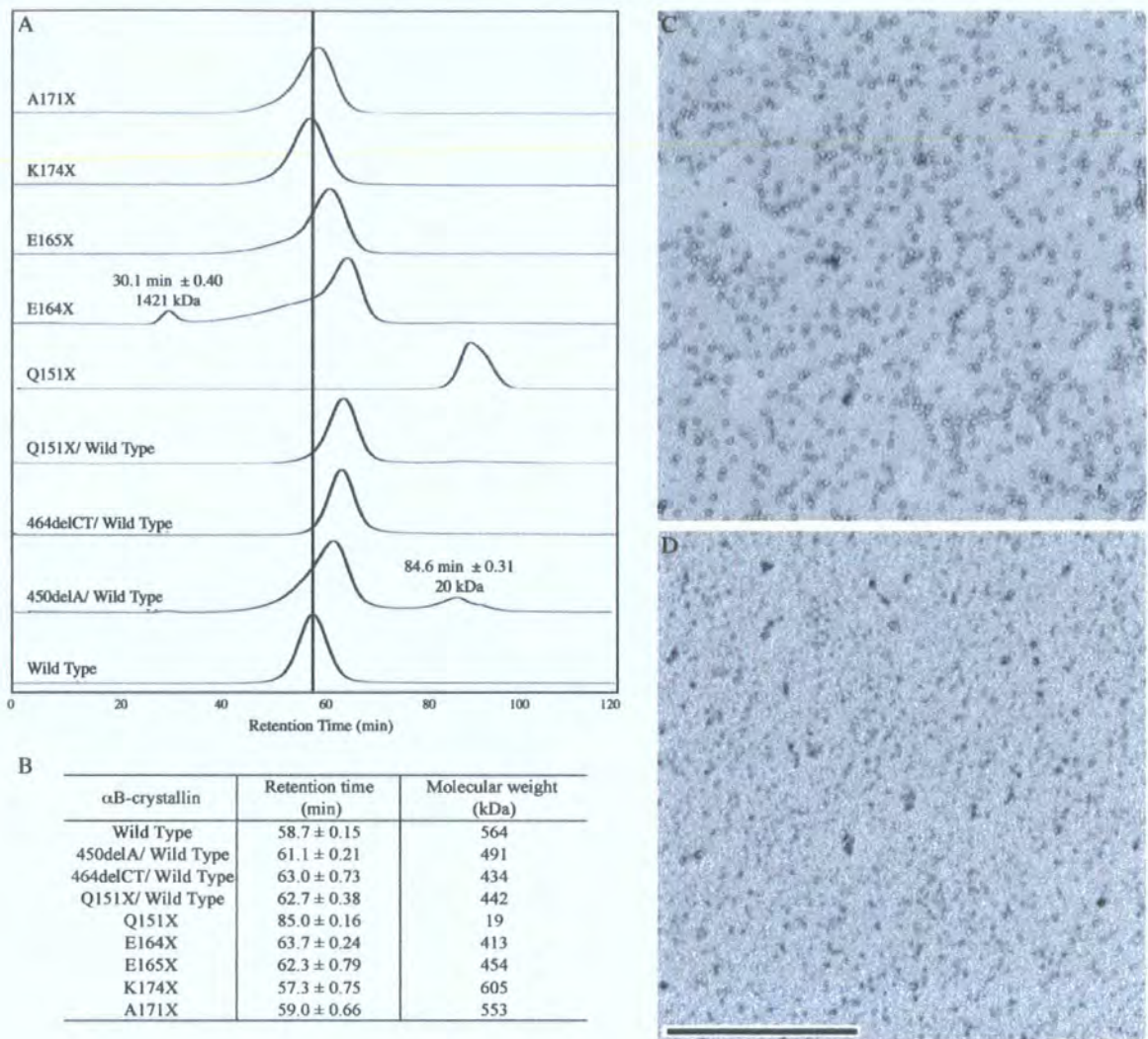
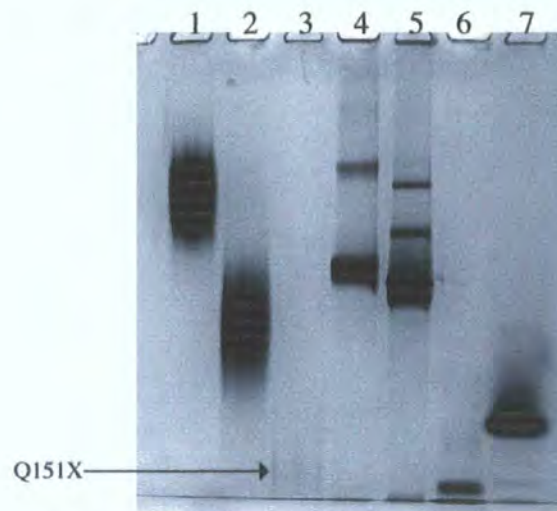


Figure 4.3. Effect of the C-terminal mutations upon the oligomerisation of α B-crystallin. The elution profiles of the various α B-crystallins were determined on a 290 x 10mm Superose 6 column (A). The elution characteristics of the various mutants are plotted relative to those obtained for wild type α B-crystallin (wild type), as highlighted by the vertical line indicating the retention time of the oligomeric complex, which is the major and only peak resolved in the wild type α B-crystallin sample. Additional minor species seen in E164X and 450delA/ wild type α B-crystallin are highlighted. A summary of the retention times and Mwt (B) is shown for the major peak resolved during SEC of the wild type α B-crystallin and other constructs. The retention times and Mwt of minor peaks are included in the figure as appropriate. The retention times (\pm SD) were calculated from the average of three cycles of SEC, from which the Mwt was determined. Negative stained images of wild type (C) and Q151X α B-crystallin (D) were obtained by transmission electron microscopy and illustrate the absence of characteristic particles in the Q151X α B-crystallin sample, in agreement with the SEC data. Bar = 500nm

Non-denaturing gel electrophoresis also confirmed that the Q151X mutation dramatically altered its electrophoretic mobility under non-denaturing conditions (see Figure 4.4). Figure 4.4 shows the increased mobility of the wild type (lane 1) when associated with the Q151X α B-crystallin (lane 2) and the mobility of the Q151X α B-crystallin is increased further when analysed as a homogenous complex (lane 3) suggesting a significantly smaller oligomer, which supports the altered oligomerisation observed in Figure 4.3.



Lane	Sample Details	Molecular Weight (kDa)
1	Wild Type α B-crystallin	564
2	Q151X/ Wild Type α B-crystallin	442
3	Q151X	18
4	Thyroglobulin	725
5	GroEL	700
6	BSA	62
7	Carbonic anhydrase	29

Figure 4.4. Native gel electrophoresis of the Q151X α B-crystallin oligomer. Analysis of Q151X α B-crystallin oligomer size, relative to wild type and Q151X/ wild type α B-crystallin. High and low Mwt calibrators are shown in lanes 4-7. All lanes represent a 20 μ g loading with the exception of the Q151X α B-crystallin (1.0 μ g) where the nature of the Q151X α B-crystallin refolding limits the available level of protein for analysis.

4.3.2. EFFECT OF THE C-TERMINAL MUTATIONS UPON THE SECONDARY STRUCTURE AND OLIGOMERISATION OF α B-CRYSTALLIN.

Circular Dichroism (CD) spectroscopy was performed to identify Far UVCD spectra of the α B-crystallin mutants (see Figure 4.5). The Far UVCD of wild type α B-crystallin showed a single broad minima, between 208 and 217nm, indicative of a protein rich in β -sheet (Figure 4.5A), which is consistent with previously reported data (Bova et al., 1999; Ghosh et al., 2006a; Horwitz et al., 2004; Pasta et al., 2003; Sreelakshmi and Sharma, 2006).

The Q151X mutation in α B-crystallin had the most significant effect upon the Far UVCD characteristics of α B-crystallin (Figure 4.5.A), due to a very significant red-shift of the minima to 217nm and a ~50% reduction in magnitude, relative to the wild type α B-crystallin, suggestive of a significant loss of secondary structure. Similar shifts have been seen for C-terminal truncation mutants of α A-crystallin (Rajan et al., 2006). A 1:1 molar mixture of Q151X with α B-crystallin wild type produced a spectrum that was clearly biased toward the Q151X α B-crystallin, indicative of the dominant nature of this mutation. Of the other mutants studied, the E164X and E165X mutants were intermediate in their effects upon negative ellipticity as compared to the Q151X mutant. This intermediate effect is likely associated with the extent of the C-terminal truncations of E164X and E165X α B-crystallin relative to Q151X α B-crystallin and suggests a less significant loss of secondary structure.

Interestingly, the E164X mutant showed a red-shift in the minimum indicating that the deletion of the second of the two glutamic acid residues in the REEK-motif does introduce a detectable change in secondary structure as well as introducing increased insolubility as discussed in Section 3.3.4. The frame-shift mutation, 464delCT α B-crystallin, introduced a small blue-shift of the minimum to 208nm and the appearance of a shoulder at approximately 223 nm, both of which are indicative of increased helicity. This increase may be the result of helix formation by the novel C-terminal sequence.

Both the K174X and A171X truncation mutants and the 450delA frameshift mutant have Far UVCD spectra very similar to the wild type α B-crystallin. The A171X and K174X α B-crystallin are similar in shape and magnitude and contained broad minima

between 208 and 217nm. The 450delA/ wild type α B-crystallin show increased negative ellipticity and a shift in minima to 208nm.

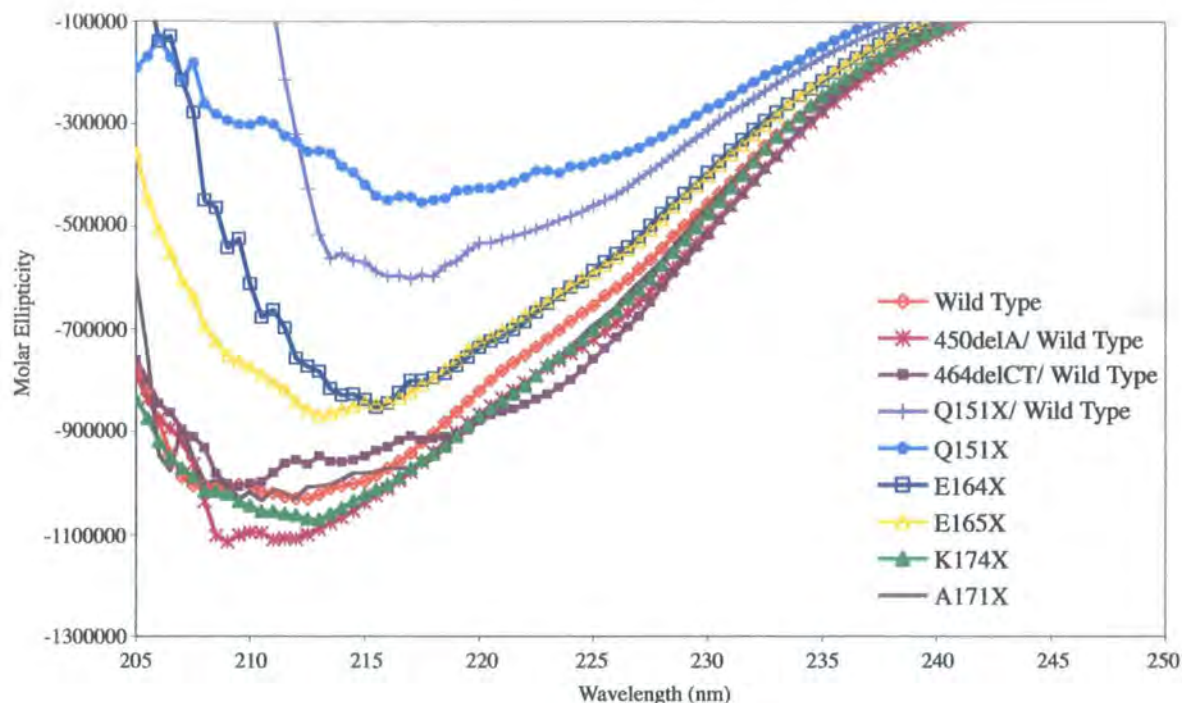


Figure 4.5. Circular dichroism of wild type α B-crystallin and the C-terminal extension mutants. The Far UVCD spectra (205-250nm) for each mutant protein were the average of four spectra. Protein concentrations were determined by Bicinchoninic Acid (BCA) assay. The Far UVCD signal was converted to molar ellipticity expressed as $\text{deg.cm}^2.\text{dmol}^{-1}$ to normalise for slight differences in molecular mass between the wild type and the other α B-crystallin constructs. The Far UVCD spectra of wild type, A171X and K174X α B-crystallin are similar in shape and magnitude and contained broad minima between 208 and 217nm. The 450delA/ wild type and 464delCT/ wild type α B-crystallin mixtures show increased negative ellipticity and a shift in minima to 208nm. Truncation of the C-terminal extension results in the loss of secondary structure reflected by a decrease in negative ellipticity and a shift in wavelength minima (E164X, E165X, Q151X, Q151X/ wild type) with the most dramatic effects seen for Q151X α B-crystallin.

The effects of the C-terminal extension mutants upon oligomerisation and secondary structure were further highlighted by investigating the changes in relative exposed hydrophobicity. The probe, bis-ANS, has a low fluorescence quantum yield in aqueous solution however, this increases dramatically upon binding to surface-exposed hydrophobic regions. As can be seen in Figure 4.6, all the α B-crystallin mutants bound more bis-ANS relative to the wild-type α B-crystallin, except for the Q151X mutant,

which bound substantially less. As all the mutants except Q151X α B-crystallin formed oligomers (see Figure 4.3A), it suggests that the increase in exposed hydrophobic surfaces arose from changes within their respective oligomeric structures. The reason why Q151X α B-crystallin binds so little bis-ANS was probably due the combined effects of decreased oligomerisation and loss of secondary structure. This was tested by examining the bis-ANS binding properties of the wild-type protein under mildly denaturing conditions (2M guanidinium hydrochloride (Gdn-HCl)), which had been shown previously to eject α B-crystallin from native α -crystallin oligomers and to cause a significant loss of secondary structure (Doss-Pepe et al., 1998). The presence of the Gdn-HCl greatly reduced the bis-ANS binding to wild-type α B-crystallin, with the fluorescence intensity dropping almost as low as that obtained for Q151X α B-crystallin alone.

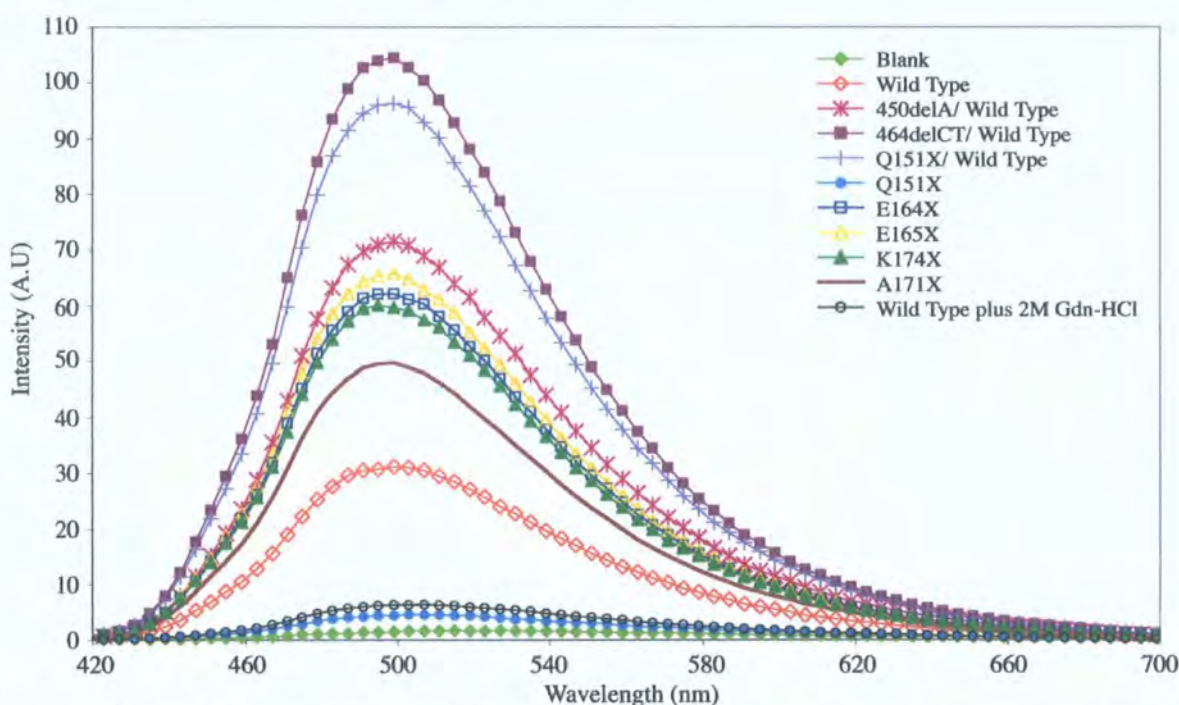


Figure 4.6. Bis-ANS fluorescence binding properties of the α B-crystallin mutants. The effect of the C-Terminal mutations upon the relative exposed hydrophobicity was performed using bis-ANS to bind to surface exposed hydrophobic regions on the mutant and wild type α B-crystallin. Protein concentrations were determined by A280nm using extinction coefficients specific for each mutant α B-crystallin (see Table 2.12). Each protein was analysed at 1 μ M in the presence of a 10-fold molar excess of bis-ANS. The excitation wavelength was 410 nm and emission spectra were collected between 420–700 nm. All spectra are the average of 10 individual scans. The resulting exposed hydrophobicity is increased for all mutants relative to the wild type α B-crystallin, with the exception of the Q151X mutant.

4.3.3. LOSS IN HEAT STABILITY OF α B-CRYSTALLIN CORRELATES WITH CHANGES IN SECONDARY STRUCTURE.

In order to understand further the consequences of an altered C-terminal extension of α B-crystallin upon structure and function, the stability under heat denaturing conditions was determined (see Figure 4.7). These data show that the two most unstable mutants are the E164X and E165X α B-crystallin because both the onset of aggregation and optical signal (OD_{360}) was very significantly increased compared to wild type α B-crystallin for these two mutants. The E164X mutant began to aggregate at 46°C, some 30°C lower than the wild type protein. The E165X mutant was notable for the rapidity of aggregation when initiated at 57°C, whilst the Q151X mutant was notable in its failure to develop a strong OD_{360} signal, despite the very significant decrease in stability indicated by the increased turbidity at 53°C. This signal reached a maximum at 55°C and remained constant until the conclusion of the assay.

The absence of the stabilising C-terminal ‘tail’ and the partial removal the interaction site $_{155}\text{PERTIPITREE}_{165}$ are a result of the E164X and E165X mutations. Deletion of this interactive site was shown to cause high levels of instability in α B-crystallin (Ghosh et al., 2006d) and perhaps the exposure of this region had a detrimental effect on the heat stability of these mutants. Surprisingly, the complete removal of this sequence seemed to confer enhanced heat stability upon the Q151X α B-crystallin relative to the E164X α B-crystallin. The significantly reduced oligomer size observed for the Q151X α B-crystallin (see Section 4.3.1, Figure 4.3) contributed towards the variation in OD_{360} signal observed, as the Q151X α B-crystallin oligomer (19 kDa) was 22-24 times smaller than E164X α B-crystallin (413 kDa) and the E165X α B-crystallin (454 kDa) respectively (see Figure 4.3B), thus the aggregates formed are less prone to sedimentation. The two shorter C-terminal truncations (K174X, A171X), showed decreased stability, but were the most stable of the mutants studied.

These data suggest a correlation between altered secondary structure and decreased heat stability. This trend is also seen for the two frame-shift mutants, (450delA/ wild type and 464delCT/ wild type α B-crystallin) that were more stable than the three shortest mutants, but less stable than either the A171X or K174X α B-crystallin truncation constructs. These data also support the observations with regards to the changes in

oligomerisation, where the Q151X α B-crystallin, despite being relatively unstable produces an optical signal that remains consistently low relative to the other mutants, highlighting the variations in light scatter, thus the size of aggregates formed under the assay conditions.

These data correlate with more conservative changes in secondary structure as detected by Far UVCD spectroscopy for the two frame-shift mutants (Figure 4.5A) and the largely unchanged spectra for the A171X and K174X mutants.

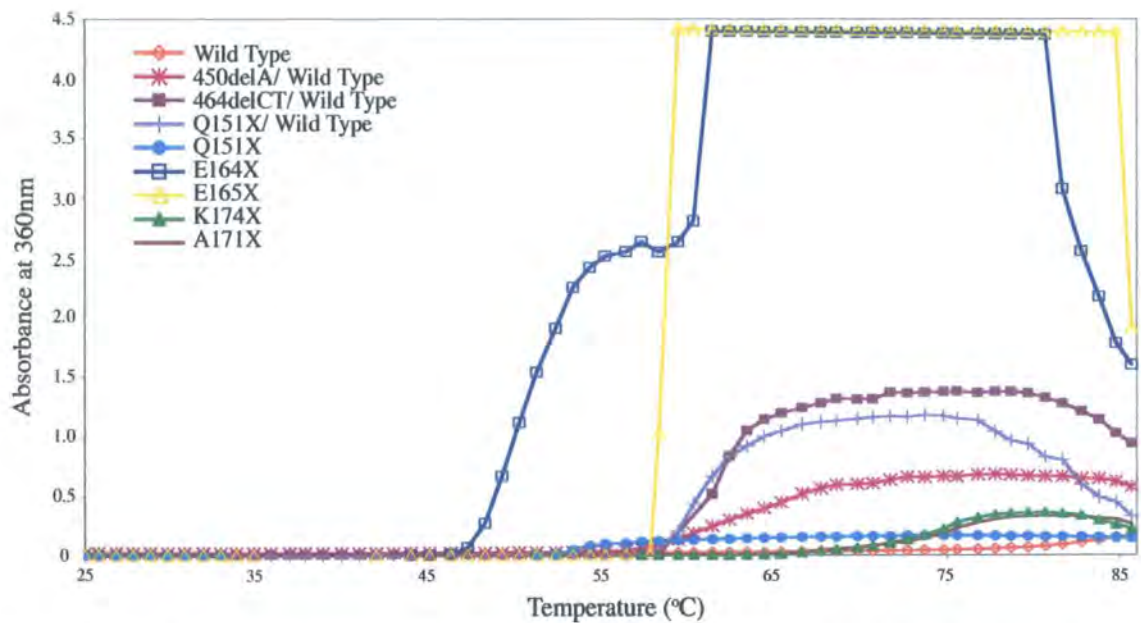


Figure 4.7. Thermal stability of wild type and C-terminal extension mutants of α B-crystallin. The effect of the C-terminal extension mutations on the heat induced aggregation of α B-crystallin was measured at 360nm over the temperature range 25 °- 86°C. The temperature was increased at a 1°C/min over 1 h. Wild type and mutant α B-crystallins were assayed at 0.1 mg/ml. Notice the significantly reduced stability of the E164X, Q151X and E165X α B-crystallin mutants.

4.3.4. EFFECT OF C-TERMINAL EXTENSION MUTATIONS UPON THE CHAPERONE ACTIVITY OF α B-CRYSTALLIN.

Citrate synthase and insulin chaperone assays were used to determine the effects of the α B-crystallin C-terminal extension mutations on the chaperone capabilities of the modified α B-crystallin mutants. Each assay was performed three times at a 4:1 mass ratio of substrate: α B-crystallin to produce an average chaperone activity for each substrate as shown for Citrate synthase (see Figure 4.8A) and Insulin (see Figure 4.9A). The percentage inhibition achieved was calculated from the end point level of aggregation (represented by AU at 360nm) of each mutant α B-crystallin as a percentage of the wild type α B-crystallin activity. The triplicates for Citrate Synthase are shown in Appendix 3, Figure A10.1 and Table A10.1 and for the Insulin assay Appendix 3, Figure A10.2 and Table A10.2.

Based on the effects of the mutations on protein secondary structure and heat stability it was predicted that E164X, E165X and Q151X α B-crystallin would exhibit the least activity in these assays. The chaperone activity achieved by these mutants in a citrate synthase aggregation assay (see Figure 4.8B) showed that whilst E164X α B-crystallin was indeed the worst of all the α B-crystallin constructs, (-57% inhibition) none of the other C-terminal extension constructs performed worse than the wild type protein (100% inhibition). Indeed, the E165X α B-crystallin (313%) was slightly better than the wild type protein and Q151X α B-crystallin (755%) was one of the best. In fact, the combination of Q151X and wild type α B-crystallin was the best chaperone in the citrate synthase assay (1263% inhibition).

Another surprise from the citrate synthase chaperone assay was the relative performance of the two frame-shift mutants, 450delA and 464delCT α B-crystallin, both of which performed better in combination with wild type α B-crystallin than the wild type α B-crystallin alone, (625 % and 216% inhibition respectively). These data show that the disease causing mutations in α B-crystallin (Q151X, 450delA and 464delCT) all retain significant chaperone activity, surpassing the potential of the wild type protein alone for this client protein in this particular chaperone assay.

In contrast to the results with citrate synthase, all the C-terminal extension mutants performed worse than the wild type α B-crystallin in the insulin based chaperone assay (see Figure 4.9A). In this assay, the three most heat-sensitive α B-crystallin mutants, E164X, E165X and Q151X α B-crystallin, increased protein aggregation compared to wild type α B-crystallin (-138, -8 and -45% inhibition respectively (see Figure 4.9B)). An equimolar mixture of Q151X and wild type α B-crystallin (47% inhibition) retained significant chaperone activity of Q151X α B-crystallin, but it was still one of the poorer chaperones in this assay. The K174X (93%) and A171X (93%) mutants had chaperone activities that most closely resembled the wild type α B-crystallin (100%) and even the two frame-shift mutants 450delA and 464delCT α B-crystallin in their respective combinations with wild type α B-crystallin, still possessed credible activities, (68 % and 78 % inhibition respectively).

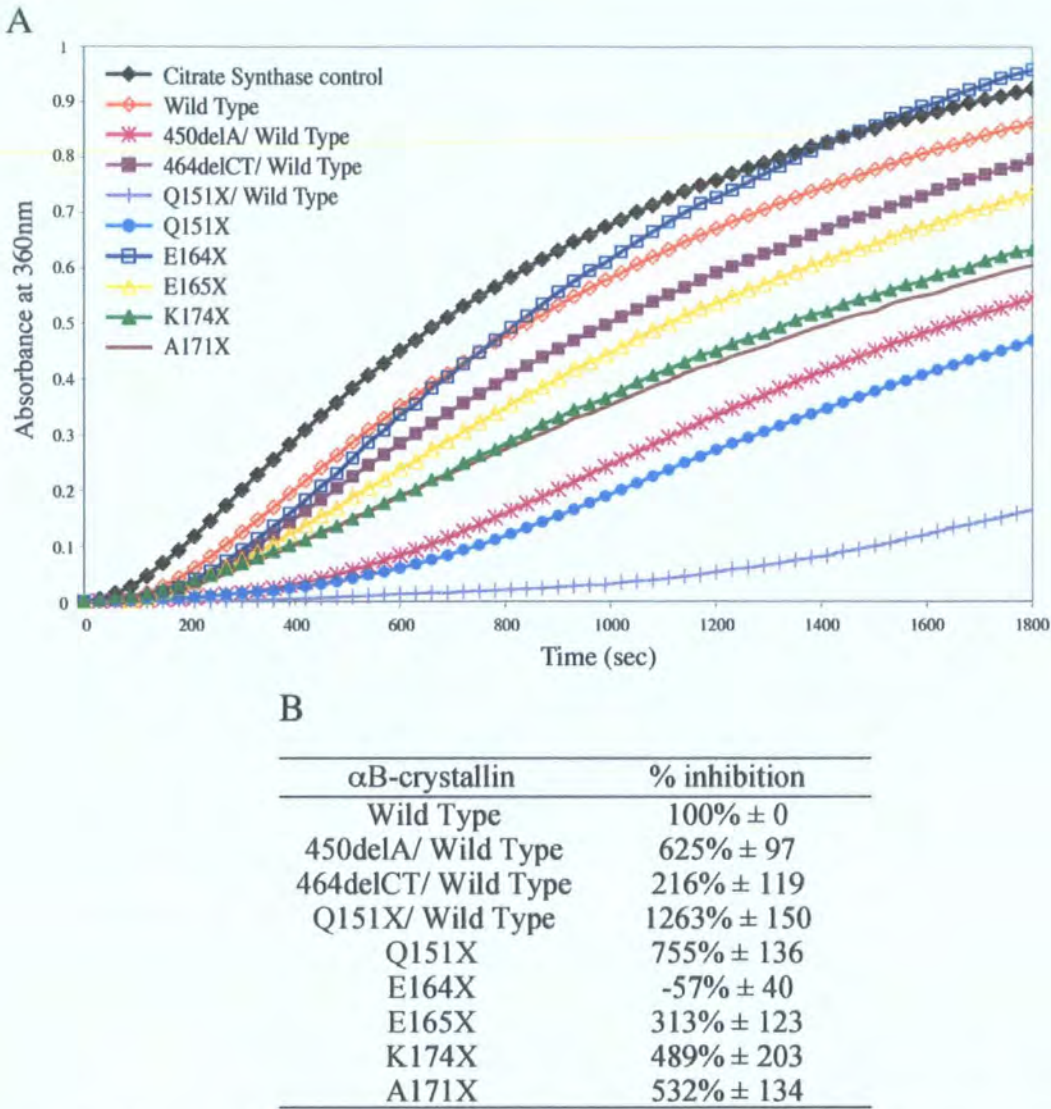
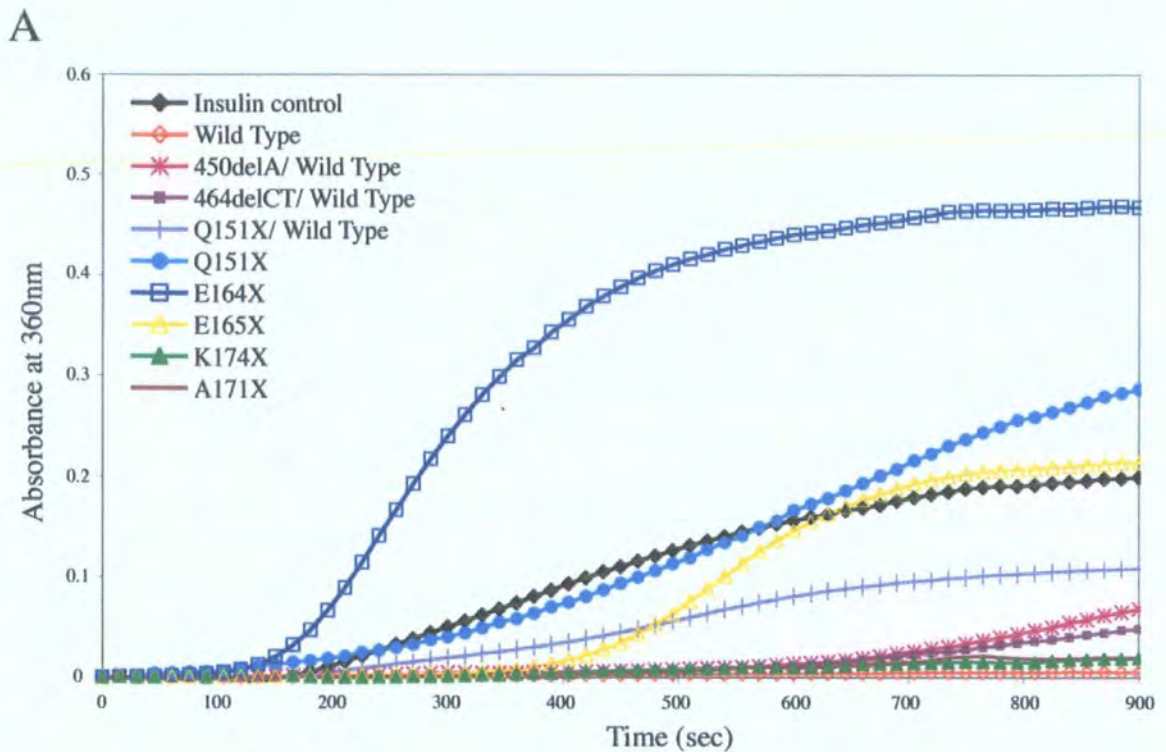


Figure 4.8. Mean aggregation of Citrate Synthase in the presence of wild type and mutant α B-crystallins. The effect of wild type and mutant α B-crystallin on the thermal aggregation of Citrate synthase, over a 30 min period at 42 °C was measured using OD₃₆₀ (A). A 4:1 molar ratio of substrate: chaperone was used. The relative inhibition of citrate synthase aggregation (B) by the C-terminal extension mutants was calculated from the end point level of aggregation of each mutant as a % of that observed for the wild type α B-crystallin alone (100% inhibition). The data shown are the mean (\pm SD) values taken from three independent experiments (see Appendix 3, Figure A3.1 and Table A3.1 for details of the complete data sets).



B

α B-crystallin	% inhibition
Wild Type	100% \pm 0
450delA/ Wild Type	68% \pm 5
464delCT/ Wild Type	78% \pm 2
Q151X/ Wild Type	47% \pm 8
Q151X	-45% \pm 11
E164X	-138% \pm 14
E165X	-8% \pm 6
K174X	93% \pm 1
A171X	93% \pm 2

Figure 4.9. Mean aggregation of insulin in the presence of wild type and mutant α B-crystallins. The effect of wild type and mutant α B-crystallin on reduction-induced aggregation of insulin (C), over a 15min period at 37°C was measured using OD₃₆₀. A 4:1 molar ratio of substrate: chaperone was used. The relative inhibition of insulin aggregation (B) by the C-terminal extension mutants was calculated from the end point level of aggregation of each mutant as a % of that observed for the wild type α B-crystallin alone (100% inhibition). The data shown are the mean (\pm SD) values taken from three independent experiments (see Appendix 3, Figure A3.2 and Table A3.2 for details of the complete data sets).

4.3.5. ABILITY OF THE DISEASE CAUSING α B-CRYSTALLIN MUTANTS TO INHIBIT DESMIN FILAMENT AGGREGATION.

One of the characteristic histopathological features of the human myopathies caused by some of the mutations in α B-crystallin under investigation in this study is the presence of aggregates of desmin filaments (Schroder et al., 2007; Vicart et al., 1998) It was therefore decided to analyse the ability of the α B-crystallin mutants in this study to prevent desmin filament-filament associations using an assay developed to investigate the cell biological effects of the R120G mutation in α B-crystallin (Perng et al., 2004). The assay takes advantage of the fact that IFs interact with each other in solution (Bousquet et al., 2001; Perng et al., 2004) and this can be measured by sedimentation assay. The presence of a mutant protein that interacts with desmin filaments, for example R120G α B-crystallin, activity encourages more filament-filament associations and therefore increases the proportion of pelletable desmin. The assays were performed at the physiologically relevant temperature of 37°C and control conditions of 20°C (see Figure 4.12) and 44°C (see Figure 4.13). Initially all samples were analysed at 0.2 mg/ml with the exception of the Q151X α B-crystallin, whose limited yield only allowed an assay concentration of 0.1 mg/ml. To eliminate any interactions that may have been caused by mass effects, the assay was repeated at the physiologically relevant temperature of 37°C with all samples at 0.1 mg/ml (see Figure 4.10). This resulted in a small loss of binding and chaperone function, but did not affect the general pattern of interaction between the mutants. Thus, the control assay at 20°C and 44°C show the relative effects of temperature on binding between the mutants at these temperatures and also the Q151X α B-crystallin at 37°C. The assay at 37°C shows the relative effects of the C-terminal mutations on binding at this physiologically relevant temperature, but is not a direct comparison between the mutants (with the exception of the Q151X α B-crystallin) at the various control assay temperatures.

At the physiologically relevant temperature of 37°C, both the Q151X and 464delCT α B-crystallin mixed with wild type displayed desmin filament associations similar to the wild type alone, whereas the 450delA-wild type protein mixture was significantly more effective than R120G α B-crystallin in inducing this filament

association, highlighting the dominant effect of the 450delA mutation over the wild type α B-crystallin (Figure 4.10A).

In stark contrast to these results, the Q151X α B-crystallin was the most effective chaperone of all the disease causing mutants and was also better than wild type α B-crystallin in reducing the proportion of pelletable desmin (Figure 4.10A). Most of the Q151X mutant (80%) co-sedimented with desmin in the pellet fraction (see Figure. 4.10B and C) and resulted in a 25% decrease in the amount of pelletable desmin, relative to the wild type α B-crystallin. The chaperone activity of the Q151X α B-crystallin was also evident at 20°C where more than half the Q151X α B-crystallin was bound to the desmin filaments (see Figure 4.12B and C) and the proportion of pelletable desmin was less than the wild type (see Figure 4.12A).

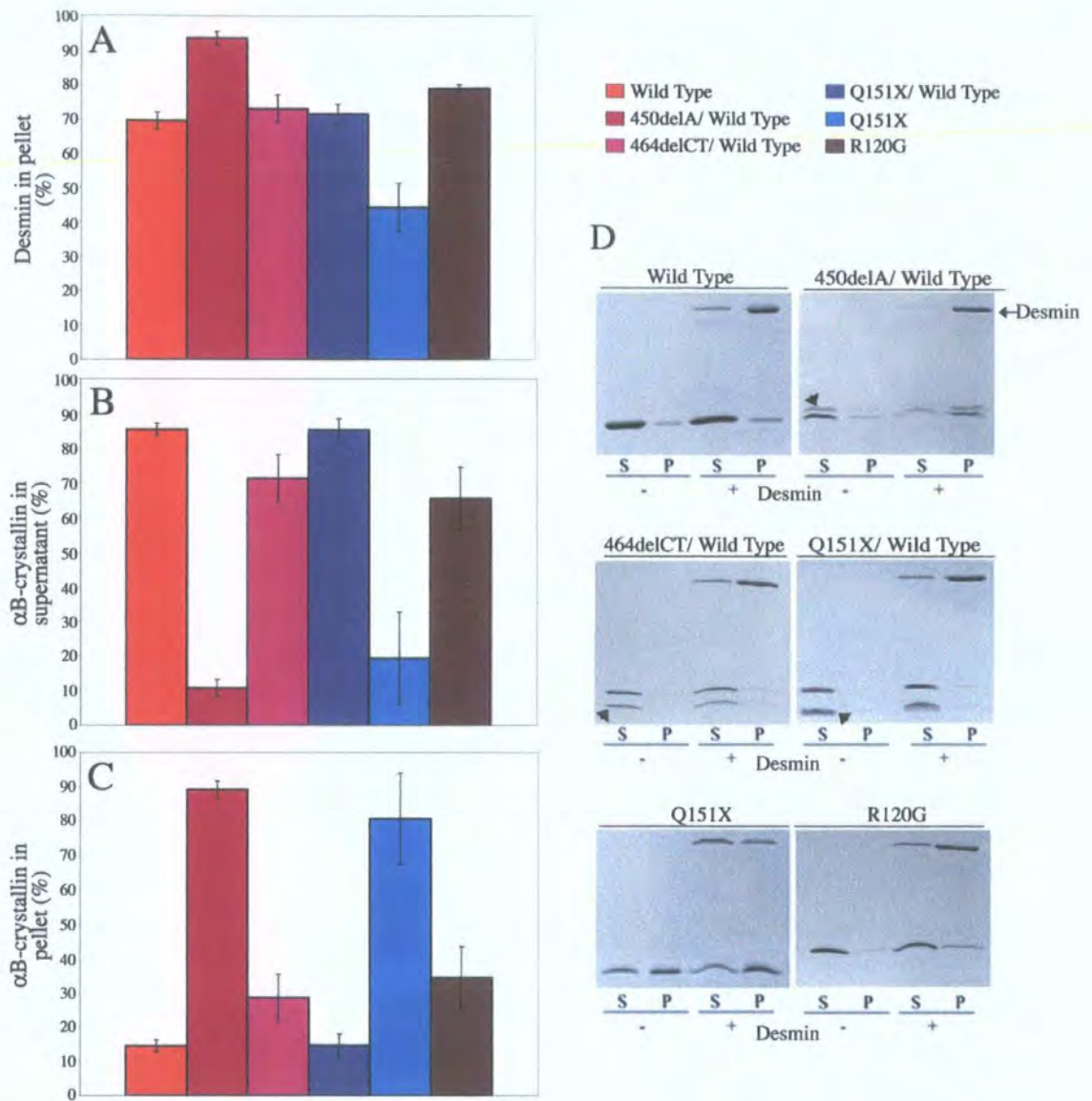


Figure 4.10. Sedimentation assay to investigate the prevention of desmin filament aggregation in the presence of various α B-crystallins at 37°C. (A-C) shows the % desmin pelleted (A), the % α B-crystallin wild type and mutants remaining soluble in the presence of desmin (B), and the % of the total α B-crystallin pelleted in the presence of desmin (C), following low speed centrifugation (2500 x g). These data were calculated from SDS-PAGE data of the desmin binding assays. (D) An example of the data used to calculate these values for wild type and mutant α B-crystallin. Those mutants associated with wild type are (450delA, 464delCT and Q151X) identified with arrowhead. These data illustrate the ability of the Q151X α B-crystallin to prevent desmin filament aggregation.

To show that the effects of Q151X α B-crystallin were not due to an inhibition of desmin filament assembly per se, negatively stained samples were analysed by electron microscopy (see Figure 4.11) and the presence of abundant 10 nm filaments confirmed. When compared to desmin assembled in the presence of wild type α B-crystallin (see

Figure 4.11A), the absence of α B-crystallin particles in the Q151X containing sample was also immediately apparent (see Figure 4.11B), confirming independently the data in Figure 4.3A and D.

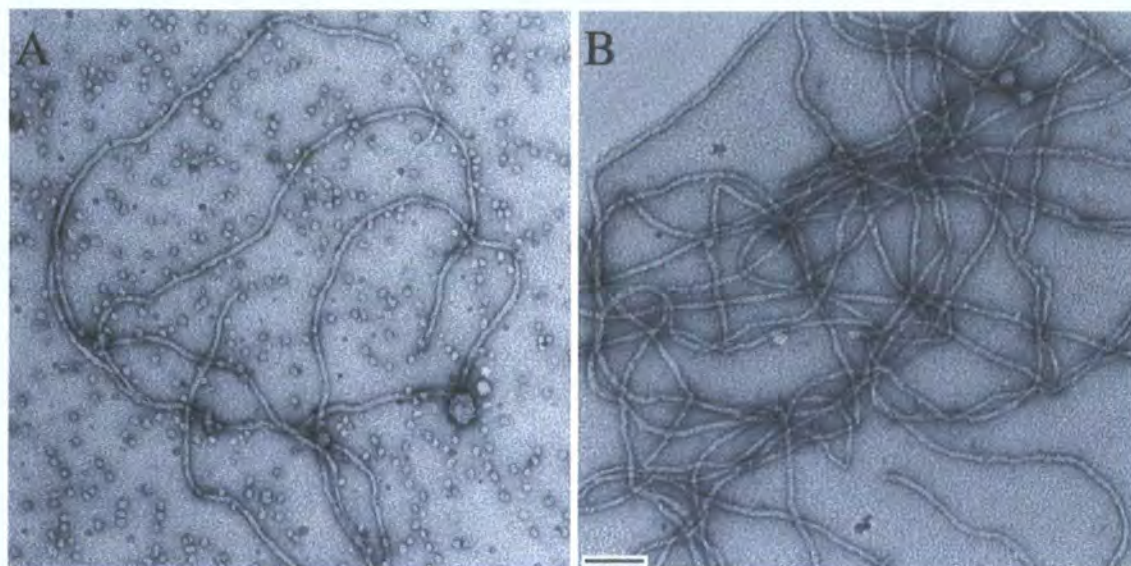


Figure 4.11. Desmin Filament assembly in the presence of wild type and Q151X α B-crystallin. Images obtained by electron microscopy of negatively stained samples of the assembled filaments for desmin assembled in the presence of wild type (A) and Q151X (B) α B-crystallin are shown to show that the addition of both chaperones has not dramatically altered filament morphology or length. Notice the lack of crystallin particles in the Q151X sample. Bar = 100nm.

Mixing Q151X with wild type α B-crystallin in an equimolar ratio reduced this binding to desmin filaments at 37°C (see Figure 4.10B and C) and restored the levels of pelletable desmin to those obtained in the presence of wild type α B-crystallin (see Figure 4.10A). In contrast, the 450delA mutant was clearly dominant over the wild type α B-crystallin as there was not only increased binding to the filaments (see Figure 4.10B and C), but also a significant increase in the proportion of pelletable desmin (Figure 4.10A). These data indicate that the increased binding of 450delA α B-crystallin induces more filament-filament interactions resulting in more desmin in the pellet. Interestingly all the mutant α B-crystallins exhibited elevated binding to desmin filaments (see Figure 4.10C) compared to the wild type α B-crystallin, but under these assay conditions (0.1mg/ml desmin @ 37°C), the Q151X and 450delA α B-crystallin had opposite effects upon the promotion of filament-filament interactions.

The chaperone activity of α B-crystallin is enhanced at elevated temperatures (Datta and Rao, 1999; Koretz et al., 1998; Raman and Rao, 1994; Raman and Rao, 1997). At temperatures greater than 37°C, chaperone activity is elevated by an increase in the subunit dynamics with elevated association and dissociation rate of subunits (Liu et al., 2006a). This stress related signal causes a shift in the equilibrium constant and activates further binding of substrate to the chaperones (Shashidharamurthy et al., 2005), as observed from 20°C to 44°C, where we see an increased binding of the mutants to the desmin filaments (see Figure 4.12C and 4.13C respectively). This enhanced binding was accompanied by increased desmin filament-filament associations shown by increased levels of desmin in the pellet (see Figure 4.12A and 4.13A). The most significant increase in filament-filament associations was observed for the Q151X α B-crystallin, where the amount of pelleted desmin at 37°C doubled at 44°C (see Figure 4.13A) despite only a slight increase in binding between the Q151X α B-crystallin and the desmin filaments (see Figure 4.13 B and C).

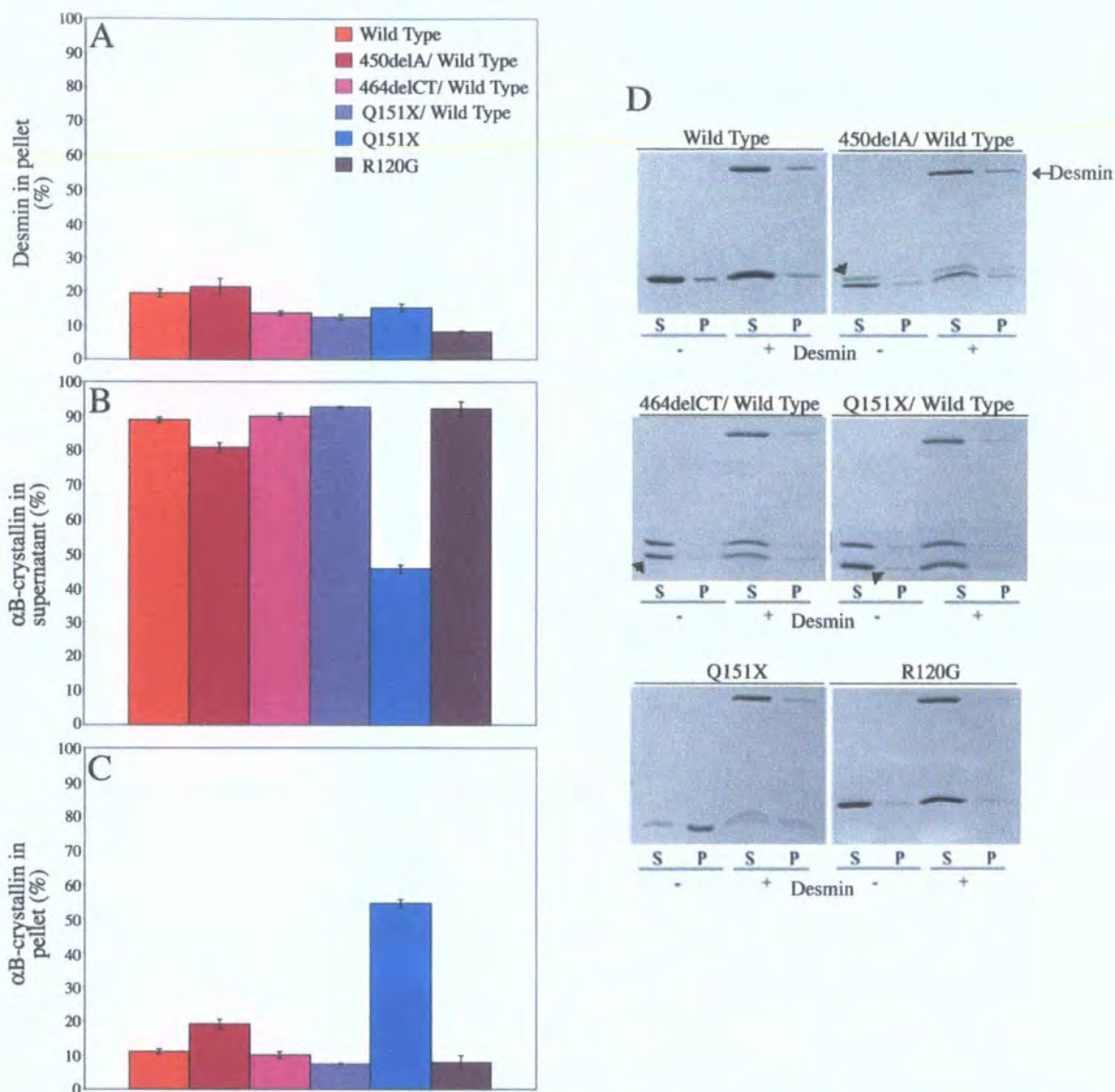


Figure 4.12. Sedimentation assay to investigate the prevention of desmin filament aggregation in the presence of various α B-crystallins at 20°C. (A-C) shows the % desmin pelleted (A), the % α B-crystallin wild type and mutants remaining soluble in the presence of desmin (B), and the % of the total α B-crystallin pelleted in the presence of desmin (C), following low speed centrifugation (2500 x g). These data were calculated from SDS-PAGE data of the desmin binding assays. (D) An example of the data used to calculate these values for wild type and mutant α B-crystallin. Those mutants associated with wild type are (450delA, 464delCT and Q151X) identified with arrowhead.

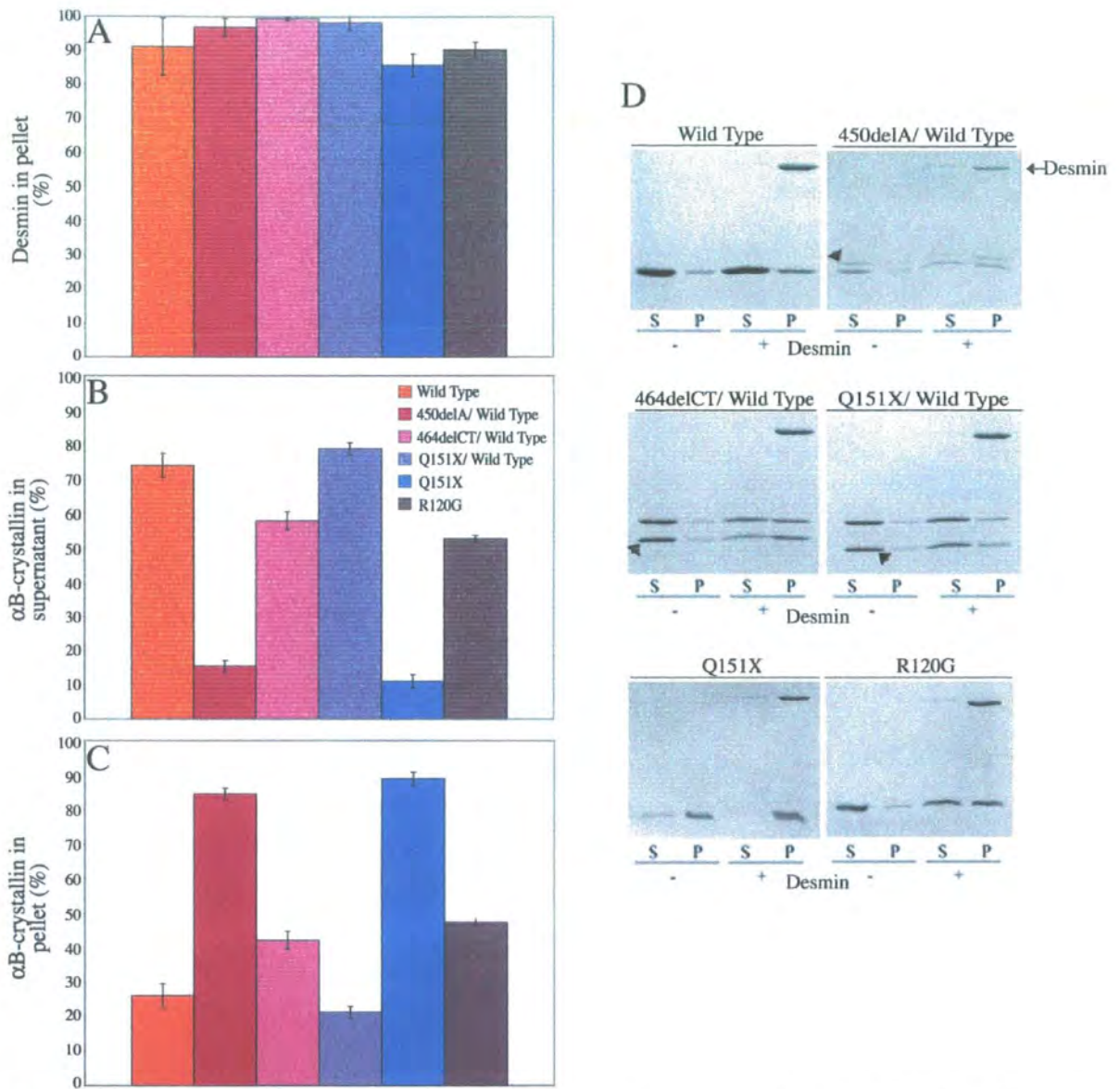


Figure 4.13. Sedimentation assay to investigate the prevention of desmin filament aggregation in the presence of various α B-crystallins at 44°C. (A-C) shows the % desmin pelleted (A), the % α B-crystallin wild type and mutants remaining soluble in the presence of desmin (B), and the % of the total α B-crystallin pelleted in the presence of desmin (C), following low speed centrifugation (2500 x g). These data were calculated from SDS-PAGE data of the desmin binding assays. (D) An example of the data used to calculate these values for wild type and mutant α B-crystallin. Those mutants associated with wild type are (450delA, 464delCT and Q151X) identified with arrowhead.

4.4. DISCUSSION

The C-terminal extension is proposed to play an important role in maintaining solubility and preventing aggregation of the α B-crystallin oligomer. Chapter 3 discussed how the sequential truncation of the C-terminal extension resulted in an equally sequential loss of solubility, with the greatest effect upon solubility being observed with the disease causing mutants. These disease mutants produced the most extreme modifications, where either the whole C-terminal extension was removed (Q151X) or completely altered by frame shift mutation (450delA and 464delCT), thus affecting both the flexible 'tail' and the non-flexible region of the C-terminal extension. The data suggest that perhaps additional regions in the non-flexible C-terminal extension also conferred an additional level of solubility to the complex through a different mechanism.

In order to gain understanding of this mechanism, I wanted to investigate the effect of the C-terminal mutations upon structure and function, which included the characterisation of the relative chaperone function, oligomerisation properties, secondary structure, exposed hydrophobicity and thermal stability. This characterisation aimed to not only provide understanding of the mechanism that links the C-terminal extension with the chaperone function, oligomeric properties and solubility, but to also explain how mutations of this C-terminal, not only cause disease, but result in phenotypic variation.

The consensus view that has emerged from recent studies on mammalian sHSPs is that the C-terminal extension is important for oligomerisation and chaperone function (Andley et al., 1996; Ghosh et al., 2005; Rajan et al., 2006; Thampi and Abraham, 2003).

Characterisation of the disease causing mutants and the series of C-terminal truncation constructs of α B-crystallin in this Chapter has shown that, whilst the C-terminal extension was essential for subunit interactions involved in oligomerisation, it showed a surprising inhibitory effect upon the chaperone function. Infact, for the Q151X α B-crystallin, the removal of the entire C-terminal extension significantly enhanced the chaperone function of α B-crystallin for some client proteins suggesting it is not essential for chaperone activity.

These data, combined with the previous observations in Chapter 3, that all three disease-causing mutations (450delA, 464delCT and Q151X) in the C-terminal extension

destabilise α B-crystallin and increase its tendency to self-aggregate, suggest it is this destabilisation rather than a catastrophic loss of chaperone activity, that is a major factor in disease development.

4.4.1. REMOVAL OF THE C-TERMINAL EXTENSION REDUCES α B-CRYSTALLIN OLIGOMERISATION, BUT NOT CHAPERONE ACTIVITY.

The data presented in this Chapter shows the effects of sequentially truncating this domain (K174, A171, E165, E164 and Q151X), upon both aspects for α B-crystallin. It shows that deletion of the last 5 residues can improve chaperone activity in the citrate synthase assay without dramatically changing the secondary structure or oligomerisation of α B-crystallin. Truncations (E164X, E165X) in the conserved REEK-motif (Rajan et al., 2006) decreased chaperone activity and oligomerisation, although this coincided with more polydispersity for the oligomer as judged by SEC (see Figure 4.3A). The removal of the C-terminal extension by the Q151X mutation produced a construct with the best chaperone activity profile of all the individual proteins investigated (see Figures 4.8 and 4.11) despite the most significant changes in secondary structure (see Figure 4.5) exposed hydrophobicity (see Figure 4.6) and altered oligomerisation (see Figure 4.3 and 4.4). Whilst these results are in broad agreement with the consensus for other mammalian sHSPs, they demonstrate that the removal of the C-terminal extension from residue 151 prevents oligomerisation (at concentrations less than 0.1mg/ml), but not at the expense of chaperone function for α B-crystallin. Indeed the citroconylation of full length α B-crystallin achieves similar results and together with these data strongly support the conclusion that oligomerisation is not required for α B-crystallin chaperone activity (Horwitz et al., 2004).

4.4.2. THE C-TERMINAL EXTENSION IS NOT ESSENTIAL FOR CHAPERONE ACTIVITY AND IS INHIBITORY FOR SOME CLIENT PROTEINS

The chaperone activity of α B-crystallin mutants for client protein citrate synthase illustrated that even the removal of only the terminal two lysines was sufficient to significantly increase the chaperone activity of α B-crystallin above the level of the wild type. The Q151X most surprisingly was not only an efficient chaperone despite its' extreme truncation and inherent instability, but was seen to actually improve chaperone activity for citrate synthase and also desmin, in stark contrast to the effect of removing a similar region from α A-crystallin where chaperone activity was lost (Andley et al., 1996; Thampi and Abraham, 2003). The C-terminal extension deleted by the Q151X mutation includes the IX(I/V) motif (de Jong et al., 1998), which is part of β -strand 10 (Kim et al., 1998a; van Montfort et al., 2001) that has been shown to be both part of a client protein binding site α B₁₅₇₋₁₆₄ (Ghosh et al., 2005) and an oligomerisation sequence α B₁₅₅₋₁₆₅ (Ghosh and Clark, 2005) in α B-crystallin (see Figure 4.1). This is removed by all three disease causing mutations, including Q151X, but retained in the other α B-crystallin mutants. Glycine substitutions in the IX(I/V) motif not only increased oligomerisation and polydispersity of α B-crystallin, but also significantly increased chaperone activity (Pasta et al., 2004). The data presented for Q151X α B-crystallin and the other truncation constructs suggest that the client protein binding site that embraces the IX(I/V) motif sequence (Ghosh and Clark, 2005; Pasta et al., 2004) is not only dispensable for activity, but that it could actually inhibit chaperone function as its removal actually increased activity for Q151X (citrate synthase, \sim 7.5 fold; desmin, \sim 2 fold). Partial removal of this site in E164X significantly inhibits chaperone activity for citrate synthase and insulin (citrate synthase, \sim 0.5 fold; Insulin, \sim 1.4 fold) and is slightly improved by extension of the site in the E165X (citrate synthase, \sim 3.1 fold; Insulin, \sim 0.1 fold). A 3D model of α B-crystallin (see Figure 4.2) has suggested that the C-terminal extension potentially acts as a 'cap' on an important oligomerisation and client protein binding site, namely the β 3- β 8- β 9 interface (Ghosh et al., 2006a). This region also interacts with the β 4 strand, which is important in sHSP oligomerisation as seen from the crystal structure of sHSP16.9 (van Montfort et al., 2001), but it is also critical for chaperone activity (Ghosh et al., 2006a). In

fact reducing α B-crystallin to just its α -crystallin domain spanning residues 57-157, which still includes the β 3- β 8- β 9 surface, retained significant chaperone activity, but this construct only formed dimers and could not oligomerise (Feil et al., 2001) due to the absence of the subunit interaction sequences of the N-Terminal (α B₃₇₋₅₄) and the C-terminal (α B₁₅₅₋₁₆₅), which have been linked with higher order assembly (Ghosh et al., 2005).

It is easy to explain these observations and also data for the Q151X α B-crystallin mutant, in terms of how the removal of this C-terminal extension 'cap' as proposed in the model (Ghosh et al., 2006a) could allow substrate to bind more readily and thus enhance chaperone function, whilst also decreasing oligomer size. The data presented supports this model and also add an interesting new dimension, suggesting that the C-terminal extension actually limits the full potential of α B-crystallin chaperone activity.

4.4.3. AGGREGATION OF α B-CRYSTALLIN IS ENCOURAGED BY THE REMOVAL OF THE C-TERMINAL EXTENSION.

In Chapter 3, I discussed the role of the C-terminal extension as a solubiliser of the α B-crystallin complex. The strong tendency of Q151X to aggregate at protein concentrations greater than 0.1 mg/ml and its very low refolding yield, along with the other aggregation prone disease mutants and E164X and E165X, which saw the removal of the flexible ‘tail’ supported the idea that the C-terminal extension played an important role in preventing the uncontrolled self-aggregation of α B-crystallin (Aquilina et al., 2004). The conclusion was that the flexible C-terminal ‘tail’ was essential to produce a stable α B-crystallin complex and that perhaps additional regions in the non flexible region of the C-terminal extension also conferred an additional level of solubility to the complex, through a mechanism that also involved the oligomerisation and chaperone function (Ghosh et al., 2006d). The C-terminal extension can influence the structure and function of α B-crystallin apart from the solubilising function that is generally attributed to this region. It appears that this region can have either inter- or intramolecular tertiary interactions that contribute significantly to the function (Pasta et al., 2002). In sHSP16.9, the IX(I/V) motif from one subunit lays in a hydrophobic groove between β 4 and β 8 strands of the other interacting monomer. Although α B-crystallin has similar structural features, including the conserved IX(I/V) motif in its C-terminal extension, the oligomers it forms are more polydisperse (Aquilina et al., 2004; Haley et al., 2000; Kim et al., 1998b) compared to either sHSP16.5 or sHSP16.9, suggesting that the precise detail for the interactions of the C-terminal extension in α B-crystallin will vary, not least due to the different hinge sequences between β -strands 9 and 10 (van Montfort et al., 2001). The strong tendency of Q151X α B-crystallin to aggregate suggests that the C-terminal extension actually prevents such errant subunit associations to favour instead oligomerisation. Therefore, the non-flexible C-terminal extension confers a level of stability to the α B-crystallin in addition to the solubilising ‘tail’ through a mechanism, which provides an interactive arm for oligomerisation and acts as a ‘cap’ over the interactive substrate binding β 3- β 6- β 9 region.

4.4.4. REDUCED PROTEIN STABILITY AND UNCONTROLLED SELF-AGGREGATION UNDERLIES THE MOLECULAR BASIS OF THE Q151X, 450DELA AND 464DELCT MUTATIONS.

To fully understand the role of C-terminal extension in the disease mechanisms causing phenotypic variation required characterisation of not only the solubility (see Chapter 3), but also of the chaperone activity and oligomerisation properties of these C-terminal mutations. This additional characterisation helped to provide a link between the structural and functional properties of the C-terminal mutants and the potential molecular basis of associated disease phenotypes.

The partial loss of the C-terminal extension due to the E164X and E165X and the complete loss due to the Q151X mutation in α B-crystallin dramatically altered the secondary (see Figure 4.5) and tertiary structure of the protein (see Figure 4.3). These truncations significantly destabilised the protein as seen from the heat stability assay (see where the E164X and E165X rapidly formed substantially larger aggregates than Q151X Figure 4.7) as supported by the variations in complex size and oligomeric characteristics (see Figure 4.3). This truncation of the C-terminal extension, which removes the flexible solubilising 'tail', showed a dramatic increase in the tendency to self-aggregate in vitro (see Chapter 3, Section 3.3.4) and in vivo (see Chapter 3, Section 3.3.5). However, the Q151X α B-crystallin, even in the presence of equimolar wild type, had significantly altered secondary structure (see Figure 4.5) which affected α B-crystallin oligomerisation (see Figure 4.3) and reduced refold yields (see Chapter 3, Section 3.3.4).

The Q151X mutation was dominant over the wild type protein in its effects upon heat stability, solubility and secondary structure. These data suggest that the strong tendency to self-aggregate as a result of reduced stability is potentially an important factor in disease development. Data for both 450delA and 464delCT also suggest that it is a similar loss in protein stability that causes cataract and myofibrillar myopathy respectively. Both mutants can only be refolded in the presence of wild type α B-crystallin and even then the temperature stabilities of the mixtures are reduced by some 20 °C compared to the wild type protein alone. Both the 450delA and 464delCT mutations introduced novel C-terminal peptides that have no homology to the existing C-terminal extension of α B-crystallin (see Figure 4.1B). Both mutations changed the oligomerisation

of wild type α B-crystallin and neither mutant/wild type mixture was an effective chaperone in either the desmin (see Figure 4.12) or insulin (see Figure 4.9) assays. Therefore loss of chaperone activity could also potentially contribute to the development of disease for these two mutants, as suggested in the case of amyloidogenesis, the chaperone ability is crucial for preventing fibril formation. The aggregation of α B-crystallin has been shown to have all the characteristics of fibrils associated with the family of amyloid diseases and that under destabilising conditions conversion of α B-crystallin into fibrils could contribute towards the disease pathology (Meehan et al., 2007).

The data suggest that the mechanism of disease associated with C-terminal mutants is influenced by an effect upon solubility and chaperone activity, however it is still not possible to draw a link between structure and function of the α B-crystallin and its phenotypic heterogeneity. The three disease-causing mutations in the C-terminal extension of α B-crystallin (Q151X, 450delA and 464delCT) are restricted in their pathology to either the lens (450delA (Berry et al., 2001)) or muscle (Q151X, 464delCT; (Selcen and Engel, 2003) and yet α B-crystallin is very highly expressed in both tissues (Kato et al., 1991). This is a familiar trend for α B-crystallin mutations and even the most recently published mutation, D140N, causes only lens cataract (Liu et al., 2006b). Thus far, R120G α B-crystallin is the only mutation that has produced both lens and muscle pathologies (Vicart et al., 1998), but this is not to say that sub-clinical pathology can be totally excluded for the other mutations, including Q151X, as tissue biopsies from apparently unaffected tissues were not analysed. Aggregation is a key histopathological feature of the Q151X mutation (Selcen and Engel, 2003) concurring with the data from the transient transfection and cell fractionation studies (see Chapter 3, Section 3.3.5) and so, this provides a plausible mechanism to support a potential dominant negative effect of the mutation by inhibiting the chaperone function of wild type α B-crystallin via co-aggregation with mutant Q151X as implicated from the in vitro refolding studies in Chapter 3, Section 3.3.4.

4.5. CHAPTER'S CONCLUSIONS

In Chapter 3 it was clear that the flexible C-terminal 'tail' was essential to produce a soluble α B-crystallin complex. A recent study however, showed how additional regions in the non-flexible region of the C-terminal extension conferred an additional level of solubility to the complex through a mechanism that also involved the oligomerisation and chaperone function (Ghosh et al., 2006d).

Therefore, in this chapter I wanted to understand how the C-terminal extension influences the chaperone function, oligomeric properties and solubility, with the aim of finding a link to the mechanism that not only causes disease but also results in varying pathology.

This Chapter has shown that the C-terminal extension influences both the structure and function of α B-crystallin in addition to the solubilising function that is generally attributed to this region.

The C-terminal extension is primarily involved in subunit-subunit interactions required for oligomerisation and is not essential for chaperone activity. The C-terminal extension can actually inhibit client substrate binding by 'capping' the β 3- β 8- β 9 interface in the α -domain, which is the interactive site for substrate binding. I have also suggested that the potential molecular mechanism behind the pathology of the disease causing mutants is a function of the reduced protein stability and uncontrolled self-aggregation caused by the alterations to the C-terminal extensions. The link however, between these findings and the mechanism, which causes the observed variations in phenotype, remains unclear and requires further investigation.

CHAPTER 5

THE RELATIONSHIP BETWEEN SUBUNIT DYNAMICS AND THE OLIGOMERISATION OF WILD TYPE α B-CRYSTALLIN

5.1. AIMS

In this Chapter, I have investigated the relationship between the subunit dynamics of wild type α B-crystallin and oligomerisation, hoping to provide further insight into the role played by this domain in the efficient chaperoning of client proteins. The polydisperse assembly of wild type α B-crystallin exists as part of a dynamic equilibrium with a constant exchange of subunits between the oligomer and a pool of subunits (Bova et al., 1997; Bova et al., 2000; Van Den Oetelaar, 1990), which have been suggested as potential active units of chaperone activity (Aquilina, 2005; Aquilina et al., 2003; Bova et al., 2000). The subunit dynamics of α B-crystallin are affected by various factors such as temperature and pH, however one of the factors important in the rate of reactions is protein concentration, which determines the frequency of collision of subunits and subsequently the rate of subunit exchange. In this chapter, I wanted to analyse the effect of protein concentration of wild type α B-crystallin upon oligomerisation, with the aim to further understand the relationship between subunit dynamics and the mechanism of chaperone activity.

In Chapter 4, I discussed how chaperone activity is reliant upon the presence of the α -domain β 3- β 8- β 9 surface for client protein interaction, thus dissociation of α B-crystallin subunits from the oligomer would increase exposure of this interface to client proteins. Similarly, the literature suggests that under conditions of stress there is an increased level of dissociation of α B-crystallin subunits from the oligomer to prevent the aggregation of unfolding or denatured proteins. The argument for this theory is not only supported by the data in Chapter 4 which observed an increase in chaperone activity for the Q151X α B-crystallin which appears monomeric, but would also be strengthened by the isolation and characterisation of an active pool of dissociated subunits. Thus far however, under normal physiological conditions it is impossible to isolate significant amount of monomers, dimers, or tetramers of α -crystallin (Horwitz et al., 2004).

5.2. INTRODUCTION

In the lens, α -crystallin subunits self-associate through subunit exchange to form polydisperse assemblies that function as chaperones, however the α A- and α B-crystallin subunits may play different roles both in the α -crystallin heteroaggregate and as separate proteins under stress conditions (Datta and Rao, 1999; Kamei and Matsuura, 2002). Whilst the subunit dynamics that influence the complex assembly of human α A and α B-crystallin are important in the regulation of chaperone activity (Bova et al., 1997; Liu et al., 2006; Shashidharamurthy et al., 2005; Spinozzi et al., 2006; Studer and Narberhaus, 2000) a study has shown the rate of subunit exchange is not the critical parameter in determining efficient chaperone behaviour for mammalian α A-crystallin (Aquilina, 2005). The polydisperse assemblies of both α A and α B-crystallin exist as part of a dynamic equilibrium with a constant exchange of subunits between the oligomer and a pool of subunits (Bova et al., 1997; Van Den Oetelaar, 1990). For α A-crystallin, a study revealed a quaternary structure of α A-crystallin consisting of small multimers of α A-crystallin subunits (trimer or tetramer) in a dynamic equilibrium with the oligomeric complex (Bova et al., 2000). Similarly for α B-crystallin, Aquilina et al. (2003) observed the formation of α B-crystallin oligomers that contained odd and even numbers of subunits implying both dimeric and non-dimeric quaternary interactions form the basic building block of oligomerisation and that these monomers or dimers may constitute the active units of chaperone activity in dynamic exchange with the oligomer (Aquilina et al., 2003; Aquilina et al., 2004). Thus far, under normal physiological conditions, however it is impossible to isolate significant amount of monomers, dimers, or tetramers of α B-crystallin (Horwitz et al., 2004) to enable further investigation of these potential active units and their role in chaperone activity.

The relationship between chaperone activity, subunit dynamics and oligomer assembly remain unresolved and the mechanism by which this chaperone function occurs is not fully understood, however, a number of theories exist to explain the relationship between oligomerisation state, chaperone activity and the influential factors which induce subunit exchange and regulate chaperone activity.

5.2.1. THEORIES FOR THE ROLE OF OLIGOMERISATION AND SUBUNIT DYNAMICS IN CHAPERONE ACTIVITY

The theories for the role of oligomerisation and subunit dynamics in chaperone activity suggest that oligomerisation is essential for efficient chaperone activity and that dissociation of subunits from the oligomeric state is required for chaperone function, whilst others suggest that the oligomeric complex is the active unit of chaperone activity and that no dissociation is required. There have been a number of studies showing support for both the oligomerisation and the dissociation theory of chaperone function.

5.2.1.1. Dissociation Theory

The theory of dissociation suggests the oligomer dissociates into smaller subunits such as monomers, dimers or multimers exposing hydrophobic surfaces enabling binding (Haslbeck et al., 1999; Van Montfort et al., 2001a). Loosening of subunit organisation may lead to more dynamic properties enhancing the available chaperone sites for target proteins. (Pasta et al., 2003). Once substrate (client protein) binding has occurred the subunits may re-associate into large soluble complexes that interact with ATP-dependant refolding machinery such as HSP70 (van Montfort et al., 2001b). Liu et.al. (2006) proposed that the subunits act as a one way irreversible 'sink' that traps the unfolded proteins (Liu et al., 2006). Another proposal suggests a different mechanism where α B-crystallin molecules are assembled into large insoluble protein aggregates that enable the subsequent disaggregation and refolding by the ATP dependant refolding machinery (Haslbeck et al., 2005).

Narberhaus states that oligomerisation is a pre-requisite for chaperone function and subunit exchange (Narberhaus, 2002) and acts as a supply of subunits, which dissociate to form the soluble pool of the active unit of chaperone activity. Some studies, however suggest this oligomerisation may not be necessary for chaperone function. The unit of subunit exchange between closely related oligomers is a dimer (Stamler et al., 2005) and interestingly, a truncated form of α B-crystallin (α B₅₇₋₁₅₇), which exists as a dimer still shows activity as a chaperone (Feil et al., 2001), suggesting that that the native oligomeric

state of α B-crystallin may not be essential for chaperone function and that multimerisation above a dimer is not required (Feil et al., 2001).

Horwitz et al. (2004), used citroconylation to disrupt the oligomeric state of α A and α B-crystallin and induce the dissociation of subunits. After this treatment the α B-crystallin oligomerisation was shown to be concentration dependant with monomers and dimers forming at 0.01 mg/ml, while at concentrations > 0.5 mg/ml tetramers are the major species. α A-crystallin is mostly tetrameric at any concentration following citroconylation. This study observed similar chaperone activity for the tetramers and monomers to the wild type suggesting that oligomerisation was not essential for chaperone activity (Horwitz et al., 2004).

5.2.1.2. Chaperone assisted stabilisation of α B-crystallin via subunit exchange

Some studies have identified another pre-requisite for efficient chaperone function. The binding of an alternative chaperone in conjunction with subunit dissociation acts to stabilise α B-crystallin thus promoting its role as a chaperone. HSP27 interacts with α A and α B-crystallin *in vivo*, but to a greater extent with α B-crystallin. In non-lenticular tissues HSP27 is expressed with α B-crystallin rather than α A-crystallin and may serve to stabilise α B-crystallin in non-lenticular tissues by co-localisation with α B-crystallin under both normal conditions and in a stressed or diseased state (Zantera et al., 1992). The likely mechanism of α B-crystallin protection by HSP27 is subunit exchange similar to the stabilising effect α A-crystallin has with α B-crystallin in the lens (Horwitz et al., 1999; Sun et al., 1998). One study by Bova et al. (2000), discusses two mechanisms for the subunit exchange between α A-crystallin and HSP27 including firstly, the continuous association and dissociation of subunits as a result of a collision between oligomers and secondly, the continuous dissociation and reassociation of the exchange unit (Bova et al., 2000).

5.2.1.3. Oligomer Theory

A number of studies have proposed that the oligomer is the active unit of chaperone activity. One study showed that the oligomer remains intact as it binds substrate on its surface and no subunit exchange is necessary (Kim et al., 2003). Initial cross-linking studies with α -crystallin have shown an oligomer α -crystallin is an efficient chaperone (Sharma and Ortwerth, 1995). Later studies which, involved preventing dissociation by cross-linking α B-crystallin, illustrated how the cross-linked α B-crystallin proved a more effective chaperone than native α B-crystallin. This study concluded that chaperone activity is a surface phenomenon and dissociation is not required for full activity (Augusteyn, 2004).

Avilov et al. (2004) used surface plasmon resonance (SPR) to study the interactions between oligomeric α -crystallin and its individual subunits with unfolded proteins. Immobilization at the sensor chip allowed the study of isolated α -crystallin subunits under physiological conditions for the first time and showed that α -crystallin subunits, in contrast to α -crystallin oligomers did not bind unfolded protein. These data indicated that quaternary structure of α -crystallin is necessary for its chaperone-like activity (Avilov et al., 2004). A recent contrasting SPR study was able to identify various influential factors, which affect α B-crystallin subunit interactions including pH and temperature. This utilised a layer of α B crystallin subunits adsorbed onto the surface of a sensor chip and a solution of α B crystallin was then flowed over the surface-bound subunits. The associations between individual subunits were analysed under varying conditions of acidity, temperature and oxidative stress and illustrated binding even at the monomeric level (Liu et al., 2006).

5.2.2. INFLUENTIAL FACTORS AFFECTING SUBUNIT DYNAMICS, OLIGOMERISATION AND CHAPERONE ACTIVITY

Interconversion of the oligomer between multiple states is the underlying mechanism of regulation of chaperone function, however, the relationship between chaperone activity, subunit dynamics and assembly remain unresolved.

In order to understand the mechanism regulating subunit dynamics, oligomerisation and chaperone activity it is important to understand what factors activate the mechanisms of subunit exchange, oligomer dissociation and exposure of interactive regions, whilst considering how these changes relate to the theories of chaperone activity.

We know that α B-crystallin interacts with a broad range of proteins, including itself and its homolog α A-crystallin, and is up regulated during conditions of stress including heat shock, low pH and oxidative stress (Datta and Rao, 1999; Liu et al., 2006; Pasta et al., 2003) . These stress conditions mediated by other factors have been shown to affect the subunit dynamics, oligomerisation and chaperone activity of α B-crystallin and include temperature, pH, phosphorylation and ATP. Divalent metal ions such as calcium, magnesium, copper and zinc have been found to influence chaperone activity but show no effect upon the subunit dynamics of α B-crystallin (del Valle et al., 2002; Duncan and Jacob, 1984; Ganadu et al., 2004; Marini et al., 1995).

5.2.2.1. Phosphorylation

Phosphorylation of α -crystallin has been reported variously to have no effect on chaperone activity (Carver et al., 1996; Nicholl and Quinlan, 1994), to reducing chaperone activity (Aquilina et al., 2004; Kamei et al., 2001) and to cause a decrease in oligomeric size (Moroni and Garland, 2001).

Both α A- and α B-crystallin polypeptides are phosphorylated on serine residues 19, 45, and 59 by cAMP-dependent and cAMP-independent mechanisms. The cAMP-independent pathway is an autophosphorylation that has been demonstrated *in vitro*, depends on magnesium and requires cleavage of ATP (Kantorow and Piatigorsky, 1998; Miesbauer et al., 1994). These phosphorylated forms are not only important because of their abundance in aging lenses and the implications for cataract but also because they have been identified in patients with degenerative brain disease (Kato et al., 2001). A study by Aquilina et al. (2004) found that phosphorylation of Ser-45 increases polydispersity of α B-crystallin, which stems from disruption of the dimeric substructure and changes in the subunit dynamics within the polydisperse α B-crystallin assembly (Aquilina et al., 2004).

In U373 MG human glioma cells, α B-crystallin was observed as large oligomers with apparent molecular masses about 500 kDa and the oligomerization size was reduced after phosphorylation of all three Ser sites (19, 45 and 59). Phosphorylation of α B-crystallin caused dissociation of large oligomers to smaller sizes of molecules and reduction of chaperone-like activity (Ito et al., 2001). The α -crystallin polypeptides differ with respect to their abilities to undergo cAMP-dependent phosphorylation, with preference given to the α B-crystallin chain. These differences and complexities in α -crystallin phosphorylations, coupled with the differences in expression patterns of the two α -crystallin polypeptides, are consistent with the idea that each polypeptide has distinctive structural and metabolic roles (Kantorow and Piatigorsky, 1998).

5.2.2.2. Temperature

Studies have shown that temperature significantly influences subunit exchange of α B-crystallin subunits. The chaperone activity of α B crystallin was enhanced at elevated temperatures,(Datta and Rao, 1999; Koretz et al., 1998; Raman and Rao, 1994; Raman and Rao, 1997). Heat shock raised the demand for chaperone function and led to the exposure of hydrophobic chaperone sites by subunit exchange (Shashidharamurthy et al., 2005). At temperatures greater than 37°C, chaperone activity was elevated and an increase in the subunit dynamics with elevated association and dissociation rate of subunits was observed (Liu et al., 2006). This stress-related signal causes a shift in the subunit exchange equilibrium constant and activates binding of substrate to the chaperones. (Shashidharamurthy et al., 2005)

Studies attempting to evaluate chaperone activity as a function of temperature showed that the polydispersity of the α B-crystallin oligomer increased at elevated temperatures in the presence of insulin, urea and thiocyanate (Spinozzi et al., 2006). The changes in polydispersity occurred in three stages, the first transition at temperatures greater than 37°C affects activity but size is not affected until the temperature has elevated above 42°C and above 60°C there is a large structural reorganisation (Spinozzi et al., 2006). At elevated temperatures the demand for chaperone activity is increased and an increase in oligomer size may be explained by the reassociation of substrate bound subunits into the oligomer.

Circular dichroism studies by Datta et al. (1999), showed some tertiary structural changes in α A-crystallin above 50°C, but α B-crystallin shows significant alteration of tertiary structure by 45°C. The study demonstrated that despite a high degree of sequence homology and their generally accepted structural similarity, α B-crystallin is much more sensitive to temperature-dependent structural perturbation than α A-crystallin or α -crystallin and shows differences in its chaperone-like properties. These differences appear to be relevant to temperature-dependent enhancement of chaperone-like activity of α -crystallin and indicate different roles for the two proteins both in α -crystallin heteroaggregate and as separate proteins under stress conditions (Datta and Rao, 1999).

5.2.2.3. pH

A recent study observed that under acidic conditions, the interaction between α B crystallin subunits increased with a higher association rate and a lower dissociation rate, suggesting that the formation of stable oligomeric assemblies of α B-crystallin was favoured under acidic pH conditions. At pH values lower than pH 7.0 chaperone activity was reduced but association was increased, however dissociation was decreased. These findings suggested that dynamic and rapid subunit exchange may regulate chaperone activity (Liu et al., 2006). The pH dependence of the subunit-subunit interactions of α B crystallin was independent of temperature. α B-crystallin is more sensitive to changes in pH than is α A-crystallin and is found in degenerating brain tissues where pH conditions are acidic (van Rijk and Bloemendal, 2000; Yun et al., 2002) and α B crystallin is found to be co-localized in high Mwt insoluble cytotoxic aggregates, neuritic plaques, amyloid- β peptides and other aggregating proteins as observed in neurofibrillary tangles and plaques in brains of Alzheimer's patients as well as cataracts in the elderly (Cobb and Petrash, 2002; Liang, 2000; Mao et al., 2001; Pan et al., 1993). In vitro studies have further shown that the binding affinity of α B-crystallin to actin and desmin filaments increases considerably at slightly acidic pH of pH 6.5, consistent with the findings of Liu et al., (2006) where increased associations resulted in the formation of stable complexes at pH<7.0 and was found to effectively prevent the tendency of actin filaments to form aggregates at acidic pH. These in vitro data suggest a protective role of α B-crystallin during stress conditions such as ischemia of the heart. Crystallin could prevent the aggregation of filaments, which might occur during the acidification of the cytosol and lead eventually to irreversible structural damage (Bennardini et al., 1992; Chiesi et al., 1990). A study by Koretz et al. (1998), revealed CD spectra, which indicated that acidic conditions led to some degree of unfolding and that this unfolding correlates directly with functionality (Koretz et al., 1998).

5.2.2.4. ATP

α B-crystallin and other sHSP's have traditionally been thought of as ATP independent chaperones, however a recent study has identified the β 4- β 8 groove in α B-crystallin as an interaction site for ATP (Ghosh et al., 2006c). Upon binding of ATP there is an effect on the subunit dynamics caused by conformational changes via disruption of the interaction between the C-terminal and the normally buried β 4- β 8 chaperone interface, leading to an increased association with unfolding substrates and enhancement of chaperone activity (Ghosh et al., 2006c). An earlier study demonstrated an ATP-dependent structural modification in the core α -crystallin domain of α B-crystallin (Muchowski et al., 1999).

A functional relationship between ATP and chaperone-like activity for α -crystallin was suggested when an interaction between ATP and bovine α -crystallin was observed (Palmisano et al., 1995; Reddy et al., 1992) and some studies have shown the binding of ATP to α -crystallin and not its hydrolysis was required to enhance chaperone activity (Biswas and Das, 2004).

A model for chaperone activity of small heat shock proteins by van Montfort et al. (2001) proposed that ATP causes sHSPs to release substrates, which are then renatured by other larger heat shock proteins. Once substrate binding has occurred the subunits may reassociate into large soluble complexes that interact with ATP-dependant refolding machinery such as HSP70 (van Montfort et al., 2001b). A similar role has been proposed for ATP in α -crystallin chaperone activity. A study implied that multiple ATP molecules bind to each subunit and/or ATP causes a more compact α -crystallin structure. Such a conformational change could release a bound substrate via both direct displacement and a global conformational change (Hasan et al., 2002).

5.2.2.5. Affinity

The collective response of the interactive domains of sHSPs determines selectivity for similar subunits, unfolding substrate proteins, or filaments in the dynamic equilibrium model for the function of sHSPs *in vivo* (Liu et al., 2006). The selective rather than specific nature of the interactions between sHSPs and unfolded substrate proteins appears to be a function of the amount of unfolding and exposed hydrophobic surface of the substrates in response to stress (Liu et al., 2006). Perhaps both dissociated subunits and oligomer have the ability to chaperone but it's the level of stress, which dictates the level of protein unfolding, thus the required oligomerisation state.

Dissociation affects the exposure of sites with varying levels of affinity for the substrate. Ghosh and Clarke (2005) suggested multiple domains of varying affinity of α B-crystallin, giving the ability to adapt the exposure of surfaces depending on the severity of the demand for chaperone and level of stress, i.e. unfolded or partially unfolded proteins (Ghosh et al., 2005). Continuing investigation of the relative binding affinities of interactive domains in human α B crystallin will characterize the collective interactions used in molecular recognition and selection mechanisms of the sHSPs (Ghosh et al., 2006d).

Understanding the relationships between oligomer assembly, subunit dynamics and chaperone activity will help gain further insight into the mechanism that induces and influences chaperone function. The existing oligomer theory (Augusteyn, 2004; Avilov et al., 2004; Kim et al., 2003; Sharma and Ortwerth, 1995) and dissociation theory (Feil et al., 2001; Haslbeck et al., 1999; Horwitz et al., 2004; Liu et al., 2006; Narberhaus, 2002; Pasta et al., 2003; Stämmler et al., 2005) explaining the relationship between oligomerisation state, subunit dynamics and chaperone activity along with the extensive studies performed to characterise the interactive regions exposed during subunit dissociation (Bhattacharyya et al., 2006; Ghosh and Clark, 2005; Ghosh et al., 2005; Ghosh et al., 2006a; Ghosh et al., 2006b; Ghosh et al., 2006c; Ghosh et al., 2006d; Sreelakshmi et al., 2004; Sreelakshmi and Sharma, 2005; Sreelakshmi and Sharma, 2006), suggest that the dissociation and subunit exchange is a pre requisite for chaperone function

and is not consistent with the oligomer theory. This supports the theory that there may be a soluble pool in constant equilibrium and dynamic exchange with the oligomer (Bova et al., 1997; Bova et al., 2000; Van Den Oetelaar, 1990), which have been suggested as potential active units of chaperone activity (Aquilina, 2005; Aquilina et al., 2003; Bova et al., 2000).

The subunit dynamics and oligomerisation of α B-crystallin are affected by various factors such as phosphorylation, temperature, pH and ATP, however one of the factors important in the rate of reactions is protein concentration, which determines the frequency of collision of subunits and subsequently the rate of subunit exchange. In this chapter, I aim to analyse the effect of protein concentration of α B-crystallin upon oligomerisation, with the aim to further understand the relationship between subunit dynamics and the mechanism of chaperone activity, whilst investigating the existence of a soluble pool of α B-crystallin subunits and its potential as the active unit of chaperone activity.

5.3. RESULTS

The investigation of the effect of α B-crystallin concentration upon oligomerisation involved the use of a Superose 6 SEC column with a Merck Hitachi HPLC system with injection valve. Initial experiments identified peak material, which appeared consistently at the end of the 93.3 min separation range of the column. Buffer blank SEC with various buffers including Tris, ammonium acetate and NaPO_4 all identified the peak material at approximately 93 min, as did conditions using 1M NaCl, confirming it was not caused by a buffer component or by hydrophobic interactions with the column matrix.

Further analysis of the system confirmed that the 93 min peak was an effect introduced by the injection valve, and interfered with the UV detection because of the low level of sensitivity at which, the experiments were performed.

Immunoblotting analysis also revealed that separation of α B-crystallin wild type resolved an unknown α B-crystallin species past the separation range of the column independent to the 93 min peak. (For full details see Appendix 4).

The results contained within this section focus upon (i) the effect of α B-crystallin concentration upon oligomerisation and (ii) the characterisation of an unknown α B-crystallin species past the separation range of the column.

5.3.1. THE EFFECT OF α B-CRYSTALLIN CONCENTRATION UPON OLIGOMERISATION AND POLYDISPERSITY

Horwitz et al. (2004), using citroconylation showed that α B-crystallin oligomerisation is concentration dependant with monomers and dimers forming at 0.01 mg/ml while at concentrations > 0.5 mg/ml tetramers are the major species. This study suggests that the increased concentration causes a shift in the equilibrium and activates association of subunits. Here I investigated the effect of α B-crystallin concentration upon oligomerisation by repeated separation (rechromatography) of the wild type α B-crystallin oligomer by SEC (see Section 2.8.2). The first cycle involved the separation of 500 μ g of wild type α B-crystallin (2 mg/ml) and the resolved oligomer fraction was stored *intermediately* overnight at ambient temperature 20°C before the second cycle of separation. This was repeated for a total of 4 cycles to achieve appropriate falls in concentration and enable the subsequent effect upon oligomerisation. Based on absorbance data, cycle 2 represented a 0.25 mg/ml solution and cycles 3 and 4 represented a 0.1 mg/ml and 0.01 mg/ml solution respectively (see Figure 5.1).

The first cycle (see Figure 5.1A) shows the α B-crystallin oligomer as a symmetrical peak at 57.4 min. The four cycles of SEC showed a change in the oligomerisation of wild type α B-crystallin as the concentration decreases. The peak height of the Cycle 2 oligomer (see Figure 5.1B) suggests a dilution of approx 8X to a predicted dilution of 0.25 mg/ml, however there is no effect upon oligomerisation with the retention time being consistent with cycle 1 and the peak area for cycle 1 and 2 both being 100%. Cycle 3 represented an approx 0.1 mg/ml solution and had the most interesting effect upon oligomerisation. Figure 5.1C shows the introduction of a shoulder on the leading edge of the oligomer peak at 49.8 min representing 10% of the total wild type mixture and the presence of 1.02 % of high Mwt material at 27.6 min (see Table 5.1). The oligomer peak appears less symmetrical and represents 88.36 % of the wild type α B-crystallin. The presence of these additional peaks and the asymmetry of the oligomer peak suggest that the fall in α B-crystallin wild type concentration has increased the polydispersity of the wild type oligomer.

Further dilution by recycling fraction 55-60 min from Cycle 3 results in a shift in retention time from 57.6 min in Cycle 3 to 60.2 min for Cycle 4 (see Figure 5.1D) and is suggestive of a smaller oligomer. The polydispersity appears more like that seen for Cycle 1 and 2 with the oligomer peak regaining its symmetry. Any additional peaks however, of lower or higher Mwt may not be observed due to the level of sensitivity.

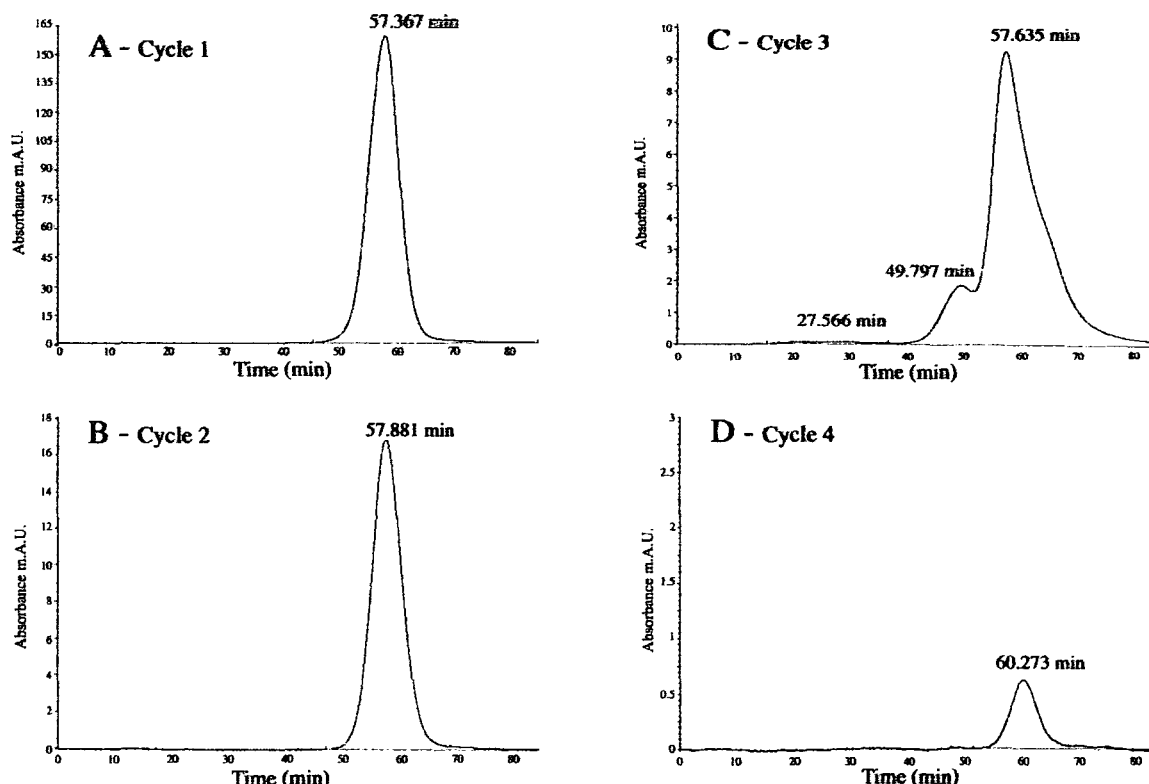


Figure 5.1. The effect of decreasing concentration upon the oligomerisation of wild type α B-crystallin at ambient temperature (20°C). Wild type α B-crystallin was separated by analytical SEC using a 26 ml Superose 6 column in 10mM Tris-HCl, 100mM NaCl, pH7.4 at 2 mg/ml (A) and the fraction collected between 55-60 min was recycled over the SEC column for a further 3 cycles (B-D) in order to see the effect of dilution upon the oligomerisation characteristics. Cycle 2 (B) represents an α B-crystallin concentration equivalent to 0.5 mg/ml, with Cycle 3 (C) and cycle 4 (D) representing 0.1 mg/ml and 0.01 mg/ml respectively. Samples for rechromatography at 20°C were stored overnight at 20°C.

Table 5.1. Integration data for Figure 5.1

Cycle	Time (min)	Height (mA.U)	Peak Area (%)
1	57.367	132.74	100
2	57.881	16.94	100
3	27.566	0.07	1.02
	49.797	1.87	10.62
	57.635	9.28	88.36
4	60.273	0.62	100

At ambient temperature, a fall in α B-crystallin concentration from 2 mg/ml to 0.25 mg/ml had no effect upon oligomerisation or polydispersity. Subsequent dilutions to 0.1 mg/ml resulted in a significant increase in polydispersity and further dilution to 0.01 mg/ml saw a decrease in the oligomer size represented by a shift in retention time.

The four cycles in Figure 5.1 were repeated this time with incubation of α B-crystallin at 4°C prior to SEC analysis performed at ambient temperature with storage of samples at 4°C between cycles. The low temperature will reduce the rate of association and dissociation and perhaps amplify the effects of concentration on polydispersity at 0.1 mg/ml.

The α B-crystallin oligomer is consistent through cycles 1 and 2 (see Figure 5.2A and B) and not until the third cycle do we observe a change in the polydispersity. Additional peaks relatively small in height were observed at 19.2, 39.3 and 73.6 min (see Figure 5.2C) with peak areas of 12.36%, 1.93% and 6.04% respectively (see Table 5.2). It is worth noting however, that the void volume of the column is 30 min at which proteins of 2000 kDa are observed (see Appendix 2). The oligomer peak remains symmetrical. At ambient temperature cycle 3 showed a greater effect upon polydispersity of the oligomer as well as the introduction of additional peaks (see Figure 5.1C), also under conditions of high ionic strength at ambient temperature (performed to assess the interaction characteristics of the 93 min peak material with the column matrix), cycle 3 showed an additional peak at 81.6 min (see Appendix 4, Figure A4.1C).

The data supports the theory that there is a critical concentration below which, there is a change in subunit equilibrium resulting in the formation of oligomers smaller in size with greater polydispersity.

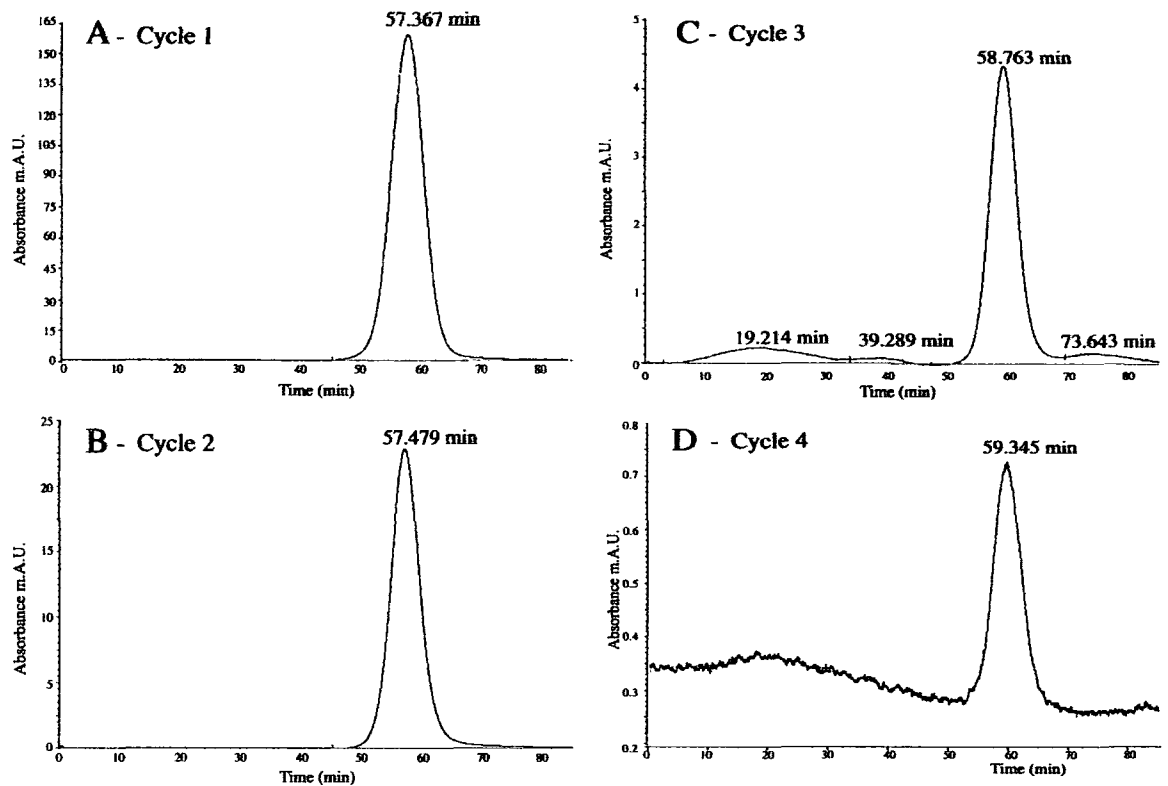


Figure 5.2. The effect of decreasing concentration upon the oligomerisation of wild type α B-crystallin at 4°C. Wild type α B-crystallin was separated by analytical SEC using a 26 ml Superose 6 column in 10mM Tris-HCl, 100mM NaCl, pH 7.4 at 2 mg/ml (A) and the fraction collected between 55-60 min was recycled over the SEC column for a further 3 cycles (B-D) in order to see the effect of dilution upon the oligomerisation characteristics. Cycle 2 (B) represents an α B-crystallin concentration equivalent to 0.25 mg/ml, with Cycle 3 (C) and cycle 4 (D) representing 0.1 mg/ml and 0.01 mg/ml respectively. Samples for rechromatography at 20°C were stored overnight at 4°C.

Table 5.2. Integration data for Figure 5.2

Cycle	Time (min)	Height (m.A.U)	Peak Area (%)
1	57.367	132.74	100
2	57.479	22.87	100
3	19.214	0.22	12.36
	39.289	0.08	1.93
	58.763	4.09	79.68
	73.643	0.15	6.04
4	59.345	0.423	100

A series of SEC experiments were performed similar to previous runs, however, the oligomer will not be recycled to achieve the dilution, instead the wild type α B-crystallin sample at 2 mg/ml was diluted to achieve the range of concentrations prior to SEC separation, with the aim to reproduce the changes in oligomerisation observed in figures 5.1 and 5.2. The samples were prepared immediately before loading and were at ambient temperature. Previous SEC experiments incubated the samples overnight at ambient (see Figure 5.1) or 4°C (see Figure 5.2) before rechromatography. The dilutions used were based upon the approx dilutions observed during rechromatography and included 2 mg/ml, 0.5 mg/ml, 0.1 mg/ml and 0.01 mg/ml (see Figure 5.3).

At 2 mg/ml the oligomer is represented by a sharp symmetrical peak and subsequent dilution to ≤ 0.5 mg/ml results in a broadening of the oligomer peak suggestive of increased polydispersity (see Figures 5.3A-D). Unlike previous SEC cycle 3 data at approx 0.1 mg/ml (see Figure 5.1C and Figure 5.2C) the SEC for the 0.1 mg/ml α B-crystallin shown in Figure 5.3C produced one species, being the wild type oligomer. At 0.01 mg/ml the α B-crystallin oligomer peak is similar in symmetry to the 2 mg/ml α B-crystallin, however, shows a shift in retention time from 58.8 min to 56.9 min (see Figure 5.3 A and D respectively). The most significant shift in retention is the 0.5 mg/ml sample showing 56.6 min with the 0.1 mg/ml sample showing a slightly smaller shift to 57.2 min (see Table 5.3).

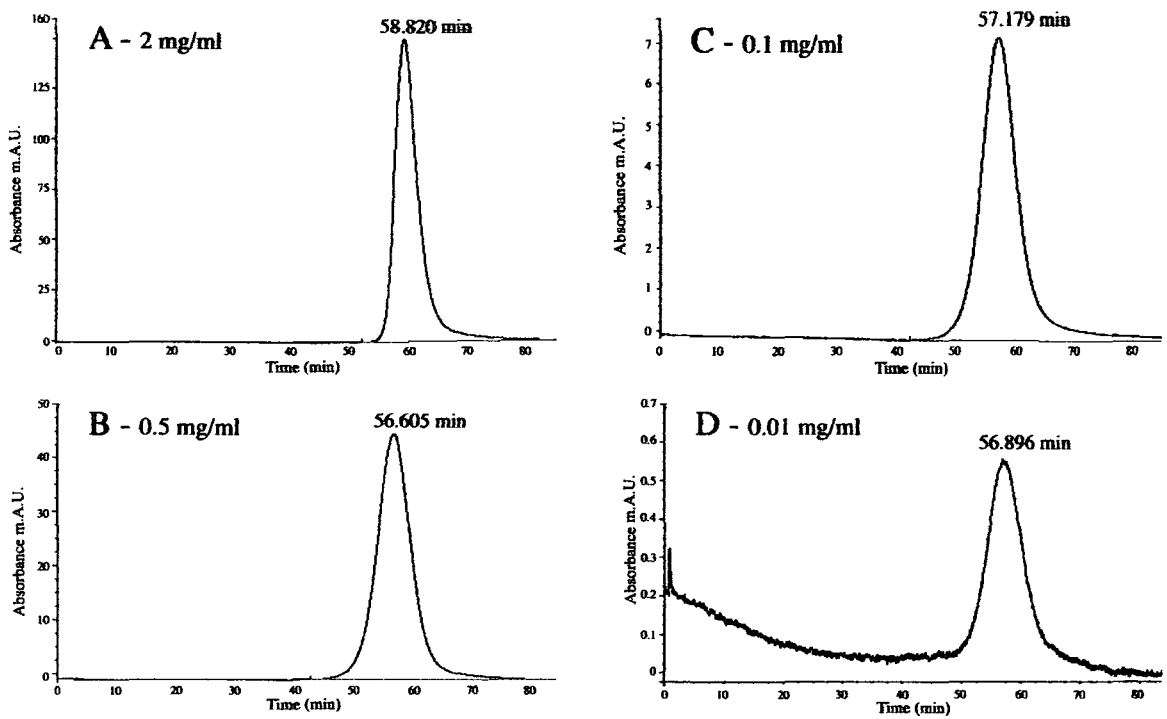


Figure 5.3. The effect of decreasing concentration upon the oligomerisation of wild type α B-crystallin at 20°C. Wild type α B-crystallin was separated by analytical SEC using a 26 ml Superose 6 column in 10mM Tris-HCl, 100mM NaCl, pH7.4 at 2 mg/ml (A). A second SEC separation using 0.5 mg/ml wild type α B-crystallin (B) was run without overnight incubation of the sample. Further concentrations at 0.1 mg/ml (C) and 0.01 mg/ml were analysed.

Table 5.3. Integration data for Figure 5.3

Cycle	Time (min)	Height (mA.U)	Peak Area (%)
1	58.820	151.46	100
2	56.605	44.93	100
3	57.179	7.15	100
4	56.896	0.49	100

The α B-crystallin concentration has an effect upon the oligomerisation of wild type α B-crystallin shown by changes in oligomeric size and polydispersity with the most significant changes in polydispersity observed at α B-crystallin concentrations of approx 0.1 mg/ml. The storage temperatures of ambient and 4°C and time of incubation induced variations in the polydispersity between data sets proving that the oligomerisation of α B-crystallin is in constant dynamic exchange, which can be influenced by external factors.

5.3.2. IDENTIFICATION OF AN UNKNOWN MWT α B-CRYSTALLIN SPECIES

The nature of the 93 min peak was determined to be an artefact (for full details see Appendix 4), however the separation of α B-crystallin wild type by SEC resolved an unknown α B-crystallin species past the separation range of the column independent to the 93 min peak by immunoblotting analysis (see Figure 5.4).

The observation of an unknown α B-crystallin species combined with evidence of a dynamic exchange (see Section 5.3.1) posed the question whether there was a presence of low Mwt complexes that were actively dissociated as part of the mechanism of chaperone activity, activated by the changes in concentration and temperature. The species could however, also represent a denatured form of α B-crystallin that binds to the column and is retained even in the presence of 1M NaCl (see Appendix 4, Figure A4.1) and a range of running conditions. In contrast, it could represent an active form of α B-crystallin that binds to either the column or denatured protein attached to the column, thus changing its elution properties. The α B-crystallin, whether in an active or denatured form may be displaced when more α B-crystallin is provided.

In this section I aimed to further investigate this species by isolating the material, which would enable the characterisation of the unknown α B-crystallin species. Firstly, I wanted to confirm the presence of this species at the end of the separating range of the column.

I aimed to confirm that there was an unknown Mwt species, which may represent a low Mwt complex in equilibrium with the oligomer that may be active in the chaperone function of α B-crystallin. I wanted to exclude the possibilities that the species was due to additional binding to the column of active or denatured forms and confirm that it was not a function of the injection system.

A series of experiments were performed, which compared the presence of the unknown Mwt species between a Superose 6 column with the Merck Hitachi HPLC system and a HW55S column of the same dimensions with manual injection using a peristaltic pump. This aimed to firstly confirm the presence of an unknown Mwt species

and secondly that the species was not a product of external factors such as the column matrix or injection systems. To strengthen the identification of the α B-crystallin species at such a low level of sensitivity, an α B-crystallin specific ELISA was utilised in conjunction with immunoblotting and UV detection (For development and optimisation of the α B-crystallin ELISA, see Appendix 5).

A 2 mg/ml (500 μ g) wild type solution was analysed by SEC using the original system as used in Section 5.3.1. Figure 5.4 illustrates the presence of a species in the tail of the α B-crystallin oligomer. The tail begins at 75 min (see Figure 5.4A) and focusing on the Absorbance signal in the region 88-120 min we can see two additional peaks at 100 min and 112 min (see Figure 5.4B). The immunoblotting data confirms the resolution of another α B-crystallin species, peaking between 108-110 min (see Figure 5.4C), however, with a greater sensitivity, the ELISA identifies numerous species with the largest eluting between 102-116 min (see Figure 5.4D).

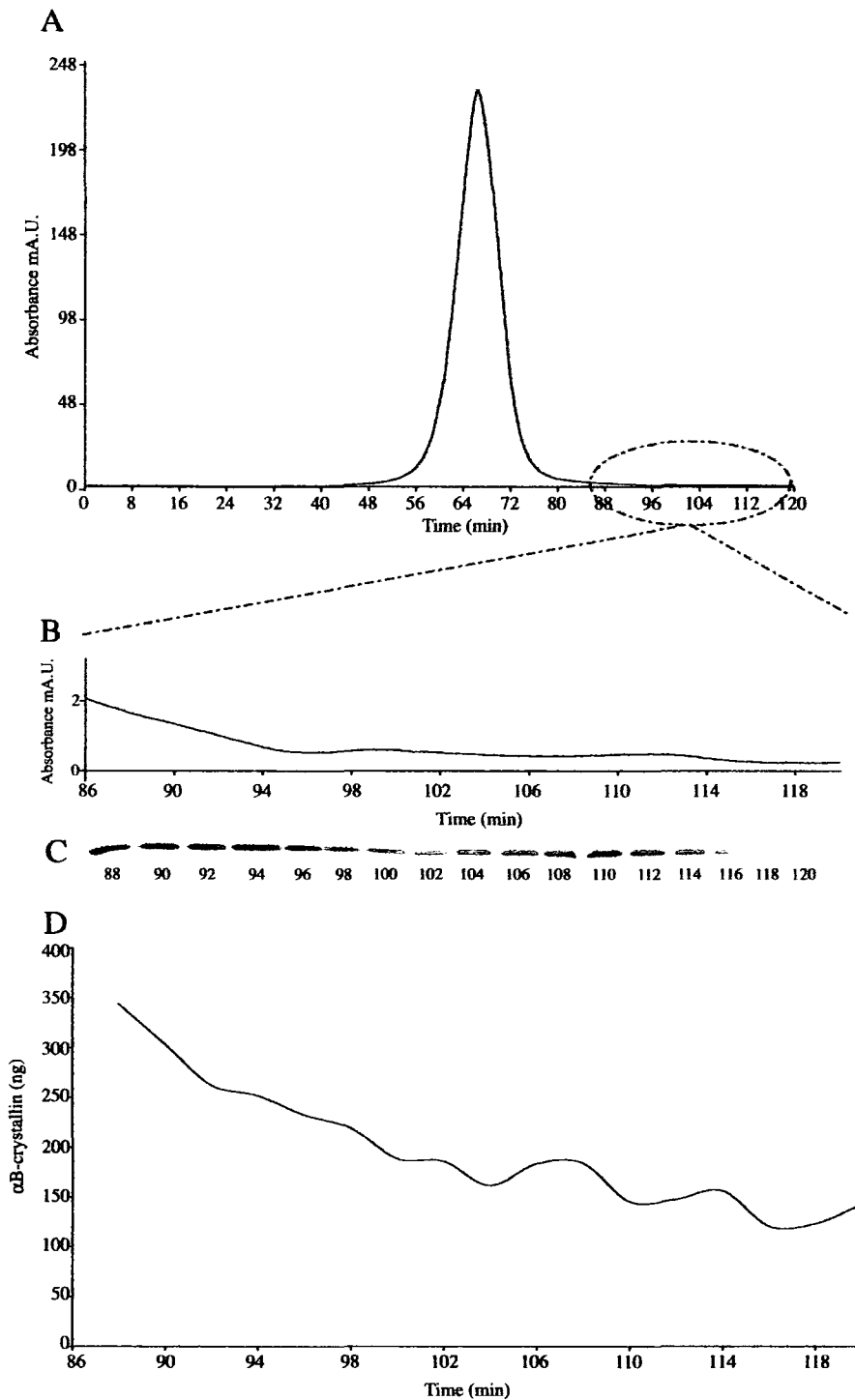


Figure 5.4. Characterisation of tail material from a 2 mg/ml α B-crystallin load onto a 23ml Superose 6 column. The column was run at 15 cm/hr and fractions were collected in 0.4 ml volume. (A) Shows the elution profile for the SEC separation. (B) Shows a zoomed in region of the elution from 86-120 min, which identifies resolution of two additional peaks at 100 min and 112 min. Western Blotting (C) and ELISA data (D) confirms that there is a definite rise in α B-crystallin signal during this region.

The outcome of this experiment with the additional analysis confirmed that there was an unknown α B-crystallin species in the tail of the α B-crystallin oligomer, which elutes past the separation range of the column (93 min).

The identification of this unknown Mwt species using a different matrix of HW55S and a manual injection system and peristaltic pump with would further confirm that the peak was not a function of the injection system or specific to the column matrix. A 2 mg/ml wild type α B-crystallin solution was loaded directly onto the bed of a 23 ml HW55S column and eluted using a peristaltic pump (see Figure 5.5). Resulting analysis shows an oligomer peak of similar height and retention time to that seen in Figure 5.4A with a tail starting at 80 min (see Figure 5.5A). Magnification of the UV data for the tail region of 88-144 min suggests a slight increase in signal between approx. 116-128 min (see Figure 5.5B). Once again the UV data does not provide sufficient sensitivity to be able to confirm the resolution of another α B-crystallin species, however, the immunoblotting illustrates an increase in α B-crystallin levels peaking at the 114 min fraction, which encompasses eluant between 112-114 min. Increased assay sensitivity achieved with the α B-crystallin ELISA identifies additional species peaking at 108, 114 and 120 min, similar to the Superose 6 run from Figure 5.4D, which saw peaks at 102, 108 and 114 min.

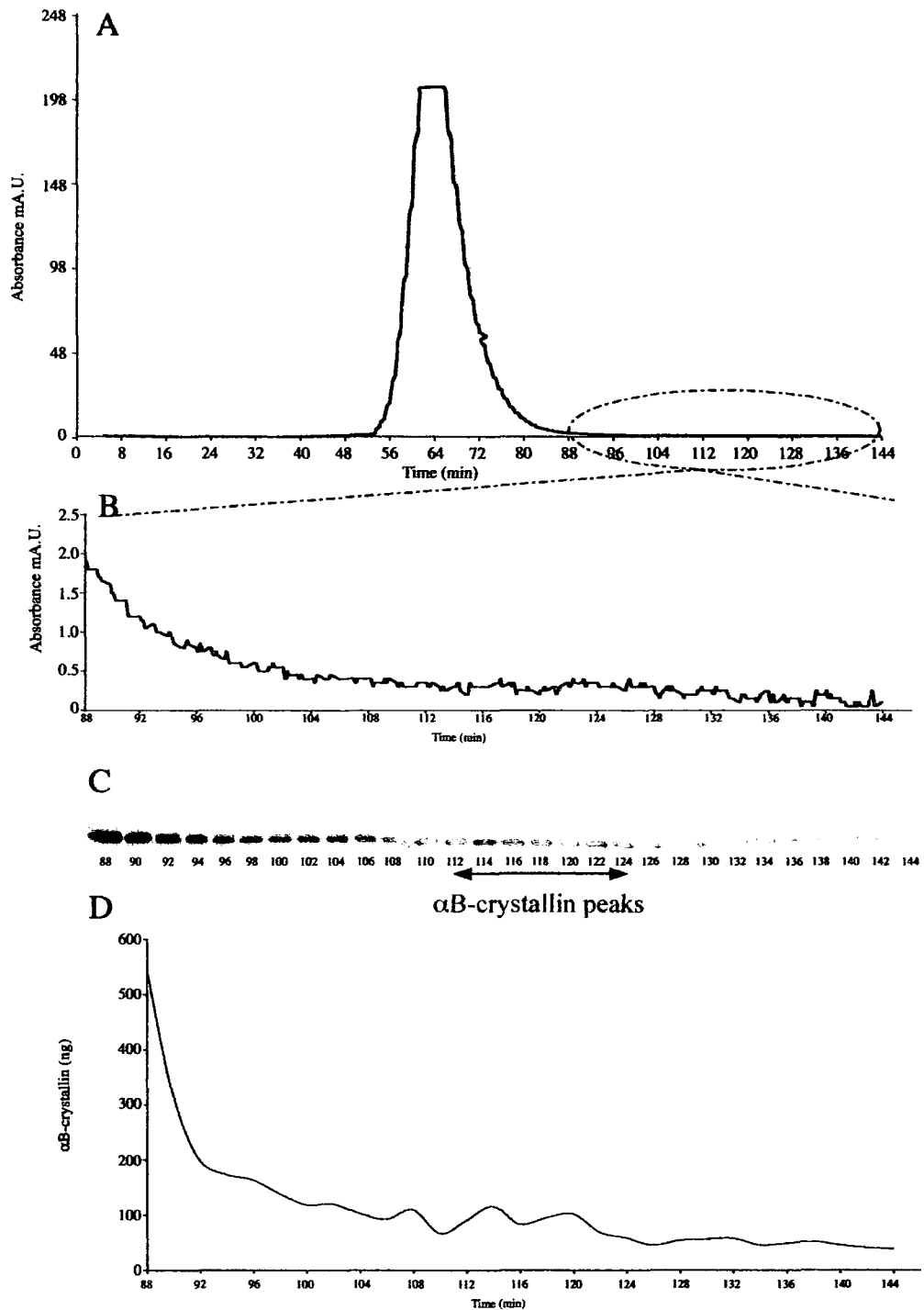


Figure 5.5. Characterisation of tail material from a 2 mg/ml α B-crystallin load onto a HW55S 23ml column. The column was run at 15 cm/hr using a peristaltic pump and fractions were collected in 0.4 ml volume. (A) Shows the elution profile for the SEC separation. (B) Shows a zoomed in region of the elution from 88-144 min, which identifies resolution of additional peaks. Western Blotting (C) and ELISA data (D) confirms that there is a definite rise in α B-crystallin signal during this region.

These data confirm that there is an unknown α B-crystallin species present in the tail region of the oligomer peak and the retention time is suggestive of a low Mwt multimer or potentially monomer.

The current theories of chaperone activity are supportive of the dissociation and association of α B-crystallin subunits between the oligomer and the active pool of active chaperones. These data may identify the active pool of chaperone activity and it could potentially be a more effective chaperone than a wild type solution, which is 99.9% oligomeric. The question remained whether this species was monomeric or multimeric and required characterisation.

5.3.3. CHARACTERISATION OF THE UNKNOWN α B-CRYSTALLIN SPECIES

Small scale SEC analysis of wild type α B-crystallin (see section 5.3.2) confirmed the presence of an unknown α B-crystallin species at the ng level.

Previously, I posed the question, whether there was a presence of low Mwt complexes that were actively dissociated as part of the mechanism of chaperone activity or whether the unknown Mwt species could represent a denatured form of α B-crystallin that binds to the column. The unknown Mwt species may also represent an active form of α B-crystallin that binds to either the column or denatured protein attached to the column and this α B-crystallin, whether in an active or denatured form may be displaced when more α B-crystallin is provided. The unknown Mwt species, however, has been observed for both Superose 6 and HW55S matrices showing the effect is independent to the type of column matrix utilised (see Section 5.3.2).

In order to determine the size of this species, thus confirming whether the unknown Mwt species was a low Mwt complex, a scaled up analytical SEC was carried out using a load of 125 mg (see Section 5.3.3.2). (Purification of the wild type α B-crystallin is detailed in Section 5.3.3.1). This separation should provide a sample of the unknown Mwt species at a higher concentration (see section 5.3.3.1), suitable for characterisation by ELISA, UV and immunoblotting (see Section 5.3.3.2) and allow investigation of the potential of the unknown Mwt species as a chaperone. Previously, fractions from the small scale runs had been analysed by Tandem mass spectrometry, a two step procedure which involves the selection of specific assemblies in the gas phase and inducing their dissociation through collisions with argon atoms to produce fragment ions. The dislodging of individual subunits from the non covalent assemblies results in a redistribution of charge on the products, therefore the range and the relative populations of the different oligomers that constitute a polydisperse assembly be can defined (Aquilina et al., 2003). Unfortunately, the system sensitivity was not sufficient to detect the unknown Mwt species at the ng level, therefore it may not be sufficient for analysis of the large scale fractions.

An alternative method involved crosslinking to fix the multimeric conformation of the unknown Mwt species, then visualisation of the cross linked species by immunoblotting to confirm the size of the complex present (see Section 5.3.3.5). (Optimisation of the cross linking process is detailed in Section 5.3.3.4).

Finally, the rechromatography of fractions containing the unknown Mwt species, on the 23 ml Superose 6 analytical SEC column was performed to investigate whether the protein would again elute at the end of the separation range or elute in the position of the oligomer (see Section 5.3.3.3). This would confirm that the species was a low Mwt complex rather than another form of α B-crystallin and strengthen the argument that the species is part of the mechanism of chaperone activity. The current theories of chaperone activity are supportive of the dissociation and association of α B-crystallin subunits between the oligomer and the active pool of active chaperones. Characterisation of the chaperone activity may identify the active pool of chaperone function and it could potentially be a more effective chaperone than a wild type solution, which is 99.9% oligomeric

5.3.3.1. Large scale purification of α B-crystallin

Preliminary experiments showed that the amount of unknown Mwt species could be increased by raising the concentration of the α B-crystallin load material, although the relative peak heights of the unknown Mwt species and the oligomer remained constant (data not shown).

The minimum concentration required for chaperone assays is 0.1 mg/ml, therefore the SEC was scaled up accordingly in order to recover the unknown Mwt species at the required concentration of 0.1 mg/ml. ELISA data for the 26 ml HW55S SEC showed a concentration of 247 ng/ml (total 197 ng) in the unknown Mwt species (see Figure 5.5D). Therefore, to achieve a concentration of 0.1 mg/ml, theoretically a 400x increase α B-crystallin load would be sufficient, which equates to 200 mg. Based on previous wild type purifications, a 0.8 L culture resulted in a final SEC pool of 16 mg. The efficiency of the lysis has been shown to be less than 100% efficient in the past, therefore to increase the yield of wild type a 0.25 mg/ml solution of lysozyme was added to the bacterial cells of a 6 L culture to aid the release of α B-crystallin from the cells. The 6 L culture was the maximum volume, which could be processed as one batch. The purification is illustrated in Figure 5.6.

The IEX purification clearly shows the resolution of the wild type from other contaminating proteins (see Figure 5.6A-B) and SDS PAGE analysis of the appropriate fractions confirms the major peak to be α B-crystallin and subsequently fractions 8-24 were pooled to give a total of 260 mg α B-crystallin (by A280). Further purification by SEC using a 413 ml HW55S column resulted in a single peak (data not shown) and subsequent fraction analysis by SDS PAGE identified α B-crystallin enriched fractions, however, two additional proteins were co-eluted in the major peak fractions (pool 1) with a further proteins being observed in the tail fractions (pools 2 and 3) (see Figure 5.6D). To identify the nature of these additional bands, immunoblotting was performed using the 2D2B6 purified monoclonal α B-crystallin antibody, and visualisation confirmed that the bands identified by SDS PAGE in pool 1 were all positive for α B-crystallin. These additional α B-crystallin positive bands are consistent with those observed with wild type α B-crystallin SEC pool at 1 L scale (see Section 3.3.3.1, Figure 3.7). The band present at 30 kDa seen in pools 2 and 3 did not test positive for α B-crystallin. Therefore, I decided

to only proceed to the characterisation of the unknown α B-crystallin species with pool 1, despite the amount of α B-crystallin I would lose by dismissing pools 2 and 3. Concentration determination confirmed that Pool 1 contained 125 mg of α B-crystallin (by A280), thus 135 mg α B-crystallin was lost in pools 2 and 3. Despite requiring 200 mg of load material for the large scale analytical SEC, I decided to proceed as a 250X scale up was still a large enough increase to potentially amplify this unknown Mwt species for characterisation.

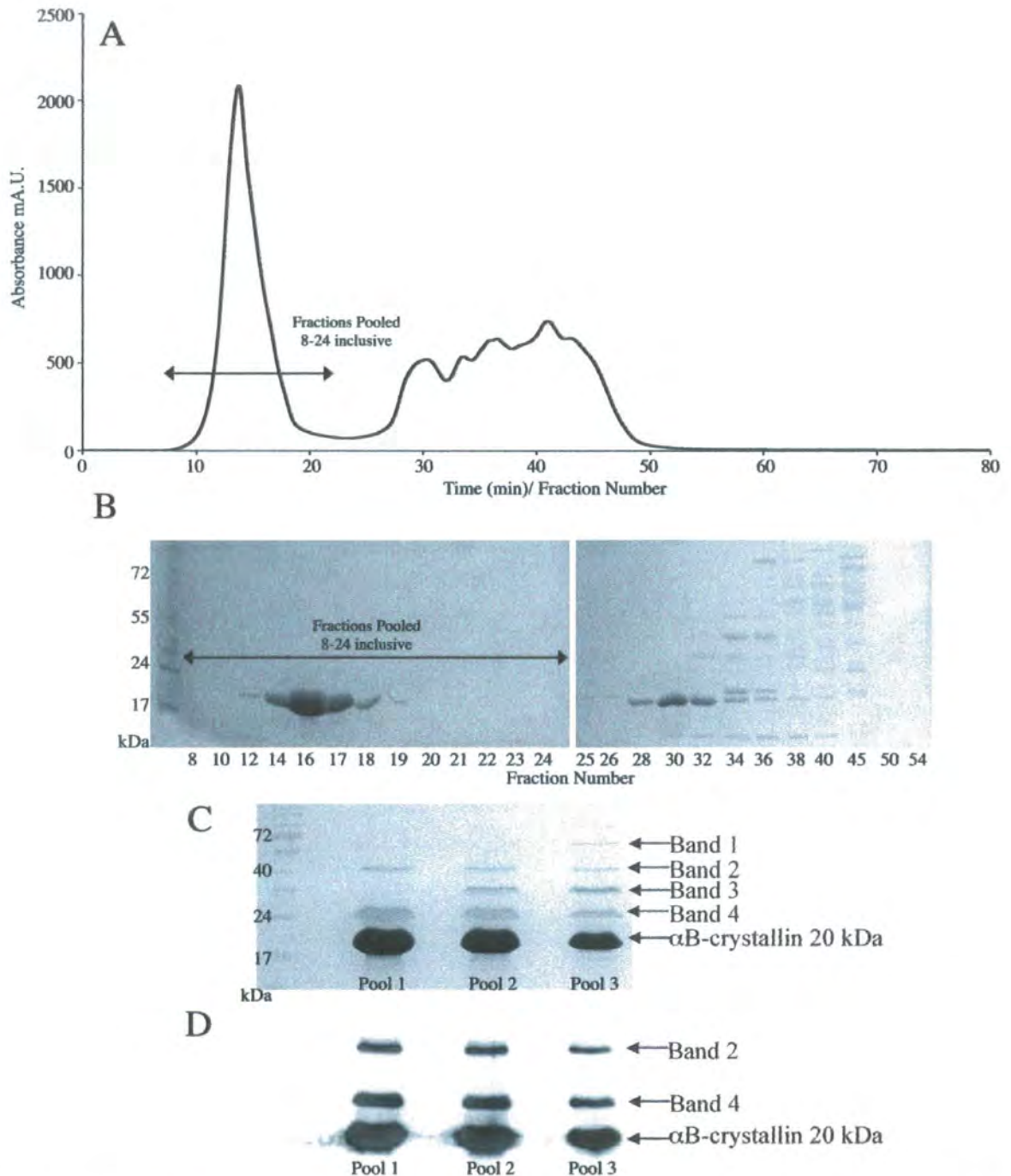


Figure 5.6. Large Scale purification of wild type α B-crystallin. A 6 L culture of BL-21 cells expressing wild type α B-crystallin were lysed and the lysate purified by IEX chromatography using a 68 ml Fractogel TMAE EMD(s) column (13x2.6cm). The resulting IEX profile (A) and SDS PAGE analysis of fractions (B) indicate that fractions 8-24 inclusive were α B-crystallin enriched and were subsequently pooled. The SEC was performed on a 413 ml HW55S column using a peristaltic pump and from individual fraction analysis three pools were prepared (D) with each pool containing various unknown bands (bands 1-4). Immunoblotting of the pools confirmed bands 2 and 4 were α B-crystallin, thus pool 1 was entirely α B-crystallin positive. Pools 2 and 3 contained unknown protein at approx 30 kDa (band 3) and pool 3 at approx 60 kDa (band 1)(C).

5.3.3.2. Identification of unknown α B-crystallin species by UV, immunoblotting and ELISA.

The 125 mg wild type solution was applied to the 413 ml HW55S SEC column at 0.6 ml/min and 8 ml fractions were collected and analysed. Figure 5.7 illustrates the relative UV, ELISA and immunoblotting data for this run. As seen previously at the 0.5 mg scale, the UV data shows a predominant oligomer peak (see Figure 5.7A) with a tail that shows some variation in signal (see Figure 5.7 B). This suggests the resolution of additional α B-crystallin species. Immunoblotting confirms the presence of an α B-crystallin species, in the tail of the oligomer and peaks at fraction 26 (see Figure 5.7C).

The high sensitivity of the ELISA assay illustrates the α B-crystallin peak, which shows an increase from 3000-6700 ng in fraction 24. The peak encompasses fractions 23-25, which contain 12165 ng of α B-crystallin in 24 ml by ELISA giving a concentration of 0.00051 mg/ml. Fraction 24 was the most concentrated fraction at 0.00084 mg/ml (total 0.0067 mg). The equivalent fraction from the 0.5 mg run (see Figure 5.5D) was 0.00029 mg/ml, which confirms only a 3x increase in concentration of the unknown Mwt species was observed by increasing the load by 250x, however the yield of α B-crystallin in this fraction increased 58x from 114.8 ng to 6734.7 ng. The resolution of this material was greater in the 125 mg run where a significant peak was observed, compared to the 0.5 mg run where numerous peaks between 106-122 min were resolved with the peak at 114 min being the most concentrated. Fraction 24 from the 125 mg run represents 78% of a column volume and fraction 114 from the 0.5 mg run represents 88% of a column volume.

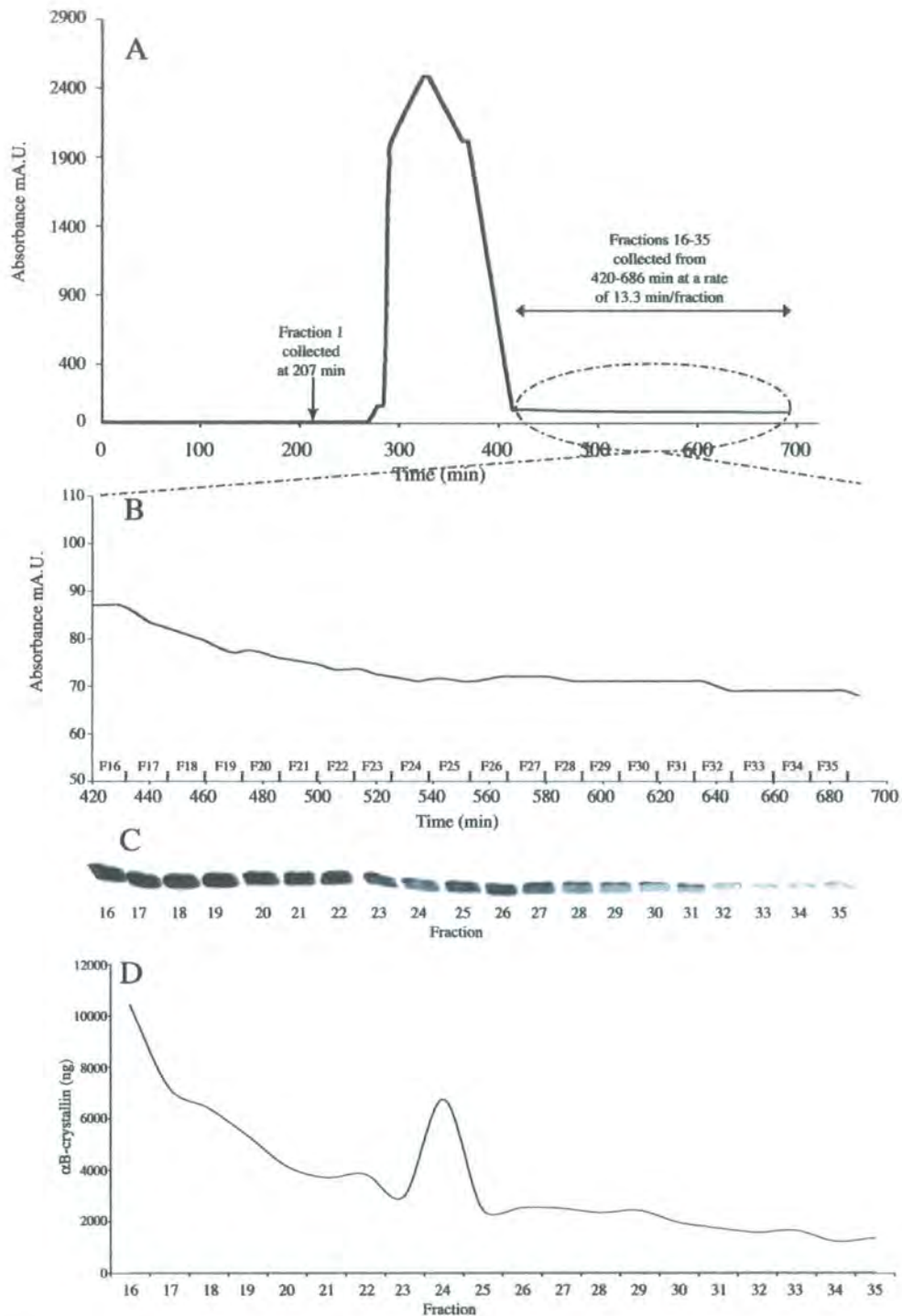


Figure 5.7. Characterisation of tail material from a 31.25mg/ml α B-crystallin load onto a HW55S 413ml column. Column was flowed at 7.5cm/hr using a peristaltic pump and fractions were collected in 8ml volume. (A) Shows the elution profile for the SEC separation, where resolution of any tail material is not evident. (B) Shows a zoomed in region of the elution from Fraction 16-35 (420-690min) which identifies the resolution of additional peaks. Western Blotting (C) and ELISA data (D) confirms that there is a definite rise in α B-crystallin signal during this region.

These runs are summarised in Table 5.4.

Table 5.4. Comparison of unknown Mwt species between 125 mg and 0.5 mg SEC runs

Details of unknown Mwt species peak	Large scale (125 mg)	Small scale (0.5 mg)
Concentration ng/ml	841.8	286.9
Total ng	6734.7	114.8
% CV	78	88
% yield	0.0054	0.022

The aim of the large scale run was to produce a fraction of the α B-crystallin species of sufficient concentration to allow characterisation of the species size and its chaperone function. It was evident from the ELISA data (see Figure 5.7D) that the material in fraction 24 was too dilute to perform any chaperone function assays. However, despite the low concentration, there was a sufficient amount for rechromatography of fraction 24 using the analytical 23 ml Superose 6 SEC column. The position of the resulting peak would determine whether the unknown Mwt species of fraction 24 was a low Mwt complex. Fraction 8 containing the oligomer was diluted to the same concentration as fraction 24 to act as a control sample for the visualisation of oligomer at the diluted concentration. This would allow me to confirm whether any of the low Mwt complexes had reassociated into the oligomer.

5.3.3.3. Characterisation of unknown α B-crystallin species by rechromatography of fractions

Rechromatography of fraction 24 was carried out ensuring that the sample temperature has remained constant, thus avoiding any potential associations that could lead to multimerisation. The appearance of a peak at the end of the separation range in the rechromatography run would confirm the material is a low Mwt species and not another form of α B-crystallin oligomer. The control involved analysis of fraction 8, which represented the oligomer peak from the 125 mg run and was used to show the levels of low Mwt species present in a fraction of the major peak (see Figure 5.8A). Magnification of the late peak at 100.7 min clearly shows the resolution of a peak in the oligomer fraction of peak height 2.7 mA.U. (see Figure 5.8B).

A 1/5000 dilution of Fraction 8, equivalent to the concentration of Fraction 24 was also analysed to determine the level of sensitivity of the UV at this dilution. This diluted sample showed a late peak at 91.9 min at similar peak height 2.9 mA.U (see Figure 5.8C), which is a difficult observation to explain. There is also evidence of a small oligomer peak even at this level of dilution at 59 min therefore the UV detection is sensitive enough to detect potential reassociation of the unknown Mwt species to an oligomeric complex in Fraction 24.

Analysis of the neat sample of Fraction 24 resulted in a peak at 96.3 min of 0.13 mA.U and showed no evidence of an oligomer peak confirming the α B-crystallin has not reassociated into the oligomer at this concentration (see Figure 5.8D) and adds support to the theory that this is potentially monomeric or dimeric. To amplify this signal and to assess the effect of concentration on the potential for reassociation, the fraction was spin concentrated 12 fold. However it seems that some loss of material occurred by binding to the membrane as suggested by the peak height being lower than the neat sample at 0.03 mA.U (see Figure 5.8E). There is a slight peak shift to 97.3 min from the 96.3 min observed with the neat fraction 24 sample, which is suggestive of a smaller protein.

Previous issues with the interference of the 93 min peak were evident in the blank consistent with Section 5.3.1.1. All the rechromatography samples were blank corrected and did not directly interfere with analysis as any low Mwt species observed, ran later at

96.3 min, 97.6 and 100.7 (A-B) and earlier at 91.9 min (see Figure 5.8D, E, A-B and C respectively).

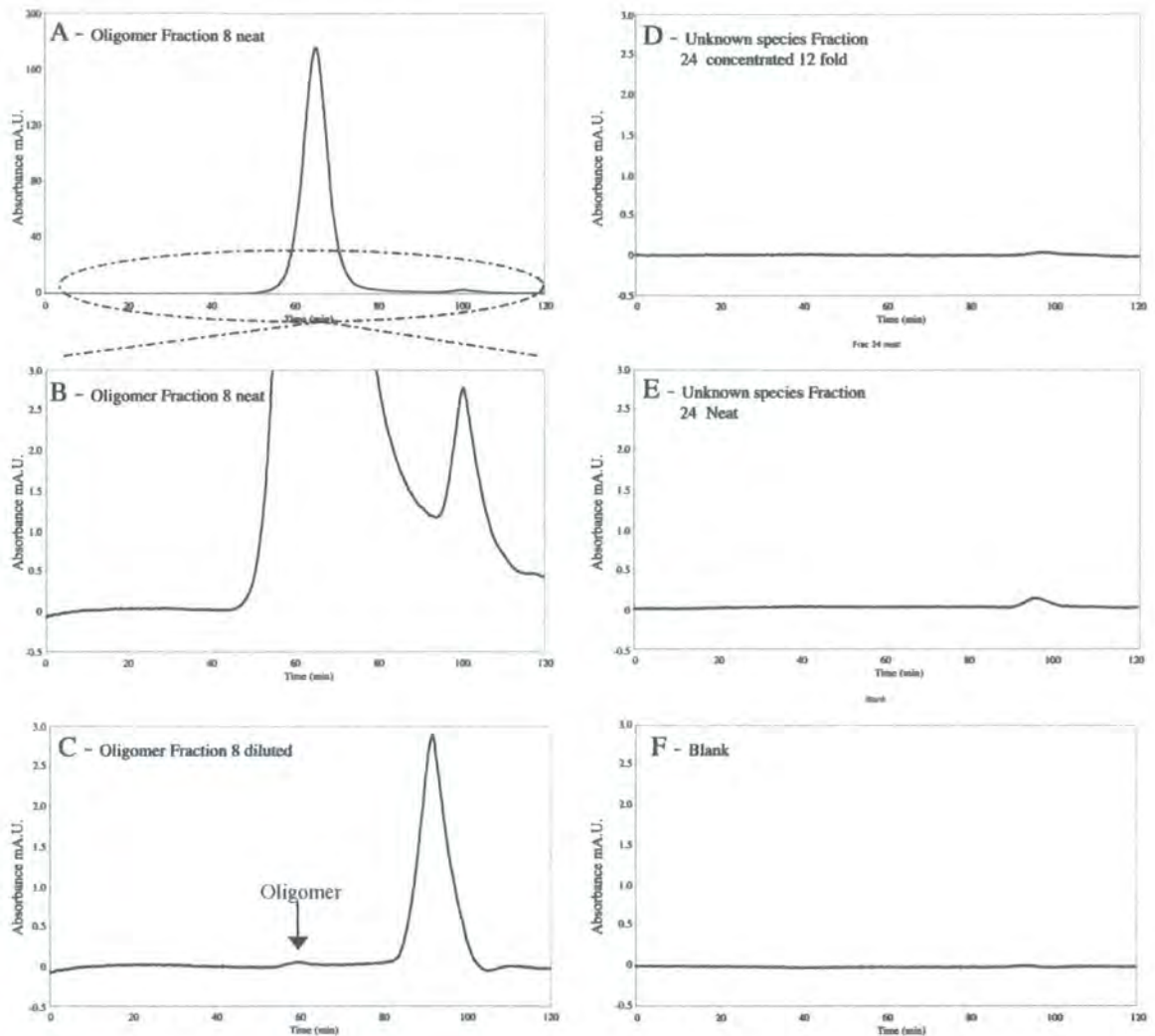


Figure 5.8. Rechromatography of the unknown α B-crystallin. Fraction 24 from the large scale analytical SEC was analysed by 26 ml Superose 6 SEC column to determine whether this material, which runs at the end of the separation range actually resolves in the corresponding position during rechromatography. The fraction representing the oligomer peak (Fraction 8) was also analysed as a control to show the levels of low MW species present in a fraction of the major peak (A). Magnification of the late peak at 100.7 min clearly shows the resolution of a peak in the oligomer fraction (B). A 1/5000 dilution of Fraction 8, equivalent to Fraction 24 shows the late peak at 91.9 min at similar peak height 2.9 mAU (C). There is also evidence of a small oligomer peak even at this level of dilution at 59 min. Fraction 24 analysis shows a peak at 96.3 min and no evidence of an oligomer peak (D). To amplify this signal the fraction was spin concentrated 12 fold, however it seems that some loss of material has occurred on the membrane with the peak height being lower than the neat sample (E). Previous issues with the interference of the 93 min peak were evident in the blank with a small peak shown at 93 min, however all samples were blank corrected. Any low MW species observed, ran later at 96.3 min (D) 97.6 (E) and 100.7 (A-B) and earlier at 91.9 min (C).

5.3.3.4. Optimisation of cross-linking conditions for the analysis of α B-crystallin unknown Mwt species

Crosslinking optimisation studies had investigated the efficiency of various cross-linking agents to achieve intermolecular crosslinking of α B-crystallin. The cross linking would analyse the multimerisation of the unknown α B-crystallin species relative to the cross linked wild type α B-crystallin oligomer and may provide some variation indicative of a separate species. Optimisation of the cross linking aimed to investigate conditions, which would produce a sample at the stage of cross-linking where intermediate complexes were present such as dimer and tetramer, and not just the highest level of association, being the oligomer.

Initial crosslinking optimisation investigated the use of the reversible cross linker, Dimethyl 3,3'-dithiobispropionimidate•2 HCl (DTBP), which is a homobifunctional, cleavable and membrane permeable cross linker. It contains an amine-reactive imidoester at each end of an 11.9 Å spacer arm. The imidoesters react with primary amines at pH 8.0 to form stable amidine bonds. Several primary amines are present in the side chain of lysine residues and the N-terminal that are available as targets for imidoester crosslinking. The imidoamide reaction product does not alter the overall charge of the protein, potentially retaining the native conformation and activity of the protein (Pierce Instruction Manual 0668.1).

A number of conditions were used in order to achieve the optimal cross-linking with DTBP however all proved unsuccessful therefore, the non-cleavable analogue of DTBP, Dimethyl Suberimidate•2 HCl (DMS) was analysed. DMS has essentially identical cross-linking activity towards primary amines and has a similar length spacer arm of 11 Å compared to DTBP, which is 11.9 Å. A cross-linking experiment was performed at 20°C using 1.0, 0.5 and 0.1 mg/ml DMS with 0.2 mg/ml α B-crystallin over 0, 30, 60 and 120 min to gain an initial assessment of the efficiency of DMS as a cross-linker of α B-crystallin (see Figure 5.9).

DMS successfully cross-links α B-crystallin resulting in low Mwt complexes with predominant complexes migrating to positions indicating dimer, trimer and perhaps octomer at 160 kDa. There is no evidence of complete cross-linking, which would be suggested by the presence of a band in the stacking gel, as the oligomer (564 kDa) would

be too large to enter the separating gel. Figure 5.9 shows that all the protein has entered the separating gel, which suggests that the DMS does not result in complete cross-linking of α B-crystallin under these conditions. The full range of cross-linking intermediates are necessary to fully understand any potential differences that may be observed in cross-linked samples of the unknown α B-crystallin species.

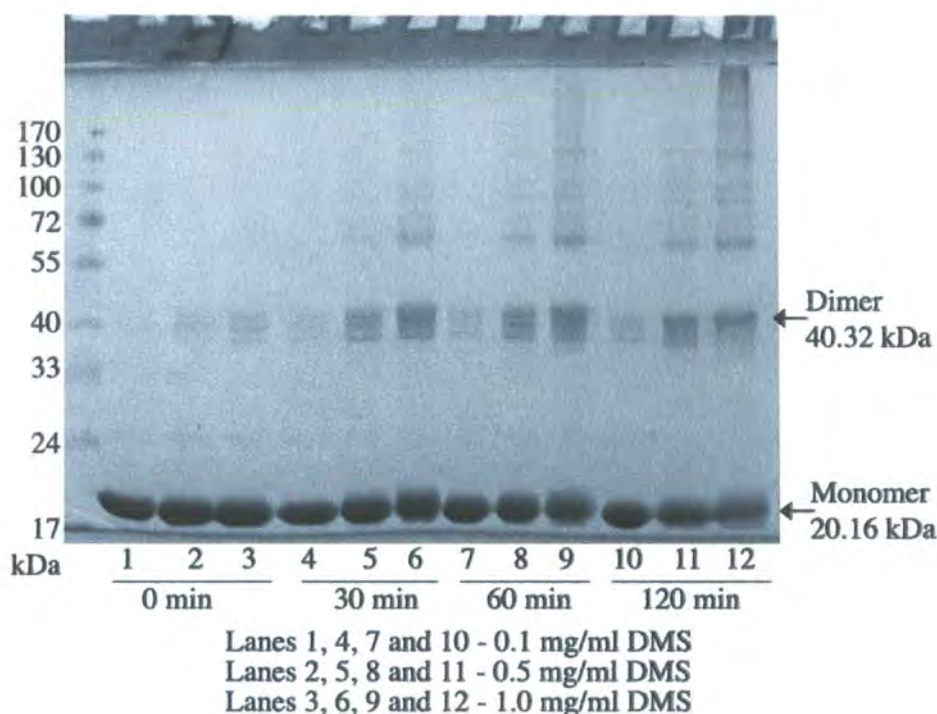
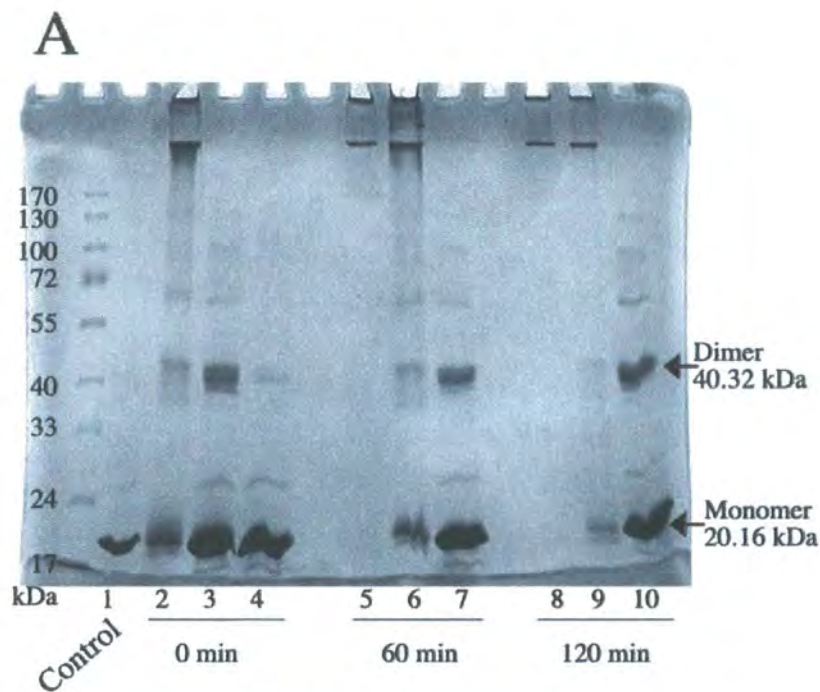


Figure 5.9. Cross-linked α B-crystallin wild type oligomer by DMS. A range of DMS concentrations of 1.0, 0.5 and 0.1 mg/ml were used with a 0.2 mg/ml α B-crystallin at 20°C over a time course of 120 min. The greater the DMS is in excess the more cross-linking is observed as evident by looking at the dimer bands in lanes 3, 6, 9 and 12. A strong band can be seen at approx 60 kDa indicative of trimer. All proteins have entered the separating gel suggesting there is no 560 kDa oligomer present, thus cross-linking is not complete.

Glutaraldehyde (GA) has been used as an efficient reagent in achieving intermolecular cross-linking with α B-crystallin (Augusteyn, 2004). GA is an amine reactive bifunctional cross-linker and has a 5 Å spacer arm, compared to DTBP (11.9 Å) and DMS (11 Å), which limits the ability to covalently link molecules that are more distant from each other (Krohn et al., 2002). A 0.2 mg/ml α B-crystallin solution was incubated at 20°C with 0.1%, 0.01% and 0.001% GA (v/v) for 0, 60 and 120 min and subsequent analysis following precipitation, by SDS PAGE was performed (see Figure 5.10A). The GA has successfully produced a range of cross-linked α B-crystallin species. At 0.1% (lane 2), even at 0 min there are high Mwt species, which are too large to enter the separating gel thus, indicate the 564 kDa oligomer. Also at 0 min 0.01% and 0.001%

(lane 3 and 4 respectively) GA cross-linked samples show signs of dimer at 40 kDa but are still predominantly monomer. After 60 min, the 0.1% sample is completely cross-linked (lane 5) and the 0.01% sample shows the oligomer and also intermediate complexes of predominantly dimer and monomer (lane 6). The 0.001% GA cross-linked sample looks similar to the 0 min GA cross-linked sample with the introduction of faint bands at 60 kDa and 80 kDa indicative of trimer and tetramer (lane 7). After 120 min, the 0.01% sample has almost completely cross-linked with a faint presence of monomer remaining (lane 9), however the 0.001% sample was still showing intermediate complexes, which suggests this concentration of GA is efficient for the identification of cross-linked dimeric complexes (lane 10).



Lanes 2, 5 and 8 - 0.1% glutaraldehyde

Lanes 3, 6 and 9 - 0.01% glutaraldehyde

Lanes 4, 7 and 10 - 0.001% glutaraldehyde

B

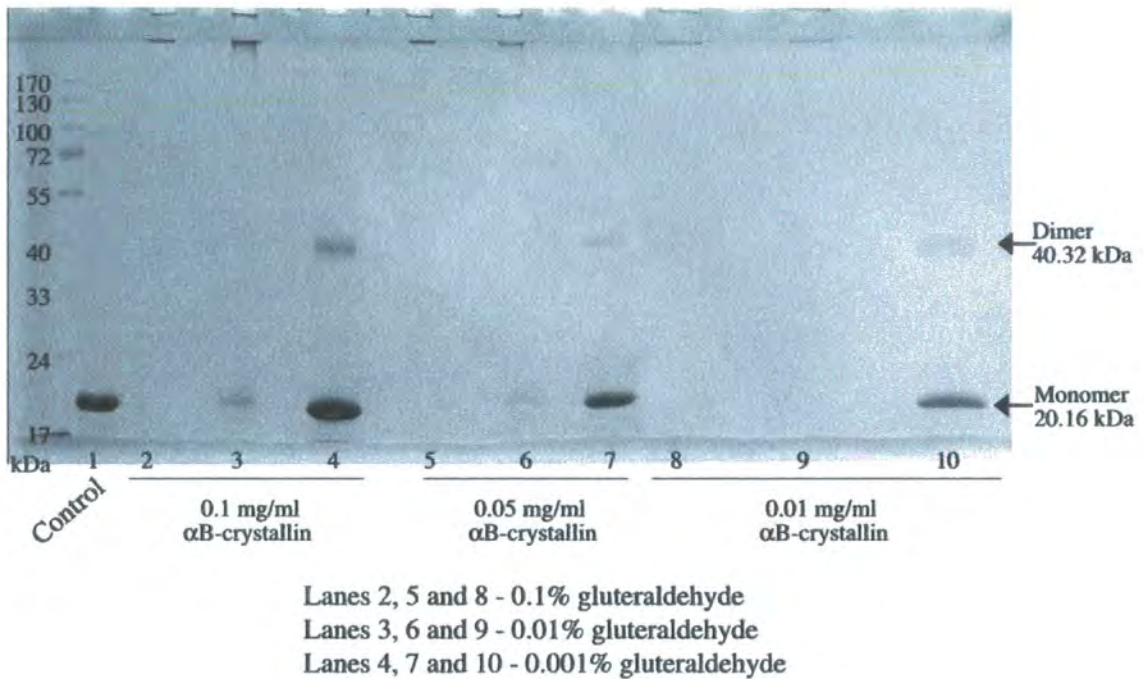


Figure 5.10. Cross-linking of α B-crystallin wild type oligomer by glutaraldehyde. A range of glutaraldehyde concentrations of 0.1, 0.01 and 0.001% (v/v) were used with 0.2 mg/ml α B-crystallin solution at 20°C over 0, 60 and 120 min (A). Cross-linking was successful and the experiment was repeated to optimise the cross-linking conditions for low α B-crystallin concentrations, representing potential fractions of the unknown α B-crystallin species from the large scale SEC (B). The SDS PAGE shows complete crosslinking for 0.1% and 0.01% glutaraldehyde samples and the presence of dimer at 0.001% (lanes 4, 7 and 10). The presence of other bands of varying MW cannot be detected at the level of sensitivity offered by SDS PAGE. The control shows the untreated wild type oligomer (control lane).

In order to investigate the efficiency of cross-linking of α B-crystallin at levels similar to the unknown Mwt species fractions, a range of α B-crystallin concentrations were cross-linked and analysed. Predicted concentrations of the unknown Mwt species following scale-up were approx. 0.05-0.1 mg/ml, therefore 0.1, 0.05 and 0.01mg/ml solutions of α B-crystallin were incubated at 20°C with 0.1%, 0.01% and 0.001% GA (v/v) for 60 min (see Figure 5.10B). It is evident that at all α B-crystallin concentrations, a 0.001% GA solution was sufficient to produce dimer at 40.32 kDa (lanes 4, 7 and 10), however only the 0.01% (lanes 3 and 6) and 0.1% (lanes 2 and 5) solutions **resulted in complete cross-linking**. The low α B-crystallin concentrations make it difficult to visualise

any potential intermediate complexes, thus the experiment was repeated and analysis by immunoblotting to achieve the higher level of sensitivity required (see Figure 5.11A).

A range of GA concentrations of 0.1, 0.01 and 0.001% (v/v) were used with a range of low α B-crystallin concentration solutions at 20°C over 60 min including 0.1, 0.05 and 0.01 mg/ml (see Figure 5.11A). The immunoblotting shows the 0.1% GA results in complete cross-linking at all α B-crystallin concentrations (lanes 1, 4 and 7) as indicated in Figure 5.10B. The 0.01% GA shows intermediate complexes as well as oligomer and monomer (lanes 2, 5 and 8). The 0.001% GA results in a range of complexes, however shows no evidence of oligomer (lanes 3, 6 and 9). The excess GA in the 0.01 mg/ml sample (lane 8) compared with 0.1 mg/ml and 0.05 mg/ml (lanes 2 and 5 respectively) is sufficient to complete the cross linking with the lower concentration of α B-crystallin. The variation in concentration is reflected by the intensity of the dimer bands.

Ideal cross-linking conditions, which will be applied to the unknown Mwt species fractions, would show the range of complexes from monomer to dimer through to the oligomer for the wild type solution (see Figure 5.11A, lane 5). These conditions can then be used effectively as a standard to compare the relative cross-linking of the unknown Mwt species to assess any variations in multimerisation.

To achieve cross-linking of similar quality to the 0.05 mg/ml with 0.01% GA (see Figure 5.11B, lane 5), but with the 0.01 mg/ml, a time course for the 0.01 mg/ml α B-crystallin solution was analysed over 0, 60 and 120 min (see Figure 5.11B). Lane 9 shows that even after 120 min the 0.001% GA does not achieve complete cross-linking, whereas the 0.1% and 0.01% GA are both complete (lanes 7 and 8 respectively). The intermediate complexes can be seen in Lane 5, which represents 0.01% GA after 60 min incubation at 20°C, although the lower Mwt bands are relatively faint compared with the 0.05 mg/ml α B-crystallin sample under the same conditions (see Figure 5.11B, lane 5).

These data suggest that at α B-crystallin concentrations from 0.2 mg/ml (see Figure 5.11A, lane 6) to 0.1, 0.05 and 0.01 mg/ml (see Figure 5.11A, lanes 2, 5 and 8), an incubation of 60 min at 20°C with 0.01% GA was sufficient to cross-link α B-crystallin multimers. From these data, I conclude that crosslinking with GA under the optimised conditions will allow me to assess any variations in multimerisation or complex size in the unknown α B-crystallin species relative to the wild type as the protein oligomer can be

detected. The unknown α B-crystallin species would be detected if it was present as an oligomer and also any variations in multimerisation achieved by crosslinking would be evident and signify a α B-crystallin species different to the wild type oligomer.

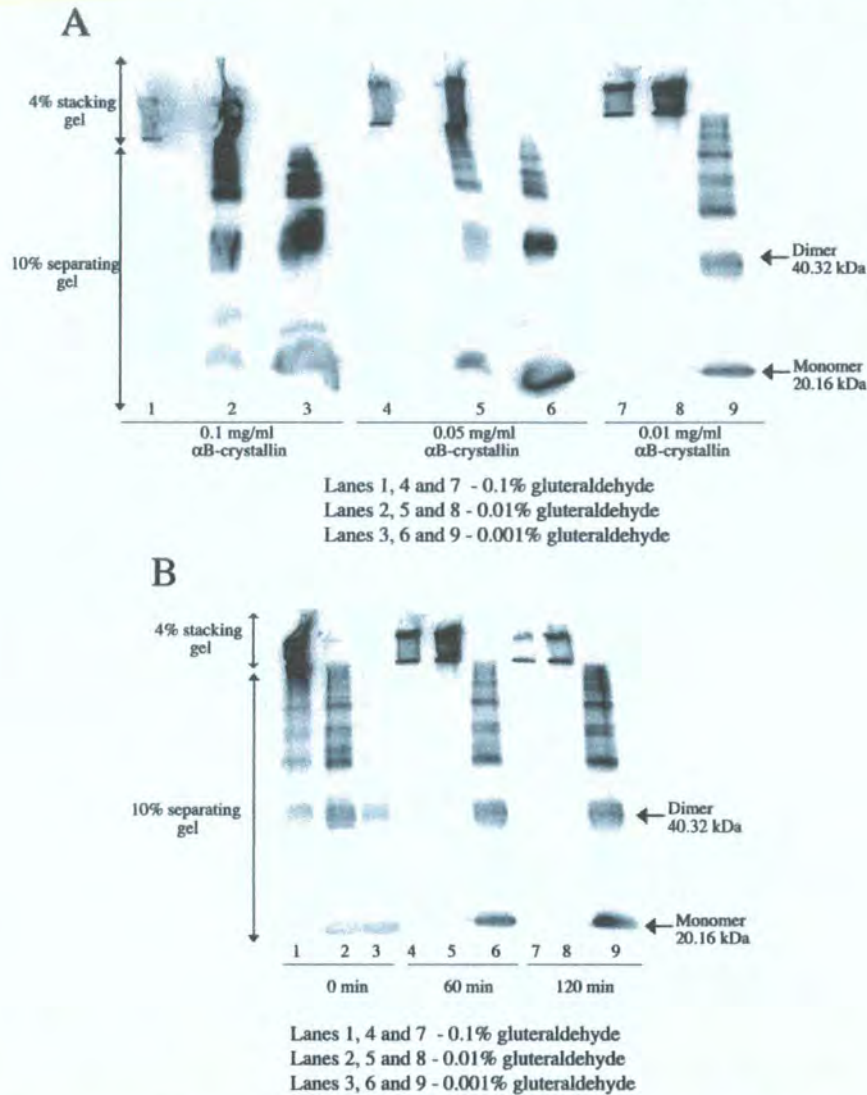


Figure 5.11. Immunoblotting of Cross-linked α B-crystallin wild type oligomer by glutaraldehyde. A range of glutaraldehyde concentrations of 0.1, 0.01 and 0.001% (v/v) were used with a range of low α B-crystallin concentration solutions at 20°C over 60 min (A). The immunoblotting shows the 0.1% glutaraldehyde results in complete cross-linking at all α B-crystallin concentrations (lanes 1, 4 and 7). The 0.01% glutaraldehyde shows intermediate complexes as well as oligomer and monomer (lanes 2, 5 and 8). The 0.001% glutaraldehyde results in a range of complexes, however shows no evidence of oligomer (lanes 3, 6 and 9). The variation in concentration is reflected by the intensity of the dimer bands. A time course for the 0.01 mg/ml α B-crystallin solution was analysed over 0, 60 and 120 min (B). Lane 9 shows that even after 120 min the 0.001% glutaraldehyde does not achieve complete cross-linking, whereas the 0.1% and 0.01% glutaraldehyde are both complete (lanes 7 and 8 respectively). Lane 5 shows, both oligomer, dimer and monomer under conditions of 0.01% (v/v) glutaraldehyde after 60 min.

5.3.3.5. Cross-linking analysis of the α B-crystallin unknown Mwt species

The conditions optimised for cross-linking α B-crystallin between 0.2 and 0.01 mg/ml was applied to fractions encompassing fraction 24, the fraction containing the peak of the unknown Mwt species confirmed by ELISA (see Figure 5.7D). Encompassing fractions included fractions 18, 23-25 and 29. As with the rechromatography (see Section 5.3.3.2.2) fraction 8 of the oligomer peak was cross-linked, as a control along with the 1/5000 dilution of fraction 8 to allow a relative comparison between the resulting cross-linked species produced from fraction 8 and the unknown Mwt species fractions.

The SEC was run with 0.2M Ammonium Acetate, thus the fractions had to be dialysed into PBS for 60 h to ensure there were no residual primary amines present from the eluant buffer, which would compete with the cross-linking reaction. Dialysates were incubated for 60 min with 0.01% GA (v/v) prior to precipitation for immunoblotting (see Figure 5.12). Initial immunoblotting showed no evidence of any higher Mwt bands in the fractions, or more interestingly in diluted fraction 8 (consistent with Figure 5.8C), despite the neat fraction 8 showing cross-linking consistent with the optimisation studies (see Figure 5.12A). The immunoblotting was repeated to enhance the visualisation of any potential higher Mwt bands but showed no improvement on the initial blotting (see Figure 5.12B). The repeat confirmed that fraction 8 shows evidence of efficient cross-linking, although large amounts of monomer remain, at time point 0 min with 0.01% GA, therefore this level of GA should be sufficient to efficiently cross-link the α B-crystallin present in the unknown Mwt species fractions and the diluted fraction 8.

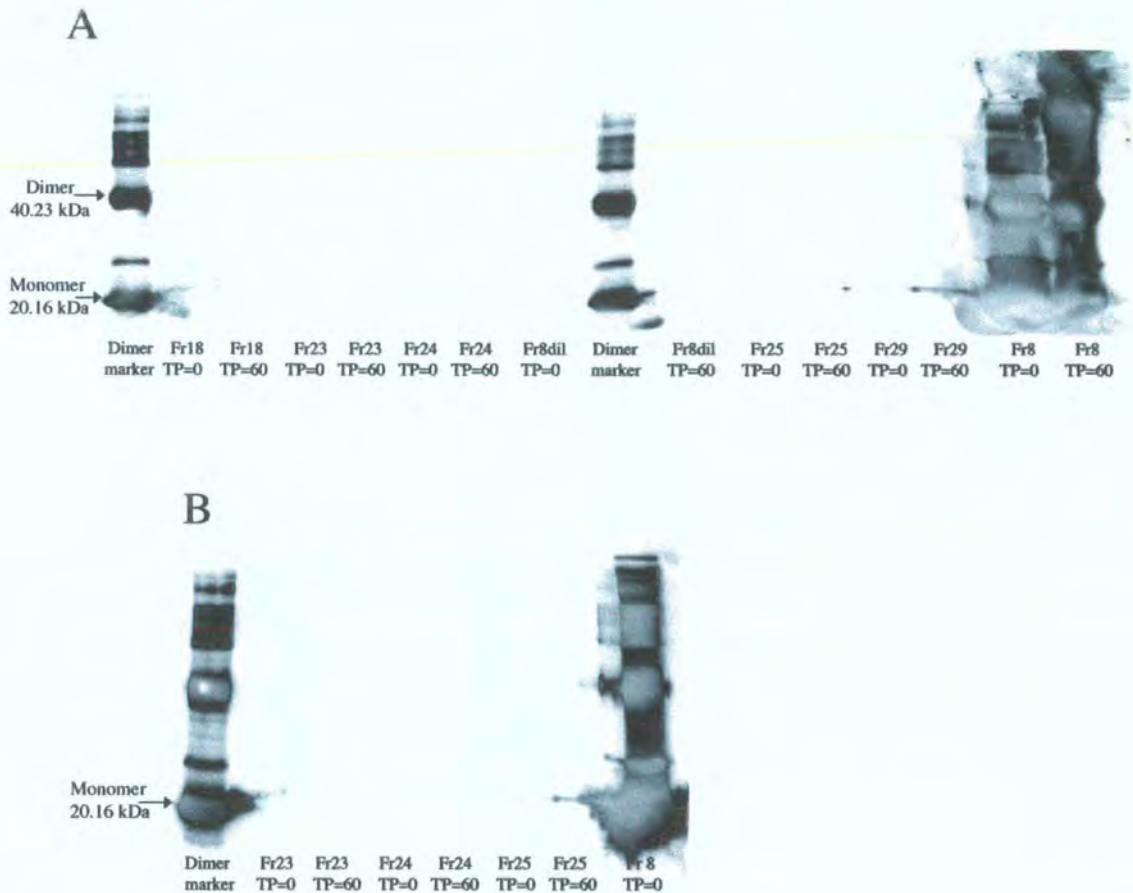


Figure 5.12. Immunoblotting of Cross-linked α B-crystallin unknown Mwt species. Cross-linking analysis of unknown Mwt species fractions and oligomer fraction from the large scale analytical SEC (A). Fractions encompassing the unknown Mwt species peak (Fr 24) and the oligomer peak of similar dilution (Fr 8dil) all show a single band corresponding to the monomer at 20.16 kDa following cross-linking with 0.01% GA (v/v) for 1hr at 20C. (25ul loaded and blotted with purified α B monoclonal 2D2B6 (1/1000) and (HRP 1/1000). Fr 8 shows higher MW species after 60 min (TP=60) however the same fraction diluted 1/5000 looks similar to the unknown Mwt species fractions. To detect any higher MW bands a repeat analysis was performed (B) with increased antibody and HRP levels (25ul loaded and blotted with purified α B monoclonal 2D2B6 (1/100) and HRP (1/500). Repeat analysis suggested no multimeric species present in the fractions.

One factor, which could be influential in the efficiency of the cross-linking, is the concentration of the unknown Mwt species fractions. Predicting 0.05-0.1 mg/ml, fraction 24 containing the peak material was actually 0.00084 mg/ml, some 12x lower than the optimised cross-linking for α B-crystallin at 0.01 mg/ml. This would mean there was an

excess of GA in the unknown Mwt species samples, thus complete cross-linking would be likely, however Figure 5.12B clearly shows no presence of a oligomeric band. The extremely low concentrations combined with limitations of the GA to covalently link molecules that are more distant from each due to a spacer of only 5 Å increase the possibility that the molecules are not cross-linking. The low concentrations make it very difficult to categorically state that there are no other Mwt complexes present.

5.4. DISCUSSION

5.4.1. THE POLYDISPERSITY OF THE WILD TYPE α B-CRYSTALLIN OLIGOMER IS DEPENDANT UPON CONCENTRATION

An important feature of α B-crystallin and other sHSPs is the ability to self associate and form mono- or polydisperse assemblies through a mechanism of subunit dynamics, however the relationship between the subunit dynamics, oligomerisation and chaperone activity remain unresolved (Liu et al., 2006). Many factors have been shown to influence the subunit dynamics as discussed extensively in the Introduction (see Section 5.2), which subsequently has an impact upon the oligomerisation and chaperone function. These include temperature (Datta and Rao, 1999; Koretz et al., 1998; Liu et al., 2006; Raman and Rao, 1994; Raman and Rao, 1997; Shashidharamurthy et al., 2005; Spinozzi et al., 2006), pH (Koretz et al., 1998; Liu et al., 2006; van Rijk and Bloemendal, 2000; Yun et al., 2002), divalent cation influences (del Valle et al., 2002; Duncan and Jacob, 1984; Ganadu et al., 2004; Marini et al., 1995), ATP (Biswas and Das, 2004; Ghosh et al., 2006c; Liu et al., 2006; Muchowski and Clark, 1998; Palmisano et al., 1995; Reddy et al., 1992), and phosphorylation (Aquilina et al., 2004; Kamei et al., 2001; Kantorow and Piatigorsky, 1998; Moroni and Garland, 2001).

One of the factors important in the rate of reactions is the concentration, which determines the frequency of collision of subunits and subsequently the rate of subunit exchange and oligomerisation. Bova suggested that for α A-crystallin the association/dissociation rate was independent of concentration, implying that the exchange of subunits is not due to the collision of the oligomers but is most likely a dissociation mechanism (Bova et al., 2000). Here I aimed to analyse the effect of protein concentration of α B-crystallin upon oligomerisation with the aim to further understand the effect external factors may have upon subunit dynamics and the mechanism of chaperone function.

In this study, I have shown that at α B-crystallin concentrations of approx 0.1 mg/ml there is an increase in polydispersity with complexes of both increased and reduced size. Further dilution to approx 0.01 mg/ml results in a reduction in the oligomeric complex size of the main α B-crystallin peak.

The investigation of the effect of α B-crystallin concentration upon oligomerisation involved recycling of the oligomer peak material under various conditions. Initial investigations of the effect of concentration on oligomerisation showed that on the third cycle (approx 0.1 mg/ml) there was resolution of additional peaks. At 20°C there was the introduction of a shoulder on the leading edge of the oligomer peak at 49.8 min and a species at 27.6 min. The oligomer peak (57.6 min) was broader and appeared less symmetrical to the wild type in cycles 1 and 2 (approx 2.0 and 0.5 mg/ml respectively). The presence of these additional peaks and the asymmetry of the oligomer peak suggest that the dilution increased the polydispersity of the wild type oligomer. The fourth cycle (approx 0.01 mg/ml) resulted in a symmetrical but smaller oligomer peak (60.3 min) suggesting that a further fall in α B-crystallin concentration affected the ability to form the oligomer observed at higher concentrations.

At 4°C it was intended that the low temperature would reduce the rate of association and dissociation and perhaps amplify the effects of concentration upon polydispersity at 0.1 mg/ml. Similarly to the oligomerisation observed at 20°C, the α B-crystallin oligomer is consistent through cycles 1 and 2. At the third cycle a change in the polydispersity was evident with additional peaks relatively small in height, being observed at 19.2, 39.3 and this time a smaller complex at 73.6 min. The oligomer peak remains similar in symmetry to cycle 1 and 2. At 20°C, dilution of α B-crystallin oligomer to 0.1 mg/ml in cycle 3 showed a greater effect upon polydispersity of the oligomer peak where at 4°C a smaller complex was resolved at 73.6 min. Under conditions of high ionic strength at 20°C, cycle 3 (approx 0.1 mg/ml) however, showed an additional peak representing a smaller complex at 81.6 min (see Appendix 4, Figure A4.1).

Further dilution to 0.01 mg/ml at 20°C, 4°C and under conditions of high ionic strength, resulted in a smaller broader oligomer peak. Here, the dilution reaches a level, which results in an effect upon the size of the oligomer as well as the polydispersity.

These data suggest that the reduction in concentration to 0.1 mg/ml reduces the rate of associations and dissociations, which results in the appearance of additional species through increased polydispersity. At even lower concentrations of 0.01 mg/ml the rate of subunit exchange is further reduced and combined with a further fall in the frequency of collisions we observe a negative effect upon the ability of the α B-crystallin to fully oligomerise.

These data support the theory that there is a critical concentration for α B-crystallin oligomerisation. In equilibrium there would be constant exchange of α B-crystallin subunits between the oligomer and a pool of α B-crystallin subunits. This has been observed for α A-crystallin where a study revealed a quaternary structure of α A crystallin consisting of small multimers of α A crystallin subunits (trimer or tetramer) in a dynamic equilibrium with the oligomeric complex (Bova et al., 2000).

The concentration of α B-crystallin subunits in the pool, at this equilibrium is referred to as the critical concentration, also referred to as the concentration of α B subunits required for oligomer formation (Lewin, 2007). When the total concentration of subunits is below the critical concentration only monomer will exist. In contrast, when the total concentration of subunits is greater than the critical concentration oligomer will form (Lewin, 2007).

As observed from the data shown, at concentrations above the critical concentration the oligomer will form at rates that depend linearly on the concentration of subunits in solution, thus resulting in the formation of a range of intermediate complexes of varying size. In its native state, α B-crystallin consists primarily of oligomers containing 24-33 subunits, with a dominant species being composed of 28 subunits (consistent with these data where α B-crystallin has a Mwt of 564 kDa (see Figure 4.3)). Additionally, low levels of oligomers as small as a 10-mer and as large as a 40-mer were observed (Aquilina et al., 2003; Benesch et al., 2006). The formation of sHSPs oligomers from plants, yeast and bacteria have been shown to consist of dimeric building blocks, which have been proposed as the active unit involved in chaperone activity and to contribute towards their monodispersity (Narberhaus, 2002; van Montfort et al., 2001b). In wheat sHSP16.5, the IX(I/V) motif of the C-terminal interacts with the β 4 and β 8 strands of another monomer to form the higher order dodecameric double disk quaternary structure observed in the crystal structure (van Montfort et al., 2001b). While α B-crystallin contains the same three structural domains found in *M.jannaschii* ssHSP16.5 and wheat sHSP16.9, the complex assembly of human α B-crystallin is larger and more polydisperse than the two sHSPs that have been crystallised and cryo-electron microscopy studies showed that α B-crystallin has an asymmetric variable quaternary structure consisting of 32 subunits with a central cavity (Feil et al., 2001; Haley et al., 1998). The

variable quaternary structure of α B-crystallin is consistent with the polydispersity of the oligomer and with the dynamic nature of α B-crystallin (Haley et al., 1998). Aquilina et al. (2003) observed the formation of α B-crystallin oligomers that contained odd and even numbers of subunits implying both dimeric and non-dimeric quaternary interactions form the basic building block of oligomerisation and that these monomers or dimers may constitute the active units of chaperone activity (Aquilina et al., 2003; Aquilina et al., 2004).

The data shown here suggests increased polydispersity is associated with a fall in α B-crystallin concentration revealing additional oligomers of both higher and lower Mwt relative to the 564 kDa oligomer. The nature of α B-crystallin oligomer formation which sees a distribution of oligomers from a 10-mer up to a 40-mer with the primary oligomers consisting of 24-33-mers and a dominant 28-mer species highlights the natural polydispersity of α B-crystallin and indicates how the associations of α B-crystallin subunits allows the formation of a wide range of oligomeric complexes, which is increased under conditions of lowered concentration. Figure 5.13 indicates the many possible intermediate α B-crystallin oligomers, which may form as a function of the polydispersity to achieve the distributions observed by Aquilina (Aquilina et al., 2003).

The temperature and time of incubation also show variations in the polydispersity adding support to theory that the oligomer of α B-crystallin is in constant dynamic exchange, which can be influenced by external factors (Datta and Rao, 1999; Koretz et al., 1998; Liu et al., 2006; Raman and Rao, 1994; Raman and Rao, 1997; Shashidharamurthy et al., 2005; Spinozzi et al., 2006). The effect of changes in polydispersity upon the function of α B-crystallin as a chaperone remains unclear. The chaperone activity improves with a smaller complex size as observed in Chapter 4 with the Q151X α B-crystallin (see Section 4.4.2), suggesting that the polydispersity resulting from a dynamic subunit exchange rate may be more important than complex size in regulating the chaperone activity of α B-crystallin and sHSPs by regulating the exposure of the interactive sites involved in the binding of client proteins (Datta and Rao, 2000; Lindner et al., 2000; Liu et al., 2006; Shashidharamurthy et al., 2005). In the α B-crystallin oligomer, the interactive site for chaperone activity and substrate binding is the β 3- β 8- β 9 interface (Ghosh et al., 2006a), which may be buried in the oligomer and inaccessible to unfolding

proteins. This leads to the hypothesis that dissociation of α B-crystallin complexes is required for effective chaperone activity. Changes in the polydispersity may influence chaperone activity by increasing or reducing the exposure of this interactive region depending on the size of the additional complexes.

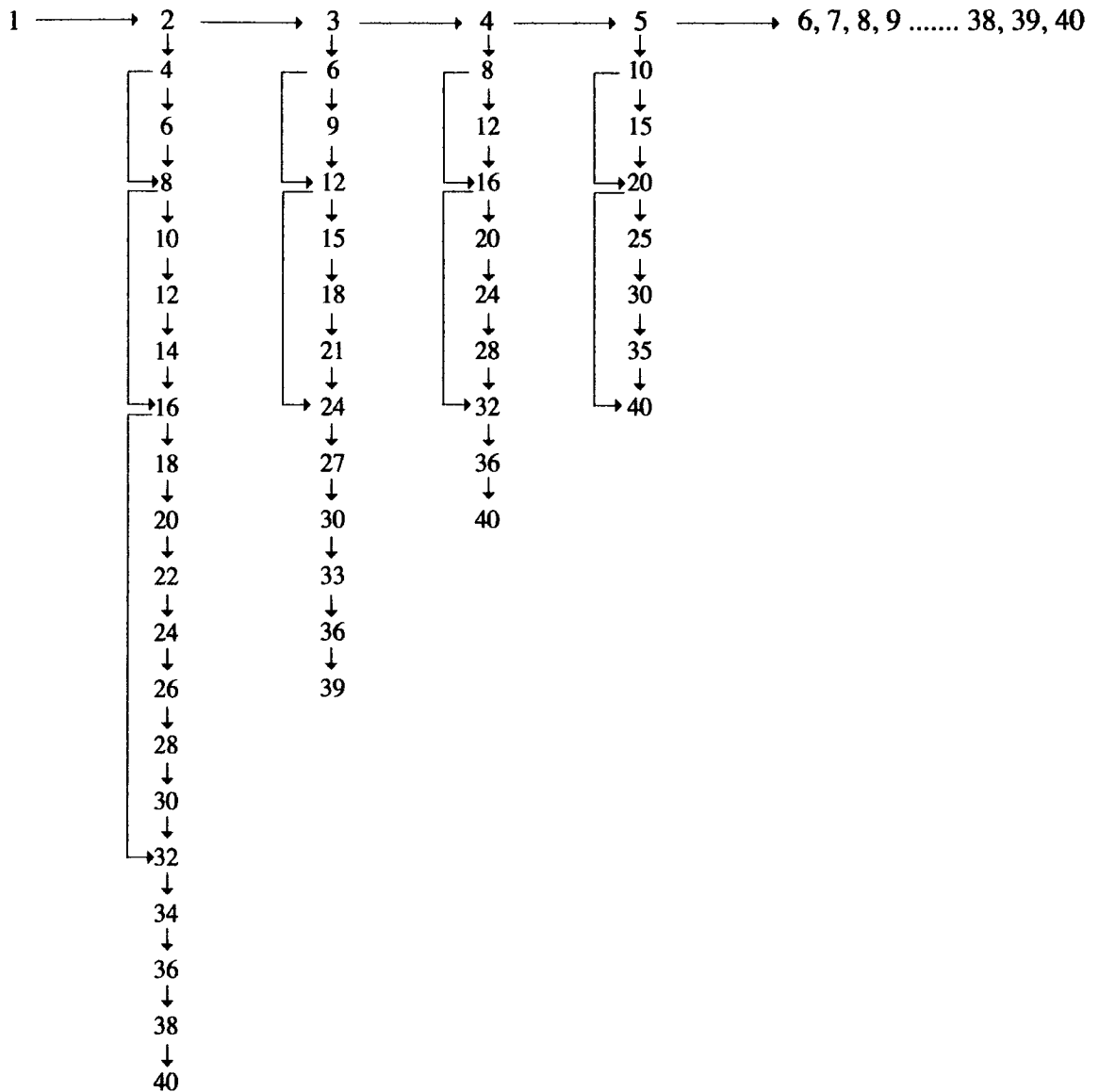


Figure 5.13. Schematic representation of the possible oligomeric assembly of α B-crystallin. The potential primary associations that may occur during oligomerisation are highlighted to indicate how the distribution of α B-crystallin oligomers may occur to achieve a polydisperse molecule. The building block of oligomerisation is believed to be the monomer, yet following monomeric associations multimers may associate to form larger complexes. The associations of multimeric complexes gives rise to a number of possible associations that may occur to achieve 10-mers, 24-33-mers and 40-mers and also the additional complexes observed at lowered α B-crystallin protein concentrations.

5.4.2. A LOW MWT α B-CRYSTALLIN SPECIES ISOLATED FROM THE α B-CRYSTALLIN OLIGOMER COULD POTENTIALLY BE THE ACTIVE UNIT OF CHAPERONE ACTIVITY

Preliminary analysis of the α B-crystallin oligomer tail identified the presence of an additional α B-crystallin species past the separation range of the column, independent of the type of column matrix and pump system utilised. Evidence of a dynamic exchange resulting in additional species at concentrations lower than 0.1 mg/ml (see Section 5.3.1) supports the theory that this α B-crystallin could potentially be a low Mwt complex representative of an active pool of subunits that are dissociated as part of the mechanism of chaperone activity or present in a dynamic exchange with the oligomer. This isolation supports the theory that dissociation of subunits from the oligomer is required for efficient chaperone activity and that the oligomer acts as a 'reservoir' of α B-crystallin subunits, which are in constant dynamic exchange with the active pool of subunits, under native conditions (Horwitz et al., 2004; Liu et al., 2006; Narberhaus, 2002; van Montfort et al., 2001b). The dynamic exchange is increased under conditions of stress where the demand for the chaperone activity is greater resulting in increased subunit exchange. For example, heat shock raises the demand for chaperone function and leads to the exposure of hydrophobic chaperone sites by subunit exchange (Shashidharamurthy et al., 2005). Under acidic conditions, the interaction between α B crystallin subunits increased with a higher association rate and a lower dissociation rate (Liu et al., 2006).

The isolation of this unknown Mwt species allows further characterisation, which is required to identify the size of this species

To fully understand the role of the unknown Mwt α B-crystallin species in subunit dynamics and chaperone activity it is important to characterise the size of this species and also investigate the relative chaperone activity and its role in oligomerisation.

The isolation of the potential active unit of chaperone activity aimed to investigate the relative chaperone activities of the unknown Mwt species and the wild type solution, which contained a mixture of predominantly oligomer with trace amounts of the unknown Mwt species. The unknown Mwt species could potentially be a more effective

chaperone than the oligomer, thus, the isolation and amplification of this species could challenge the wild type as a chaperone.

Resolution of the unknown Mwt species from a scaled up SEC yielded a protein concentration of 0.00084 mg/ml, therefore the chaperone assays could not be performed as they required a minimum concentration of unknown Mwt species of approx 0.05-0.1 mg/ml. The recovery of the unknown Mwt species can be increased albeit disproportionately, however, there is limitation to the potential concentration that can be achieved. This suggests that the presence and isolation of the species is a function of the low concentration. In section 5.3.1, I discussed how concentrations of α B-crystallin below 0.1 mg/ml induced increased polydispersity and a smaller oligomer size. Perhaps a higher concentration of the unknown Mwt species would result in a different species caused by a change in the subunit dynamics, thus the reassociation of subunits to form larger oligomeric complexes.

Subsequent characterisation of the unknown Mwt species at 0.00084 mg/ml concentration involved rechromatography to assess the size of the species. Typically size determination could be carried out using Tandem Mass Spectrometry (Aquilina et al., 2003; Benesch et al., 2006), however the technique required sample material of significantly greater concentration.

A low Mwt species was observed by a peak at 96.3 min and showed no evidence of an oligomer peak. The oligomer fraction was diluted to the same concentration as the unknown Mwt species resulted in a definite oligomer peak at 58 min. These data confirmed the α B-crystallin had not reassociated into the oligomer and any oligomer, if present in the unknown Mwt fraction, would be detected at this level of sensitivity. This data combined with the data showing there is a presence of the unknown Mwt species from SEC with various matrices and systems, confirms that the unknown Mwt α B-crystallin species is of a very low Mwt and is not a product of interactions of denatured or active forms of α B-crystallin with the column or denatured proteins attached to the column, that may subsequently be displaced by the presence of additional α B-crystallin. This adds support to the theory that this low Mwt species of α B-crystallin is potentially the monomeric or dimeric active unit of chaperone activity.

Further characterisation of the low Mwt α B-crystallin species by cross-linking analysis aimed to identify any relative differences in oligomerisation between the wild type oligomer and the low Mwt species, which may be significant when considering the potential role of the low Mwt species in the chaperone activity. Using optimised cross-linking conditions, the low Mwt species showed only monomer similar to the diluted oligomer control, however, the neat oligomer fraction showed cross-linking consistent with optimisation studies. The absence of any Mwt species above monomer in the low Mwt species fractions and the diluted oligomer control could be symptomatic of a number of conditions. If the monomer was the major cross-linked species, then visualisation at such a low protein concentration of any lower intensity oligomer bands of the low Mwt species and diluted oligomer control may not be possible. The GA however, was added at a concentration that was sufficient to produce predominantly oligomer at α B-crystallin solutions of 0.01 mg/ml, thus the monomer should be the band of lowest intensity and higher multimers should be greater in intensity and easily visible. The monomers that we see representing the cross-linked low Mwt species and diluted oligomer control could be real monomers, however, the rechromatography of the diluted oligomer fraction confirmed at this low concentration that oligomer was present. Finally, the combination of low concentration and the limitations of the 5 Å spacer arm of GA in forming links with distant subunits could have had an inhibitory effect upon the cross-linking efficiency. The crosslinking data investigating the relative differences in oligomerisation between the wild type oligomer and the low Mwt species was not conclusive due to limitations caused by the low protein concentrations being analysed.

Therefore, the characterisation of the unknown α B-crystallin species suggests that it has a very low Mwt and may be monomeric or a small multimer. This supports the theory that the species may be the active unit of chaperone activity in constant equilibrium and dynamic exchange with the oligomer. However, it has not been possible to categorically confirm the size of the species or the efficiency as a chaperone due to the limitations provided by a low concentration of the unknown Mwt species yielded from the scaled-up SEC. It appears that the presence of this species is a function of the low concentration, thus making it very difficult to potentially achieve a concentration that

would allow analysis of the chaperone function and complex size determination by mass spectrometry. The development of matrix-assisted laser desorption ionization (MALDI) mass spectrometry has permitted the determination of the molecular mass of proteins up to the 105-Da range with an accuracy of 0.1-0.01%, requiring only picomoles or sub picomoles of material (Beavis and Chait, 1990; Juhasz and Biemann, 1994; Karas, 1987), however, the tandem mass spectrometry system specific for the analysis of oligomeric complexes (Aquilina et al., 2003; Benesch et al., 2006; Benesch and Robinson, 2006) was not sensitive enough to detect the low Mwt α B-crystallin species at the current concentration of 0.00084 mg/ml. An alternative method for determining molecular weight is Analytical ultracentrifugation. With analytical centrifugation, the sedimentation equilibrium is most commonly used for Mwt determination, where the solute particles do not pellet at the bottom of the cell. Instead they redistribute over time with increasing concentration as the distance from the centre of rotation increases. After an appropriate period of time, the process of diffusion equals the process of sedimentation (called the sedimentation equilibrium). Measurement of the solute concentration at different time points leads to the determination of the molar weight of the sedimenting solute (Ralston, 1993). For a typical sedimentation equilibrium experiment, 150 μ l of sample with an OD at 280 nm of 0.3 is required, which for α B-crystallin is approx 0.4 mg/ml, however with less protein available it is suggested that a lower wavelength (e.g. 220 nm) can be used (Beckman, Model XL-A Training Guide, Beckman Instruments Inc, CA, USA). Analytical centrifugation has been typically performed at protein concentrations of 0.25 mg/ml or above (Bunkoczi et al., 2007; Chang et al., 1996; Li et al., 2007; Yu et al., 2004), however concentrations of 0.06mg/ml have also been utilised (Schar et al., 2008). Therefore, the Mwt determination of the low Mwt α B-crystallin species at 0.00084 mg/ml could potentially be achieved by Analytical ultracentrifugation but will require further analysis.

5.5. CHAPTER'S CONCLUSIONS

The aim of this chapter was to investigate the effect of concentration upon the oligomerisation of α B-crystallin. By the end of this Chapter, I have confirmed that the reduction of α B-crystallin concentration below 0.1 mg/ml results in increased polydispersity and the appearance of additional high and low Mwt species independent of temperature. Further reduction in α B-crystallin concentration to 0.01 mg/ml shows a smaller oligomeric complex size. These studies resulted in the identification of a low Mwt α B-crystallin species in the late tail region of the oligomer. This low Mwt α B-crystallin could potentially be the active unit of chaperone activity in constant equilibrium and dynamic exchange with the oligomer but this will require further analysis. Further characterisation was hindered by the disproportionate increase in concentration (3X) achieved by scale-up (125X) and suggested that the appearance of this species may be a function of the low concentration and as Horwitz observed in 2004, under normal physiological conditions, it is impossible to isolate significant amount of monomers, dimers, or tetramers of α -crystallin (Horwitz et al., 2004). Confirmation of the size of the low Mwt α B-crystallin remains difficult without a higher concentration, which may be slightly improved, albeit disproportionately by further scale up of the SEC process. Alternatively, analytical ultracentrifugation may be a successful technique for the Mwt determination of this species. Confirmation of the size of the low Mwt α B-crystallin would perhaps help understand the mechanism involved in the relationship between oligomerisation, subunit dynamics and chaperone function.

CHAPTER 6

CONCLUSION

6.1. STUDY SUMMARY

To date, the role of the C-terminal extension of α B-crystallin upon solubility, structure and function and the relationship with disease has not been investigated. In this study, the systematic analysis of the role of the C-terminal extension of α B-crystallin aimed to investigate the hypothesis that the C-terminal region in α B-crystallin is important for solubility, structure and function of the protein. This study also aimed to find a link between the role of the C-terminus and the symptoms of disease, thus providing a potential explanation of whether the three mutations (450delA, Q151X and 464delCT) cause the various diseases via the loss of chaperone function or perhaps by a different mechanism. The nature of the disease mutants is to form aggregates within the lens (450delA, E164X) and muscle tissue (464delCT and Q151X) thus, providing a link between the effect of a severely altered C-terminal and the solubility of the expressed protein. Elucidation of the mechanism of disease may help understand the phenotypic variation observed with mutations of α B-crystallin. Further understanding of the mechanism of chaperone function with regards to the oligomerisation state and subunit dynamics aimed to provide further understanding of the role this plays in efficient chaperoning of client proteins.

The findings of this study showed that the flexible C-terminal extension was essential to produce a stable α B-crystallin complex as the sequential removal of the C-terminal resulted in aggregation of the mutants. . The mutants displayed a varying level of insolubility during the refold process as a function of the severity of the alterations to the C-terminal extension. The disease mutants 450delA, 464delCT and Q151X along with the post translational modification (PTM) E164X proved the most insoluble and indicated that the non flexible region was also influential upon complex solubility through a different mechanism involving oligomerisation and chaperone function, suggesting a relationship between the role of the C-terminal extension and disease.

The C-terminal extension has been shown to be primarily involved in subunit-subunit interactions required for oligomerisation and was not essential for chaperone activity. The C-terminal extension can actually inhibit client substrate binding by 'capping' the $\beta 3$ - $\beta 8$ - $\beta 9$ interface in the α -domain, which is the interactive site for substrate binding. The findings in Chapters 3 and 4 suggested that the potential molecular mechanism behind the pathology of the disease causing mutants is a function of the reduced protein stability and uncontrolled self-aggregation caused by the alterations to the C-terminal extensions and not caused by a loss of chaperone activity as illustrated by the efficiency of the Q151X α B-crystallin as a chaperone. The link however, between these findings and the mechanism, which causes the variations in phenotypic expression, remains unclear and requires further investigation.

In chapter 5, I identified a potentially low Mwt species of α B-crystallin that maybe important for effective chaperone activity. This species may be an active unit of chaperone activity, however in this study I was unable to confirm the size of the species therefore the implications of this species upon chaperone function remain unresolved.

6.2. IMPLICATIONS FOR THE CELLULAR FUNCTIONS OF α B-CRYSTALLIN

The identified physiological roles of α B-crystallin include regulator of IF networks, regulators of apoptosis, transcriptional regulators, genome stability and proteasome function.

The findings of this study propose that the chaperone function of the wild type α B-crystallin is inhibited via coaggregation with the destabilised mutants, suggesting several possible consequences for cellular function (see Figure 6.1), which are discussed below.

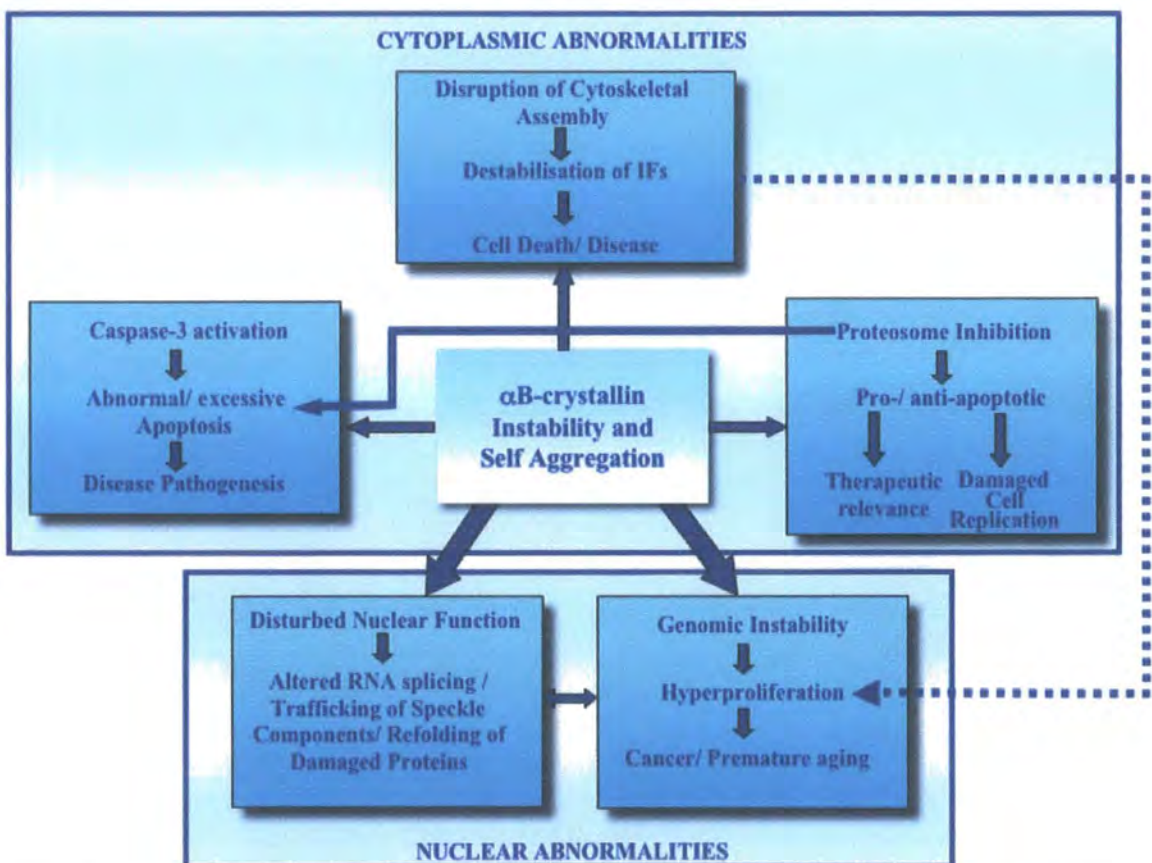


Figure 6.1. Effect of coaggregation upon the physiological function of α B-crystallin. The inability for α B-crystallin to perform its cellular functions could cumulatively play a role in disease pathogenesis. The loss of α B-crystallin has potential cytoplasmic and nuclear consequences including altered nuclear function and genome instability, abnormal apoptosis, proteasome inhibition and disruption of the cytoskeletal assembly.

6.2.1. CYTOPLASMIC EFFECTS

α B-crystallin participates in the dynamic assembly, disassembly, reorganisation and stabilisation of the filamentous cytoskeleton during cell development and cell differentiation (Bennardini et al., 1992; Ghosh et al., 2007; Nicholl and Quinlan, 1994). Disruption of the cytoskeletal assembly is one of the early effects of any stress that can ultimately lead to cell death thus, maintaining the individuality of IFs by controlling filament-filament interactions (Perng, 1999) and assisting in the formation of IF networks in cells (Perng et al., 2004) by α B-crystallin is essential for a functioning cytoskeleton. The absence of wild type α B-crystallin, caused by co-aggregation with the disease causing mutants, would lead to the disruption of the cytoskeletal assembly via aggregation of IFs, as observed for desmin in diseases with muscle phenotype including DRM and MM (see Figure 6.1).

α B-crystallin is thought to participate broadly in the regulation of muscle cell death by suppressing myogenic differentiation and the activation of caspase-3 (Kamradt et al., 2002), which plays a central role in the execution of apoptosis (Cryns and Yuan, 1998). The induction of caspase-3 during myogenesis might be required for the ablation of differentiation-incompetent myoblasts (Ikeda et al., 2006). Loss of α B-crystallin by co-aggregation would remove the ability to inhibit caspase-3 activation and myogenic differentiation, subsequently leading to excessive apoptosis (see Figure 6.1), which has been shown to be a feature of various diseases including cancer, autoimmune diseases, neurodegenerative diseases muscular atrophy, Parkinson's disease, Alzheimer's and ischaemia (Elmore, 2007). Apoptosis has also been associated with human cataractogenesis where various factors, which cause cataractogenesis, also trigger lens epithelial cell apoptosis. In fact, death precedes development of lens opacification and apoptotic cells are found in human cataractous lenses (Yan et al., 2006). Thus, it is evident that an abnormal apoptosis mechanism caused by the expression of an α B-crystallin disease causing mutant could contribute towards the pathology observed for the 450delA, Q151X and 464delCT α B-crystallin mutations.

Apoptosis is further linked with α B-crystallin, albeit indirectly, via its role in the proteasome-mediated degradation of selected proteins (den Engelsman et al., 2003; Parcellier et al., 2005). The co-aggregation of α B-crystallin with the mutant α B-

crystallins may inhibit proteasome function as it is active in the mechanism that destines proteins for ubiquitin-dependant degradation (den Engelsman et al., 2003). The inhibition of the proteasome activates the apoptotic pathway dependant on the stress kinase cJUN N-terminal kinase (JNK) and simultaneously induces synthesis of the protective protein HSP72, which suppresses JNK (Meriin et al., 1998). Meriin et al. (1998) suggested the balance between these two activities could define whether pro- or anti-apoptotic action of the inhibitors would dominate (see Figure 6.1) (Meriin et al., 1998).

Proteasome inhibitors have been demonstrated to cause complex effects on programmed cell death and while inhibition is usually pro-apoptotic (Drexler, 1997; Orłowski, 1999; Wojcik, 1999), under certain conditions it prevents apoptosis triggered by harmful stimuli (Grimm et al., 1996; Meriin et al., 1998; Sadoul et al., 1996). Proteasome inhibition could have clinical therapeutic relevance and has been linked to effective anti-tumour activity inducing apoptosis by disrupting the regulated degradation of pre-growth cell cycle proteins (Adams et al., 1999) and also in pancreatic cancer (Shah et al., 2001), nonhodgkin's lymphoma (O'Connor, 2005) and psoriasis (Zollner et al., 2002). Studies have also shown that proteasome inhibition protects lens epithelial cells against interferon induced apoptosis and correlates with increased expression of sHSPs and implicates sHSPs as mediators of the protective effect of proteasome inhibition (Awasthi and Wagner, 2005).

s-IBM (inclusion body mitosis) the most common muscle disease of patients aged 50 and above, features the accumulation of intra-muscle fiber multi-protein aggregates similar to Alzheimer's disease (Askanas and Engel, 2006). The reduction of 26S proteasome activity was recently demonstrated within s-IBM muscle fibers (Fratta et al., 2005) and α B-crystallin was shown immunohistochemically to be abnormally accumulated in muscle fibers of s-IBM. It was proposed that increased α B-crystallin expression precedes other abnormalities in s-IBM muscle fibers (Banwell and Engel, 2000). HSP27 and α B-crystallin are increased, phosphorylated and localised in aggresomes when proteasome activity is inhibited (Ito et al., 2002).

There is a link between the accumulation of α B-crystallin within the muscle and lens fibers and the activity of both the proteasome and apoptosis, which may be part of a mechanism, contributing towards the onset of MM and cataract caused by the 450delA, 464delCt and Q151X α B-crystallin mutants.

6.2.2. NUCLEAR EFFECTS

The identification of α B-crystallin as a nuclear speckle component in unstressed cells suggests a constitutive function for this chaperone in the nucleus where a role in transcription is possible (van den IJssel et al., 2003). Speckles are linked to transcriptional activity and are thought to be transit or storage sites for splicing components where dynamic protein interactions are important (Bellini and Gall, 1999; Phair and Misteli, 2000; Sleeman et al., 2001; Sleeman and Lamond, 1999; Yin et al., 2001). Heat stress invokes the formation of intranuclear granules comprising protein chaperones (Velazquez and Lindquist, 1984) and sHSPs are effective in accelerating the recovery of cells with nuclear aggregates (Kampinga et al., 1994). The possible role of α B-crystallin in transcription can not be discriminated between a chaperoning role restricted to protein-protein interactions, a facilitator of protein traffic through the speckle compartment or even a direct role in RNA splicing itself, however the role involves unstressed cells suggesting it is essential for efficient nuclear function (van den IJssel et al., 2003). The mutation R120G has been shown to inhibit the accumulation of α B-crystallin into nuclear speckles, which could affect the nuclear function of α B-crystallin (van den IJssel et al., 2003). Similarly the co-aggregation of wild type α B-crystallin with C-terminal mutants 450delA, Q151X, 464delCT α B-crystallin may effect the nuclear function and contribute towards the development of a muscle phenotype but not cataract as an effect upon nuclear function would not implicate the lens fiber cells due removal of the nuclei during organogenesis (Harding, 1991). Perhaps a similar mechanism involving nuclear function and transcriptional regulation occurs with the R157H mutant leading to DCM, however the effect of the mutation on the structure and function is yet to be elucidated.

There is mounting evidence that transcription and genomic instability are linked processes (Aguilera, 2002; Tini, 2002) and transcription has been proven to be important in the maintenance of genome integrity and in the induction of genetic instability and diversity (Aguilera, 2002). The maintenance of primary DNA sequence and the preservation of chromosomal ploidy and structure are important factors in genome stability (Hartwell et al., 1994). The loss of α B-crystallin enhances genome instability and hyperproliferation (Andley et al., 2001), and provides a further link suggesting that α B-crystallin regulates cell division (Andley et al., 2001; Andley et al., 2000; Fujita et al.,

2004). In fact, α B-crystallin is associated with the regulation of actin filament dynamics *in vivo* (Singh et al., 2007) and connections between remodelling of the actin cytoskeleton and the control of cell proliferation have been suggested to play a role in a pathway through which an aberrant actin cytoskeleton can cause epithelial hyperproliferation in corneal cells (Ikeda, 2003). Because lens epithelial cells grow throughout a lifetime and the lens is exposed to light induced stress it is likely that mechanisms may be present to protect these cells for a lifetime of exposure to metabolic and environmental stress (Andley et al., 2000). Genomic instability is a hallmark of many syndromes, which include neurodegeneration, cancer, premature aging and immunodeficiency (Andley et al., 2001).

The implications of aggregated α B-crystallin upon the various cellular functions of α B-crystallin reveal the complex mechanisms that can be influenced, and potentially play an important role in the generation of the disease phenotype. Consideration of these cellular effects can be made in conjunction with other factors to discuss in Section 6.3, the unresolved mechanism of phenotypic variation associated with α B-crystallin C-terminal mutations.

6.3. POTENTIAL MECHANISMS OF PHENOTYPIC HETEROGENEITY ASSOCIATED WITH α B-CRYSTALLIN

The mechanism of disease associated with C-terminal mutants is influenced by an effect upon solubility and chaperone activity, however it is still not possible to draw a link between structure and function of the α B-crystallin and its phenotypic heterogeneity.

The three disease-causing mutations in the C-terminal extension of α B-crystallin (Q151X, 450delA and 464delCT) are restricted in their pathology to either the lens (450delA) (Berry et al., 2001)) or muscle (Q151X and 464delCT) (Selcen and Engel, 2003)) and yet α B-crystallin is very highly expressed in both tissues (Kato et al., 1991). This is a familiar trend for α B-crystallin mutations and even the most recently published mutation (R157H) causes DCM alone (Inagaki et al., 2006) and D140N, causes only lens cataract (Liu et al., 2006b). Thus far, R120G α B-crystallin is the only mutation that has produced both lens and muscle pathologies (Vicart et al., 1998), although both R120G and D140N mutations result in similar structure changes (Liu et al., 2006b). This is not to say that sub-clinical pathology can be totally excluded for the other mutations, including Q151X, as tissue biopsies from apparently unaffected tissues were not analysed.

Liu et al. (2006) suggested that perhaps the dominant negative effect of the D140N mutation is one of the major mechanisms of the cataract phenotype and that mutant α B-crystallin was rapidly degraded in muscles, which have active proteolytic systems (Liu et al., 2006b). It was also suggested that due to the low expression levels observed in the muscle compared to the lens, the mutant α B-crystallin may not reach levels necessary for inhibiting chaperone activity of wild type α B-crystallin and other sHSPs (Liu et al., 2006b). This proposal does not reflect the findings of this thesis, which suggest it is the self aggregation rather than a loss of chaperone function that leads to the disease onset (see Chapter 4).

The 450delA α B-crystallin causes isolated congenital cataract and has no muscle phenotype, whereas the Q151X and the 464delCT α B-crystallin cause symptoms associated with MM but not cataract. This suggests that perhaps one factor that may be influential in the phenotypic expression is the tissue specific associations of α B-crystallin.

HSP27 interacts with α A and α B-crystallin *in vivo*, but to a greater extent with α B-crystallin. In non-lenticular tissues HSP27 is expressed with α B-crystallin rather than α A-crystallin and may serve to stabilise α B-crystallin in non-lenticular tissues by co-localisation with α B-crystallin under both normal conditions and in a stressed or diseased state (Zantema et al., 1992).

Perhaps the 450delA mutation causes a dominant negative effect not only on the wild type α B-crystallin but also causes co-aggregation of the α A-crystallin oligomer, thus causing cataract. If the 450delA mutation caused such an effect then it is likely that a muscle phenotype would also be observed, as the stabilising α A-crystallin is not present in muscle tissue, however this is not the case. The significantly lower expression levels observed in non-lenticular tissues may be such that the tissue specific α B-crystallin stabilising partner HSP27 is able to chaperone any aggregating α B-crystallin and prevent any pathological effect, alternatively the co-aggregation observed in muscle tissue may be the result of a completely different mechanism. The concern, however is if the HSP27 can stabilise the 450delA α B-crystallin aggregates then the Q151X and 464delCT α B-crystallin in theory should also be stabilised by the HSP27 aggregates, yet a muscle phenotype is characteristic of these mutations with no cataract. Perhaps, a combination of the concentration in the lens and the size of the 450delA α B-crystallin aggregates are responsible for the aggregation of the α A-crystallin and cataract. The MM mutants especially the Q151X are smaller complexes without an extended C-terminal and perhaps the α A-crystallin can efficiently chaperone the aggregated mutants to maintain the refractive properties of the lens. The muscle phenotype could be a function of a disrupted or abnormal association mechanism between α B-crystallin and HSP27.

The potential contribution towards the onset of disease caused by the disturbance of the other cellular functions of α B-crystallin (see Section 6.2) may help explain the mechanism of phenotypic heterogeneity. The potential role of α B-crystallin in the nuclear functions such as protein-protein interactions, facilitator of protein traffic through the speckle compartment and a direct role in RNA splicing (van den IJssel et al., 2003), suggests that loss of α B-crystallin through self aggregation could affect the nuclear function of α B-crystallin. The lens fiber cells however, do not contain nuclei due to

programmed loss of cellular organelles during differentiation (Harding, 1991) and provides a significant variation between lenticular and non-lenticular tissue. Any physiological consequence of altered nuclear function caused by α B-crystallin mutation would not be observed in the lens fiber cells, thus providing a possible explanation for the Q151X and 464delCT phenotypic expression.

The disturbance of the apoptosis mechanism has been shown to have specific effects on the lens epithelial cells, which eventually result in cataractogenesis (Yan et al., 2006). First, lens epithelial cell death interrupts the life long growth of human lenses, therefore contributing towards the thinness of cataract lenses (Goodman, 1964; Laursen and Fledelius, 1979), and the lower density of epithelial cells in the cataract lenses (Karim et al., 1987; Konofsky et al., 1987). Secondly, depletion of individual or patches of lens epithelial cells will eliminate homeostatic epithelial cell control of the underlying fiber cells leading to impairment of the integrity and transparency of these of these fiber cells (Spector, 1991). Thus induction of apoptosis due to the inhibition of the α B-crystallin function in the apoptotic mechanism may initiate cataract formation. Subsequently, this effect would not affect muscle tissue and perhaps the mutant 450delA α B-crystallins can be stabilised by association with HSP27.

It is important to consider the wider biological context of phenotypic variation and the association with disease. Thus far, four sHSPs have been associated with disease and include α A-, α B-crystallin, HSP27 and HSP22 (Selcen and Engel, 2003; Tang et al., 2005a; Tang et al., 2005b; Vicart et al., 1998). Interestingly the mutations of both HSP22 and HSP27 also display phenotypic variation and lead to the onset of various neuropathies and muscle related disorders. Mutations in genes encoding the IF nuclear lamins and associated proteins cause a wide spectrum of diseases sometimes called "laminopathies." (Pigliucci, 2003; Worman and Bonne, 2007). Recently, 5 missense mutations in HSP27 have been identified to cause Charcot-Marie-Tooth disease (CMT) type 2F and distal hereditary motor neuropathy (dHMN) (Evgrafov et al., 2004; Harding and Thomas, 1980a; Harding and Thomas, 1980b; Ismailov SM, 2001; Suter and Scherer, 2003; Tang et al., 2005a).

Mutations of the HSP22 gene (HSPB8) co-segregate perfectly with either the CMT phenotype (De Jonghe, 1998; Tang et al., 2005b; Timmerman et al., 1992) or the dHMN

phenotype (Carra et al., 2005); (Irobi et al., 2004) (Morrow and Tanguay, 2003; Soti and Csermely, 2003). Tang suggested that the dysfunction of HSP22 leads to the formation of aggregates that may block axonal transport (Tang et al., 2005b). The different regions, such as the anterior horn cells or peripheral nerves, in which the aggregates are deposited may be associated with the different phenotypes, i.e., CMT and dHMN (Tang et al., 2005b). Kasakov suggested that mutations in the $\beta 5$ – $\beta 7$ loop of HSP22 located on the border of an intrinsically disordered region and the $\beta 7$ -strand affect the structure of HSP22 and its chaperone-like activity. This explains why mutations in this part of different sHSPs (αA -, αB -crystallin, HSP27 and HSP22), induce deleterious effects and are associated with different congenital diseases (Kasakov et al., 2007).

Phenotypic variation has been studied for many years beginning in 1942, when C.H. Waddington proposed a new mechanism of evolutionary change, which he termed “genetic assimilation” (Waddington, 1942; Waddington, 1961). The idea was that certain environmental or genetic factors can disrupt the normally canalized (i.e., stable) course of development of living organisms. This disruption may then generate phenotypic variation that could allow a population to persist in a novel or stressful environment until new mutations would eventually let natural selection fix (“assimilate”) the advantageous phenotypic variants (Pigliucci, 2003). Epigenetic variation is often overlooked as a source of phenotypic variation for natural or artificial selection. Strong theoretical arguments in favour of the importance of epigenetic mechanisms have been discussed (Cubas et al., 1999; Hollick et al., 1997; Jablonka, 2002; Jacobsen and Meyerowitz, 1997; Jacobsen et al., 2000; Kermicle et al., 1995; Martienssen et al., 1990; Martienssen and Baron, 1994; McClintock, 1951; Pigliucci and Murren, 2003; Soppe et al., 2000; Stokes et al., 2002).

In recent years, the heat shock response has been suggested to play a role in phenotypic evolution, whereby chaperones acting as “capacitors” of morphological change, provide a molecular basis for Waddington’s genetic assimilation. (Queitsch et al., 2000; Rutherford and Lindquist, 1998). The malfunctioning of molecular chaperones may result in uncovering genetic variation however, the molecular basis of this phenomenon remains largely unknown (Bobula et al., 2006; Sangster et al., 2004). In 1998, Rutherford et al., provided first evidence for an explicit molecular mechanism, involving the

molecular chaperone HSP90, that assists the process of evolutionary change in response to the environment (Queitsch et al., 2002; Rutherford et al., 2007a; Rutherford et al., 2007b; Rutherford, 2007; Rutherford and Lindquist, 1998; Salathia and Queitsch, 2007). Fully functional HSP90 stabilises wild type phenotypes by suppressing underlying genetic and epigenetic variation (Salathia and Queitsch, 2007; Samakovli et al., 2007). Further discoveries identified a similar role for other chaperones such as HSP70 (which works in conjunction with HSP90) and HSP60 in other organisms (Fares et al., 2002). Additionally, overexpression of the chaperonin GroEL has been shown to buffer the fitness effects of deleterious polymorphisms in *E.coli* (Fares et al., 2002) and GroE overexpression suppresses many mutations (Fayet et al., 1986; Jenkins et al., 1986). In recent years the idea has emerged that not only chaperones but a large number of other proteins may also regulate the diversity of the phenotype (Bergman and Siegal, 2003; Csermely, 2004; Csermely and Soti, 2006).

Molecular chaperones can mask the negative effects of mutations but the mechanism of such buffering need not be direct. A plausible role of chaperones is to stabilise genetic networks, thus making them more tolerant to malfunctioning of their constituents. (Hartman et al., 2001; Hermisson and Wagner, 2004; Kirschner and Gerhart, 1998; Siegal and Bergman, 2002; Wagner, 2005). Thus, the ability to resist genetic perturbations results from the ability to cope with environmental challenges (Rutherford and Lindquist, 1998).

The mechanism of phenotypic heterogeneity remains unresolved. Phenotypic expression of the C-terminal α B-crystallin mutations (450delA, Q151X and 464delT) may be a function of combined factors including effect upon cellular functions and the destabilisation of genetic networks, the effect of the mutation upon tissue specific associations and finally the propensity to self-aggregate. Further analysis of the mechanism is required to gain understanding of the phenotypic variation.

6.4. FUTURE WORK

Several questions remain unresolved and could be answered by further analyses.

6.4.1. Phenotypic Heterogeneity

The mechanism of phenotypic variation remains unresolved for C-terminal mutations of α B-crystallin. Investigation of this mechanism would involve analysis of the relative associations of α A-, α B-crystallin and HSP27 between the C-terminal mutant α B-crystallins upon the stability and refolding efficiency of the formed complexes. Further characterisation of the complexes would initially analyse relative chaperone function, thermostability, secondary structure and quaternary structure.

Analysis of these associations in a mammalian cell environment would provide an indication of the relative effects the C-terminal α B-crystallin mutants have upon solubility and cellular localisation. These experiments may provide a correlation between altered associations, the type of stabilising chaperone present, the mutation and expressed phenotype.

Protein aggregates containing α B-crystallin and desmin are typical features of patients with MM. In Chapter 4, I investigated the effect of the C-terminal mutants upon desmin filament assembly *in vitro*, but did not investigate this effect further in a mammalian cell environment. Transient co-transfection of the α B-crystallin mutants and desmin into MCF7 cells, where there is no endogenous α B-crystallin, may show variations in the formation of desmin filaments, which may show a correlation with the disease phenotype. Further more, transient transfection of desmin, α A- and α B-crystallin using a cell line where 450delA α B-crystallin is endogenous may also help towards explaining the phenotypic heterogeneity by analysing the relative effects upon desmin stability.

6.4.2. Additional congenital α B-crystallin mutant characterisation

The naturally occurring mutations of α B-crystallin not analysed in this thesis include the P20S (Liu et al., 2006a), R157H (Inagaki et al., 2006) and D140N (Liu et al., 2006b) point mutations, which cause congenital isolated cataract, dilated cardiomyopathy (DCM) and isolated lamellar cataract respectively. All three mutations affect individual chaperone sites (see Figure 4.1A), with the R157H mutation occurring in the C-terminal extension, the D140N mutation affecting the α -crystallin domain and the P20S in the N-terminal. Subsequent characterisation of these mutants would provide further insight towards the relationship between the structure and function of α B-crystallin and the relationship with disease and phenotypic heterogeneity. These mutants also provide three further subjects in investigating the relative associations between mutant α B-crystallins and stabilising α A-, α B-crystallin and HSP27 proteins.

6.4.3. Refolding efficiency

One of the limitations of characterisation, observed especially for the Q151X α B-crystallin, is the concentration of mutant protein achieved during the refolding. Thus, further optimisation of the refolding process would be necessary to improve the current yields, which range from 1.4% (Q151X α B-crystallin) to 12.0% (E164X α B-crystallin) (see Table 3.11). Refolding of the 450delA and 464delCT α B-crystallin as homogenous protein solutions would provide data directly comparable to the wild type α B-crystallin and the other α B-crystallin mutants, which are refolded without the presence of the stabilising wild type α B-crystallin. Current refolding protocol utilises a dilution method, which reduces both the urea and protein concentration prior to dialysis at 16°C (see Section 2.7.3). Further investigation of these parameters may help optimise the refolding yield.

6.4.4. The effect of α B-crystallin concentration upon oligomerisation and polydispersity

In Chapter 5, the increased polydispersity of wild type α B-crystallin at concentrations below 0.1 mg/ml and the appearance of additional oligomeric complexes of varying size were observed during SEC at ambient temperature. The separation by SEC performed at 4°C may increase polydispersity, although samples stored intermittently at 4°C prior to SEC at ambient temperature showed no additional polydispersity, compared to samples stored at ambient temperature. Relative chaperone activities of the various oligomeric complexes, resulting from increasing polydispersity, may provide an insight into the relationship between efficient chaperone function and complex size. Data of this nature would provide evidence for proving or disproving the theories of chaperone activity discussed in Chapter 5. This investigation may also extend to the incorporation of other factors, which have been shown to affect the oligomerisation characteristics of α B-crystallin such as low pH, phosphorylation and oxidative stress (see Section 5.2.2.)

6.4.5. Characterisation of the potential unit of chaperone activity

Elucidation of the Mwt of the unknown α B-crystallin species, isolated from the tail region of an α B-crystallin SEC separation, would help determine its potential as an active unit of chaperone activity. Preferably Mass Spectrometry would be utilised to determine the nature of the unknown α B-crystallin species, however, the type of characterisation method to be utilised is limited due to the very low protein concentration of the species recovered from the SEC. It may be that immunoblotting of a native SDS-PAGE, analysing the tail region of the SEC separation, could provide evidence of the monomeric species considering a native SDS-PAGE successfully illustrated the Q151X α B-crystallin mutant, which is predicted to be monomeric (see Figure 4.4). In Section 5.4.2, I discussed how further scale up would increase the protein concentration, but disproportionately, therefore characterisation at the current low protein concentration would be preferred. Such characterisation using the technique of analytical ultracentrifugation has been utilised at concentrations as low as 0.06 mg/ml, therefore may be successful in providing the Mwt data required. Further scale up would be an option if

analytical centrifugation proved unsuccessful. Confirmation of the size of the unknown α B-crystallin species would prompt similar analyses of the C-terminal α B-crystallin mutants in order to assess the presence of a similar species.

APPENDIX 1

ASSEMBLY AND BLAST ANALYSIS OF MUTANT α B-CRYSTALLIN BACTERIAL AND MAMMALIAN EXPRESSION CONSTRUCTS FOR CHAPTER 3

A1.1 THE PROMOTER AND MULTIPLE CLONING SEQUENCES OF VECTORS USED FOR MUTAGENESIS AND CLONING

Figure A1.1. The promoter and multiple cloning sequences of pGEM®-T Easy

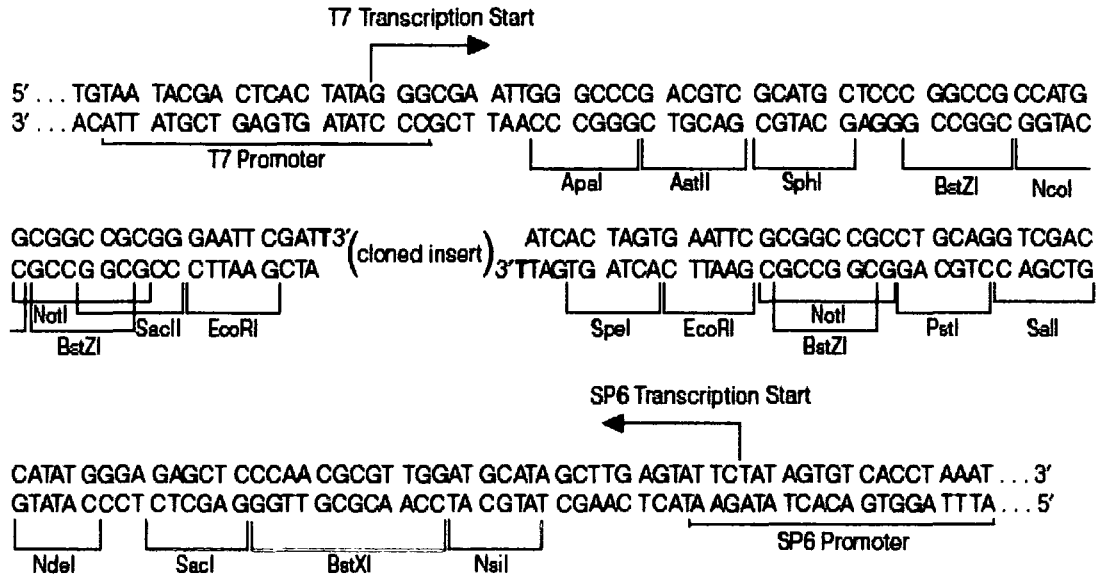


Figure A1.1. The promoter and multiple cloning sequence of the pGEM®-T and pGEM®-T Easy Vectors. The top strand of the sequence shown corresponds to the RNA synthesized by T7 RNA polymerase. The bottom strand corresponds to the RNA synthesized by SP6 RNA polymerase (Taken from Promega Technical Manual TM042, Promega, Southampton, UK).

Figure A1.2. The promoter and multiple cloning sequences of pET23d(+)

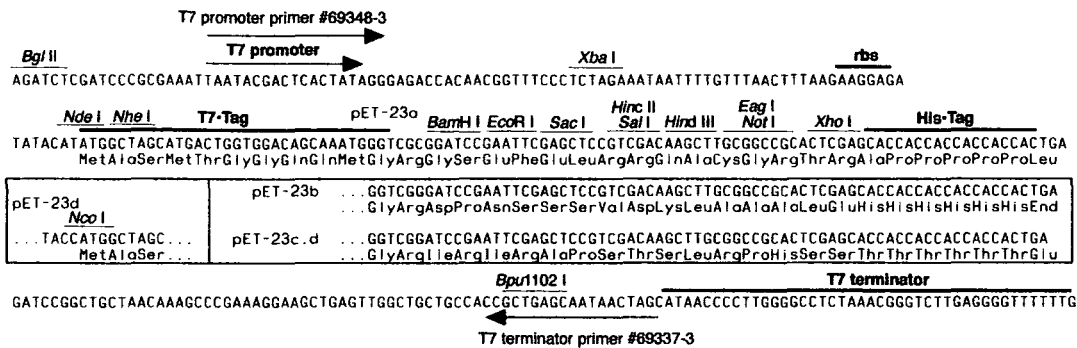


Figure A1.2. The maps for pET23b(+), pET23c(+), and pET23d(+) are the same as pET23a(+) (shown) with the following exceptions: pET23b(+) is a 3665bp plasmid; subtract 1bp from each site beyond *Bam*HI at 198. pET23c(+) is a 3664bp plasmid; subtract 2bp from each site beyond *Bam*HI at 198. pET23d(+) is a 3663bp plasmid; the *Bam*HI site is in the same reading frame as in pET23c(+). An *Nco*I site is substituted for the *Nde*I site with a net 1bp deletion at position 238 of pET23c(+). As a result, *Nco*I cuts pET23d(+) at 234, and *Nhe*I cuts at 228. For the rest of the sites, subtract 3bp from each site beyond position 239 in pET23a(+). *Nde*I does not cut pET-23d(+). Note also that *Sty*I is not unique in pET23d(+). (Taken from Novagen Technical Bulletin TB051, Novagen, WI, USA).

Figure A1.3. The promoter and multiple cloning sequences of pcDNA3.1(-)

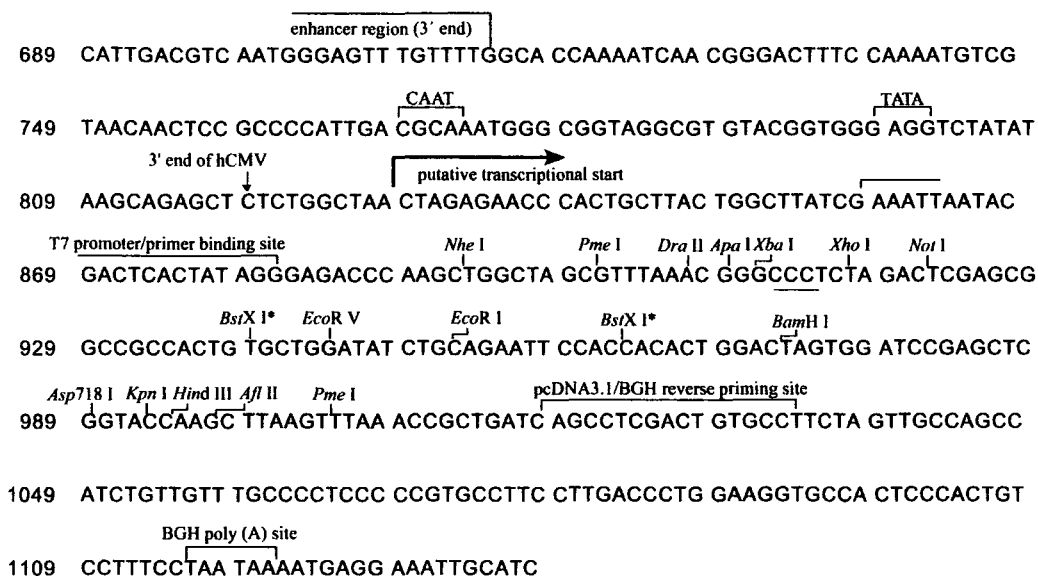


Figure A1.3. The multiple cloning site for pcDNA3.1(-). Restriction sites are labelled to indicate cleavage site. The *Xba*I site contains an internal stop codon (TGTAGA). The multiple cloning site has been confirmed by sequencing and functional testing by Invitrogen. (Taken from Invitrogen Technical manual 081401, Invitrogen, Paisley, UK).

A1.2 ASSEMBLY OF Q151X α B-CRYSTALLIN CONSTRUCT BY SDM

Initial SDM optimisation followed the manufacturers guidelines utilizing the proof reading capabilities of pfu Turbo polymerase. This enzyme failed to generate a PCR product of the correct size. Further SDM PCR reactions utilised Taq polymerase with primer combinations including T7 promoter/Q151X reverse primer (reaction 1) and Q151X forward primer/ T7 terminator (reaction 2). Both combinations produced the pET23d(+) vector of required size 4159 bp (see Figure A1.4A). *DpnI* digested DNA from the Q151X forward primer/ T7 terminator reaction was proliferated to allow confirmation of the Q151X mutant insert by screening using *NcoI/StuI* digestion. From 8 colonies selected of transformants, two constructs showed *NcoI/StuI* digest fragments representing the Q151X insert (see Figure A1.4B, lane 10 and 12; construct 1 and 2 respectively). Subsequent sequencing and BLAST analysis of the two constructs confirmed the presence of the mutant Q151X insert, however, construct 1 had two random base changes at 413c-t and 430c-t (see Figure A1.5). Clone 2 BLAST data (see Figure A1.6) showed a cytosine insertion at 470, however this insertion was downstream to the stop codon introduced at codon 151, therefore the plasmid DNA was a suitable candidate for use in protein expression.

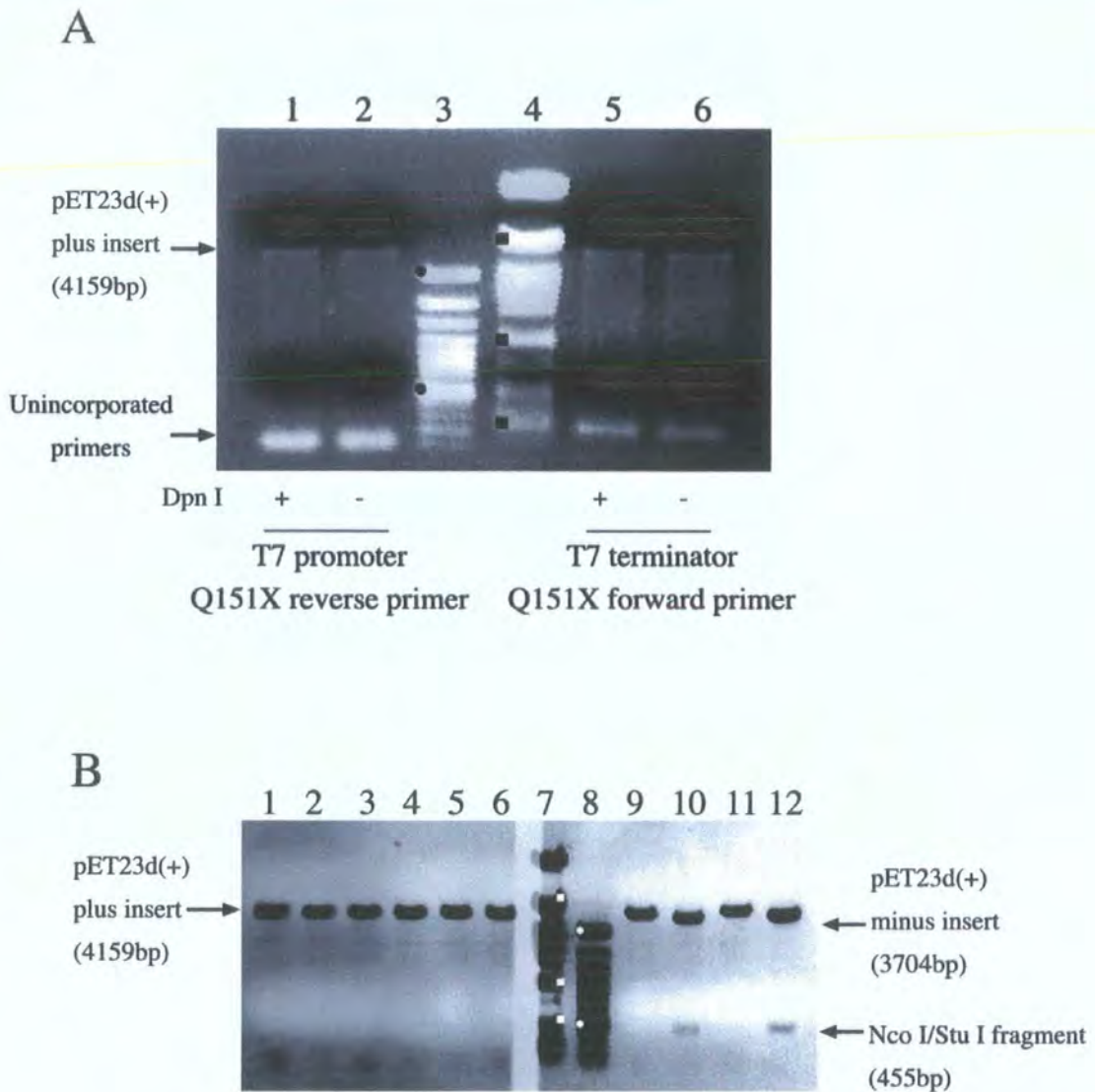


Figure A1.4. SDM PCR for insertion of mutant α B-crystallin into pET23d(+) bacterial expression vector. (A) confirms the correctly sized pET23d(+) vector (approx 4159 bp) produced using Taq polymerase and T7 promoter/ Q151X reverse primer (lanes 1 and 2) and vice versa (lanes 5 and 6). Unincorporated primers bands are more intense in lanes 1 and 2, suggesting the mutagenesis may be more successful in lanes 5 and 6. This DNA was proliferated. DNA ladders λ *Pst*I (lane 4, black box- 339, 805, 4749bp) and 100bp GeneRuler (lane 3, black circle- 500 and 3000bp). (B) Successful incorporation of the mutant Q151X insert is confirmed by the presence of NcoI/ StuI fragments (455bp) (lane 10 and 11) in DNA purified from the respective transformants, with sequencing and BLAST analysis confirming the clone in lane 12 to be suitable for protein expression despite an insertion downstream to the mutated stop codon. DNA ladders λ *Pst*I (lane 7, white box- 514, 805, 5077bp) and 100bp GeneRuler (lane 8, white circle- 500 and 3000bp).

Figure A1.5. BLAST data for Q151X insert in pET23d(+) Construct 1

Stu I in BOLD (AGGCCT)

Pink - random substitution

Green - insertion/ deletion

Red - Wild Type Methionine and wt stop codon

Blue-SDM mutation

Underlined -primer sequence

```

-24 GACCCCTCAC ACTCACCTAG CCACCATGA CATCGCCATC CACCACCCCT GGATCCGCCG
 36 CCCCTTCTTT CTTTCCACT CCCCAGCCG CCTCTTTGAC CAGTTCTTCG GAGAGCACCT
 96 GTTGGAGTCT GATCTTTTCC CGACGTCTAC TTCCCTGAGT CCCTTCTACC TTCGGCCACC
156 CTCCTTCCTG CGGGCACCCA GCTGGTTTGA CACTGGACTC TCAGAGATGC GCCTGGAGAA
216 GGACAGGTTT TCTGTCAACC TGGATGTGAA GCACTTCTCC CCAGAGGAAC TCAAAGTTAA
276 GGTGTTGGGA GATGTGATTG AGGTGCATGG AAAACATGAA GAGCGCCAGG ATGAACATGG
336 TTTTCATCTCC AGGGAGTTCC ACAGGAAATA CCGGATCCCA GCTGATGTAG ACCCTCTCAC
396 CATTACTTCA TCCCTGTTAT CTGATGGGGT CCTCATGTG AATGGACCAA GGAAATAGGC
456 CTCTGGCCCT GAGCGCACCA TTCCCATCAC CCGTGAAGAG AAGCCTGCTG TCACCGCAGC
516 CCCCAAGAAA TAGATGCCCT TTCTTGAATT GCATTTTTTA AAACAAGAAA GTTCCCCAC
576 CAGTGAATGA AAGTCTTGTG ACTAGTGCTG AAGCTTATTA ATGCTAAGGG CAGGCCCAA
636 TTATCAAGCT AATAAAATAT CATTCAGCAA C

```

Figure A1.6. BLAST data for Q151X insert in pET23d(+) Construct 2

Homo sapiens crystallin, alpha B (CRYAB), mRNA

Length = 691

Score = 1025 bits (517), Expect = 0.0

Identities = 530/533 (99%), Gaps = 1/533 (0%)

Strand = Plus / Minus

```

QUERY: 116 TCTATTTCTTGGGGGCTGCGGTGACAGCAGGCTTCTCTTCACGGGTGATGGGAATGGTGC 175
      |||
SBJCT: 554 TCTATTTCTTGGGGGCTGCGGTGACAGCAGGCTTCTCTTCACGGGTGATGGGAATGGTGC 495

QUERY: 176 CGCTCAGGGCCAGAGGCCTATTTCTTGGTCCATTACAGTGAGGACCCCATCAGATGAC 235
      |||
SBJCT: 494 -GCTCAGGGCCAGAGACCTGTTTCTTGGTCCATTACAGTGAGGACCCCATCAGATGAC 436

QUERY: 236 AGGGATGAAGTAATGGTGAGAGGGTCTACATCAGCTGGGATCCGGTATTTCTGTGGAAC 295
      |||
SBJCT: 435 AGGGATGAAGTAATGGTGAGAGGGTCTACATCAGCTGGGATCCGGTATTTCTGTGGAAC 376

QUERY: 296 TCCCTGGAGATGAAACCATGTTTCATCCTGGCGCTCTTCATGTTTTCCATGCACCTCAATC 355
      |||
SBJCT: 375 TCCCTGGAGATGAAACCATGTTTCATCCTGGCGCTCTTCATGTTTTCCATGCACCTCAATC 316

QUERY: 356 ACATCTCCCAACACCTTAACTTTGAGTTCTCTGGGAGAAAGTGCTTCACATCCAGGTTG 415
      |||
SBJCT: 315 ACATCTCCCAACACCTTAACTTTGAGTTCTCTGGGAGAAAGTGCTTCACATCCAGGTTG 256

QUERY: 416 ACAGAGAACCTGTCTTCTCCAGGCGCATCTCTGAGAGTCCAGTGTCAAACCAGCTGGGT 475
      |||
SBJCT: 255 ACAGAGAACCTGTCTTCTCCAGGCGCATCTCTGAGAGTCCAGTGTCAAACCAGCTGGGT 196

QUERY: 476 GCCCGCAGGAAGGAGGGTGGCCGAAGGTAGAAGGGACTCAGGGAAGTAGACGTCGGGAAA 535
      |||
SBJCT: 195 GCCCGCAGGAAGGAGGGTGGCCGAAGGTAGAAGGGACTCAGGGAAGTAGACGTCGGGAAA 136

QUERY: 536 AGATCAGACTCCAACAGGTGCTCTCCGAAGAAGTGGTCAAAGAGGCGGCTGGGGGAGTGG 595
      |||
SBJCT: 135 AGATCAGACTCCAACAGGTGCTCTCCGAAGAAGTGGTCAAAGAGGCGGCTGGGGGAGTGG 76

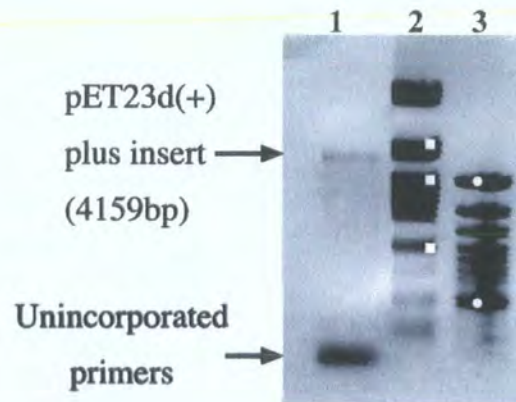
QUERY: 596 AAAGGAAAGAAGGGGCGGCGGATCCAGGGGTGGTGGATGGCGATGTCCATGGT 648
      |||
SBJCT: 75 AAAGGAAAGAAGGGGCGGCGGATCCAGGGGTGGTGGATGGCGATGTCCATGGT 23

```

A1.3 ASSEMBLY OF E165X α B-CRYSTALLIN BY SDM

The optimisation of the SDM process for the Q151X mutant has shown that the Taq polymerase enzyme is successful in generating the mutated PCR product. Initial SDM reverted back to the manufacturers guidelines by utilising forward and reverse complementary primers to incorporate the E165X mutation. The PCR resulted in a correctly sized pET23d(+) band of 4159bp (see Figure A1.7.A, lane 1), therefore this PCR product was *DpnI* digested and proliferated in DH5 α cells. Purified DNA was screened using an *NcoI/HindIII* digest to assess the presence of the mutant insert of expected size 497bp. The pET23d(+) vector contains a *HindIII* site downstream to the insert, therefore unsuccessful constructs still containing the wild type α B-crystallin insert will also produce a digest fragment of an expected size of 559bp as clarified in Figure A1.7.B. The digestion identified 5 constructs, which potentially could be viable for protein expression. The constructs were sequenced and compared for fidelity to the GenBank data base entry (accession no. NM001885), using BLAST software. This revealed that construct 2 and 10 (see Figure A1.7.B, lane 2 and lane 12 respectively) although containing a polymorphism point mutation at C474T, the codon remained threonine, therefore was viable for protein expression (see Figure A1.8 and A8.9 respectively).

A



B

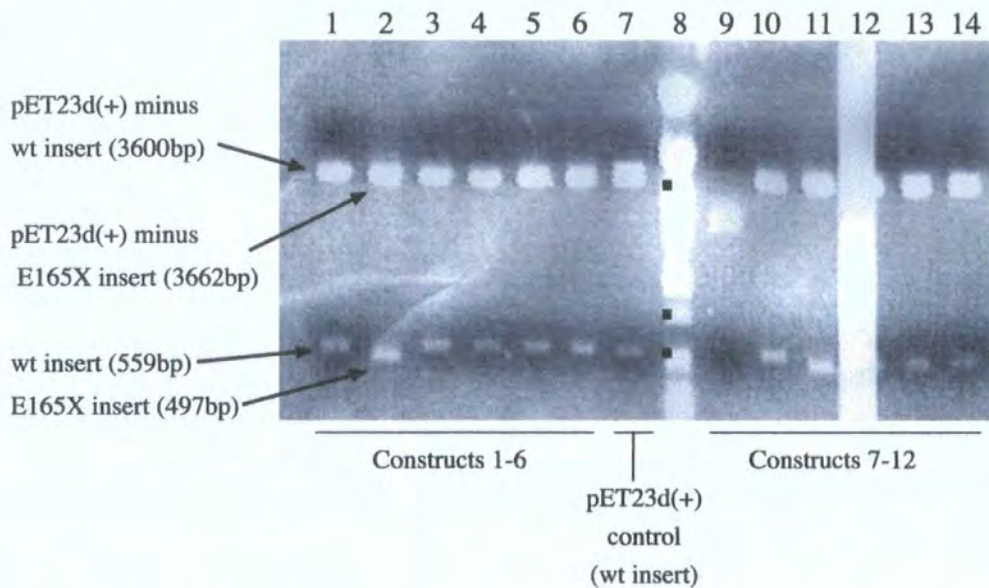


Figure A1.7. PCR mutagenesis of E165X mutant construct assembly. PCR conditions successful in producing a correctly sized pET23d(+) vector (approx 4159bp lane 1). DNA ladders λ *Pst*I (lane 2, white box- 805, 2838, 5077bp) and 100bp GeneRuler (lane 3, white circle- 500 and 3000bp). (B) Restriction enzyme digestion (*Nco*I/*Hind*III) of potentially viable E165X constructs. Screening identified the constructs, which contained the E165X α B-crystallin insert (lanes 2 and 11-14) by a 497bp fragment leaving a pET23d(+) vector of 3662bp. Constructs where SDM failed to incorporate the E165X mutation contain a pET23d(+) vector of 3600bp, and a digest fragment of 559bp (lanes 1, 3-6 and 9-10). Construct 7 appears incomplete. DNA ladders λ *Pst*I (lane 8, black box- 514, 805, 2838bp). The overexposure through lane 12 was a function of the Biorad Gel Doc 2000.

Figure A1.8. BLAST data for E165X insert in pET23d(+) Construct 2

Hind III in BOLD (AAGCTT)

Pink - random substitution

Green - insertion/ deletion

Red - Wild Type Methionine and wt stop codon

Blue-SDM mutation

Underlined -primer sequence

*= polymorphism

Homo sapiens crystallin, alpha B (CRYAB), mRNA

Length = 691

Score = 1025 bits (517), Expect = 0.0

Identities = 528/532 (99%)

Strand = Plus / Plus

```

Query: 57  ACCATGGACATCGCCATCCACCACCCCTGGATCCGCCGCCCTTCTTTCTTTTCCACTCC 116
          |||
SBJCT: 23  ACCATGGACATCGCCATCCACCACCCCTGGATCCGCCGCCCTTCTTTCTTTTCCACTCC 82

QUERY: 117  CCCAGCCGCCTCTTTGACCAGTTCTTCGGAGAGCACCTGTTGGAGTCTGATCTTTTCCCG 176
          |||
SBJCT: 83  CCCAGCCGCCTCTTTGACCAGTTCTTCGGAGAGCACCTGTTGGAGTCTGATCTTTTCCCG 142

QUERY: 177  ACGTCTACTTCCCTGAGTCCCTTCTACCTTCGGCCACCTCCTTCCTGCGGGCACCCAGC 236
          |||
SBJCT: 143  ACGTCTACTTCCCTGAGTCCCTTCTACCTTCGGCCACCTCCTTCCTGCGGGCACCCAGC 202

QUERY: 237  TGGTTTGACACTGGACTCTCAGAGATGCGCCTGGAGAAGGACAGGTTCTCTGTCAACCTG 296
          |||
SBJCT: 203  TGGTTTGACACTGGACTCTCAGAGATGCGCCTGGAGAAGGACAGGTTCTCTGTCAACCTG 262

QUERY: 297  GATGTGAAGCACTTCTCCCCAGAGGAACCAAAGTTAAGGTGTTGGGAGATGTGATTGAG 356
          |||
SBJCT: 263  GATGTGAAGCACTTCTCCCCAGAGGAACCAAAGTTAAGGTGTTGGGAGATGTGATTGAG 322

QUERY: 357  GTGCATGGAAAACATGAAGAGCGCCAGGATGAACATGGTTTCATCTCCAGGGAGTTCCAC 416
          |||
SBJCT: 323  GTGCATGGAAAACATGAAGAGCGCCAGGATGAACATGGTTTCATCTCCAGGGAGTTCCAC 382

QUERY: 417  AGGAAATACCGGATCCAGCTGATGTAGACCCTCTCACCATTACTTCATCCCTGTCATCT 476
          |||
SBJCT: 383  AGGAAATACCGGATCCAGCTGATGTAGACCCTCTCACCATTACTTCATCCCTGTCATCT 442

QUERY: 477  GATGGGGTCCTCACTGTGAATGGACCAAGGAAACAGGTCTCTGGCCCTGAGCGCACT*ATT 536
          |||
SBJCT: 443  GATGGGGTCCTCACTGTGAATGGACCAAGGAAACAGGTCTCTGGCCCTGAGCGCACC*ATT 502

QUERY: 537  CCCATCACCCGTGAATAGAGCTTGCTGTCACCNCAGCCCCAAGAAATAGA 588
          |||
SBJCT: 503  CCCATCACCCGTGAAGAGAGCCTGCTGTCACCGCAGCCCCAAGAAATAGA 554

```

Figure A1.9. BLAST data for E165X insert in pET23d(+) Construct 10

Homo sapiens crystallin, alpha B (CRYAB), mRNA

Length = 691

Score = 1031 bits (520), Expect = 0.0

Identities = 529/532 (99%)

Strand = Plus / Plus

```

QUERY: 56  ACCATGACATCGCCATCCACCACCCCTGGATCCGCCGCCCTTCTTTCCTTTCCACTCC 115
          |||
SBJCT: 23  ACCATGACATCGCCATCCACCACCCCTGGATCCGCCGCCCTTCTTTCCTTTCCACTCC 82

QUERY: 116 CCCAGCCGCCTCTTTGACCAGTTCTTCGGAGAGCACCTGTTGGAGTCTGATCTTTTCCCG 175
          |||
SBJCT: 83  CCCAGCCGCCTCTTTGACCAGTTCTTCGGAGAGCACCTGTTGGAGTCTGATCTTTTCCCG 142

QUERY: 176 ACGTCTACTTCCCTGAGTCCCTTCTACCTTCGGCCACCCTCCTTCTGCGGGCACCCAGC 235
          |||
SBJCT: 143 ACGTCTACTTCCCTGAGTCCCTTCTACCTTCGGCCACCCTCCTTCTGCGGGCACCCAGC 202

QUERY: 236 TGGTTTGACACTGGACTCTCAGAGATGCGCCTGGAGAAGGACAGGTTCTCTGTCAACCTG 295
          |||
SBJCT: 203 TGGTTTGACACTGGACTCTCAGAGATGCGCCTGGAGAAGGACAGGTTCTCTGTCAACCTG 262

QUERY: 296 GATGTGAAGCACTTCTCCCAGAGGAAC TCAAAGTTAAGGTGTTGGGAGATGTGATTGAG 355
          |||
SBJCT: 263 GATGTGAAGCACTTCTCCCAGAGGAAC TCAAAGTTAAGGTGTTGGGAGATGTGATTGAG 322

QUERY: 356 GTGCATGGAAAACATGAAGAGCGCCAGGATGAACATGGTTTCATCTCCAGGGAGTCCAC 415
          |||
SBJCT: 323 GTGCATGGAAAACATGAAGAGCGCCAGGATGAACATGGTTTCATCTCCAGGGAGTCCAC 382

QUERY: 416 AGGAAATACCGGATCCCAGCTGATGTAGACCCTCTCACCATTACTTCATCCCTGTCATCT 475
          |||
SBJCT: 383 AGGAAATACCGGATCCCAGCTGATGTAGACCCTCTCACCATTACTTCATCCCTGTCATCT 442

QUERY: 476 GATGGGGTCCTCACTGTGAATGGACCAAGGAAACAGGTCTCTGGCCCTGAGCGCACT* ATT 535
          |||
SBJCT: 443 GATGGGGTCCTCACTGTGAATGGACCAAGGAAACAGGTCTCTGGCCCTGAGCGCACT* ATT 502

QUERY: 536 CCCATCACCCGTGAATAGAAAGCTTGCTGTCACCGCAGCCCCCAAGAAA TAGA 587
          |||
SBJCT: 503 CCCATCACCCGTGAAGAGAAGCTTGCTGTCACCGCAGCCCCCAAGAAA TAGA 554

```

A1.4 ASSEMBLY OF 464DELCT α B-CRYSTALLIN

PCR mutagenesis experiments involved the production of the 464delCT α B-crystallin mutant insert with 3'A overhangs for subsequent ligation into the pGEM®-T Easy vector (see Figure A1.10.A). The 464delCT mutant does not contain a suitable unique restriction site, hence an *EcoRI* site in the pGEM®-T Easy vector downstream from the ligation site was utilised (see Figure A1.1). DNA from selected transformants was purified and the presence of the mutation assessed using an *NcoI/EcoRI* digest to screen for fragments of expected size 498bp (see Figure A1.10.B). Screening suggested that 11 out of the 12 clones contained the 464delCT mutant insert. Subsequent sequencing and BLAST analysis identified constructs 8, 10 and 11 (shown in lanes 9, 10 and 12 respectively) contained the 464delCT mutant insert with no additional mutations incurred when compared to the GenBank data base entry (accession no. NM001885) for human α B-crystallin

Construct 8 (see Figure A1.11) was subcloned into pET23d(+) using an *NcoI/EcoRI* digest. The multiple cloning region of pET23d(+) is shown in Figure A1.2. The presence of the mutation was assessed using the *NcoI/EcoRI* digest on purified constructs to screen for fragments of expected 464delCT insert size of 498bp (see Figure A1.10.C). Of 11, constructs 1, 2, 3 and 5 indicated the presence of a low intensity fragment at 498bp (lanes 1, 2, 3 and 5 respectively, see arrowhead). Subsequent sequencing and BLAST analysis of the 4 constructs confirmed the 464delCT insert had successfully been subcloned into the pET23d(+) vector in construct 2 with no unwanted sequence changes, when compared to the GenBank data base entry (accession no. NM001885) for human α B-crystallin. Construct 2 was viable for protein expression. (see Figure A1.12).

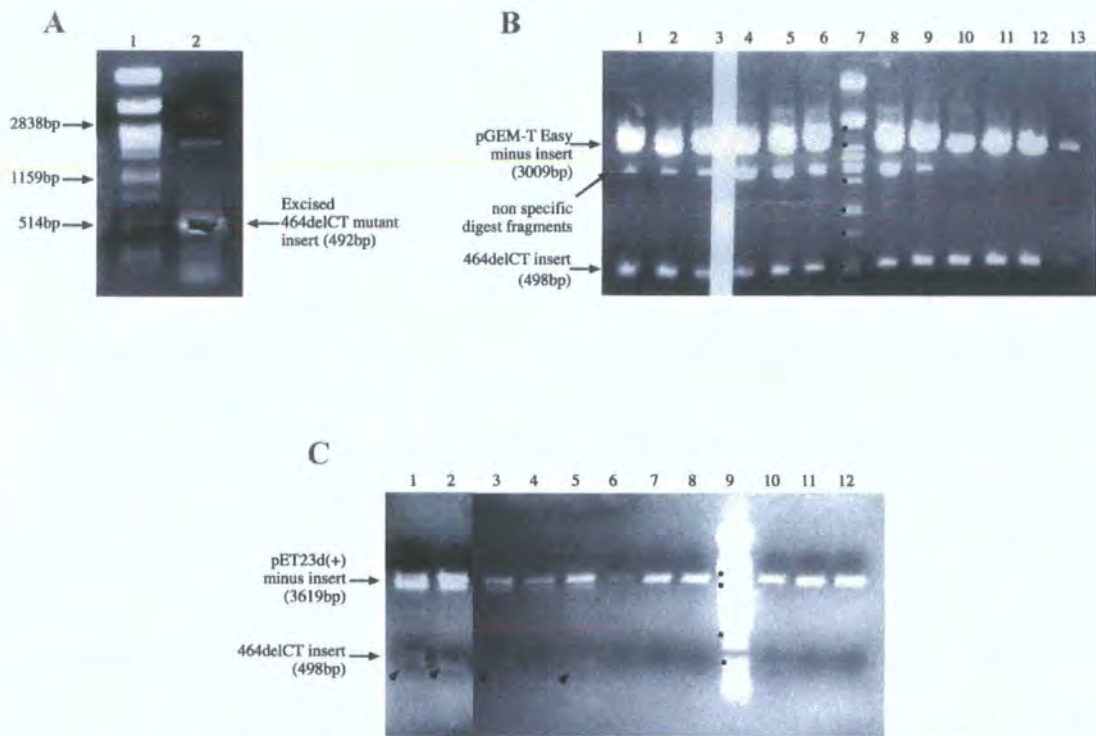


Figure A1.10. Assembly of 464delCT α B-crystallin construct using pGEM®-T Easy vector system. PCR mutagenesis produced a PCR product of 492bp (A) that was purified and ligated into using pGEM®-T Easy vector. The efficiency of the ligation was assessed using an *NcoI/EcoRI* digest screen (B), which suggested 11 out of 12 selected constructs contained the 464delCT insert. Sequencing confirmed constructs shown in lanes 9, 10 and 12 contained the 464delCT mutant insert. . DNA ladder λ *PstI* (Figure A1.10.B, lane 7, black circle- 514, 805, 1159, 1700, 2838 and 4507bp) The overexposure through lane 3 was a function of the Biorad Gel Doc 2000. The 464delCT insert (Figure 3.5 B, lane 9) was subcloned into the pET23d(+) vector. Purified DNA was screened (C) using *NcoI/EcoRI* digestion and suggested the 464delCT insert was present in constructs shown in lanes 1, 2, 3 and 5 at 498bp (see arrowhead). Sequencing confirmed the construct in lane 2 contained the 464delCT insert with no additional mutations, therefore was viable for protein expression. DNA ladder λ *PstI* (Figure A1.10.C lane 9, black circle- 514, 1159, 2838 and 4507bp).

Figure A1.11. BLAST data for 464delCT insert in pGEM-T Easy-Construct 8

Pink - random substitution

Green - insertion/ deletion

Red - Wild Type Methionine and wt stop codon

Blue-SDM mutation

Underlined -primer sequence

*= polymorphism

Homo sapiens crystallin, alpha B (CRYAB), mRNA

Length=691Length=691

Score = 959 bits (484), Expect = 0.0

Identities = 493/495 (99%), Gaps = 2/495 (0%)

Strand=Plus/Plus

```

Query  52  ACCATGGACATCGCCATCCACCACCCCTGGATCCGCCGCCCTTCTTTCCTTTCCACTCC  111
          |||
Sbjct  23  ACCATGGACATCGCCATCCACCACCCCTGGATCCGCCGCCCTTCTTTCCTTTCCACTCC  82

Query  112 CCCAGCCGCCTCTTTGACCAGTTCTTCGGAGAGCACCTGTTGGAGTCTGATCTTTTCCCG  171
          |||
Sbjct  83  CCCAGCCGCCTCTTTGACCAGTTCTTCGGAGAGCACCTGTTGGAGTCTGATCTTTTCCCG  142

Query  172  ACGTCTACTTCCCTGAGTCCCTTCTACCTTCGGCCACCTCCTTCCTGCGGGCACCCAGC  231
          |||
Sbjct  143  ACGTCTACTTCCCTGAGTCCCTTCTACCTTCGGCCACCTCCTTCCTGCGGGCACCCAGC  202

Query  232  TGGTTTGACACTGGACTCTCAGAGATGCGCCTGGAGAAGGACAGGTTCTCTGTCAACCTG  291
          |||
Sbjct  203  TGGTTTGACACTGGACTCTCAGAGATGCGCCTGGAGAAGGACAGGTTCTCTGTCAACCTG  262

Query  292  GATGTGAAGCACTTCTCCCCAGAGGAACTCAAAGTTAAGGTGTTGGGAGATGTGATTGAG  351
          |||
Sbjct  263  GATGTGAAGCACTTCTCCCCAGAGGAACTCAAAGTTAAGGTGTTGGGAGATGTGATTGAG  322

Query  352  GTGCATGGAAAACATGAAGAGCGCCAGGATGAACATGGTTTCATCTCCAGGGAGTTCCAC  411
          |||
Sbjct  323  GTGCATGGAAAACATGAAGAGCGCCAGGATGAACATGGTTTCATCTCCAGGGAGTTCCAC  382

Query  412  AGGAAATACCGGATCCCAGCTGATGTAGACCCTCTCACCATTACTTCATCCCTGTCATCT  471
          |||
Sbjct  383  AGGAAATACCGGATCCCAGCTGATGTAGACCCTCTCACCATTACTTCATCCCTGTCATCT  442

Query  472  GATGGGGTCCTCACTGTGAATGGACCAAGGAAACAGGTCTCTGGCC--GAGCGCACCATT  529
          |||
Sbjct  443  GATGGGGTCCTCACTGTGAATGGACCAAGGAAACAGGTCTCTGGCCBTGAGCGCACCATT  502

Query  530  CCCATCACCCGTGAA  544
          |||
Sbjct  503  CCCATCACCCGTGAA  517

```


Figure A1.12. BLAST data for 464delCT insert in pET23d(+)-Construct 2

Homo sapiens crystallin, alpha B (CRYAB), mRNA
 Length=691
 Score = 954 bits (481), Expect = 0.0
 Identities = 492/495 (99%), Gaps = 2/495 (0%)
 Strand=Plus/Minus

```

Query 115  TTCACGGGTGATGGGAATGGTGCCTC--GGCCAGAGACCTGTTTCCTTGGTCCATTAC 172
          |||
Sbjct 517  TTCACGGGTGATGGGAATGGTGCCTCAGGGCCAGAGACCTGTTTCCTTGGTCCATTAC 458

Query 173  AGTGAGGACCCCATCAGATGACAGGGATGAAGTAATGGTGAGAGGGTCTACATCAGCTGG 232
          |||
Sbjct 457  AGTGAGGACCCCATCAGATGACAGGGATGAAGTAATGGTGAGAGGGTCTACATCAGCTGG 398

Query 233  GATCCGGTATTTCCTGTGGAACCTCCCTGGAGATGAAACCATGTTTCATCTGGCGCTCTTC 292
          |||
Sbjct 397  GATCCGGTATTTCCTGTGGAACCTCCCTGGAGATGAAACCATGTTTCATCTGGCGCTCTTC 338

Query 293  ATGTTTTCCATGCACCTCAATCACATCTCCCAACACCTTAACCTTGAGTTCCTCTGGGGA 352
          |||
Sbjct 337  ATGTTTTCCATGCACCTCAATCACATCTCCCAACACCTTAACCTTGAGTTCCTCTGGGGA 278

Query 353  GAAGTGCTTCACATCCAGGTTGACAGAGAACCTGTCCTTCTCCAGGCGCATCTCTGAGAG 412
          |||
Sbjct 277  GAAGTGCTTCACATCCAGGTTGACAGAGAACCTGTCCTTCTCCAGGCGCATCTCTGAGAG 218

Query 413  TCCAGTGTCAAACCAGCTGGGTGCCCGCAGGAAGGAGGGTGGCCGAAGGTAGAAGGGACT 472
          |||
Sbjct 217  TCCAGTGTCAAACCAGCTGGGTGCCCGCAGGAAGGAGGGTGGCCGAAGGTAGAAGGGACT 158

Query 473  CAGGGAAGTAGACGTCGGGAAAAGATCAGACTCCAACAGGTGCTCTCCGAAGAACTGGTC 532
          |||
Sbjct 157  CAGGGAAGTAGACGTCGGGAAAAGATCAGACTCCAACAGGTGCTCTCCGAAGAACTGGTC 98

Query 533  AAAGAGGCGGCTGGGGGAGTGGAAAGGAAAGAGGGGCGCGGATCCAGGGGTGGTGGAT 592
          |||
Sbjct 97  AAAGAGGCGGCTGGGGGAGTGGAAAGGAAAGAGGGGCGCGGATCCAGGGGTGGTGGAT 38

Query 593  GGCGATGTCCATGGT 607
          |||
Sbjct 37  GGCGATGTCCATGGT 23
  
```

A1.5 ASSEMBLY OF E164X α B-CRYSTALLIN

PCR mutagenesis experiments involved the production of the E164X α B-crystallin mutant insert with 3'A overhangs for subsequent ligation into the pGEM®-T Easy vector. The E164X mutant contains a unique PstI restriction site downstream to the stop codon. DNA from selected transformants was screened using an *NcoI/PstI* digest to identify fragments of expected size 506bp (see Figure A1.13.A). Screening suggested that 5 out of the 8 clones contained the E164X mutant insert. Subsequent sequencing and BLAST analysis confirmed all 5 constructs contained the E164X mutant insert.

Construct 4 (see, Figure A1.14) was subcloned into pET23d(+) using an *NcoI/EcoRI* digest. The presence of the E164X mutation was assessed using the *NcoI/PstI* digest on purified constructs to screen for fragments of expected E164X insert size of 506bp (see Figure A1.13.B). Of 6, constructs 1, 2, 3 and 4 indicated the presence of a low intensity fragment at 506bp (lanes 1, 2, 3 and 4 respectively). Subsequent sequencing and BLAST analysis of the 4 constructs confirmed the E164X insert had successfully been subcloned into the pET23d(+) vector in construct 1-3 with no unwanted sequence changes, (see, Figure A.15.). Construct 1 would be used for protein expression.

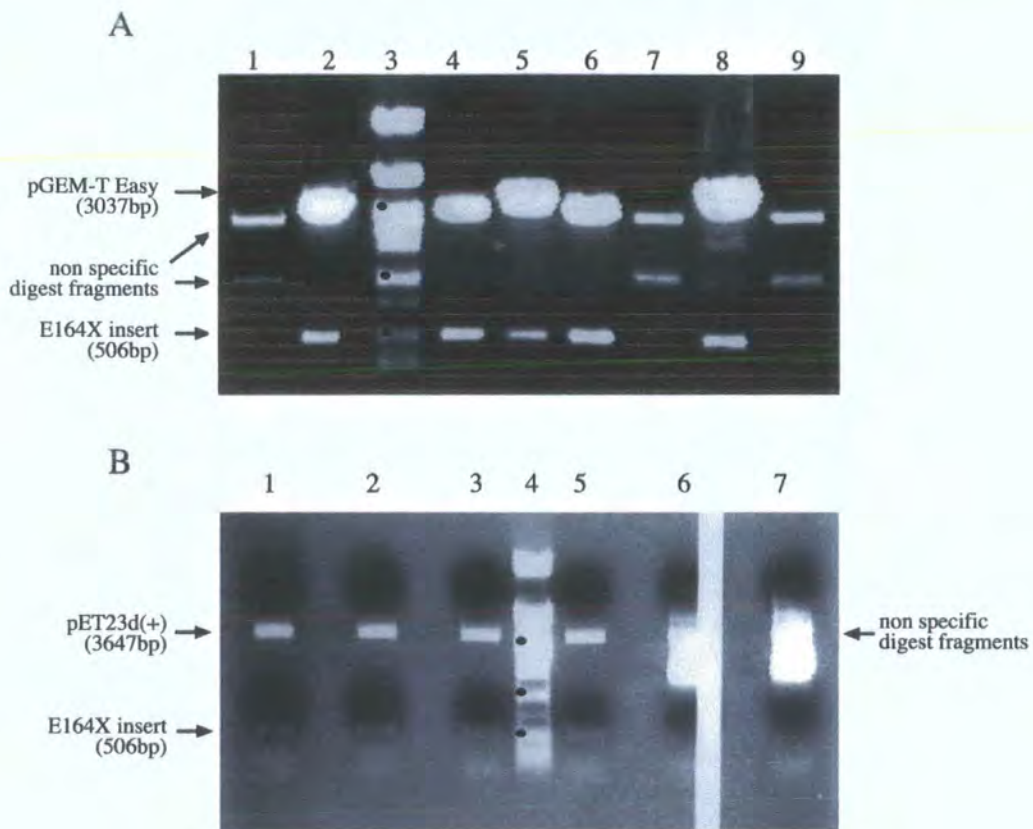


Figure A1.13. Assembly of E164X α B-crystallin construct using pGEM®-T Easy vector system. PCR mutagenesis produced a PCR product of 528bp that was purified and ligated into using pGEM®-T Easy vector. The efficiency of the ligation was assessed using an *NcoI/PstI* digest screen (A), which suggested 5 out of 8 selected constructs contained the E164X insert. Sequencing confirmed constructs 2, 3, 4, 5 and 7 shown in lanes 2, 4, 5, 6 and 8 respectively contained the E164X mutant insert. Construct 4 (Figure A1.13A, lane 5) was subcloned into the pET23d(+) vector. Purified DNA was screened (B) using *NcoI/PstI* digestion and suggested the E164X insert was present in constructs 1-4 shown in lanes 1, 2, 3 and 5 respectively at 506bp. Sequencing confirmed constructs 1-3 contained the E164X insert with no additional mutations, therefore were viable for protein expression. DNA ladder λ *PstI* (Figure A1.13.A lane 3; Figure A1.13.B, lane 4-black circle- 514, 1159 and 2838bp). The overexposure through lane 6 was a function of the Biorad Gel Doc 2000.

Figure A1.14. BLAST data for E164X insert in pGEM-T Easy-Construct 4

Pst I highlighted in bold (CTGCAG)

Pink - random substituton

Green - insertion/ deletion

Red - Wild Type Methionine and wt stop codon

Blue-SDM mutation

Underlined -primer sequence

*****= polymorphism

Homo sapiens crystallin, alpha B (CRYAB), mRNA

Length=691

Score = 1021 bits (515), Expect = 0.0

Identities = 524/527 (99%), Gaps = 0/527 (0%)

Strand=Plus/Plus

```

Query  51  ACCATGGACATCGCCATCCACCACCCCTGGATCCGCCGCCCTTCTTTCTTTCCACTCC  110
      |||
Sbjct  23  ACCATGGACATCGCCATCCACCACCCCTGGATCCGCCGCCCTTCTTTCTTTCCACTCC  82

Query  111  CCCAGCCGCCCTCTTTGACCAGTCTTCGGAGAGCACCTGTTGGAGTCTGATCTTTCCCG  170
      |||
Sbjct  83  CCCAGCCGCCCTCTTTGACCAGTCTTCGGAGAGCACCTGTTGGAGTCTGATCTTTCCCG  142

Query  171  ACGTCTACTTCCCTGAGTCCCTTCTACCTTCGCCACCCCTCCTTCCTGCGGGCACCCAGC  230
      |||
Sbjct  143  ACGTCTACTTCCCTGAGTCCCTTCTACCTTCGCCACCCCTCCTTCCTGCGGGCACCCAGC  202

Query  231  TGGTTTGACACTGGACTCTCAGAGATGCGCCTGGAGAAGGACAGGTTCTGTCAACCTG  290
      |||
Sbjct  203  TGGTTTGACACTGGACTCTCAGAGATGCGCCTGGAGAAGGACAGGTTCTGTCAACCTG  262

Query  291  GATGTGAAGCACTTCTCCCCAGAGGAACTCAAAGTTAAGGTGTTGGGAGATGTGATTGAG  350
      |||
Sbjct  263  GATGTGAAGCACTTCTCCCCAGAGGAACTCAAAGTTAAGGTGTTGGGAGATGTGATTGAG  322

Query  351  GTGCATGGAAAACATGAAGAGCGCCAGGATGAACATGGTTTCATCTCCAGGGAGTTCCAC  410
      |||
Sbjct  323  GTGCATGGAAAACATGAAGAGCGCCAGGATGAACATGGTTTCATCTCCAGGGAGTTCCAC  382

Query  411  AGGAAATACCGGATCCCAGCTGATGTAGACCCCTCTCACCATTACTTCATCCCTGTCATCT  470
      |||
Sbjct  383  AGGAAATACCGGATCCCAGCTGATGTAGACCCCTCTCACCATTACTTCATCCCTGTCATCT  442

Query  471  GATGGGGTCCTCACTGTGAATGGACCAAGGAAACAGGTCTCTGGCCCTGAGCGCACCATT  530
      |||
Sbjct  443  GATGGGGTCCTCACTGTGAATGGACCAAGGAAACAGGTCTCTGGCCCTGAGCGCACCATT  502

Query  531  CCCATCACCCTGTAAGAGAAGCCTGCAGTCCCGCAGCTCCCAAGAA  577
      |||
Sbjct  503  CCCATCACCCTGTAAGAGAAGCCTGCAGTCCCGCAGCTCCCAAGAA  549

```

Figure A1.15. BLAST data for E164X insert in pET23d(+)-Construct 1

Homo sapiens crystallin, alpha B (CRYAB), mRNA
 Length=691
 Score = 1021 bits (515), Expect = 0.0
 Identities = 524/527 (99%), Gaps = 0/527 (0%)
 Strand=Plus/Plus

```

Query   51   ACCATGGACATCGCCATCCACCACCCCTGGATCCGCCGCCCTTCTTTCTTTCCACTCC   110
          |||
Sbjct   23   ACCATGGACATCGCCATCCACCACCCCTGGATCCGCCGCCCTTCTTTCTTTCCACTCC   82

Query   111  CCCAGCCGCCTCTTTGACCAGTTCTTCGGAGAGCACCTGTTGGAGTCTGATCTTTTCCCG   170
          |||
Sbjct   83   CCCAGCCGCCTCTTTGACCAGTTCTTCGGAGAGCACCTGTTGGAGTCTGATCTTTTCCCG   142

Query   171  ACGTCTACTTCCCTGAGTCCCTTCTACCTTCGGCCACCCTCCTTCCTGCGGGCACCCAGC   230
          |||
Sbjct   143  ACGTCTACTTCCCTGAGTCCCTTCTACCTTCGGCCACCCTCCTTCCTGCGGGCACCCAGC   202

Query   231  TGGTTTGACACTGGACTCTCAGAGATGCGCCTGGAGAAGGACAGGTTCTCTGTCAACCTG   290
          |||
Sbjct   203  TGGTTTGACACTGGACTCTCAGAGATGCGCCTGGAGAAGGACAGGTTCTCTGTCAACCTG   262

Query   291  GATGTGAAGCACTTCTCCCCAGAGGAACTCAAAGTTAAGGTGTTGGGAGATGTGATTGAG   350
          |||
Sbjct   263  GATGTGAAGCACTTCTCCCCAGAGGAACTCAAAGTTAAGGTGTTGGGAGATGTGATTGAG   322

Query   351  GTGCATGGAAAACATGAAGAGCGCCAGGATGAACATGGTTTCATCTCCAGGGAGTTCAC   410
          |||
Sbjct   323  GTGCATGGAAAACATGAAGAGCGCCAGGATGAACATGGTTTCATCTCCAGGGAGTTCAC   382

Query   411  AGGAAATACCGGATCCCAGCTGATGTAGACCCTCTCACCATTACTTCATCCCTGTCATCT   470
          |||
Sbjct   383  AGGAAATACCGGATCCCAGCTGATGTAGACCCTCTCACCATTACTTCATCCCTGTCATCT   442

Query   471  GATGGGGTCCTCACTGTGAATGGACCAAGGAAACAGGTCTCTGGCCCTGAGCGCACCATTT   530
          |||
Sbjct   443  GATGGGGTCCTCACTGTGAATGGACCAAGGAAACAGGTCTCTGGCCCTGAGCGCACCATTT   502

Query   531  CCCATCACCCGTTAAGAGAAGCCTGCAAGTCACCGCAGCTCCCAAGAA   577
          |||
Sbjct   503  CCCATCACCCGTTAAGAGAAGCCTGCTGTCACCGCAGCCCCCAAGAA   549

```

A1.6 ASSEMBLY OF A171X α B-CRYSTALLIN

PCR mutagenesis experiments involved the production of the A171X α B-crystallin mutant insert with 3'A overhangs for subsequent ligation into the pGEM®-T Easy vector. The A171X mutant contains a unique *SacI* restriction site downstream from the stop codon. This site was used to screen DNA from selected transformants using an *NcoI/SacI* digest to identify fragments of expected size 512bp (see Figure A1.16.A). Screening suggested that 7 out of the 8 clones contained the A171X mutant insert. Subsequent sequencing and BLAST analysis confirmed constructs 2, 3, 4, 6 and 8 shown in Figure 3.7A, lanes 2, 3, 4, 6 and 9 respectively, contained the A171X mutant insert.

Construct 2 (see Figure A1.17) was subcloned into pET23d(+) using an *NcoI/EcoRI* digest. The ligation of the A171X mutant insert was confirmed using the *NcoI/SacI* digest on purified constructs to screen for fragments of expected A171X insert size of 512bp (see Figure A1.16.B). All 6 constructs indicated the presence of a low intensity fragment at 512bp (lanes 1, 2, 3, 5, 6 and 7 respectively). Subsequent sequencing and BLAST analysis of constructs 1-5 confirmed the A171X insert had successfully been subcloned into the pET23d(+) vector in construct 2 and 3 with no unwanted sequence changes, (see Figure A1.18). Construct 2 would be used for protein expression.

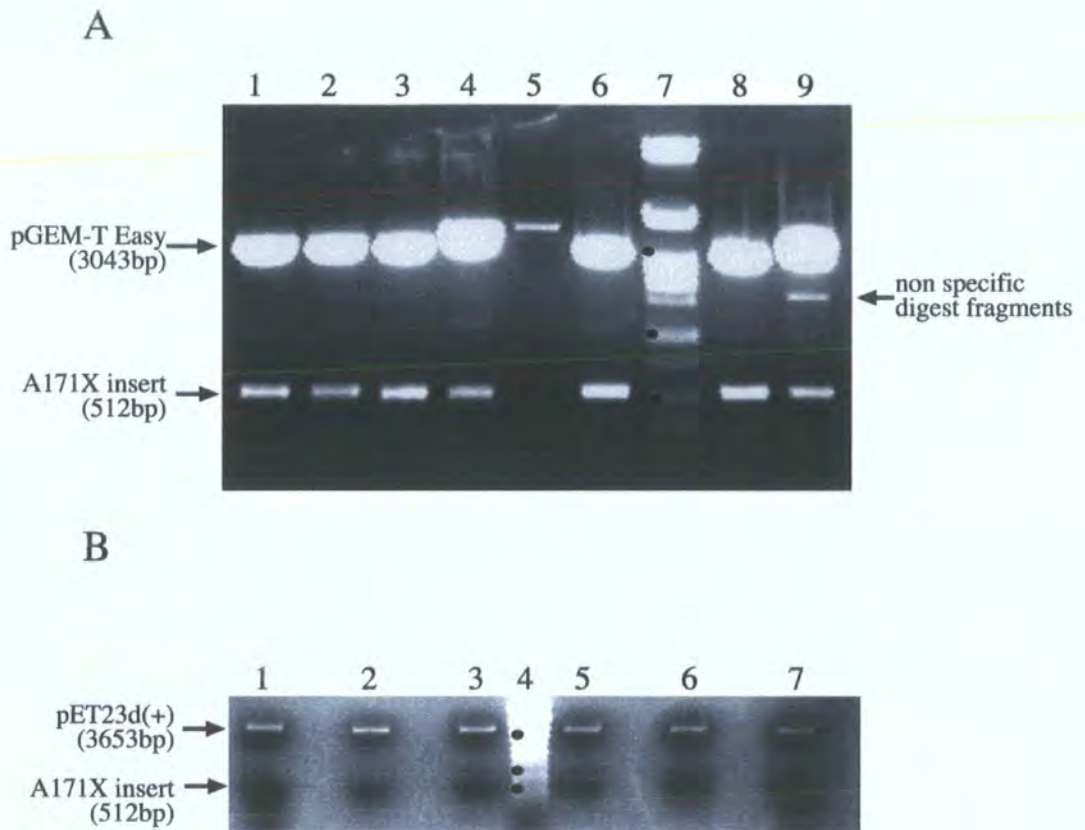


Figure A1.16. Assembly of A171X α B-crystallin construct using pGEM®-T Easy vector system. PCR mutagenesis produced a PCR product of 540bp that was purified and ligated into using pGEM®-T Easy vector. The efficiency of the ligation was assessed using an *NcoI/SacI* digest screen (A), which suggested 7 out of 8 selected constructs contained the A171X insert. Sequencing confirmed constructs 2, 3, 4, 6 and 8 shown in lanes 2, 3, 4, 6 and 9 respectively contained the A171X mutant insert. Construct 2 (Figure A1.16.A, lane 2) was subcloned into the pET23d(+) vector. Purified DNA was screened (B) using *NcoI/SacI* digestion and suggested the A171X insert was present in constructs 1-6 shown in lanes 1, 2, 3, 5, 6 and 7 respectively at 512bp. Sequencing confirmed constructs 2 and 3 contained the A171X insert with no additional mutations, therefore were viable for protein expression. DNA ladder λ *PstI* (Figure A1.16.A lane 7; Figure A1.16.B, lane 4-black circle- 514, 1159 and 2838bp).

Figure A1.17. BLAST data for A171X insert in pGEM-T Easy-Construct 2

Sac I highlighted in bold (GAGCTC)

Pink - random substitution

Green - insertion/ deletion

Red - Wild Type Methionine and wt stop codon

Blue-SDM mutation

Underlined -primer sequence

*= polymorphism

Homo sapiens crystallin, alpha B (CRYAB), mRNA

Length=691

Score = 1041 bits (525), Expect = 0.0

Identities = 534/537 (99%), Gaps = 0/537 (0%)

Strand=Plus/Minus

```

Query  60  GGGCATCTATTTCTTGGGGAGCTCAGGTGACAGCAGGCTTCTCTTCACGGGTGATGGGAAT  119
      |||
Sbjct  559  GGGCATCTATTTCTTGGGGGCTGCGGTGACAGCAGGCTTCTCTTCACGGGTGATGGGAAT  500

Query  120  GGTGCGCTCAGGGCCAGAGACCTGTTTCCTTGGTCCATTACAGTGAGGACCCCATCAGA  179
      |||
Sbjct  499  GGTGCGCTCAGGGCCAGAGACCTGTTTCCTTGGTCCATTACAGTGAGGACCCCATCAGA  440

Query  180  TGACAGGGATGAAGTAATGGTGAGAGGGTCTACATCAGCTGGGATCCGGTATTTCTGTG  239
      |||
Sbjct  439  TGACAGGGATGAAGTAATGGTGAGAGGGTCTACATCAGCTGGGATCCGGTATTTCTGTG  380

Query  240  GAACTCCCTGGAGATGAAACCATGTTTCATCCTGGCGCTCTTCATGTTTCCATGCACCTC  299
      |||
Sbjct  379  GAACTCCCTGGAGATGAAACCATGTTTCATCCTGGCGCTCTTCATGTTTCCATGCACCTC  320

Query  300  AATCACATCTCCCAACACCTTAACCTTGGAGTTCCTCTGGGGAGAAGTGCTTCACATCCAG  359
      |||
Sbjct  319  AATCACATCTCCCAACACCTTAACCTTGGAGTTCCTCTGGGGAGAAGTGCTTCACATCCAG  260

Query  360  GTTGACAGAGAACCTGTCCTTCTCCAGGCGCATCTCTGAGAGTCCAGTGTCAAACCAGCT  419
      |||
Sbjct  259  GTTGACAGAGAACCTGTCCTTCTCCAGGCGCATCTCTGAGAGTCCAGTGTCAAACCAGCT  200

Query  420  GGGTGCCCGCAGGAAGGAGGGTGGCCGAAGGTAGAAGGGACTCAGGGAAGTAGACGTCGG  479
      |||
Sbjct  199  GGGTGCCCGCAGGAAGGAGGGTGGCCGAAGGTAGAAGGGACTCAGGGAAGTAGACGTCGG  140

Query  480  GAAAAGATCAGACTCCAACAGGTGCTCTCCGAAGAACTGGTCAAAGAGGCGGCTGGGGGA  539
      |||
Sbjct  139  GAAAAGATCAGACTCCAACAGGTGCTCTCCGAAGAACTGGTCAAAGAGGCGGCTGGGGGA  80

Query  540  GTGGAAAGGAAAGAAGGGGCGCGGATCCAGGGGTGGTGGATGGCGATGTCCATGGT  596
      |||
Sbjct  79  GTGGAAAGGAAAGAAGGGGCGCGGATCCAGGGGTGGTGGATGGCGATGTCCATGGT  23

```


Homo sapiens crystallin, alpha B (CRYAB), mRNA
Length=691
Score = 1035 bits (522), Expect = 0.0
Identities = 533/537 (99%), Gaps = 0/537 (0%)
Strand=Plus/Minus

Query	108	GGGCATCTATTCTTTGGGAGCTCAGGTGACAGCAGGCTTCTCTTCACGGGTGATGGGAAT	167
Sbjct	559	GGGCATCTATTCTTTGGGGGCTGCGGTGACAGCAGGCTTCTCTTCACGGGTGATGGGAAT	500
Query	168	GGTGCGCTCAGGGCCAGAGACCTGTTTCCTTGGTCCATTACAGTGAGGACCCCATCAGA	227
Sbjct	499	GGTGCGCTCAGGGCCAGAGACCTGTTTCCTTGGTCCATTACAGTGAGGACCCCATCAGA	440
Query	228	TGACAGGGATGAAGTAATGGTGAGAGGGTCTACATCAGCTGGGATCCGGTATTTCTGTG	287
Sbjct	439	TGACAGGGATGAAGTAATGGTGAGAGGGTCTACATCAGCTGGGATCCGGTATTTCTGTG	380
Query	288	GAAC TCCCTGGAGATGAAACCATGTTTCATCTGGCGCTCTTCATGTTTTCCATGCACCTC	347
Sbjct	379	GAAC TCCCTGGAGATGAAACCATGTTTCATCTGGCGCTCTTCATGTTTTCCATGCACCTC	320
Query	348	AATCACATCTCCCAACACCTTAACTTTGAGTTCTCTGGGGAGAAGTGCTTCACATCCAG	407
Sbjct	319	AATCACATCTCCCAACACCTTAACTTTGAGTTCTCTGGGGAGAAGTGCTTCACATCCAG	260
Query	408	GTTGACAGAGAACCTGTCCTTCTCCAGGCGCATCTCTGAGAGTCCAGTGTCAAACCAGCT	467
Sbjct	259	GTTGACAGAGAACCTGTCCTTCTCCAGGCGCATCTCTGAGAGTCCAGTGTCAAACCAGCT	200
Query	468	GGGTGCCCCGAGGAAGGAGGGTGGCCGAAGGTAGAAGGGA CT CANGGAAGTAGACGTCGG	527
Sbjct	199	GGGTGCCCCGAGGAAGGAGGGTGGCCGAAGGTAGAAGGGA CT CAGGGAAGTAGACGTCGG	140
Query	528	GAAAAGATCAGACTCCAACAGGTGCTCTCCGAAGAACTGGTCAAAGAGGCGGCTGGGGGA	587
Sbjct	139	GAAAAGATCAGACTCCAACAGGTGCTCTCCGAAGAACTGGTCAAAGAGGCGGCTGGGGGA	80
Query	588	GTGGAAAGGAAAGAAAGGGGGCGCGGATCCAGGGGTGGTGGATGGCGATGTC CAT TGGT	644
Sbjct	79	GTGGAAAGGAAAGAAAGGGGGCGCGGATCCAGGGGTGGTGGATGGCGATGTC CAT TGGT	23

A1.7 ASSEMBLY OF K174X α B-CRYSTALLIN

PCR mutagenesis experiments involved the production of the K174X α B-crystallin mutant insert with 3'A overhangs for subsequent ligation into the pGEM®-T Easy vector. The K174X mutant contains a unique *SacII* restriction site upstream to the stop codon. DNA from selected transformants was purified and presence of the K174X mutation was assessed using an *NcoI/SacII* digest to screen for fragments of expected size 514bp (see Figure A1.19.A). Screening suggested that all 12 constructs contained the K174X mutant insert. Subsequent sequencing and BLAST analysis of 2, 3, 4, 5 and 11 confirmed constructs 2 and 5 shown in Figure A1.19.A, lanes 2 and 5 respectively, contained the K174X mutant insert.

Construct 2 (see Figure A1.20) was subcloned into pET23d(+) using an *NcoI/EcoRI* digest. The ligation of the K174X mutant insert was assessed using the *NcoI/SacII* digest on purified constructs to screen for fragments of expected K174X insert size of 514bp (see Figure A1.19.B). Constructs 1, 2 and 4 indicated the presence of a low intensity fragment at 514bp (lanes 2, 3 and 5 respectively see arrow head). Subsequent sequencing and BLAST analysis of constructs 1, 2 and 5 confirmed the K174X insert had successfully been subcloned into the pET23d(+) vector in construct 1 with no unwanted sequence changes, (see Figure A1.21). Construct 1 would be used for protein expression and subcloning into pcDNA3.1(-) vector for transient expression in mammalian cells.

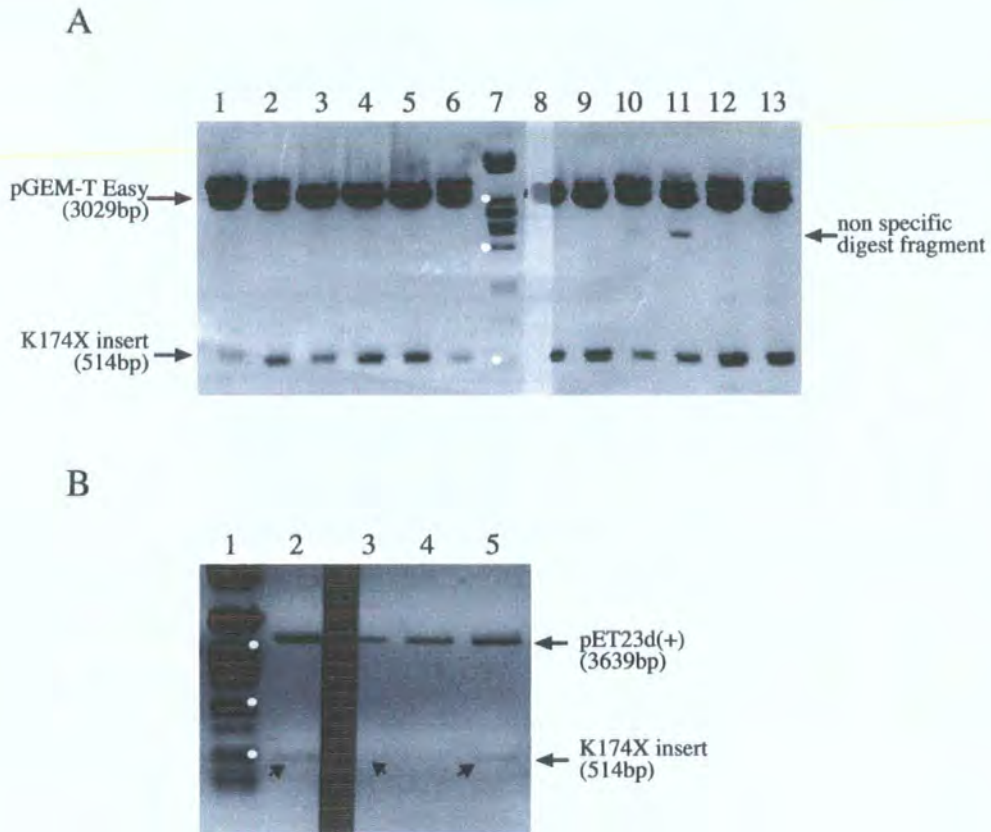


Figure A1.19. Assembly of K174X α B-crystallin construct using pGEM®-T Easy vector system. PCR mutagenesis produced a PCR product of 528bp that was purified and ligated into using pGEM®-T Easy vector. The efficiency of the ligation was assessed using an *NcoI/SacII* digest screen (A), which suggested all 12 constructs contained the K174X insert. Sequencing confirmed constructs 2, and 5 shown in lanes 2, and 5 respectively contained the K174X mutant insert. Construct 2 (Figure A1.19.A, lane 2) was subcloned into the pET23d(+) vector. Purified DNA was screened (B) using *NcoI/SacII* digestion and suggested the K174X insert was present in constructs 1, 2 and 4 shown in lanes 2, 3, and 5 respectively at 514bp. Sequencing confirmed constructs 1 contained the K174X insert with no additional mutations, therefore were viable for protein expression. DNA ladder λ *PstI* (Figure A1.19.A lane 7; Figure A1.19.B, lane 1-white circle- 514, 1159 and 2838bp). The overexposure through Figure A1.19.B lane 3 was a function of Biorad Gel Doc 2000.

Figure A1.20. BLAST data for K174X insert in pGEM-T Easy-Construct 2

Sac II highlighted in bold (CCGCGG)

Pink - random substitution

Green - insertion/ deletion

Red - Wild Type Methionine and wt stop codon

Blue-SDM mutation

Underlined -primer sequence

* = polymorphism

```

Homo sapiens crystallin, alpha B (CRYAB), mRNA
Length=691
Score = 1019 bits (514), Expect = 0.0
Identities = 522/525 (99%), Gaps = 0/525 (0%)
Strand=Plus/Minus
Query 48 TTCTAGGGGGCCGCGGTGACAGCAGGCTTCTCTTACGGGTGATGGGAATGGTGCGCTCA 107
| | | | | | | | | | | | | | | | | | | | | | | | | | | | | | | | | | | | | | | |
Sbjct 549 TTCTTGGGGGCTGCGGTGACAGCAGGCTTCTCTTACGGGTGATGGGAATGGTGCGCTCA 490
Query 108 GGGCCAGAGACCTGTTTCCCTTGGTCCATTACAGTGAGGACCCATCNGATGACAGGGAT 167
| | | | | | | | | | | | | | | | | | | | | | | | | | | | | | | | | | | | | | | |
Sbjct 489 GGGCCAGAGACCTGTTTCCCTTGGTCCATTACAGTGAGGACCCATCAGATGACAGGGAT 430
Query 168 GAAGTAATGGTGAGAGGGTCTACATCAGCTGGGATCCGGTATTTCTGTGGAACCTCCCTG 227
| | | | | | | | | | | | | | | | | | | | | | | | | | | | | | | | | | | | | | | |
Sbjct 429 GAAGTAATGGTGAGAGGGTCTACATCAGCTGGGATCCGGTATTTCTGTGGAACCTCCCTG 370
Query 228 GAGATGAAACCATGTTTCATCCTGGCGCTCTTCATGTTTTCCATGCACCTCAATCACATCT 287
| | | | | | | | | | | | | | | | | | | | | | | | | | | | | | | | | | | | | | | |
Sbjct 369 GAGATGAAACCATGTTTCATCCTGGCGCTCTTCATGTTTTCCATGCACCTCAATCACATCT 310
Query 288 CCCAACACCTTAACTTTGAGTTCTCTGGGGAGAAGTGCTTCACATCCAGGTTGACAGAG 347
| | | | | | | | | | | | | | | | | | | | | | | | | | | | | | | | | | | | | | | |
Sbjct 309 CCCAACACCTTAACTTTGAGTTCTCTGGGGAGAAGTGCTTCACATCCAGGTTGACAGAG 250
Query 348 AACCTGTCCTTCTCCAGGCGCATCTCTGAGAGTCCAGTGTCAAACCAGCTGGGTGCCCGC 407
| | | | | | | | | | | | | | | | | | | | | | | | | | | | | | | | | | | | | | | |
Sbjct 249 AACCTGTCCTTCTCCAGGCGCATCTCTGAGAGTCCAGTGTCAAACCAGCTGGGTGCCCGC 190
Query 408 AGGAAGGAGGGTGGCCGAAGGTAGAAGGGACTCAGGGAAGTAGACGTCGGGAAAAGATCA 467
| | | | | | | | | | | | | | | | | | | | | | | | | | | | | | | | | | | | | | | |
Sbjct 189 AGGAAGGAGGGTGGCCGAAGGTAGAAGGGACTCAGGGAAGTAGACGTCGGGAAAAGATCA 130
Query 468 GACTCCAACAGGTGCTCTCCGAAGAACTGGTCAAAGAGGCGGCTGGGGAGTGGAAGGA 527
| | | | | | | | | | | | | | | | | | | | | | | | | | | | | | | | | | | | | | | |
Sbjct 129 GACTCCAACAGGTGCTCTCCGAAGAACTGGTCAAAGAGGCGGCTGGGGAGTGGAAGGA 70
Query 528 AAGAAGGGGCGCGGATCCAGGGGTGGTGGATGGCGATGTCATG 572
| | | | | | | | | | | | | | | | | | | | | | | | | | | | | | | | | | | | | | | |
Sbjct 69 AAGAAGGGGCGCGGATCCAGGGGTGGTGGATGGCGATGTCATG 25

```

Figure A1.21. BLAST data for K174X insert in pET23d(+)-Construct 1

Homo sapiens crystallin, alpha B (CRYAB), mRNA
Length=691

Score = 1029 bits (519), Expect = 0.0
Identities = 525/527 (99%), Gaps = 0/527 (0%)
Strand=Plus/Minus

```

Query 113  TTCTAGGGGGCCGCGGTGACAGCAGGCTTCTCTTCACGGGTGATGGGAATGGTGCGCTCA 172
          |||
Sbjct 549  TTCTTGGGGGCTGCGGTGACAGCAGGCTTCTCTTCACGGGTGATGGGAATGGTGCGCTCA 490

Query 173  GGGCCAGAGACCTGTTTCCTTGGTCCATTACAGTGAGGACCCCATCAGATGACAGGGAT 232
          |||
Sbjct 489  GGGCCAGAGACCTGTTTCCTTGGTCCATTACAGTGAGGACCCCATCAGATGACAGGGAT 430

Query 233  GAAGTAATGGTGAGAGGGTCTACATCAGCTGGGATCCGGTATTTCTGTGGAACCTCCCTG 292
          |||
Sbjct 429  GAAGTAATGGTGAGAGGGTCTACATCAGCTGGGATCCGGTATTTCTGTGGAACCTCCCTG 370

Query 293  GAGATGAAACCATGTTTCATCCTGGCGCTCTTCATGTTTTCATGCACCTCAATCACATCT 352
          |||
Sbjct 369  GAGATGAAACCATGTTTCATCCTGGCGCTCTTCATGTTTTCATGCACCTCAATCACATCT 310

Query 353  CCCAACACCTTAACTTTGAGTTCCTCTGGGGAGAAGTGCTTCACATCCAGGTTGACAGAG 412
          |||
Sbjct 309  CCCAACACCTTAACTTTGAGTTCCTCTGGGGAGAAGTGCTTCACATCCAGGTTGACAGAG 250

Query 413  AACCTGTCCTTCTCCAGGCGCATCTCTGAGAGTCCAGTGTCAAACCAGCTGGGTGCCCGC 472
          |||
Sbjct 249  AACCTGTCCTTCTCCAGGCGCATCTCTGAGAGTCCAGTGTCAAACCAGCTGGGTGCCCGC 190

Query 473  AGGAAGGAGGGTGCGCCGAAGGTAGAAGGGACTCAGGGAAGTAGACGTCGGGAAAAGATCA 532
          |||
Sbjct 189  AGGAAGGAGGGTGCGCCGAAGGTAGAAGGGACTCAGGGAAGTAGACGTCGGGAAAAGATCA 130

Query 533  GACTCCAACAGGTGCTCTCCGAAGAACTGGTCAAAGAGGCGGCTGGGGGAGTGGAAGGA 592
          |||
Sbjct 129  GACTCCAACAGGTGCTCTCCGAAGAACTGGTCAAAGAGGCGGCTGGGGGAGTGGAAGGA 70

Query 593  AAGAAGGGGCGCGGATCCAGGGGTGGTGGATGGCGATGTCCATGGT 639
          |||
Sbjct 69  AAGAAGGGGCGCGGATCCAGGGGTGGTGGATGGCGATGTCCATGGT 23

```

A1.8 SUBCLONING α B-CRYSTALLIN CONSTRUCTS INTO THE MAMMALIAN EXPRESSION VECTOR pCDNA3.1(-)

In order to express the α B-crystallin mutants in mammalian cells by transient transfection, the inserts were subcloned from the pET23d(+) bacterial expression vector into pcDNA3.1(-) using an *Xba*I/*Hind*III digest. Subsequent screening utilised an *Apa*I/*Hind*III digest, where *Apa*I is unique to the pcDNA3.1(-) vector, thus confirming the efficient ligation of the mutant insert, but also the presence of the target vector pcDNA3.1 (-). The multiple cloning region of pcDNA3.1(-) is shown in Figure A1.3. The screening process for the ligations of each α B-crystallin mutant is shown in Figure A1.22.

The 464delCT screen suggested constructs 1, 2, 4 and 5 (see Figure A1.22.A, lanes 1, 2, 5 and 6 respectively) contained the correct mutant insert. Sequencing and BLAST analysis of constructs 2, 4 and 5 confirmed that all three constructs contained the correct insert with no unwanted sequences when compared for fidelity to the GenBank data base entry (accession no. NM001885) for human α B-crystallin. The BLAST sequence for construct 2 is shown in Figure A1.23.

The 450delA screen suggested constructs 1, 3, 4, 5 and 6 (see Figure A1.22.B, lanes 1, 3, 5, 6 and 7 respectively) contained the correct mutant insert. Sequencing and BLAST analysis of constructs 3 and 4 confirmed that both constructs contained the correct insert with no unwanted sequences. The BLAST sequence for construct 3 is shown in Figure A1.24.

The K174X screen suggested constructs 1- 6 (see Figure A1.22.C, lanes 1-3 and 5-7 respectively) contained the correct mutant insert. Sequencing and BLAST analysis of constructs 1-3 confirmed that all constructs contained the correct insert with unwanted sequences. The BLAST sequence for construct 1 is shown in Figure A1.25.

The Q151X screen, suggested constructs 1- 6 (see Figure A1.22.D, lanes 1-3 and 5-7 respectively) contained the correct mutant insert. Sequencing and BLAST analysis of constructs 1-3 confirmed that all constructs contained the correct insert with no unwanted sequences. The BLAST sequence for construct 1 is shown in Figure A1.26. (The Q151X mutant insert contains a guanine insertion downstream from the stop codon, seen previously in Figure A1.6, which does not affect the viability of the mutant DNA).

The E164X screen, suggested constructs 1- 12 (see Figure A1.22.E, lanes 1-3, 5-10 and 12-14 respectively) contained the correct mutant insert. Sequencing and BLAST analysis of constructs 4, 5, 10 and 11 confirmed that all four constructs contained the correct insert with no unwanted sequences. . The BLAST sequence for construct 4 is shown in Figure A1.27.

The A171X screen, suggested constructs 2, 3, 4, 7, 10 and 11 (see Figure A1.22.F, lanes 2, 3, 5, 8, 12 and 13 respectively) contained the correct mutant insert. Sequencing and BLAST analysis of constructs 2, 7, 10 and 11 confirmed that constructs 2, 7 and 10 contained the correct insert with unwanted sequences. . The BLAST sequence for construct 2 is shown in Figure A1.28.

Finally, the E165X screen, suggested constructs 1-10 and 12 (see Figure A1.22.G, lanes 1-6, 8-11 and 13 respectively) contained the correct mutant insert. Sequencing and BLAST analysis of constructs 1-5 confirmed that all five constructs contained the correct insert with no unwanted sequences. . The BLAST sequence for construct 1 is shown in Figure A1.29.

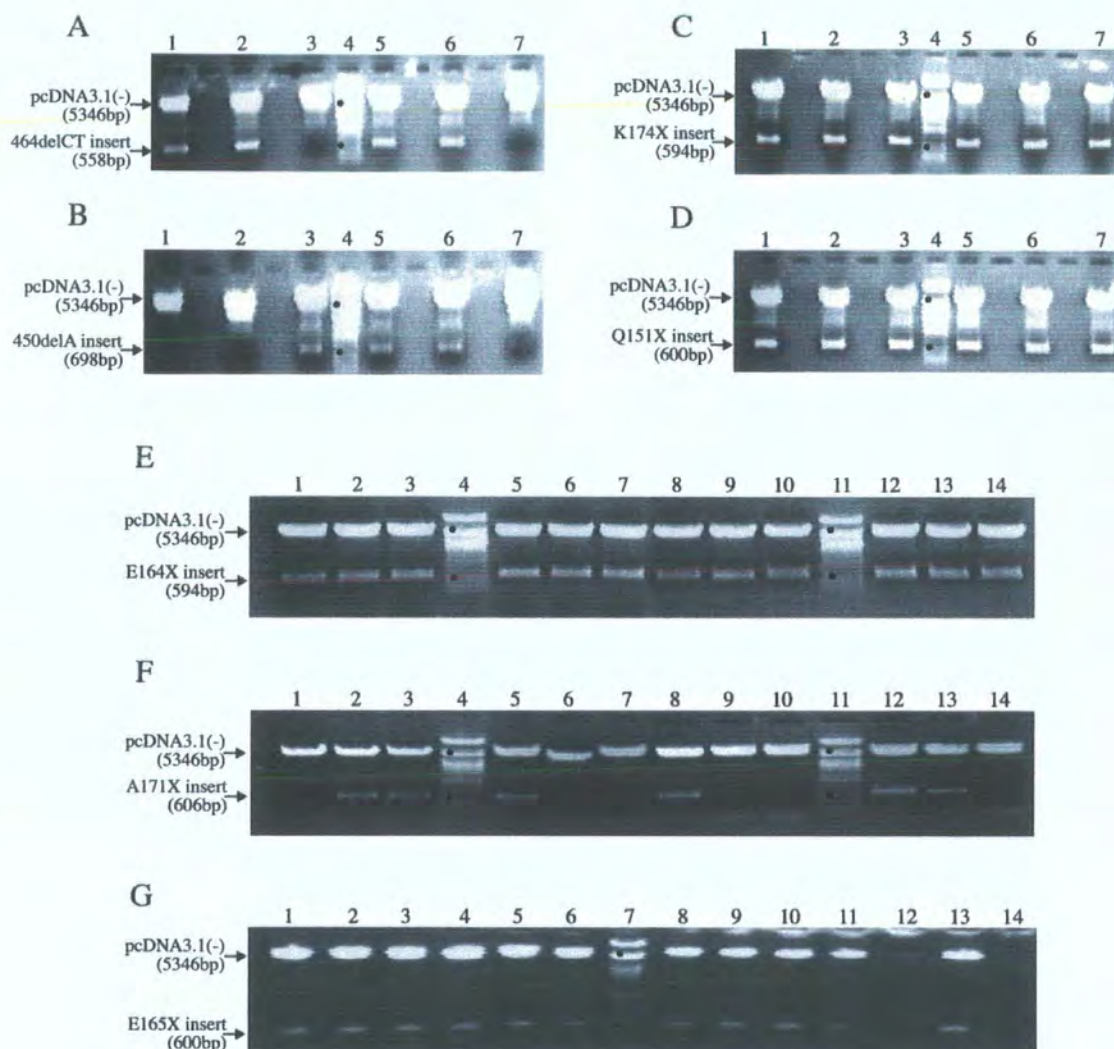


Figure A1.22. Subcloning of α B-crystallin constructs from pET23d(+) into the vector pcDNA3.1(-). Mutant inserts were ligated into pcDNA3.1(-) from pET23d(+) using *XbaI/HindIII* restriction digestion. Screening was performed with *ApaI/HindIII* digestion where the *ApaI* is specific to pcDNA3.1(-). Sequencing identified the constructs for each mutant that contained the correct insert with no additional mutations, therefore were viable for expression in mammalian cells. DNA ladder λ *PstI* -black circle- 514 and 5077bp.

Figure A1.23. BLAST data for 464delCT insert in pcDNA3.1(-) - Construct 2

Pink - random substitution

Green - insertion/ deletion

Red - Wild Type Methionine and wt stop codon

Blue-SDM mutation

Underlined -primer sequence

*= polymorphism

Homo sapiens crystallin, alpha B (CRYAB), mRNA

Length=691

Score = 959 bits (484), Expect = 0.0

Identities = 493/495 (99%), Gaps = 2/495 (0%)

Strand=Plus/Plus

```

Query 71  ACCATGGACATCGCCATCCACCACCCCTGGATCCGCCGCCCTTCTTTCCCTTTCCACTCC 130
          |||
Sbjct 23  ACCATGGACATCGCCATCCACCACCCCTGGATCCGCCGCCCTTCTTTCCCTTTCCACTCC 82

Query 131 CCCAGCCGCCTCTTTGACCAGTCTTTCGGAGAGCACCTGTTGGAGTCTGATCTTTTCCCG 190
          |||
Sbjct 83  CCCAGCCGCCTCTTTGACCAGTCTTTCGGAGAGCACCTGTTGGAGTCTGATCTTTTCCCG 142

Query 191 ACGTCTACTTCCCTGAGTCCCTTCTACCTTCGGCCACCCTCCTTCCTGCGGGCACCCAGC 250
          |||
Sbjct 143 ACGTCTACTTCCCTGAGTCCCTTCTACCTTCGGCCACCCTCCTTCCTGCGGGCACCCAGC 202

Query 251 TGGTTTGACACTGGACTCTCAGAGATGCGCCTGGAGAAGGACAGGTTCTCTGTCAACCTG 310
          |||
Sbjct 203 TGGTTTGACACTGGACTCTCAGAGATGCGCCTGGAGAAGGACAGGTTCTCTGTCAACCTG 262

Query 311 GATGTGAAGCACTTCTCCCCAGAGGAACCTCAAAGTTAAGGTGTTGGGAGATGTGATTGAG 370
          |||
Sbjct 263 GATGTGAAGCACTTCTCCCCAGAGGAACCTCAAAGTTAAGGTGTTGGGAGATGTGATTGAG 322

Query 371 GTGCATGGAAAACATGAAGAGCGCCAGGATGAACATGGTTTCATCTCCAGGGAGTTCCAC 430
          |||
Sbjct 323 GTGCATGGAAAACATGAAGAGCGCCAGGATGAACATGGTTTCATCTCCAGGGAGTTCCAC 382

Query 431 AGGAAATACCGGATCCCAGCTGATGTAGACCTCTCACCATTACTTCATCCCTGTCATCT 490
          |||
Sbjct 383 AGGAAATACCGGATCCCAGCTGATGTAGACCTCTCACCATTACTTCATCCCTGTCATCT 442

Query 491 GATGGGGTCTCACTGTGAATGGACCAAGGAAACAGGTCTCTGGCC--GAGCGCACCATT 548
          |||
Sbjct 443 GATGGGGTCTCACTGTGAATGGACCAAGGAAACAGGTCTCTGGCCCTGAGCGCACCATT 502

Query 549 CCCATCACCCGTGAA 563
          |||
Sbjct 503 CCCATCACCCGTGAA 517

```

Figure A1.24. BLAST data for 450delA insert in pcDNA3.1(-) - Construct 3

Homo sapiens crystallin, alpha B (CRYAB), mRNA
 Length=691
 Score = 1203 bits (607), Expect = 0.0
 Identities = 614/615 (99%), Gaps = 1/615 (0%)
 Strand=Plus/Plus

```

Query 70  ACCATGGACATCGCCATCCACCACCCCTGGATCCGCCGCCCTTCTTTCTTTCCACTCC 129
          ||||||||||||||||||||||||||||||||||||||||||||||||||||
Sbjct 23  ACCATGGACATCGCCATCCACCACCCCTGGATCCGCCGCCCTTCTTTCTTTCCACTCC 82

Query 130 CCCAGCCGCCTCTTTGACCAGTTCTTCGGAGAGCACCTGTTGGAGTCTGATCTTTCCCG 189
          ||||||||||||||||||||||||||||||||||||||||||||||||||||
Sbjct 83  CCCAGCCGCCTCTTTGACCAGTTCTTCGGAGAGCACCTGTTGGAGTCTGATCTTTCCCG 142

Query 190 ACGTCTACTTCCCTGAGTCCCTTCTACCTTCGGCCACCCCTCCTTCCTGCGGGCAGCCAGC 249
          ||||||||||||||||||||||||||||||||||||||||||||||||||||
Sbjct 143 ACGTCTACTTCCCTGAGTCCCTTCTACCTTCGGCCACCCCTCCTTCCTGCGGGCAGCCAGC 202

Query 250 TGGTTTGACACTGGACTCTCAGAGATGCGCCTGGAGAAGGACAGGTTCTGTCAACCTG 309
          ||||||||||||||||||||||||||||||||||||||||||||||||||||
Sbjct 203 TGGTTTGACACTGGACTCTCAGAGATGCGCCTGGAGAAGGACAGGTTCTGTCAACCTG 262

Query 310 GATGTGAAGCACTTCTCCCCAGAGGAACCTCAAAGTTAAGGTGTTGGGAGATGTGATTGAG 369
          ||||||||||||||||||||||||||||||||||||||||||||||||||||
Sbjct 263 GATGTGAAGCACTTCTCCCCAGAGGAACCTCAAAGTTAAGGTGTTGGGAGATGTGATTGAG 322

Query 370 GTGCATGGAAAACATGAAGAGCGCCAGGATGAACATGGTTTCATCTCCAGGGAGTTCCAC 429
          ||||||||||||||||||||||||||||||||||||||||||||||||||||
Sbjct 323 GTGCATGGAAAACATGAAGAGCGCCAGGATGAACATGGTTTCATCTCCAGGGAGTTCCAC 382

Query 430 AGGAAATACCGGATCCCAGCTGATGTAGACCCCTCTCACCATTACTTTCATCCCTGTCATCT 489
          ||||||||||||||||||||||||||||||||||||||||||||||||||||
Sbjct 383 AGGAAATACCGGATCCCAGCTGATGTAGACCCCTCTCACCATTACTTTCATCCCTGTCATCT 442

Query 490 GATGGGGTCTCACTGTGAATGGACCAAGG-AACAGGTCTCTGGCCCTGAGCGCACCATT 548
          ||||||||||||||||||||||||||||||||||||||||||||||||||||
Sbjct 443 GATGGGGTCTCACTGTGAATGGACCAAGGAAACAGGTCTCTGGCCCTGAGCGCACCATT 502

Query 549 CCCATCACCCGTGAAGAGAAGCCTGCTGTCACCGCAGCCCCCAAGAAATAGATGCCCTTT 608
          ||||||||||||||||||||||||||||||||||||||||||||||||||||
Sbjct 503 CCCATCACCCGTGAAGAGAAGCCTGCTGTCACCGCAGCCCCCAAGAAATAGATGCCCTTT 562

Query 609 CTTGAATTGCATTTTTTTAAAACAAGAAAGTTTCCCCACCAGTGAATGAAAGTCTTGTGAC 668
          ||||||||||||||||||||||||||||||||||||||||||||||||||||
Sbjct 563 CTTGAATTGCATTTTTTTAAAACAAGAAAGTTTCCCCACCAGTGAATGAAAGTCTTGTGAC 622

Query 669 TAGTGCTGAAGCTTA 683
          ||||||||||||
Sbjct 623 TAGTGCTGAAGCTTA 637

```

TAA = new stop codon caused by a frameshift due to the 450delA

Figure A1.25. BLAST data for K174X insert in pcDNA3.1(-) - Construct 1

Sac II highlighted in **bold** (CCGCGG)

Homo sapiens crystallin, alpha B (CRYAB), mRNA
 Length=691
 Score = 1029 bits (519), Expect = 0.0
 Identities = 525/527 (99%), Gaps = 0/527 (0%)
 Strand=Plus/Plus

```

Query 71  ACCATGGACATCGCCATCCACCACCCCTGGATCCGCCGCCCTTCTTTCTTTCCACTCC 130
          |||
Sbjct 23  ACCATGGACATCGCCATCCACCACCCCTGGATCCGCCGCCCTTCTTTCTTTCCACTCC 82

Query 131 CCCAGCCGCCTCTTTGACCAGTTCTTCGGAGAGCACCTGTTGGAGTCTGATCTTTTCCC 190
          |||
Sbjct 83  CCCAGCCGCCTCTTTGACCAGTTCTTCGGAGAGCACCTGTTGGAGTCTGATCTTTTCCC 142

Query 191 ACGTCTACTTCCCTGAGTCCCTTCTACCTTCGGCCACCCTCCTTCCTGCGGGCACCCAGC 250
          |||
Sbjct 143 ACGTCTACTTCCCTGAGTCCCTTCTACCTTCGGCCACCCTCCTTCCTGCGGGCACCCAGC 202

Query 251 TGGTTTGACACTGGACTCTCAGAGATGCGCCTGGAGAAGGACAGGTTCTCTGTCAACCTG 310
          |||
Sbjct 203 TGGTTTGACACTGGACTCTCAGAGATGCGCCTGGAGAAGGACAGGTTCTCTGTCAACCTG 262

Query 311 GATGTGAAGCACTTCTCCCCAGAGGAACTCAAAGTTAAGGTGTTGGGAGATGTGATTGAG 370
          |||
Sbjct 263 GATGTGAAGCACTTCTCCCCAGAGGAACTCAAAGTTAAGGTGTTGGGAGATGTGATTGAG 322

Query 371 GTGCATGGAAAACATGAAGAGCGCCAGGATGAACATGGTTTCATCTCCAGGGAGTTCAC 430
          |||
Sbjct 323 GTGCATGGAAAACATGAAGAGCGCCAGGATGAACATGGTTTCATCTCCAGGGAGTTCAC 382

Query 431 AGGAAATACCGGATCCCAGCTGATGTAGACCTCTCACCATTACTTCATCCCTGTCATCT 490
          |||
Sbjct 383 AGGAAATACCGGATCCCAGCTGATGTAGACCTCTCACCATTACTTCATCCCTGTCATCT 442

Query 491 GATGGGGTCCTCACTGTGAATGGACCAAGGAAACAGGTCTCTGGCCCTGAGCGCACCATT 550
          |||
Sbjct 443 GATGGGGTCCTCACTGTGAATGGACCAAGGAAACAGGTCTCTGGCCCTGAGCGCACCATT 502

Query 551 CCCATCACCCGTGAAGAGAAGCCTGCTGTCACCGCGGCCCCTAGAA 597
          |||
Sbjct 503 CCCATCACCCGTGAAGAGAAGCCTGCTGTCACCGCAGCCCCAAGAA 549
  
```

Figure A1.26. BLAST data for Q151X insert in pcDNA3.1(-) - Construct 1

Stu I highlighted in **BOLD (AAGCCT)**

Homo sapiens crystallin, alpha B (CRYAB), mRNA

Length=691

Score = 1025 bits (517), Expect = 0.0

Identities = 530/533 (99%), Gaps = 1/533 (0%)

Strand=Plus/Plus

```

Query   70   ACCATGGACATCGCCATCCACCACCCCTGGATCCGCCGCCCTTCTTTCCCTTTCCACTCC   129
          |||
Sbjct   23   ACCATGGACATCGCCATCCACCACCCCTGGATCCGCCGCCCTTCTTTCCCTTTCCACTCC   82

Query   130   CCCAGCCGCCTCTTTGACCAGTTCTTCGGAGAGCACCTGTTGGAGTCTGATCTTTTCCCG   189
          |||
Sbjct   83   CCCAGCCGCCTCTTTGACCAGTTCTTCGGAGAGCACCTGTTGGAGTCTGATCTTTTCCCG   142

Query   190   ACGTCTACTTCCCTGAGTCCCTTCTACCTTCGGCCACCCTCCTTCCTGCGGGCACCCAGC   249
          |||
Sbjct   143   ACGTCTACTTCCCTGAGTCCCTTCTACCTTCGGCCACCCTCCTTCCTGCGGGCACCCAGC   202

Query   250   TGGTTTGACACTGGACTCTCAGAGATGCGCCTGGAGAAGGACAGGTTCTCTGTCAACCTG   309
          |||
Sbjct   203   TGGTTTGACACTGGACTCTCAGAGATGCGCCTGGAGAAGGACAGGTTCTCTGTCAACCTG   262

Query   310   GATGTGAAGCACTTCTCCCCAGAGGAACTCAAAGTTAAGGTGTTGGGAGATGTGATTGAG   369
          |||
Sbjct   263   GATGTGAAGCACTTCTCCCCAGAGGAACTCAAAGTTAAGGTGTTGGGAGATGTGATTGAG   322

Query   370   GTGCATGGAAAACATGAAGAGCGCCAGGATGAACATGGTTTCATCTCCAGGGAGTTCCAC   429
          |||
Sbjct   323   GTGCATGGAAAACATGAAGAGCGCCAGGATGAACATGGTTTCATCTCCAGGGAGTTCCAC   382

Query   430   AGGAAATACCGGATCCCAGCTGATGTAGACCCTCTCACCATTACTTCATCCCTGTCATCT   489
          |||
Sbjct   383   AGGAAATACCGGATCCCAGCTGATGTAGACCCTCTCACCATTACTTCATCCCTGTCATCT   442

Query   490   GATGGGGTCCTCACTGTGAATGGACCAAGGAAATAGGCCTCTGGCCCTGAGCGCACCAT   549
          |||
Sbjct   443   GATGGGGTCCTCACTGTGAATGGACCAAGGAAACAGGTCTCTGGCCCTGAGC-GCACCAT   501

Query   550   TCCCATCACCCGTGAAGAGAAGCCTGCTGTCAACCGCAGCCCCCAAGAAATAGA   602
          |||
Sbjct   502   TCCCATCACCCGTGAAGAGAAGCCTGCTGTCAACCGCAGCCCCCAAGAAATAGA   554

```


Figure A1.27. BLAST data for E164X insert in pcDNA3.1(-) - Construct 4Pst I highlighted in **bold** (CTGCAG)

Homo sapiens crystallin, alpha B (CRYAB), mRNA

Length=691

Score = 1021 bits (515), Expect = 0.0

Identities = 524/527 (99%), Gaps = 0/527 (0%)

Strand=Plus/Plus

```

Query  62  ACCATGGACATCGCCATCCACCACCCCTGGATCCGCCGCCCTTCTTTCCTTTCCACTCC 121
          |||
Sbjct  23  ACCATGGACATCGCCATCCACCACCCCTGGATCCGCCGCCCTTCTTTCCTTTCCACTCC 82

Query  122  CCCAGCCGCCCTCTTTGACCAGTTCTTCGGAGAGCACCTGTTGGAGTCTGATCTTTTCCCG 181
          |||
Sbjct  83  CCCAGCCGCCCTCTTTGACCAGTTCTTCGGAGAGCACCTGTTGGAGTCTGATCTTTTCCCG 142

Query  182  ACGTCTACTTCCCTGAGTCCCTTCTACCTTCGGCCACCCTCCTTCCTGCGGGCACCCAGC 241
          |||
Sbjct  143  ACGTCTACTTCCCTGAGTCCCTTCTACCTTCGGCCACCCTCCTTCCTGCGGGCACCCAGC 202

Query  242  TGGTTTGACACTGGACTCTCAGAGATGCGCCTGGAGAAGGACAGGTTCTCTGTCAACCTG 301
          |||
Sbjct  203  TGGTTTGACACTGGACTCTCAGAGATGCGCCTGGAGAAGGACAGGTTCTCTGTCAACCTG 262

Query  302  GATGTGAAGCACTTCTCCCCAGAGGAACCAAAGTTAAGGTGTTGGGAGATGTGATTGAG 361
          |||
Sbjct  263  GATGTGAAGCACTTCTCCCCAGAGGAACCAAAGTTAAGGTGTTGGGAGATGTGATTGAG 322

Query  362  GTGCATGGAAAACATGAAGAGCGCCAGGATGAACATGGTTTCATCTCCAGGGAGTTCAC 421
          |||
Sbjct  323  GTGCATGGAAAACATGAAGAGCGCCAGGATGAACATGGTTTCATCTCCAGGGAGTTCAC 382

Query  422  AGGAAATACCGGATCCCAGCTGATGTAGACCCTCTCACCATTACTTCATCCCTGTCTCT 481
          |||
Sbjct  383  AGGAAATACCGGATCCCAGCTGATGTAGACCCTCTCACCATTACTTCATCCCTGTCTCT 442

Query  482  GATGGGGTCTCACTGTGAATGGACCAAGGAAACAGGTCTCTGGCCCTGAGCGCACCATT 541
          |||
Sbjct  443  GATGGGGTCTCACTGTGAATGGACCAAGGAAACAGGTCTCTGGCCCTGAGCGCACCATT 502

Query  542  CCCATACCCGTTAAGAGAAGCCTGCAGTCACCGCAGCTCCCAAGAA 588
          |||
Sbjct  503  CCCATACCCGTGAAGAGAAGCCTGCTGTCACCGCAGCCCCCAAGAA 549

```

Figure A1.28. BLAST data for A171X insert in pcDNA3.1(-) - Construct 2

Sac I highlighted in **bold** (GAGCTC)

Homo sapiens crystallin, alpha B (CRYAB), mRNA

Length=691

Score = 1041 bits (525), Expect = 0.0

Identities = 534/537 (99%), Gaps = 0/537 (0%)

Strand=Plus/Plus

```

Query   63   ACCATGGACATCGCCATCCACCACCCCTGGATCCGCCGCCCTTCTTTCCTTTCCACTCC   122
          |||
Sbjct   23   ACCATGGACATCGCCATCCACCACCCCTGGATCCGCCGCCCTTCTTTCCTTTCCACTCC   82

Query   123  CCCAGCCGCCCTCTTTGACCAGTTCTTCGGAGAGCACCTGTTGGAGTCTGATCTTTTCCCG   182
          |||
Sbjct   83   CCCAGCCGCCCTCTTTGACCAGTTCTTCGGAGAGCACCTGTTGGAGTCTGATCTTTTCCCG   142

Query   183  ACGTCTACTTCCCTGAGTCCCTTCTACCTTCGGCCACCCTCCTTCCTGCGGGCACCCAGC   242
          |||
Sbjct   143  ACGTCTACTTCCCTGAGTCCCTTCTACCTTCGGCCACCCTCCTTCCTGCGGGCACCCAGC   202

Query   243  TGGTTTGACACTGGACTCTCAGAGATGCGCCTGGAGAAGGACAGGTTCTCTGTCAACCTG   302
          |||
Sbjct   203  TGGTTTGACACTGGACTCTCAGAGATGCGCCTGGAGAAGGACAGGTTCTCTGTCAACCTG   262

Query   303  GATGTGAAGCACTTCTCCCCAGAGGAACTCAAAGTTAAGGTGTTGGGAGATGTGATTGAG   362
          |||
Sbjct   263  GATGTGAAGCACTTCTCCCCAGAGGAACTCAAAGTTAAGGTGTTGGGAGATGTGATTGAG   322

Query   363  GTGCATGGAAAACATGAAGAGCGCCAGGATGAACATGGTTTCATCTCCAGGGAGTTCCAC   422
          |||
Sbjct   323  GTGCATGGAAAACATGAAGAGCGCCAGGATGAACATGGTTTCATCTCCAGGGAGTTCCAC   382

Query   423  AGGAAATACCGGATCCCAGCTGATGTAGACCCTCTCACCATTACTTCATCCCTGTCATCT   482
          |||
Sbjct   383  AGGAAATACCGGATCCCAGCTGATGTAGACCCTCTCACCATTACTTCATCCCTGTCATCT   442

Query   483  GATGGGTCTCTCACTGTGAATGGACCAAGGAAACAGGTCTCTGGCCCTGAGCGCACCATT   542
          |||
Sbjct   443  GATGGGTCTCTCACTGTGAATGGACCAAGGAAACAGGTCTCTGGCCCTGAGCGCACCATT   502

Query   543  CCCATCACCCGTGAAGAGAAGCCTGCTGTCACCTTGAGCTCCCAAGAAATAGATGCCC   599
          |||
Sbjct   503  CCCATCACCCGTGAAGAGAAGCCTGCTGTCACCTGCAGCCCCAAGAAATAGATGCCC   559

```


Figure A1.29. BLAST data for E165X insert in pcDNA3.1(-) - Construct 1

Hind III is highlighted in **BOLD** (AAGCTT)

Homo sapiens crystallin, alpha B (CRYAB), mRNA
 Length=691
 Score = 979 bits (494), Expect = 0.0
 Identities = 500/502 (99%), Gaps = 0/502 (0%)
 Strand=Plus/Plus

```

Query 17  ACCATGGACATCGCCATCCACCACCCCTGGATCCGCCGCCCTTCTTTCCCTTCCACTCC 76
          ||||||||||||||||||||||||||||||||||||||||||||||||||||||||
Sbjct 23  ACCATGGACATCGCCATCCACCACCCCTGGATCCGCCGCCCTTCTTTCCCTTCCACTCC 82

Query 77  CCCAGCCGCCTCTTTGACCAGTTCTTCGGAGAGCACCTGTTGGAGTCTGATCTTTTCCCG 136
          ||||||||||||||||||||||||||||||||||||||||||||||||||||||||
Sbjct 83  CCCAGCCGCCTCTTTGACCAGTTCTTCGGAGAGCACCTGTTGGAGTCTGATCTTTTCCCG 142

Query 137  ACGTCTACTTCCCTGAGTCCCTTCTACCTTCGGCCACCCTCCTTCCTGCGGGCACCCAGC 196
          ||||||||||||||||||||||||||||||||||||||||||||||||||||||||
Sbjct 143  ACGTCTACTTCCCTGAGTCCCTTCTACCTTCGGCCACCCTCCTTCCTGCGGGCACCCAGC 202

Query 197  TGGTTTGACACTGGACTCTCAGAGATGCGCCTGGAGAAGGACAGGTTCTCTGTCAACCTG 256
          ||||||||||||||||||||||||||||||||||||||||||||||||||||||||
Sbjct 203  TGGTTTGACACTGGACTCTCAGAGATGCGCCTGGAGAAGGACAGGTTCTCTGTCAACCTG 262

Query 257  GATGTGAAGCACTTCTCCCCAGAGGAACTCAAAGTTAAGGTGTTGGGAGATGTGATTGAG 316
          ||||||||||||||||||||||||||||||||||||||||||||||||||||||||
Sbjct 263  GATGTGAAGCACTTCTCCCCAGAGGAACTCAAAGTTAAGGTGTTGGGAGATGTGATTGAG 322

Query 317  GTGCATGGAAAACATGAAGAGCGCCAGGATGAACATGGTTTCATCTCCAGGGAGTTCCAC 376
          ||||||||||||||||||||||||||||||||||||||||||||||||||||||||
Sbjct 323  GTGCATGGAAAACATGAAGAGCGCCAGGATGAACATGGTTTCATCTCCAGGGAGTTCCAC 382

Query 377  AGGAAATACCGGATCCCAGCTGATGTAGACCCTCTCACCATTACTTCATCCCTGTCATCT 436
          ||||||||||||||||||||||||||||||||||||||||||||||||||||||||
Sbjct 383  AGGAAATACCGGATCCCAGCTGATGTAGACCCTCTCACCATTACTTCATCCCTGTCATCT 442

Query 437  GATGGGGTCTCACTGTGAATGGACCAAGGAAACAGGTCTCTGGCCCTGAGCGCACT*ATT 496
          ||||||||||||||||||||||||||||||||||||||||||||||||||||||||
Sbjct 443  GATGGGGTCTCACTGTGAATGGACCAAGGAAACAGGTCTCTGGCCCTGAGCGCACC*ATT 502

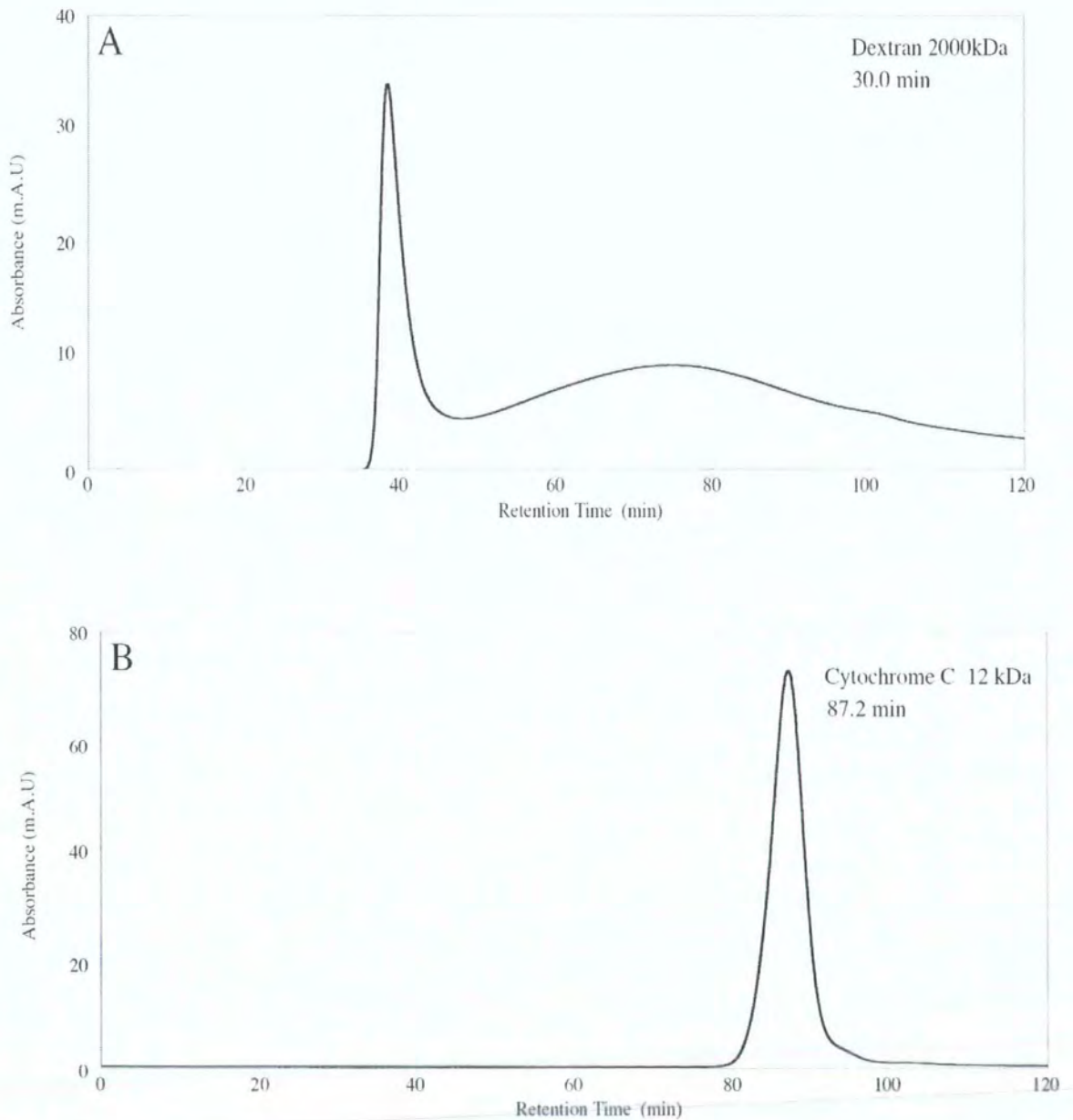
Query 497  CCCATCACCCGTGAATAGAAGC 518
          |||||||||||
Sbjct 503  CCCATCACCCGTGAAGGAGAAGC 524
  
```

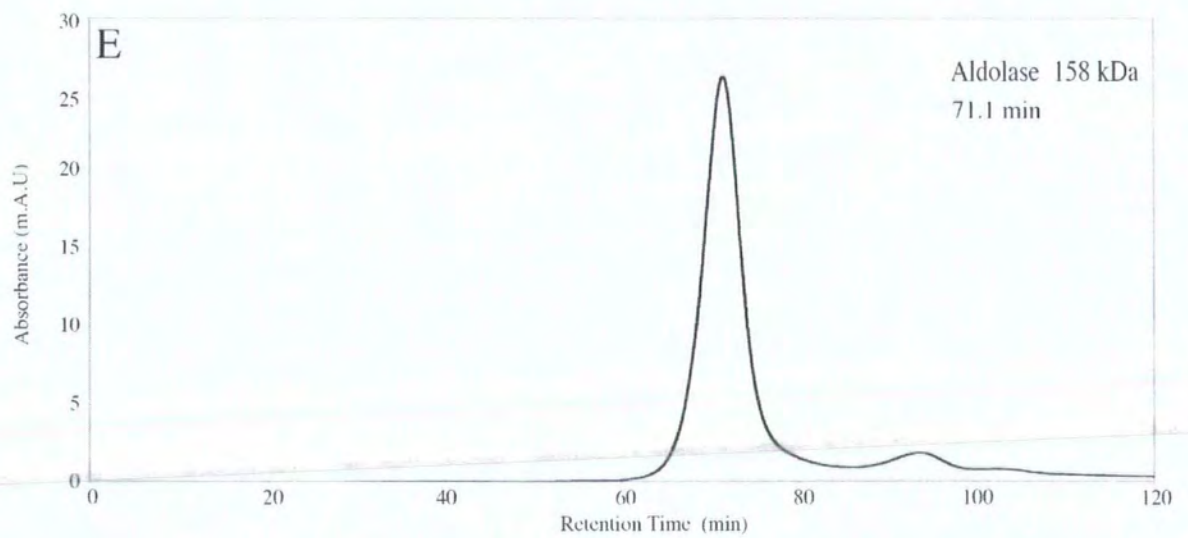
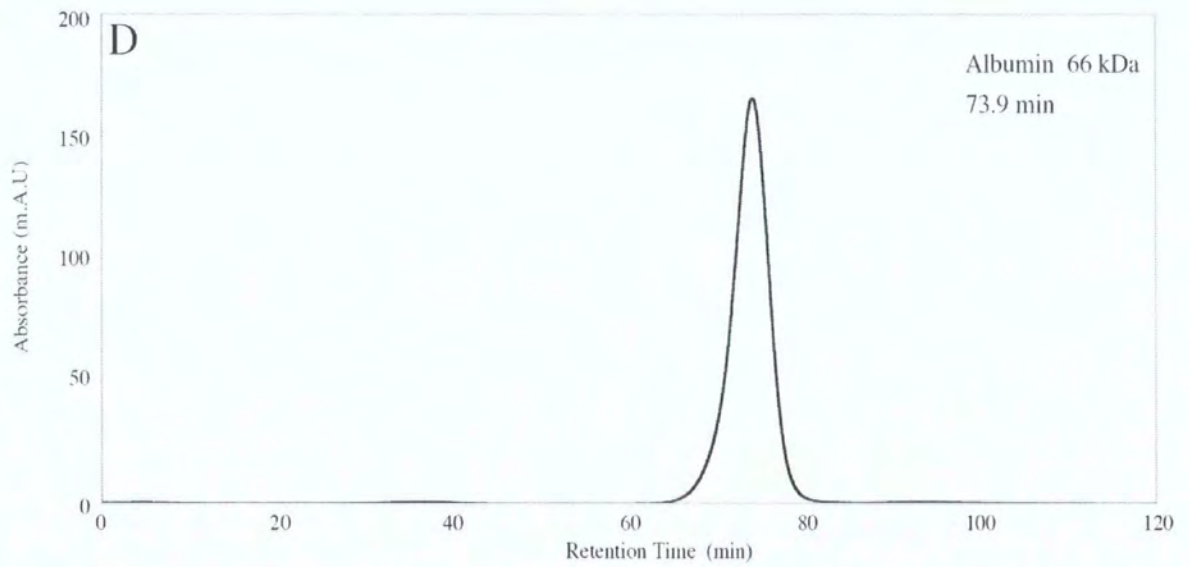
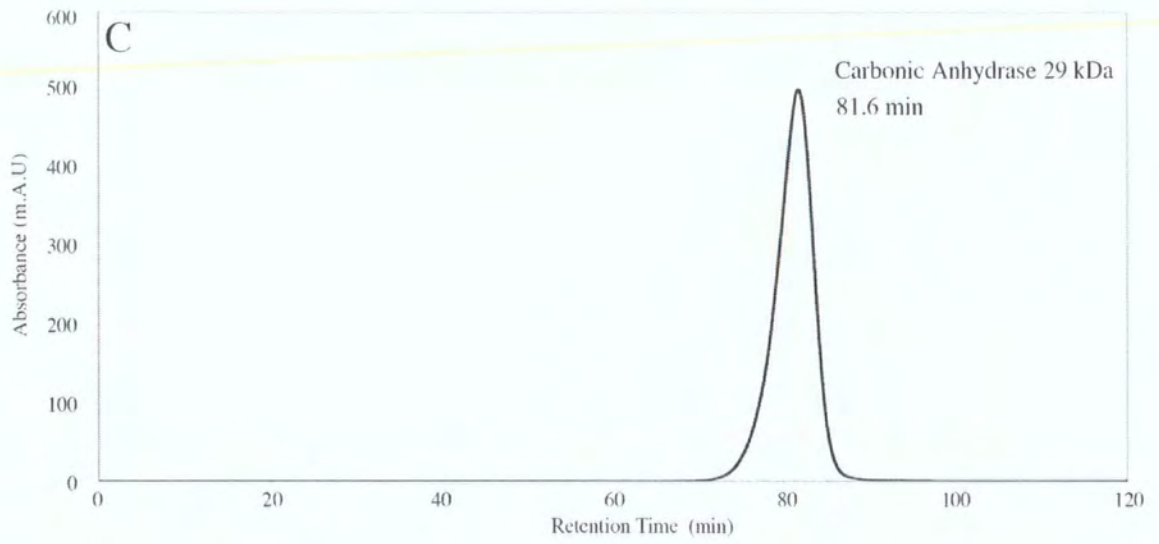
APPENDIX 2

CALIBRATION OF ANALYTICAL SEC COLUMN AND MOLECULAR WEIGHT DETERMINATION OF α B-CRYSTALLIN MUTANTS FOR CHAPTER 4 (SECTION 4.3.1).

A2.1 CALIBRATION OF SUPEROSE 6 ANALYTICAL SEC COLUMN

The SEC calibrator profiles are shown in Figure A2.1 (A-H). The retention times were used to generate a calibration curve (see Figure A2.2), from which the Mwt of each α B-crystallin mutant was calculated, (see Chapter 4.3.1, Table 4.2).





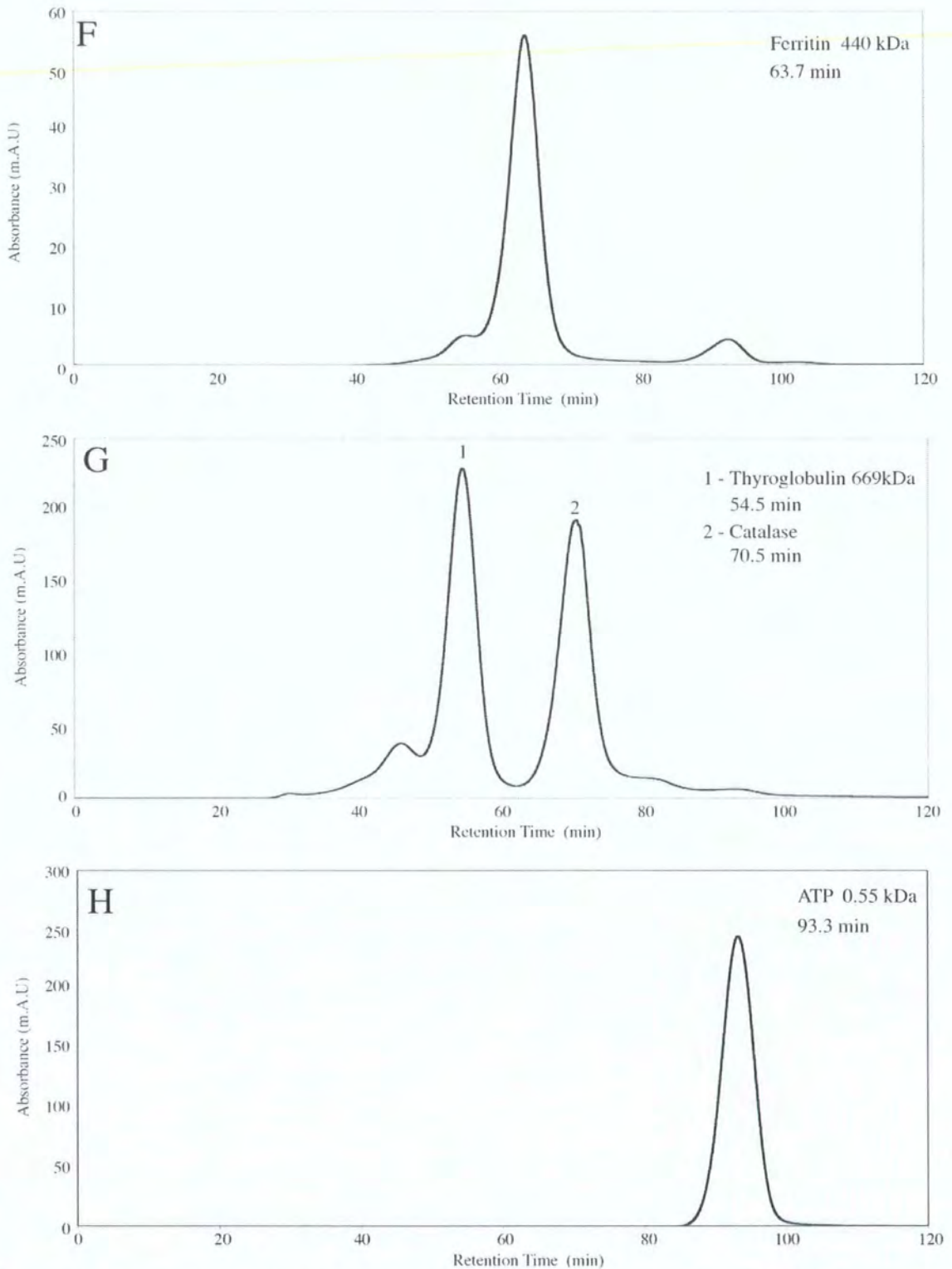


Figure A2.1 The SEC calibrator profiles for calibration of the analytical SEC column. A range of calibrators, from the low Mwt Cytochrome C at 12 kDa (B), to the high Mwt Thyroglobulin at 669 kDa (G). The void volume of the SEC column was determined using Dextran at 2000 kDa (A). The separation range of the column was determined using ATP (H).

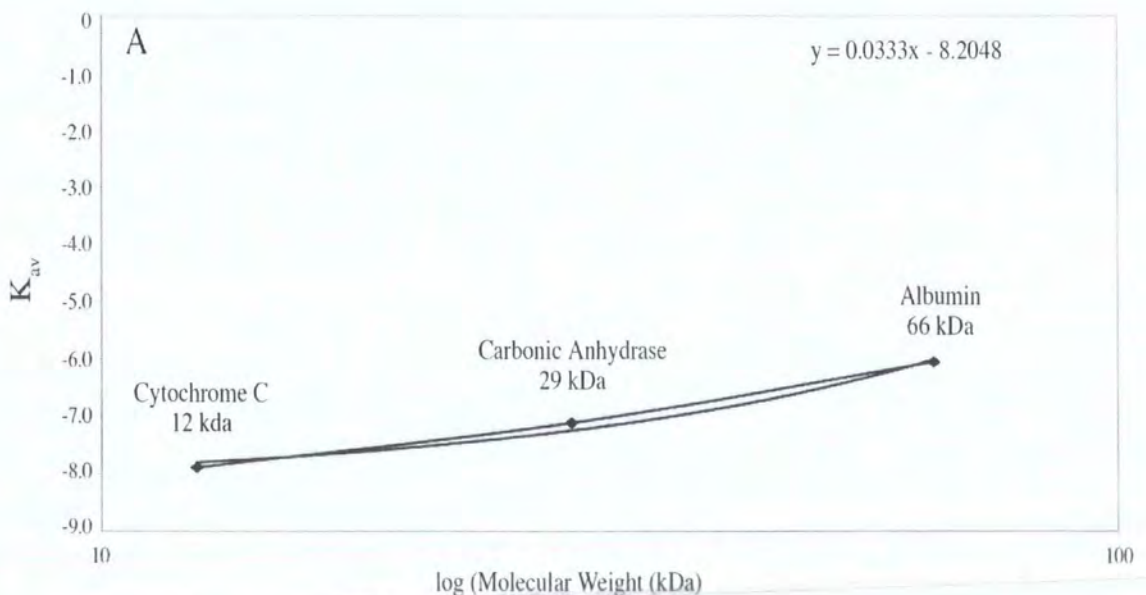
A2.2 MOLECULAR WEIGHT DETERMINATION OF α B-CRYSTALLIN MUTANTS

A calibration curve of K_{av} versus log molecular weight was prepared using the data from Figure A2.1 and the following equation:

$$K_{av} = \frac{V_e - V_o}{V_c - V_o}$$

Where V_e = elution volume as retention time, V_o = column void volume, V_c = geometric column volume.

Separate calibration curves of low Mwt calibrators (see Figure A2.2.A) and high Mwt calibrators (see Figure A2.2.B) were prepared to allow accurate Mwt determination for α B-crystallin mutants with retention times at both the low and high range of calibration.



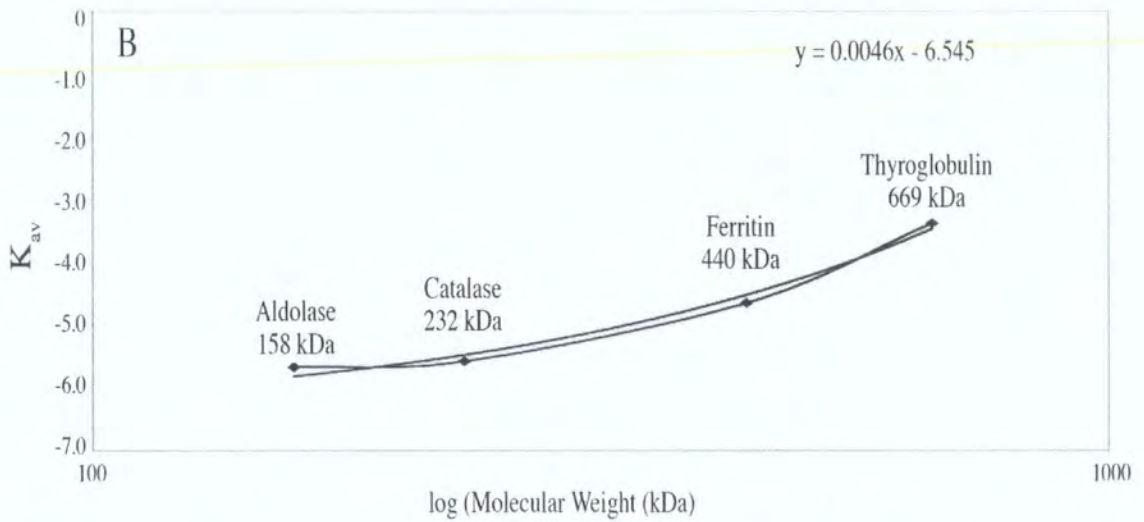


Figure A2.2. SEC calibration curves for Mwt determination. The calibration curves of low Mwt calibrators (A) and high Mwt calibrators (B) are shown with a linear trendline. The equations required for calculations of unknown Mwt α B-crystallin mutants at both the low range (A) and high range (B) are shown.

The α B-crystallin mutants Mwt were calculated, using the appropriate curve for the resulting retention time. For example, for mutants with retention times between 30–72 min the high Mwt calibration curve was used and retention times between 72–93 min the low Mwt calibration curve was used (see Chapter 4, Section 4.3.1).

APPENDIX 3

CHAPERONE ASSAY DATA SETS FOR CHAPTER 4

(SECTION 4.3.4)

A3.1 CITRATE SYNTHASE ASSAY TRIPLICATE DATA SETS FOR FIGURE 4.7

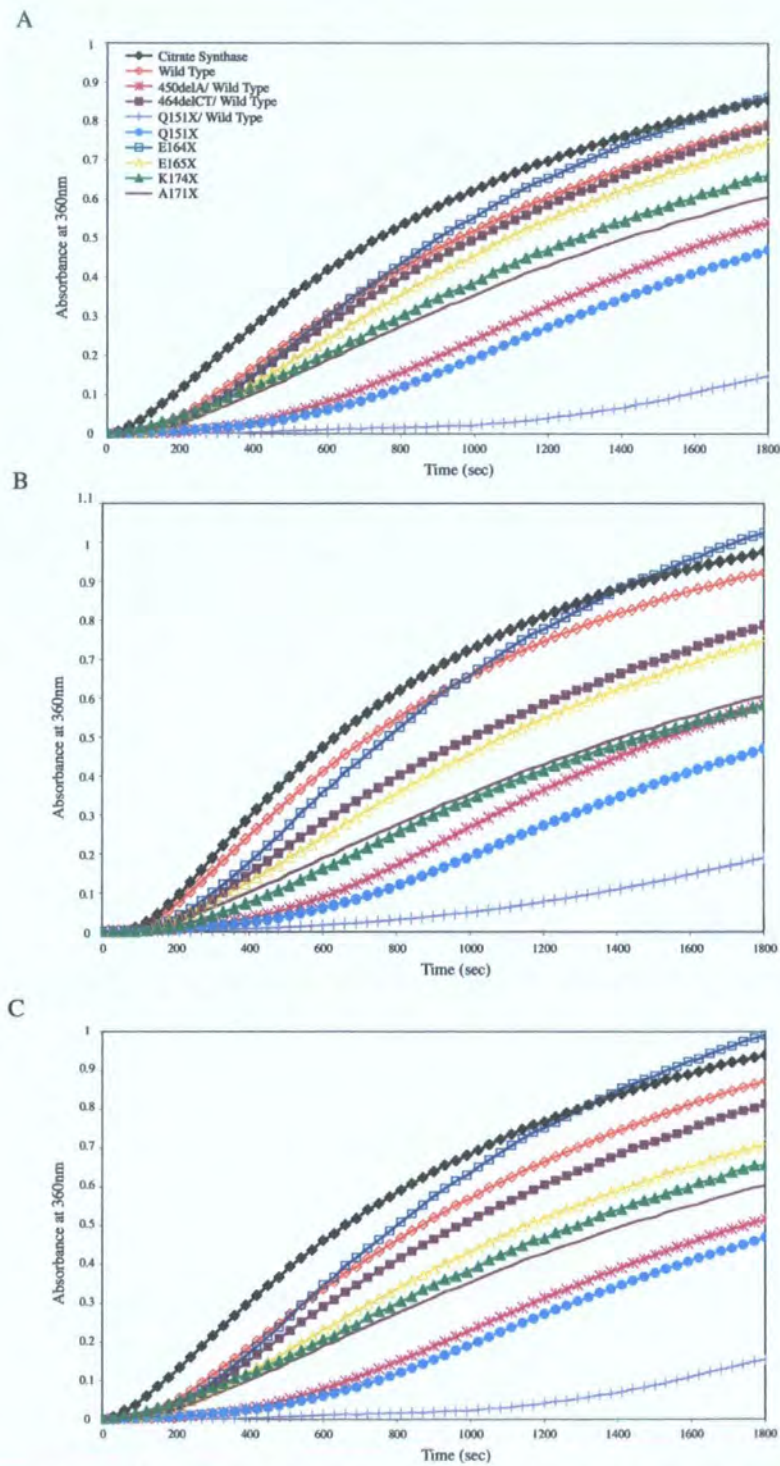


Figure A3.1. Triplicate data set of Citrate synthase assays. The three data sets were averaged to produce Figure 4.7A and B

Table A3.1. Inhibition data for the Citrate Synthase assay. The percentage inhibition for assays A, B and C from Figure A3.1 A, B and C respectively, are detailed with the subsequent average and standard deviations used in Figure 4.7B.

α B-crystallin	Inhibition (%)			Standard Deviation	Average Inhibition (%)
	Assay A	Assay B	Assay C		
Wild Type	100%	100%	100%	0%	100%
450delA/ Wild Type	525%	719%	632%	97%	625%
464delCT/ Wild Type	113%	347%	188%	119%	216%
Q151X/ Wild Type	1181%	1437%	1172%	150%	1263%
Q151X	641%	924%	702%	149%	755%
E164X	-11%	-86%	-75%	40%	-57%
E165X	178%	418%	342%	123%	313%
K174X	327%	717%	423%	203%	489%
A171X	416%	678%	501%	134%	532%

A3.2 INSULIN ASSAY TRIPLICATE DATA SETS FOR FIGURE 4.8

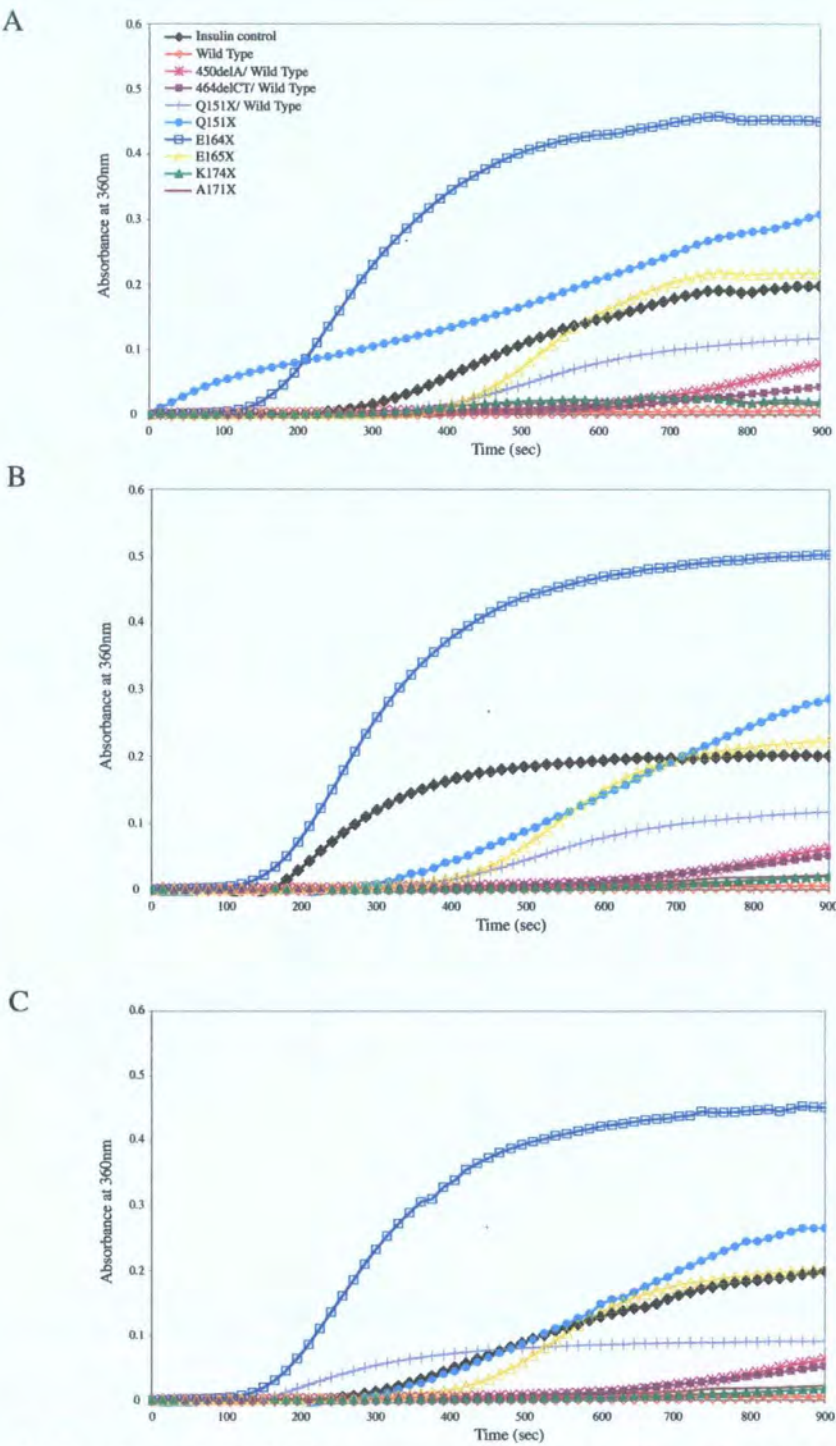


Figure A3.2. Triplicate data set of Insulin assays. The three data sets were averaged to produce Figure 4.8A and B.

Table A3.2. Inhibition data for the Insulin assay. The percentage inhibition for assays A, B and C from Figure A3.2 A, B and C respectively, are detailed with the subsequent average and standard deviations used in Figure 4.8B.

α B-crystallin	Inhibition (%)			Standard Deviation	Average Inhibition (%)
	Assay A	Assay B	Assay C		
Wild Type	100%	100%	100%	0%	100%
450delA/ Wild Type	62%	71%	70%	5%	68%
464delCT/ Wild Type	81%	76%	76%	2%	78%
Q151X/ Wild Type	42%	43%	56%	8%	47%
Q151X	-57%	-44%	-34%	11%	-45%
E164X	-131%	-154%	-130%	14%	-138%
E165X	-10%	-12%	-1%	6%	-8%
K174X	93%	92%	94%	1%	93%
A171X	95%	92%	92%	2%	93%

APPENDIX 4

CHARACTERISATION OF THE NATURE OF THE 93 MIN

PEAK RESOLVED DURING ANALYTICAL SEC OF

α B-CRYSTALLIN FOR CHAPTER 6 (SECTION 6.3.1).

A4.1 THE NATURE OF THE 93 MIN PEAK MATERIAL

The investigation of the effect of α B-crystallin concentration upon oligomerisation involved the use of a Superose 6 SEC column with a Merck Hitachi HPLC system with injection valve. Initial experiments identified a peak, which appeared consistently at the end of the 93.3 min separation range of the column but showed variations in peak heights. Blank runs with various buffers including Tris, ammonium acetate and sodium phosphate all identified the 93 min peak, confirming it was not caused by a buffer component.

The potential interaction of α B-crystallin with the column matrix was assessed by using the SEC protocol shown in Figure 5.1 under conditions of 1M NaCl (see Figure A4.1). This involved SEC analysis of 500 μ g wild type α B-crystallin at 2 mg/ml to isolate the oligomeric species, which was then reinjected onto the SEC for subsequent analysis. This was repeated for a total of four cycles to allow the identification of any 93 min peak material. This data also provided a comparable data set for the effect of α B-crystallin concentration upon oligomerisation shown in Figure 5.1.

Figure A4.1 confirms that the high ionic strength does not prevent the presence of the 93 min peak, which is present in all four cycles of SEC. The oligomer peak in cycle 4 shifted slightly indicated by a larger retention time similar to the shift shown in Figure 5.1. The wild type α B-crystallin also appears more polydisperse in cycle 3 (approx 0.1 mg/ml) (see Figure A4.1C), which is similar to the polydispersity shown in Figure 5.1C.

The peak height of the 93 min peak is variable and is not proportional to the amount of α B-crystallin applied as the 93 min peak in cycle 4 (approx 0.01 mg/ml) has a height of 0.524 mA.U compared to 0.296 mA.U. observed in cycle 2 (approx 0.5 mg/ml) (see Table A4.1).

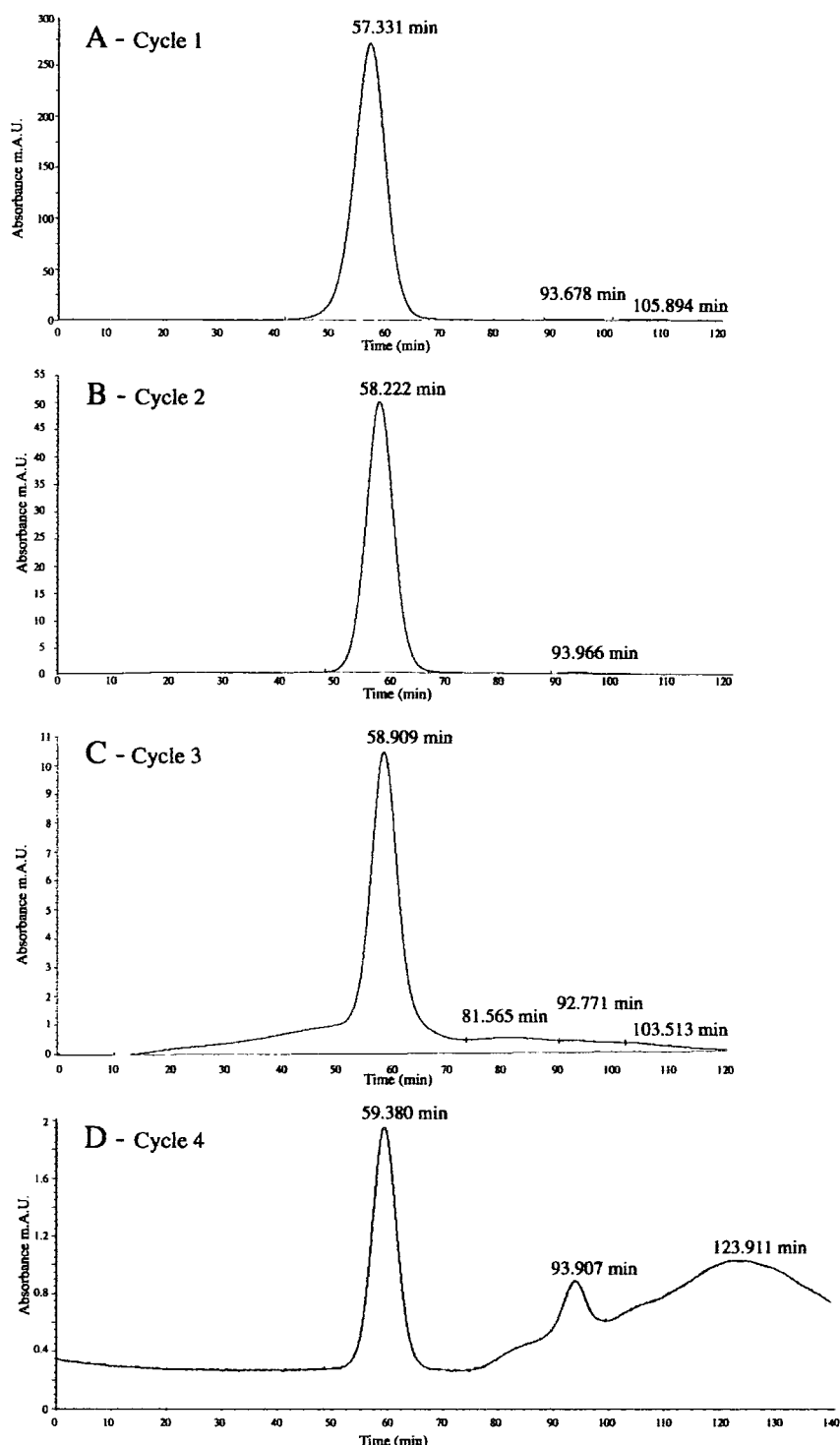


Figure A4.1. The effect of decreasing concentration upon the oligomerisation of wild type α B-crystallin under conditions of 1M NaCl. Wild type α B-crystallin at 2 mg/ml was analysed by analytical SEC (A) and the fraction collected between 55-60 min was recycled over the SEC column for a further 3 cycles (B-C) in order to see the effect of dilution upon the oligomerisation characteristics. The SEC were performed in 1M NaCl in order to determine whether the presence of the 93 min peak was a product of hydrophobic interactions with the column matrix.

Table A4.1. Integration data for Figure A4.1.

Cycle	Time (min)	Height (mA.U)	Peak Area (%)
Cycle 1	57.331	271.505	99.68
	93.678	0.734	0.22
	105.894	0.299	0.1
Cycle 2	58.222	49.503	99.57
	93.966	0.296	0.43
Cycle 3	58.909	9.754	84.91
	81.565	0.505	7.64
	92.771	0.39	4.21
	103.513	0.305	3.24
Cycle 4	59.38	1.683	31.74
	93.907	0.524	15.85
	123.911	0.519	52.41

With the consistent appearance of the 93 min peak, the question still remaining was whether the 93 min peak was in fact α B-crystallin and was due to increased subunit dynamics induced by decreasing α B-crystallin concentration.

The presence of the 93 min peak in blank runs of the α B-crystallin solvent (10mM Tris-HCl, 1mM EGTA, 5mM EDTA, 150mM NaCl, pH7.5 and in blank runs of 0.2M ammonium acetate and 10mM sodium phosphate, pH7.0 suggest that it is not caused by buffer components, therefore could it be due to α B-crystallin carry over in between runs.

In order to determine the nature of the 93 min peak, the SEC column was sanitised and underwent extensive equilibration for 72 h, after which 5 consecutive blank runs were performed prior to separation of the wild type α B-crystallin (2 mg/ml) (pre α B-crystallin blanks). Following separation a further blank was performed (post α B-crystallin blank) and the appropriate fractions encompassing the 93 min peak were probed for α B-crystallin (see Figure A4.2). The first blank shows the greatest peak height of 2.5 mA.U (see Figure A4.2A, Table A4.2) following the equilibration, and declines to a consistent

height of approx 0.15 mA.U for blanks 2-5 (see Figure A4.2B-E, Table A4.2). On application of wild type α B-crystallin (see Figure A4.2F) the peak height is 2.2 mA.U and there is an additional peak resolved at 100.6 min, which is similar to blank 5 which also showed a peak of retention time of 103.5 min. The post wild type blank (see Figure A4.2G) also shows the two peaks and the 93 min peak has a peak height of 0.2 mA.U. The 93 min peak fractions from all the blanks and the wild type SEC were probed for the presence of α B-crystallin, along with the oligomer peak produced in Figure A4.2F. Figure A4.2H (lanes 2-6) showed that there was no α B-crystallin in the 93 min peak material for blanks 1-5 (see Figure A4.2A-E). The α B-crystallin present in the oligomer peak was represented by a strong band in lane 7, and fractions encompassing 90-105 min (lanes 8-10 respectively) clearly indicate the presence of α B-crystallin as do 90-105 min fractions for the post wild type blank (lanes 11-13 respectively). The interesting point is that although blank 1 has a greater peak height of 2.5 mA.U compared to 2.2 mA.U for the wild type 93min peak, there is no α B-crystallin signal. The post wild type blank (lanes 11-13) with a peak height of 0.2 mA.U (see Figure A4.2G), despite being a tenth of the size of the 93 min peak in blank 1 shows a weak α B-crystallin signal. Therefore, it seems that the 93 min peak is not representative of protein, as it is consistently in blanks where there is no protein present in the system. The size of the 93 min peak also shows random variability in peak height independent to the type of mobile phase in use, therefore suggest that it is a function of the instrument and not biological in nature. The presence of α B-crystallin in fractions 90-105 min (see Figure A4.3H, lanes 8-10) confirms that there is the presence of a low molecular weight α B-crystallin complex past the separation range of the column, however it is not represented by the 93 min peak resulting from the Absorbance

data. The calibrated SEC column gives a retention time of 87.2 min for 12 kDa Cytochrome C (see Appendix 2).

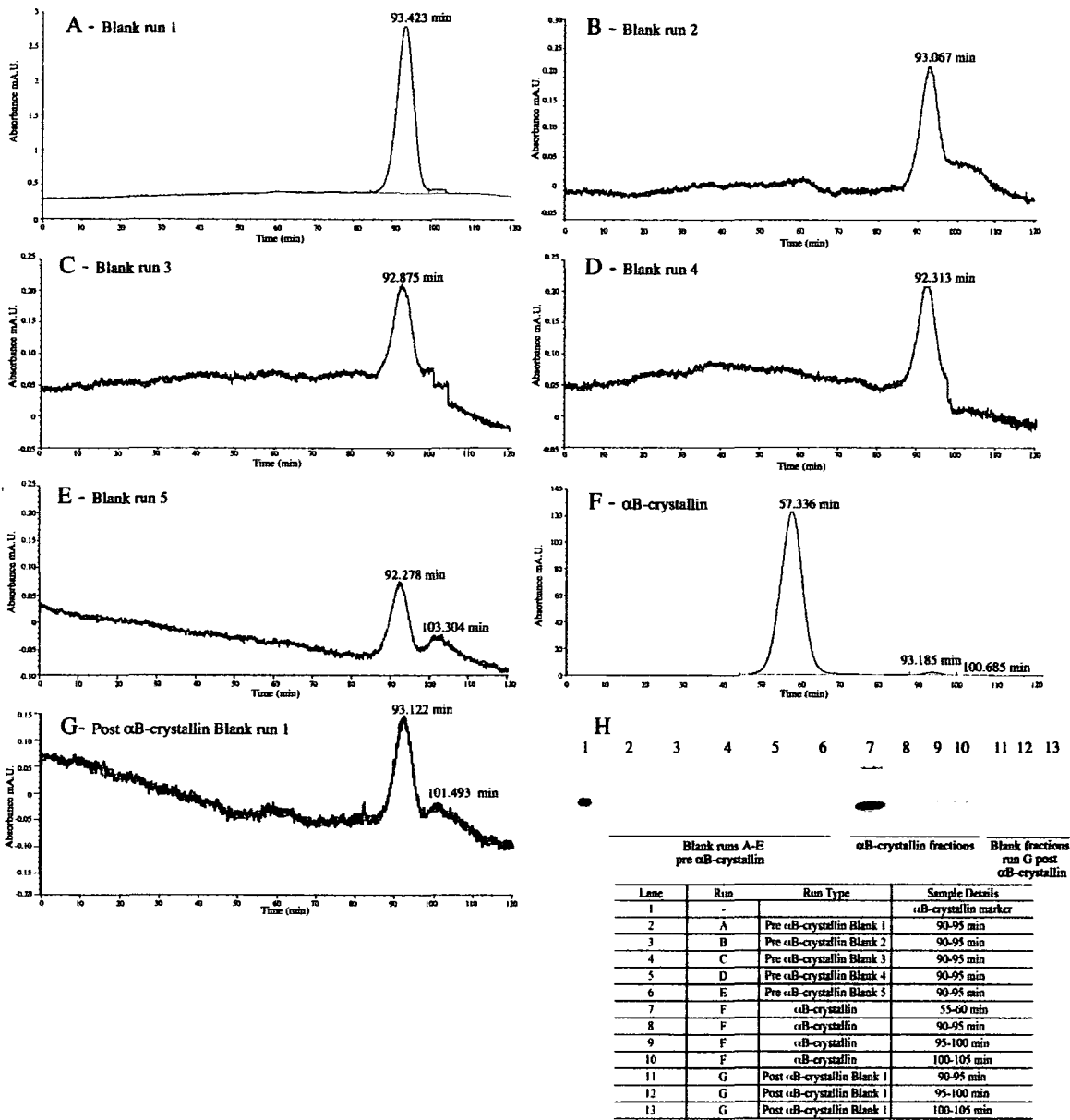


Figure A4.2. Analysis of the 93 min peak of the Superose 6 SEC analytical column. A total of 5 blanks runs (A-E) were performed prior to analysis of the wild type αB-crystallin (F) using 10mM Tris-HCl, 1mM EGTA, 5mM EDTA, 150mM NaCl, pH7.5. A post wild type blank was performed (G). Appropriate fractions were probed for αB-crystallin (H).

Table A4.2. Relative peak heights of 93 min peaks from Figure A4.2

Run	Peak height (mA.U)
Blank 1	2.50
Blank 2	0.22
Blank 3	0.15
Blank 4	0.16
Blank 5	0.15
Wild type α B-crystallin	2.20
Post wild type Blank 1	0.20

The 93 min peak appears to be a function of the HPLC instrument, and the point at which irregularities could most likely be introduced would be the injection valve. Therefore, the effect of the injection valve upon the presence of the peak was investigated (see Figure A4.3). A blank run was performed with and without physical injection of buffer (see Figure A4.3A and B respectively). The blank run without injection showed a steady decline of A280 over the 120 min time course, however once the injection was introduced the 93 min peak was again evident. There was no α B-crystallin present in the 93 min peak of the blank (see Figure A4.3D, lanes 4-6) as confirmed by immunoblotting, but was obvious in the equivalent fractions for the wild type α B-crystallin (see Figure A4.3D, lanes 8-10). This result was reproducible for alternative injection valves.

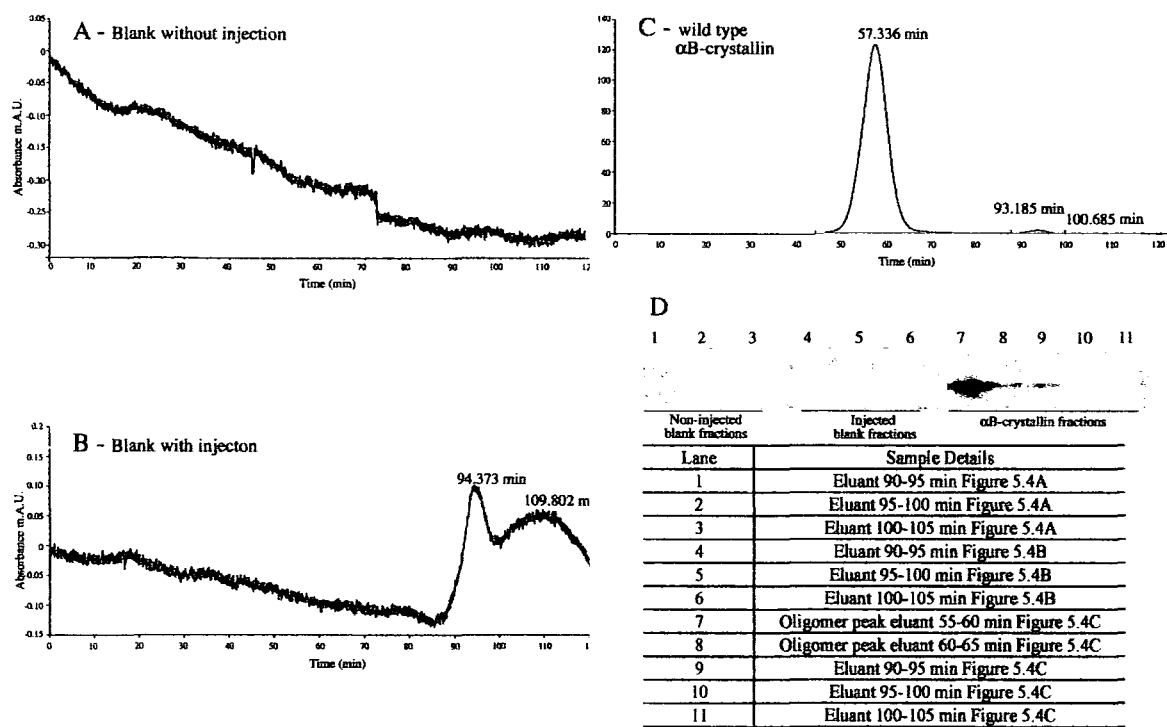


Figure A4.3. The effect of the injection upon the presence of the 93 min peak. A blank run was performed without injection (A) by turning of the valve and a second blank was injected (B). The wild type α B-crystallin was analysed (C) and fractions from the runs A-C were probed for α B-crystallin (D). Both blanks show no evidence of α B-crystallin despite the peak height of the 93 min peak for run B being above the level of sensitivity required for immunoblotting detection. The presence of α B-crystallin in 90-105 min fractions is evident in lanes 8-10 (D).

Therefore, I can conclude that the 93 min peak is an artefact introduced by injection of sample into the injection valve and interferes with the UV detection because of the level of sensitivity at which the experiments are performed. The immunoblotting of SEC fractions of wild type α B-crystallin show that there was resolution of an unknown α B-crystallin species past the separation range of the column.

APPENDIX 5

DEVELOPMENT OF AN α B-CRYSTALLIN ELISA ASSAY

FOR THE DETECTION AND QUANTITATION OF SEC

FRACTIONS FROM CHAPTER 5

A5.1 DEVELOPMENT OF AN α B-CRYSTALLIN ELISA

The development of this assay was carried with the help and support of ImmunoDiagnostics Limited. The development aimed to produce a sandwich assay rather than a competitive assay, where two antibodies bind to epitopes that do not overlap on the antigen. This can be accomplished with either two monoclonal antibodies that recognise discrete sites or one batch of affinity purified polyclonal antibodies or one monoclonal and one polyclonal antibody for the same antigen.

The capture antibody is bound to the solid phase, after which the antigen is added and allowed to complex with the bound antibody. The detection antibody, conjugated to an enzyme completes the sandwich and the assay is quantitated by measuring the amount of labelled detection antibody bound to the matrix through the use of a colourimetric substrate.

The major advantage of this format is that the antigen does not require prior purification and the assays are very specific, however not all antibodies can be used. Monoclonal antibody combinations must be qualified as matched pairs meaning they can recognise separate epitopes on the antigen so they do not hinder each other's binding. (Chemicon Technical information-Introduction to Antibodies-ELISA <http://www.chemicon.com/resource/ANT101/a2C.asp>). The assay format is illustrated in Figure A5.1.

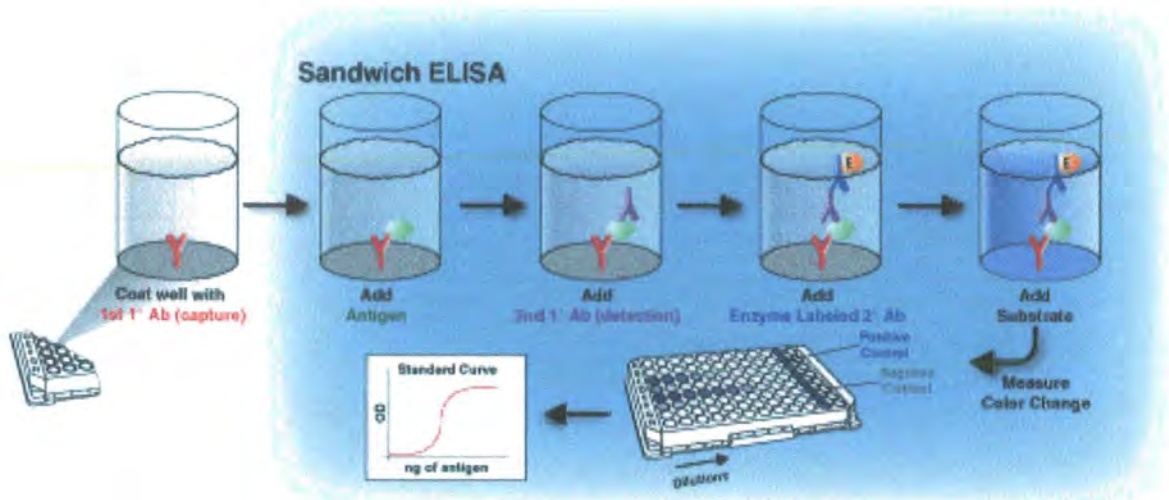


Figure A5.1. A typical sandwich ELISA assay. The capture antibody is bound to the microtitre plate well and complexed with the antigen. The antigen is quantitated using a second antibody labelled with enzyme for detection using a colourimetric substrate. (Figure taken from Chemicon Technical information-Introduction to Antibodies –ELISA <http://www.chemicon.com/resource/ANT101/a2C.asp>)

In order to develop a highly sensitive and reliably accurate ELISA, a series of optimisation experiments were performed looking at a number of criteria. These conditions can be separated into five categories:

- (I) Assay type, including the simultaneous assay, where the antigen and conjugate are simultaneously placed in contact with the antibody. The second assay was the split assay, which typically is of greater sensitivity as the antigen is incubated with the antibody prior to addition of the conjugate and both components are present in twice the volume as those seen in the simultaneous assay simply due to the limitations of well size.
- (II) Coating antibody, Both the α B-crystallin Mab and Pab were coated onto 96-well plates to allow analysis of both combinations
- (III) Conjugated antibody, Both the α B-crystallin Mab and Pab were conjugated to analyse the quality of α B-crystallin detection with both combinations

- (IV) Type of conjugate, Both Biotinylation and HRP conjugation were carried out with both the Mab and the Pab to investigate the best assay combinations.
- (V) Concentration of plate coat antibody, two sets of plates for each antibody were prepared at 2 and 5 mg/L to optimise the sensitivity of the assay.

Optimisation of the assay conditions and of the combinations of the different assay components were aiming to produce a high quality reliable and sensitive α B-crystallin ELISA.

A5.1.1 Purification and conjugation of α B-crystallin Mab and Pab

The culture and harvest of Hybridoma cells, expressing α B-crystallin Mab 2D2B6 clone of α B-crystallin produced 180 ml of cell supernatant, which was subsequently purified on a PROSEP® G Affinity chromatography column (10 x 100mm Omnifit). The amount of purified Mab recovered was 20.1 mg (determined by A280), however losses occurred following the spin concentration to 1 mg/ml, resulting in a final yield of 14.5 mg.

The α B-crystallin Pab was a rabbit polyclonal antibody, clone 3148 generated to the C-terminal decapeptide KPAVTAAPKK. A 1ml aliquot was purified by ammonium sulphate precipitation and PD-10 purification resulting in 6.6 mg at a stock concentration of 1 mg/ml.

For ELISA development, both Biotin and HRP conjugates of the Mab were to be prepared. Biotinylated and HRP conjugated Mab were produced at a stock concentration of 25 μ g/ml.

A5.1.2 Titration of α B-crystallin Mab and Pab HRP conjugates

In order to find the optimal conditions for α B-crystallin detection and quantitation a titration of α B-crystallin Mab and Pab HRP conjugates from 125ng/ml to 1000ng/ml was performed. The antigen used was purified α B-crystallin wild type, which was used to produce a calibration curve ranging from 0-100 ng/ml. Other variables used are the concentration of antibody coated on the plate, (2mg/L and 5mg/L) and the type of capture antibody (Mab or Pab α B-crystallin). The final variable was the type of ELISA utilised, (Split or simultaneous assay).

In order to investigate the success of the assay under all the conditions, 8 assays were carried out and included:

- Assay 1: Simultaneous assay - Mab capture (2 g/L)-Pab:HRP detection
- Assay 2: Simultaneous assay - Mab capture (5 g/L)- Pab:HRP detection
- Assay 3: Split assay - Mab capture (2 g/L)- Pab:HRP detection
- Assay 4: Split assay - Mab capture (5 g/L)- Pab:HRP detection
- Assay 5: Simultaneous assay - Pab capture (2 g/L)- Mab:HRP detection
- Assay 6: Simultaneous assay - Pab capture (5 g/L)- Mab:HRP detection
- Assay 7: Split assay - Pab capture (2 g/L)- Mab:HRP detection
- Assay 8: Split assay - Pab capture (5 g/L)- Mab:HRP detection

The results for the Pab HRP detection are shown in Figure A5.2 and for Mab HRP detection in Figure A5.3.

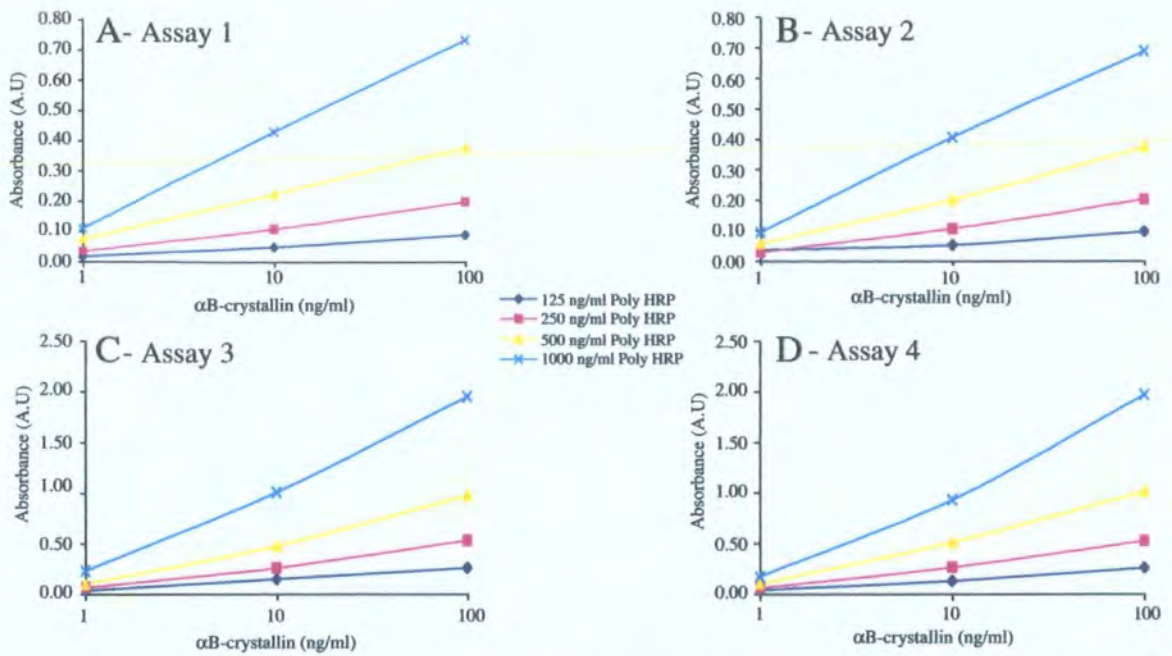


Figure A5.2. Titration Pab HRP conjugates on plates with 0-100 ng/ml α B-crystallin. Assay 1 and 2 (A and B respectively) are simultaneous assays using Mab capture and Pab: HRP detection with 2 g/L (A) or 5 g/L (B) capture antibody. Assay 3 and 4 (C and D respectively) are split with 2 g/L (C) or 5 g/L (D) capture antibody.

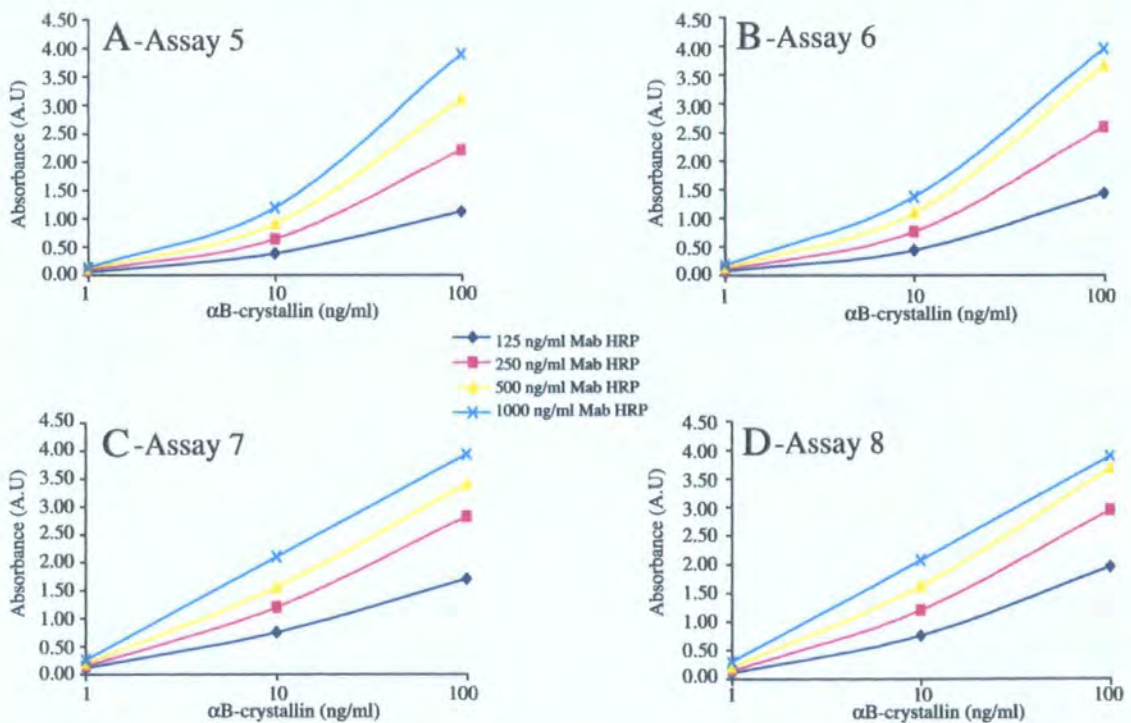


Figure A5.3. Titration of Mab HRP conjugates on plates with 0-100 ng/ml α B-crystallin. Assay 5 and 6 (A and B respectively) are simultaneous assays using Pab capture and Mab: HRP detection with 2 g/L (A) or 5 g/L (B) capture antibody. Assay 7 and 8 (C and D respectively) are split with 2 g/L (C) or 5 g/L (D) capture antibody.

The relative signal achieved using the 2 mg/L and 5 mg/L capture antibody concentration is comparable for assays using the same conjugate. Figures A5.3A and C at 2 g/L compared with Figure A5.2 B and D at 5 g/L, illustrate the similarities in signal between the split and simultaneous assay where the 1000 ng/ml Poly HRP achieves an A.U value of approx 0.75 A.U. This pattern is also observed for the Mab HRP titration (see Figure A5.3), however, the 1000 ng/ml Mab HRP achieves a signal of approx 4.0 A.U suggesting that using the Pab as a capture antibody produces an assay of significantly greater sensitivity than the Mab capture antibody. Utilising the split assay can increase the sensitivity of the Mab capture assay from 0.75 A.U to approx 2.0 A.U (see Figure A5.2 C and D), however still remains significantly lower in sensitivity to the Pab capture assay (see Figures A5.3C and D). Additionally, the Mab capture also results in a relatively higher level of non-specific binding confirmed by similar A.U values for the 0 ng/ml and 1 ng/ml α B-crystallin.

So far the optimisation had identified the 2 g/L Pab capture as the most sensitive assays for the α B-crystallin detection (see Figures A5.3 A and C). Assays 5 and 7 suggest the optimal level of Mab: HRP conjugate is 250 ng/ml in the simultaneous assay. This combination produces a signal range up to 2.0 A.U for detection of 100 ng/ml α B-crystallin. Any signal above 2.0 A.U cannot be considered as reliable data. The 125 ng/ml of Mab :HRP although providing a detection range under 2.0 A.U only achieves 1.0 A.U in the simultaneous assay (see Figure A5.3A) and 1.50 A.U in the split assay (see Figure A5.3C), thus not maximising the potential detection range. The simultaneous assay appears to be the optimal assay format, compared with the split assay where, a 250 ng/ml Mab: HRP signal achieves an output of 2.60 A.U for 100 ng/ml α B-crystallin detection thus is out of range. The split assay also shows a lower level of sensitivity for the detection of low concentrations of α B-crystallin between 1-10 ng/ml (see Figure A5.3C).

The optimised assay conditions for the detection of α B-crystallin at levels between 100ng/ml – 1.27ng/ml utilises a 2 mg/L Poly capture with a 250 ng/ml Mab: HRP conjugate detection in a Simultaneous assay.

A5.1.2.1 Initial assessment of relative sensitivity between Mab: HRP and Mab:Biotin detection of α B-crystallin

An initial assay was performed to assess the relative difference in sensitivity of the Mab: HRP and Mab: Biotin assays, by varying the Mab: Biotin concentrations whilst looking at various Avidin: HRP concentrations. This was aiming to give an initial assessment of the sensitivity achieved using biotinylated Mab (see Figure A5.4).

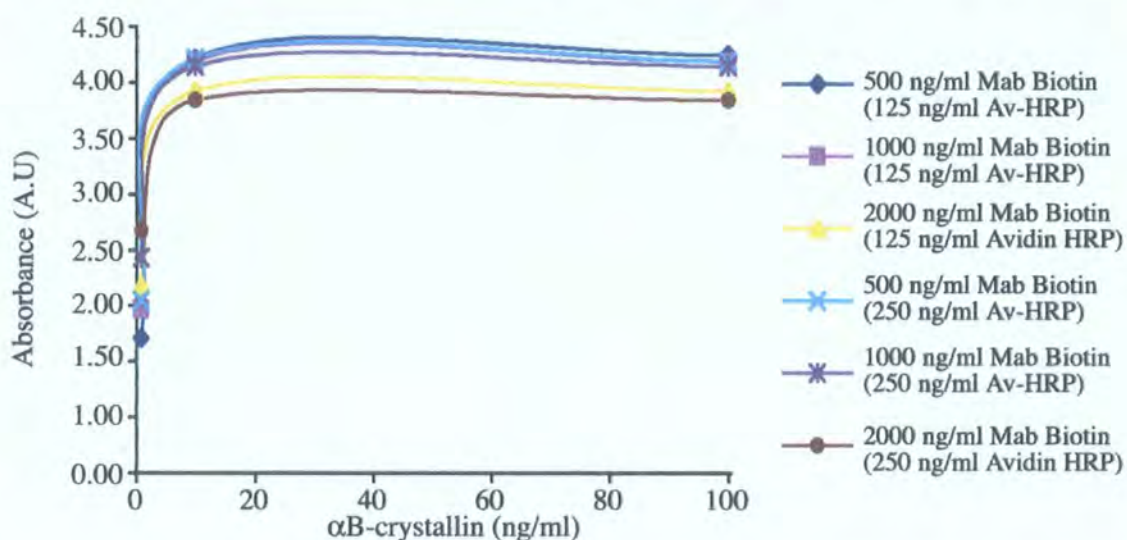


Figure A5.4. The specific signal of a Poly capture assay with titrated Mab Biotin and Av-HRP levels. To assess the relative sensitivity of Biotin conjugated Mab and HRP, this assay analysed 500 ng/ml-2000 ng/ml Mab Biotin at two levels of Av-HRP, 125 ng/ml and 250 ng/ml.

The Assay utilised a 2 mg/L Poly coated plate with the simultaneous assay method. The absorbance readings shown in Figure A5.4 are above 2.0 A.U suggesting the Mab: Biotin levels used are too high resulting in an assay with greater sensitivity than is required for detection of α B-crystallin. The variation of Avidin-HRP concentration does not significantly affect the signal achieved. Reduction of the Mab: Biotin concentration and utilisation of a 250 ng/ml Av-HRP solution where 50 % is unlabelled Avidin to 50% labelled Avidin HRP should result in a lower sensitivity of the assay.

This initial assessment of the Biotin sensitivity allowed the comparison of absorbance achieved with 500 ng/ml Mab Biotin (see Figure A5.4) and Mab HRP (see Figure A5.3A for 10ng/ml of α B-crystallin is 0.896A.U and 3.697A.U respectively. This

revealed that the Mab: Biotin assay has a four fold higher sensitivity than the Mab: HRP assay and would allow detection of analyte at levels below 10ng/ml. Further optimisation was required to test this hypothesis.

A5.1.2.2 Optimisation of Mab: Biotin concentration and α B-crystallin standard curve

Section 6.3.3 confirmed that the Mab: Biotin detection method results in a four fold increase in sensitivity for α B-crystallin relative to the Mab: HRP. Figure A5.4 showed that a 500 ng/ml Mab: Biotin concentration combined with 125 ng/ml Av-HRP produced a signal in strength that was greatly above the detection limit.

Therefore, further optimisation of the Mab: Biotin assay included titration of Mab: Biotin from 125ng/ml to 500ng/ml and also increased the standard range from 100ng/ml–1.27 ng/ml to 100 ng/ml–0.1 pg/ml in order to identify the lower limits of sensitivity of the Mab: Biotin assay. A compromise for the level of Avidin required for optimal α B-crystallin detection is a solution of 50% HRP labelled Avidin and 50% unlabelled Avidin to a final concentration of 250 ng/ml. These data are shown in Figure A5.5.

Figure A5.5A suggests that the Mab: Biotin assay is too sensitive for the detection of α B-crystallin at concentrations above 10ng/ml regardless of the Mab: Biotin concentration and above 6 ng/ml the 250 ng/ml Mab: biotin produces a signal greater than 2.0 A.U (see Figure A5.5B). At α B-crystallin concentrations below 1.0 ng/ml an appropriate calibration curve is evident (see Figure A5.5C).

The 500 ng/ml concentration of Mab: Biotin has a limiting affect on the assay resulting in a relatively low signal compared to the 125 ng/ml and the 250 ng/ml Mab: Biotin. The 250ng/ml Mab: Biotin achieves the optimal standard curve and allows detection of α B-crystallin in the range 6.0–0.10 ng/ml at 250ng/ml Mab: Biotin, (see Figure A5.5B and C).

The optimised assay conditions for the detection of α B-crystallin at levels between 6.0 ng/ml–0.1 ng/ml utilises a 2 mg/L Poly capture with a 250 ng/ml Mab: Biotin conjugate in association with Av/Av-HRP (50% labelled) detection of 250 ng/ml in a simultaneous assay.

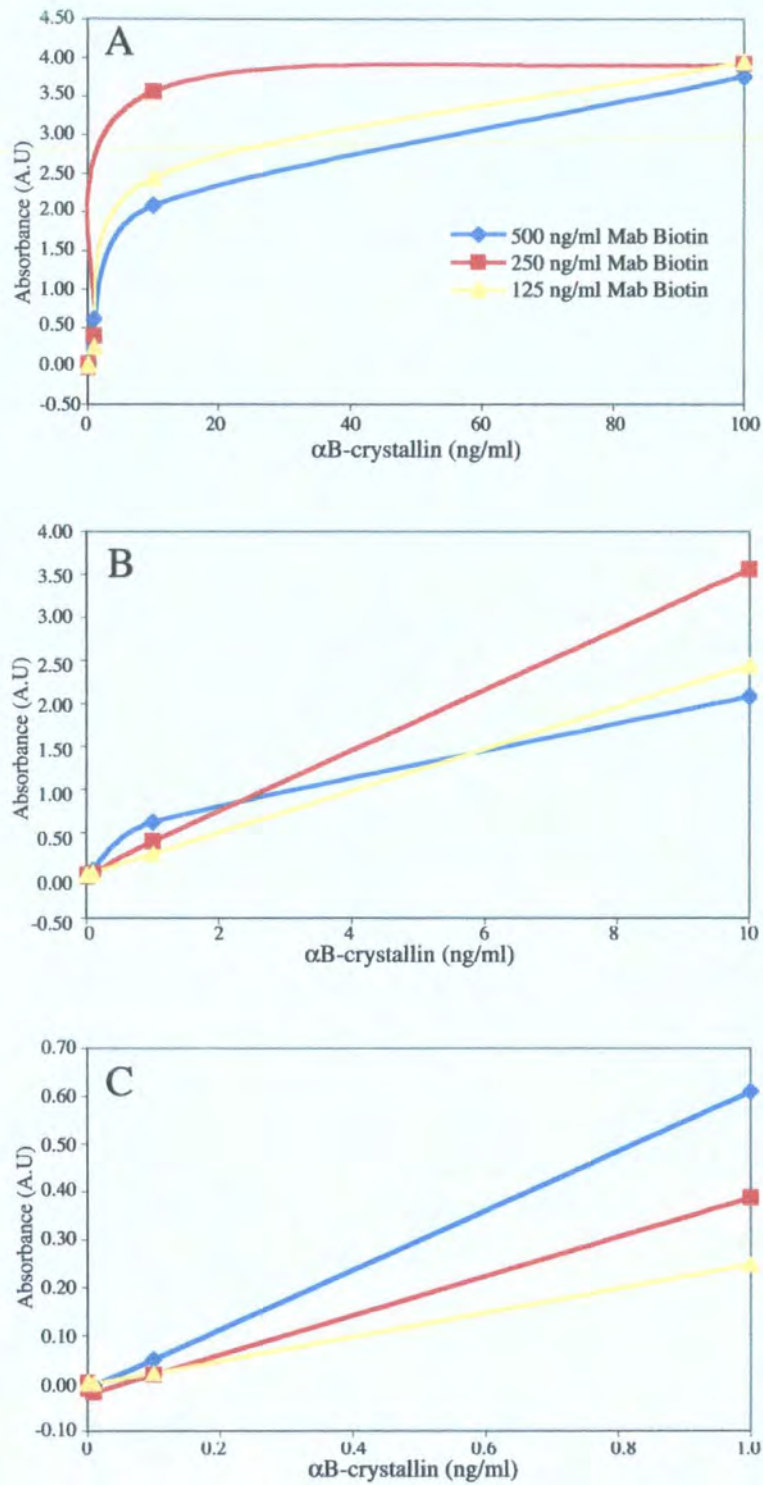


Figure A5.5. Optimisation of the α B-crystallin Mab Biotin Simultaneous ELISA. The Mab:Biotin concentrations of 125, 250 and 500 ng/ml were used with 250 ng/ml Av-HRP to assess the relative sensitivities of α B-crystallin detection. The lower limit of α B-crystallin that could be detected was investigated and the detected signal from 0.1-100 ng/ml (A), 0.1-10 ng/ml (B) and 0.1-1.0 ng/ml (C) showed that α B-crystallin at the pg level was accurately detected.

A5.1.3 The use of ELISA for potential quantification α B-crystallin protein isolated in SEC fractions

One of the aims of this chapter was to be able to develop a working α B-crystallin ELISA of greater sensitivity than immunoblotting to allow quantification of low level α B-crystallin in SEC fractions. Here I tested the ability of the ELISA to accurately quantify the presence of α B-crystallin in SEC fractions from a typical 500 μ g load on the 26 ml Superose 6 SEC column. I also investigated the appropriate dilutions for each stage of the SEC elution and subsequently depending on the sensitivity required, which Mab: conjugate was required.

A5.1.3.1 Quantification α B-crystallin in SEC fractions using Mab: HRP

A typical elution will result in the major oligomeric species at 57 min followed by an unknown low Mwt multimeric/monomeric species at approx as shown in Figure A5.6. Thus the dilutions required and most appropriate Mab: conjugate will reflect the relative peak areas.

Initial analysis investigated the efficiency of the less sensitive Mab: HRP assay. This assay optimised conditions for the detection of α B-crystallin at levels between 100ng/ml – 1.27ng/ml utilising a 2 mg/L Poly capture with a 250 ng/ml Mab: HRP conjugate detection in a Simultaneous assay. The samples analysed included 2 fractions encompassing the major oligomeric peak (oligomer 1 and 2) and three fractions encompassing the low Mwt species (low Mwt 1, 2 and 3). These fractions provide a typical range of α B-crystallin concentrations that would require quantitation.

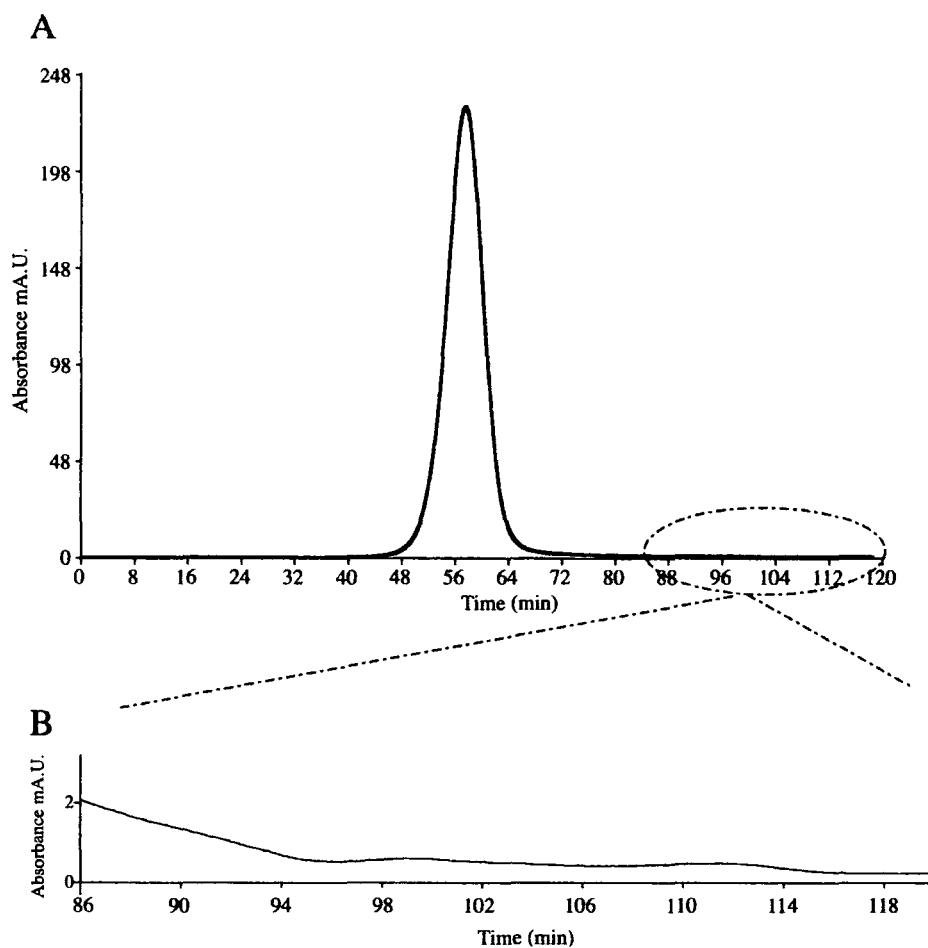


Figure A5.6. A typical 500 μg SEC elution profile. The range of αB -crystallin concentrations resulting in this SEC are evident by the absorbance data for specific regions. The oligomer peak (A) is some 250x greater in peak height than the low Mwt species highlighted in B.

The fractions were assayed at a range of dilutions aiming to produce a signal within the central region of the standard curve and the resulting quantitation data is shown in Table A5.1. Oligomer fraction 1 encompasses 55-60 min of the elution, whilst Oligomer fraction 2 encompasses 60-65 min. the low Mwt fractions encompass 90-95 min (fraction 1), 95-100 min (fraction 2) and 100-105 min (fraction 3) (see Figure A5.6).

Table A5.1. Quantitation of Oligomer and 93min peak material from 500 μ g α B-crystallin load using Mab: HRP

Peak and Fraction	Dilution	Observed ng/ml	Total ng/ml	Mean total ng/ml	Mean total μ g/ml
Oligomeric fraction 1	5000	59.3	296500	305750	306
Oligomeric fraction 1	50000	6.3	315000		
Oligomeric fraction 2	5000	35	175000	175000	175
Oligomeric fraction 2	50000	3.5	175000		
Low Mwt fraction 1	10	11.0	110	245	0.25
Low Mwt fraction 1	100	3.8	380		
Low Mwt fraction 1	1000	<1.27	<1.27		
Low Mwt fraction 2	10	5.5	55	108	0.11
Low Mwt fraction 2	100	1.6	160		
Low Mwt fraction 2	1000	<1.27	<1.27		
Low Mwt fraction 3	10	4.5	45	93	0.10
Low Mwt fraction 3	100	1.4	140		
Low Mwt fraction 3	1000	<1.27	<1.27		

Table A5.1 details the quantitation achieved and shows that the dilutions for the oligomeric fractions especially the 5000x, results in observed ng/ml values of α B-crystallin within the standard curve. The 50000x dilution results in ng/ml values at the low limits of the curve therefore an optimal dilution series for these samples would be 1:5000 and 1:25000.

The low Mwt fraction analysis indicates that a 1000x dilution is too large for α B-crystallin concentrations at this level of sensitivity and thus the absorbance readings were lower than the lower limits of the standard curve (< 1.27 ng/ml). The 100x dilution is just above this limit whereas the 10x dilution produces values that are more reliable. Based on these observations it is evident that a 2x and 10x dilution would provide data which could be reliably and accurately converted to α B-crystallin concentrations in these low Mwt fractions. These assays were repeated for fractions from a 125 μ g, 25 μ g and 2.5 μ g SEC load however, the assay was not of sufficient sensitivity to be able to accurately quantify the low Mwt fractions. It was however feasible method of quantitation for the oligomeric fractions and the data is shown in Table A5.2.

Table A5.2. Quantitation of Oligomer and 93min peak material from 125µg αB-crystallin load using Mab: HRP

Peak and Fraction	Load (µg)	Dilution	Observed ng/ml	Total ng/ml	Mean total ng/ml	Mean total µg/ml
Oligomeric fraction 1	125	500	93.9	46950	61975	62.0
Oligomeric fraction 1	125	5000	15.4	77000		
Oligomeric fraction 2	125	500	32.3	16150	17825	18.0
Oligomeric fraction 2	125	5000	3.9	19500		
Oligomeric fraction 1	25	50	89.6	4480	5820	5.8
Oligomeric fraction 1	25	500	26.8	13400		
Oligomeric fraction 2	25	50	69.9	3495	3323	3.3
Oligomeric fraction 2	25	500	6.3	3150		
Oligomeric fraction 1	2.5	10	10.1	101	101	0.10
Oligomeric fraction 1	2.5	100	1.0	< 1.27		
Oligomeric fraction 2	2.5	10	3.4	34	34	0.03
Oligomeric fraction 2	2.5	100	0.2	< 1.27		

Table A5.2 details the quantitation achieved and shows that the dilutions for the oligomeric fractions results in observed ng/ml values for αB-crystallin within the standard curve. The 2.5 µg SEC resulted in observed ng/ml values for αB-crystallin at the low limits of the standard curve when using a 100x dilution, however valid data is produced with a 10x dilution and perhaps a 2x dilution would be an appropriate second dilution for these fractions.

As we have seen previously in section 11.1.2.2, the Mab: Biotin conjugate achieves a four fold increase in sensitivity allowing quantification αB-crystallin protein at 5ng/ml –100pg/ml concentrations, thus the experiment was repeated to assess how the sensitivity observed during optimisation transferred to the quantitation of αB-crystallin

fractions and if the quantitation of the oligomer and especially the low Mwt fractions is enhanced using the Mab: Biotin.

Development of an ELISA for the analysis of α B-crystallin in SEC fractions of a wide range of protein concentrations has been successful. However, further optimisation is required using the Mab: Biotin assay in order to quantify those fractions with low Mwt species of α B-crystallin.

A5.1.3.2 Quantification α B-crystallin in SEC fractions using Mab: Biotin

The Mab: HRP assay provides an assay of appropriate sensitivity for the quantitation of the oligomeric fractions, which avoids excessive dilutions of fraction samples to provide a signal within the calibration curve. However, the low Mwt fractions require an assay of increased sensitivity and we know the Mab: Biotin can provide this. I also wanted to assess the level of dilution required to quantify the oligomeric fractions in this assay (see Table A5.3).

Table A5.3. Quantitation of Oligomer and 93min peak material from 500 μ g α B-crystallin load using Mab: Biotin.

Peak and Fraction	Dilution	Observed pg/ml	Total Ng/ml	Mean total ng/ml	Mean total μ g/ml
Oligomeric fraction 1	1000000	184.1	184100	184100	184.1
Oligomeric fraction 1	5000000	42.9	<128 pg/ml		
Oligomeric fraction 2	1000000	121.3	<128 pg/ml	121300	121.3
Oligomeric fraction 2	5000000	16.4	<128 pg/ml		
Low Mwt fraction 1	100	934.1	93.4	85.1	0.09
Low Mwt fraction 1	500	153.3	76.7		
Low Mwt fraction 2	10	4362.1	43.6	42.1	0.04
Low Mwt fraction 2	100	406.3	40.6		
Low Mwt fraction 2	500	56.0	<128 pg/ml		
Low Mwt fraction 3	10	3648.6	36.5	35.1	0.04
Low Mwt fraction 3	100	336.5	33.7		
Low Mwt fraction 3	500	85.7	<128 pg/ml		

Table A5.3 details the quantitation achieved and shows that the dilutions for the low Mwt species fractions results in observed pg/ml for α B-crystallin within the standard curve. An optimal dilution series for these samples appears to be 1:10 and 1:100. The oligomeric fractions were assayed at a substantial dilution of 1×10^6 and 5×10^6 , which proved too excessive and only produced a signal within the calibration curve for fraction 1.

This signal was itself towards the lower limit of the calibration range. It appears that dilutions of 5×10^5 and 5×10^4 would be sufficient to provide viable absorbance data for quantification, some 10x greater than dilutions required with the Mab: HRP. It is evident that both Mab conjugates can be used for quantification of α B-crystallin in the oligomer fractions and choice would depend perhaps on the available sample volume required to achieve the respective dilutions. The quantification of the low Mwt fractions with the Mab: Biotin proves to be an effective method for assay of 500 μ g SEC fractions. The assay is sensitive between 5000-128 pg/ml, therefore the quantification of the 125, 25 and 2.5 μ g SEC fractions was investigated. At the 2.5 μ g SEC level it was interesting to analyse the oligomeric fractions along with the low Mwt fractions.

Table A5.4 details the quantitation achieved and suggests the optimal dilutions for quantitation of α B-crystallin at the varying levels of SEC load. The 125 μ g SEC low Mwt fractions require a neat and 3x dilution; the 25 μ g SEC fractions require a neat and 2x dilution. Interestingly, the 2.5 μ g SEC fractions appear to require a larger dilution relative to the 25 μ g SEC fractions, of 2.5x and 5x. The oligomeric fractions of the 2.5 μ g SEC show viable absorbance data with this Mab: Biotin assay. The variations observed between the 2.5 μ g and 25 μ g SEC quantification highlights the dynamic characteristics of α B-crystallin with decreasing concentration as discussed in Chapter 5.

Table A5.4. Quantitation of 93min peak material from 125µg αB-crystallin load using Mab: Biotin.

Peak and fraction	Load (µg)	Observed pg/ml	Dilution	Total ng/ml	Mean total ng/ml
Low Mwt fraction 1	125	233.7	3	0.7	0.7
Low Mwt fraction 1	125	95.2	10	< 128 pg/ml	
Low Mwt fraction 2	125	451.2	3	1.4	2.9
Low Mwt fraction 2	125	429.9	10	4.3	
Low Mwt fraction 3	125	115.4	3	< 128 pg/ml	1.3
Low Mwt fraction 3	125	133.2	10	1.3	
Low Mwt fraction 1	25	129.6	3	0.4	0.4
Low Mwt fraction 1	25	36.9	10	< 128 pg/ml	
Low Mwt fraction 2	25	223.1	3	0.7	0.7
Low Mwt fraction 2	25	26.1	10	< 128 pg/ml	
Low Mwt fraction 3	25	41.7	3	< 128 pg/ml	N/a
Low Mwt fraction 3	25	15.2	10	< 128 pg/ml	
Oligomer fraction 1	2.5	2119.3	10	21.2	27
Oligomer fraction 1	2.5	1090	30	32.7	
Oligomer fraction 2	2.5	133.2	10	1.3	1.3
Oligomer fraction 2	2.5	103.6	30	< 128 pg/ml	
Low Mwt fraction 1	2.5	210.1	2.5	0.5	2.1
Low Mwt fraction 1	2.5	731.2	5	3.7	
Low Mwt fraction 2	2.5	644.4	2.5	1.6	2.3
Low Mwt fraction 2	2.5	569.6	5	2.9	
Low Mwt fraction 3	2.5	156.9	2.5	0.4	2.0
Low Mwt fraction 3	2.5	728.8	5	3.6	

Investigating the feasibility of using the αB-crystallin ELISA for the analysis and quantitation of αB-crystallin present in SEC fractions with a wide range of concentrations resulted in the identification of appropriate dilutions for optimal detection in the Mab: Biotin and Mab: IIRP assays.

The development of an ELISA assay for the detection and quantitation of α B-crystallin has resulted in 2 assays optimised for varying levels of sensitivity. The simultaneous Mab: HRP assay is optimised to the 5-100ng/ml level, for oligomer samples from runs 500 μ g, 125 μ g and 25 μ g and low Mwt samples from 500 μ g, and 125 μ g runs. For fractions of lower α B-crystallin concentration, the Mab: Biotin assay is preferred with sensitivity from 5ng/ml – 128 pg/ml. Although this work has identified appropriate dilutions it is not always possible to assume the α B-concentration of particular fractions and selected dilutions may not produce absorbance data sufficiently within the calibration range, therefore re-assaying with amended dilutions may be required. However, this work has also shown that the α B-crystallin ELISA is a feasible means of quantifying α B-crystallin at any level of sensitivity.

The Mab: Biotin detection system is a powerful tool for the analysis of the tail material of α B-crystallin analytical SEC elutions, to determine the presence of additional α B-crystallin species of low Mwt as discussed in Chapter 5 (see Section 5.3.2-5.3.3). The Mab: Biotin ELISA produced repeatable, reliable and accurate quantification of α B-crystallin in the SEC fractions to aid the investigation of the subunit dynamics of α B-crystallin, which was supported by immunoblotting and Absorbance data performed in conjunction with the ELISA.

APPENDIX 6

PUBLICATIONS

Truncation of α B-Crystallin by the Myopathy-causing Q151X Mutation Significantly Destabilizes the Protein Leading to Aggregate Formation in Transfected Cells^{*§}

Received for publication, August 3, 2007, and in revised form, January 29, 2008 Published, JBC Papers in Press, January 29, 2008, DOI 10.1074/jbc.M706453200

Victoria H. Hayes[‡], Glyn Devlin[§], and Roy A. Quinlan^{‡1}

From the [‡]School of Biological and Biomedical Sciences, South Road Science Site, Durham University, Durham DH1 3LE and the [§]Department of Chemistry, University of Cambridge, Lensfield Road, Cambridge CB2 1EW, United Kingdom

Here we investigate the effects of a myopathy-causing mutation in α B-crystallin, Q151X, upon its structure and function. This mutation removes the C-terminal domain of α B-crystallin, which is expected to compromise both its oligomerization and chaperone activity. We compared this to two other α B-crystallin mutants (450delA, 464delCT) and also to a series of C-terminal truncations (E164X, E165X, K174X, and A171X). We find that the effects of the Q151X mutation were not always as predicted. Specifically, we have found that although the Q151X mutation decreased oligomerization of α B-crystallin and even increased some chaperone activities, it also significantly destabilized α B-crystallin causing it to self-aggregate. This conclusion was supported by our analyses of both the other disease-causing mutants and the series of C-terminal truncation constructs of α B-crystallin. The 450delA and 464delCT mutants could only be refolded and assayed as a complex with wild type α B-crystallin, which was not the case for Q151X α B-crystallin. From these studies, we conclude that all three disease-causing mutations (450delA, 464delCT, and Q151X) in the C-terminal extension destabilize α B-crystallin and increase its tendency to self-aggregate. We propose that it is this, rather than a catastrophic loss of chaperone activity, which is a major factor in the development of the reported diseases for the three disease-causing mutations studied here. In support of this hypothesis, we show that Q151X α B-crystallin is found mainly in the insoluble fraction of cell extracts from transiently transfected cells, due to the formation of cytoplasmic aggregates.

The crystallins were first identified as the major proteins of the eye lens and their subsequent classification into α -, β -, and γ -crystallins (1) allowed different functional properties to be assigned to the α - and β -crystallin groups (2). The α -crystallins are two distinct proteins derived from two separate genes, α A- and α B-crystallin (2). Whereas α A-crystallin is almost entirely lens specific (3), α B-crystallin is expressed widely in

other tissues, most notably astrocytes (4) and muscle (5). In the early 1980s, pioneering work from Klemenz and co-workers (6) and Horwitz (7) laboratories established that α B-crystallin was a protein chaperone and a member of the small heat shock protein (sHSP)² family, that is now known to comprise 10 different human proteins (8).

When the first mutation (R120G) in α B-crystallin was reported, it was found to cause both cataract and desmin-related myopathy in the affected patients (9). Characteristic histopathological aggregates of the muscle intermediate filament protein desmin were observed (9), strongly suggesting that there is an important functional interaction between intermediate filaments and α B-crystallin. Subsequent analyses showed that the R120G α B-crystallin mutation induced increased binding for desmin intermediate filaments (10), providing an explanation for the formation of the desmin aggregates in the muscles of the affected individuals. Coincidentally, mutations in desmin also induced filament aggregation (11, 12) and these aggregates also contained α B-crystallin (12). Collectively, these data suggest that one of the functions of α B-crystallin is to chaperone intermediate filaments and their networks in cells (10, 13, 14).

Subsequently, three other mutations in the C-terminal extension were reported for α B-crystallin, but in contrast to the R120G mutation, none caused both cataract and myopathy. The first of these was the 450delA mutation that is associated only with cataract and resulted in a 184-residue product where the coding sequence of the C-terminal extension was altered from residue 150 onwards (15). This region is distal to the β -strand 9 and proximal to the conserved hydrophobic IX(I/V) motif (16) that forms part of β -strand 10 in the crystal structure of the archaeal HSP16.5 (17). Two other mutations were then reported (Q151X and 464delCT) that cause myopathy and not cataract (18) that either truncated (Q151X) or substituted the C-terminal extension from residue 155 (464delCT). The fact that all three mutations delete a known substrate interaction site (157–164) (19) and a region important in the oligomerization of α B-crystallin itself (155–166) (20) support the hypothesis that this region in α B-crystallin is important to both the structure and function of the protein. Very recently, a C-terminal point mutation (R157H) (21) was reported, lending further

This work was supported by a Biotechnology and Biological Sciences Research Council (BBSRC) and ImmunoDiagnostics Systems BBSRC CASE award (to V. H. H.) and National Institutes of Health NINDS Grant P01NS42803 (to R. A. Q.). The costs of publication of this article were defrayed in part by the payment of page charges. This article must therefore be hereby marked "advertisement" in accordance with 18 U.S.C. Section 1734 solely to indicate this fact.

§ The on-line version of this article (available at <http://www.jbc.org>) contains supplemental Figs. S1–S4.

To whom correspondence should be addressed. Fax: 44-191-334-1201; E-mail: r.a.quinlan@durham.ac.uk.

² The abbreviations used are: sHSP, small heat shock protein; bis-ANS, 4,4'-dianilino-1,1'-binaphthyl-5,5'-disulfonic acid; MWCO, molecular weight cut off; SEC, size exclusion chromatography.

TABLE 1
Oligonucleotide primer sequence details used for introduction of the α B-crystallin mutations

The unique restriction enzyme sites incorporated into the primer design are highlighted in bold text. Q151X and E165X were introduced using site-directed mutagenesis (SDM) requiring complementary forward (5'-3') and reverse (3'-5') primers. The 464delCT, K174X, A171X, and E164X mutant mRNA were amplified using a forward primer overlapping the pET23d insertion site and the 5' end of the template wild type α B-crystallin. Reverse primers were complementary to the 3' end of the template wild type α B-crystallin and incorporated the mutation and unique restriction sites to assist screening, using the available software (DNA_Analysis_Frame). A suitable restriction enzyme site was not available for the 464delCT mutation.

Mutant α B-crystallin	Restriction enzyme site	Primer sequence (5'-3')
Q151X	StuI	Forward primer: gtgaatggaccaaggaaat aggcct ctggccctgagcgcacc Reverse primer: ggtgcgctcagggccag aggcct atttctcttggtccattcac
E165X	HindIII	Forward primer: attcccatcaccgtgaataga agcctt gctgtccaccgcagccccc Reverse primer: gggggctgcggtgacagca agcctt ctattcacgggtgatgggaat
464delCT	NA ^a	Forward primer: taccatggacatcgccatccaccacc Reverse primer: tcacgggtgatgggaatggtgcgctcggccagagacctgtttcc
K174X	SacII	Forward primer: taccatggacatcgccatccaccacc Reverse primer: ctaggggg ccg cggtgacagcaggcttc
A171X	SacI	Forward primer: taccatggacatcgccatccaccacc Reverse primer: gggcattctatttcttggg agctc agggtgacagcaggcttctc
E164X	PstI	Forward primer: taccatggacatcgccatccaccacc Reverse primer: cttgggagctgcggtgactg caggctt ctcttaacgggtgatgggaatggt

^a NA, not applicable.

support to this conclusion. Thus far, the effect of such extensive deletions (Q151X) combined with altered C-terminal sequences (450delA and 464CT) upon α B-crystallin structure and function have not been investigated.

In other sHSPs, the C-terminal domain has been shown to be very important to both oligomerization and chaperone function and therefore the expectation is that the C-terminal extension mutations would similarly affect α B-crystallin. Removal of the 17 most C-terminal residues of α A-crystallin reduced its chaperone activity and induced the formation of larger oligomers (22). In two crystal structures of sHSPs (HSP16.5 (17) and HSP16.9 (23)), the C-terminal extension makes contact with a hydrophobic patch on neighboring protein subunits, strengthening the dimer-dimer interaction in the oligomer (23). The sequence between β -strands 9 and 10 of the C-terminal extension contains a hinge that likely contributes to the size polydispersity of the different sHSPs by allowing packing geometries to vary while maintaining common interaction surfaces (23). Some naturally occurring sHSPs lack a C-terminal extension and in such cases the oligomerization is restricted, as seen for Tsp36 from the tapeworm *Taenia saginata*, which forms dimers and tetramers, but is functional as a chaperone (24). Likewise, removal of the short C-terminal extension from *Methanococcus janashii* HSP16.5 resulted in reduced oligomerization, but the retention of chaperone activity (25). This is quite contrary to the closely related lens chaperone α A-crystallin that naturally co-oligomerizes with α B-crystallin in the lens. Stepwise removal of C-terminal sequences from α A-crystallin, including the REEK motif, not only reduced oligomerization, but also resulted in the sequential loss of chaperone activity (26), despite the fact that the IX(I/V) motif was retained in the mutants investigated. Mutations of lysine and glutamic acid residues in the C-terminal extension can improve chaperone

activity against amyloid fibril formation providing a potential application of α B-crystallin in the treatment of amyloid-related diseases (27). In α B-crystallin, there has not been any systematic analysis of the role of the C-terminal extension and therefore no potential explanation of whether the three mutations (450delA, Q151X, and 464delCT) cause the various diseases via the loss of chaperone function or perhaps by a different mechanism.

In this study, we have analyzed the effects of the Q151X, 464delCT, and 450delA upon the oligomerization and chaperone activity of α B-crystallin. For comparison, we have also assessed the activity of a series of α B-crystallin constructs truncated at residues Lys¹⁷⁴, Ala¹⁷¹, Glu¹⁶⁵, and Glu¹⁶⁴ to sequentially remove important regions of the C-terminal extension and therefore help us understand the effect of the Q151X mutation. With respect to the role of the C-terminal extension in oligomerization, our data show similar results to those obtained for α A-crystallin (28). Interestingly, the chaperone function of Q151X is actually increased in some *in vitro* chaperone assays. The ability of Q151X α B-crystallin to resist self-aggregation is, however, very greatly diminished, a trend that is further enhanced by the 464delCT and 450delA mutations, which are only stable in the presence of wild type α B-crystallin. These data show that like other sHSPs, the C-terminal extension is important for oligomerization. Its removal increases the tendency of α B-crystallin to self-aggregate.

EXPERIMENTAL PROCEDURES

Construction of α B-Crystallin Mutants

Primers (Table 1; Sigma Genosys, UK) were designed based on the mRNA sequence for wild type human α B-crystallin (DDBJ/EMBL/GenBank entry NM_001885) and were used to

Removal of C-terminal Extension Induces α B-Crystallin Aggregation

generate the mutants listed, using wild type α B-crystallin as a template for PCR mutagenesis. With the exception of the Q151X and E165X mutations, the amplified products were cloned into the vector pGEM[®]-T Easy (Promega). After verification of the sequences, the mutant α B-crystallin constructs were subcloned into the NcoI and EcoRI sites of the expression vector pET23d (Invitrogen). The Q151X and E165X mutations were introduced into pET23d by site-directed mutagenesis (Stratagene) using complementary primers (see Table 1). Constructs were sequenced and compared for fidelity to the GenBank[™] data base (accession number NM001885).

Protein Expression and Purification of α B-Crystallin Mutants

Proteins were recombinantly expressed in *Escherichia coli* strain BL21 (pLysS). The wild type α B-crystallin, K174X and A171X proteins were prepared essentially as described (29), but adding polyethyleneimine (final concentration 0.1% (w/v)) to remove contaminating DNA (10, 30) before purification by ion exchange chromatography on a Fractogel TMAE column. Peak fractions were pooled and then dialyzed into 20 mM Tris-HCl, 100 mM NaCl, pH 7.4, in preparation for size exclusion chromatography on a Fractogel EMD BioSEC Superformance column (60 \times 1.6 cm; VWR, UK).

All other mutant α B-crystallins formed inclusion bodies, and were purified essentially as described (31). These were dissolved in 10 mM Tris-HCl, 6 M urea, 1 mM EDTA, pH 8.0, 0.2 mM phenylmethylsulfonyl fluoride, 1 mM dithiothreitol and then purified by ion exchange chromatography (29) on a Fractogel TMAE column.

Fractions containing α B-crystallin were pooled and sometimes concentrated using an Amicon Ultra Centrifugal filter device 10K MWCO (Millipore, Bedford, MA). Concentrations of the purified proteins were determined using BCA Protein Assay reagent kit (Pierce) unless otherwise stated.

Refolding of α B-Crystallin Mutants following Inclusion Body Purification

In the Presence of Wild Type α B-Crystallin

The 450delA, 464delCT, and Q151X were refolded in the presence of wild type α B-crystallin. Wild type α B-crystallin was dialyzed for 16 h at 4 °C into 10 mM Tris-HCl, 6 M urea, 1 mM EDTA, pH 8.0, 1 mM dithiothreitol. Protein concentration of the wild type and mutant α B-crystallin were determined by OD₂₈₀ (extinction coefficients were determined using the Emboss Pepstats program) and then mixed in a 1:1 ratio.

Diluted Refold Protocol (450delA/Wild Type, Q151X/Wild Type, E164X, and Q151X)

The protein mixture was diluted to 0.25 mg/ml in 10 mM Tris-HCl, 6 M urea, 1 mM EDTA, pH 8.0, 1 mM dithiothreitol followed by an additional 6-fold dilution to 1 M urea in refold buffer (10 mM Tris-HCl, 5 mM EDTA, 1 mM EGTA, 150 mM NaCl, pH 7.5) prior to dialysis against the same buffer for 4 h at 6 °C. The dialysate was partially concentrated using Amicon Ultra Centrifugal filter device 10K MWCO (Millipore) and centrifuged for 2 h at 4 °C at 250,000 \times g in the Beckman Optima MAX Ultracentrifuge MLA-80 rotor (Beckman Instruments

Inc., Fullerton, CA). The supernatant was further concentrated to a suitable volume.

Undiluted Refolding Protocol (464delCT/Wild Type, E165X)

The protein mixture was dialyzed into refold buffer for 4 h at 16 °C. The dialysate was centrifuged for 2 h at 4 °C at 250,000 \times g in the Beckman Optima MAX Ultracentrifuge MLA-80 rotor (Beckman Instruments Inc.) and the supernatant concentrated to give the desired protein concentration.

Characterization of α B-Crystallin Mutants

Analytical Size Exclusion Chromatography (SEC)

Purified α B-crystallin proteins were analyzed using a Superose 6 column (290 \times 10 mm) at a flow rate of 0.2 ml/min at room temperature using a Merck-Hitachi Biochromatography system. The data were analyzed using Chromeleon 6.30 software (Sunnyvale, CA).

Mass Spectrometry for Molecular Weight Determination

Purified proteins were loaded onto a MassPREP desalting cartridge (Waters, Elstree, Herts, UK) to remove buffer contaminants. The protein was eluted with 70% (v/v) acetonitrile, 0.5% (v/v) formic acid at 0.2 ml/min and introduced into a Waters Q-TOF Premier mass spectrometer operating in positive electrospray mode, with a cone voltage of 40 V. Spectra were externally calibrated using sodium formate, then corrected for drift using a leucine enkephalin lockspray. Multiply charged protein ions were deconvoluted using the manufacturer-supplied MaxEnt1 software, to determine protein mass.

CD Spectroscopy

Far UV CD spectra of wild type and mutant α B-crystallin were recorded in a cuvette with 0.1-cm path length at room temperature using a Jasco J-810 spectropolarimeter. Samples were at a concentration of 0.2–0.3 mg/ml, with the exception of Q151X, assayed at 0.1 mg/ml due to the low yield of soluble protein. Samples were assayed in 10 mM Tris, 150 mM NaCl, 5 mM EDTA, 1 mM EGTA, pH 7.5. Four data sets were collected for each sample and averaged, by continuous scanning at 100 nm/min, between wavelengths 190 and 250 nm. The UV CD spectra were baseline corrected using spectra of the buffer. The CD spectra were normalized and expressed as molar ellipticity.

Thermal Stability Assay

Absorbance at 360 nm over a temperature gradient of 25–86 °C at 1 °C/min ramp rate was continuously monitored using the Beckman DU640 spectrophotometer. Samples were assayed at 0.1 mg/ml.

In Vitro Protein Chaperone Assays

Citrate Synthase—A 200- μ l volume of citrate synthase from porcine heart (Sigma) was dialyzed for 16 h at 4 °C against 50 mM Tris-HCl, 2 mM EDTA, pH 8.0, and diluted to 0.49 mg/ml. The assay mixture contained citrate synthase and α B-crystallin at a 4:1 ratio of substrate:chaperone in 220 μ l. Time-dependant light scattering was measured at 360 nm every 15 s over 30 min at 42 °C using a Beckman DU640 spectrophotometer.

Removal of C-terminal Extension Induces α B-Crystallin Aggregation

Insulin Assay—A 20-mg aliquot of insulin from bovine pancreas (Sigma) was reconstituted in 100 mM NaSO₄, 20 mM NaPO₄, pH 6.9 (Insulin buffer), and solubilized by the addition of 30% (v/v) acetic acid and gentle mixing for 15 min. The insulin solution was dialyzed for 16 h at 4 °C against the insulin buffer and the dialysate was centrifuged for 1 min at 13,000 \times g in an Eppendorf bench top centrifuge (5417R; Eppendorf, Hamburg, Germany). The insulin concentration was determined from the measured OD₂₈₀ using its extinction coefficient ($(A_{280/5840}) \times 5600 = \text{mg/ml}$). Insulin was mixed with α B-crystallin at a 4:1 ratio and the change in light scattering was measured at 360 nm every 15 s over a period of 15 min at 37 °C using a Beckman DU640 spectrophotometer.

Bis-ANS Fluorescence Measurements

α B-Crystallin variant proteins were incubated in 10 mM Tris, 150 mM NaCl, 5 mM EDTA, 1 mM EGTA, pH 7.5, at a protein concentration of 1 μ M and in the presence of a 10-fold molar excess of bis-ANS (4,4'-dianilino-1,1'-binaphthyl-5,5'-disulfonic acid, purchased from Invitrogen). Samples were allowed to equilibrate for 1 h at room temperature prior to the acquisition of fluorescence spectra on a Varian Cary Eclipse fluorescence spectrophotometer. The excitation wavelength was 410 nm and emission was collected between 420 and 700 nm with excitation and emission slit widths of 5 nm and a scan speed of 600 nm/min. All spectra are the average of 10 individual scans.

In Vitro Desmin Filament Assembly and Cosedimentation Assay

In vitro assembly and cosedimentation assays were carried out essentially as described (10). Recombinant human desmin was a kind gift from Dr. Ming Der Perng (Durham, UK). Wild type or mutant α B-crystallin was mixed with desmin in low ionic strength buffer at a 1:1 mass ratio at 0.1 mg/ml. After filament assembly, samples were separated into pellet and supernatant fractions by high speed centrifugation (80,000 \times g for 30 min at 20 °C in a Beckman TLS-55 rotor (Beckman Instruments Inc., Fullerton, CA)) as described (10) to pellet assembled desmin filament and the associated α B-crystallin. To investigate the ability of the three α B-crystallin mutants and the other C-terminal truncation constructs to prevent filament-filament interactions *in vitro*, an additional low-speed centrifugation assay was used (2500 \times g for 15 min in a bench top centrifuge) as described previously (10). The pellet and supernatant fractions were analyzed by 12% (w/v) SDS-PAGE (32) and protein bands visualized by Coomassie Blue staining. The amount of protein in the supernatant and pellet fractions were analyzed by a luminescent image analyzer (LAS-1000plus; Fuji Film, Tokyo, Japan) and quantified using the Image Gauge software (version 4.0; Fuji Film).

Cell Cultures and Transient Transfection Assays

MCF7 cells were maintained as described previously (10). Wild type and mutant α B-crystallin were subcloned into the mammalian expression vector pcDNA3.1 (Invitrogen) from the bacterial expression vector pET23d, using XbaI and HindIII. Transient transfection of these cells was achieved using Gene-juice transfection reagent (Novagen) according to manufacturer's protocol. Cells were allowed to recover for 24 h before processing for immunofluorescence microscopy, cell fractionation, and immunoblotting.

Cell Fractionation, SDS-PAGE, and Immunoblotting

Cells grown on 10-cm dishes were washed twice with phosphate-buffered saline before being lysed with 1 ml of extraction buffer (phosphate-buffered saline, 0.5% (v/v) Triton X-100) by repeatedly passing through a 25-gauge needle. Following incubation on ice for 15 min, the lysates were clarified by centrifugation 18,000 \times g for 10 min at 4 °C. The resulting supernatant and pellet fractions were solubilized in equal volumes of Laemmli sample buffer before SDS-PAGE and immunoblotting analysis as described (10). Membranes were probed with a panel of purified mouse monoclonal anti- α B-crystallin 2D2B6 and monoclonal anti-HSP27 antibody, ER-D5, as described (10). Antibody labeling was detected by enhanced chemiluminescence using a luminescent image analyzer (LAS-1000plus; Fuji Photo Film (UK), London, United Kingdom).

Immunofluorescence Microscopy

Cells were processed as described previously (10). The primary antibodies used in this study were rabbit polyclonal anti- α B-crystallin, a synthetic peptide corresponding to human α B-crystallin residues 1–10 (MDIAIHHPWI) conjugated to hemocyanin (1:200; Chemicon Ab1546) and monoclonal mouse anti-keratin LE41 (1:1; CRUK). Samples were analyzed using an Axioplan fluorescence microscope (Carl Zeiss, Jena, Germany). Images were obtained using a confocal Axiovert 200M microscope and LSM 510 META software (both Zeiss, Germany). Optical sections were set to \sim 1.0 μ m. Images were processed and prepared for figures using Adobe Photoshop 8.0 (Adobe Systems). Quantitation of the α B-crystallin phenotypes was by visual assessment of the cells.

RESULTS

Expression and Purification of the C-terminal Extension α B-Crystallin Mutants—An overview of the C-terminal extension mutants in comparison to wild type α B-crystallin is presented (Fig. 1A). It shows the relationship of the various mutations and truncations to the structural features of the C-terminal extension and also summarizes the consequences of the two frameshift mutations, 450delA and 464delCT, that cause inherited cataract (15) and myofibrillar myopathy (18), respectively. In addition to the three disease-causing mutations (Q151X, 450delA, and 464delCT), a series of C-terminal extension truncation constructs were also expressed and purified (Fig. 1B). All the mutants except A171X and K174X were purified from inclusion bodies. The predicted mass of each of the expressed proteins was confirmed by mass spectrometry measurements (Fig. 1C). Whereas Q151X, E164X, and E165X could be refolded successfully without the addition of wild type α B-crystallin, both 450delA and 464delCT could only be refolded in its presence. When refolded with an equimolar ratio of α B-crystallin, \sim 7% of 450delA and 10% of 464delCT remained soluble (Fig. 1D). Although Q151X α B-crystallin could be refolded in the absence of wild type α B-crystallin, the yield could be increased some 7-fold when the wild type protein

Removal of C-terminal Extension Induces α B-Crystallin Aggregation

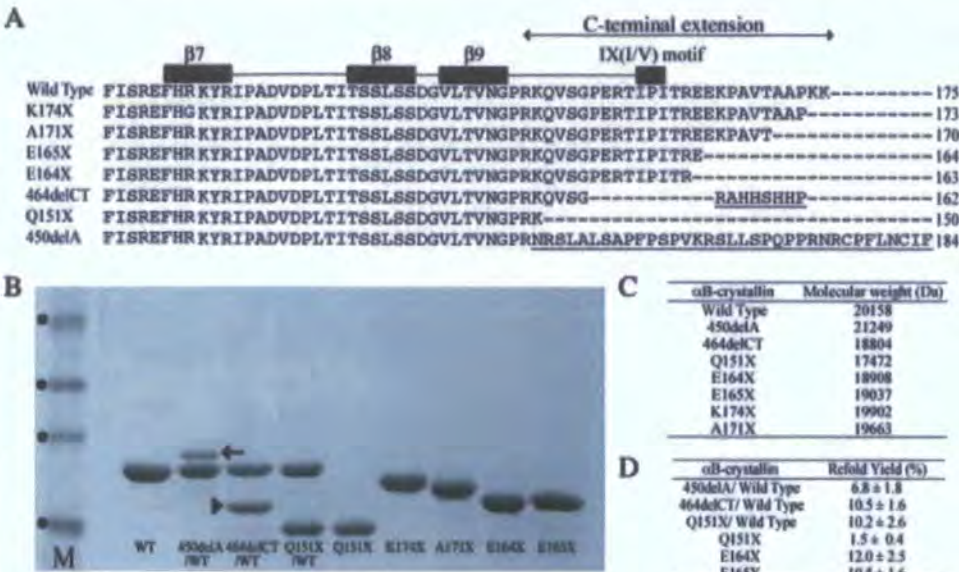


FIGURE 1. Details of the α B-crystallin mutants and their characterization by SDS-PAGE. Structural alignment of the C-terminal extensions of α B-crystallin mutants (A) includes the C-terminal extension from residue 149 (24), and β -sheets and the IX(I/V) motif are indicated as black boxes. The β 7 sequence spans residues 118–123 (FHRKYR), β 8 sequence spans residues 134–138 (TSSLS), and β 9 sequence spans residues 142–148 (VLTVNGP). The highly conserved IX(I/V) motif includes residues 159–161 (IPI). The C-terminal extension consists of residues 149–175 (RKQVSGPERTIPITREEKPAVTAAPKK). The 450delA (arrow) and 464delCT (arrowhead) mutants could not be produced as individual soluble proteins and therefore were refolded in the presence of wild type α B-crystallin. Molecular weight markers (track M) are indicated (●) in order of increasing relative mobility (40, 33, 24, and 17 kDa). The relative molecular weights of the wild type and mutant α B-crystallins (C) were confirmed by mass spectrometry and compared with values calculated from the amino acid sequences using the Emboss Pepstats program. D, refolding yields for α B-crystallin truncation constructs and mutants purified from inclusion bodies.

was included. These data show the disease-causing mutations seriously affect the solubility of α B-crystallin.

The K174X construct removes the two most C-terminal lysine residues and would be expected to retain the secondary structural characteristics and oligomerization characteristics of α B-crystallin (33). The electrophoretic mobility of this K174X mutant was increased relative to the wild type α B-crystallin (Fig. 1B) and is in agreement with previous observations for C-terminal-deleted forms of α B-crystallin (34–37). Removal of the 5 most C-terminal residues generated the A171X mutant and is equivalent to the truncated form of α B-crystallin found in normal rat lenses (38), bovine lenses (39), and in rat models of diabetic cataracts (40). Another C-terminal-truncated form of α B-crystallin (E164X) has 12 residues removed from the C terminus and this has been detected in normal rat lenses (41). This truncation deletes the pair of glutamic acid residues at positions 164 and 165 that are part of the REEK motif in α A-crystallin that have been shown to be important in oligomerization (26). It is also equivalent to the 10-residue C-terminal-truncated form of α A-crystallin (40).

Truncation of the C-terminal Extension Reduces α B-Crystallin Oligomerization—Wild type α B-crystallin formed oligomers that were equivalent to 564 kDa, as calculated from the size exclusion chromatography data, agreeing with previously published data (42). The oligomer population was consistent between different preparations as shown by dynamic light scattering (supplementary data Fig. S1). The sequential truncation of the C-terminal extension of α B-crystallin produces a steady

decrease in oligomer size (Fig. 2A). The shortest construct Q151X α B-crystallin produces a peak with very significantly increased elution volume (Fig. 2B) and represents the most dramatic reduction in oligomerization observed for all the constructs studied. This effect on Q151X oligomerization is obvious when the negative stained electron micrographs of wild type and Q151X α B-crystallin are compared (Fig. 2, C and D, respectively). Notice the absence of particles in the Q151X sample (Fig. 2D) relative to the wild type (Fig. 2C).

Deletion of the two C-terminal lysines (K174X) did not alter significantly the oligomerization of α B-crystallin, as previously reported (33). Removal of 5 C-terminal residues, however, reduced the apparent size of the main peak, as did the removal of both 11 (E165X) and 12 (E164X) residues. In the case of the latter two truncation mutants, there is evidence of increased polydispersity as indicated by the very noticeable shoulder on the main peak for the E165X construct and the presence of

an additional peak at the void volume of the column for the E164X construct. The elution volume of the main peak is increased, suggestive of reduced mean size for α B-crystallin oligomers. These data suggest that residues Glu¹⁶⁴–Glu¹⁶⁵ also contribute to α B-crystallin oligomerization.

The two frameshift mutants 450delA and 464delCT remained insoluble unless they were refolded in the presence of wild type α B-crystallin. As seen from the elution profiles in Fig. 2A, the presence of these mutant proteins decreased the oligomer size of the wild type α B-crystallin. SDS-PAGE analysis (Fig. 1B) revealed that the wild type α B-crystallin is present in excess compared with 450delA α B-crystallin, yet this excess was not sufficient to retain the elution characteristics of the wild type protein. In fact, this proved to be the maximum ratio compatible with protein solubility for the 450delA-wild type α B-crystallin complex and is in stark contrast to 464delCT α B-crystallin, where a 1:1 mixture with wild type α B-crystallin was entirely soluble. The presence of the 450delA α B-crystallin also increased the polydispersity of the main peak, as seen by the shoulder and the additional small peak with a predicted molecular weight equivalent to α B-crystallin dimers.

The 450delA mutation introduces a unique 33-residue polypeptide completely unrelated to the C-terminal extension of wild type α B-crystallin (Fig. 1A) and quite clearly this frameshift sequence has a significant effect upon the oligomerization of α B-crystallin. It is, however, the Q151X mutation that has the most dramatic effect, with the complete removal of the single peak equivalent to the 564-kDa oligomer and the appear-

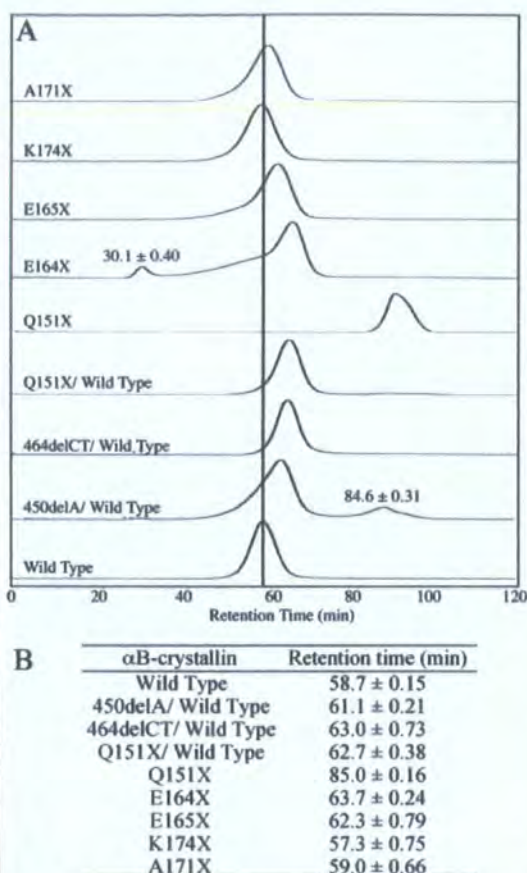


FIGURE 2. Effect of the Q151X mutation upon the oligomerization of α B-crystallin. The elution profiles of the various α B-crystallins were determined on a 290 × 10-mm Superose 6 column (A). The elution characteristics of the various mutants are plotted relative to those obtained for wild type α B-crystallin (wild type), as highlighted by the vertical line indicating the retention time of the oligomeric complex, which is the major and only peak resolved in the wild type α B-crystallin sample. Additional minor species seen in E164X and 450delA/wild type are highlighted. A summary of the retention times (B) is shown for the major peak resolved during SEC of the wild type α B-crystallin and other constructs. The retention times of minor peaks are included in the figure as appropriate. The retention times (\pm S.D.) were calculated from the average of three cycles of SEC. Negative stained images of wild type (C) and Q151X α B-crystallin (D) were obtained by transmission electron microscopy and illustrate the absence of characteristic particles in the Q151X sample, in agreement with the SEC data. Bar, 500 nm.

ance of a peak with elution characteristics predicted to be equivalent to a monomer. Non-denaturing gel electrophoresis also confirmed that the Q151X mutation dramatically altered its electrophoretic mobility under non-denaturing conditions in line with significantly altered oligomerization (supplementary data Fig. 2).

Effect of the C-terminal Mutations upon the Secondary Structure and Oligomerization of α B-Crystallin—CD spectroscopy of wild type α B-crystallin showed a single, broad minima, between 208 and 217 nm, indicative of a protein rich in β sheet (Fig. 3), which is consistent with previously reported data (42–46). The Q151X mutation had the most significant effect upon the far UV CD characteristics of α B-crystallin (Fig. 3), due to a very significant red shift of the minima to 217 nm and a ~50% reduction in magnitude, suggestive of a significant loss of secondary structure. Similar shift patterns have been seen for C-terminal truncation mutants of α A-crystallin (26). A 1:1 molar mixture of Q151X with α B-crystallin wild type produced a spectrum that was clearly biased toward the Q151X, indicative of the dominant nature of this mutation.

Of the other mutants studied, the E164X and E165X mutants were intermediate in their effects upon negative ellipticity as compared with the Q151X mutant. This intermediate effect is likely associated with the extent of the C-terminal truncations of E164X, E165X relative to Q151X, and suggests a less significant loss of secondary structure. Interestingly, the E164X mutant showed a red shift in the minimum indicating that the deletion of the second of the two glutamic acid residues in the REEK motif does introduce a detectable change in secondary structure. A recent study showed an R163X mutant with significantly altered secondary structure compared with the wild type (27). The frameshift mutation, 464delCT, introduced a small blue shift of the minimum to 208 nm and the appearance of a shoulder at ~223 nm, both of which are indicative of increased helicity. This increase may be the result of helix formation by the novel C-terminal sequence. Both the K174X and A171X truncation mutants and the 450delA frameshift mutant have far UV CD spectra very similar to the wild type α B-crystallin.

Loss in Heat Stability of α B-Crystallin Correlates with Changes in Secondary Structure—To probe the consequences of the altered secondary sequence characteristics of the

α B-crystallin C-terminal extension mutants, their heat stability was determined (Fig. 4). These data show that the two most unstable mutants are E164X and E165X because both the onset and optical signal was very significantly increased compared with wild type α B-crystallin for these two mutants. The E164X mutant began to aggregate at 46 °C, some 30 °C lower than the wild type protein. The E165X mutant was notable for the rapidity of aggregation when initiated at 57 °C, whereas the Q151X mutant was notable in its failure to develop a strong OD₃₆₀ signal, despite the very significant decrease in stability indicated by the increased turbidity at 53 °C. This signal reached a maximum at 55 °C and remained constant until the conclusion of the assay. The two shorter C-terminal truncations (K174X and A171X), showed decreased stability, but were the most stable of the constructs studied.

These data suggest a correlation between altered secondary structure and decreased heat stability. This trend is also seen for the two frameshift mutants (450delA/wild type and 464delCT/wild type) that were more stable than the three shortest constructs, but less stable than either the A171X or K174X trunca-

Removal of C-terminal Extension Induces α B-Crystallin Aggregation

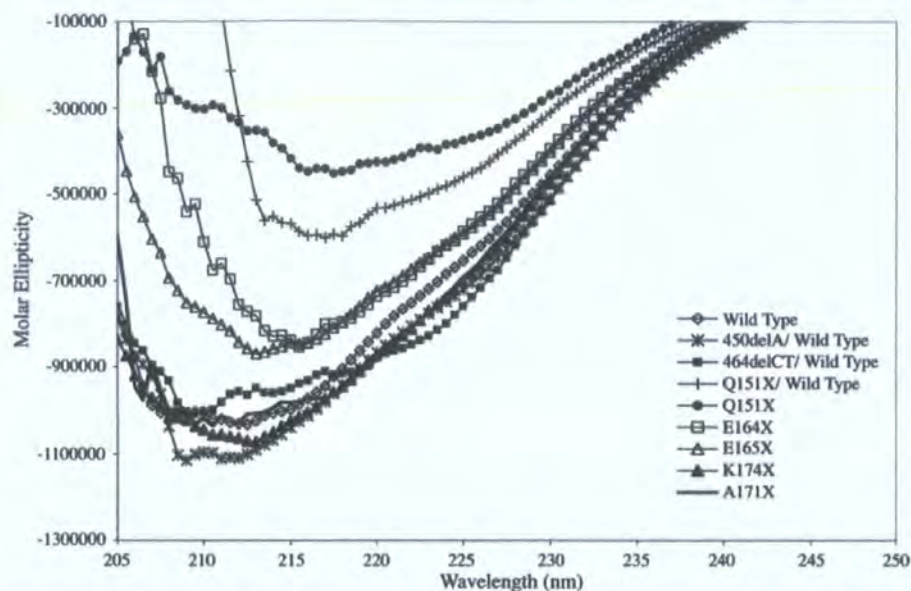


FIGURE 3. Circular dichroism of wild type α B-crystallin and the C-terminal extension mutants. Far UV CD spectra (205–250 nm) for each protein were the average of four spectra. The far UV CD signal was converted to molar ellipticity expressed as degree/cm²/dmol⁻¹ to normalize for slight differences in molecular mass between the wild type and the other α B-crystallin constructs. The far UV CD spectra of wild type, A171X, and K174X are similar in shape and magnitude and contained broad minima between 208 and 217 nm. The 450delA/wild type and 464delCT/wild type mixtures show increased negative ellipticity and a shift in minima to 208 nm. Truncation of the C-terminal extension results in the loss of secondary structure reflected by a decrease in negative ellipticity and a shift in wavelength minima (E164X, E165X, Q151X, and Q151X/wild type), with the most dramatic effects seen for Q151X.

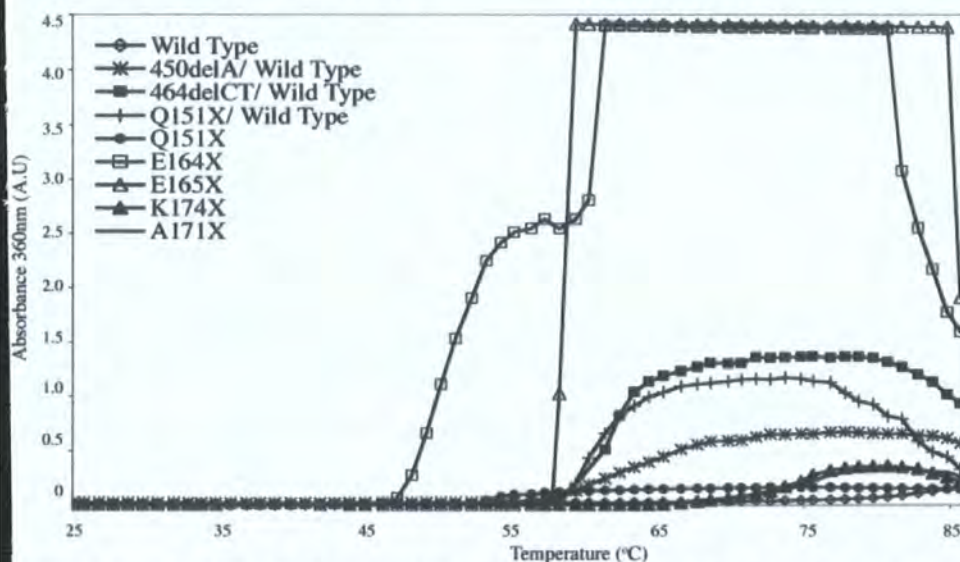


FIGURE 4. Thermal stability of wild type and C-terminal extension mutants of α B-crystallin. The effect of the C-terminal extension mutations on the heat-induced aggregation of α B-crystallin was measured at 360 nm over the temperature range 25–86 °C. The temperature was increased at a 1 °C/min over 1 h. Wild type and mutant α B-crystallins were assayed at 0.1 mg/ml. Notice the significantly reduced stability of the E164X, Q151X, and E165X α B-crystallin mutants.

ion constructs. These data correlate with more conservative changes in secondary structure as detected by far UV CD spectroscopy for the two frameshift mutants (Fig. 3) and the largely unchanged spectra for the A171X and K174X mutants.

Effect of C-terminal Extension Mutants upon Exposed Hydrophobicity—The probe, bis-ANS, has a low fluorescence quantum yield in aqueous solution, however, this increases dramatically upon binding to surface-exposed hydrophobic regions. As can be seen in Fig. 5, all the α B-crystallin mutants

bind more bis-ANS relative to the wild type α B-crystallin, except for the Q151X mutant, which binds substantially less. As all the mutants except Q151X α B-crystallin form oligomers (Fig. 2), we infer from these data that the increase in exposed hydrophobic surfaces arise from changes within their respective oligomeric structures. The reason why Q151X α B-crystallin binds so little bis-ANS is probably due the combined effects of decreased oligomerization and loss of secondary structure. We tested this by examining the bis-ANS binding properties of the wild type protein under mildly denaturing conditions (2 M guanidinium hydrochloride), which have been shown previously to eject α B-crystallin from native α -crystallin oligomers and to cause a significant loss of secondary structure (47). Indeed the presence of the guanidinium hydrochloride greatly reduced the bis-ANS binding to wild type α B-crystallin, with the fluorescence intensity dropping almost as low as that obtained for Q151X α B-crystallin alone.

Effect of C-terminal Extension Mutations upon α B-Crystallin Chaperone Activity—Citrate synthase (Fig. 6A) and insulin (Fig. 6C) chaperone assays were used to determine the effects of the α B-crystallin C-terminal extension mutations. Our expectation was that the observed chaperone activity would correlate with the effects of the mutations on protein secondary structure and heat stability. We predicted that E164X, E165X, and Q151X would exhibit the least activity in this assay. The chaperone activity achieved by these mutants in a citrate synthase aggregation assay (Fig. 6B) showed that whereas E164X was indeed the worst of all

the α B-crystallin constructs (–57% inhibition) none of the other C-terminal extension constructs performed worse than the wild type protein (100% inhibition). Indeed, the E165X (313%) was slightly better than the wild type protein and Q151X (755%) was one of the best. In fact, the combination of Q151X and wild type α B-crystallin was the best chaperone in the citrate synthase assay (1263% inhibition).

Another surprise from the citrate synthase chaperone assay was the relative performance of the two frameshift mutants,

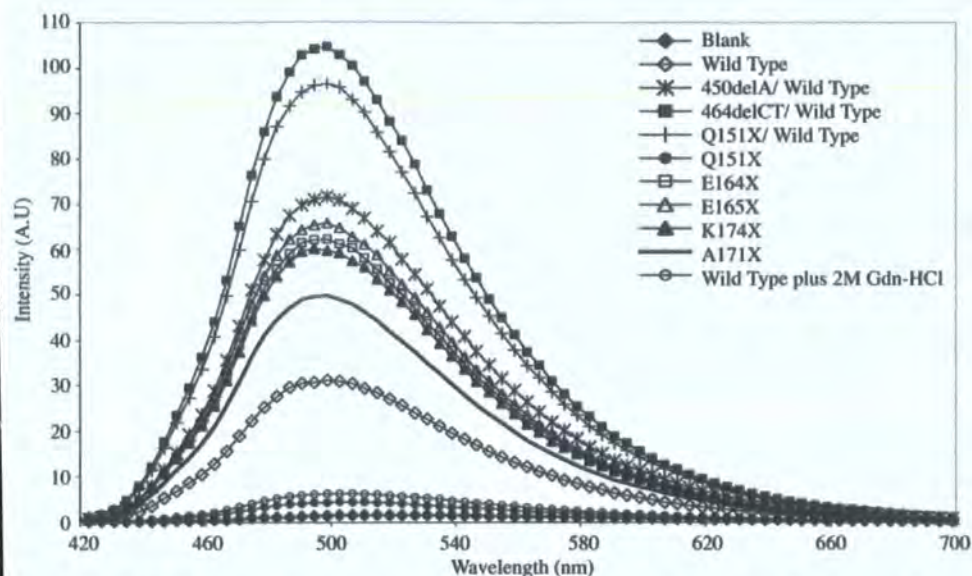


FIGURE 5. Bis-ANS fluorescence binding properties of α B-crystallin mutants. The effect of the C-terminal mutations upon the relative exposed hydrophobicity was performed using bis-ANS to bind to surface-exposed hydrophobic regions on the mutant and wild type α B-crystallin. Each protein was analyzed at 1 μ M in the presence of a 10-fold molar excess of bis-ANS. The excitation wavelength was 410 nm and emission spectra were collected between 420 and 700 nm. All spectra are the average of 10 individual scans. The resulting exposed hydrophobicity is increased for all mutants relative to the wild type α B-crystallin, with the exception of the Q151X mutant.

450delA and 464delCT, both of which performed better in combination with wild type α B-crystallin than the wild type α B-crystallin alone (625 and 216% inhibition, respectively). These data show that the disease-causing mutations in α B-crystallin (Q151X, 450delA, and 464delCT) all retain significant chaperone activity, surpassing the potential of the wild type protein alone for this client protein in this particular chaperone assay.

In contrast to the results with citrate synthase, all the C-terminal extension mutants performed worse than the wild type α B-crystallin in the insulin-based chaperone assay (Fig. 6C). In this assay, the three most heat-sensitive α B-crystallin mutants, E164X, E165X, and Q151X, increased protein aggregation compared with wild type α B-crystallin (–138, –8, and –45% inhibition, respectively (Fig. 6D)). An equimolar mixture of Q151X and wild type α B-crystallin (47% inhibition) retained significant chaperone activity of Q151X, but it was still one of the poorer chaperones in this assay. The K174X (93%) and A171X (93%) mutants had chaperone activities that most closely resembled the wild type α B-crystallin (100%) and even the two frameshift mutants, 450delA and 464delCT, in their respective combinations with wild type α B-crystallin, still possessed credible activities (68 and 78% inhibition, respectively).

Ability of the Disease-causing α B-Crystallin Mutants to Inhibit Desmin Filament Aggregation—One of the characteristic histopathological features of the human myopathies caused by some of the mutations in α B-crystallin under investigation in this study is the presence of aggregates of desmin filaments (9, 12). It was therefore decided to analyze the ability of the α B-crystallin mutants in this study to prevent desmin filament-filament associations (Fig. 7), using an assay developed to investigate the cell biological effects of the R120G mutation in α B-crystallin (10).

The assay takes advantage of the fact that intermediate filaments interact with each other in solution (10, 48) and this can be measured by sedimentation assay. The presence of a mutant protein that interacts with desmin filaments, for example, R120G α B-crystallin, activity encourages more filament-filament associations and therefore increases the proportion of pelletable desmin. Both Q151X and 464delCT α B-crystallin when mixed with wild type displayed desmin filament associations similar to wild type alone, whereas the 450delA/wild type protein mixture was significantly more effective than R120G α B-crystallin in inducing this filament association, highlighting the dominant effect of the 450delA mutation over the wild type α B-crystallin (Fig. 7).

In stark contrast to these results, the Q151X α B-crystallin was the most effective chaperone of all the disease-causing mutants and was also better than wild type α B-crystallin in reducing the proportion of pelletable desmin (Fig. 7A). Most of the Q151X mutant co-sedimented with desmin in the pellet fraction (cf. Fig. 7, B and C). Mixing Q151X with wild type α B-crystallin in an equimolar ratio reduced this binding to desmin filaments (cf. Fig. 7, B and C) and restored the levels of pelletable desmin to those obtained in the presence of wild type α B-crystallin (Fig. 7A). In contrast, the 450delA mutant was clearly dominant over the wild type α B-crystallin as there was not only increased binding to the filaments (cf. Fig. 7, B and C), but also a significant increase in the proportion of pelletable desmin (Fig. 7A). We interpret these data to indicate that the increased binding of 450delA α B-crystallin induces more filament-filament interactions resulting in more desmin in the pellet. Interestingly all the mutant α B-crystallins exhibited elevated binding to desmin filaments (Fig. 7C), but under these assay conditions (0.1 mg/ml desmin at 37 °C), the Q151X and 450delA α B-crystallin had opposite effects upon the promotion of filament-filament interactions.

To show that the effects of Q151X α B-crystallin were not due to an inhibition of desmin filament assembly *per se*, negatively stained samples were analyzed by electron microscopy (Fig. 7E) and the presence of abundant 10-nm filaments confirmed. When compared with desmin assembled in the presence of wild type α B-crystallin (Fig. 7D), the absence of α B-crystallin particles in the Q151X containing sample was also immediately apparent, confirming independently the data in Fig. 2, A and D.

Cytoplasmic Aggregate Formation of Selected α B-Crystallin Mutants in MCF7 Cells—The *in vitro* assays show that the Q151X mutant increased some chaperone activities, but also significantly destabilized the protein causing it to aggregate. We then decided to investigate the behavior of Q151X α B-crys-

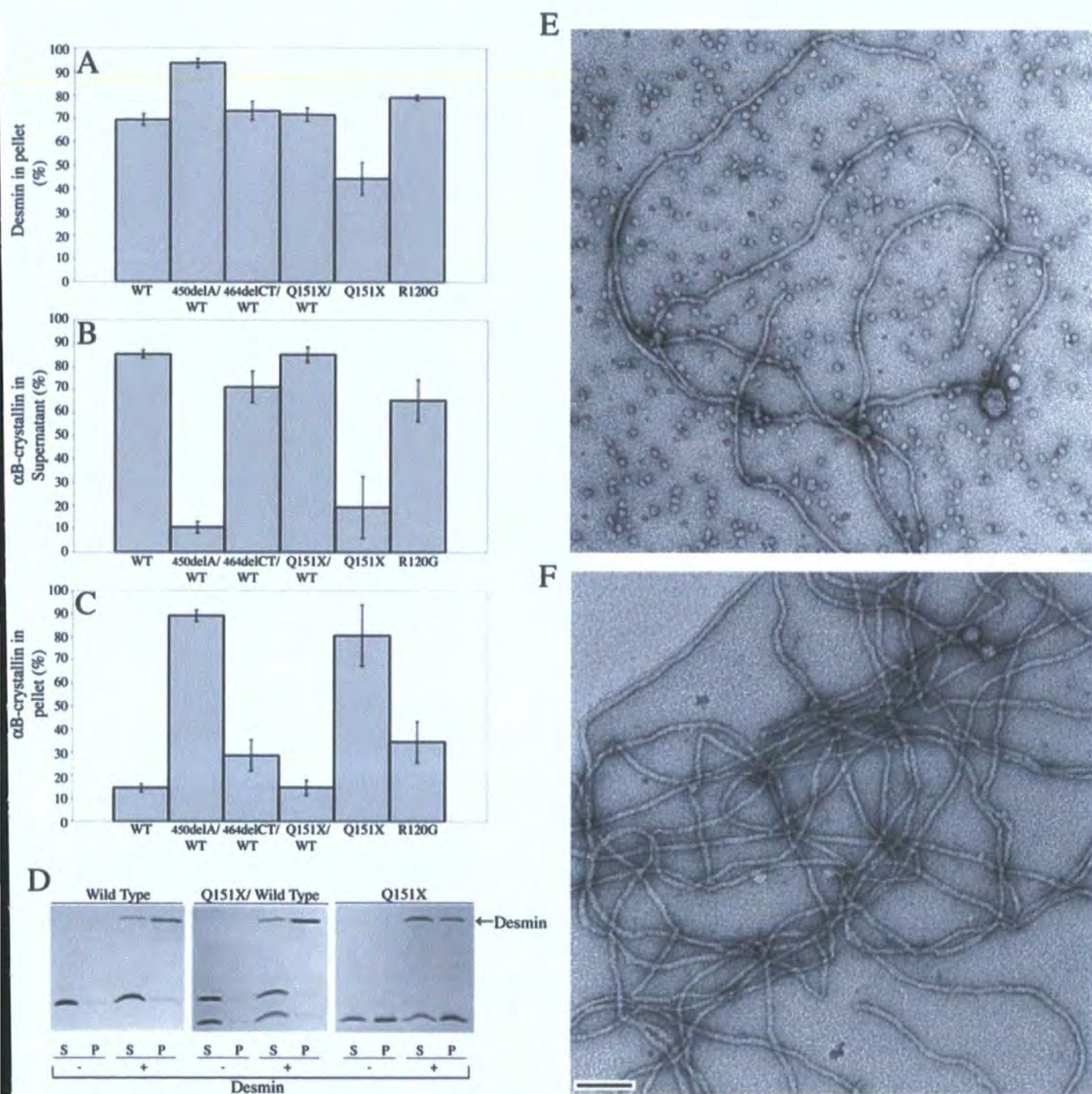


FIGURE 7. Sedimentation assay to investigate the prevention of desmin filament aggregation in the presence of various α B-crystallins at 37 °C. A–C shows the % desmin pelleted (A), the % α B-crystallin wild type and mutants remaining soluble in the presence of desmin (B), and the % of the total α B-crystallin pelleted in the presence of desmin (C), following low-speed centrifugation (2500 \times g). These data were calculated from SDS-PAGE data of the desmin binding assays. D, an example of the data used to calculate these values for wild type, Q151X/wild type, and Q151X α B-crystallin. These data illustrate the ability of the Q151X α B-crystallin to prevent desmin filament aggregation. Images obtained by electron microscopy of negatively stained samples of the assembled filaments for desmin assembled in the presence of wild type (E) and Q151X (F) α B-crystallin are shown to show that the addition of both chaperones has not dramatically altered filament morphology or length. Notice the lack of crystallin particles in the Q151X sample. Bar, 100 nm. S, supernatant; P, pellet.

increases the tendency of α B-crystallin to self-aggregate, even in a cellular environment.

DISCUSSION

Removal of the C-terminal Extension Reduces α B-Crystallin Oligomerization, but Not Chaperone Activity—The consensus view that has emerged from recent studies on mammalian

sHSPs is that the C-terminal extension is important for oligomerization and chaperone function (19, 22, 26, 28). The study presented here is the first to investigate the effects of sequentially truncating this domain (Lys¹⁷⁴, Ala¹⁷¹, Glu¹⁶⁵, and Glu¹⁶⁴) upon both aspects for α B-crystallin. It shows that deletion of the last 5 residues can improve chaperone activity in the citrate synthase assay without dramatically changing the sec-

Removal of C-terminal Extension Induces α B-Crystallin Aggregation

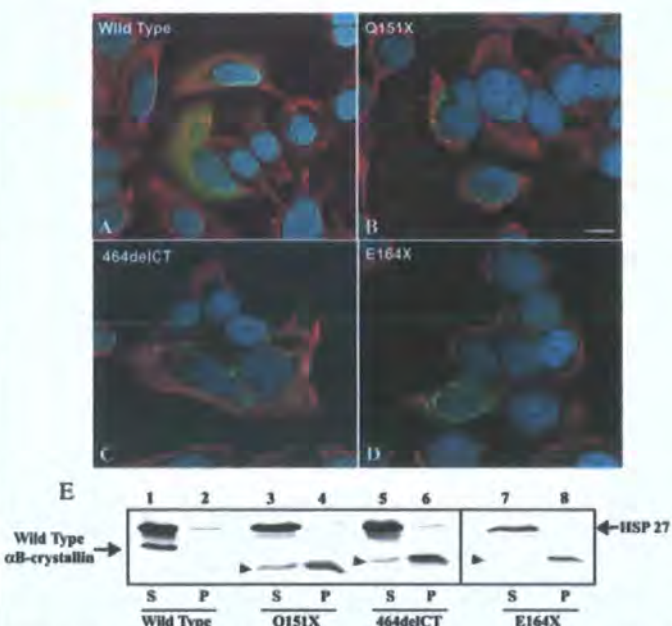


FIGURE 8. Decreased solubility and increased aggregation potential of Q151X α B-crystallin is revealed by transient transfection into MCF7 cells. A–D, MCF7 cells transiently transfected with wild type (A), Q151X (B), 464delCT (C), or E164X (D) α B-crystallin were fixed at 24 h post-transfection and processed for immunofluorescence microscopy. The subcellular distribution of α B-crystallin and keratin were visualized by double labeling with monoclonal anti-keratin (red channel) and polyclonal anti- α B-crystallin antibodies (green channel). A–D are merged images, showing the superimposition of the green, red, and blue (4',6-diamidino-2-phenylindole staining) channels. Images are individual optical sections acquired using a confocal laser scanning microscope (Zeiss 510). Cells expressing wild type α B-crystallin (A) showed the expected cytoplasmic distribution of α B-crystallin. In contrast, cells expressing mutant α B-crystallin resulted in the formation of cytoplasmic aggregates of α B-crystallin (B–D). Notice that 464delCT aggregates are scattered throughout the cytoplasm, whereas the Q151X and E164X aggregates locate to the perinuclear region of the cell. Bars, 10 μ m. Immunoblotting analysis (E) of α B-crystallin transiently transfected in MCF7 cells shows a shift in solubility for the mutant α B-crystallins. At 24 h post-transfection, cells were extracted with detergent buffer followed by centrifugation at $18,000 \times g$ for 10 min at 4 $^{\circ}$ C. The resulting supernatant (S) and pellet (P) fractions were analyzed by SDS-PAGE followed by immunoblotting analysis using anti-HSP 27 (loading control) and α B-crystallin antibodies. The blot was developed using enhanced chemiluminescence. Whereas wild type α B-crystallin was almost entirely soluble (E, lane 1, labeled S), Q151X (lane 4), 464delCT (lane 6), and E164X (lane 8) were found mostly in the pellet fractions (labeled P) of cell extracts. The relative electrophoretic mobility of mutant α B-crystallins is denoted by the arrowhead (\blacktriangleright). Like wild type α B-crystallin, HSP27 was also largely present in the supernatant fractions (E, lanes 2, 4, and 6, labeled P). These data are representative of three experiments.

secondary structure or oligomerization of α B-crystallin. Truncations (E164X, E165X) in the conserved REEK motif (26) decreased chaperone activity and oligomerization, although this coincided with more polydispersity for the oligomer as judged by size exclusion chromatography (Fig. 2). The removal of the C-terminal extension by the Q151X mutation produced a construct with the best chaperone activity profile of all the individual protein clients investigated (Figs. 6 and 7) despite the most significant changes in secondary structure (Fig. 3), bis-ANS binding (Fig. 5), and altered oligomerization (Fig. 2).

Whereas these results are in broad agreement with the consensus for other mammalian sHSPs, they demonstrate that the removal of the C-terminal extension from residue 151 prevents oligomerization (at concentrations less than 0.1 mg/ml), but not at the expense of chaperone function for α B-crystallin.

Indeed the citroconylation of full-length α B-crystallin achieves similar results and together with these data strongly support the conclusion that oligomerization is not required for α B-crystallin chaperone activity (42).

Deletion of the C-terminal Extension by the Q151X Mutation Increases Chaperone Activity for Some Client Proteins—The somewhat surprising observation is that the Q151X mutation actually improved chaperone activity for some client proteins (desmin and citrate synthase), in stark contrast to the effect of removing a similar region from α A-crystallin where chaperone activity was lost (22, 28).

The C-terminal extension deleted by the Q151X mutation includes the IX(I/V) motif (16), which is part of β -strand 10 (17, 23), that has been shown to be both part of a client protein binding site (19) and an oligomerization sequence (20) in α B-crystallin. This is removed by all three disease-causing mutations, including Q151X, but retained in the other truncation constructs (Fig. 1). Glycine substitutions in the IX(I/V) motif not only increased oligomerization and polydispersity of α B-crystallin, but also significantly increased chaperone activity (52). The data we have presented for Q151X α B-crystallin and the other truncation constructs suggest that the client protein binding site that embraces the IX(I/V) motif (19, 53) is not only dispensable for activity, but that it could actually inhibit chaperone function as its removal actually increased activity (citrate synthase, ~ 7.5 -fold; desmin, ~ 2 -fold).

A three-dimensional model of α B-crystallin has suggested that the C-terminal extension potentially acts as a "cap" on an important oligomerization and client protein binding site, namely the β 3- β 8- β 9 interface (46). This region also interacts with the β 4 strand, which is important in sHSP oligomerization as seen from the crystal structure of HSP16.9 (23), but it is also critical for chaperone activity (46). In fact reducing α B-crystallin to just its α -crystallin domain spanning residues 57–157, which still includes the β 3- β 8- β 9 surface, retained chaperone activity, but this construct only formed dimers and could not oligomerize (54). It is easy to explain these observations and also our data on the Q151X α B-crystallin mutant, in terms of how the removal of this C-terminal extension cap as proposed in the model (46) could allow substrate to bind more readily and thus enhance chaperone function while also decreasing oligomer size. The data we have presented here support this model and also add an interesting dimension. Our data also suggest that the C-terminal extension actually limits the full potential of α B-crystallin chaperone activity for some client proteins.

Aggregation of α B-Crystallin Encouraged by the Removal of the C-terminal Extension—The strong tendency of Q151X to aggregate at protein concentrations greater than 0.1 mg/ml and its very low refolding yield (Fig. 1D), suggests another potential role played by the C-terminal extension in preventing the uncontrolled self-aggregation of α B-crystallin (55). From the available sHSP crystal structures (17, 23), the C-terminal extension is solvent exposed and contributes to the higher order assembly of the oligomer (23, 56–58). In HSP16.9, the IX(I/V) motif from one subunit lays in a hydrophobic groove between β 4 and β 8 strands of the other interacting monomer. Although α B-crystallin has similar structural features, including the con-

served IX(I/V) motif in its C-terminal extension (Fig. 1A), the oligomers it forms are more polydisperse (55, 59, 60) compared with either HSP16.5 or HSP16.9, suggesting that the precise detail for the interactions of the C-terminal extension in α B-crystallin will vary, not least due to the different hinge sequences between β -strands 9 and 10 (23). The strong tendency of Q151X α B-crystallin to aggregate suggests that the C-terminal extension actually prevents such potential errant associations to favor instead oligomerization.

Reduced Protein Stability and Uncontrolled Self-aggregation Underlies the Molecular Basis of the Q151X, 450delA, and 464delCT Mutations—The loss of the C-terminal extension due to the Q151X mutation in α B-crystallin dramatically altered the secondary (Fig. 3) and tertiary structure of the protein (Fig. 2). This mutant was significantly destabilized as seen from the heat stability assay (Fig. 4) and showed a dramatic increase in the tendency to self-aggregate *in vitro* (Fig. 1) and *in vivo* (Fig. 8). Only a small proportion of Q151X α B-crystallin (~1%, Fig. 1D) remained soluble after refolding. Even in the presence of equimolar wild type α B-crystallin, the mixture had significantly altered secondary structure (Fig. 2), which affected α B-crystallin oligomerization (Fig. 3) and reduced refold yields (Fig. 1D). The Q151X mutation was dominant over the wild type protein in its effects upon heat stability, solubility, and secondary structure. These data suggest that the strong tendency to self-aggregate as a result of reduced stability is potentially an important factor in disease development.

Our data for both 450delA and 464delCT also suggest that it is a similar loss in protein stability that causes cataract and myofibrillar myopathy, respectively. Both mutants can only be refolded in the presence of wild type α B-crystallin and even then the temperature stabilities of the mixtures are reduced by some 20 °C compared with the wild type protein alone. Both the 450delA and 464delCT mutations introduced novel C-terminal peptides that have no homology to the existing C-terminal extension of α B-crystallin (Fig. 1A). Both mutations changed the oligomerization of wild type α B-crystallin and neither mutant/wild type mixture was an effective chaperone in either the desmin (Fig. 7) or insulin (Fig. 6, C and D) assays. Indeed, the 450delA mutation actively promoted filament-filament interactions for desmin, as reported previously for R120G α B-crystallin (10) and, under the assay conditions here, 450delA was more efficient than R120G in this activity. Therefore the loss of chaperone activity coupled with sequestration by client proteins could both contribute to the development of disease in the case of these two mutants. We suggest, however, that the aggregation of α B-crystallin is a key feature that offers potential for gain of function via its amyloidogenic potential (61).

The most difficult observation to explain regarding the Q151X mutation is its muscle-specific effect, which restricts the pathology to myofibrillar myopathy (18). In fact all three disease-causing mutations in the C-terminal extension of α B-crystallin (Q151X, 450delA, and 464delCT) are restricted in their pathology to either the lens (450delA (15)) or muscle (Q151X, 464delCT; (18)) and yet α B-crystallin is very highly expressed in both tissues (5). This is a familiar trend for α B-crystallin mutations and even the most recently published mutation, D140N, causes only lens cataract (62). Thus far,

R120G α B-crystallin is the only mutation that has produced both lens and muscle pathologies (9), but this is not to say that subclinical pathology can be totally excluded for the other mutations, including Q151X, as tissue biopsies from apparently unaffected tissues were not analyzed. Aggregation is a key histopathological feature of the Q151X mutation (18) concurring with our transient transfection and cell fractionation studies (Fig. 8) and so, this provides a plausible mechanism to support a potential dominant negative effect of the mutation by inhibiting the chaperone function of wild type α B-crystallin via coaggregation with mutant Q151X as implicated from our *in vitro* studies (Fig. 1).

Acknowledgments—We thank Terry Gibbons for technical support and Ming Der Perng for helpful discussions. We thank Cait MacPhee (Dept. of Physics, University of Edinburgh) for discussions and David Dixon for mass spectrometry analyses of recombinant proteins.

REFERENCES

- Morner, C. (1894) *Hoppe-Seyler's Z. Physiol. Chem.* **18**, 61–106
- Bloemendal, H., and de Jong, W. W. (1991) *Prog. Nucleic Acids Res. Mol. Biol.* **41**, 259–281
- Kato, K., Shinohara, H., Kurobe, N., Goto, S., Inaguma, Y., and Ohshima, K. (1991) *Biochim. Biophys. Acta* **1080**, 173–180
- Iwaki, T., Kume-Iwaki, A., Liem, R. K., and Goldman, J. E. (1991) *Kidney Int.* **40**, 52–56
- Kato, K., Shinohara, H., Kurobe, N., Inaguma, Y., Shimizu, K., and Ohshima, K. (1991) *Biochim. Biophys. Acta* **1074**, 201–208
- Klemenz, R., Frohli, E., Steiger, R. H., Schafer, R., and Aoyama, A. (1991) *Proc. Natl. Acad. Sci. U. S. A.* **88**, 3652–3656
- Horwitz, J. (1992) *Proc. Natl. Acad. Sci. U. S. A.* **89**, 10449–10453
- Kappe, G., Verschuure, P., Philipsen, R. L., Staalduinen, A. A., Van de Boogaart, P., Boelens, W. C., and De Jong, W. W. (2001) *Biochim. Biophys. Acta* **1520**, 1–6
- Vicart, P., Caron, A., Guicheney, P., Li, Z., Prevost, M. C., Faure, A., Chateau, D., Chapon, F., Tome, F., Dupret, J. M., Paulin, D., and Fardeau, M. (1998) *Nat. Genet.* **20**, 92–95
- Perng, M. D., Wen, S. F., van den IJssel, P., Prescott, A. R., and Quinlan, R. A. (2004) *Mol. Biol. Cell* **15**, 2335–2346
- Goldfarb, L. G., Park, K. Y., Cervenakova, L., Gorokhova, S., Lee, H. S., Vasconcelos, O., Nagle, J. W., Semino-Mora, C., Sivakumar, K., and Dalakas, M. C. (1998) *Nat. Genet.* **19**, 402–403
- Schroder, R., Vrabie, A., and Goebel, H. H. (2007) *J. Cell. Mol. Med.* **11**, 416–426
- Nicholl, I. D., and Quinlan, R. A. (1994) *EMBO J.* **13**, 945–953
- Perng, M. D., Cairns, L., van den IJssel, P., Prescott, A., Hutcheson, A. M., and Quinlan, R. A. (1999) *J. Cell Sci.* **112**, 2099–2112
- Berry, V., Francis, P., Reddy, M. A., Collyer, D., Vithana, E., MacKay, I., Dawson, G., Carey, A. H., Moore, A., Bhattacharya, S. S., and Quinlan, R. A. (2001) *Am. J. Hum. Genet.* **69**, 1141–1145
- de Jong, W. W., Caspers, G. J., and Leunissen, J. A. (1998) *Int. J. Biol. Macromol.* **22**, 151–162
- Kim, K. K., Kim, R., and Kim, S. H. (1998) *Nature* **394**, 595–599
- Selcen, D., and Engel, A. G. (2003) *Ann. Neurol.* **54**, 804–810
- Ghosh, J. G., Estrada, M. R., and Clark, J. I. (2005) *Biochemistry* **44**, 14854–14869
- Ghosh, J. G., and Clark, J. I. (2005) *Protein Sci.* **14**, 684–695
- Inagaki, N., Hayashi, T., Arimura, T., Koga, Y., Takahashi, M., Shibata, H., Teraoka, K., Chikamori, T., Yamashina, A., and Kimura, A. (2006) *Biochem. Biophys. Res. Commun.* **342**, 379–386
- Andley, U. P., Mathur, S., Griest, T. A., and Petrash, J. M. (1996) *J. Biol. Chem.* **271**, 31973–31980
- van Montfort, R. L., Basha, E., Friedrich, K. L., Slingsby, C., and Vierling, E. (2001) *Nat. Struct. Biol.* **8**, 1025–1030

Removal of C-terminal Extension Induces α B-Crystallin Aggregation

24. Stamler, R., Kappe, G., Boelens, W., and Slingsby, C. (2005) *J. Mol. Biol.* **353**, 68–79

25. Kim, R., Lai, L., Lee, H. H., Cheong, G. W., Kim, K. K., Wu, Z., Yokota, H., Marqusee, S., and Kim, S. H. (2003) *Proc. Natl. Acad. Sci. U. S. A.* **100**, 8151–8155

26. Rajan, S., Chandrashekar, R., Aziz, A., and Abraham, E. C. (2006) *Biochemistry* **45**, 15684–15691

27. Treweek, T. M., Ecroyd, H., Williams, D. M., Meehan, S., Carver, J. A., and Walker, M. J. (2007) *PLoS ONE* **2**, e1046

28. Thampi, P., and Abraham, E. C. (2003) *Biochemistry* **42**, 11857–11863

29. Perng, M. D., Muchowski, P. J., van den IJssel, P., Wu, G. J. S., Clark, J. I., and Quinlan, R. A. (1999) *J. Biol. Chem.* **274**, 33235–33243

30. Horwitz, J., Huang, Q. L., Ding, L., and Bova, M. P. (1998) *Methods Enzymol.* **290**, 365–383

31. Quinlan, R. A., Moir, R. D., and Stewart, M. (1989) *J. Cell Sci.* **93**, 71–83

32. Laemmli, U. (1970) *Nature* **227**, 680–685

33. Plater, M. L., Goode, D., and Crabbe, M. J. (1996) *J. Biol. Chem.* **271**, 28558–28566

34. He, S., Pan, S., Wu, K., Amster, I. J., and Orlando, R. (1995) *J. Mass Spectrom.* **30**, 424–431

35. Smith, J. B., Shun-Shin, G. A., Sun, Y., Miesbauer, L. R., Yang, Z., Yang, Z., Zhou, X., Schwedler, J., and Smith, D. L. (1995) *J. Protein Chem.* **14**, 179–188

36. Jimenez-ASENSIO, J., Colvis, C. M., Kowalak, J. A., Douglas-Tabor, Y., Dattiles, M. B., Moroni, M., Mura, U., Rao, C. M., Balasubramanian, D., Janjani, A., and Garland, D. (1999) *J. Biol. Chem.* **274**, 32287–32294

37. Colvis, C. M., Douglas-Tabor, Y., Werth, K. B., Vieira, N. E., Kowalak, J. A., Janjani, A., Yergey, A. L., and Garland, D. L. (2000) *Electrophoresis* **21**, 2219–2227

38. Ueda, Y., Duncan, M. K., and David, L. L. (2002) *Investig. Ophthalmol. Vis. Sci.* **43**, 205–215

39. Van Kleef, S. M., Willems-Thijssen, W., and Hoenders, H. J. (1976) *Eur. J. Biochem.* **66**, 477–483

40. Thampi, P., Hassan, A., Smith, J. B., and Abraham, E. C. (2002) *Investig. Ophthalmol. Vis. Sci.* **43**, 3265–3272

41. Ueda, Y., Fukiage, C., Shih, M., Shearer, T. R., and David, L. L. (2002) *Mol. Cell. Proteomics* **1**, 357–365

42. Horwitz, J., Huang, Q., and Ding, L. (2004) *Exp. Eye Res.* **79**, 817–821

43. Bova, M. P., Yaron, O., Huang, Q., Ding, L., Haley, D. A., Stewart, P. L., and Horwitz, J. (1999) *Proc. Natl. Acad. Sci. U. S. A.* **96**, 6137–6142

44. Sreelakshmi, Y., and Sharma, K. K. (2006) *Mol. Vis.* **12**, 581–587

45. Pasta, S. Y., Raman, B., Ramakrishna, T., and Rao, Ch. M. (2003) *J. Biol. Chem.* **278**, 51159–51166

46. Ghosh, J. G., Estrada, M. R., and Clark, J. I. (2006) *Biochemistry* **45**, 9878–9886

47. Doss-Pepe, E. W., Carew, E. L., and Koretz, J. F. (1998) *Exp. Eye Res.* **67**, 657–679

48. Bousquet, O., Ma, L., Yamada, S., Gu, C., Idei, T., Takahashi, K., Wirtz, D., and Coulombe, P. A. (2001) *J. Cell Biol.* **155**, 747–754

49. Munoz-Marmol, A. M., Strasser, G., Isamat, M., Coulombe, P. A., Yang, Y., Roca, X., Vela, E., Mate, J. L., Coll, J., Fernandez-Figueras, M. T., Navas-Palacios, J. J., Ariza, A., and Fuchs, E. (1998) *Proc. Natl. Acad. Sci. U. S. A.* **95**, 11312–11317

50. Zantema, A., Verlaan-De Vries, M., Maasdam, D., Bol, S., and van der Eb, A. (1992) *J. Biol. Chem.* **267**, 12936–12941

51. Simon, S., Fontaine, J. M., Martin, J. L., Sun, X., Hoppe, A. D., Welsh, M. J., Benndorf, R., and Vicart, P. (2007) *J. Biol. Chem.* **282**, 34276–34287

52. Pasta, S. Y., Raman, B., Ramakrishna, T., and Rao, Ch. M. (2004) *Mol. Vis.* **10**, 655–662

53. Ghosh, J. G., Houck, S. A., and Clark, J. I. (2008) *Int. J. Biochem. Cell Biol.* **40**, 954–967

54. Feil, I. K., Malfois, M., Hendle, J., van Der Zandt, H., and Svergun, D. I. (2001) *J. Biol. Chem.* **276**, 12024–12029

55. Aquilina, J. A., Benesch, J. L., Ding, L. L., Yaron, O., Horwitz, J., and Robinson, C. V. (2004) *J. Biol. Chem.* **279**, 28675–28680

56. White, H. E., Orlova, E. V., Chen, S., Wang, L., Ignatiou, A., Gowen, B., Stromer, T., Franzmann, T. M., Haslbeck, M., Buchner, J., and Saibil, H. R. (2006) *Structure* **14**, 1197–1204

57. Kennaway, C. K., Benesch, J. L., Gohlke, U., Wang, L., Robinson, C. V., Orlova, E. V., Saibil, H. R., and Keep, N. H. (2005) *J. Biol. Chem.* **280**, 33419–33425

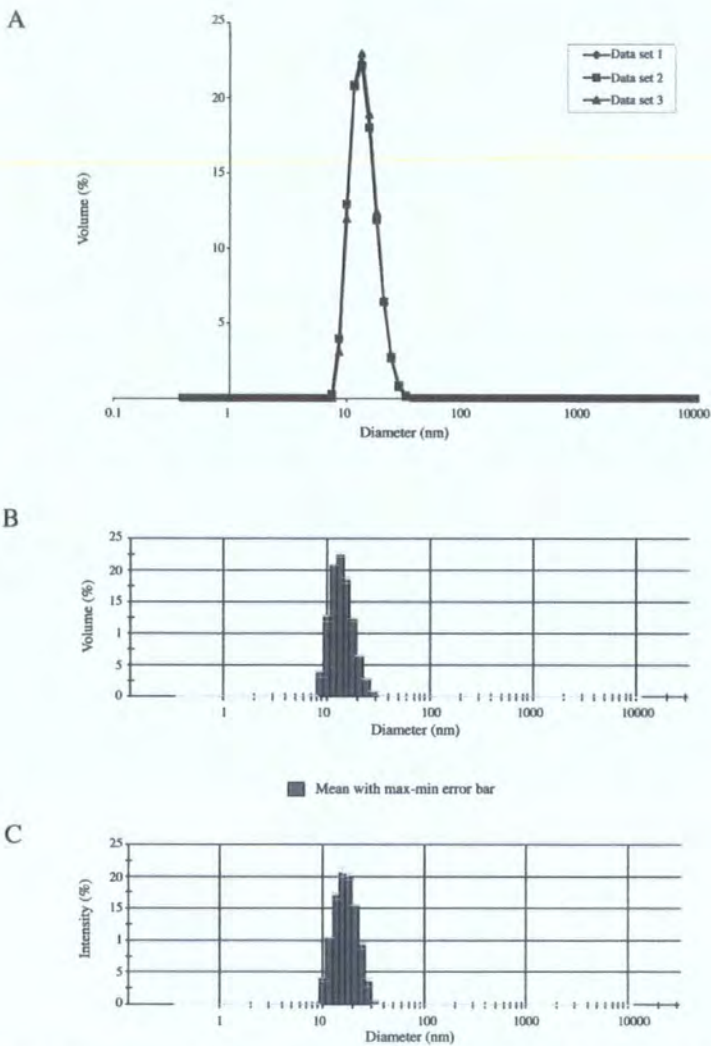
58. Kim, R., Kim, K. K., Yokota, H., and Kim, S. H. (1998) *Proc. Natl. Acad. Sci. U. S. A.* **95**, 9129–9133

59. Haley, D. A., Bova, M. P., Huang, Q. L., McHaourab, H. S., and Stewart, P. L. (2000) *J. Mol. Biol.* **298**, 261–272

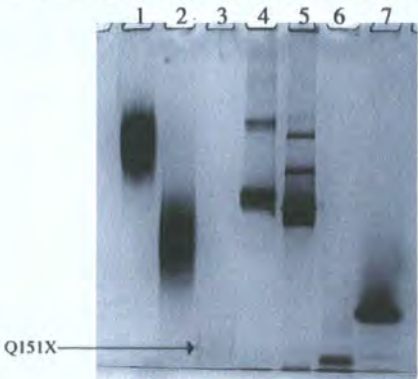
60. Haley, D. A., Horwitz, J., and Stewart, P. L. (1998) *J. Mol. Biol.* **277**, 27–35

61. Meehan, S., Knowles, T. P., Baldwin, A. J., Smith, J. F., Squires, A. M., Clements, P., Treweek, T. M., Ecroyd, H., Tartaglia, G. G., Vendruscolo, M., Macphree, C. E., Dobson, C. M., and Carver, J. A. (2007) *J. Mol. Biol.* **372**, 470–484

62. Liu, Y., Zhang, X., Luo, L., Wu, M., Zeng, R., Cheng, G., Hu, B., Liu, B., Liang, J. J., and Shang, F. (2006) *Investig. Ophthalmol. Vis. Sci.* **47**, 1069–1075

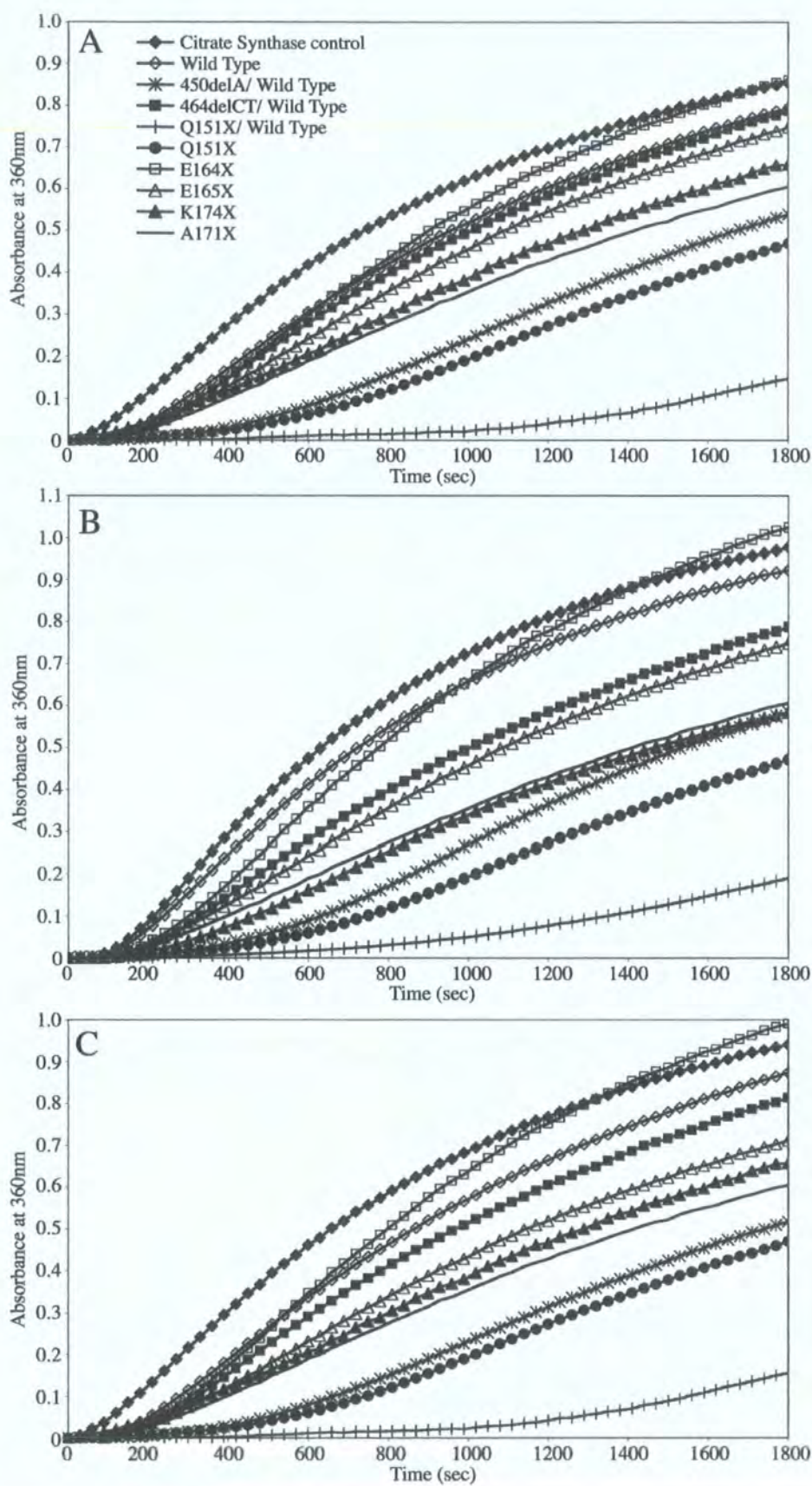


Supplementary Figure 1. Dynamic Light Scattering analyses of α B-crystallin wild type. The data shown represents the average of 3 runs, each of which consisted of 5 data accumulations. Supplementary Figure 1A shows the 3 data sets overlayed and confirms that the wild type oligomer accounts for 100% of the protein in the SEC pool. Figure 1B shows the corresponding histogram and (C) represents the intensity or level of light scattering produced by the α B-crystallin wild type.

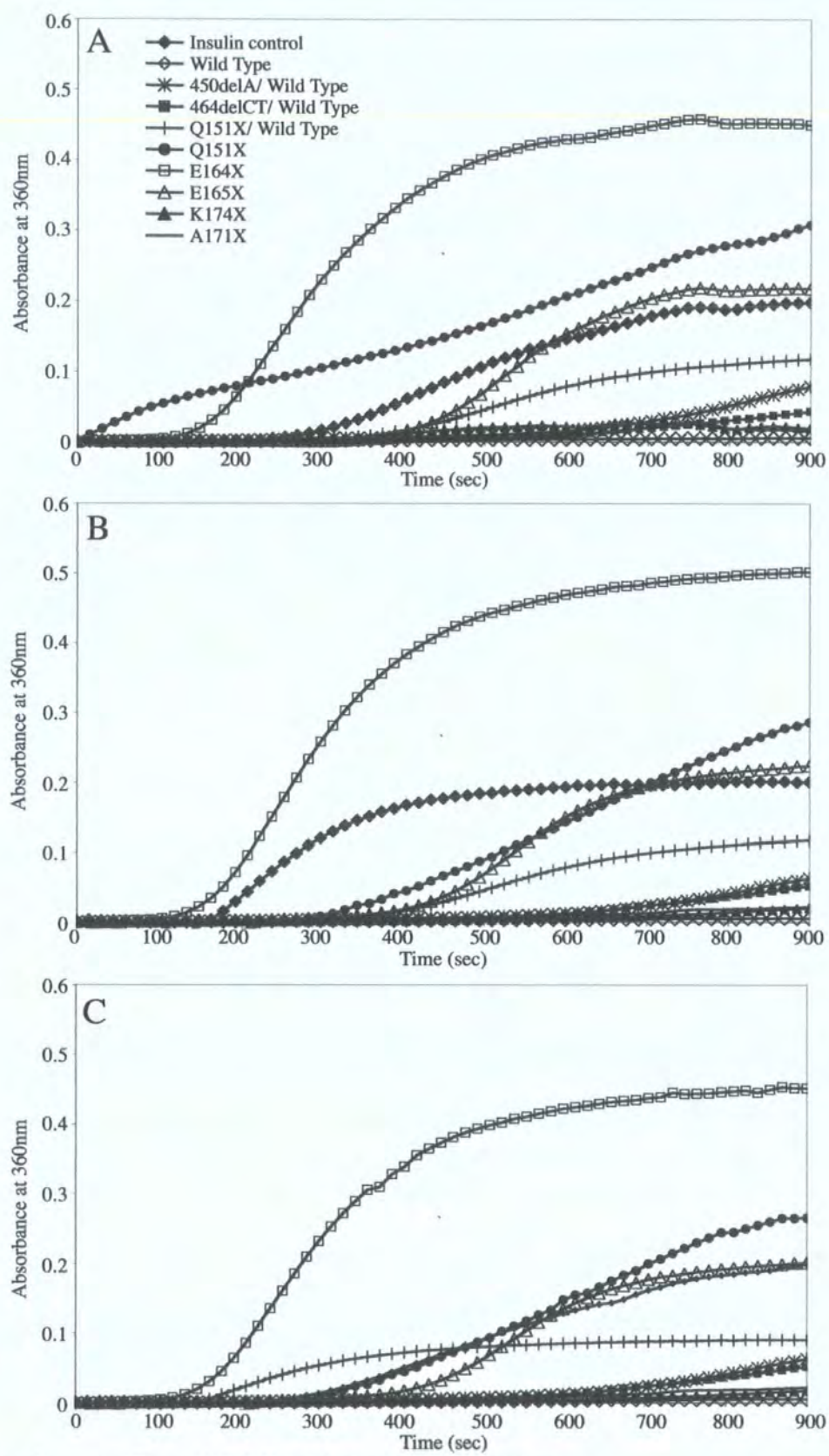


Lane	Sample Details	Molecular Weight (kDa)
1	Wild Type α B-crystallin	564
2	Q151X/ Wild Type α B-crystallin	442
3	Q151X	18
4	Thyroglobulin	725
5	GroEL	700
6	BSA	62
7	Carbonic anhydrase	29

Supplementary Figure 2. Native gel electrophoresis of the Q151X α B-crystallin oligomer. Analysis of Q151X α B-crystallin oligomer size, relative to wild type and Q151X/ wild type α B-crystallin. High and low Mwt calibrators are shown in lanes 4-7. All lanes represent a 20 μ g loading with the exception of the Q151X α B-crystallin (1.0 μ g) where the nature of the Q151X α B-crystallin refolding limits the available level of protein for analysis.



Supplementary Figure 3. Triplicate data set of Citrate synthase assays.



Supplementary Figure 4. Triplicate data set of Insulin assays.

REFERENCES

- Adams, J.M., Huang, D.C., Puthalakath, H., Bouillet, P., Vairo, G., Moriishi, K., Hausmann, G., O'Reilly, L., Newton, K., Ogilvy, S., Bath, M.L., Print, C.G., Harris, A.W., Strasser, A. and Cory, S. (1999) Control of apoptosis in hematopoietic cells by the Bcl-2 family of proteins. *Cold Spring Harb Symp Quant Biol*, 64, 351-358. α
- Aguilera, A. (2002) The connection between transcription and genomic instability. *EMBO J*, 21, 195-201.
- Andley, U.P., Mathur, S., Griest, T.A. and Petrash, J.M. (1996) Cloning, expression, and chaperone-like activity of human α A-crystallin. *J Biol Chem*, 271, 31973-31980.
- Andley, U.P., Patel, H.C. and Xi, J.H. (2002) The R116C mutation in α A-crystallin diminishes its protective ability against stress-induced lens epithelial cell apoptosis. *J Biol Chem*, 277, 10178-10186.
- Andley, U.P., Song, Z., Wawrousek, E.F., Brady, J.P., Bassnett, S. and Fleming, T.P. (2001) Lens epithelial cells derived from α B-crystallin knockout mice demonstrate hyperproliferation and genomic instability. *Faseb J*, 15, 221-229.
- Andley, U.P., Song, Z., Wawrousek, E.F., Fleming, T.P. and Bassnett, S. (2000) Differential protective activity of α A- and α B-crystallin in lens epithelial cells. *J Biol Chem*, 275, 36823-36831.
- Apple, D.J., Peng, Q., Visessook, N., Werner, L., Pandey, S.K., Escobar-Gomez, M., Ram, J., Whiteside, S.B., Schoderbeck, R., Ready, E.L. and Guindi, A. (2000) Surgical prevention of posterior capsule opacification. Part 1: Progress in eliminating this complication of cataract surgery. *J Cataract Refract Surg*, 26, 180-187.
- Aquilina, J.A. (2005) Subunit Exchange of Polydisperse Proteins. *The Journal of Biological Chemistry*, 280, 14485-14491.
- Aquilina, J.A., Benesch, J.L., Bateman, O.A., Slingsby, C. and Robinson, C.V. (2003) Polydispersity of a mammalian chaperone: mass spectrometry reveals the population of oligomers in α B-crystallin. *Proc Natl Acad Sci U S A*, 100, 10611-10616.
- Aquilina, J.A., Benesch, J.L., Ding, L.L., Yaron, O., Horwitz, J. and Robinson, C.V. (2004) Phosphorylation of α B-crystallin alters chaperone function through loss of dimeric substructure. *J Biol Chem*, 279, 28675-28680.
- Arai, H. and Atomi, Y. (1997) Chaperone activity of α B-crystallin suppresses tubulin aggregation through complex formation. *Cell Struct Funct*, 22, 539-544.
- Askanas, V. and Engel, W.K. (2006) Inclusion-body myositis: a myodegenerative conformational disorder associated with A β , protein misfolding, and proteasome inhibition. *Neurology*, 66, S39-48.
- Augusteyn, R.C. (2004a) α -crystallin: a review of its structure and function. *Clin Exp Optom*, 87, 356-366.
- Augusteyn, R.C. (2004b) Dissociation is not required for α -crystallin's chaperone function. *Exp Eye Res*, 79, 781-784.
- Augusteyn, R.C., Stevens, A. (1998) Macromolecular Structure of the Eye lens. *Progress in Polymer Science*, 23, 375-413.
- Avilov, S.V., Aleksandrov, N.A. and Demchenko, A.P. (2004) Quaternary structure of α -crystallin is necessary for the binding of unfolded proteins: a surface plasmon resonance study. *Protein Pept Lett*, 11, 41-48.

- Awasthi, N. and Wagner, B.J. (2005) Upregulation of heat shock protein expression by proteasome inhibition: an antiapoptotic mechanism in the lens. *Invest Ophthalmol Vis Sci*, 46, 2082-2091.
- Aziz, A., Santhoshkumar, P., Sharma, K.K. and Abraham, E.C. (2007) Cleavage of the C-terminal serine of human α A-crystallin produces α A1-172 with increased chaperone activity and oligomeric size. *Biochemistry*, 46, 2510-2519.
- Bardwell, J.C. and Craig, E.A. (1988) Ancient heat shock gene is dispensable. *J Bacteriol*, 170, 2977-2983.
- Barral, J.M., Broadley, S.A., Schaffar, G. and Hartl, F.U. (2004) Roles of molecular chaperones in protein misfolding diseases. *Semin Cell Dev Biol*, 15, 17-29.
- Beavis, R.C. and Chait, B.T. (1990) High-accuracy molecular mass determination of proteins using matrix-assisted laser desorption mass spectrometry. *Anal Chem*, 62, 1836-1840.
- Bellini, M. and Gall, J.G. (1999) Coilin shuttles between the nucleus and cytoplasm in *Xenopus* oocytes. *Mol Biol Cell*, 10, 3425-3434.
- Benesch, J.L., Aquilina, J.A., Ruotolo, B.T., Sobott, F. and Robinson, C.V. (2006) Tandem mass spectrometry reveals the quaternary organization of macromolecular assemblies. *Chem Biol*, 13, 597-605.
- Benesch, J.L. and Robinson, C.V. (2006) Mass spectrometry of macromolecular assemblies: preservation and dissociation. *Curr Opin Struct Biol*, 16, 245-251.
- Bennardini, F., Wrzosek, A. and Chiesi, M. (1992) α B-crystallin in cardiac tissue. Association with actin and desmin filaments. *Circ Res*, 71, 288-294.
- Bergman, A. and Siegal, M.L. (2003) Evolutionary capacitance as a general feature of complex gene networks. *Nature*, 424, 549-552.
- Berry, V., Francis, P., Kaushal, S., Moore, A. and Bhattacharya, S. (2000) Missense mutations in MIP underlie autosomal dominant 'polymorphic' and lamellar cataracts linked to 12q. *Nat Genet*, 25, 15-17.
- Berry, V., Francis, P., Reddy, M.A., Collyer, D., Vithana, E., MacKay, I., Dawson, G., Carey, A.H., Moore, A., Bhattacharya, S.S. and Quinlan, R.A. (2001) α B crystallin gene (CRYAB) mutation causes dominant congenital posterior polar cataract in humans. *Am J Hum Genet*, 69, 1141-1145.
- Bhat, S.P. and Nagineni, C.N. (1989) α B subunit of lens-specific protein α -crystallin is present in other ocular and non-ocular tissues. *Biochem Biophys Res Commun*, 158, 319-325.
- Bhattacharyya, J., Padmanabha Udupa, E.G., Wang, J. and Sharma, K.K. (2006) Mini- α B-crystallin: a functional element of α B-crystallin with chaperone-like activity. *Biochemistry*, 45, 3069-3076.
- Billingsley, G., Santhiya, S.T., Paterson, A.D., Ogata, K., Wodak, S., Hosseini, S.M., Manisastry, S.M., Vijayalakshmi, P., Gopinath, P.M., Graw, J. and Heon, E. (2006) CRYBA4, a novel human cataract gene, is also involved in microphthalmia. *Am J Hum Genet*, 79, 702-709.
- Biswas, A. and Das, K.P. (2004) Role of ATP on the interaction of α -crystallin with its substrates and its implications for the molecular chaperone function. *J Biol Chem*, 279, 42648-42657.
- Bloemendal, H., de Jong, W., Jaenicke, R., Lubsen, N.H., Slingsby, C. and Tardieu, A. (2004) Ageing and vision: structure, stability and function of lens crystallins. *Prog Biophys Mol Biol*, 86, 407-485.

- Bloemendal, H. and de Jong, W.W. (1991) Lens proteins and their genes. *Prog Nucleic Acid Res Mol Biol*, 41, 259-281.
- Boelens, W.C., Croes, Y., de Ruwe, M., de Reu, L. and de Jong, W.W. (1998) Negative charges in the C-terminal domain stabilize the α B-crystallin complex. *J Biol Chem*, 273, 28085-28090.
- Bobula, J., Tomala, K., Jez, E., Wloch, D.M., Borts, R.H. and Korona, R. (2006) Why molecular chaperones buffer mutational damage: a case study with a yeast Hsp40/70 system. *Genetics*, 174, 937-944.
- Bousquet, O., Ma, L., Yamada, S., Gu, C., Idei, T., Takahashi, K., Wirtz, D. and Coulombe, P.A. (2001) The nonhelical tail domain of keratin 14 promotes filament bundling and enhances the mechanical properties of keratin intermediate filaments in vitro. *J Cell Biol*, 155, 747-754.
- Bova, M.P., Ding, L.L., Horwitz, J. and Fung, B.K. (1997) Subunit exchange of α A-crystallin. *J Biol Chem*, 272, 29511-29517.
- Bova, M.P., McHaourab, H.S., Han, Y. and Fung, B.K. (2000) Subunit exchange of small heat shock proteins. Analysis of oligomer formation of α A-crystallin and Hsp27 by fluorescence resonance energy transfer and site-directed truncations. *J Biol Chem*, 275, 1035-1042.
- Bova, M.P., Yaron, O., Huang, Q., Ding, L., Haley, D.A., Stewart, P.L. and Horwitz, J. (1999) Mutation R120G in α B-crystallin, which is linked to a desmin-related myopathy, results in an irregular structure and defective chaperone-like function. *Proc Natl Acad Sci U S A*, 96, 6137-6142.
- Bradley, R.H., Ireland, M.E. and Maisel, H. (1979) Age changes in the skeleton of the human lens. *Acta Ophthalmol (Copenh)*, 57, 461-469.
- Bron, A.J., Vrensen, G.F., Koretz, J., Maraini, G. and Harding, J.J. (2000) The ageing lens. *Ophthalmologica*, 214, 86-104.
- Bu, L., Jin, Y., Shi, Y., Chu, R., Ban, A., Eiberg, H., Andres, L., Jiang, H., Zheng, G., Qian, M., Cui, B., Xia, Y., Liu, J., Hu, L., Zhao, G., Hayden, M.R. and Kong, X. (2002) Mutant DNA-binding domain of HSF4 is associated with autosomal dominant lamellar and Marner cataract. *Nat Genet*, 31, 276-278.
- Bullard, B., Ferguson, C., Minajeva, A., Leake, M.C., Gautel, M., Labeit, D., Ding, L., Labeit, S., Horwitz, J., Leonard, K.R. and Linke, W.A. (2004) Association of the chaperone α B-crystallin with titin in heart muscle. *J Biol Chem*, 279, 7917-7924.
- Bunkoczi, G., Salah, E., Filippakopoulos, P., Fedorov, O., Muller, S., Sobott, F., Parker, S.A., Zhang, H., Min, W., Turk, B.E. and Knapp, S. (2007) Structural and functional characterization of the human protein kinase ASK1. *Structure*, 15, 1215-1226.
- Carra, S., Sivilotti, M., Chavez Zobel, A.T., Lambert, H. and Landry, J. (2005) HspB8, a small heat shock protein mutated in human neuromuscular disorders, has in vivo chaperone activity in cultured cells. *Hum Mol Genet*, 14, 1659-1669.
- Carver, J.A. (1999) Probing the structure and interactions of crystallin proteins by NMR spectroscopy. *Prog Retin Eye Res*, 18, 431-462.
- Carver, J.A., Aquilina, J.A., Truscott, R.J. and Ralston, G.B. (1992) Identification by ^1H NMR spectroscopy of flexible C-terminal extensions in bovine lens α -crystallin. *FEBS Lett*, 311, 143-149.
- Carver, J.A., Guerreiro, N., Nicholls, K.A. and Truscott, R.J. (1995) On the interaction of α -crystallin with unfolded proteins. *Biochim Biophys Acta*, 1252, 251-260.

- Carver, J.A. and Lindner, R.A. (1998) NMR spectroscopy of α -crystallin. Insights into the structure, interactions and chaperone action of small heat-shock proteins. *Int J Biol Macromol*, 22, 197-209.
- Carver, J.A., Nicholls, K.A., Aquilina, J.A. and Truscott, R.J. (1996) Age-related changes in bovine α -crystallin and high-molecular-weight protein. *Exp Eye Res*, 63, 639-647.
- Caspers, G.J., Leunissen, J.A. and de Jong, W.W. (1995) The expanding small heat-shock protein family, and structure predictions of the conserved " α -crystallin domain". *J Mol Evol*, 40, 238-248.
- Cenciarelli, C., Chiaur, D.S., Guardavaccaro, D., Parks, W., Vidal, M. and Pagano, M. (1999) Identification of a family of human F-box proteins. *Curr Biol*, 9, 1177-1179.
- Chang, Z., Primm, T.P., Jakana, J., Lee, I.H., Serysheva, I., Chiu, W., Gilbert, H.F. and Quioco, F.A. (1996) Mycobacterium tuberculosis 16-kDa antigen (Hsp16.3) functions as an oligomeric structure in vitro to suppress thermal aggregation. *J Biol Chem*, 271, 7218-7223.
- Chavez Zobel, A.T., Loranger, A., Marceau, N., Theriault, J.R., Lambert, H. and Landry, J. (2003) Distinct chaperone mechanisms can delay the formation of aggresomes by the myopathy-causing R120G α B-crystallin mutant. *Hum Mol Genet*, 12, 1609-1620.
- Cheng, C.Y., Yen, M.Y., Chen, S.J., Kao, S.C., Hsu, W.M. and Liu, J.H. (2001) Visual acuity and contrast sensitivity in different types of posterior capsule opacification. *J Cataract Refract Surg*, 27, 1055-1060.
- Chiesi, M., Longoni, S. and Limbruno, U. (1990) Cardiac α -crystallin. III. Involvement during heart ischemia. *Mol Cell Biochem*, 97, 129-136.
- Christen, W.G., Glynn, R.J., Chew, E.Y. and Buring, J.E. (2007) Vitamin E and Age-Related Cataract in a Randomized Trial of Women. *Ophthalmology*.
- Ciechanover, A. (1998) The ubiquitin-proteasome pathway: on protein death and cell life. *Embo J*, 17, 7151-7160.
- Ciechanover, A. (2001) Linking ubiquitin, parkin and synphilin-1. *Nat Med*, 7, 1108-1109.
- Cobb, B.A. and Petrash, J.M. (2002) α -Crystallin chaperone-like activity and membrane binding in age-related cataracts. *Biochemistry*, 41, 483-490.
- Colvis, C.M., Douglas-Tabor, Y., Werth, K.B., Vieira, N.E., Kowalak, J.A., Janjani, A., Yergey, A.L. and Garland, D.L. (2000) Tracking pathology with proteomics: identification of in vivo degradation products of α B-crystallin. *Electrophoresis*, 21, 2219-2227.
- Conley, Y.P., Erturk, D., Keverline, A., Mah, T.S., Keravala, A., Barnes, L.R., Bruchis, A., Hess, J.F., FitzGerald, P.G., Weeks, D.E., Ferrell, R.E. and Gorin, M.B. (2000) A juvenile-onset, progressive cataract locus on chromosome 3q21-q22 is associated with a missense mutation in the beaded filament structural protein-2. *Am J Hum Genet*, 66, 1426-1431.
- Cryns, V. and Yuan, J. (1998) Proteases to die for. *Genes Dev*, 12, 1551-1570.
- Csermely, P. (2004) Strong links are important, but weak links stabilize them. *Trends Biochem Sci*, 29, 331-334.
- Csermely, P. and Soti, C. (2006) Cellular networks and the aging process. *Arch Physiol Biochem*, 112, 60-64.
- Cubas, P., Vincent, C. and Coen, E. (1999) An epigenetic mutation responsible for natural variation in floral symmetry. *Nature*, 401, 157-161.

- Cvekl, A. and Piatigorsky, J. (1996) Lens development and crystallin gene expression: many roles for Pax-6. *Bioessays*, 18, 621-630.
- Dahlman, J.M., Margot, K.L., Ding, L., Horwitz, J. and Posner, M. (2005) Zebrafish α -crystallins: protein structure and chaperone-like activity compared to their mammalian orthologs. *Mol Vis*, 11, 88-96.
- Datta, S.A. and Rao, C.M. (1999) Differential temperature-dependent chaperone-like activity of α A- and α B-crystallin homoaggregates. *J Biol Chem*, 274, 34773-34778.
- Datta, S.A. and Rao, C.M. (2000) Packing-induced conformational and functional changes in the subunits of α -crystallin. *J Biol Chem*, 275, 41004-41010.
- de Jong, W.W., Caspers, G.J. and Leunissen, J.A. (1998) Genealogy of the α -crystallin--small heat-shock protein superfamily. *Int J Biol Macromol*, 22, 151-162.
- de Jong, W.W., Leunissen, J.A., Leenen, P.J., Zweers, A. and Versteeg, M. (1988) Dogfish α -crystallin sequences. Comparison with small heat shock proteins and Schistosoma egg antigen. *J Biol Chem*, 263, 5141-5149.
- De Jonghe, P., Timmerman, V., Van Broeckhoven, C. (1998) 2nd Workshop of the European CMT Consortium: 53rd ENMC International Workshop on Classification and Diagnostic Guidelines for Charcot-Marie-Tooth Type 2 (CMT2-HMSN II) and Distal Hereditary Motor Neuropathy (distal HMN-Spinal CMT) 26-28 September 1997, Naarden, The Netherlands. *Neuromuscul Disord*, 8, 426-431.
- De Rijk, E.P., Van Rijk, A.F., Van Esch, E., De Jong, W.W., Wesseling, P. and Bloemendal, H. (2000) Demyelination and axonal dystrophy in α A-crystallin transgenic mice. *Int J Exp Pathol*, 81, 271-282.
- del Valle, L.J., Escribano, C., Perez, J.J. and Garriga, P. (2002) Calcium-induced decrease of the thermal stability and chaperone activity of α -crystallin. *Biochim Biophys Acta*, 1601, 100-109.
- Delcourt, C., Dupuy, A.M., Carriere, I., Lacroux, A. and Cristol, J.P. (2005) Albumin and transthyretin as risk factors for cataract: the POLA study. *Arch Ophthalmol*, 123, 225-232.
- den Engelsman, J., Keijsers, V., de Jong, W.W. and Boelens, W.C. (2003) The small heat-shock protein α B-crystallin promotes FBX4-dependent ubiquitination. *J Biol Chem*, 278, 4699-4704.
- Deretic, D., Aebersold, R.H., Morrison, H.D. and Papermaster, D.S. (1994) α A- and α B-crystallin in the retina. Association with the post-Golgi compartment of frog retinal photoreceptors. *J Biol Chem*, 269, 16853-16861.
- Derham, B.K. and Harding, J.J. (1999) α -crystallin as a molecular chaperone. *Prog Retin Eye Res*, 18, 463-509.
- Dickerson, J.E., Jr., Dotzel, E. and Clark, A.F. (1997) Steroid-induced cataract: new perspective from in vitro and lens culture studies. *Exp Eye Res*, 65, 507-516.
- Doss-Pepe, E.W., Carew, E.L. and Koretz, J.F. (1998) Studies of the denaturation patterns of bovine α -crystallin using an ionic denaturant, guanidine hydrochloride and a non-ionic denaturant, urea. *Exp Eye Res*, 67, 657-679.
- Drexler, H.C. (1997) Activation of the cell death program by inhibition of proteasome function. *Proc Natl Acad Sci U S A*, 94, 855-860.
- Dubin, R.A., Wawrousek, E.F. and Piatigorsky, J. (1989) Expression of the murine α B-crystallin gene is not restricted to the lens. *Mol Cell Biol*, 9, 1083-1091.
- Duncan, G. and Jacob, T.J. (1984) Calcium and the physiology of cataract. *Ciba Found Symp*, 106, 132-152.

- Durrant, A. (1962) The environmental induction of heritable change in *Linum*. *Heredity*, 17, 27-61.
- Ehrnsperger, M., Lilie, H., Gaestel, M. and Buchner, J. (1999) The dynamics of Hsp25 quaternary structure. Structure and function of different oligomeric species. *J Biol Chem*, 274, 14867-14874.
- Ellis, R.J. and Minton, A.P. (2003) Cell biology: join the crowd. *Nature*, 425, 27-28.
- Elmore, S. (2007) Apoptosis: a review of programmed cell death. *Toxicol Pathol*, 35, 495-516.
- Evgrafov, O.V., Mersiyanova, I., Irobi, J., Van Den Bosch, L., Dierick, I., Leung, C.L., Schagina, O., Verpoorten, N., Van Impe, K., Fedotov, V., Dadali, E., Auer-Grumbach, M., Windpassinger, C., Wagner, K., Mitrovic, Z., Hilton-Jones, D., Talbot, K., Martin, J.J., Vasserman, N., Tverskaya, S., Polyakov, A., Liem, R.K., Gettemans, J., Robberecht, W., De Jonghe, P. and Timmerman, V. (2004) Mutant small heat-shock protein 27 causes axonal Charcot-Marie-Tooth disease and distal hereditary motor neuropathy. *Nat Genet*, 36, 602-606.
- Fain, O. (2004) [Vitamin C deficiency]. *Rev Med Interne*, 25, 872-880.
- Fares, M.A., Ruiz-Gonzalez, M.X., Moya, A., Elena, S.F. and Barrio, E. (2002) Endosymbiotic bacteria: groEL buffers against deleterious mutations. *Nature*, 417, 398.
- Fayet, O., Louarn, J.M. and Georgopoulos, C. (1986) Suppression of the *Escherichia coli* dnaA46 mutation by amplification of the groES and groEL genes. *Mol Gen Genet*, 202, 435-445.
- Feil, I.K., Malfois, M., Hendle, J., van Der Zandt, H. and Svergun, D.I. (2001) A novel quaternary structure of the dimeric α -crystallin domain with chaperone-like activity. *J Biol Chem*, 276, 12024-12029.
- Fernando, P., Heikkila, J.J. (2000) Functional characterisation of *Xenopus* small heat shock protein, Hsp3-C: the carboxyl end is required for stability and chaperone activity. *Cell Stress & Chaperones*, 5, 148-159.
- Francis, P.J., Berry, V., Bhattacharya, S.S. and Moore, A.T. (2000) The genetics of childhood cataract. *J Med Genet*, 37, 481-488.
- Francis, P.J., Berry, V., Moore, A.T. and Bhattacharya, S. (1999) Lens biology: development and human cataractogenesis. *Trends Genet*, 15, 191-196.
- Fratta, P., Engel, W.K., McFerrin, J., Davies, K.J., Lin, S.W. and Askanas, V. (2005) Proteasome inhibition and aggresome formation in sporadic inclusion-body myositis and in amyloid-beta precursor protein-overexpressing cultured human muscle fibers. *Am J Pathol*, 167, 517-526.
- Fujita, Y., Ohto, E., Katayama, E. and Atomi, Y. (2004) α B-Crystallin-coated MAP microtubule resists nocodazole and calcium-induced disassembly. *J Cell Sci*, 117, 1719-1726.
- Ganadu, M.L., Aru, M., Mura, G.M., Coi, A., Mlynarz, P. and Kozlowski, H. (2004) Effects of divalent metal ions on the α B-crystallin chaperone-like activity: spectroscopic evidence for a complex between copper(II) and protein. *J Inorg Biochem*, 98, 1103-1109.
- Geisler, N. and Weber, K. (1981) Comparison of the proteins of two immunologically distinct intermediate-sized filaments by amino acid sequence analysis: desmin and vimentin. *Proc Natl Acad Sci USA*, 78, 4120-4123.
- Georgopoulos, C. (2004) In vivo analysis of the overlapping functions of DnaK and trigger factor. *EMBO Rep*, 5, 195-200.

- Ghosh, J.G. and Clark, J.I. (2005a) Insights into the domains required for dimerization and assembly of human α B crystallin. *Protein Sci*, 14, 684-695.
- Ghosh, J.G., Estrada, M.R. and Clark, J.I. (2005b) Interactive domains for chaperone activity in the small heat shock protein, human α B crystallin. *Biochemistry*, 44, 14854-14869.
- Ghosh, J.G., Estrada, M.R. and Clark, J.I. (2006a) Structure-based analysis of the beta8 interactive sequence of human α B crystallin. *Biochemistry*, 45, 9878-9886.
- Ghosh, J.G., Estrada, M.R., Houck, S.A. and Clark, J.I. (2006b) The function of the β 3 interactive domain in the small heat shock protein and molecular chaperone, human α B crystallin. *Cell Stress Chaperones*, 11, 187-197.
- Ghosh, J.G., Houck, S.A. and Clark, J.I. (2007) Interactive sequences in the stress protein and molecular chaperone human α B crystallin recognize and modulate the assembly of filaments. *Int J Biochem Cell Biol*, 39, 1804-1815.
- Ghosh, J.G., Houck, S.A., Doneanu, C.E. and Clark, J.I. (2006c) The β 4- β 8 Groove Is an ATP-interactive Site in the α -Crystallin Core Domain of the Small Heat Shock Protein, Human α B Crystallin. *J Mol Biol*, 364, 364-375.
- Ghosh, J.G., Shenoy, A.K., Jr. and Clark, J.I. (2006d) N- and C-Terminal Motifs in Human α B Crystallin Play an Important Role in the Recognition, Selection, and Solubilization of Substrates. *Biochemistry*, 45, 13847-13854.
- Glass, C.K. and Rosenfeld, M.G. (2000) The coregulator exchange in transcriptional functions of nuclear receptors. *Genes Dev*, 14, 121-141.
- Goodman, H. (1964) Senile changes of the lens and the vitreous. *Am J Ophthalmol*, 57, 1-13.
- Gounari, F., Merdes, A., Quinlan, R., Hess, J., FitzGerald, P.G., Ouzounis, C.A. and Georgatos, S.D. (1993) Bovine filensin possesses primary and secondary structure similarity to intermediate filament proteins. *J Cell Biol*, 121, 847-853.
- Grainger, R.M. (1992) Embryonic lens induction: shedding light on vertebrate tissue determination. *Trends Genet*, 8, 349-355.
- Granzier, H.L. and Labeit, S. (2004) The giant protein titin: a major player in myocardial mechanics, signaling, and disease. *Circ Res*, 94, 284-295.
- Graw, J. (2003) The genetic and molecular basis of congenital eye defects. *Nat Rev Genet*, 4, 876-888.
- Grimm, L.M., Goldberg, A.L., Poirier, G.G., Schwartz, L.M. and Osborne, B.A. (1996) Proteasomes play an essential role in thymocyte apoptosis. *Embo J*, 15, 3835-3844.
- Groenen, P.J., Merck, K.B., de Jong, W.W. and Bloemendal, H. (1994) Structure and modifications of the junior chaperone α -crystallin. From lens transparency to molecular pathology. *Eur J Biochem*, 225, 1-19.
- Gupta, R. and Srivastava, O.P. (2004) Deamidation affects structural and functional properties of human α A-crystallin and its oligomerization with α B-crystallin. *J Biol Chem*, 279, 44258-44269.
- Guruprasad, K. and Kumari, K. (2003) Three-dimensional models corresponding to the C-terminal domain of human α A- and α B-crystallins based on the crystal structure of the small heat-shock protein HSP16.9 from wheat. *Int J Biol Macromol*, 33, 107-112.

- Haley, D.A., Bova, M.P., Huang, Q.L., McHaourab, H.S. and Stewart, P.L. (2000) Small heat-shock protein structures reveal a continuum from symmetric to variable assemblies. *J Mol Biol*, 298, 261-272.
- Haley, D.A., Horwitz, J. and Stewart, P.L. (1998) The small heat-shock protein, α B-crystallin, has a variable quaternary structure. *J Mol Biol*, 277, 27-35.
- Hamamichi, S., Kosano, H., Nakai, S., Ogiwara-Umeda, I. and Nishigori, H. (2003) Involvement of hepatic glucocorticoid receptor-mediated functions in steroid-induced cataract formation. *Exp Eye Res*, 77, 575-580.
- Harding, J.J. (1991) Post-translational modification of lens proteins in cataract. *Lens Eye Toxic Res*, 8, 245-250.
- Harding, A.E. and Thomas, P.K. (1980a) The clinical features of hereditary motor and sensory neuropathy types I and II. *Brain*, 103, 259-280.
- Harding, A.E. and Thomas, P.K. (1980b) Hereditary distal spinal muscular atrophy. A report on 34 cases and a review of the literature. *J Neurol Sci*, 45, 337-348.
- Harrington, V., McCall, S., Huynh, S., Srivastava, K. and Srivastava, O.P. (2004) Crystallins in water soluble-high molecular weight protein fractions and water insoluble protein fractions in aging and cataractous human lenses. *Mol Vis*, 10, 476-489.
- Hartman, J.L.t., Garvik, B. and Hartwell, L. (2001) Principles for the buffering of genetic variation. *Science*, 291, 1001-1004.
- Hartwell, L., Weinert, T., Kadyk, L. and Garvik, B. (1994) Cell cycle checkpoints, genomic integrity, and cancer. *Cold Spring Harb Symp Quant Biol*, 59, 259-263.
- Hasan, A., Smith, D.L. and Smith, J.B. (2002) α -crystallin regions affected by adenosine 5'-triphosphate identified by hydrogen-deuterium exchange. *Biochemistry*, 41, 15876-15882.
- Haslbeck, M., Walke, S., Stromer, T., Ehrnsperger, M., White, H.E., Chen, S., Saibil, H.R. and Buchner, J. (1999) Hsp26: a temperature-regulated chaperone. *Embo J*, 18, 6744-6751.
- Hayashi, L.C. (1998) Ultraviolet radiation and cataract: A review. *Asia Pac J Public Health*.
- Head, M.W., Corbin, E. and Goldman, J.E. (1993) Overexpression and abnormal modification of the stress proteins α B-crystallin and HSP27 in Alexander disease. *Am J Pathol*, 143, 1743-1753.
- Head, M.W. and Goldman, J.E. (2000) Small heat shock proteins, the cytoskeleton, and inclusion body formation. *Neuropathol Appl Neurobiol*, 26, 304-312.
- Heon, E., Priston, M., Schorderet, D.F., Billingsley, G.D., Girard, P.O., Lubsen, N. and Munier, F.L. (1999) The gamma-crystallins and human cataracts: a puzzle made clearer. *Am J Hum Genet*, 65, 1261-1267.
- Hermisson, J. and Wagner, G.P. (2004) The population genetic theory of hidden variation and genetic robustness. *Genetics*, 168, 2271-2284.
- Hess, J.F., Casselman, J.T. and FitzGerald, P.G. (1993) cDNA analysis of the 49 kDa lens fiber cell cytoskeletal protein: a new, lens-specific member of the intermediate filament family? *Curr Eye Res*, 12, 77-88.
- Hess, J.F., Casselman, J.T. and FitzGerald, P.G. (1996) Gene structure and cDNA sequence identify the beaded filament protein CP49 as a highly divergent type I intermediate filament protein. *J Biol Chem*, 271, 6729-6735.
- Hess, J.F., Casselman, J.T., Kong, A.P. and FitzGerald, P.G. (1998) Primary sequence, secondary structure, gene structure, and assembly properties suggests that the lens-

- specific cytoskeletal protein filensin represents a novel class of intermediate filament protein. *Exp Eye Res*, 66, 625-644.
- Hiller, R., Sperduto, R.D., Podgor, M.J., Wilson, P.W., Ferris, F.L., 3rd, Colton, T., D'Agostino, R.B., Roseman, M.J., Stockman, M.E. and Milton, R.C. (1997) Cigarette smoking and the risk of development of lens opacities. The Framingham studies. *Arch Ophthalmol*, 115, 1113-1118.
- Hollick, J.B., Dorweiler, J.E. and Chandler, V.L. (1997) Paramutation and related allelic interactions. *Trends Genet*, 13, 302-308.
- Horwitz, J. (1992) α -crystallin can function as a molecular chaperone. *Proc Natl Acad Sci USA*, 89, 10449-10453.
- Horwitz, J. (1993) Proctor Lecture. The function of α -crystallin. *Invest Ophthalmol Vis Sci*, 34, 10-22.
- Horwitz, J. (2003) α -crystallin. *Exp Eye Res*, 76, 145-153.
- Horwitz, J., Emmons, T. and Takemoto, L. (1992) The ability of lens α -crystallin to protect against heat-induced aggregation is age-dependent. *Curr Eye Res*, 11, 817-822.
- Horwitz, J., Huang, Q. and Ding, L. (2004) The native oligomeric organization of α -crystallin, is it necessary for its chaperone function? *Exp Eye Res*, 79, 817-821.
- Ikeda, R., Yoshida, K., Ushiyama, M., Yamaguchi, T., Iwashita, K., Futagawa, T., Shibayama, Y., Oiso, S., Takeda, Y., Kariyazono, H., Furukawa, T., Nakamura, K., Akiyama, S., Inoue, I. and Yamada, K. (2006) The small heat shock protein α B-crystallin inhibits differentiation-induced caspase 3 activation and myogenic differentiation. *Biol Pharm Bull*, 29, 1815-1819.
- Inagaki, N., Hayashi, T., Arimura, T., Koga, Y., Takahashi, M., Shibata, H., Teraoka, K., Chikamori, T., Yamashina, A. and Kimura, A. (2006) α B-crystallin mutation in dilated cardiomyopathy. *Biochem Biophys Res Commun*, 342, 379-386.
- Inaguma, Y., Hasegawa, K., Goto, S., Ito, H. and Kato, K. (1995) Induction of the synthesis of hsp27 and α B crystallin in tissues of heat-stressed rats and its suppression by ethanol or an α 1-adrenergic antagonist. *J Biochem*, 117, 1238-1243.
- Ingolia, T.D. and Craig, E.A. (1982) Four small *Drosophila* heat shock proteins are related to each other and to mammalian α -crystallin. *Proc Natl Acad Sci USA*, 79, 2360-2364.
- Inoue, A., Takahashi, M., Hatta, Y., Okamoto, H. (1994) Developmental regulation of Islet-1 mRNA expression during neuronal differentiation in embryonic zebrafish. *Dev. Dyn*, 199, 1-11.
- Ionasescu, V., Searby, C., Sheffield, V.C., Roklina, T., Nishimura, D. and Ionasescu, R. (1996) Autosomal dominant Charcot-Marie-Tooth axonal neuropathy mapped on chromosome 7p (CMT2D). *Hum Mol Genet*, 5, 1373-1375.
- Irobi, J., Van Impe, K., Seeman, P., Jordanova, A., Dierick, I., Verpoorten, N., Michalik, A., De Vriendt, E., Jacobs, A., Van Gerwen, V., Vennekens, K., Mazanec, R., Tournev, I., Hilton-Jones, D., Talbot, K., Kremensky, I., Van Den Bosch, L., Robberecht, W., Van Vandeckerckhove, J., Van Broeckhoven, C., Gettemans, J., De Jonghe, P. and Timmerman, V. (2004) Hot-spot residue in small heat-shock protein 22 causes distal motor neuropathy. *Nat Genet*, 36, 597-601.
- Ismailov SM, F.V., Dadali EL. (2001) A new locus for autosomal dominant Charcot-Marie-Tooth disease type 2 (CMT2F) maps to chromosome 7q11-q21. *Eur J Hum Genet*, 9, 646-650.

- Ito, H., Kamei, K., Iwamoto, I., Inaguma, Y., Garcia-Mata, R., Sztul, E. and Kato, K. (2002) Inhibition of proteasomes induces accumulation, phosphorylation, and recruitment of HSP27 and α B-crystallin to aggresomes. *J Biochem*, 131, 593-603.
- Ito, H., Kamei, K., Iwamoto, I., Inaguma, Y., Nohara, D. and Kato, K. (2001) Phosphorylation-induced change of the oligomerization state of α B-crystallin. *J Biol Chem*, 276, 5346-5352.
- Itoh-Satoh, M., Hayashi, T., Nishi, H., Koga, Y., Arimura, T., Koyanagi, T., Takahashi, M., Hohda, S., Ueda, K., Nouchi, T., Hiroe, M., Marumo, F., Imaizumi, T., Yasunami, M. and Kimura, A. (2002) Titin mutations as the molecular basis for dilated cardiomyopathy. *Biochem Biophys Res Commun*, 291, 385-393.
- Iwaki, T., Kume-Iwaki, A., Liem, R.K. and Goldman, J.E. (1989) α B-crystallin is expressed in non-lenticular tissues and accumulates in Alexander's disease brain. *Cell*, 57, 71-78.
- Iwamoto, T., Kagawa, Y., Naito, Y., Kuzuhara, S. and Kojima, M. (2004) Steroid-induced diabetes mellitus and related risk factors in patients with neurologic diseases. *Pharmacotherapy*, 24, 508-514.
- Jablonska, E., Matzke, M., Thieffry, D., Speybroeck, L.V. (2002) the genome in context: Biologists and philosophers on epigenetics. *Bioessays*, 24, 392-394.
- Jacob, R.F., Cenedella, R.J. and Preston Mason, R. (2000) Determination of human eye lens membrane structure by xray diffraction analysis. *The Rigaku Journal*, 17.
- Jacob, T.J. (1999) The relationship between cataract, cell swelling and volume regulation. *Prog Retin Eye Res*, 18, 223-233.
- Jacobsen, S.E. and Meyerowitz, E.M. (1997) Hypermethylated SUPERMAN epigenetic alleles in arabidopsis. *Science*, 277, 1100-1103.
- Jacobsen, S.E., Sakai, H., Finnegan, E.J., Cao, X. and Meyerowitz, E.M. (2000) Ectopic hypermethylation of flower-specific genes in Arabidopsis. *Curr Biol*, 10, 179-186.
- Jamieson, R.V., Perveen, R., Kerr, B., Carette, M., Yardley, J., Heon, E., Wirth, M.G., van Heyningen, V., Donnai, D., Munier, F. and Black, G.C. (2002) Domain disruption and mutation of the bZIP transcription factor, MAF, associated with cataract, ocular anterior segment dysgenesis and coloboma. *Hum Mol Genet*, 11, 33-42.
- Jenkins, A.J., March, J.B., Oliver, I.R. and Masters, M. (1986) A DNA fragment containing the groE genes can suppress mutations in the Escherichia coli dnaA gene. *Mol Gen Genet*, 202, 446-454.
- Jimenez-Asensio, J., Colvis, C.M., Kowalak, J.A., Douglas-Tabor, Y., Datiles, M.B., Moroni, M., Mura, U., Rao, C.M., Balasubramanian, D., Janjani, A. and Garland, D. (1999) An atypical form of α B-crystallin is present in high concentration in some human cataractous lenses. Identification and characterization of aberrant N- and C-terminal processing. *J Biol Chem*, 274, 32287-32294.
- Johnson, A.B. and Bettica, A. (1989) On-grid immunogold labeling of glial intermediate filaments in epoxy-embedded tissue. *Am J Anat*, 185, 335-341.
- Juhasz, P. and Biemann, K. (1994) Mass spectrometric molecular-weight determination of highly acidic compounds of biological significance via their complexes with basic polypeptides. *Proc Natl Acad Sci U S A*, 91, 4333-4337.
- Kamei, A., Hamaguchi, T., Matsuura, N. and Masuda, K. (2001) Does post-translational modification influence chaperone-like activity of α -crystallin? I. Study on phosphorylation. *Biol Pharm Bull*, 24, 96-99.
- Kamei, A. and Matsuura, N. (2002) Analysis of crystallin-crystallin interactions by surface plasmon resonance. *Biol Pharm Bull*, 25, 611-615.

- Kampinga, H.H., Brunsting, J.F., Stege, G.J., Konings, A.W. and Landry, J. (1994) Cells overexpressing Hsp27 show accelerated recovery from heat-induced nuclear protein aggregation. *Biochem Biophys Res Commun*, 204, 1170-1177.
- Kamradt, M.C., Chen, F., Sam, S. and Cryns, V.L. (2002) The small heat shock protein α B-crystallin negatively regulates apoptosis during myogenic differentiation by inhibiting caspase-3 activation. *J Biol Chem*, 277, 38731-38736.
- Kannabiran, C., Wawrousek, E., Sergeev, Y., Rao, G. N., Kaiser-Kupfer, M., Hejtmancik, J. F. (1999) Mutation of beta A3/A1 crystallin gene in autosomal dominant zonular cataract with sutural opacities results in a protein with single globular domain. *Ophthalm. Vis. Sci.*, 40.
- Kantorow, M. and Piatigorsky, J. (1998) Phosphorylations of α A- and α B-crystallin. *Int J Biol Macromol*, 22, 307-314.
- Karas, M., Bachmann, D., Bahr, U. & Hillenkamp, F. (1987) Matrix-Assisted Ultraviolet Laser Desorption of Non-Volatile Compounds. *International Journal of Mass spectrometry Ion Processes*, 78, 53-68.
- Karim, A.K., Jacob, T.J. and Thompson, G.M. (1987) The human anterior lens capsule: cell density, morphology and mitotic index in normal and cataractous lenses. *Exp Eye Res*, 45, 865-874.
- Kasakov, A.S., Bukach, O.V., Seit-Nebi, A.S., Marston, S.B. and Gusev, N.B. (2007) Effect of mutations in the β 5- β 7 loop on the structure and properties of human small heat shock protein HSP22 (HspB8, H11). *Febs J*, 274, 5628-5642.
- Kato, K., Inaguma, Y., Ito, H., Iida, K., Iwamoto, I., Kamei, K., Ochi, N., Ohta, H. and Kishikawa, M. (2001) Ser-59 is the major phosphorylation site in α B-crystallin accumulated in the brains of patients with Alexander's disease. *J Neurochem*, 76, 730-736.
- Kato, K., Ito, H., Kamei, K., Inaguma, Y., Iwamoto, I. and Saga, S. (1998) Phosphorylation of α B-crystallin in mitotic cells and identification of enzymatic activities responsible for phosphorylation. *J Biol Chem*, 273, 28346-28354.
- Kato, K., Shinohara, H., Goto, S., Inaguma, Y., Morishita, R. and Asano, T. (1992) Copurification of small heat shock protein with α B crystallin from human skeletal muscle. *J Biol Chem*, 267, 7718-7725.
- Kato, K., Shinohara, H., Kurobe, N., Goto, S., Inaguma, Y. and Ohshima, K. (1991) Immunoreactive α A crystallin in rat non-lenticular tissues detected with a sensitive immunoassay method. *Biochim Biophys Acta*, 1080, 173-180.
- Kelly, S.P., Thornton, J., Edwards, R., Sahu, A. and Harrison, R. (2005) Smoking and cataract: review of causal association. *J Cataract Refract Surg*, 31, 2395-2404.
- Kermicle, J.L., Eggleston, W.B. and Alleman, M. (1995) Organization of paramutagenicity in R-stippled maize. *Genetics*, 141, 361-372.
- Krohn, N.M., Yanagisawa, S. and Grasser, K.D. (2002) Specificity of the stimulatory interaction between chromosomal HMGB proteins and the transcription factor Dof2 and its negative regulation by protein kinase CK2-mediated phosphorylation. *J Biol Chem*, 277, 32438-32444.
- Kim, K.K., Kim, R. and Kim, S.H. (1998a) Crystal structure of a small heat-shock protein. *Nature*, 394, 595-599.
- Kim, R., Kim, K.K., Yokota, H. and Kim, S.H. (1998b) Small heat shock protein of *Methanococcus jannaschii*, a hyperthermophile. *Proc Natl Acad Sci U S A*, 95, 9129-9133.

- Kim, R., Lai, L., Lee, H.H., Cheong, G.W., Kim, K.K., Wu, Z., Yokota, H., Marqusee, S. and Kim, S.H. (2003) On the mechanism of chaperone activity of the small heat-shock protein of *Methanococcus jannaschii*. *Proc Natl Acad Sci U S A*, 100, 8151-8155.
- King, R.J., Finley, J.R., Coffey, A.I., Millis, R.R. and Rubens, R.D. (1987) Characterization and biological relevance of a 29-kDa, oestrogen receptor-related protein. *J Steroid Biochem*, 27, 471-475.
- Kirkwood, T.B. and Austad, S.N. (2000) Why do we age? *Nature*, 408, 233-238.
- Kirschner, M. and Gerhart, J. (1998) Evolvability. *Proc Natl Acad Sci U S A*, 95, 8420-8427.
- Klein, B.E., Klein, R., Linton, K.L. and Franke, T. (1993) Cigarette smoking and lens opacities: the Beaver Dam Eye Study. *Am J Prev Med*, 9, 27-30.
- Klein, R., Klein, B.E., Wong, T.Y., Tomany, S.C. and Cruickshanks, K.J. (2002) The association of cataract and cataract surgery with the long-term incidence of age-related maculopathy: the Beaver Dam eye study. *Arch Ophthalmol*, 120, 1551-1558.
- Klemenz, R., Frohli, E., Steiger, R.H., Schafer, R. and Aoyama, A. (1991) α B-crystallin is a small heat shock protein. *Proc Natl Acad Sci U S A*, 88, 3652-3656.
- Kojima, M., Shui, Y.B., Murano, H., Nagata, M., Hockwin, O., Sasaki, K. and Takahashi, N. (2002) Low vitamin E level as a subliminal risk factor in a rat model of prednisolone-induced cataract. *Invest Ophthalmol Vis Sci*, 43, 1116-1120.
- Konofsky, K., Naumann, G.O. and Guggenmoos-Holzmamm, I. (1987) Cell density and sex chromatin in lens epithelium of human cataracts. Quantitative studies in flat preparation. *Ophthalmology*, 94, 875-880.
- Koretz, J.F., Doss, E.W. and LaButti, J.N. (1998) Environmental factors influencing the chaperone-like activity of α -crystallin. *Int J Biol Macromol*, 22, 283-294.
- Krishnaiah, S., Vilas, K., Shamanna, B.R., Rao, G.N., Thomas, R. and Balasubramanian, D. (2005) Smoking and its association with cataract: results of the Andhra Pradesh eye disease study from India. *Invest Ophthalmol Vis Sci*, 46, 58-65.
- Kyhse-Andersen, J. (1984) Electrophoretic transfer of multiple gels: a simple apparatus without buffer tank for rapid transfer of proteins from polyacrylamide to nitrocellulose. *J Biochem Biophys Methods*, 10, 203-209.
- Laemmli, U.K. (1970) Cleavage of structural proteins during the assembly of the head of bacteriophage T4. *Nature*, 227, 680-685.
- Launay, N., Goudeau, B., Kato, K., Vicart, P. and Lilienbaum, A. (2006) Cell signaling pathways to α B-crystallin following stresses of the cytoskeleton. *Exp Cell Res*, 312, 3570-3584.
- Laursen, A.B. and Fledelius, H. (1979) Variations of lens thickness in relation to biomicroscopic types of human senile cataract. *Acta Ophthalmol (Copenh)*, 57, 1-13.
- Leroux, M.R., Ma, B.J., Batelier, G., Melki, R. and Candido, E.P. (1997) Unique structural features of a novel class of small heat shock proteins. *J Biol Chem*, 272, 12847-12853.
- Lewin, B. (2007) *Cells*. Jones and Bartlett.
- Lewis, G.P., Erickson, P.A., Kaska, D.D. and Fisher, S.K. (1988) An immunocytochemical comparison of Muller cells and astrocytes in the cat retina. *Exp Eye Res*, 47, 839-853.

- Li, Y., Chirgadze, D.Y., Bolanos-Garcia, V.M., Sibanda, B.L., Davies, O.R., Ahnesorg, P., Jackson, S.P. and Blundell, T.L. (2007) Crystal structure of human XLF/Cernunnos reveals unexpected differences from XRCC4 with implications for NHEJ. *Embo J*.
- Liang, J.J. (2000) Interaction between beta-amyloid and lens α B-crystallin. *FEBS Lett*, 484, 98-101.
- Liao, J.H., Lee, J.S. and Chiou, S.H. (2002) C-terminal lysine truncation increases thermostability and enhances chaperone-like function of porcine α B-crystallin. *Biochem Biophys Res Commun*, 297, 309-316.
- Lin, P., Smith, D.L. and Smith, J.B. (1997) In vivo modification of the C-terminal lysine of human lens α B-crystallin. *Exp Eye Res*, 65, 673-680.
- Lindblad, B.E., Hakansson, N., Philipson, B. and Wolk, A. (2007) Alcohol consumption and risk of cataract extraction: a prospective cohort study of women. *Ophthalmology*, 114, 680-685.
- Lindner, R.A., Carver, J.A., Ehrnsperger, M., Buchner, J., Esposito, G., Behlke, J., Lutsch, G., Kotlyarov, A. and Gaestel, M. (2000) Mouse Hsp25, a small shock protein. The role of its C-terminal extension in oligomerization and chaperone action. *Eur J Biochem*, 267, 1923-1932.
- Litt, M., Carrero-Valenzuela, R., LaMorticella, D.M., Schultz, D.W., Mitchell, T.N., Kramer, P. and Maumenee, I.H. (1997) Autosomal dominant cerulean cataract is associated with a chain termination mutation in the human β -crystallin gene CRYBB2. *Hum Mol Genet*, 6, 665-668.
- Litt, M., Kramer, P., LaMorticella, D.M., Murphey, W., Lovrien, E.W. and Weleber, R.G. (1998) Autosomal dominant congenital cataract associated with a missense mutation in the human α -crystallin gene CRYAA. *Hum Mol Genet*, 7, 471-474.
- Liu, M., Ke, T., Wang, Z., Yang, Q., Chang, W., Jiang, F., Tang, Z., Li, H., Ren, X., Wang, X., Wang, T., Li, Q., Yang, J., Liu, J. and Wang, Q.K. (2006a) Identification of a CRYAB mutation associated with autosomal dominant posterior polar cataract in a Chinese family. *Invest Ophthalmol Vis Sci*, 47, 3461-3466.
- Liu, Y., Zhang, X., Luo, L., Wu, M., Zeng, R., Cheng, G., Hu, B., Liu, B., Liang, J.J. and Shang, F. (2006b) A novel α B-crystallin mutation associated with autosomal dominant congenital lamellar cataract. *Invest Ophthalmol Vis Sci*, 47, 1069-1075.
- Liu, L., Ghosh, J.G., Clark, J.I. and Jiang, S. (2006c) Studies of α B crystallin subunit dynamics by surface plasmon resonance. *Anal Biochem*, 350, 186-195.
- Lois, N., Dawson, R., McKinnon, A.D. and Forrester, J.V. (2003) A new model of posterior capsule opacification in rodents. *Invest Ophthalmol Vis Sci*, 44, 3450-3457.
- Ma, Z., Hanson, S.R., Lampi, K.J., David, L.L., Smith, D.L. and Smith, J.B. (1998) Age-related changes in human lens crystallins identified by HPLC and mass spectrometry. *Exp Eye Res*, 67, 21-30.
- Mackay, D., Ionides, A., Kibar, Z., Rouleau, G., Berry, V., Moore, A., Shiels, A. and Bhattacharya, S. (1999) Connexin46 mutations in autosomal dominant congenital cataract. *Am J Hum Genet*, 64, 1357-1364.
- Mackay, D.S., Boskovska, O.B., Knopf, H.L., Lampi, K.J. and Shiels, A. (2002) A nonsense mutation in CRYBB1 associated with autosomal dominant cataract linked to human chromosome 22q. *Am J Hum Genet*, 71, 1216-1221.
- Maisel, H. (1985) *The Ocular Lens*. Marcel Dekker, New York.

- Maisel, H. and Perry, M.M. (1972) Electron microscope observations on some structural proteins of the chick lens. *Exp Eye Res*, 14, 7-12.
- Mangan, S. and Alon, U. (2003) Structure and function of the feed-forward loop network motif. *Proc Natl Acad Sci USA*, 100, 11980-11985.
- Mao, J.J., Katayama, S., Watanabe, C., Harada, Y., Noda, K., Yamamura, Y. and Nakamura, S. (2001) The relationship between α B-crystallin and neurofibrillary tangles in Alzheimer's disease. *Neuropathol Appl Neurobiol*, 27, 180-188.
- Marini, I., Bucchioni, L., Voltarelli, M., Del Corso, A. and Mura, U. (1995) α -crystallin-like molecular chaperone against the thermal denaturation of lens aldose reductase: the effect of divalent metal ions. *Biochem Biophys Res Commun*, 212, 413-420.
- Martienssen, R., Barkan, A., Taylor, W.C. and Freeling, M. (1990) Somatic heritable switches in the DNA modification of Mu transposable elements monitored with a suppressible mutant in maize. *Genes Dev*, 4, 331-343.
- Martienssen, R. and Baron, A. (1994) Coordinate suppression of mutations caused by Robertson's mutator transposons in maize. *Genetics*, 136, 1157-1170.
- Masaki, S. and Watanabe, T. (1992) cDNA sequence analysis of CP94: rat lens fiber cell beaded-filament structural protein shows homology to cytokeratins. *Biochem Biophys Res Commun*, 186, 190-198.
- McCarty, C. and Taylor, H. (2002) A Review of the Epidemiologic Evidence Linking Ultraviolet Radiation and Cataracts.
- McClintock, B. (1951) Chromosome organization and genic expression. *Cold Spring Harb Symp Quant Biol*, 16, 13-47.
- McLaren, A.J., Marshall, S.E., Haldar, N.A., Mullighan, C.G., Fuggle, S.V., Morris, P.J. and Welsh, K.I. (1999) Adhesion molecule polymorphisms in chronic renal allograft failure. *Kidney Int*, 55, 1977-1982.
- Medawar, P. (1952) An unsolved problem in biology.
- Meehan, S., Knowles, T.P., Baldwin, A.J., Smith, J.F., Squires, A.M., Clements, P., Treweek, T.M., Ecroyd, H., Tartaglia, G.G., Vendruscolo, M., Macphee, C.E., Dobson, C.M. and Carver, J.A. (2007) Characterisation of amyloid fibril formation by small heat-shock chaperone proteins human α A-, α B- and R120G α B-crystallins. *J Mol Biol*, 372, 470-484.
- Meriin, A.B., Gabai, V.L., Yaglom, J., Shifrin, V.I. and Sherman, M.Y. (1998) Proteasome inhibitors activate stress kinases and induce Hsp72. Diverse effects on apoptosis. *J Biol Chem*, 273, 6373-6379.
- Miesbauer, L.R., Zhou, X., Yang, Z., Yang, Z., Sun, Y., Smith, D.L. and Smith, J.B. (1994) Post-translational modifications of water-soluble human lens crystallins from young adults. *J Biol Chem*, 269, 12494-12502.
- Mignot, C., Delarasse, C., Escaich, S., Della Gaspera, B., Noe, E., Colucci-Guyon, E., Babinet, C., Pekny, M., Vicart, P., Boespflug-Tanguy, O., Dautigny, A., Rodriguez, D. and Pham-Dinh, D. (2007) Dynamics of mutated GFAP aggregates revealed by real-time imaging of an astrocyte model of Alexander disease. *Exp Cell Res*, 313, 2766-2779.
- Minassian, D.C., Mehra, V. and Jones, B.R. (1984) Dehydrational crises from severe diarrhoea or heatstroke and risk of cataract. *Lancet*, 1, 751-753.
- Miyake, K., Ota, I., Miyake, S. and Horiguchi, M. (1998) Liquefied aftercataract: a complication of continuous curvilinear capsulorhexis and intraocular lens implantation in the lens capsule. *Am J Ophthalmol*, 125, 429-435.

- Moroni, M. and Garland, D. (2001) In vitro dephosphorylation of α -crystallin is dependent on the state of oligomerization. *Biochim Biophys Acta*, 1546, 282-290.
- Morrow, G. and Tanguay, R.M. (2003) Heat shock proteins and aging in *Drosophila melanogaster*. *Semin Cell Dev Biol*, 14, 291-299.
- Moscona, A.A., Fox, L., Smith, J. and Degenstein, L. (1985) Antiserum to lens antigens immunostains Muller glia cells in the neural retina. *Proc Natl Acad Sci U S A*, 82, 5570-5573.
- Muchowski, P.J. and Clark, J.I. (1998) ATP-enhanced molecular chaperone functions of the small heat shock protein human α B crystallin. *Proc Natl Acad Sci U S A*, 95, 1004-1009.
- Muchowski, P.J., Hays, L.G., Yates, J.R., 3rd and Clark, J.I. (1999) ATP and the core " α -Crystallin" domain of the small heat-shock protein α B-crystallin. *J Biol Chem*, 274, 30190-30195.
- Mörner, C. (1894) *Z. physiol. Chemie*, 18, 61-106.
- Nakamura, T., Sasaki, H., Nagai, K., Fujisawa, K., Sasaki, K., Suzuki, K. and Tsugawa, R. (2003) Influence of cyclosporin on steroid-induced cataracts after renal transplantation. *Jpn J Ophthalmol*, 47, 254-259.
- Narberhaus, F. (2002) α -crystallin-type heat shock proteins: socializing minichaperones in the context of a multichaperone network. *Microbiol Mol Biol Rev*, 66, 64-93; table of contents.
- Naze, P., Vuillaume, I., Destee, A., Pasquier, F. and Sablonniere, B. (2002) Mutation analysis and association studies of the ubiquitin carboxy-terminal hydrolase L1 gene in Huntington's disease. *Neurosci Lett*, 328, 1-4.
- Nene, V., Dunne, D.W., Johnson, K.S., Taylor, D.W. and Cordingley, J.S. (1986) Sequence and expression of a major egg antigen from *Schistosoma mansoni*. Homologies to heat shock proteins and α -crystallins. *Mol Biochem Parasitol*, 21, 179-188.
- Nicholl, I.D. and Quinlan, R.A. (1994) Chaperone activity of α -crystallins modulates intermediate filament assembly. *Embo J*, 13, 945-953.
- O'Connor, O.A. (2005) Targeting histones and proteasomes: new strategies for the treatment of lymphoma. *J Clin Oncol*, 23, 6429-6436.
- Orii, H., Agata, K., Sawada, K., Eguchi, G. and Maisel, H. (1993) Evidence that the chick lens cytoskeletal protein CP 49 belongs to the family of intermediate filament proteins. *Curr Eye Res*, 12, 583-588.
- Orlowski, R.Z. (1999) The role of the ubiquitin-proteasome pathway in apoptosis. *Cell Death Differ*, 6, 303-313.
- Palmisano, D.V., Groth-Vasselli, B., Farnsworth, P.N. and Reddy, M.C. (1995) Interaction of ATP and lens α -crystallin characterized by equilibrium binding studies and intrinsic tryptophan fluorescence spectroscopy. *Biochim Biophys Acta*, 1246, 91-97.
- Pan, S., Wu, K., Liang, S. and Li, S. (1993) [Relations between opacification of lens protein and pH]. *Yan Ke Xue Bao*, 9, 179-182.
- Parcellier, A., Schmitt, E., Brunet, M., Hammann, A., Solary, E. and Garrido, C. (2005) Small heat shock proteins HSP27 and α B-crystallin: cytoprotective and oncogenic functions. *Antioxid Redox Signal*, 7, 404-413.
- Pasta, S.Y., Raman, B., Ramakrishna, T. and Rao Ch, M. (2002) Role of the C-terminal extensions of α -crystallins. Swapping the C-terminal extension of α -crystallin to

- α B-crystallin results in enhanced chaperone activity. *J Biol Chem*, 277, 45821-45828.
- Pasta, S.Y., Raman, B., Ramakrishna, T. and Rao Ch, M. (2003) Role of the conserved SRLFDQFFG region of α -crystallin, a small heat shock protein. Effect on oligomeric size, subunit exchange, and chaperone-like activity. *J Biol Chem*, 278, 51159-51166.
- Pasta, S.Y., Raman, B., Ramakrishna, T. and Rao Ch, M. (2004) The IXI/V motif in the C-terminal extension of α -crystallins: alternative interactions and oligomeric assemblies. *Mol Vis*, 10, 655-662.
- Pastor-Valero, M., Fletcher, A.E., De Stavola, B.L. and Chaques-Alepuz, V. (2007) Years of sunlight exposure and cataract: a case-control study in a Mediterranean population. *BMC Ophthalmol*, 7, 18.
- Patteau, F., Bourcier, T., Naacke, H., Allahdadi, H., Borderie, V. and Laroche, L. (2003) [Posterior subcapsular cataract in a case of ulcerative colitis treated with corticosteroid enema]. *J Fr Ophthalmol*, 26, 834-836.
- Perng, M.D., Zhang, Q. and Quinlan, R.A. (2007) Insights into the beaded filament of the eye lens. *Exp Cell Res*, 313, 2180-2188.
- Perng, M.D., Cairns, L., van den Issel, P., Prescott, A.M., Hutcheson, C., Quinlan, R.A. (1999) Intermediate filament interactions can be altered by HSP27 and α B-crystallin. *J. Cell. Sci*, 112, 2099-2122.
- Perng, M.D., Muchowski, P.J., van den IJssel, P.R., Wu, G.J.S., Hutcheson, A.M., Clark, J.I. and Quinlan, R.A. (1999) The Cardiomyopathy and Lens Cataract Mutation in α B-crystallin alters its Protein Structure, chaperone activity and interaction with intermediate filaments *in Vitro*. *J Biol Chem*, 274, 33235-33243.
- Perng, M.D. and Quinlan, R.A. (2005) Seeing is believing! The optical properties of the eye lens are dependent upon a functional intermediate filament cytoskeleton. *Exp Cell Res*, 305, 1-9.
- Perng, M.D., Wen, S.F., van den, I.P., Prescott, A.R. and Quinlan, R.A. (2004) Desmin aggregate formation by R120G α B-crystallin is caused by altered filament interactions and is dependent upon network status in cells. *Mol Biol Cell*, 15, 2335-2346.
- Peterson, J.J., Young, M.M. and Takemoto, L.J. (2004) Probing α -crystallin structure using chemical cross-linkers and mass spectrometry. *Mol Vis*, 10, 857-866.
- Phair, R.D. and Misteli, T. (2000) High mobility of proteins in the mammalian cell nucleus. *Nature*, 404, 604-609.
- Piatigorsky, J. (1981) Lens differentiation in vertebrates. A review of cellular and molecular features. *Differentiation*, 19, 134-153.
- Pigliucci, M. (2003) Epigenetics is back! Hsp90 and phenotypic variation. *Cell Cycle*, 2, 34-35.
- Pigliucci, M. and Murren, C.J. (2003) Perspective: Genetic assimilation and a possible evolutionary paradox: can macroevolution sometimes be so fast as to pass us by? *Evolution Int J Org Evolution*, 57, 1455-1464.
- Plater, M.L., Goode, D. and Crabbe, M.J. (1996) Effects of site-directed mutations on the chaperone-like activity of α B-crystallin. *J Biol Chem*, 271, 28558-28566.
- Pras, E., Frydman, M., Levy-Nissenbaum, E., Bakhan, T., Raz, J., Assia, E.I. and Goldman, B. (2000) A nonsense mutation (W9X) in CRYAA causes autosomal recessive cataract in an inbred Jewish Persian family. *Invest Ophthalmol Vis Sci*, 41, 3511-3515.

- Queitsch, C., Hong, S.W., Vierling, E. and Lindquist, S. (2000) Heat shock protein 101 plays a crucial role in thermotolerance in *Arabidopsis*. *Plant Cell*, 12, 479-492.
- Queitsch, C., Sangster, T.A. and Lindquist, S. (2002) Hsp90 as a capacitor of phenotypic variation. *Nature*, 417, 618-624.
- Rafferty, N.S. (1985) *The Ocular Lens*. Marcel Dekker, New York.
- Rajan, S., Chandrashekar, R., Aziz, A. and Abraham, E.C. (2006) Role of Arginine-163 and the (163)REEK(166) Motif in the Oligomerization of Truncated α A-Crystallins. *Biochemistry*, 45, 15684-15691.
- Raju, P., George, R., Ve Ramesh, S., Arvind, H., Baskaran, M. and Vijaya, L. (2006) Influence of tobacco use on cataract development. *Br J Ophthalmol*, 90, 1374-1377.
- Ralston, G.B. (1993) *Analytical Ultracentrifugation Volume 1 Beckman Instruments, Inc*, California.
- Ramaekers, F.C., Dunia, I., Dodemont, H.J., Benedetti, E.L. and Bloemendal, H. (1982) Lenticular intermediate-sized filaments: biosynthesis and interaction with plasma membrane. *Proc Natl Acad Sci USA*, 79, 3208-3212.
- Ramaekers, F.C., Osborn, M., Schmid, E., Weber, K., Bloemendal, H. and Franke, W.W. (1980) Identification of the cytoskeletal proteins in lens-forming cells, a special epitheloid cell type. *Exp Cell Res*, 127, 309-327.
- Raman, B. and Rao, C.M. (1994) Chaperone-like activity and quaternary structure of α -crystallin. *J Biol Chem*, 269, 27264-27268.
- Raman, B. and Rao, C.M. (1997) Chaperone-like activity and temperature-induced structural changes of α -crystallin. *J Biol Chem*, 272, 23559-23564.
- Raso, S.W., King, J. (2000) *Protein Folding and Human Disease*. Oxford University Press.
- Reddy, G.B., Reddy, P.Y., Vijayalakshmi, A., Kumar, M.S., Suryanarayana, P. and Sesikeran, B. (2002) Effect of long-term dietary manipulation on the aggregation of rat lens crystallins: role of α -crystallin chaperone function. *Mol Vis*, 8, 298-305.
- Reddy, M.C., Palmisano, D.V., Groth-Vasselli, B. and Farnsworth, P.N. (1992) 31P NMR studies of the ATP/ α -crystallin complex: functional implications. *Biochem Biophys Res Commun*, 189, 1578-1584.
- Richardson, P.J. (1996) Assessment of myocardial damage in dilated cardiomyopathy. *Eur Heart J*, 17, 489-490.
- Rideout, H.J., Larsen, K.E., Sulzer, D. and Stefanis, L. (2001) Proteasomal inhibition leads to formation of ubiquitin/ α -synuclein-immunoreactive inclusions in PC12 cells. *J Neurochem*, 78, 899-908.
- Rutherford, S., Hirate, Y. and Swalla, B.J. (2007a) The Hsp90 capacitor, developmental remodeling, and evolution: the robustness of gene networks and the curious evolvability of metamorphosis. *Crit Rev Biochem Mol Biol*, 42, 355-372.
- Rutherford, S., Knapp, J.R. and Csermely, P. (2007b) Hsp90 and developmental networks. *Adv Exp Med Biol*, 594, 190-197.
- Rutherford, S., Knapp, J.R., Csermely, P. (2007) *Molecular Aspects of the StressResponse; Chaperones, Membranes and Networks*. Springer, New York.
- Rutherford, S.L. (2003) Between genotype and phenotype: protein chaperones and evolvability. *Nat Rev Genet*, 4, 263-274.
- Rutherford, S.L. and Lindquist, S. (1998) Hsp90 as a capacitor for morphological evolution. *Nature*, 396, 336-342.

- Sadoul, R., Fernandez, P.A., Quiquerez, A.L., Martinou, I., Maki, M., Schroter, M., Becherer, J.D., Irmeler, M., Tschopp, J. and Martinou, J.C. (1996) Involvement of the proteasome in the programmed cell death of NGF-deprived sympathetic neurons. *Embo J*, 15, 3845-3852.
- Salathia, N. and Queitsch, C. (2007) Molecular mechanisms of canalization: Hsp90 and beyond. *J Biosci*, 32, 457-463.
- Samakovli, D., Thanou, A., Valmas, C. and Hatzopoulos, P. (2007) Hsp90 canalizes developmental perturbation. *J Exp Bot*, 58, 3513-3524.
- Sandilands, A. (1995) Characterisation of the intermediate filament proteins filensin and CP49 within the eye lens. University of Dundee, Dundee, Vol. Ph.D.
- Sandilands, A., Prescott, A.R., Carter, J.M., Hutcheson, A.M., Quinlan, R.A., Richards, J. and FitzGerald, P.G. (1995) Vimentin and CP49/filensin form distinct networks in the lens which are independently modulated during lens fibre cell differentiation. *J Cell Sci*, 108 (Pt 4), 1397-1406.
- Sandilands, A., Prescott, A.R., Wegener, A., Zoltoski, R.K., Hutcheson, A.M., Masaki, S., Kuszak, J.R. and Quinlan, R.A. (2003) Knockout of the intermediate filament protein CP49 destabilises the lens fibre cell cytoskeleton and decreases lens optical quality, but does not induce cataract. *Exp Eye Res*, 76, 385-391.
- Sangster, T.A., Lindquist, S. and Queitsch, C. (2004) Under cover: causes, effects and implications of Hsp90-mediated genetic capacitance. *Bioessays*, 26, 348-362.
- Sangster, T.A. and Queitsch, C. (2005) The HSP90 chaperone complex, an emerging force in plant development and phenotypic plasticity. *Curr Opin Plant Biol*, 8, 86-92.
- Sawada, K., Agata, K., Yoshiki, A. and Eguchi, G. (1993) A set of anti-crystallin monoclonal antibodies for detecting lens specificities: β -crystallin as a specific marker for detecting lentoidogenesis in cultures of chicken lens epithelial cells. *Jpn J Ophthalmol*, 37, 355-368.
- Schar, C.R., Blouse, G.E., Minor, K.H. and Peterson, C.B. (2008) A deletion mutant of vitronectin lacking the somatomedin B domain exhibits residual pai-1-binding activity. *J Biol Chem*.
- Schroder, R., Vrabie, A. and Goebel, H.H. (2007) Primary desminopathies. *J Cell Mol Med*, 11, 416-426.
- Selcen, D. and Engel, A.G. (2003) Myofibrillar myopathy caused by novel dominant negative α B-crystallin mutations. *Ann Neurol*, 54, 804-810.
- Selcen, D., Ohno, K. and Engel, A.G. (2004) Myofibrillar myopathy: clinical, morphological and genetic studies in 63 patients. *Brain*, 127, 439-451.
- Selkoe, D.J. (2003a) Aging, amyloid, and Alzheimer's disease: a perspective in honor of Carl Cotman. *Neurochem Res*, 28, 1705-1713.
- Selkoe, D.J. (2003b) Folding proteins in fatal ways. *Nature*, 426, 900-904.
- Semina, E.V., Ferrell, R.E., Mintz-Hittner, H.A., Bitoun, P., Alward, W.L., Reiter, R.S., Funkhauser, C., Daack-Hirsch, S. and Murray, J.C. (1998) A novel homeobox gene PITX3 is mutated in families with autosomal-dominant cataracts and ASMD. *Nat Genet*, 19, 167-170.
- Shah, S.A., Potter, M.W., McDade, T.P., Ricciardi, R., Perugini, R.A., Elliott, P.J., Adams, J. and Callery, M.P. (2001) 26S proteasome inhibition induces apoptosis and limits growth of human pancreatic cancer. *J Cell Biochem*, 82, 110-122.
- Shah, S.P., Dineen, B., Jadoon, Z., Bourne, R., Khan, M.A., Johnson, G.J., De Stavola, B., Gilbert, C. and Khan, M.D. (2007) Lens opacities in adults in pakistan: prevalence and risk factors. *Ophthalmic Epidemiol*, 14, 381-389.

- Shalini, V.K., Luthra, M., Srinivas, L., Rao, S.H., Basti, S., Reddy, M. and Balasubramanian, D. (1994) Oxidative damage to the eye lens caused by cigarette smoke and fuel smoke condensates. *Indian J Biochem Biophys*, 31, 261-266.
- Sharma, K.K. and Ortwerth, B.J. (1995) Effect of cross-linking on the chaperone-like function of α -crystallin. *Exp Eye Res*, 61, 413-421.
- Shashidharamurthy, R., Koteiche, H.A., Dong, J. and McHaourab, H.S. (2005) Mechanism of chaperone function in small heat shock proteins: dissociation of the HSP27 oligomer is required for recognition and binding of destabilized T4 lysozyme. *J Biol Chem*, 280, 5281-5289.
- Shibata, S., Natori, Y., Nishihara, T., Tomisaka, K., Matsumoto, K., Sansawa, H. and Nguyen, V.C. (2003) Antioxidant and anti-cataract effects of Chlorella on rats with streptozotocin-induced diabetes. *J Nutr Sci Vitaminol (Tokyo)*, 49, 334-339.
- Shiels, A., Bennett, T.M., Knopf, H.L., Yamada, K., Yoshiura, K., Niikawa, N., Shim, S. and Hanson, P.I. (2007) CHMP4B, a novel gene for autosomal dominant cataracts linked to chromosome 20q. *Am J Hum Genet*, 81, 596-606.
- Shiels, A., Mackay, D., Ionides, A., Berry, V., Moore, A. and Bhattacharya, S. (1998) A missense mutation in the human connexin50 gene (GJA8) underlies autosomal dominant "zonular pulverulent" cataract, on chromosome 1q. *Am J Hum Genet*, 62, 526-532.
- Shinohara, T., White, H., Mulhern, M.L. and Maisel, H. (2007) Cataract: window for systemic disorders. *Med Hypotheses*, 69, 669-677.
- Shroff, N.P., Cherian-Shaw, M., Bera, S. and Abraham, E.C. (2000) Mutation of R116C results in highly oligomerized α A-crystallin with modified structure and defective chaperone-like function. *Biochemistry*, 39, 1420-1426.
- Siegal, M.L. and Bergman, A. (2002) Waddington's canalization revisited: developmental stability and evolution. *Proc Natl Acad Sci U S A*, 99, 10528-10532.
- Siezen, R.J., Bindels, J.G. and Hoenders, H.J. (1978) The quaternary structure of bovine α -crystallin. Size and charge microheterogeneity: more than 1000 different hybrids? *Eur J Biochem*, 91, 387-396.
- Simon, S., Fontaine, J.M., Martin, J.L., Sun, X., Hoppe, A.D., Welsh, M.J., Benndorf, R. and Vicart, P. (2007a) Myopathy-associated α B-crystallin Mutants: Abnormal Phosphorylation, intracellular location and Interactions with other small heat shock proteins. *J Biol Chem*, 282, 34276-34287.
- Simon, S., Michiel, M., Skouri-Panet, F., Lechaire, J.P., Vicart, P. and Tardieu, A. (2007b) Residue R120 is essential for the quaternary structure and functional integrity of human α B-crystallin. *Biochemistry*, 46, 9605-9614.
- Singh, B.N., Rao, K.S., Ramakrishna, T., Rangaraj, N. and Rao Ch, M. (2007) Association of α B-crystallin, a small heat shock protein, with actin: role in modulating actin filament dynamics in vivo. *J Mol Biol*, 366, 756-767.
- Sleeman, J.E., Ajuh, P. and Lamond, A.I. (2001) snRNP protein expression enhances the formation of Cajal bodies containing p80-coilin and SMN. *J Cell Sci*, 114, 4407-4419.
- Sleeman, J.E. and Lamond, A.I. (1999) Newly assembled snRNPs associate with coiled bodies before speckles, suggesting a nuclear snRNP maturation pathway. *Curr Biol*, 9, 1065-1074.
- Smulders, R., Carver, J.A., Lindner, R.A., van Boekel, M.A., Bloemendal, H. and de Jong, W.W. (1996) Immobilization of the C-terminal extension of bovine α A-crystallin reduces chaperone-like activity. *J Biol Chem*, 271, 29060-29066.

- Soppe, W.J., Jacobsen, S.E., Alonso-Blanco, C., Jackson, J.P., Kakutani, T., Koornneef, M. and Peeters, A.J. (2000) The late flowering phenotype of *fwa* mutants is caused by gain-of-function epigenetic alleles of a homeodomain gene. *Mol Cell*, 6, 791-802.
- Soti, C. and Csermely, P. (2003) Aging and molecular chaperones. *Exp Gerontol*, 38, 1037-1040.
- Spector, A. (1991) *The lens and oxidative stress*, London.
- Spinozzi, F., Mariani, P., Rustichelli, F., Amenitsch, H., Bennardini, F., Mura, G.M., Coi, A. and Ganadu, M.L. (2006) Temperature dependence of chaperone-like activity and oligomeric state of α B-crystallin. *Biochim Biophys Acta*, 1764, 677-687.
- Sreelakshmi, Y., Santhoshkumar, P., Bhattacharyya, J. and Sharma, K.K. (2004) α A-crystallin interacting regions in the small heat shock protein, α B-crystallin. *Biochemistry*, 43, 15785-15795.
- Sreelakshmi, Y. and Sharma, K.K. (2005) Recognition sequence 2 (residues 60-71) plays a role in oligomerization and exchange dynamics of α B-crystallin. *Biochemistry*, 44, 12245-12252.
- Sreelakshmi, Y. and Sharma, K.K. (2006) The interaction between α A- and α B-crystallin is sequence-specific. *Mol Vis*, 12, 581-587.
- Stamler, R., Kappe, G., Boelens, W. and Slingsby, C. (2005) Wrapping the α -crystallin domain fold in a chaperone assembly. *J Mol Biol*, 353, 68-79.
- Stark, A., Brennecke, J., Bushati, N., Russell, R.B. and Cohen, S.M. (2005) Animal MicroRNAs confer robustness to gene expression and have a significant impact on 3'UTR evolution. *Cell*, 123, 1133-1146.
- Stege, G.J., Renkawek, K., Overkamp, P.S., Verschuure, P., van Rijk, A.F., Reijnen-Aalbers, A., Boelens, W.C., Bosman, G.J. and de Jong, W.W. (1999) The molecular chaperone α B-crystallin enhances amyloid beta neurotoxicity. *Biochem Biophys Res Commun*, 262, 152-156.
- Stephan, D.A., Gillanders, E., Vanderveen, D., Freas-Lutz, D., Wistow, G., Baxevas, A.D., Robbins, C.M., VanAuken, A., Quesenberry, M.I., Bailey-Wilson, J., Juo, S.H., Trent, J.M., Smith, L. and Brownstein, M.J. (1999) Progressive juvenile-onset punctate cataracts caused by mutation of the gammaD-crystallin gene. *Proc Natl Acad Sci USA*, 96, 1008-1012.
- Stoevring, B., Frederiksen, J.L. and Christiansen, M. (2007) CRYAB promoter polymorphisms: influence on multiple sclerosis susceptibility and clinical presentation. *Clin Chim Acta*, 375, 57-62.
- Stokes, T.L., Kunkel, B.N. and Richards, E.J. (2002) Epigenetic variation in Arabidopsis disease resistance. *Genes Dev*, 16, 171-182.
- Studer, S. and Narberhaus, F. (2000) Chaperone activity and homo- and hetero-oligomer formation of bacterial small heat shock proteins. *J Biol Chem*, 275, 37212-37218.
- Sulochana, K.N., Punitham, R. and Ramakrishnan, S. (2002) Effect of cigarette smoking on cataract: Antioxidant enzymes and constituent minerals in the lens and blood of humans. *Indian Journal of Pharmacology* 2002, 34, 428-431.
- Sun, H., Ma, Z., Li, Y., Liu, B., Li, Z., Ding, X., Gao, Y., Ma, W., Tang, X., Li, X. and Shen, Y. (2005) Gamma-S crystallin gene (CRYGS) mutation causes dominant progressive cortical cataract in humans. *J Med Genet*, 42, 706-710.
- Sun, T.X., Akhtar, N. and Liang, J.J. (1998) Conformational change of human lens insoluble α -crystallin. *J Protein Chem*, 17, 679-684.

- Suter, U. and Scherer, S.S. (2003) Disease mechanisms in inherited neuropathies. *Nat Rev Neurosci*, 4, 714-726.
- Takemoto, L., Horwitz, J. and Emmons, T. (1992) Oxidation of the N-terminal methionine of lens α -A crystallin. *Curr Eye Res*, 11, 651-655.
- Tamaoka, A., Mizusawa, H., Mori, H. and Shoji, S. (1995) Ubiquitinated α B-crystallin in glial cytoplasmic inclusions from the brain of a patient with multiple system atrophy. *J Neurol Sci*, 129, 192-198.
- Tang, B., Liu, X., Zhao, G., Luo, W., Xia, K., Pan, Q., Cai, F., Hu, Z., Zhang, C., Chen, B., Zhang, F., Shen, L., Zhang, R. and Jiang, H. (2005a) Mutation analysis of the small heat shock protein 27 gene in chinese patients with Charcot-Marie-Tooth disease. *Arch Neurol*, 62, 1201-1207.
- Tang, B.S., Zhao, G.H., Luo, W., Xia, K., Cai, F., Pan, Q., Zhang, R.X., Zhang, F.F., Liu, X.M., Chen, B., Zhang, C., Shen, L., Jiang, H., Long, Z.G. and Dai, H.P. (2005b) Small heat-shock protein 22 mutated in autosomal dominant Charcot-Marie-Tooth disease type 2L. *Hum Genet*, 116, 222-224.
- Taylor, A., Zuliani, A.M., Hopkins, R.E., Dallal, G.E., Treglia, P., Kuck, J.F. and Kuck, K. (1989) Moderate caloric restriction delays cataract formation in the Emory mouse. *Faseb J*, 3, 1741-1746.
- Thampi, P. and Abraham, E.C. (2003) Influence of the C-terminal residues on oligomerization of α A-crystallin. *Biochemistry*, 42, 11857-11863.
- Thampi, P., Hassan, A., Smith, J.B. and Abraham, E.C. (2002) Enhanced C-terminal truncation of α A- and α B-crystallins in diabetic lenses. *Invest Ophthalmol Vis Sci*, 43, 3265-3272.
- Timmerman, V., Raeymaekers, P., Nelis, E., De Jonghe, P., Muylle, L., Ceuterick, C., Martin, J.J. and Van Broeckhoven, C. (1992) Linkage analysis of distal hereditary motor neuropathy type II (distal HMN II) in a single pedigree. *J Neurol Sci*, 109, 41-48.
- Tomokane, N., Iwaki, T., Tateishi, J., Iwaki, A. and Goldman, J.E. (1991) Rosenthal fibers share epitopes with α B-crystallin, glial fibrillary acidic protein, and ubiquitin, but not with vimentin. Immunoelectron microscopy with colloidal gold. *Am J Pathol*, 138, 875-885.
- Treweek, T.M., Ecroyd, H., Williams, D.M., Meehan, S., Carver, J.A. and Walker, M.J. (2007) Site-Directed Mutations in the C-Terminal Extension of Human α B-Crystallin Affect Chaperone Function and Block Amyloid Fibril Formation. *PLoS ONE*, 2, e1046.
- Treweek, T.M., Rekas, A., Lindner, R.A., Walker, M.J., Aquilina, J.A., Robinson, C.V., Horwitz, J., Perng, M.D., Quinlan, R.A. and Carver, J.A. (2005) R120G α B-crystallin promotes the unfolding of reduced α -lactalbumin and is inherently unstable. *Febs J*, 272, 711-724.
- Ueda, Y., Duncan, M.K. and David, L.L. (2002a) Lens proteomics: the accumulation of crystallin modifications in the mouse lens with age. *Invest Ophthalmol Vis Sci*, 43, 205-215.
- Ueda, Y., Fukiage, C., Shih, M., Shearer, T.R. and David, L.L. (2002b) Mass measurements of C-terminally truncated α -crystallins from two-dimensional gels identify Lp82 as a major endopeptidase in rat lens. *Mol Cell Proteomics*, 1, 357-365.

- Valero, M.P., Fletcher, A.E., De Stavola, B.L., Vioque, J. and Alepuz, V.C. (2002) Vitamin C is associated with reduced risk of cataract in a Mediterranean population. *J Nutr*, 132, 1299-1306.
- van den IJssel, P., Wheelock, R., Prescott, A., Russell, P. and Quinlan, R.A. (2003) Nuclear speckle localisation of the small heat shock protein α B-crystallin and its inhibition by the R120G cardiomyopathy-linked mutation. *Exp Cell Res*, 287, 249-261.
- Van Den Oetelaar, P., Van Someren PFHM., Thomson, JA., Siezen, RJ. & Hoenders, HJ. (1990) A dynamic quaternary structure of bovine α -crystallin as indicated from intermolecular exchange of subunits. *Biochemistry*, 29, 3488-3493.
- Van Montfort, R., Slingsby, C. and Vierling, E. (2001a) Structure and function of the small heat shock protein/ α -crystallin family of molecular chaperones. *Adv Protein Chem*, 59, 105-156.
- van Montfort, R.L., Basha, E., Friedrich, K.L., Slingsby, C. and Vierling, E. (2001b) Crystal structure and assembly of a eukaryotic small heat shock protein. *Nat Struct Biol*, 8, 1025-1030.
- van Noort, J.M., van Sechel, A.C., van Stipdonk, M.J. and Bajramovic, J.J. (1998) The small heat shock protein α B-crystallin as key autoantigen in multiple sclerosis. *Prog Brain Res*, 117, 435-452.
- van Rijk, A.F. and Bloemendal, H. (2000) α B-crystallin in neuropathology. *Ophthalmologica*, 214, 7-12.
- Van Rijk, A.F., Sweers, M.A., Merckx, G.F., Lammens, M. and Bloemendal, H. (2003) Pathogenesis of axonal dystrophy and demyelination in α A-crystallin-expressing transgenic mice. *Int J Exp Pathol*, 84, 91-99.
- Velazquez, J.M. and Lindquist, S. (1984) hsp70: nuclear concentration during environmental stress and cytoplasmic storage during recovery. *Cell*, 36, 655-662.
- Vicart, A., Lefebvre, T., Imbert, J., Fernandez, A. and Kahn-Perles, B. (2006) Increased chromatin association of Sp1 in interphase cells by PP2A-mediated dephosphorylations. *J Mol Biol*, 364, 897-908.
- Vicart, P., Caron, A., Guicheney, P., Li, Z., Prevost, M.C., Faure, A., Chateau, D., Chapon, F., Tome, F., Dupret, J.M., Paulin, D. and Fardeau, M. (1998) A missense mutation in the α B-crystallin chaperone gene causes a desmin-related myopathy. *Nat Genet*, 20, 92-95.
- Virgolici, B. and Popescu, L. (2006) [Risk factors in cataract]. *Oftalmologia*, 50, 3-9.
- Waddington, C.H. (1942) Canalization of development and the inheritance of acquired characteristics. *Nature*, 150, 563-565.
- Waddington, C.H. (1952) Genetic assimilation of an acquired character. *Evolution*, 7, 118-126.
- Waddington, C.H. (1961) Genetic Assimilation. *Advances in Genetics*, 10, 257-290.
- Wagner, A. (2005) Robustness, evolvability, and neutrality. *FEBS Lett*, 579, 1772-1778.
- Walker, M.J., Feather, K.D., Davis, P.D. and Hines, K.K. (1995) A new enhanced chemiluminescent substrate for the development of the horseradish peroxidase label in Western blotting applications. *Journal of NIH research*.
- West, S.K. and Valmadrid, C.T. (1995) Epidemiology of risk factors for age-related cataract. *Surv Ophthalmol*, 39, 323-334.
- Wojcik, C. (1999) Inhibition of the proteasome as a therapeutic approach. *Drug Discov Today*, 4, 188-189.

- Worman, H.J. and Bonne, G. (2007) "Laminopathies": a wide spectrum of human diseases. *Exp Cell Res*, 313, 2121-2133.
- Xi, J., Farjo, R., Yoshida, S., Kern, T.S., Swaroop, A. and Andley, U.P. (2003) A comprehensive analysis of the expression of crystallins in mouse retina. *Mol Vis*, 9, 410-419.
- Yan, Q., Liu, J.P. and Li, D.W. (2006) Apoptosis in lens development and pathology. *Differentiation*, 74, 195-211.
- Yin, X., Landay, M.F., Han, W., Levitan, E.S., Watkins, S.C., Levenson, R.M., Farkas, D.L. and Prochownik, E.V. (2001) Dynamic in vivo interactions among Myc network members. *Oncogene*, 20, 4650-4664.
- Yu, C.M., Chang, G.G., Chang, H.C. and Chiou, S.H. (2004) Cloning and characterization of a thermostable catfish α B-crystallin with chaperone-like activity at high temperatures. *Exp Eye Res*, 79, 249-261.
- Yun, S.J., Hahm, D.H. and Lee, E.H. (2002) Immobilization stress induces the expression of α B-crystallin in rat hippocampus: implications of glial activation in stress-mediated hippocampal degeneration. *Neurosci Lett*, 324, 45-48.
- Zantema, A., Verlaan-De Vries, M., Maasdam, D., Bol, S. and van der Eb, A. (1992) Heat shock protein 27 and α B-crystallin can form a complex, which dissociates by heat shock. *J Biol Chem*, 267, 12936-12941.
- Zhang, L.Y., Yam, G.H., Fan, D.S., Tam, P.O., Lam, D.S. and Pang, C.P. (2007) A novel deletion variant of gammaD-crystallin responsible for congenital nuclear cataract. *Mol Vis*, 13, 2096-2104.
- Zodpey, S.P., Ughade, S.N., Khanolkar, V.A. and Shrikhande, S.N. (1999) Dehydrational crisis from severe diarrhoea and risk of age-related cataract. *J Indian Med Assoc*, 97, 13-15, 24.
- Zollner, T.M., Podda, M., Pien, C., Elliott, P.J., Kaufmann, R. and Boehncke, W.H. (2002) Proteasome inhibition reduces superantigen-mediated T cell activation and the severity of psoriasis in a SCID-hu model. *J Clin Invest*, 109, 671-679.

4. APPENDIX 4-CHARACTERISATION OF THE NATURE OF THE 93 MIN PEAK RESOLVED DURING ANALYTICAL SEC OF αB-CRYSTALLIN FOR CHAPTER 6 (SECTION 6.3.1).....	307
A4.1 THE NATURE OF THE 93 MIN PEAK MATERIAL.....	308
5. APPENDIX 5-DEVELOPMENT OF AN αB-CRYSTALLIN ELISA ASSAY FOR THE DETECTION AND QUANTITATION OF SEC FRACTIONS FROM CHAPTER 5.....	315
A5.1 DEVELOPMENT OF AN α B-CRYSTALLIN ELISA.....	316
A5.1.1 Purification and conjugation of α B-crystallin Mab and Pab.....	318
A5.1.2 Titration of α B-crystallin Mab and Pab HRP conjugates.....	319
A5.1.3 The use of ELISA for potential quantification α B-crystallin protein isolated in SEC fractions.....	325
6. APPENDIX 6-PUBLICATIONS.....	333
REFERENCES.....	350

4. APPENDIX 4-CHARACTERISATION OF THE NATURE OF THE 93 MIN PEAK RESOLVED DURING ANALYTICAL SEC OF αB-CRYSTALLIN FOR CHAPTER 6 (SECTION 6.3.1).....	307
A4.1 THE NATURE OF THE 93 MIN PEAK MATERIAL.....	308
5. APPENDIX 5-DEVELOPMENT OF AN αB-CRYSTALLIN ELISA ASSAY FOR THE DETECTION AND QUANTITATION OF SEC FRACTIONS FROM CHAPTER 5.....	315
A5.1 DEVELOPMENT OF AN α B-CRYSTALLIN ELISA.....	316
A5.1.1 Purification and conjugation of α B-crystallin Mab and Pab.....	318
A5.1.2 Titration of α B-crystallin Mab and Pab HRP conjugates.....	319
A5.1.3 The use of ELISA for potential quantification α B-crystallin protein isolated in SEC fractions.....	325
6. APPENDIX 6-PUBLICATIONS.....	333
REFERENCES.....	350

4. APPENDIX 4-CHARACTERISATION OF THE NATURE OF THE 93 MIN PEAK RESOLVED DURING ANALYTICAL SEC OF αB-CRYSTALLIN FOR CHAPTER 6 (SECTION 6.3.1).....	307
A4.1 THE NATURE OF THE 93 MIN PEAK MATERIAL.....	308
5. APPENDIX 5-DEVELOPMENT OF AN αB-CRYSTALLIN ELISA ASSAY FOR THE DETECTION AND QUANTITATION OF SEC FRACTIONS FROM CHAPTER 5.....	315
A5.1 DEVELOPMENT OF AN α B-CRYSTALLIN ELISA.....	316
A5.1.1 Purification and conjugation of α B-crystallin Mab and Pab.....	318
A5.1.2 Titration of α B-crystallin Mab and Pab HRP conjugates.....	319
A5.1.3 The use of ELISA for potential quantification α B-crystallin protein isolated in SEC fractions.....	325
6. APPENDIX 6-PUBLICATIONS.....	333
REFERENCES.....	350

